THE MORPHOLOGY AND PHYSIOLOGY OF INSECT CHEMOSENSORY SYSTEMS – ITS ORIGIN AND EVOLUTION

EDITED BY: Rui Tang and Xin-Cheng Zhao
PUBLISHED IN: Frontiers in Physiology, Frontiers in Ecology and Evolution and Frontiers in Neuroanatomy

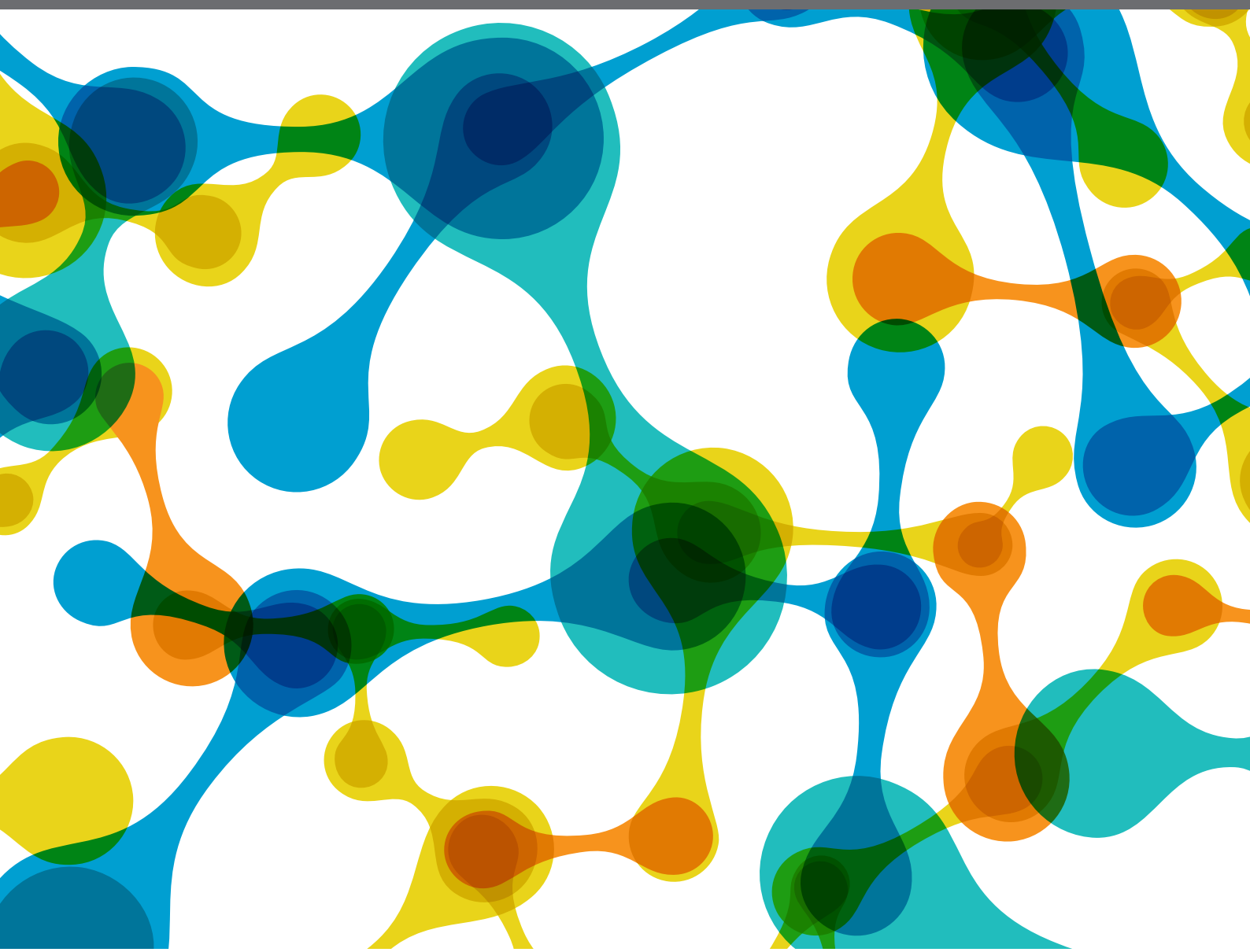

frontiers Research Topics

Frontiers eBook Copyright Statement

The copyright in the text of individual articles in this eBook is the property of their respective authors or their respective institutions or funders. The copyright in graphics and images within each article may be subject to copyright of other parties. In both cases this is subject to a license granted to Frontiers.

The compilation of articles constituting this eBook is the property of Frontiers.

Each article within this eBook, and the eBook itself, are published under the most recent version of the Creative Commons CC-BY licence. The version current at the date of publication of this eBook is CC-BY 4.0. If the CC-BY licence is updated, the licence granted by Frontiers is automatically updated to the new version.

When exercising any right under the CC-BY licence, Frontiers must be attributed as the original publisher of the article or eBook, as applicable.

Authors have the responsibility of ensuring that any graphics or other materials which are the property of others may be included in the CC-BY licence, but this should be checked before relying on the CC-BY licence to reproduce those materials. Any copyright notices relating to those materials must be complied with.

Copyright and source acknowledgement notices may not be removed and must be displayed in any copy, derivative work or partial copy which includes the elements in question.

All copyright, and all rights therein, are protected by national and international copyright laws. The above represents a summary only. For further information please read Frontiers' Conditions for Website Use and Copyright Statement, and the applicable CC-BY licence.

ISSN 1664-8714
ISBN 978-2-83250-489-5
DOI 10.3389/978-2-83250-489-5

About Frontiers

Frontiers is more than just an open-access publisher of scholarly articles: it is a pioneering approach to the world of academia, radically improving the way scholarly research is managed. The grand vision of Frontiers is a world where all people have an equal opportunity to seek, share and generate knowledge. Frontiers provides immediate and permanent online open access to all its publications, but this alone is not enough to realize our grand goals.

Frontiers Journal Series

The Frontiers Journal Series is a multi-tier and interdisciplinary set of open-access, online journals, promising a paradigm shift from the current review, selection and dissemination processes in academic publishing. All Frontiers journals are driven by researchers for researchers; therefore, they constitute a service to the scholarly community. At the same time, the Frontiers Journal Series operates on a revolutionary invention, the tiered publishing system, initially addressing specific communities of scholars, and gradually climbing up to broader public understanding, thus serving the interests of the lay society, too.

Dedication to Quality

Each Frontiers article is a landmark of the highest quality, thanks to genuinely collaborative interactions between authors and review editors, who include some of the world's best academicians. Research must be certified by peers before entering a stream of knowledge that may eventually reach the public - and shape society; therefore, Frontiers only applies the most rigorous and unbiased reviews.
Frontiers revolutionizes research publishing by freely delivering the most outstanding research, evaluated with no bias from both the academic and social point of view. By applying the most advanced information technologies, Frontiers is catapulting scholarly publishing into a new generation.

What are Frontiers Research Topics?

Frontiers Research Topics are very popular trademarks of the Frontiers Journals Series: they are collections of at least ten articles, all centered on a particular subject. With their unique mix of varied contributions from Original Research to Review Articles, Frontiers Research Topics unify the most influential researchers, the latest key findings and historical advances in a hot research area! Find out more on how to host your own Frontiers Research Topic or contribute to one as an author by contacting the Frontiers Editorial Office: frontiersin.org/about/contact

THE MORPHOLOGY AND PHYSIOLOGY OF INSECT CHEMOSENSORY SYSTEMS – ITS ORIGIN AND EVOLUTION

Topic Editors:
Rui Tang, Guangdong Academy of Science (CAS), China
Xin-Cheng Zhao, Henan Agricultural University, China

Citation: Tang, R., Zhao, X.-C., eds. (2022). The Morphology and Physiology of Insect Chemosensory Systems – Its Origin and Evolution.
Lausanne: Frontiers Media SA. doi: 10.3389/978-2-83250-489-5

Table of Contents

frontiers | Frontiers in Neuroanatomy

TYPE Editorial
PUBLISHED 29 September 2022
DOI 10.3389/fnana.2022.1024927

Check for updates

OPEN ACCESS

EDITED AND REVIEWED BY
Javier DeFelipe,
Polytechnic University of Madrid, Spain

*CORRESPONDENCE
Rui Tang
tangr@giz.gd.cn
Xin-Cheng Zhao
xincheng@henau.edu.cn

RECEIVED 22 August 2022
ACCEPTED 02 September 2022
PUBLISHED 29 September 2022

CITATION
Tang R and Zhao X-C (2022) Editorial: The morphology and physiology of insect chemosensory systems – Its origin and evolution.
Front. Neuroanat. 16:1024927.
doi: 10.3389/fnana.2022.1024927

COPYRIGHT
© 2022 Tang and Zhao. This is an open-access article distributed under the terms of the Creative Commons Attribution License (CC BY). The use, distribution or reproduction in other forums is permitted, provided the original author(s) and the copyright owner(s) are credited and that the original publication in this journal is cited, in accordance with accepted academic practice. No use, distribution or reproduction is permitted which does not comply with these terms.

Editorial: The morphology and physiology of insect chemosensory systems – Its origin and evolution

Rui Tang [1]* and Xin-Cheng Zhao [2]*

[1]Guangdong Key Laboratory of Animal Conservation and Resource Utilization, Guangdong Public Laboratory of Wild Animal Conservation and Utilization, Institute of Zoology, Guangdong Academy of Sciences, Guangzhou, China, [2]Henan International Laboratory for Green Pest Control/College of Plant Protection, Henan Agricultural University, Zhengzhou, China

KEYWORDS

insect, chemosensory system, morphology, physiology, neural pathway, omics

Editorial on the Research Topic
The morphology and physiology of insect chemosensory systems – Its origin and evolution

Insects rely heavily on the ancient chemosensory modality to colonize in the environment. To date, the huge diversity of insect species and their special adaptations to distinct ecological niches are mostly driven by key environmental cues, species-specific neural pathways, and functional repertoires of several biological macromolecule classes. These essential elements contain an indispensable clue from which modern phenotype-to-molecular study scenarios were established. The chemosensory circuits and physiological traits in insect species can reflect protein-ligand interactions at the molecular level and *vice versa*. As such, the omic-based reverse chemical ecology has been swiftly improved along with the classic chemical ecology. Information on either side can help us gain knowledge of the other side, and provide information to help solve the riddle of how certain chemosensory traits emerged and evolved in insects. This Research Topic aims to seek morphological, physiological, and molecular features in insect chemosensory system toward allelochemicals and provide the linkage between architectures and innervated/environmental causes which forged the insect populations over time.

Inter- and intra-species communication

Pre-mating sex communication in Lepidoptera is one of the most representative modules to understand chemical-driven behavioral decisions in insects. In the sex pheromone detection processes, sex pheromone molecule (SPM), pheromone receptor (PR), co-receptor (ORco), pheromone binding protein (PBP), sensory neuron membrane protein (SNMP), and pheromone degradation enzyme (PDE) play individual and

cooperative roles. The review from Yang et al. summarized SPR/ORco from 10 families of Lepidopteran insects regarding the receptor-ligand clustering, protein topologies, and updated pheromone signaling pathways. Future interests of the area are expected to explore the cryo-EM structure of SPR and the SPR-ligand docking pattern from a biophysical perspective.

The function of peripheral neurons in recognizing sex pheromones provides fundamental knowledge for us to link species ecology with biological molecules and innervated circuits. The work of Wang et al. filled this gap in the oriental armyworm *Mythimna separata*. The trichoid sensilla (TS) from both sexes of adults were classified into four types after carrying out single sensillum recording (SSR) tests. The neurons within the TS were further characterized, and corresponding PRs were speculated according to later functional deorphanizations of receptors.

The odorant coding to aromatics in insect pollinators is important in understanding insect-plant interactions. Dong et al. studied the syrphid fly *Eupeodes corollae* in terms of antennal sensillar clustering, ultrastructural characterization, and SSR firing patterns, by providing results from SEM, TEM, and SSR, respectively. Sensillar types and structures of the species were described in detail, and a sensilla basiconica (SB) answering to methyl eugenol was identified.

The host acceptances of insects can be determined largely by detecting plant metabolites with taste. Sun et al. showed that larvae of the generalist *Helicoverpa armigera* and the specialist *H. assulta* had distinct herbivore inducing and responding patterns toward host molecules. Components including saccharides, amino acids, and other secondary metabolites elicited varied feeding responses between the two species. The firing patterns of gustatory receptor neurons (GRNs) in the maxillary styloconic sensilla were found to be consistent with the differences in feeding preferences between the two species.

Insect chemosensory genes in the era of omics

Development and host ranges influence gene expressions in insects. The work presented by Tian et al. utilized weighted gene co-expression network analysis (WGCNA) to construct gene co-expression networks in the whitefly *Bemisia tabaci*. Co-expression modules related to host plant selection were identified by cross checking with transcriptomic data from various tissues.

The mature RNA-seq technology is by far the most convenient way to tackle spatial-temporal functional annotations of chemosensory genes in insects. The work from Liu et al. analyzed tissue- and gender-wise transcriptome of *Chilo sacchariphagus* and identified a panel of comprehensive chemoreception-related family genes. Annotations were further evaluated by phylogenetic analysis and real-time expression profiling.

It is essential to link peripheral architectures with associated chemosensory genes. The work on the orange spiny whitefly *Aleurocanthus spiniferus* provided by Gao et al. unveiled antennal sensillar types and chemosensory gene annotations of the species. The expression profiling of selected chemosensory genes at different developmental stages was further examined and mapped to transcriptomes.

Aldehyde oxidases (AOXs) are common detoxifying enzymes in several organisms. In insects, AOXs act in xenobiotic metabolism and as odorant-degrading enzymes (ODEs). In the work of Godoy et al., novel *AOX* families were reported by checking 18 genomes from moths and butterflies. Odorant-degrading functions of the two clades were estimated through phylogenetic tests, involving both plant volatiles and sex pheromones, respectively.

In insects, odorant binding proteins (OBPs) form a vital chemosensory family which is involved in transporting hydrophobic odor molecules from the external environment to receptor neurons. By providing a comparative genomic analysis using the codling moth *Cydia pomonella*, Huang et al. described evolution traits of *OBPs* in the species. Possible distant ancestral OBPs were found lost, and the expansion of OBPs was speculated to have resulted from tandem duplications.

Ligand binding properties are major concerns in exploring insect OBPs. Jiang et al. characterized this family within *Aphidius gifuensis*, which was the most common endoparasitoids of the field aphids, by providing evidence from transcriptomes, expression profiling, gene cloning, and competitive ligand binding assays. It showed that OBPs abundantly expressed in the legs of this species were responsible for binding an analog of (E)-β-farnesene, which has a known function in aphid ecology.

Insect-plant interactions are also initiated from protein-ligand binding of OBPs in herbivores. Hong et al. identified an antennal-specific OBP within the jujube bud weevil *Pachyrhinus yasumatsui via* transcriptomic analysis, and further evaluated this protein in a binding test. A broad ligand recognition pattern was found with the tested OBP, and essential amino acid residues for binding were estimated *via* modeling and docking simulations.

Expanding methodologies and aspects

Electrophysiological tests can never be too precise. Li et al. reported on a new electroantennogram (EAG) recording technique for evaluation of electrophysiological responses of antennal lamellae of *Pseudosymmachia flavescens* to sex pheromones and host-plant-related compounds. EAG responses were recorded simultaneously from each lamella and the closed antennal club. This has provided a method to separate EAG

channels of lamellae in the scarab beetles or other possible insects with unconventional antennal morphology.

Land to freshwater transitions occurred in many lineages within the insect tree of life. Whether chemosensory gene repertoires of aquatic insects remained essentially unchanged or underwent more or less drastic modifications to cope with physico-chemical constraints associated with life underwater remains virtually unknown. Montagné et al. provided the transcriptome of chemosensory organs of the diving beetle *Rhantus suturalis* and described OBP and OR expansions specific to diving beetles. These duplicated genes tend to be expressed in palps rather than in antennae, suggesting a possible adaptation with respect to the land-to-water transition.

Chemosensory-related genes are expressed in various tissues, including non-sensory organs, and they play diverse roles. Insect OBPs and CSPs have been detected in various tissues as well as olfactory organs. They are involved in carrying semiochemicals that have various roles, such as in reproduction, regeneration, development, nutrition, anti-inflammatory action, and vision. The work by Chen et al. showed that OBPs and CSPs existed in the brains of oriental armyworm adults, by providing transcriptomic analysis and sex-biased expression profiling. This may help us understand novel functions and ligand targets of insect chemosensory proteins.

Neuroanatomical studies are regularly done in adults of agricultural pests, but brain structures from larvae are rarely reported. Zhang et al. targeted the important fall armyworm species and traced the serotonergic and serotonergic neural networks within the larval brain and gnathal ganglion. Morphological mapping and segmentation were conducted with the above neuropils of the species. Wiring of serotonergic neurons were described in detail.

Conclusion

To conclude, the current hot spots in insect chemosensory research include pheromone-based behavioral driving and multi-trophic interaction mechanisms. Next-generation omics and iterative analytic tools have granted us vast data to explore and a unique chance to trace evolutionary milestones among species. We have harvested novel results, views, and prospects within this topic that they will inspire further studies on precise neural pathways, functional deorphanizations, and adaptation history of chemoreception in insects.

Author contributions

RT and X-CZ drafted and finalized this document.

Funding

This report was supported by Guangzhou Science and Technology Project (No. 202201010039) and GDAS Special Project of Science and Technology Development (2022GDASZH-2022010106).

Acknowledgments

We would like to express our sincere thanks to all colleagues who contributed to this topic, covering most focal areas in the research landscapes of modern insect chemoreception. We also thank all reviewers and affiliated editors working in the science community who supported us by producing consistent and high-quality publications. Last but not least, we are grateful to Frontiers editorial and supporting units for all their help and encouragement during our work.

Conflict of interest

The authors declare that the research was conducted in the absence of any commercial or financial relationships that could be construed as a potential conflict of interest.

Publisher's note

All claims expressed in this article are solely those of the authors and do not necessarily represent those of their affiliated organizations, or those of the publisher, the editors and the reviewers. Any product that may be evaluated in this article, or claim that may be made by its manufacturer, is not guaranteed or endorsed by the publisher.

frontiers in Physiology

ORIGINAL RESEARCH
published: 05 March 2021
doi: 10.3389/fphys.2021.636353

Transcriptome Characterization and Expression Analysis of Chemosensory Genes in *Chilo sacchariphagus* (Lepidoptera Crambidae), a Key Pest of Sugarcane

Jianbai Liu[1], Huan Liu[1,2], Jiequn Yi[1], Yongkai Mao[1], Jihu Li[1], Donglei Sun[1], Yuxing An[1] and Han Wu[1]**

[1] *Guangdong Engineering Research Center for Pesticide and Fertilizer, Institute of Bioengineering, Guangdong Academy of Sciences, Guangzhou, China,* [2] *College of Horticulture and Plant Protection, Henan University of Science and Technology, Luoyang, China*

Insect chemoreception involves many families of genes, including odourant/pheromone binding proteins (*OBP/PBPs*), chemosensory proteins (*CSPs*), odourant receptors (*ORs*), ionotropic receptors (*IRs*), and sensory neuron membrane proteins (*SNMPs*), which play irreplaceable roles in mediating insect behaviors such as host location, foraging, mating, oviposition, and avoidance of danger. However, little is known about the molecular mechanism of olfactory reception in *Chilo sacchariphagus,* which is a major pest of sugarcane. A set of 72 candidate chemosensory genes, including 31 *OBPs/PBPs*, 15 *CSPs*, 11 *ORs*, 13 *IRs*, and two *SNMPs*, were identified in four transcriptomes from different tissues and genders of *C. sacchariphagus*. Phylogenetic analysis was conducted on gene families and paralogs from other model insect species. Quantitative real-time PCR (qRT-PCR) showed that most of these chemosensory genes exhibited antennae-biased expression, but some had high expression in bodies. Most of the identified chemosensory genes were likely involved in chemoreception. This study provides a molecular foundation for the function of chemosensory proteins, and an opportunity for understanding how *C. sacchariphagus* behaviors are mediated via chemical cues. This research might facilitate the discovery of novel strategies for pest management in agricultural ecosystems.

Keywords: *Chilo sacchariphagus*, transcriptome, chemosensory genes, gene expression, phylogenetic analysis

OPEN ACCESS

Edited by:
Xin-Cheng Zhao,
Henan Agricultural University, China

Reviewed by:
Peng He,
Guizhou University, China
Fanghai Wang,
Sun Yat-sen University, China

****Correspondence:***
Yuxing An
yanxing888@126.com
Han Wu
antenna1217@163.com

Specialty section:
This article was submitted to Invertebrate Physiology, a section of the journal Frontiers in Physiology

Received: *01 December 2020*
Accepted: *04 January 2021*
Published: *05 March 2021*

Citation:
Liu J, Liu H, Yi J, Mao Y, Li J, Sun D, An Y and Wu H (2021) Transcriptome Characterization and Expression Analysis of Chemosensory Genes in Chilo sacchariphagus (Lepidoptera Crambidae), a Key Pest of Sugarcane. Front. Physiol. 12:636353. doi: 10.3389/fphys.2021.636353

INTRODUCTION

Insects, the most diverse and successful group of animals on earth, have existed for more than 350 million years (Stork, 1993; Chen et al., 2018); they not only affect the natural environment but also influence human life and productivity in many ways. A sophisticated chemosensory system makes insect prominence among other animals for their survival and reproduction (Leal, 2013).

Abbreviations: OR, odorant receptor; IR, ionotropic receptor; PBP, pheromone binding protein; OBP, odorant binding protein; CSP, chemosensory protein; SNMP, sensory neuron membrane protein; GO, gene ontology; FPKM, fragments per kb per million fragments; FDR, false discovery rate.

Chemoreception plays a critical role in many insect behaviors, including behaviors to avoid harm from predators or the surrounding environment, behaviors to detect locations for oviposition or hosts, searching for food or mates, and interspecific communication (Stocker, 1994; Hildebrand, 1995; Grosse-Wilde et al., 2011; Zhang et al., 2015). The recognition of chemical signals depends on peripheral chemosensory systems (Vieira and Rozas, 2011; Zhang et al., 2016). External chemical ligands are recognized by binding and membrane receptor proteins located in the antennae, which have many kinds of sensilla, and then translated into electrical signals to the central nervous system (Robertson et al., 2003; Ramdya and Benton, 2010). Chemoreception in insects is mediated via many proteins, including odourant binding proteins (OBPs), pheromone binding proteins (PBPs), chemosensory proteins (CSPs), odourant receptors (ORs), ionotropic receptors (IRs), and sensory neuron membrane proteins (SNMPs) (Leal, 2013; Pelosi et al., 2014, 2018; Wicher, 2014; Butterwick et al., 2018; He et al., 2019b).

Insect OBPs, small water-soluble proteins with molecular masses of approximately 14 kDa that were first found in *Antheraea polyphemus* (Vogt and Riddiford, 1981), are present at high concentrations in the sensillum lymph (Vogt and Riddiford, 1981; Pelosi et al., 2006). OBPs act as a liaison between external chemicals and ORs (Leal, 2005), recognizing hydrophobic odourants and delivering them to olfactory receptors (ORs) on olfactory sensory neurone (OSN) membranes (Pelosi et al., 2006; Xu et al., 2009; Leal, 2013), which is the first and key step in the process of olfaction. CSPs, which were found to be soluble binding proteins (Gong et al., 2007), are abundant in the sensillum lymph (Vogt and Riddiford, 1981; Prestwich, 1996; Pophof, 2004; Grosse-Wilde et al., 2006; Lautenschlager et al., 2007; Leal, 2007; Laughlin et al., 2008; Kaissling, 2009) and also expressed in many organs and tissues, such as antennae, wings, legs, maxillary palps, and labial palps, with the function of affecting chemoreception (Jacquinjoly et al., 2001; Jin et al., 2005; González et al., 2009; Pelletier and Leal, 2011; Gu et al., 2013; Zhang et al., 2014). PBPs, a kind of special odor-binding protein that can dissolve and transport fat-soluble pheromones through hydrophilic lymph (Vogt and Riddiford, 1981; Wojtasek and Leal, 1999), are expressed around the time of eclosion (Gyorgyi et al., 1988).

Insect ORs, a member of a novel family of seven-transmembrane proteins located in the dendrite membrane of OSNs with a reversed membrane topology compared to that of G-protein coupled vertebrate ORs (intracellular N-terminus and extracellular C-terminus) (Clyne et al., 1999; Benton et al., 2006), were first found and identified in *Drosophila melanogaster* (Clyne et al., 1999; Vosshall et al., 1999). In the process of insect olfactory signal transduction, OR and ORCO form a complex of odourant-gated ion channels that play a fundamental role in the conversion of chemical signals to electrical signals (Larsson et al., 2004; Jones et al., 2005; Sato et al., 2008; Smart et al., 2008; Wicher et al., 2008; Butterwick et al., 2018; Fandino et al., 2019).

Ionotropic receptors, belonging to the ionotropic glutamate receptor (iGluR) family of ion channels with three transmembrane domains (M1, M2, and M3), have been shown to be involved in chemosensation (Benton et al., 2009; Croset et al., 2010; Abuin et al., 2011; Bengtsson et al., 2012; Andersson et al., 2013; Tang et al., 2020). Two or three IR genes were co-expressed in an IR-expressing neuron (Benton et al., 2009). IRs are extensively distributed in many insect species, including *D. melanogaster*, *Cydia pomonella*, *Chrysoperla sinica*, *Bactrocera dorsalis*, and *Dendroctonus valens* (Benton et al., 2009; Bengtsson et al., 2012; Gu et al., 2015; Li et al., 2015; Wu et al., 2015), and show relatively high homology across species (Chiu et al., 1999). In insects, IRs are thought to be used for sensing chemicals in the surrounding environment and function during the process of taste perception (Chiu et al., 1999; Benton et al., 2009; Croset et al., 2010).

Sensory neuron membrane proteins, located on dendrite cilia in insects, belong to the CD36 family of two-transmembrane domain membrane proteins (Rogers et al., 2001; Hu et al., 2016). Insect SNMPs can usually be divided into two subfamilies: SNMP1 and SNMP2, while in a recent study, SNMP3 has been found in lepidopteran. SNMP1, with specific expression on pheromone-specific OSNs in the insect antennae, was thought to have a pheromone detection function (Vogt et al., 2009); the function of SNMP2 has not yet been clarified; while is specifically SNMP3 is biased-expressed in the larval midgut, which may be involved in functioning immunity response to virus and bacterial infections the silkworm (Zhang et al., 2020).

Chilo saccharaphagus Bojeris, a lepidopteran of the Pyralidae family, is one of the most dangerous pests for sugarcane. Their larvae cause damage by mining the seedlings and stems of sugarcane; this species also harms sorghum, corn and other crops. *C. saccharaphagus* causes great economic losses to the sugar industry every year in China, as well as in South Africa, India, Swaziland, and other countries and regions (Bezuidenhout et al., 2008; Geetha et al., 2010). At present, research on the sugarcane cane borer is mainly focused on identifying resistant varieties, determining the resistance mechanisms of sugarcane and developing biological control techniques (including the utilization of *Trichogramma chilonis* Ishii, pheromones, and pathogenic nematodes) (Nibouche and Tibère, 2010; Nibouche et al., 2012; Sallam et al., 2016). Chemoreception plays an irreplaceable role in the foraging, mating, oviposition and other behaviors of *C. saccharaphagus*, which are vital for its survival in the natural environment. However, few reports have been published on this topic, including on the characterization and function of chemosensory genes and the mechanisms of chemosensory recognition.

In this study, we sequenced and analyzed the *C. saccharaphagus* adult antennal transcriptomes using the Illumina HiSeq^{TM} 4000 platform. Seventy-two chemoreception-related genes were identified in total, including 31 *OBP/PBPs*, 15 *CSPs*, 11 *ORs*, 13 *IRs*, and two *SNMPs*, by analyzing the transcriptome data. Our aim was to identify chemoreception-related genes in this pest insect species, which is destructive to the sugarcane production and sugar industry in China, across Asia and in the Pacific and India. We intend to provide a theory for an improved understanding of how *C. saccharaphagus* recognizes, locates, forages, and mates.

MATERIALS AND METHODS

Insects

The eggs of *C. saccharaphagus*, obtained from a wild field, were reared at 27 ± 1°C with 75 ± 5% relative humidity and a 14 L:10 D photoperiod at Guangdong Engineering Research Center for Pesticide and Fertilizer, Institute of Bioengineering, Guangdong Academy of Sciences, Guangzhou, China. Larvae were reared on an artificial diet under the same conditions. After at least three generations, newly emerged male and female adult *C. saccharaphagus* were chosen as experimental subjects. After pupation, male and female pupae were separated and fed with 10% sugar solution. Antennae of unmated male and female individuals were collected 2 days after eclosion, immediately frozen in liquid nitrogen, and stored at −80°C. Antennae with intact structure were removed using tweezers.

cDNA Library Construction, Transcriptome Sequencing, Assembly and Functional Annotation

Twenty pairs of antennae and 20 body tissues (without antennae) from male and female of *C. saccharaphagus* were used for RNA extraction. For each sample, total RNA was extracted using TRIzol reagents (Invitrogen, United States) according to the manufacturer's instructions. RNase-free DNase I (Takara Biotechnology Co., Ltd., Dalian, China) was used to remove contaminating genomic DNA. The quantity and quality of RNA were assessed by agarose gel electrophoresis and on a Bioanalyzer 2100 system (Agilent Technologies, United States). RNA with high purity, concentration and integrity was chosen for cDNA library construction and final Illumina sequencing at Gene Denovo Biotechnology Company (Guangzhou, China). The cDNA was then tested for quality and sequenced on an Illumina HiSeq^{TM} 4000 platform as 150 bp paired-end reads.

The obtained raw reads were processed to remove adapters, primers, low-quality sequences, and ambiguous "N" nucleotides. Then, quality assessment of the clean data was carried out by Q30, and the GC content and sequence duplication level were calculated. Clean data were assembled into contigs using Trinity software and subsequently assembled into transcripts using the De Bruijn graph method. The assembled transcripts were further clustered to form unigenes by using the TGI Clustering Tool (Quackenbush et al., 2001; Pertea et al., 2003).

The annotation of all unigenes was performed by BLASTx against a pooled database containing protein entries from the National Center for Biotechnology Information non-redundant protein (NCBI-NR), Swiss-Prot, Gene Ontology (GO), Clusters of Orthologous Groups (COG), and Kyoto Encyclopedia of Genes and Genomes (KEGG) databases with an *E*-value $< 10^{-5}$. After amino acid sequence prediction, annotation of unigenes was obtained using HMMER software (Eddy, 1998), and Gene Ontology (GO) annotations were determined by Blast2GO. In addition, WEGO (Ye et al., 2006) was utilized to perform GO functional classification and evaluate the distribution of gene functions at the macro level. Unigene functions were also predicted by aligning their sequences with the COG database.

Phylogenetic Analysis

The amino acid sequence alignment of the candidate chemosensory-related genes of *C. saccharaphagus* was performed using CLUSTALX 2.0 (Larkin et al., 2007). The candidate OBPs, PBPs, CSPs, ORs, IRs, and SNMPs of *C. saccharaphagus* were chosen for phylogenetic analysis along with genes from model organisms Lepidoptera (*Manduca sexta* and *Bombyx mori*), Diptera (*D. melanogaster*), and Hymenoptera (*Apis mellifera*) species. Phylogenetic trees were constructed by the neighbor-joining method, as implemented in MEGA6.0 software. Node support was assessed using a bootstrap procedure with 1000 replicates (Tamura et al., 2013). Phylogenetic trees were colored and arranged using FigTree (Version: 1.4.2).

Expression Analysis by Real-Time Quantitative PCR (qRT-PCR)

Real-time quantitative PCR (qRT-PCR) was performed to verify the expression of candidate chemosensory genes. Tissue samples were collected from *C. saccharaphagus* adults 2 days after eclosion in three biological replicates, and total RNA was extracted as described above. One microgram of total RNA from the transcriptome samples was subjected to reverse transcription in a total reaction volume of 20 μL according to the manufacturer's instructions (PrimeScript^{TM} RT Reagent Kit, Takara, Japan) to obtain the first-strand cDNAs. With the manual for the SYBR Green I Master (Roche Diagnostics Ltd., Lewes, United Kingdom), qRT-PCR was processed in 10 μL reaction volumes [1 μL cDNA (2 ng/μL), 5 μL SYBR Green I Master, 0.5 μL/primer, and 3 μL ddH_2O] on a LightCycler® 480 real-time PCR system (Roche Diagnostics Ltd.) with the following program: denaturation at 95°C for 5 min followed by 40 cycles of 5 s at 95°C, 20 s at 60°C, and 20 s at 72°C. β-*actin* was used as the internal reference gene, and each gene was tested in triplicate. The relative expression levels of the candidate chemosensory genes normalized to the internal control gene were calculated using the $2^{-\Delta\Delta Ct}$ method (Livak and Schmittgen, 2001).

RESULTS

Overview of Transcriptomes

After sequencing and a subsequent quality control process, a total of 16.60 Gb of clean data were obtained from four libraries (CT: antennae of female, CS: body of female, XT: antennae of male, XS: body of male). All the transcriptome libraries generated 231891488 raw reads. A total of 57757438, 61860942, 64297952, and 47525880 clean reads were obtained for CT, CS, XT, and XS, respectively. Then, these clean reads were arranged into 41571, 45477, 41900, and 44065 unigenes for CT, CS, XT, and XS, respectively, with a mean length of 829 bp and N50 length of 1694 bp, using Trinity software (**Table 1**). The Q30 and GC content of each library were over 93.57% and 46.58%, respectively. Of the unigenes predicted, 24008 (39.96%) had a length between 200 and 300 bp, and 13785 (22.94%) were over 1000 bp in length (**Supplementary Figure 1**).

TABLE 1 | Summary of the *C. saccharaphagus* transcriptome.

Group Name	Number
200–300	24008 (39.96%)
300–500	12445 (20.71%)
500–1000	9848 (16.39%)
1000–2000	7422 (12.35%)
2000+	6361 (10.59%)
Total No. of unigenes	60084
GC percentage (%)	41.33
N50 length (bp)	1694
Maximum unigene length (bp)	23896
Minimum unigene length (bp)	201
Mean length (bp)	829

TABLE 2 | Summary of the annotations of the assembled *C. saccharaphagus* unigenes.

Category	Number of unigenses	Percentage (%)
Nr annotation	27392	45.59
SwissProt annotation	15150	25.21
KOG annotation	12996	21.63
KEGG annotation	11718	19.50
Total annotated genes	28330	47.15
Total No. of unigenes	60087	

In total, 28330 unigenes (47.15%) were annotated (**Table 2**). A total of 27392 unigenes (45.59%) were annotated in the NR database, which accounted for the largest proportion of matches, followed by the Swiss-Prot (15150, 25.21%), KOG (12996, 21.63%), and KEGG (11718, 19.50%) databases. The identity levels of the annotation match were >80.00% for 17.87% of the sequences and between 60.00 and 80.00% for 29.04% of the sequences (**Figure 1A**). According to the NR annotation, 61.64% of the unigenes were annotated with sequences from *Amyelois transitella* (18.02%), *B. mori* (9.57%), *Papilio xuthus* (7.78%), *Papilio machaon* (6.62%), *Operophtera brumata* (4.15%), *Plutella xylostella* (3.66%), *Papilio polytes* (3.27%), *Danaus plexippus* (2.33%), *Pararge aegeria* (2.31%), *Daphnia magna* (2.11%), and *Chilo suppressalis* (1.64%), and 38.54% of the unigenes were annotated with sequences from other species (**Figure 1B**). Based on the *E* value distribution of the top hits in the NR database, 33.40% and 40.31% of the sequences showed strong ($0 \leq E$-value $\leq 1.0E^{-100}$) and moderate ($1.0E^{-100} \leq E$-value $\leq 1.0E^{-20}$) homology, respectively (**Figure 1C**).

A total of 4662 unigenes were annotated with functional groups classified into 52 subcategories under three main GO categories ("biological process," "cellular component," and "molecular function") via Blast2GO and WEGO software (**Figure 2**). Among 24 subcategories in the "biological process" category, "metabolic process" and "cellular process" were predominant terms. In the "cellular component" category, "cell part" and "cell" were the most abundant GO terms. Of the 11 subcategories under the "molecular function" category, two contained the largest groups, namely, "catalytic activity" and "binding."

Identification of the Candidate Genes Related to Chemoreception

Within this transcriptome, 72 candidate genes related to chemoreception were identified, including 11 *ORs*, 31 *OBPs/PBPs*, 13 *IRs*, 15 *CSPs*, and two *SNMPs*. Twenty-eight different putative sequences encoding odourant binding proteins were identified. Most insect OBPs/PBPs were highly conserved, and 15 candidate OBPs/PBPs (CsacOBP1, CsacOBP2, CsacOBP3, CsacOBP4, CsacOBP5, CsacOBP7, CsacOBP8, CsacOBP10, CsacOBP18, CsacOBP19, CsacOBP20, CsacOBP21, CsacOBP23, CsacOBP26, and CsacPBP2) had an identity higher than 80% with OBPs/PBPs from *Chilo suppressalis*, *Danaus plexippus*, and *Amyelois transitella* (**Table 3**). According to the prediction, all the CsacOBPs/PBPs possess signal peptides with complete N-termini, except for CsacOBP3, CsacOBP7, CsacOBP12, CsacOBP15, CsacOBP18, CsacOBP25, and CsacPBP3. In the phylogenetic analysis of the OBPs/PBPs in different insect species, CsacOBPs/PBPs were spread across various branches, where they formed five small subgroups together with OBPs/PBPs from other insects (**Figure 3**). A specific branch consisting of five OBPs from *C. saccharaphagus* (CsacOBP2, CsacOBP4, CsacOBP10, CsacOBP14, and CsacOBP16) was divergent from the OBPs of other insects. The five CsacOBPs have a close relation to OBP83a, OBP56d, and OBPLOC100301497 precursor from *B. mori* and OBP83a and OBP69a from *M. sexta*. CsacOBP6, CsacOBP12, CsacOBP26, and CsacOBP27 formed a small branch that shared a close relationship to OBPfmxg18C7 precursor and OBPLOC100301495 precursor from *B. mori*; in addition, three OBPs from *C. saccharaphagus* (CsacOBP19, CsacOBP20, and CsacOBP24), two OBPs from *M. sexta* (MsexOBP99a and MsexOBP28a) and three OBPs from *B. mori* (BmorOBPLOC100301496 precursor, BmorOBP99a, and BmorOBP6) formed a small subgroup within this branch. However, a specific branch consisting of five closely related genes, *CsacPBP2*, *MsexPBP, BmorPBP* precursor, *BmorPBP*, and *BmorPBP2* partial, was divergent from other OBPs/PBPs.

Among the 11 candidate *ORs*, four were of short length (no more than 100 amino acids), and the remaining seven possessed a deduced protein longer than 200 amino acids (**Table 3**). From the prediction, three sequences (*CsacORCO*, *CsacOR1*, and *CsacOR4*) were full-length *OR* genes with intact open reading frames with a general length of 1500 bp and 5–7 transmembrane domains, which are characteristic of typical insect ORs. Compared with OBPs, the results of BLASTx revealed that the identity of these candidate ORs with known insect ORs was relatively low. Only one candidate OR (CsacORCO) had an identity higher than 80% (96%) with its closest match, while the identities of the remaining ORs ranged from 38 to 71%. Two ORs, CsacOR1 and CsacOR5, formed a small branch that was closely related to BmorOR1 and BmorOR9 from *B. mori* and MsexOR60 from *M. sexta*, and these ORs formed a distinct subgroup (**Figure 4**). Most of the splits in the tree were supported by bootstrap values, and only a few splits were unreliable.

Bioinformatic analysis led to the identification of 15 different sequences encoding candidate *CsacCSPs*. Due to their complete N-termini, all the sequences had signal peptides. The identity of

TABLE 3 | Unigenes of candidate odorant receptors, ionotropic receptors, odorant binding proteins, sensory neuron membrane proteins, and chemosensory proteins.

Gene name	Unigene reference	Blastx best hit (name)	Species	Length (bp)	ORF (aa)	E-value	Identity (%)	TMD (No.)	Signal peptide
CsacOBP1	Unigene0030060	general odorant binding protein 1	*Chilo suppressalis*	675	152	3E-101	85		Yes
CsacOBP2	Unigene0030448	general odorant binding protein 1	*Chilo suppressalis*	473	140	8.00E-80	81		Yes
CsacOBP3	Unigene0027582	odorant-binding protein 2	*Danaus plexippus*	674	183	3.00E-107	85		No
CsacOBP4	Unigene0033446	minus strand odorant-binding protein 2	*Chilo suppressalis*	740	133	2.00E-88	94		Yes
CsacOBP5	Unigene0007401	general odorant binding protein 2	*Chilo suppressalis*	731	162	1.00E-103	87		Yes
CsacOBP6	Unigene0029763	odorant-binding protein 3	*Cnaphalocrocis medinalis*	865	256	4.00E-92	52		Yes
CsacOBP7	Unigene0009252	minus strand odorant-binding protein 3	*Chilo suppressalis*	2079	196	1.00E-114	80		No
CsacOBP8	Unigene0032347	odorant-binding protein 4	*Chilo suppressalis*	744	146	2.00E-91	87		Yes
CsacOBP9	Unigene0035693	odorant-binding protein 4	*Chilo suppressalis*	999	192	1.00E-78	60		Yes
CsacOBP10	Unigene0008372	minus strand odorant-binding protein 5	*Chilo suppressalis*	1116	143	3.00E-83	85		Yes
CsacOBP11	Unigene0012927	odorant binding protein 6	*Athetis dissimilis*	496	152	2.00E-42	46		Yes
CsacOBP12	Unigene0030417	minus strand odorant-binding protein 7, partial	*Cnaphalocrocis medinalis*	786	241	1.00E-92	56		No
CsacOBP13	Unigene0037360	minus strand odorant binding protein 10	*Ostrinia furnacalis*	1460	125	3.00E-83	65		Yes
CsacOBP14	Unigene0035330	odorant binding protein 13	*Ostrinia furnacalis*	1275	192	7.00E-84	78		Yes
CsacOBP15	Unigene0006183	odorant binding protein 17, partial	*Ostrinia furnacalis*	509	165	2.00E-25	41		No
CsacOBP16	Unigene0030117	minus strand odorant-binding protein 18	*Cnaphalocrocis medinalis*	791	138	4.00E-68	75		Yes
CsacOBP17	Unigene0006733	minus strand odorant binding protein 20	*Spodoptera litura*	1740	133	1.00E-58	69		Yes
CsacOBP18	Unigene0028432	odorant-binding protein 21, partial	*Chilo suppressalis*	683	213	7.00E-98	93		No
CsacOBP19	Unigene0039894	minus strand odorant-binding protein 25	*Chilo suppressalis*	614	154	1.00E-94	90		Yes
CsacOBP20	Unigene0000195	minus strand odorant-binding protein 29, partial	*Chilo suppressalis*	521	146	1.00E-82	83		Yes
CsacOBP21	Unigene0043170	minus strand PREDICTED: general odorant-binding protein 70-like	*Amyelois transitella*	975	184	9.00E-128	96		Yes
CsacOBP22	Unigene0005874	PREDICTED: general odorant-binding protein 72-like	*Papilio xuthus*	479	121	1.00E-78	75		Yes
CsacOBP23	Unigene0005061	odorant binding protein	*Chilo suppressalis*	1051	133	1.00E-72	83		Yes
CsacOBP24	Unigene0032152	odorant binding protein	*Chilo suppressalis*	583	150	1.00E-65	71		Yes
CsacOBP25	Unigene0037021	odorant binding protein	*Chilo suppressalis*	862	174	9.00E-68	72		No
CsacOBP26	Unigene0038968	odorant-binding protein	*Chilo suppressalis*	893	256	3.00E-165	88		Yes
CsacOBP27	Unigene0029475	odorant binding protein	*Eogystia hippophaecolus*	870	239	8.00E-68	44		Yes
CsacOBP28	Unigene0042810	minus strand Odorant binding protein	*Operophtera brumata*	651	157	7.00E-87	76		Yes
CsacPBP1	Unigene0036519	minus strand pheromone binding protein 1	*Chilo suppressalis*	1123	162	6.00E-87	77		Yes
CsacPBP2	Unigene0042820	minus strand pheromone binding protein 2	*Chilo suppressalis*	1766	140	1.00E-89	80		Yes
CsacPBP3	Unigene0002457	pheromone binding protein 5	*Ostrinia furnacalis*	1604	165	1.00E-46	45		No
CsacCSP1	Unigene0012225	chemosensory protein 3	*Agrotis ipsilon*	524	120	5.00E-34	48		Yes
CsacCSP2	Unigene0004638	chemosensory protein 4	*Ostrinia furnacalis*	1431	129	7.00E-73	82		Yes
CsacCSP3	Unigene0007810	chemosensory protein 6	*Conogethes punctiferalis*	699	123	8.00E-54	63		Yes
CsacCSP4	Unigene0029070	minus strand chemosensory protein 10	*Ostrinia furnacalis*	425	121	2.00E-43	58		Yes
CsacCSP5	Unigene0001797	chemosensory protein 14	*Spodoptera exigua*	2497	333	5.00E-107	58		Yes
CsacCSP6	Unigene0007266	chemosensory protein 16	*Ostrinia furnacalis*	455	118	2.00E-36	50		Yes
CsacCSP7	Unigene0031023	chemosensory protein 18	*Ostrinia furnacalis*	547	105	2.00E-51	78		Yes
CsacCSP8	Unigene0035672	chemosensory protein 36	*Cnaphalocrocis medinalis*	860	121	6.00E-51	69		Yes

(Continued)

TABLE 3 | Continued

Gene name	Unigene reference	Blastx best hit (name)	Species	Length (bp)	ORF (aa)	*E*-value	Identity (%)	TMD (No.)	Signal peptide
CsacCSP9	Unigene0002397	chemosensory protein	*Chilo suppressalis*	523	121	3.00E-74	86		Yes
CsacCSP10	Unigene0002847	chemosensory protein, partial	*Chilo suppressalis*	1027	120	7.00E-72	89		Yes
CsacCSP11	Unigene0035354	minus strand chemosensory protein, partial	*Chilo suppressalis*	1620	167	2.00E-68	71		Yes
CsacCSP12	Unigene0001848	minus strand chemosensory protein	*Cnaphalocrocis medinalis*	1001	190	2.00E-57	59		Yes
CsacCSP13	Unigene0004808	minus strand chemosensory protein	*Cnaphalocrocis medinalis*	606	130	3.00E-69	75		Yes
CsacCSP14	Unigene0041621	chemosensory protein	*Cnaphalocrocis medinalis*	2154	121	4.00E-64	86		Yes
CsacCSP15	Unigene0033697	chemosensory protein	*Eogystia hippophaecolus*	1365	145	1.00E-51	64		Yes
CsacORCO	Unigene0033699	minus strand olfactory receptor 2	*Chilo suppressalis*	1664	342	0	96	6	
CsacOR1	Unigene0007696	odorant receptor 13a-like	*Plutella xylostella*	1651	454	2.00E-129	45	6	
CsacOR2	Unigene0011933	odorant receptor 50, partial	*Manduca sexta*	1174	365	5.00E-127	50	4	
CsacOR3	Unigene0026875	olfactory receptor 43, partial	*Cnaphalocrocis medinalis*	900	272	2.00E-90	47	3	
CsacOR4	Unigene0028620	minus strand odorant receptor	*Eogystia hippophaecolus*	1552	401	1.00E-136	49	6	
CsacOR5	Unigene0033533	minus strand odorant receptor 13a-like	*Plutella xylostella*	894	292	3.00E-61	38	4	
CsacOR6	Unigene0037945	minus strand odorant receptor 60	*Athetis dissimilis*	1428	229	2.00E-86	71	3	
CsacOR7	Unigene0023407	odorant receptor	*Eogystia hippophaecolus*	448	127	6.00E-37	43	2	
CsacOR8	Unigene0057813	odorant receptor 14, partial	*Cnaphalocrocis medinalis*	709	160	5.00E-75	68	2	
CsacOR9	Unigene0010994	minus strand olfactory receptor 40	*Cnaphalocrocis medinalis*	413	122	9.00E-65	68	2	
CsacOR10	Unigene0028643	olfactory receptor 56	*Bombyx mori*	520	107	2.00E-56	67	2	
CsacIR1	Unigene0005443	ionotropic receptor 1, partial	*Cnaphalocrocis medinalis*	781	247	3.00E-175	94	2	
CsacIR2	Unigene0030792	minus strand ionotropic receptor 1	*Heliconius melpomene rosina*	923	137	3.00E-73	67	0	
CsacIR3	Unigene0026968	ionotropic receptor	*Ostrinia furnacalis*	1003	268	2.00E-169	85	1	
CsacIR4	Unigene0038631	ionotropic receptor	*Ostrinia furnacalis*	2004	547	0	74	3	
CsacIR5	Unigene0040849	ionotropic receptor	*Ostrinia furnacalis*	2884	836	0	95	3	
CsacIR6	Unigene0045750	minus strand ionotropic receptor, partial	*Ostrinia furnacalis*	1469	233	2.00E-129	78	1	
CsacIR7	Unigene0019248	minus strand ionotropic receptor, partial	*Ostrinia furnacalis*	935	280	3.00E-151	72	3	
CsacIR8	Unigene0027705	ionotropic receptor, partial	*Dendrolimus kikuchii*	747	100	2.00E-80	55	0	
CsacIR9	Unigene0025240	ionotropic receptor	*Ostrinia furnacalis*	734	232	3.00E-102	65	0	
CsacIR10	Unigene0011763	ionotropic receptor	*Ostrinia furnacalis*	478	110	7.00E-78	72	0	
CsacIR11	Unigene0018788	ionotropic receptor	*Ostrinia furnacalis*	465	110	2.00E-61	74	0	
CsacIR12	Unigene0005556	ionotropic receptor 21a.1, partial	*Cnaphalocrocis medinalis*	415	127	2.00E-44	62	0	
CsacIR13	Unigene0019250	ionotropic receptor, partial	*Ostrinia furnacalis*	395	108	2.00E-23	37	0	
CsacSNMP1	Unigene0013065	minus strand sensory neuron membrane protein 1	*Chilo suppressalis*	1852	526	0	83	2	
CsacSNMP2	Unigene0007127	minus strand sensory neuron membrane protein 2	*Chilo suppressalis*	1896	519	0	82	1	

The putative N-terminal signal peptides and most likely cleavage sites were predicted using SignalP V3.0 (http://www.cbs.dtu.dk/services/SignalP/). The transmembrane helices in the ORs, IRs, and SNMPs were predicted using TMHMM Server v. 2.0 (http://www.cbs.dtu.dk/services/TMHMM/).

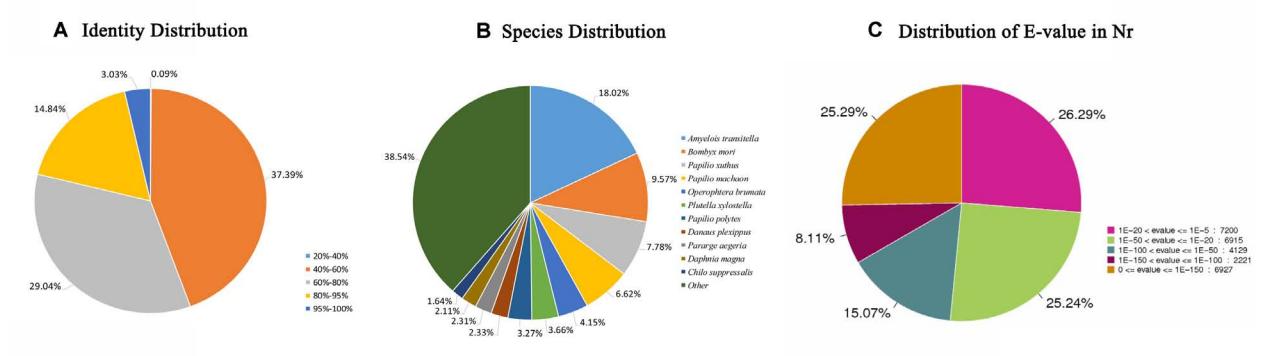

FIGURE 1 | NR classification data. **(A)** The identity distribution of the NR annotation results. **(B)** The species distribution of the NR annotation results. **(C)** The *E*-value distribution of the NR annotation results. NR, non-redundant protein database.

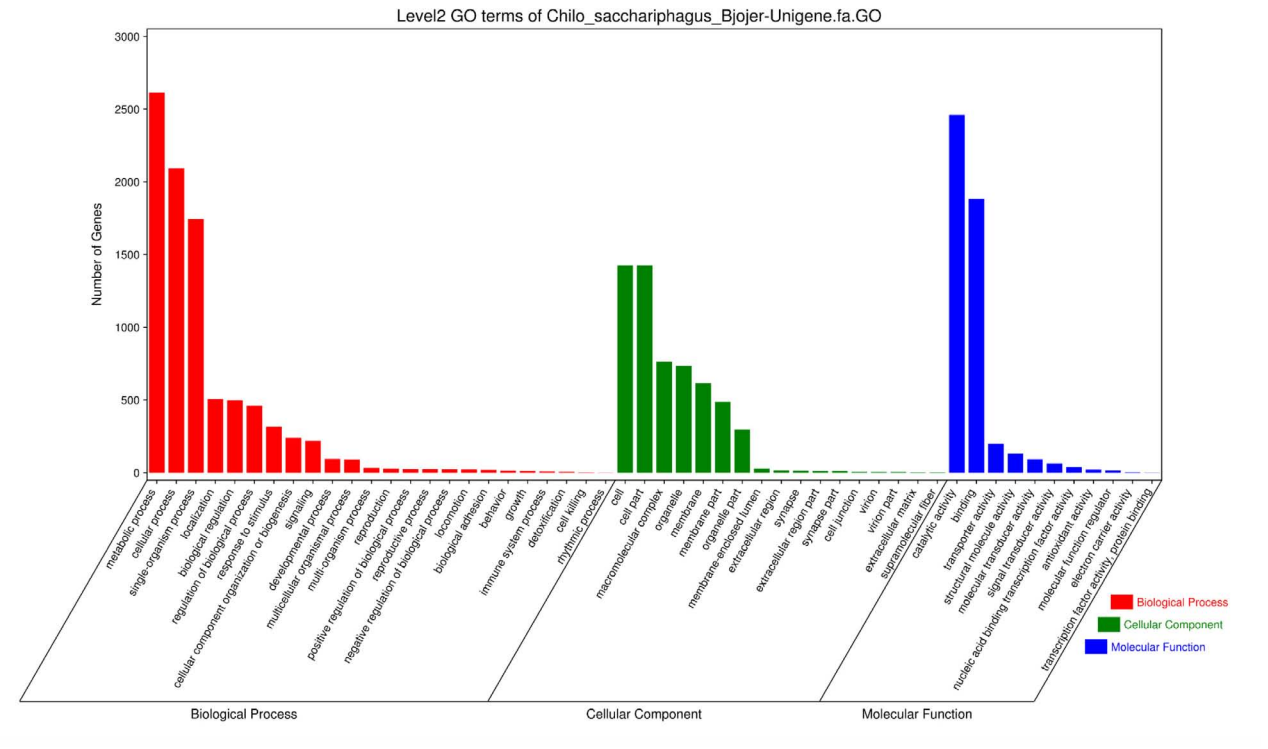

FIGURE 2 | Histogram of Gene Ontology classification of *C. saccharaphagus* unigenes. The right *y*-axis represents the number of genes in each category. The left *y*-axis represents the percentage of a specific category of genes in that main category.

the 15 CsacCSPs ranged from 48 to 89% (**Table 3**). Neighbor-joining tree analysis showed that CsacCSP13 and CsacCSP15 formed a specific branch that was close to BmorCSP1 and BmorCSP1 variant from *B. mori*. Additionally, a specific branch consisting of two CSPs from *C. saccharaphagus* (CsacCSP4 and CsacCSP10) was divergent from the CSPs of other insects, and the two CsacCSPs have a close relationship to CSP7 precursor from *B. mori* (**Figure 5**).

The putative *IR* genes in the *C. saccharaphagus* transcriptome were represented according to their similarity to known insect *IRs*. Bioinformatic analysis led to the identification of 13 candidate *IRs*, of which eight candidate IRs had higher than 70% identity with known insect IRs, and only two had identities lower than 60%. Compared with general insect IRs, which have three transmembrane domains, three IR candidates in *C. saccharaphagus* (CsacIR4, CsacIR5, and CsacIR7) were predicted to have three transmembrane domains by TMHMM2.0 (**Table 3**). In the phylogenetic analysis, CsacIR2, CsacIR7, and IRs from *M. sexta* (MsexIR1) and *D. melanogaster* (DmelIR75a, DmelIR75b, and DmelIR75c) formed a distinct subgroup, while CsacIR6, CsacIR10, and CsacIR11 formed a branch that shared a close relation to IR75d from *D. melanogaster* and IR75a,

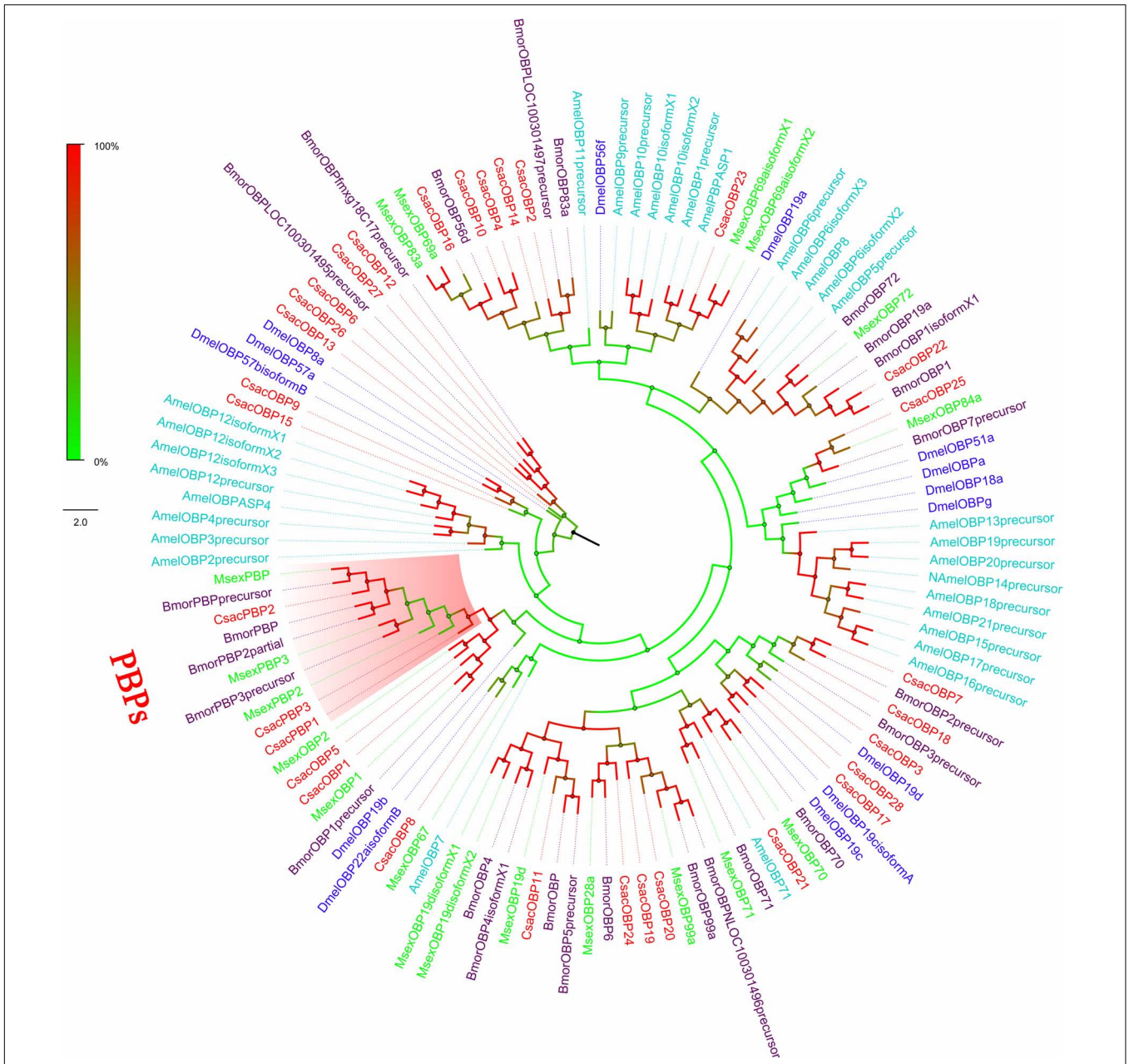

FIGURE 3 | Phylogenetic analysis of putative odourant/phenomenon binding proteins (OBP/PBPs) of *C. sacchariphagus*. The tree was constructed in MEGA6.0 using the neighbor-joining method. Genes from *C. sacchariphagus* are labeled in red. OBP/PBPs from *D. melanogaster* (Diptera) are labeled in dark blue, OBP/PBPs from *B. mori* (Lepidoptera) are labeled in purple, OBP/PBPs from *M. sexta* (Lepidoptera) are labeled in green, and OBP/PBPs from *A. mellifera* (Hymenoptera) are labeled in light blue.

IR75p.1, and IR75p.3 from *M. sexta*; additionally, CsacIR1, CsacIR3, and CsacIR12 formed a specific branch consisting of DmelIR8a, AmelIR25a MsexIR8a, MsexIR25a, and BmorIR25a with their positions in phylogenetic tree and strong bootstrap support (**Figure 6**).

Sensory neuron membrane proteins were identified in pheromone-sensitive neurons in Lepidopteran insects and are thought to function in the process of pheromone recognition (Rogers et al., 2001). Two *SNMPs* (*CsacSNMP1* and *CsacSNMP2*) were identified in our transcriptome. Both of them all have an identity of greater than 80% with SNMPs of *Chilo suppressalis* (**Table 3**). According to the phylogenetic analysis, both *C. sacchariphagus* candidate SNMPs clustered with their SNMP orthologs into separate subclades (**Figure 7**), among which CsacSNMP1, BmorSNMP1, and MsexSNMP1 formed a specific branch and CsacSNMP2 and SNMP2 from *B. mori* and *M. sexta* shared a close relationship.

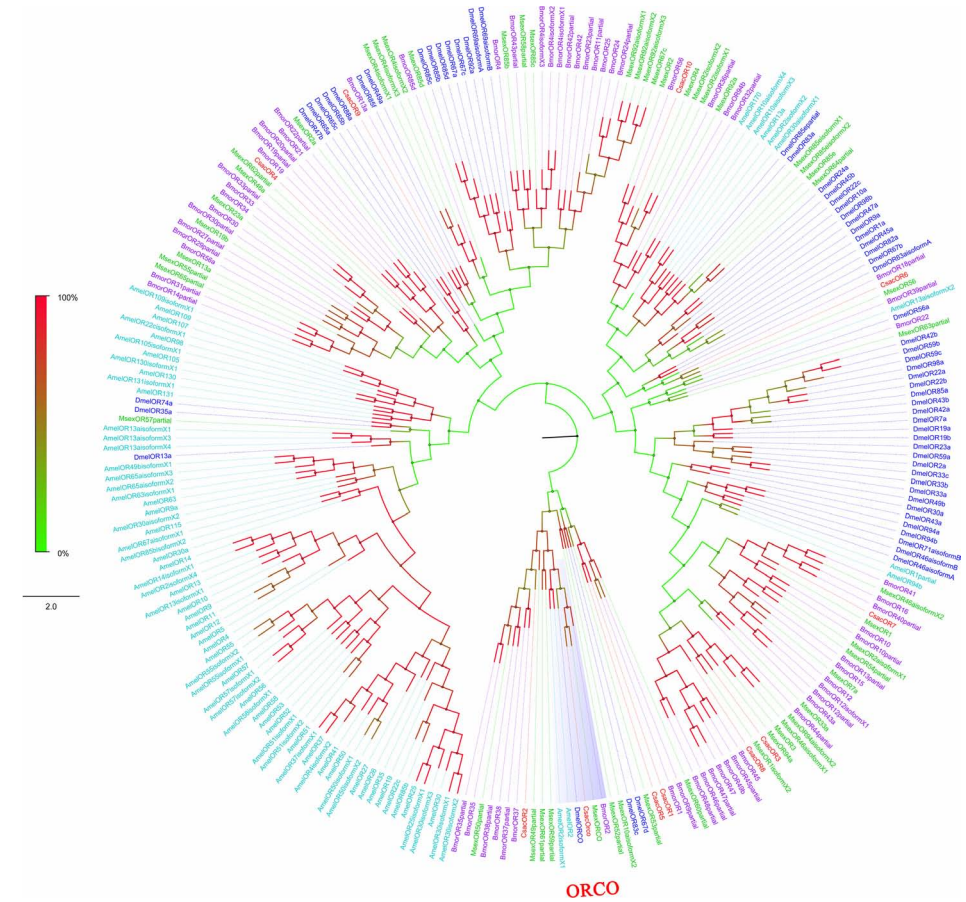

FIGURE 4 | Phylogenetic analysis of putative olfactory receptors (ORs) of *C. saccharaphagus*. The tree was constructed in MEGA6.0 using the neighbor-joining method. Genes from *C. saccharaphagus* are labeled in red. ORs from *D. melanogaster* (Diptera) are labeled in dark blue, ORs from *B. mori* (Lepidoptera) are labeled in purple, ORs from *M. sexta* (Lepidoptera) are labeled in green, and ORs from *A. mellifera* (Hymenoptera) are labeled in light blue.

Tissue- and Sex-Specific Expression of Candidate Chemosensory Genes

To validate and analyze the expression profiles of candidate chemosensory genes in different organs and tissues between male and female *C. saccharaphagus*, all candidate chemosensory genes encoding OBPs/PBPs, CSPs, ORs, IRs, and SNMPs were subjected to RT-qPCR with specific primers (**Supplementary Table 1**). The expression difference of chemosensory genes from transcriptome data was shown in heatmap (**Supplementary Figure 2**). The expression patterns of the 72 chemosensory genes were basically consistent with the FPKM values, and the data are presented as $\log_2$ values of fold changes in gene expression. According to the RT-qPCR results, a large number of chemosensory genes were antenna-predominant and showed different expression levels between males and females ($P < 0.05$). Among these genes, the expression levels of genes (*CsacOBP2/5/6/9/12/15/17/24/25/26*, *CsacPBP1/2*, *CSP2/3/4/9/10*, *CsacOR1/5/6/8/9/10*, *IR1/6/7*, and *CsacSNMP1*) were higher in male antennae than that in female antennae (**Figure 8**), whereas the opposite occurred was observed for the other genes expression (*CsacOBP1/3/4/11/19/22/23/27*, *CsacPBP3*, *CsacCSP1/5/6/7*, *CsacOR2/3/7*, *CsacIR2/3/4/11/12*, and *CsacSNMP2*) (**Figure 8**). In addition, some genes (*CsacOBP3/7/8/10/13/14/18/20/25/26/28*, *CsacCSP3/4/8/9/10/11/12/13/15*, *CsacOR1/4/6*, and *CsacIR1/4/8/9/10*) had a high expression in bodies (excluding antennae and legs) or legs (**Figure 8**).

DISCUSSION

In this study, the transcriptome of the pest *C. saccharaphagus* was analyzed using Illumina HiSeq^{TM} 4000 technology. We obtained 16.60 GB of clean data that was assembled into 60084 unigenes with a mean length of 829 bp and N50 length of 1694 bp. There were 60.67% unigenes with a length <500 bp after assembly, possibly due to the short-length sequencing capacity of Illumina sequencing. Among the 60084 unigenes, 28330 unigenes were annotated, and 52.85% of unigenes had no significant match in any of the databases searched. This phenomenon may be caused by the lack of genomic and transcriptomic information for this moth in the databases. This antennal and body transcriptome sequencing provides a dataset of chemosensory genes, including 28 *OBPs*, three *PBPs*, 15 *CSPs*, 11 *ORs*, 13 *IRs*, and two *SNMPs*.

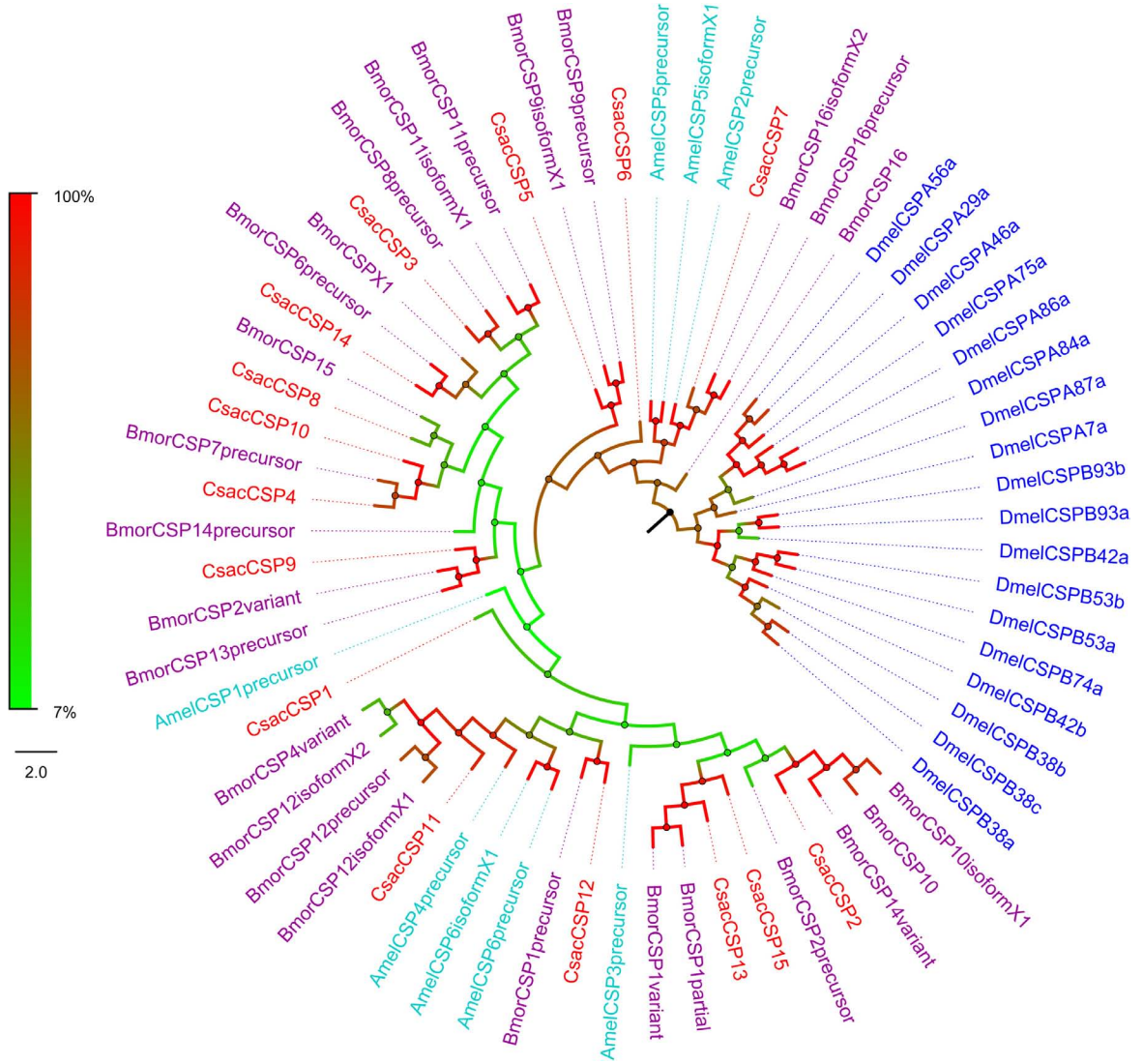

FIGURE 5 | Phylogenetic analysis of putative chemosensory proteins (CSPs) of *C. saccharaphagus*. The tree was constructed in MEGA6.0 using the neighbor-joining method. Genes from *C. saccharaphagus* are labeled in red. CSPs from *D. melanogaster* (Diptera) are labeled in dark blue, CSPs from *B. mori* (Lepidoptera) are labeled in purple, CSPs from *M. sexta* (Lepidoptera) are labeled in green, and CSPs from *A. mellifera* (Hymenoptera) are labeled in light blue.

Odourant/pheromone binding proteins interact with semiochemicals, hormones or other biologically active chemicals that enter the body through pores and then transport them to ORs located on the membranes of olfactory receptor neurons (Pelosi and Maida, 1995; Vogt, 1995; Kaissling, 1998). Fewer *OBPs/PBPs* were identified in this transcriptome of *C. saccharaphagus* (31) than in *B. mori* (44) or *D. melanogaster* (51) (Hekmat-Scafe et al., 2002; Gong et al., 2007). The difference in the number of *OBPs* might be related to the sequencing method, depth, the process of sample preparation or evolutionary differences across different species. These results are comparable to those reported for the transcriptomes of *Spodoptera littoralis* (33), *Spodoptera exigua* (34), and *Helicoverpa armigera* (26) (Liu N. Y. et al., 2012; Liu Y. et al., 2012; Poivet et al., 2013; Liu et al., 2015; Walker et al., 2019). This suggests that *C. saccharaphagus OBPs* show conservation in gene numbers. Some OBPs are conserved and have orthologous relationships with counterparts from other insects. Insect *OBPs/PBPs*, mainly expressed in the antennae, are considered to have an olfactory function. Analysis of *OBP/PBPs* expression profiles in different organs and tissues could reveal their likely functions. qRT-PCR results showed that 22 *CsacOBPs/PBPs* displayed antenna-enriched expression, indicating that these genes may play critical roles in the process of olfactory reception. Among these genes, 13 (*CsacOBP2/5/6/9/12/15/17/24/25/26/27* and *CsacPBP1/2*) were mainly expressed in male antennae, suggesting that these genes may encode proteins involved in sex-specific behaviors, including selectively sensing and transporting sex pheromones released by females in the process of molecular recognition and searching for suitable mates (Gu et al., 2013;

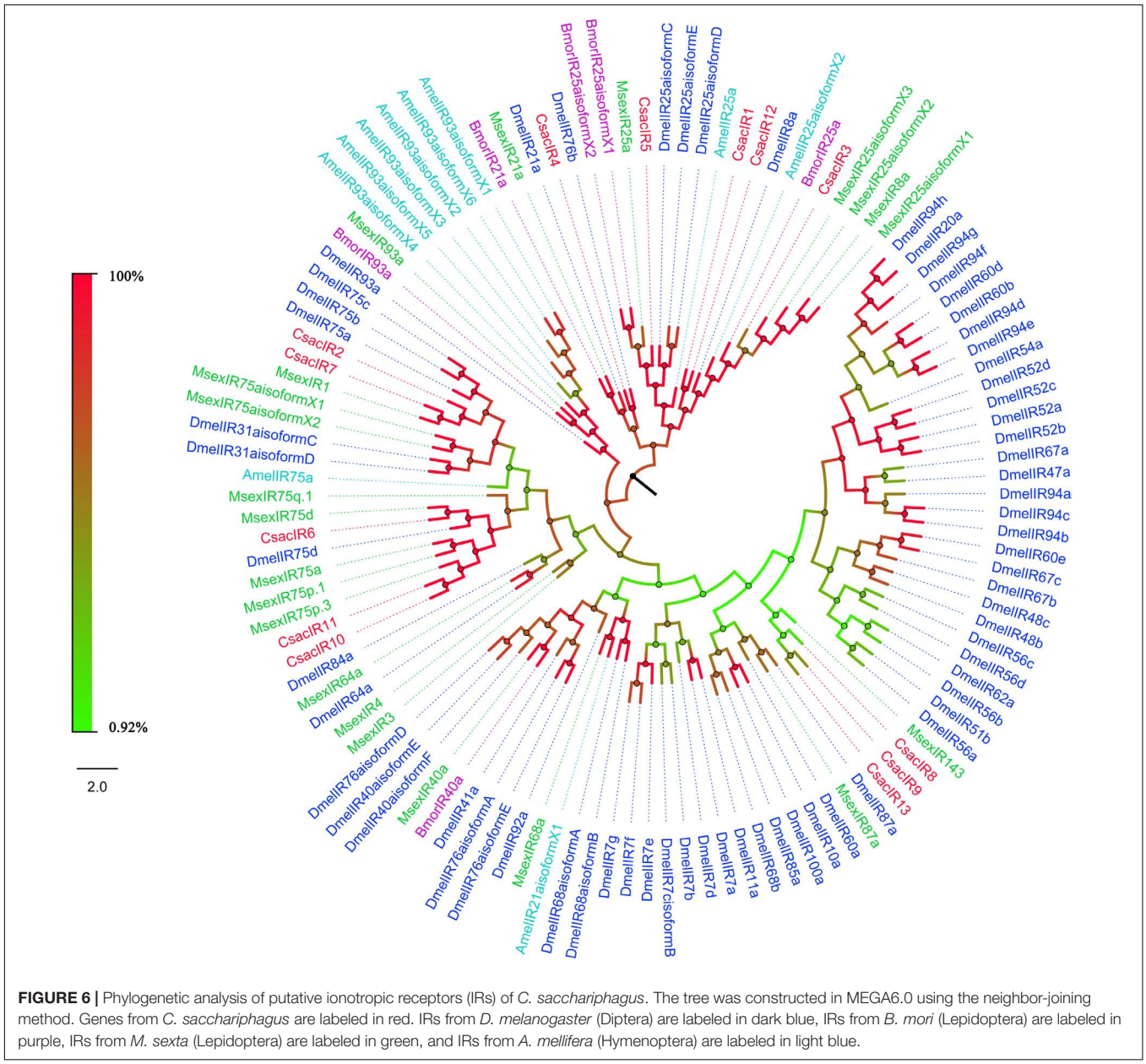

FIGURE 6 | Phylogenetic analysis of putative ionotropic receptors (IRs) of *C. sacchariphagus*. The tree was constructed in MEGA6.0 using the neighbor-joining method. Genes from *C. sacchariphagus* are labeled in red. IRs from *D. melanogaster* (Diptera) are labeled in dark blue, IRs from *B. mori* (Lepidoptera) are labeled in purple, IRs from *M. sexta* (Lepidoptera) are labeled in green, and IRs from *A. mellifera* (Hymenoptera) are labeled in light blue.

Jin et al., 2014; Chang et al., 2015; Zhu et al., 2016, 2019). Ten genes (*CsacOBP7/8/10/13/14/16/18/20/21/28*) without significant differences in expression levels between males and females may function as general odourant detectors rather than in pheromone recognition (Li et al., 2008; Pelletier and Leal, 2009; He et al., 2019a). Some genes (*CsacOBP1/3/4/11/19/22/23/27*) showed female antenna-biased expression, indicating that those OBPs may help to locate oviposition sites by recognizing chemicals from hosts, a model that is supported by previous studies of *Pieris rapae* (Renwick et al., 1992; Sato et al., 1999; Li et al., 2020).

Fifteen *CSPs* were identified in transcriptome sequencing. This number is almost equal to the number of *CSPs* in *H. armigera* (18), *Heliothis assulta* (17), *S. littoralis* (21), *B. mori* (20), and *S. exigua* (20) but much higher than that of *D. melanogaster* (4) (Wanner et al., 2004; Gong et al., 2007; Zhou et al., 2010; Poivet et al., 2013; Leitch et al., 2015; Liu et al., 2015; Zhang et al., 2015; Walker et al., 2019), indicating that the numbers of *CSP* genes differ among different species. *CSPs* exist in insect chemosensory and non-chemosensory organs and tissues, including antennae, legs, pheromone glands, and wings (Picimbon et al., 2001; Ban et al., 2003; Dani et al., 2011; Liu N. Y. et al., 2012; Wei et al., 2017). In our study, 10 *CsacCSPs* were significantly expressed in the antennae, and these CSPs might be thought to participate in general odourant recognition and perception (Pelosi et al., 2014; Jia et al., 2018). Four *CSPs* showed high expression in legs and might be associated with gustatory behaviors, such as detecting non-volatile chemicals (Jia et al., 2020).

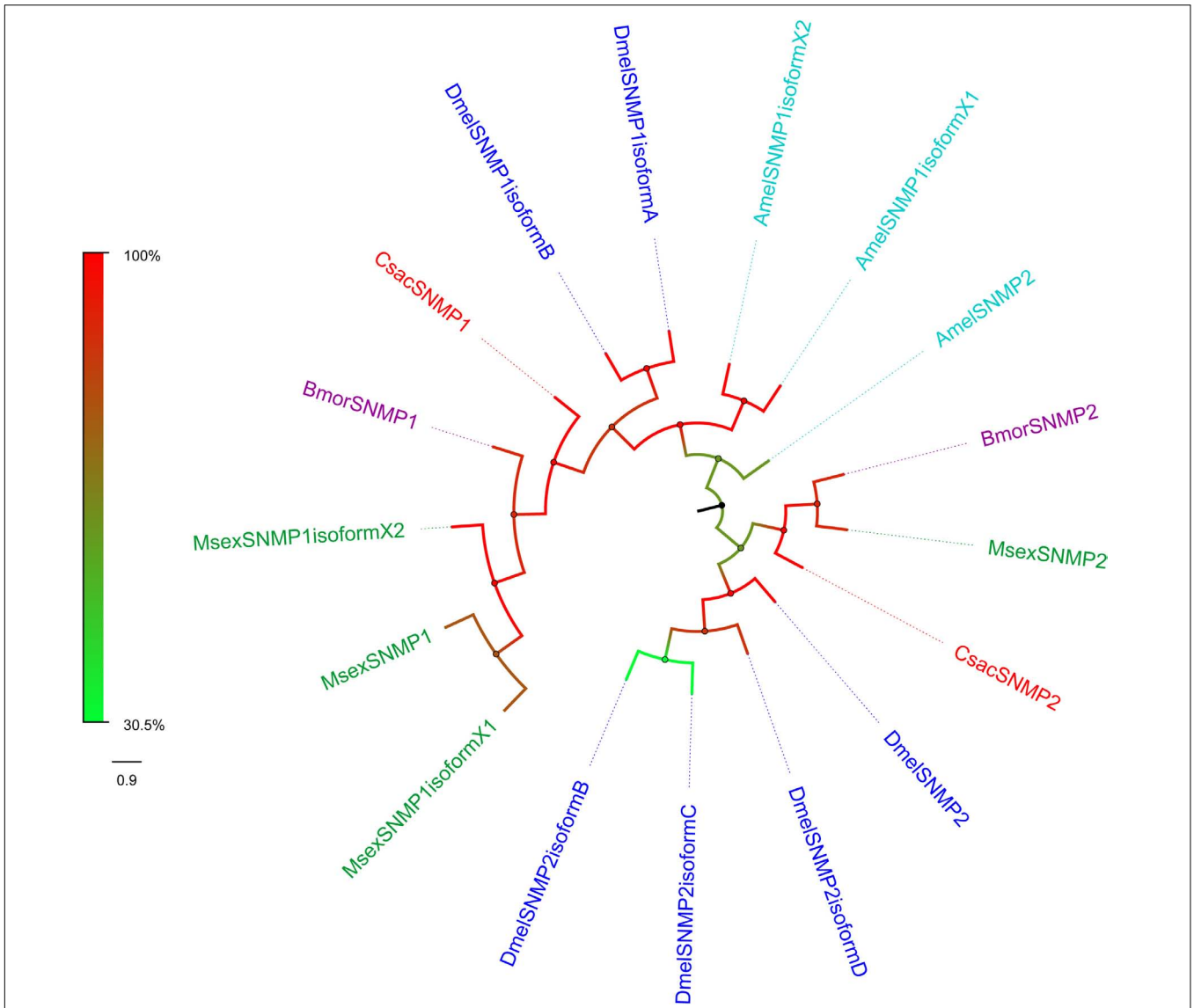

FIGURE 7 | Phylogenetic analysis of putative sensory neuron membrane proteins (SNMPs) of *C. sacchariphagus*. The tree was constructed in MEGA6.0 using the neighbor-joining method. Genes from *C. sacchariphagus* are labeled in red. SNMPs from *D. melanogaster* (Diptera) are labeled in dark blue, SNMPs from *B. mori* (Lepidoptera) are labeled in purple, SNMPs from *M. sexta* (Lepidoptera) are labeled in green, and SNMPs from *A. mellifera* (Hymenoptera) are labeled in light blue.

In the qRT-PCR analysis, some identified *CsacOBPs* and *CsacCSPs* displayed high expression in male bodies, and we speculated that these genes are likely to be involved in different functions in non-sensory organs and tissues of the insect body. Some OBPs and CSPs in male insect seminal fluid might be related to binding and releasing pheromones. In *D. melanogaster*, OBPs were found to be components of the seminal fluid (Takemori and Yamamoto, 2009); LmigCSP91 was identified to have a high expression in reproductive organs in male *Locusta migratoria* and possessed a good affinity to a kind of pheromone that is produced in the same reproductive organs (Ban et al., 2013; Zhou et al., 2013). Some OBPs are male specific and could be transferred into female bodies during the process of mating, indicating that these OBPs might function in sperm–egg communication (Findlay et al., 2008; Takemori and Yamamoto, 2009; Prokupek et al., 2010). In addition, CSPs are involved in releasing some molecules in male glands; for example, a CSP was found in large quantities in the ejaculatory apparatus, which secretes the male pheromone vaccenyl acetate (Dyanov and Dzitoeva, 1995).

Odourant receptors act as the most critical and determinate roles in insect peripheral olfactory reception (Dani et al., 2011; Leal, 2013). Eleven *ORs* were identified in our research, and this number was lower than the numbers identified in *B. mori* (72) (Gong et al., 2009), *M. sexta* (73) (Koenig et al., 2015), *H. armigera* (84) (Pearce et al., 2017), *Heliconius melpomene* (74) (Dasmahapatra et al., 2012), *D. melanogaster* (62) (Clyne et al., 1999; Gao and Chess, 1999; Robertson et al., 2003),

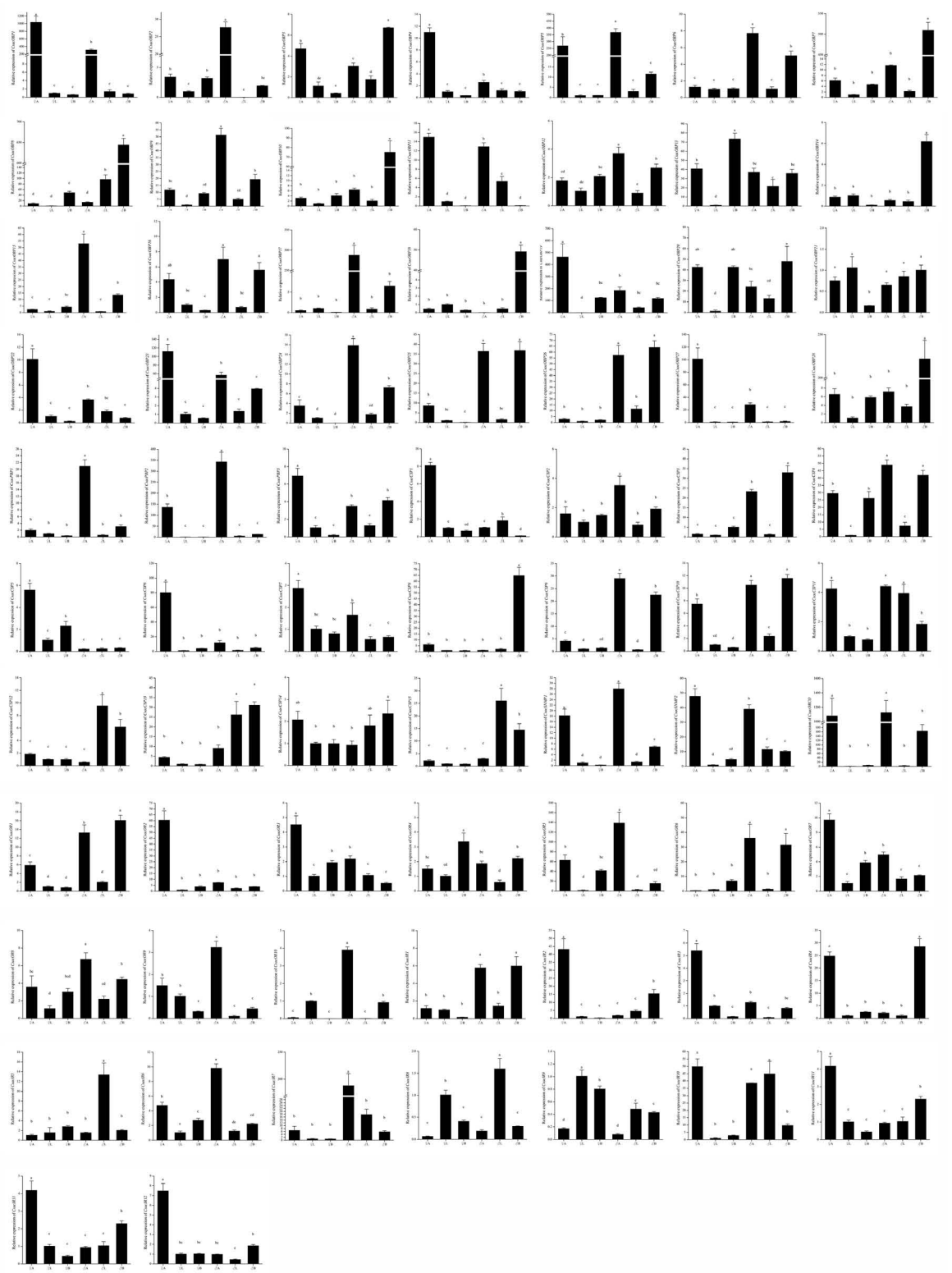

FIGURE 8 | Expression patterns of putative odourant/phenomenon binding proteins (OBP/PBPs), chemosensory proteins (CSPs), sensory neuron membrane proteins (SNMPs), odourant receptors (ORs), and ionotropic receptors (IRs) in the different tissues of *C. saccharaphagus* as determined using RT-qPCR. ♀A, female antennae; ♂A, male antennae; ♀L, female legs; ♂L, male legs; ♀B, female body (without antennae and legs); ♂B, male body (without antennae and legs). Error bars indicate SEMs from the analysis of three replicates ($P < 0.05$). The lower case letters indicate that there are significant differences between the data.

Laodelphax striatellus (133) (He et al., 2020), *Sogatella furcifera* (135) (He et al., 2018), and *A. mellifera* (170) (Robertson and Wanner, 2006), suggesting that different sequencing methods and depths may affect the outcome of studies; the lack of genomic and transcriptomic information in the databases may influence the annotation results for *C. saccharaphagus*, and some ORs expressed at low levels may be difficult to detect (Li et al., 2015; Wang et al., 2017). In the neighbor-joining tree of ORs, CsacOR1 and CsacOR5 are orthologs of BmorOR1; CsacOR4 is the ortholog of BmorOR19; and CsacOR10 clustered close to BmorOR56. In *B. mori*, OR1 is the receptor of the pheromone bombykol; OR19 can sense linalool, which is related to selection of spawning environment; and OR56, specific and highly sensitive to *cis*-jasmone, is involved in the sensing of odor molecules released by plants and signal transduction (Wanner et al., 2007; Anderson et al., 2009; Tanaka et al., 2009). The qRT-PCR results showed that *CsacOR1/5/10* were highly expressed in the male antennae, suggesting that they are highly specifically involved in the detection of sex pheromones, while *CsacOR4* has a higher expression in the female body than in the male body, indicating that it is likely involved in the regulation of female-specific behaviors, such as the localization of oviposition sites and oviposition (Xu et al., 2020). The expression of *CsacORCO*, which was highly conserved in the OR tree, was significantly antenna-specific. The different expression levels of the *ORs* in different organs and tissues and different sexes suggested that they might perform different functions, which should be further studied in the future.

Thirteen IR genes were identified in this study from *C. saccharaphagus*. The number is similar to that of *B. mori* (18), *H. armigera* (12), and *S. littoralis* (12) (Croset et al., 2010; Olivier et al., 2011; Liu Y. et al., 2012). Most CsacIRs were clustered with orthologs in *D. melanogaster*, *M. sexta*, *B. mori*, and *A. mellifera*, indicating that IRs are relatively conserved in different insect species. In *D. melanogaster*, IR84a/8a, IR76b/IR41a, IR75a/IR8a, IR64a/IR8a have been reported to sense phenylacetaldehyde and phenylacetic acid, polyamines, acetic acid, and other acids, respectively (Ai et al., 2010; Grosjean et al., 2011; Hussain et al., 2016; Prieto-Godino et al., 2016). And in *M. sexta*, MsexIR8a has been shown the function of sensing carboxylic acids 3-methylpentanoic acid and hexanoic acid (Zhang et al., 2019). In addition, DmelIR21a/IR25a have been reported to be sensitive to cool temperatures (Ni et al., 2016). The CsacIR genes showed high sequence similarity to these functionally characterized DmelIRs, indicating that they may have similar functions.

In insects, *SNMP1* is usually expressed in pheromone-sensitive OSNs and is important for pheromone perception (Jin et al., 2008; Nichols and Vogt, 2008; Vogt et al., 2009; Gomez-Diaz et al., 2016). However, *SNMP2* functions remain unclear. In the present study, two *SNMPs* were identified in *C. saccharaphagus*. Both were conserved with respect to other holometabolous insect species. They exhibited a clear antenna-predominant expression, suggesting that *CsacSNMP1* may be associated with pheromone reception.

In conclusion, 72 candidate chemosensory protein genes (31 *OBP/PBPs*, 15 *CSPs*, 11 *ORs*, 13 *IRs*, and two *SNMPs*) were first identified via transcriptome sequencing analysis in *C. saccharaphagus,* which is an important agricultural pest. This study will not only serve as a valuable resource for future research on the chemosensory system of *C. saccharaphagus* and other lepidopteran species but also contribute to the development of creative and sustainable pest management strategies involving interference with olfaction.

DATA AVAILABILITY STATEMENT

The datasets presented in this study can be found in online repositories. The names of the repository/repositories and accession number(s) can be found in the article/ **Supplementary Material**.

AUTHOR CONTRIBUTIONS

JL, HL, JY, YA, and HW conceived, coordinated, and designed the research. YM, JL, and DS assembled and analyzed the transcriptome datasets. JL and HL performed experiments. JL, JY, YA, and HW drafted the manuscript. All authors read and approved the final manuscript.

FUNDING

This work was supported by the GDAS' Project of Science and Technology Development (Grant No. 2019GDASYL-0103040) and GDAS' Project of Science and Technology Development (Grant No. 2020GDASYL-20200103056). The funders had no role in study design, data collection and analysis, decision to publish, or preparation of the manuscript.

ACKNOWLEDGMENTS

We thank M.D. students Anwen Liang (State Key Laboratory of Biocontrol, Sun Yat-sen University) for technical assistance. Thanks to Prof. Qiang Zhou (State Key Laboratory of Biocontrol, Sun Yat-sen University) for editorial assistance and comments on the manuscript.

SUPPLEMENTARY MATERIAL

The Supplementary Material for this article can be found online at: https://www.frontiersin.org/articles/10.3389/fphys.2021.636353/full#supplementary-material

Supplementary Figure 1 | Length distribution of unigenes in transcriptomes of *Chilo saccharaphagus*.

Supplementary Figure 2 | The expression difference of chemosensory genes from transcriptome data.

Supplementary Table 1 | Primers used in qRT-PCR.

REFERENCES

Abuin, L., Bargeton, B., Ulbrich, M. H., Isacoff, E. Y., Kellenberger, S., and Benton, A. R. (2011). Functional architecture of olfactory ionotropic glutamate receptors. *Neuron* 69, 44–60. doi: 10.1016/j.neuron.2010.11.042

Ai, M., Min, S., Grosjean, Y., Leblanc, C., Bell, R., Benton, R., et al. (2010). Acid sensing by the *Drosophila* olfactory system. *Nature* 468, 691–695. doi: 10.1038/nature09537

Anderson, A. R., Wanner, K. W., Trowell, S. C., Warr, C. G., Jaquin-Joly, E., Zagatti, P., et al. (2009). Molecular basis of female-specific odorant responses in *Bombyx mori*. *Insect Biochem. Mol. Biol.* 39, 189–197. doi: 10.1016/j.ibmb.2008.11.002

Andersson, M. N., Grosswilde, E., Keeling, C. I., Bengtsson, J. M., Yuen, M. M., Li, M., et al. (2013). Antennal transcriptome analysis of the chemosensory gene families in the tree killing bark beetles, Ips typographus and *Dendroctonus ponderosae* (Coleoptera: Curculionidae: Scolytinae). *BMC Genomics* 14:198. doi: 10.1186/1471-2164-14-198

Ban, L., Scaloni, A., Brandazza, A., Angeli, S., Zhang, L., Yan, Y., et al. (2003). Chemosensory proteins of *Locusta migratoria*. *Insect Mol. Biol.* 12, 125–134. doi: 10.1046/j.1365-2583.2003.00394.x

Ban, L. P., Napolitano, E., Serra, A., Zhou, X., Iovinella, I., and Pelosi, P. (2013). Identification of pheromone-like compounds in male reproductive organs of the oriental locust *Locusta migratoria*. *Biochem. Biophys. Res. Commun.* 437, 620–624. doi: 10.1016/j.bbrc.2013.07.015

Bengtsson, J. M., Trona, F., Montagné, N., Anfora, G., Ignell, R., Witzgall, P., et al. (2012). Putative chemosensory receptors of the codling moth, *Cydia pomonella*, identified by antennal transcriptome analysis. *PLoS One* 7:e31620. doi: 10.1371/journal.pone.0031620

Benton, R., Sachse, S., Michnick, S. W., and Vosshall, L. B. (2006). A typical membrane topology and heteromeric function of *Drosophila* odorant receptors in vivo. *PLoS Biol.* 4:e20. doi: 10.1371/journal.pbio.0040020

Benton, R., Vannice, K. S., Gomez-Diaz, C., and Vosshall, L. B. (2009). Variant ionotropic glutamate receptors as chemosensory receptors in *Drosophila*. *Cell* 136, 149–162. doi: 10.1016/j.cell.2008.12.001

Bezuidenhout, C. N., Goebel, R., Hull, P. J., Schulze, R. E., and Maharaj, M. (2008). Assessing the potential threat of *Chilo saccharaphagus* (Lepidoptera: Crambidae) as a pest in South Africa and Swaziland: realistic scenarios based on climatic indices. *Afr. Entomol.* 16, 86–90. doi: 10.4001/1021-3589-16.1.86

Butterwick, J. A., Del Mármol, J., Kim, K. H., Kahlson, M. A., Rogow, J. A., Walz, T., et al. (2018). Cryo-EM structure of the insect olfactory receptor Orco. *Nature* 560, 447–452. doi: 10.1038/s41586-018-0420-8

Chang, H., Liu, Y., Yang, T., Pelosi, P., Dong, S., and Wang, G. (2015). Pheromone binding proteins enhance the sensitivity of olfactory receptors to sex pheromones in *Chilo suppressalis*. *Sci. Rep.* 5:13093. doi: 10.1038/srep13093

Chen, H., Liu, J., Cui, K., Lu, Q., Wang, C., Wu, H., et al. (2018). Molecular mechanisms of tannin accumulation in *Rhus galls* and genes involved in plant-insect interactions. *Sci. Rep.* 8:9841. doi: 10.1038/s41598-018-28153-y

Chiu, J., DeSalle, R., Lam, H. M., Meisel, L., and Coruzzi, G. (1999). Molecular evolution of glutamate receptors: a primitive signaling mechanism that existed before plants and animals diverged. *Mol. Biol. Evol.* 16, 826–838. doi: 10.1093/oxfordjournals.molbev.a026167

Clyne, P. J., Warr, C. G., Freeman, M. R., Lessing, D., Kim, J., and Carlson, J. R. (1999). A novel family of divergent seven-transmembrane proteins: candidate odorant receptors in *Drosophila*. *Neuron* 22, 327–338. doi: 10.1016/s0896-6273(00)81093-4

Croset, V., Rytz, R., Cummins, S. F., Budd, A., Brawand, D., and Kaessmann, H. (2010). Ancient protostome origin of chemosensory ionotropic glutamate receptors and the evolution of insect taste and olfaction. *PLoS Genet.* 6:e1001064. doi: 10.1371/journal.pgen.1001064

Dani, F. R., Michelucci, E., Francese, S., Mastrobuoni, G., Cap-pellozza, S., Marca, G. L., et al. (2011). Odorant-binding proteins and chemosensory proteins in pheromone detection and release in the silkmoth *Bombyx mori*. *Chem. Senses* 36, 335–344. doi: 10.1093/chemse/bjq137

Dasmahapatra, K. K., Walters, J. R., Briscoe, A. D., Davey, J. W., Whibley, A., Nadeau, N. J., et al. (2012). Butterfly genome reveals promiscuous exchange of mimicry adaptations among species. *Nature* 487, 94–98. doi: 10.1038/nature11041

Dyanov, H. M., and Dzitoeva, S. G. (1995). Method for attachment of microscopic preparations on glass for in situ hybridization, PRINS and in situ PCR studies. *Biotechniques* 18, 822–826. doi: 10.1021/ic020451f

Eddy, S. R. (1998). Profile hidden markov models. *Bioinformatics* 14, 755–763. doi: 10.1093/bioinformatics/14.9.755

Fandino, R. A., Haverkamp, A., Bisch-Knaden, S., Zhang, J., Bucks, S., Nguyen, T. A. T., et al. (2019). Mutagenesis of odorant coreceptor Orco fully disrupts foraging but not oviposition behaviors in the hawkmoth *Manduca sexta*. *Proc. Natl. Acad. Sci. U.S.A.* 116, 15677–15685. doi: 10.1073/pnas.1902089116/-/DCSupplemental

Findlay, G. D., Yi, X., MacCoss, M. J., and Swanson, W. J. (2008). Proteomics reveals novel *Drosophila* seminal fluid proteins transferred at mating. *PLoS Biol.* 6:e178. doi: 10.1371/journal.pbio.0060178

Gao, Q., and Chess, A. (1999). Identification of candidate *Drosophila* olfactory receptors from genomic DNA sequence. *Genomics* 60, 31–39. doi: 10.1006/geno.1999.5894

Geetha, N., Shekinah, E. D., and Rakkiyappan, P. (2010). Comparative impact of release frequency of, *Trichogramma chilonis*, Ishii against, *Chilo saccharaphagus* indicus, (Kapur) in sugarcane. *J. Biol. Control* 23, 343–351. doi: 10.18311/jbc/2009/3687

Gomez-Diaz, C., Bargeton, B., Abuin, L., Bukar, N., Reina, J. H., Bartoi, T., et al. (2016). A CD36 ectodomain mediates insect pheromone detection via a putative tunnelling mechanism. *Nat. Commun.* 7:11866. doi: 10.1038/ncomms11866

Gong, D. P., Zhang, H. J., Zhao, P., Lin, Y., and Xiang, Z. H. (2007). Identification and expression pattern of the chemosensory protein gene family in the silkworm, *Bombyx mori*. *Insect Biochem. Mol. Biol.* 37, 266–277. doi: 10.1016/j.ibmb.2006.11.012

Gong, D. P., Zhang, H. J., Zhao, P., Xia, Q. Y., and Xiang, Z. H. (2009). The odorant binding protein gene family from the genome of silkworm, *Bombyx mori*. *BMC Genomics* 10:332. doi: 10.1186/1471-2164-10-332

González, D., Zhao, Q., Mcmahan, C., Velasquez, D., Haskins, W. E., Sponsel, V., et al. (2009). The major antennal chemosensory protein of red imported fire ant workers. *Insect Mol. Biol.* 18, 395–404. doi: 10.1111/j.1365-2583.2009.00883.x

Grosjean, Y., Rytz, R., Farine, J. P., Abuin, L., Cortot, J., Jefferis, G. S., et al. (2011). An olfactory receptor for food-derived odours promotes male courtship in *Drosophila*. *Nature* 478, 236–240. doi: 10.1038/nature10428

Grosse-Wilde, E., Kuebler, L. S., Bucks, S., Vogel, H., Wicher, D., and Hansson, B. S. (2011). Antennal transcriptome of *Manduca sexta*. *Proc. Natl. Acad. Sci. U.S.A.* 108, 7449–7454. doi: 10.1073/pnas.1017963108

Grosse-Wilde, E., Svatos, A., and Krieger, J. (2006). A pheromone-binding protein mediates the bombykol-induced activation of a pheromone receptor in vitro. *Chem. Senses* 31, 547–555. doi: 10.1093/chemse/bjj059

Gu, S. H., Zhou, J. J., Wang, G. R., Zhang, Y. J., and Guo, Y. Y. (2013). Sex pheromone recognition and immunolocalization of three pheromone binding proteins in the black cutworm moth *Agrotis ipsilon*. *Insect Biochem. Mol. Biol.* 43, 237–251. doi: 10.1016/j.ibmb.2012.12.009

Gu, X.-C., Zhang, Y.-N., Kang, K., Dong, S.-L., and Zhang, L.-W. (2015). Antennal transcriptome analysis of odorant reception genes in the red turpentine beetle (rtb), *Dendroctonus valens*. *PLoS One* 10. doi: 10.1371/journal.pone.0125159

Gyorgyi, T. K., Roby-Shemkovitz, A. J., and Lerner, M. R. (1988). Characterization and cDNA cloning of the pheromone-binding protein from the tobacco hornworm, *Manduca sexta*: a tissue-specific developmentally regulated protein. *Proc. Natl. Acad. Sci. U.S.A.* 85, 9851–9855. doi: 10.1073/pnas.85.24.9851

He, P., Chen, G. L., Li, S., Wang, J., Ma, Y. F., Pan, Y. F., et al. (2019a). Evolution and functional analysis of odorant-binding proteins in three rice planthoppers: *Nilaparvata lugens*, *Sogatella furcifera*, and *Laodelphax striatellus*. *Pest Manag. Sci.* 75, 1606–1620. doi: 10.1002/ps.5277

He, P., Durand, N., and Dong, S. L. (2019b). Editorial: insect olfactory proteins (from gene identification to functional characterization). *Front. Physiol.* 10:1313. doi: 10.3389/fphys.2019.01313

He, P., Engsontia, P., Chen, G. L., Yin, Q., Wang, J., Lu, X., et al. (2018). Molecular characterization and evolution of a chemosensory receptor gene family in three notorious rice planthoppers, *Nilaparvata lugens*, *Sogatella furcifera* and *Laodelphax striatellus*, based on genome and transcriptome analyses. *Pest Manag. Sci.* 74, 2156–2167. doi: 10.1002/ps.4912

He, P., Wang, M. M., Wang, H., Ma, Y. F., Yang, S., Li, S. B., et al. (2020). Genome-wide identification of chemosensory receptor genes in the small

brown planthopper, *Laodelphax striatellus*. *Genomics* 112, 2034–2040. doi: 10.1016/j.ygeno.2019.11.016

Hekmat-Scafe, D. S., Scafe, C. R., McKinney, A. J., and Tanouye, M. A. (2002). Genome-wide analysis of the odorant-binding protein gene family in *Drosophila melanogaster*. *Genome Res.* 12, 1357–1369. doi: 10.1101/gr.239402

Hildebrand, J. G. (1995). Analysis of chemical signals by nervous systems. *Proc. Natl. Acad. Sci. U.S.A.* 92, 67–74. doi: 10.1073/pnas.92.1.67

Hu, P., Wang, J., Cui, M., Tao, J., and Luo, Y. (2016). Antennal transcriptome analysis of the Asian longhorned beetle *Anoplophora glabripennis*. *Sci. Rep.* 6:26652. doi: 10.1038/srep26652

Hussain, A., Zhang, M., Ucpunar, H. K., Svensson, T., Quillery, E., Gompel, N., et al. (2016). Ionotropic chemosensory receptors mediate the taste and smell of polyamines. *PLoS Biol.* 14:e1002454. doi: 10.1371/journal.pbio.1002454

Jacquinjoly, E., Vogt, R. G., François, M. C., and Nagnanle, M. P. (2001). Functional and ex-pression pattern analysis of chemosensory proteins expressed in antennae and pheromonal gland of *Mamestra brassicae*. *Chem. Senses* 26, 833–844. doi: 10.1093/chemse/26.7.833

Jia, H. R., Niu, L. L., Sun, Y. F., Liu, Y. Q., and Wu, K. M. (2020). Odorant binding proteins and chemosensory proteins in *Episyrphus balteatus* (Diptera: Syrphidae): molecular cloning, expression profiling, and gene evolution. *J. Insect Sci.* 20:15. doi: 10.1093/jisesa/ieaa065

Jia, X. J., Zhang, X. F., Liu, H. M., Wang, R. Y., Zhang, T., and Gao, Y. L. (2018). Identification of chemosensory genes from the antennal transcriptome of Indian meal moth *Plodia interpunctella*. *PLoS One* 13:e0189889. doi: 10.1371/journal.pone.0189889

Jin, J. Y., Li, Z. Q., Zhang, Y. N., Liu, N. Y., and Dong, S. L. (2014). Different roles suggested by sex-biased expression and pheromone binding affinity among three pheromone binding proteins in the pink rice borer, *Sesamia inferens* (Walker) (Lepidoptera: Noctuidae). *J. Insect Physiol.* 66, 71–79. doi: 10.1016/j.jinsphys.2014.05.013

Jin, X., Brandazza, A., Navarrini, A., Ban, L., Zhang, S., Steinbrecht, R. A., et al. (2005). Expression and immunolocalisation of odorant-binding and chemosensory proteins in locusts. *Cell. Mol. Life Sci.* 62, 1156–1166. doi: 10.1007/s00018-005-5014-6

Jin, X., Ha, T. S., and Smith, D. P. (2008). SNMP is a signaling component required for pheromone sensitivity in *Drosophila*. *Proc. Natl. Acad. Sci. U.S.A.* 105, 10996–11001. doi: 10.1073/pnas.0803309105

Jones, W. D., Nguyen, T. A. T., Kloss, B., Lee, K. J., and Vosshall, L. B. (2005). Functional conservation of an insect odorant receptor gene across 250 millionyears of evolution. *Curr. Biol.* 15, 119–121. doi: 10.1016/j.cub.2005.02.007

Kaissling, K. E. (1998). Pheromone deactivation catalyzed by receptor molecules: a quantitative kinetic model. *Chem. Senses* 23, 385–395. doi: 10.1093/chemse/23.4.385

Kaissling, K. E. (2009). Olfactory perireceptor and receptor events in moths: a kinetic model revised. *J. Comp. Physiol. A* 195, 895–922. doi: 10.1007/s00359-009-0461-4

Koenig, C., Hirsh, A., Bucks, S., Klinner, C., Vogel, H., Shukla, A., et al. (2015). A reference gene set for chemosensory receptor genes of *Manduca sexta*. *Insect Biochem. Mol. Biol.* 66, 51–63. doi: 10.1016/j.ibmb.2015.09.007

Larkin, M. A., Blackshields, G., Brown, N. P., Chenna, R., McGettigan, P. A., McWilliam, H., et al. (2007). Clustal W and clustal X version 2.0. *Bioinformatics* 23, 2947–2948. doi: 10.1093/bioinformatics/btm404

Larsson, M. C., Domingos, A. I., Jones, W. D., Chiappe, M. E., Amrein, H., and Vosshall, L. B. (2004). Or83b encodes a broadly expressed odorant receptor essential for *Drosophila* olfaction. *Neuron* 43, 703–714. doi: 10.1016/j.neuron.2004.08.019

Laughlin, J. D., Ha, T. S., Jones, D. N., and Smith, D. P. (2008). Activation of pheromone-sensitive neurons is mediated by conformational activation of pheromone-binding protein. *Cell* 133, 1255–1265. doi: 10.1016/j.cell.2008.04.046

Lautenschlager, C., Leal, W. S., and Clardy, J. (2007). *Bombyx mori* pheromone-binding protein binding non-pheromone ligands: implications for pheromone recognition. *Structure* 15, 1148–1154. doi: 10.1016/j.str.2007.07.013

Leal, W. S. (2005). Pheromone reception. *Top Curr. Chem.* 240, 1–36. doi: 10.1007/b98314

Leal, W. S. (2007). Rapid binding, releaseand inactivation of insect pheromones. *Comp. Biochem. Physiol. A Mol. Integr. Physiol.* 148, S81–S81. doi: 10.1016/j.cbpa.2007.06.210

Leal, W. S. (2013). Odorant reception in insects: roles of receptors, binding proteins, and degrading enzymes. *Annu. Rev. Entomol.* 58, 373–391. doi: 10.1146/annurev-ento-120811-153635

Leitch, O., Papanicolaou, A., Lennard, C., Kirkbride, K. P., and Anderson, A. (2015). Chemosensory genes identified in the antennal transcriptome of the blowfly *Calliphora stygia*. *BMC Genomics* 16:255. doi: 10.1186/s12864-015-1466-8

Li, M. Y., Jiang, X. Y., Qi, Y. Z., Huang, Y. J., Li, S. G., and Liu, S. (2020). Identification and expression profiles of 14 odorant-binding protein genes from *Pieris rapae* (Lepidoptera: Pieridae). *J. Insect Sci.* 20, 1–10. doi: 10.1093/jisesa/ieaa087

Li, S., Picimbon, J. F., Ji, S., Kan, Y., Chuanling, Q., Zhou, J. J., et al. (2008). Multiple functions of an odorant-binding protein in the mosquito *Aedes aegypti*. *Biochem. Biophys. Res. Commun.* 372, 464–468. doi: 10.1016/j.bbrc.2008.05.064

Li, Z. Q., Zhang, S., Luo, J. Y., Wang, S. B., Wang, C. Y., Lv, L. M., et al. (2015). Identification and expression pattern of candidate olfactory genes in *Chrysoperla sinica* by antennal transcriptome analysis. *Comp. Biochem. Physiol. Part D Genom. Proteom.* 15, 28–38. doi: 10.1016/j.cbd.2015.05.002

Liu, N. Y., He, P., and Dong, S. L. (2012). Binding properties of pheromone-binding protein 1 from the common cutworm *Spodoptera litura*. *Comp. Biochem. Physiol. B Biochem. Mol. Biol.* 161, 295–302. doi: 10.1016/j.cbpb.2011.11.007

Liu, N. Y., Zhang, T., Ye, Z. F., Li, F., and Dong, S. L. (2015). Identification and characterization of candidate chemosensory gene families from *Spodoptera exigua* developmental transcriptomes. *Int. J. Biol. Sci.* 11, 1036–1048. doi: 10.7150/ijbs.12020

Liu, Y., Gu, S., Zhang, Y., Guo, Y., and Wang, G. (2012). Candidate olfaction genes identified within the *Helicoverpa armigera* antennal transcriptome. *PLoS One* 7:e48260. doi: 10.1371/journal.pone.0048260

Livak, K. J., and Schmittgen, T. D. (2001). Analysis of relative gene expression data using real time quantitative PCR and the $2^{-\Delta\Delta Ct}$, method. *Methods* 25, 402–408. doi: 10.1006/meth.2001.1262

Ni, L., Klein, M., Svec, K. V., Budelli, G., Chang, E. C., Ferrer, A. J., et al. (2016). The ionotropic receptors IR21a and IR25a mediate cool sensing in *Drosophila*. *eLife* 5:13254. doi: 10.7554/eLife.13254

Nibouche, S., Raboin, L. M., Hoarau, J. Y., D'Hont, A., and Costet, L. (2012). Quantitative trait loci for sugarcane resistance to the spotted stem borer *Chilo saccharaphagus*. *Mol. Breed.* 29, 129–135. doi: 10.1007/s11032-010-9531-0

Nibouche, S., and Tibère, R. (2010). Mechanism of resistance to the spotted stalk borer, *Chilo saccharaphagus*, in the sugarcane cultivar R570. *Entomol. Exp. Appl.* 135, 308–314. doi: 10.1111/j.1570-7458.2010.00996.x

Nichols, Z., and Vogt, R. G. (2008). The SNMP/CD36 gene family in Diptera, Hymenoptera and Coleoptera: *Drosophila melanogaster*, *D. pseudoobscura*, *Anopheles gambiae*, *Aedes aegypti*, *Apis mellifera*, and *Tribolium castaneum*. *Insect Biochem. Mol. Biol.* 38, 398–415. doi: 10.1016/j.ibmb.2007.11.003

Olivier, V., Monsempes, C., Francois, M. C., Poivet, E., and Jacquin-Joly, E. (2011). Candidate chemosensory ionotropic receptors in a Lepidoptera. *Insect Biochem. Mol. Biol* 20, 189–199. doi: 10.1111/j.1365-2583.2010.01057.x

Pearce, S. L., Clarke, D. F., East, P. D., Elfekih, S., Gordon, K. H. J., Jermiin, L. S., et al. (2017). Genomic innovations, transcriptional plasticity and gene loss underlying the evolution and divergence of two highly polyphagous and invasive *Helicoverpa* pest species. *BMC Biol.* 15:63. doi: 10.1186/s12915-017-0402-6

Pelletier, J., and Leal, W. S. (2009). Genome analysis and expression patterns of odorant-binding proteins from the southern house mosquito *Culex pipiens* quinquefasciatus. *PLoS One* 4:e6237. doi: 10.1371/journal.pone.0006237

Pelletier, J., and Leal, W. S. (2011). Characterization of olfactory genes in the antennae of the southern house mosquito, *Culex quinquefasciatus*. *J. Insect Physiol.* 57, 915–929. doi: 10.1016/j.jinsphys.2011.04.003

Pelosi, P., Iovinella, I., Felicioli, A., and Dani, F. R. (2014). Soluble proteins of chemical communication: an overview across arthropods. *Front. Physiol.* 5:320. doi: 10.3389/fphys.2014.00320

Pelosi, P., Iovinella, I., Zhu, J., Wang, G., and Dani, F. R. (2018). Beyond chemoreception: diverse tasks of soluble olfactory proteins in insects. *Biol. Rev. Cambridge Philos. Soc.* 93, 184–200. doi: 10.1111/brv.12339

Pelosi, P., and Maida, R. (1995). Odorant-binding proteins in insects. *Comp. Biochem. Physiol. Part B Biochem. Mol. Biol.* 111, 503–514. doi: 10.1016/0305-0491(95)00019-5

Pelosi, P., Zhou, J. J., Ban, L. P., and Calvello, M. (2006). Soluble proteins in insect chemical communication. *Cell Mol. Life Sci.* 63, 1658–1676. doi: 10.1007/s00018-005-5607-0

Pertea, G., Huang, X., Liang, F., Antonescu, V., Sultana, R., Karamycheva, S., et al. (2003). TIGR gene indices clustering tools (TGICL): a software system for fast clustering of largest datasets. *Bioinformatics* 19, 651–652. doi: 10.1093/bioinformatics/btg034

Picimbon, J.-F. J., Dietrich, K., Krieger, J., and Breer, H. (2001). Identity and expression pattern of chemosensory proteins in *Heliothis virescens* (Lepidoptera, Noctuidae). *Insect Biochem. Mol. Biol.* 31, 1173–1181. doi: 10.1016/s0965-1748(01)00063-7

Poivet, E., Gallot, A., Montagné, N., Glaser, N., Legeai, F., and Jacquinjoly, E. (2013). A comparison of the olfactory gene repertoires of adults and larvae in the noctuid moth *Spodoptera littoralis*. *PLoS One* 8:e60263. doi: 10.1371/journal.pone.0060263

Pophof, B. (2004). Pheromone-binding proteins contribute to the activation of olfactory receptor neurons in the silkmoths *Antheraea polyphemus* and *Bombyx mori*. *Chem. Senses* 29, 117–125. doi: 10.1093/chemse/bjh012

Prestwich, G. D. (1996). Proteins that smell: pheromone recognition and signal transduction. *Bioorg. Med. Chem.* 4, 505–513. doi: 10.1016/0968-0896(96)00033-8

Prieto-Godino, L. L., Rytz, R., Bargeton, B., Abuin, L., Arguello, J. R., Peraro, M. D., et al. (2016). Olfactory receptor pseudo-pseudogenes. *Nature* 539, 93–97. doi: 10.1038/nature19824

Prokupek, A. M., Eyun, S. I., Ko, L., Moriyama, E. N., and Harshman, L. G. (2010). Molecular evolutionary analysis of seminal receptacle sperm storage organ genes of *Drosophila melanogaster*. *J. Evol. Biol.* 23, 1386–1398. doi: 10.1111/j.1420-9101.2010.01998.x

Quackenbush, J., Cho, J., Lee, D., Liang, F., Holt, I., Karamycheva, S., et al. (2001). The TIGR gene indices: analysis of gene transcript sequences in highly sampled eukaryotic species. *Nucleic Acids Res.* 29, 159–164. doi: 10.1093/nar/29.1.159

Ramdya, P., and Benton, R. (2010). Evolving olfactory systems on the fly. *Trends Genet.* 26, 307–316. doi: 10.1016/j.tig.2010.04.004

Renwick, J. A. A., Radke, C. D., Sachdev-Gupta, K., and Städler, E. (1992). Leaf surface chemicals stimulating oviposition by *Pieris rapae* (Lepidoptera: Pieridae) on cabbage. *Chemoecology* 3, 33–38. doi: 10.1007/BF01261454

Robertson, H. M., and Wanner, K. W. (2006). The chemoreceptor superfamily in the honey bee, *Apis mellifera*: expansion of the odorant, but not gustatory, receptor family. *Genome Res.* 16, 1395–1403. doi: 10.1101/gr.5057506

Robertson, H. M., Warr, C. G., and Carlson, J. R. (2003). Molecular evolution of the insect chemoreceptor gene superfamily in *Drosophila melanogaster*. *Proc. Natl. Acad. Sci. U.S.A.* 100(Suppl. 2), 14537–14542. doi: 10.1073/pnas.2335847100

Rogers, M. E., Krieger, J., and Vogt, R. G. (2001). Antennal SNMPs (sensory neuron membrane proteins) of Lepidoptera define a unique family of invertebrate CD36-like proteins. *J. Neurobiol.* 49, 47–61. doi: 10.1002/neu.1065

Sallam, N., Achadian, E. M., Putra, L., Dianpratiwi, T., Kristini, A., Donald, D., et al. (2016). In search of varietal resistance to sugarcane moth borers in Indonesia. *Int. Sugar J.* 118, 450–452.

Sato, K., Pellegrino, M., Nakagawa, T., Nakagawa, T., Vosshall, L. B., and Touhara, K. (2008). Insect olfactory receptors are heteromeric ligand-gated ion channels. *Nature* 452, 1002–1006. doi: 10.1038/nature06850

Sato, Y., Yano, S., Takabayashi, J., and Ohsaki, N. (1999). *Pieris rapae* (Ledidoptera: Pieridae) females avoid oviposition on *Rorippa indica* plants infested by conspecific larvae. *Appl. Entomol. Zool.* 34, 333–337. doi: 10.1021/cr9001676

Smart, R., Kiely, A., Beale, M., Vargas, E., Carraher, C., Kralicek, A. V., et al. (2008). *Drosophila* odorant receptors are novel seven transmembrane domain proteins that can signal independently of heterotrimeric G proteins. *Insect Biochem. Mol. Biol.* 38, 770–780. doi: 10.1016/j.ibmb.2008.05.002

Stocker, R. F. (1994). The organization of the chemosensory system in *Drosophila melanogaster*: a review. *Cell Tissue Res.* 275, 3–26. doi: 10.1007/bf00305372

Stork, N. E. (1993). How many species are there? *Biodivers. Conserv.* 2, 215–232. doi: 10.1007/BF00056669

Takemori, N., and Yamamoto, M. T. (2009). Proteome mapping of the *Drosophila melanogaster* male reproductive system. *Proteomics* 9, 2484–2493. doi: 10.1002/pmic.200800795

Tamura, K., Stecher, G., Peterson, D., Filipski, A., and Kumar, S. (2013). MEGA6: molecular evolutionary genetics analysis version 6.0. *Mol. Biol. Evol.* 30, 2725–2729. doi: 10.1093/molbev/mst197

Tanaka, K., Uda, Y., Ono, Y., Nakagawa, T., Suwa, M., Yamaoka, R., et al. (2009). Highly selective tuning of a silkworm olfactory receptor to a key mulberry leaf volatile. *Curr. Biol.* 19, 881–890. doi: 10.1016/j.cub.2009.04.035

Tang, R., Jiang, N. J., Ning, C., Li, G. C., and Wang, C. Z. (2020). The olfactory reception of acetic acid and ionotropic receptors in the oriental armyworm, *Mythimna separata* walker. *Insect Biochem. Mol. Biol.* 118:103312. doi: 10.1016/j.ibmb.2019.103312

Vieira, F. G., and Rozas, J. (2011). Comparative genomics of the odorant-binding and chemosensory protein gene families across the Arthropoda: origin and evolutionary history of the chemosensory system. *Genome Biol. Evol.* 3, 476–490. doi: 10.1093/gbe/evr033

Vogt, R. G. (1995). "Molecular genetics of moth olfaction: a model for cellular identity and temporal assembly of the nervous system," in *Molecular Model Systems in the Lepidoptera*, eds M. Goldsmith and A. S. Wilkins (Cambridge: Cambridge University Press), 341–367. doi: 10.1017/cbo9780511529931.014

Vogt, R. G., Miller, N. E., Litvack, R., Fandino, R. A., Sparks, J., Staples, J., et al. (2009). The insect SNMP gene family. *Insect Biochem. Mol. Biol.* 39, 448–456. doi: 10.1016/j.ibmb.2009.03.007

Vogt, R. G., and Riddiford, L. M. (1981). Pheromone binding and inactivation by moth antennae. *Nature* 293, 161–613. doi: 10.1038/293161a0

Vosshall, L. B., Amrein, H., Morozov, P. S., Rzhetsky, A., and Axel, R. (1999). A spatial map of olfactory receptor expression in the *Drosophila antenna*. *Cell* 96, 725–736. doi: 10.1016/s0092-8674(00)80582-6

Walker, W. B., Roy, A., Anderson, P., Schlyter, F., Hansson, B. S., and Larsson, M. C. (2019). Transcriptome analysis of gene families involved in chemosensory function in *Spodoptera littoralis* (Lepidoptera: Noctuidae). *BMC Genomics* 20:428. doi: 10.1186/s12864-019-5815-x

Wang, B., Liu, Y., and Wang, G. R. (2017). Chemosensory genes in the antennal transcriptome of two syrphid species, *Episyrphus balteatus* and *Eupeodes corollae* (diptera: syrphidae). *BMC Genomics* 18:586. doi: 10.1186/s12864-017-3939-4

Wanner, K. W., Anderson, A. R., Trowell, S. C., Theilmann, D. A., Robertson, H. M., and Newcomb, R. D. (2007). Female-biased expression of odourant receptor genes in the adult antennae of the silkworm, *Bombyx mori*. *Insect Mol. Biol.* 16, 107–119. doi: 10.1111/j.1365-2583.2007.00708.x

Wanner, K. W., Willis, L. G., Theilmann, D. A., Isman, M. B., Feng, Q. L., and Plettner, E. (2004). Analysis of the insect os-d-like gene family. *J. Chem. Ecol.* 30, 889–911. doi: 10.1023/b:joec.0000028457.51147.d4

Wei, H. S., Li, K. B., Zhang, S., Cao, Y. Z., and Yin, J. (2017). Identification of candidate chemosensory genes by transcriptome analysis in *Loxostege sticticalis* Linnaeus. *PLoS One* 12:e0174036. doi: 10.1371/journal.pone.0174036

Wicher, D. (2014). Olfactory signaling in insects. *Prog. Mol. Biol. Transl. Sci.* 130, 37–54. doi: 10.1016/bs.pmbts.2014.11.002

Wicher, D., Schafer, R., Bauernfeind, R., Stensmyr, M. C., Heller, R., Heinemann, S. H., et al. (2008). *Drosophila* odorant receptors are both ligand-gated and cyclic-nucleotide-activated cation channels. *Nature* 452, 1007–1011. doi: 10.1038/nature06861

Wojtasek, H., and Leal, W. S. (1999). Conformational change in the pheromone-binding protein from *Bombyx mori* induced by pH and by interaction with membranes. *J. Biol. Chem.* 274, 30950–30956. doi: 10.1074/jbc.274.43.30950

Wu, Z., Zhang, H., Wang, Z., Bin, S., He, H., and Lin, J. (2015). Discovery of chemosensory genes in the oriental fruit fly, *Bactrocera dorsalis*. *PLoS One* 10:e0129794. doi: 10.1371/journal.pone.0129794

Xu, Q. Y., Wu, Z. Z., Zeng, X. N., and An, X. C. (2020). Identification and expression profiling of chemosensory genes in *Hermetia illucens* via a transcriptomic analysis. *Front. Physiol.* 11:720. doi: 10.3389/fphys.2020.00720

Xu, Y. L., He, P., Zhang, L., Fang, S. Q., Dong, S. L., Zhang, Y. J., et al. (2009). Large-scale identification of odorant-binding proteins and chemosensory proteins from expressed sequence tags in insects. *BMC Genomics* 10:632. doi: 10.1186/1471-2164-10-632

Ye, J., Fang, L., Zheng, H., Zhang, Y., Chen, J., Zhang, Z., et al. (2006). WEGO: a web tool for plotting GO annotations. *Nucleic Acids Res.* 34, 293–297. doi: 10.1093/nar/gkl031

Zhang, H. J., Xu, W., Chen, Q. M., Sun, L. N., Anderson, A., Xia, Q. Y., et al. (2020). A phylogenomics approach to characterizing sensory neuron membrane proteins (SNMPs) in Lepidoptera. *Insect Biochem. Mol. Biol.* 118, 103313. doi: 10.1016/j.ibmb.2020.103313

Zhang, J., Bisch-Knaden, S., Fandino, R. A., Yan, S., Obiero, G. F., Grosse-Wilde, E., et al. (2019). The olfactory coreceptor IR8a governs larval feces-mediated competition avoidance in a hawkmoth. *Proc. Natl. Acad. Sci. U.S.A.* 116, 21828–21833. doi: 10.1073/pnas.1913485116

Zhang, J., Wang, B., Dong, S. L., Cao, D. P., Dong, J. F., Walker, W. B., et al. (2015). Antennal transcriptome analysis and comparison of chemosensory gene families in two closely related Noctuidae moths, *Helicoverpa armigera* and *H. assulta*. *PLoS One* 10:e0117054. doi: 10.1371/journal.pone.0117054

Zhang, L. W., Kang, K., Jiang, S. C., Zhang, Y. N., and Ding, D. G. (2016). Analysis of the antennal transcriptome and insights into olfactory genes in *Hyphantria cunea* (Drury). *PLoS One* 11:e0164729. doi: 10.1371/journal.pone.0164729

Zhang, Y. N., Ye, Z. F., Yang, K., and Dong, S. L. (2014). Antenna-predominant and male-biased csp19 of *Sesamia inferens* is able to bind the female sex pheromones and host plant volatiles. *Gene* 536, 279–286. doi: 10.1016/j.gene.2013.12.011

Zhou, J. J., Vieira, F. G., He, X. L., Smadja, C., Liu, R., Rozas, J., et al. (2010). Genome annotation and comparative analyses of the odorant-binding proteins and chemosensory proteins in the pea aphid *Acyrthosiphon pisum*. *Insect. Mol. Biol.* 19, 113–122. doi: 10.1111/j.1365-2583.2009.00919.x

Zhou, X. H., Ban, L. P., Iovinella, I., Zhao, L. J., Gao, Q., Felicioli, A., et al. (2013). Diversity, abundance and sex-specific expression of chemosensory proteins in the reproductive organs of the locust *Locusta migratoria* manilensis. *Biol. Chem.* 394, 43–54. doi: 10.1515/hsz-2012-0114

Zhu, G. H., Xu, J., Cui, Z., Dong, X. T., Ye, Z. F., Niu, D. J., et al. (2016). Functional characterization of slitpbp3 in spodoptera litura by crispr/cas9 mediated genome editing. *Insect Biochem. Mol. Biol.* 75, 1–9. doi: 10.1016/j.ibmb.2016.05.006

Zhu, G. H., Zheng, M. Y., Sun, J. B., Khuhro, S. A., Yan, Q., Huang, Y., et al. (2019). CRISPR/Cas9 mediated gene knockout reveals a more important role of PBP1 than PBP2 in the perception of female sex pheromone components in *Spodoptera litura*. *Insect Biochem. Mol. Biol.* 115:103244. doi: 10.1016/j.ibmb.2019.103244

Conflict of Interest: The authors declare that the research was conducted in the absence of any commercial or financial relationships that could be construed as a potential conflict of interest.

Copyright © 2021 Liu, Liu, Yi, Mao, Li, Sun, An and Wu. This is an open-access article distributed under the terms of the Creative Commons Attribution License (CC BY). The use, distribution or reproduction in other forums is permitted, provided the original author(s) and the copyright owner(s) are credited and that the original publication in this journal is cited, in accordance with accepted academic practice. No use, distribution or reproduction is permitted which does not comply with these terms.

frontiers in Physiology

BRIEF RESEARCH REPORT
published: 13 April 2021
doi: 10.3389/fphys.2021.656649

Whitefly Network Analysis Reveals Gene Modules Involved in Host Plant Selection, Development and Evolution

Jiahui Tian[1,2], Haixia Zhan[2], Youssef Dewer[3], Biyun Zhang[2], Cheng Qu[2], Chen Luo[2], Fengqi Li[2] and Shiyong Yang[1,4]**

[1] School of Ecology and Environment, Anhui Normal University, Wuhu, China, [2] Beijing Key Laboratory of Environment Friendly Management on Fruit Diseases and Pests in North China, Institute of Plant and Environment Protection, Beijing Academy of Agriculture and Forestry Sciences, Beijing, China, [3] Bioassay Research Department, Central Agricultural Pesticide Laboratory, Agricultural Research Center, Dokki, Giza, Egypt, [4] Collaborative Innovation Center of Recovery and Reconstruction of Degraded Ecosystem in Wanjiang Basin Co-Founded by Anhui Province and Ministry of Education, Anhui Normal University, Wuhu, China

OPEN ACCESS

Edited by:
Rui Tang, Guangdong Academy of Science (CAS), China

Reviewed by:
Hao Guo, Chinese Academy of Sciences (CAS), China
Liu Fangzhou, University of Rochester, United States

***Correspondence:**
Shiyong Yang
shiyan@ahnu.edu.cn
Fengqi Li
pandit@163.com

Specialty section:
This article was submitted to Invertebrate Physiology, a section of the journal Frontiers in Physiology

Received: *21 January 2021*
Accepted: *22 March 2021*
Published: *13 April 2021*

Citation:
Tian J, Zhan H, Dewer Y, Zhang B, Qu C, Luo C, Li F and Yang S (2021) Whitefly Network Analysis Reveals Gene Modules Involved in Host Plant Selection, Development and Evolution. Front. Physiol. 12:656649. doi: 10.3389/fphys.2021.656649

Whiteflies are Hemipterans that typically feed on the undersides of plant leaves. They cause severe damage by direct feeding as well as transmitting plant viruses to a wide range of plants. However, it remains largely unknown which genes play a key role in development and host selection. In this study, weighted gene co-expression network analysis was applied to construct gene co-expression networks in whitefly. Nineteen gene co-expression modules were detected from 15560 expressed genes of whitefly. Combined with the transcriptome data of salivary glands and midgut, we identified three gene co-expression modules related to host plant selection. These three modules contain genes related to host-plant recognition, such as detoxification genes, chemosensory genes and some salivary gland-associated genes. Results of Gene Ontology and Kyoto Encyclopedia of Genes and Genomes analyses elucidated the following pathways involved in these modules: lysosome, metabolic and detoxification pathways. The modules related to the development contain two co-expression modules; moreover, the genes were annotated to the development of chitin-based cuticle. This analysis provides a basis for future functional analysis of genes involved in host-plant recognition.

Keywords: weighted gene co-expression network analysis, whitefly, development, host plant, co-expressed genes

INTRODUCTION

The whitefly *Bemisia tabaci* (Hemiptera: Aleyrodidae) is one of the most important insect pests for major crops, especially in the sub-tropical and tropical regions around the world (Liu et al., 2007; De Barro et al., 2011). Systematic studies of the *B. tabaci* reveal convincing evidence that *B. tabaci* is a complex species including at least 35 cryptic species with extensive genetic diversity (De Barro et al., 2011; Bing et al., 2013). Among them, the Middle East-Asia Minor 1 (MEAM1) and Mediterranean 1 are considered to be the most widely distributed species worldwide, causing substantial economic

damage to crops (Xu et al., 2011; Liu et al., 2012). *B. tabaci* has a wide host range with a total of 600 different plant species from different families such as: Compositae, Cruciferae, Cucurbitaceae, Euphorbiaceae, Leguminosae, Lamiaceae, Malvaceae, and Solanaceae (Mound and Halsey, 1978; Johnson et al., 1982; Elsey and Farnham, 1994; Bayhan et al., 2006; Li et al., 2011). In spite of the large-scale of host-plant use, whiteflies show diverse behavior concerning to host plant preference, oviposition, ecological adaptation as well as population size and degree of plant damage (Butler and Henneberry, 1989; Costa et al., 1991). However, the genes related to whitefly development and host-plant selection are still unknown.

One of the methods used to understand gene function and gene association from genome-wide expression is co-expression network analysis (Langfelder and Horvath, 2008; Childs et al., 2011; Liang et al., 2014). Weighted gene co-expression network analysis (WGCNA) is the most commonly used systemic biology approach used to identify the pattern of correlations among genes (Tahmasebi et al., 2019). The genes in co-expressed module, combined with functional annotations [Gene Ontology (GO) and Kyoto Encyclopedia of Genes and Genomes (KEGG)] and comparative evolution, could make the results of WGCNA more meaningful (Stuart et al., 2003; Zinkgraf et al., 2017). Thus, co-expressed modules can be helpful in understanding the function and co-expression module in genes.

In the present study, we used WGCNA analysis to construct a co-expression network among genes to identify host plant selection-related and development-related co-expression modules in the MEAM1 species of *B. tabaci*. Moreover, we accessed the function analysis and evolutionary selection pressure analysis of the key module genes.

MATERIALS AND METHODS

Data Preparation

We downloaded the genome sequence of the *B. tabaci* MEAM1 species from www.whiteflygenomics.org (download version: MEAM1_scaffold_v1.2.fa.gz) and gene annotation GFF3 file (download version: MEAM1_v1.2. gff3.gz). The publicly available whitefly RNA-Seq transcriptome datasets deposited in the NCBI SRA database were used in the analysis (**Supplementary Table 1**). Data included SRA data of whitefly fed on different host plants (Malka et al., 2018) and SRA data at different developmental stages (Zeng et al., 2018). We used the alignment tool Hisat2 version 2.1.0 to map the transcriptome sequence to the MEAM1 genome, and used featureCounts version 1.6.4 to calculate the count value of the transcriptome expression of the whitefly transcriptome of different treatments, and convert the count values of each gene into TPM expression values.

Weighted Gene Co-Expression Network Analysis

We ran the WGCNA software package on R (version 3.6.1). Before constructing the co-expression network, we filtered out samples with more than 10% missing genes, removed genes with 0 variance and genes with more than 10% missing samples. The genes were clustered into network modules using the topological overlap measure (TOM). Genes were grouped by hierarchical clustering on the basis of dissimilarity of gene connectivity (1-TOM). The co-expression clusters were produced by dynamic Mods in which the minimum size of modules was kept at 30 genes. The modules were randomly color-labeled. An adjacency matrix was built by applying a power function (β) on the Pearson correlation coefficient.

Differential Gene Expression Analysis

We used the B-biotype whitefly midgut transcriptome (SRR835757) and salivary gland transcriptome (SRR10780450) to determine the differentially expressed genes in the midgut and salivary gland of *B. tabaci*. The calculation method of TPM expression values of genes in the midgut and salivary glands is the same as above. We used the DESeq2 software package in R (version 3.6.1; Love et al., 2014) to perform the differential expression analysis of genes (**Supplementary Table 3**). According to the Benjamini-Hochberg procedure, if the *p*-value is less than 0.05 after 5% FDR and the log2Fold change is greater than 2, then the gene is considered to be differentially expressed.

Functional Annotation of Genes in Key Modules

We used the KEGG Orthology Based Annotation System (KOBAS 3.0) to perform Gene Ontology and KEGG on genes in key co-expression modules. In KOBAS, the term enrichment was defined as the Benjamini-adjusted Fisher's exact test *p*-value. A corrected *P*-value less than or equal to 0.01 was considered statistically significant (Pu et al., 2020).

Evolutionary Analysis of Homologous Genes in Key Modules

We choose *Bemisia* Mediterranean (MED or "Q" biotypes) species as the related group of *B. tabaci*. We employed OrthoFinder version 2.3.11 software program to calculate the orthologous genes in the B-and Q-biotypes of whitefly. KaKs_Calculator 2.0 was used to analyze the selection pressure of homologous genes in key modules.

RESULTS

Gene Co-Expression Network for *B. tabaci* Was Successfully Constructed

A total of 33 whitefly samples were analyzed including different developmental stages of *B. tabaci*: egg, 1–2nd instar nymphs, 3rd instar nymphs, 4th instar nymphs, males, and females. The whiteflies were fed with different host plants: sucrose-pepper, pepper, kale, eggplant, and cassava. A β value of 27 was determined to be optimal for balancing the scale-free property of the co-expression network and the sparsity of connections between genes (**Supplementary Figure 1**). A total of 19 co-expressed gene modules were identified after merging similar modules (**Figure 1A**). The network genes were then clustered and modules were detected using the dynamic tree cut method.

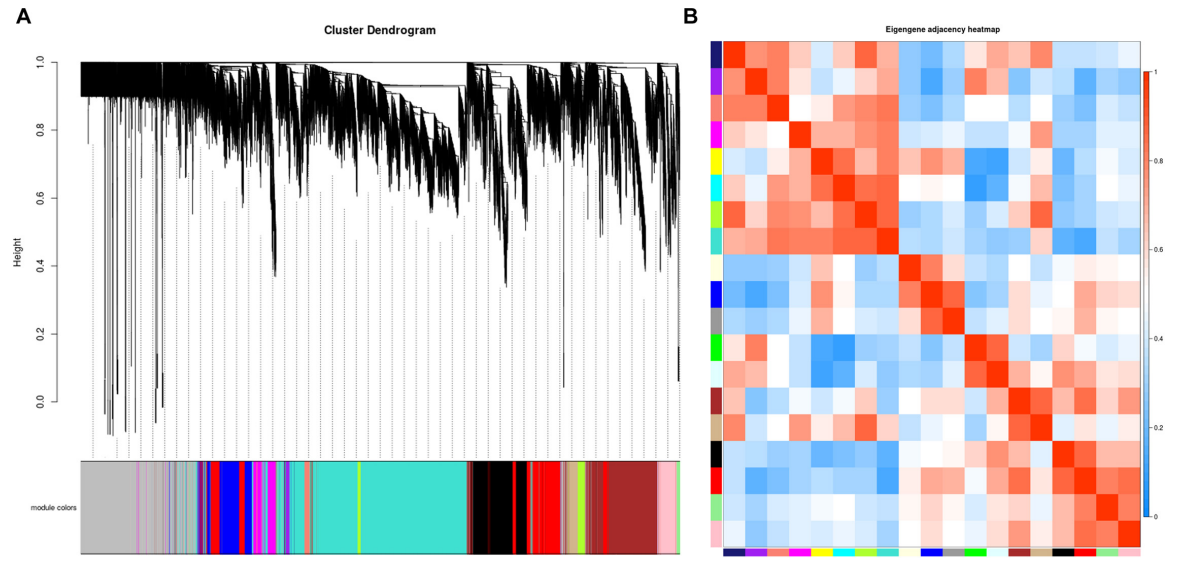

FIGURE 1 | Establishment of a co-expression network in whitefly. **(A)** Gene clustering tree (dendrogram) of 15,560 genes obtained via hierarchical clustering of topological overlapping dissimilarity. **(B)** Eigengene adjacency heatmap of the 19 modules in the network. Each row and column in the heatmap corresponds to one module (labeled in color). The scale bar on the right represents the correlation strength ranging from 0 (blue) to 1 (red).

A heatmap of eigengene correlations among the 19 modules indicated that the adjacent modules with red squares along the diagonal clustered to form several meta-modules with high correlation, suggesting that multiple modules may be involved in a similar biological process (**Figure 1B**).

Identification and Function of Host Plant Selection-Related Modules in the Whitefly

To identify the host plant selection-related modules, we performed an enrichment analysis on the genes in the co-expression module and the differentially expressed genes in the salivary glands and midgut. There were 1168 genes differentially expressed in the salivary glands. Midnight blue module and turquoise module were enriched for whitefly genes expressed in the salivary glands (**Figure 2A**). There were 1151 differentially expressed genes in the midgut. Magenta module was enriched for midgut-expressed genes (**Figure 2B**). The heatmap and characteristic value bar graph of the expression level of the module showed that the genes in the midnight blue, turquoise and magenta modules were highly expressed in different host plants (**Figures 2C–E**). Cytoscape software was used to construct a visual network based on target genes, and the first 50 connectivity genes were obtained through the cytohubba plug-in. The depth of the color represents the strength of the connection. The co-expression network of the first fifty genes in midnight blue and magenta module was shown in **Supplementary Figure 2**. To further determine the relationship between the gene-enriched modules differentially expressed in the salivary glands, midgut and host selection, we conducted GO and KEGG enrichment analyses in these three modules. From the GO annotation (**Supplementary Table 2**), the midnight blue module was associated with "neuropeptide signaling pathway (GO:0007218)," followed by "neuropeptide hormone activity (GO:0005184)," and "G protein-coupled receptor signaling pathway (GO:0007186)." The turquoise module was associated with "mitochondrial translation (GO:0032543)," followed by "ATP binding (GO:0005524)." The magenta module was associated with "peptidase activity (GO:0008233)," followed by "detoxification of zinc ion (GO:0010312)." KEGG analysis of midnight blue module genes identified "Glycosphingolipid biosynthesis – globo and isoglobo series" as the most significantly enriched metabolic pathways (**Supplementary Table 2**). KEGG analysis of turquoise module genes identified "Lysosome" and "Starch and sucrose metabolism" as the most significantly enriched metabolic pathways (**Supplementary Table 2** and **Figure 2F**). KEGG analysis of magenta module genes identified "Protein processing in endoplasmic reticulum" and "Metabolic pathways" as the most significantly enriched metabolic pathway (**Supplementary Table 2**).

Identification and Function of Development-Related Modules in the Whitefly

According to the expression heatmap and feature value bar graph of each co-expression module, the co-expression modules related to whitefly development were determined as black and red. The genes in the black module were highly co-expressed in 4th instar nymphs (**Figure 3A**), and the genes in the red module were highly co-expressed in whitefly eggs and nymphs (**Figure 3B**). The co-expression network of the first fifty genes in the two modules was shown in **Supplementary Figure 2**. To determine the functions of genes in the two key co-expression modules related to development, GO and KEGG enrichment analyses

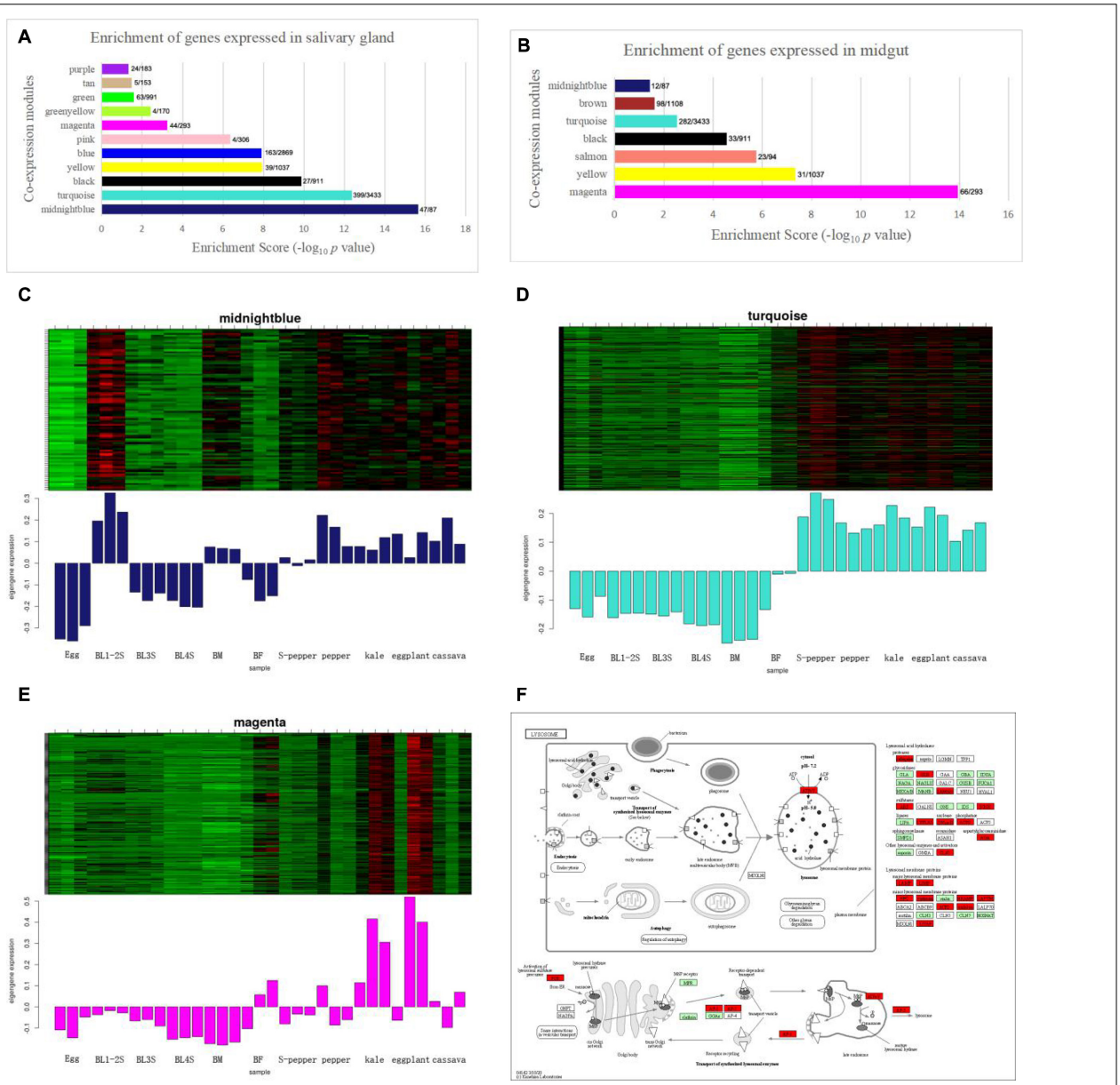

FIGURE 2 | The host plant selection-related module of whitefly is performed by WGCNA. **(A)** Enrichment scores of genes expressed in salivary gland. The *x*/*y* values above the bars indicate gene numbers in the enriched category (*x*) and module (*y*). **(B)** Enrichment scores of genes expressed in midgut. The *x*/*y* values above the bars indicate gene numbers in the enriched category (*x*) and module (*y*). **(C)** The heatmap of expression pattern of genes in midnight blue module enriched in salivary gland. **(D)** The heatmap of expression pattern of genes in turquoise module enriched in salivary gland. **(E)** The heatmap of expression pattern of genes in magenta module enriched in midgut. **(F)** The KEGG enrichment of Lysosome in turquoise module with the *P*-Value of 1.5E-09.

were performed on the black and red genes. From GO annotation (**Supplementary Table 2**), the black module was associated with "chitin-based cuticle development (GO:0040003)," followed by "regulation of membrane potential (GO:0042391)." The red module was associated with "chemical synaptic transmission (GO:0007268)," followed by "G protein-coupled amine receptor activity (GO:0008227)." KEGG analysis of black module genes identified "Pentose and glucuronate interconversions" and "Ascorbate and aldarate metabolism" as the most significantly enriched metabolic pathways (**Supplementary Table 2**). "Neuroactive ligand-receptor interaction" was the most significantly enriched metabolic pathway in the red module.

Evolution of Key Modules Related to Host Plant Selection and Development of the Whitefly

To study the evolutionary selection pressure of genes in co-expression modules related to host selection and development, we used the Q-biotype of whitefly as a relative group of

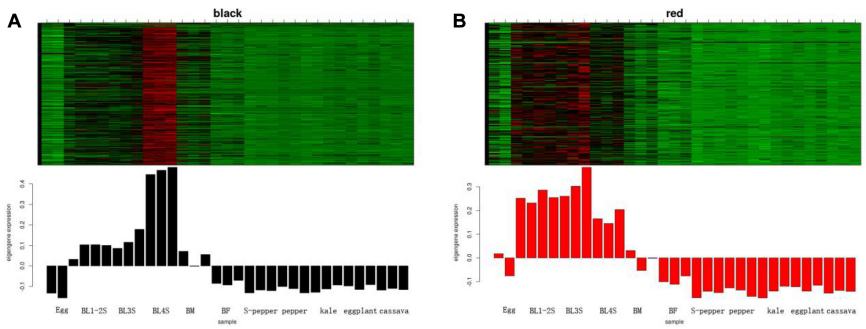

FIGURE 3 | The development-related module of whitefly is performed by WGCNA. **(A)** The heatmap of expression pattern of genes in black module. **(B)** The heatmap of expression pattern of genes in red module.

TABLE 1 | Evolutionary selection pressure of key modules related to host plant selection and development of the whitefly.

	Module	Number of co-expressed genes	Number of genes with ka/ks > 1	Max of ka/ks	Min of ka/ks	Average of ka/ks	Proportion of ka/ks > 1
Host plant-related	Midnight blue	87	2	1.2207	0.001	0.289	0.036
	Turquoise	3433	74	99	0.001	0.281	0.057
	Magenta	293	12	99	0.001	0.308	0.030
Development-related	Black	911	8	99	0.001	0.261	0.013
	Red	982	5	99	0.001	0.271	0.009

B-biotype and performed Ka/Ks analysis on the homologous genes of the two species (**Table 1**). Among the modules related to host selection, 2 genes in the midnight blue module have undergone positive selection, 74 genes in the turquoise module have undergone positive selection, and 12 genes in the magenta module have undergone positive selection. Among the three host-related modules, the turquoise module had the highest percentage of genes (0.057%) undergoing positive selection. Among the development-related modules, 8 genes in the black module have undergone positive selection, and 5 genes in the red module have undergone positive selection.

DISCUSSION

WGCNA Has Been Applied for Gene Co-Expression Network Construction in Many Species

In plant research, WGCNA identified cell-type specific and endoderm differentiation-associated gene co-expression modules (Zhan et al., 2015). Pu et al. (2020) used WGCNA to identify micro-RNAs functional modules and genes of ischemic stroke. In *Myzus persicae*, WGCNA was used to identify genes with expression levels that are highly correlated in different host plants (Chen et al., 2020). Their results showed that the DE transcripts were enriched in proteolysis (including Cathepsin B). In contrast with previous research, the module related to host plant selection was also included Cathepsin B, but we also found more genes related to host plant selection, such as Odorant-binding proteins (OBPs) and chemosensory proteins (CSPs). Moreover, 19 modules were obtained by WGCNA analysis, among which midnight blue, turquoise and magenta modules were highly correlated with host plant selection. Black and red modules were highly correlated with whitefly development.

The Differentially Expressed Genes of Saliva and the Midgut Further Validate the Modules Related to Host Plant Selection

The midgut and saliva play critical roles in mediating the interaction between herbivorous insects and their host plants (Kumar et al., 2015; Huang et al., 2020). Some proteases are highly expressed in the midgut and may reflect the ability of insects to select their appropriate host plants for development (Saikia et al., 2011). In this study, we used the EBseq package to locate genes that are differentially expressed in the salivary glands and midgut. The highly expressed genes in the salivary glands and midgut were, respectively, enriched in the identified co-expression modules. The results showed that midnight blue and turquoise were enriched in the salivary glands, and magenta was enriched in the midgut. KEGG analysis of midnight blue, turquoise and magenta showed that glycosphingolipid biosynthesis, lysosome and protein processing in the endoplasmic reticulum pathway were enriched, respectively.

Among them, lysosomal enzymes are concerned with the degradation of metabolites. Lysosomes are membrane delimited organelles serving as the cell's main digestive compartment (Appelqvist et al., 2013) and lysosome pathway enriched 50 genes. Their functions include endocytosis, phagocytosis and

autophagy. Lysosomes contain a variety of proteases and esterases that are highly expressed in the salivary glands, such as cathepsins b (CTSB). Herbivorous insects can use these cysteine proteases to break down dietary proteins, and these cysteine proteases can act as defense proteins against toxins or protease inhibitors that may be produced by host plants (Koo et al., 2008; Serbielle et al., 2009). These enzymes are very important in host selection (Huang et al., 2020; Guo et al., 2020).

Modules Related to Host Plant Selection Contain Multiple Genes Adapted to Host Plants

The host selection module contains many detoxification related genes, such as cytochrome P450 (CYPs) and UDPGT family. CYPs is an ancient superfamily of enzymes, found in all areas of life, and involved in the metabolism of a variety of substrates. These substrates play an important role in hormone synthesis, decomposition, development and detoxification (Feyereisen, 1999; Heidel-Fischer and Vogel, 2015). In previous studies, after a transfer from eggplant to cassava, pepper and kale, the P450 and UDPGT family genes were significantly enriched in the detoxification gene family of whitefly (Malka et al., 2018). And a study on the generalist aphid species, *M. persicae*, compared colonies that were reared in parallel for 1 year on *Brassica rapa* or *Nicotiana benthamiana*, the enrichment of differentially expressed genes from the P450 and UDPGT families responding to host changes (Mathers et al., 2017). This has a striking similarity to our research.

Odorant-binding proteins and CSPs play essential roles in chemical communication and host plant selection of insects (Xu et al., 2009). The modules related to host selection identified in *B. tabaci* contain several OBPs and CSPs genes. It was reported that CSP2 in *B. tabaci* can bind the plant volatiles homoterpene (E)-3,8-dimethyl-1,4,7-non-atriene (DMNT) and its analogs, which can inhibit host selection and oviposition of whitefly (Li et al., 2020). The OBP1, OBP3, and OBP4 can recognize β-ionone, a plant volatile that can inhibit the oviposition behavior of *B. tabaci* (Li et al., 2019; Wang et al., 2019). In addition, OBP2 and OBP6 were highly expressed in the heads of *B. tabaci* adults (Wang et al., 2017; Zeng et al., 2018), and in the WGCNA analysis results, OBP2 and OBP6 were identified in the midnight blue and turquoise modules, respectively. So these two OBP genes may also be involved in the identification of host plant volatiles.

Development-Related Modules Contain Multiple Genes Related to Chitin Formation

We identified two modules related to development of whitefly: black and red. In black and red modules, genes are highly expressed in nymphs. In the GO enrichment results, the *P*-values of chitin-based cuticle development (GO:0040003) and chitin-based embryonic cuticle biosynthetic process (GO:0008362) were 7.14E-19 and 7.17E-05, respectively. Insect growth and morphogenesis are strictly dependent on the ability to remodel chitin-containing structures (Merzendorfer and Zimoch, 2003). Chitin formation and degradation are essential for insect development. Not surprisingly, malfunction of chitin synthesis leads to developmental disorders that can be observed during embryogenesis. For example, in Drosophila, zygotic disruption of any one of the genes required for proper deposition and/or morphogenesis of the cuticle will result in embryonic mortality (Ostrowski et al., 2002). According to the results of WGCNA, we found co-expression modules related to whitefly development and determined the co-expressed genes related to development.

CONCLUSION

This study aimed to identify the host plant selection-related module and development-related module in the whitefly. Midnight blue, turquoise and magenta modules were related to host plant selection based on WGCNA analysis. Black and red modules were related to whitefly development. GO and KEGG analyses highlighted "Glycosphingolipid biosynthesis," "Lysosome," and "Protein processing in endoplasmic reticulum pathway," as key biological processes and metabolic pathways involved in host plant selection. The "chitin-based cuticle development" and "chitin-based embryonic cuticle biosynthetic process" were the key GO terms involved in whitefly development. This study provides a foundation for studies of the genes related to host plant selection and development in *B. tabaci*.

DATA AVAILABILITY STATEMENT

The original contributions presented in the study are included in the article/**Supplementary Material**; further inquiries can be directed to the corresponding author/s.

AUTHOR CONTRIBUTIONS

JT, SY, and FL designed the study. JT wrote the first draft of the manuscript and performed the interpretation of the results and wrote the final version of article in collaboration, which was critically revised by HZ, YD, BZ, CQ, CL, and SY. All authors approved the final version of the manuscript, and agreed to be accountable for all aspects of the work.

FUNDING

The authors thank the projects of Beijing Municipal Natural Science Foundation, grant number 6202005, and National Natural Science Foundation of China, grant numbers 31871972 and 31070338.

SUPPLEMENTARY MATERIAL

The Supplementary Material for this article can be found online at: https://www.frontiersin.org/articles/10.3389/fphys.2021.656649/full#supplementary-material

REFERENCES

Appelqvist, H., Wäster, P., Kågedal, K., and llinger, K. (2013). The lysosome: from waste bag to potential therapeutic target. *J. Mol. Cell Biol.* 5, 214–226. doi: 10.1093/jmcb/mjt022

Bayhan, E., Ulusoy, M. R., and Brown, J. K. (2006). Host range, distribution, and natural enemies of *Bemisia tabaci* 'B biotype' (Hemiptera: Aleyrodidae) in Turkey. *J. Pest Sci.* 79, 233–240. doi: 10.1007/s10340-006-0139-4

Bing, X. L., Yang, J., Zchori-Fein, E., Wang, X. W., and Liu, S. S. (2013). "Hemipteriphilus asiaticus, a newly-described whitefly symbiont," in *Proceedings of the 1st International Whitefly Symposium*, Kolymbari, 83.

Butler, G. D., and Henneberry, T. J. (1989). Migration, population increase and control of Sweetpotato whitefly with cotton seed oil sprays on lettuce. *Southwest. Entomol.* 14, 287–293.

Chen, Y., Singh, A., Kaithakottill, G. G., Mathers, T. C., Hogenhout, S. A., Gravino, M., et al. (2020). An aphid RNA transcript migrates systemically within plants and is a virulence factor. *Proc. Natl. Acad. Sci.* 117, 12763–12771.

Childs, K. L., Davidson, R. M., and Buell, C. R. (2011). Gene coexpression network analysis as a source of functional annotation for rice genes. *PLoS One* 6:e22196. doi: 10.1371/journal.pone.0022196

Costa, H. S., Brown, J. K., and Byrne, D. N. (1991). Hostplant selection by the whitefly, *Bemisia tabaci* (Genn.) (Homoptera:Aleyrodidae) under greenhouse conditions. *J. Appl. Entomol.* 112, 146–152. doi: 10.1111/j.1439-0418.1991.tb01040.x

De Barro, P. J., Liu, S.-S., Boykin, L. M., and Dinsdale, A. B. (2011). *Bemisia tabaci*: a statement of species status. *Annu. Rev. Entomol.* 56, 1–19. doi: 10.1146/annurev-ento-112408-085504

Elsey, K. D., and Farnham, M. W. (1994). Response of *Brassica oleracea* L. to *Bemisia tabaci* (Gennadius). *Hortscience* 29, 814–817.

Feyereisen, R. (1999). Insect P450 enzymes. *Annu. Rev. Entomol.* 44, 507–533. doi: 10.1146/annurev.ento.44.1.507

Guo, H., Zhang, Y., Tong, J., Ge, P., Wang, Q., Zhao, Z., et al. (2020). An aphid-secreted salivary protease activates plant defense in phloem. *Curr. Biol.* 30, 4826–4836.e7.

Heidel-Fischer, H. M., and Vogel, H. (2015). Molecular mechanisms of insect adaptation to plant secondary compounds. *Curr. Opin. Insect Sci.* 8, 8–14.

Huang, H.-J., Ye, Z.-X., Lu, G., Zhang, C.-X., Chen, J. P., and Li, J.-M. (2020). Identification of salivary proteins in the whitefly *Bemisia tabaci* by transcriptomic and LC–MS/MS analyses. *Insect Sci.* doi: 10.1111/1744-7917.12856

Johnson, M. W., Toscano, N. C., Reynolds, H. T., Sylvester, E. S., Kido, K., and Natwick, E. T. (1982). Whiteflies cause problems for southern California growers. *Calif. Agric.* 36, 24–26.

Koo, Y. D., Ahn, J. E., Salzman, R. A., Moon, J., Chi, Y. H., Yun, D. J., et al. (2008). Functional expression of an insect cathepsin B-like counter-defence protein. *Insect Mol. Biol.* 17, 235–245. doi: 10.1111/j.1365-2583.2008.00799.x

Kumar, R., Bhardwaj, U., Kumar, P., and Mazumdar-Leighton, S. (2015). Midgut serine proteases and alternative host plant utilization in *Pieris brassicae* L. *Front. Physiol.* 6:95. doi: 10.3389/fphys.2015.00095

Langfelder, P., and Horvath, S. (2008). WGCNA: an R package for weighted correlation network analysis. *BMC Bioinformatics* 9:559.

Li, F. Q., Dewer, Y., Li, D., Qu, C., and Luo, C. (2020). Functional and evolutionary characterization of chemosensory protein CSP2 in the whitefly, *Bemisia tabaci*. *Pest Manag. Sci.* 77, 378–388. doi: 10.1002/ps.6027

Li, F. Q., Li, D., Dewer, Y., Qu, C., Yang, Z., Tian, J. H., et al. (2019). Discrimination of oviposition deterrent volatile β-icconone by odorant-binding proteins 1 and 4 in the whitefly *Bemisia tabaci*. *Biomolecules* 9, 563. doi: 10.3390/biom9100563

Li, S.-J., Xue, X., Ahmed, M. Z., Ren, S.-X., Du, Y.-Z., Wu, J.-H., et al. (2011). Host plants and natural enemies of *Bemisia tabaci* (Hemiptera: Aleyrodidae) in China. *Insect Sci.* 18, 101–120. doi: 10.1111/j.1744-7917.2010.01395.x

Liang, Y. H., Cai, B., Chen, F., Wang, G., Wang, M., Zhong, Y., et al. (2014). Construction and validation of a gene co-expression network in grapevine (*Vitis vinifera*. L.). *Hortic. Res.* 1, 14040.

Liu, S.-S., Colvin, J., and De Barro, P. J. (2012). Species concepts as applied to the whitefly *Bemisia tabaci* systematics: how many species are there? *J. Integr. Agric.* 11, 176–186. doi: 10.1016/s2095-3119(12)60002-1

Liu, S. S., De Barro, P. J., Xu, J., Luan, J. B., Zang, L. S., Ruan, Y. M., et al. (2007). Asymmetric mating interactions drive widespread invasion and displacement in a whitefly. *Science* 318, 1769–1772. doi: 10.1126/science.1149887

Love, M. I., Huber, W., and Anders, S. (2014). Moderated estimation of fold change and dispersion for RNA-seq data with DESeq2. *Genome Biol.* 15:550.

Malka, O., Santos-Garcia, D., Feldmesser, E., Sharon, E., Krause-Sakate, R., Delatte, H., et al. (2018). Species-complex diversification and host-plant associations in *Bemisia tabaci*: A plant-defence, detoxification perspective revealed by RNA-Seq analyses. *Mol. Ecol.* 27, 4241–4256. doi: 10.1111/mec.14865

Mathers, T. C., Chen, Y., Kaithakottil, G., Legeai, F., Mugford, S. T., Baa-Puyoulet, P., et al. (2017). Erratum to: rapid transcriptional plasticity of duplicated gene clusters enables a clonally reproducing aphid to colonise diverse plant species. *Genome Biol.* 18:63.

Merzendorfer, H., and Zimoch, L. (2003). Chitin metabolism in insects: structure, function and regulation of chitin synthases and chitinases. *J. Exp. Biol.* 206, 4393–4412. doi: 10.1242/jeb.00709

Mound, L. A., and Halsey, S. H. (1978). *Whiteflies of the World*. London: British Museum of Natural History, 340.

Ostrowski, S., And, Dierick HA., and Bejsovec, A. (2002). Genetic control of cuticle formation during embrynic development of *Drosophila melanogaster*. *Genetics* 161, 171–182.

Pu, L., Wang, M., Li, K., Feng, T., Zheng, P., Li, S., et al. (2020). Identification micro-RNAs functional modules and genes of ischemic stroke based on weighted gene co-expression network analysis (WGCNA). *Genomics* 112, 2748–2754. doi: 10.1016/j.ygeno.2020.03.011

Saikia, M., Singh, Y. T., Bhattacharya, A., and Mazumdar-Leighton, S. (2011). Expression of diverse midgut serine proteinases in the sericigenous Lepidoptera *Antheraea assamensis* (Helfer) is influenced by choice of host plant species. *Insect Mol. Biol.* 20, 1–13. doi: 10.1111/j.1365-2583.2010.01048.x

Serbielle, C., Moreau, S., Veillard, F., Voldoire, E., Bézier, A., Mannucci, M. A., et al. (2009). Identification of parasite-responsive cysteine proteases in *Manduca sexta*. *Biol. Chem.* 390, 493–502.

Stuart, J. M., Segal, E., Koller, D., and Kim, S. K. (2003). A gene-coexpression network for global discovery of conserved genetic modules. *Science* 302, 249–255. doi: 10.1126/science.1087447

Tahmasebi, A., Ashrafi-Dehkordi, E., Shahriari, A. G., Mazloomi, S. M., and Ebrahimie, E. (2019). Integrative meta-analysis of transcriptomic responses to abiotic stress in cotton. *Prog. Biophys. Molecular Biology* 146, 112–122.

Wang, R., Hu, Y., Wei, P. L., Qu, C., and Luo, C. (2019). Molecular and functional characterization of one odorant-binding protein gene OBP3 in *Bemisia tabaci* (Hemiptera: Aleyrodidae). *J. Econ. Entomol.* 13, 299–305.

Wang, R., Li, F. Q., Zhang, W., Zhang, X., Qu, C., Tetreau, G., et al. (2017). Identification and expression profile analysis of odorant binding protein and chemosensory protein genes in *Bemisia tabaci* MED by head transcriptome. *PLoS One* 12:e0171739. doi: 10.1371/journal.pone.0171739

Xu, J., Lin, K. K., and Liu, S. S. (2011). Performance on different host plants of an alien and an indigenous *Bemisia tabaci* from China. *J. Appl. Entomol.* 135, 771–779. doi: 10.1111/j.1439-0418.2010.01581.x

Xu, Y. L., He, P., Zhang, L., Fang, S. Q., Dong, S. L., Zhang, Y. J., et al. (2009). Large-scale identification of odorant-binding proteins and chemosensory proteins from expressed sequence tags in insects. *BMC Genomics* 10:632. doi: 10.1186/1471-2164-10-632

Zeng, Y., Yang, Y. T., Wu, Q. J., Wang, S. L., Xie, W., and Zhang, Y. J. (2018). Genome-wide analysis of odorant-binding proteins and chemosensory

proteins in the sweet potato whitefly, *Bemisia tabaci*. *Insect Sci.* 26, 620–634.

Zhan, J., Thakare, D., Ma, C., Lloyd, A., Nixon, N. M., Arakaki, A. M., et al. (2015). RNA sequencing of laser-capture microdissected compartments of the maize Kernel identifies regulatory modules associated with endosperm cell differentiation. *Plant Cell* 27, 513–531. doi: 10.1105/tpc.114.135657

Zinkgraf, M., Liu, L., Groover, A., and Filkov, V. (2017). Identifying gene co-expression networks underlying the dynamic regulation of wood-forming tissues in Populus under diverse environmental conditions. *New Phytol.* 214, 1464–1478. doi: 10.1111/nph.14492

Conflict of Interest: The authors declare that the research was conducted in the absence of any commercial or financial relationships that could be construed as a potential conflict of interest.

Copyright © 2021 Tian, Zhan, Dewer, Zhang, Qu, Luo, Li and Yang. This is an open-access article distributed under the terms of the Creative Commons Attribution License (CC BY). The use, distribution or reproduction in other forums is permitted, provided the original author(s) and the copyright owner(s) are credited and that the original publication in this journal is cited, in accordance with accepted academic practice. No use, distribution or reproduction is permitted which does not comply with these terms.

frontiers in Physiology

ORIGINAL RESEARCH
published: 21 April 2021
doi: 10.3389/fphys.2021.662978

Plant Metabolites Drive Different Responses in Caterpillars of Two Closely Related *Helicoverpa* Species

Longlong Sun[1†], Wenhua Hou[1†], Jiajia Zhang[1], Yuli Dang[2], Qiuyun Yang[2], Xincheng Zhao[1], Ying Ma[2] and Qingbo Tang[1]**

[1] The Institute of Chemical Ecology and College of Plant Protection, Henan Agricultural University, Zhengzhou, China, [2] College of Agronomy, Henan Agricultural University, Zhengzhou, China

The host acceptances of insects can be determined largely by detecting plant metabolites using insect taste. In the present study, we investigated the gustatory sensitivity and feeding behaviors of two closely related caterpillars, the generalist *Helicoverpa armigera* (Hübner) and the specialist *H. assulta* (Guenée), to different plant metabolites by using the single sensillum recording technique and the dual-choice assay, aiming to explore the contribution of plant metabolites to the difference of diet breadth between the two species. The results depicted that the feeding patterns of caterpillars for both plant primary and secondary metabolites were significantly different between the two *Helicoverpa* species. Fructose, glucose, and proline stimulated feedings of the specialist *H. assulta*, while glucose and proline had no significant effect on the generalist *H. armigera*. Gossypol and tomatine, the secondary metabolites of host plants of the generalist *H. armigera*, elicited appetitive feedings of this insect species but drove aversive feedings of *H. assulta*. Nicotine and capsaicin elicited appetitive feedings of *H. assulta*, but drove aversive feedings of *H. armigera*. For the response of gustatory receptor neurons (GRNs) in the maxillary styloconic sensilla of caterpillars, each of the investigated primary metabolites induced similar responding patterns between the two *Helicoverpa* species. However, four secondary metabolites elicited different responding patterns of GRNs in the two species, which is consistent with the difference of feeding preferences to these compounds. In summary, our results of caterpillars' performance to the plant metabolites could reflect the difference of diet breadth between the two *Helicoverpa* species. To our knowledge, this is the first report showing that plant secondary metabolites could drive appetitive feedings in a generalist insect species, which gives new insights of underscoring the adaptation mechanism of herbivores to host plants.

Keywords: ***Helicoverpa armigera***, ***Helicoverpa assulta***, **plant primary metabolites, plant secondary metabolites, feeding preference, electrophysiological response, gustatory receptor neurons**

OPEN ACCESS

Edited by:
Peng He,
Guizhou University, China

Reviewed by:
Ya-Nan Zhang,
Huaibei Normal University, China
Roberto Massimo Crnjar,
University of Cagliari, Italy

***Correspondence:**
Ying Ma
maying999@126.com
Qingbo Tang
qingbotang@126.com;
qbtang@henau.edu.cn

† These authors have contributed equally to this work

Specialty section:
This article was submitted to Invertebrate Physiology, a section of the journal Frontiers in Physiology

Received: *02 February 2021*
Accepted: *16 March 2021*
Published: *21 April 2021*

Citation:
Sun L, Hou W, Zhang J, Dang Y, Yang Q, Zhao X, Ma Y and Tang Q (2021) Plant Metabolites Drive Different Responses in Caterpillars of Two Closely Related Helicoverpa Species. Front. Physiol. 12:662978. doi: 10.3389/fphys.2021.662978

INTRODUCTION

The herbivorous insects use a variety of physiological mechanisms including pre-ingestive responses (i.e., chemosensory) (Bernays et al., 2000a; Glendinning, 2002), the post-ingestive response (Montandon et al., 1987; Behmer et al., 1999; Wright et al., 2010; Simões et al., 2012), and the detoxification processes (Mao et al., 2007; Tao et al., 2012; Bretschneider et al., 2016;

Krempl et al., 2016; Tian et al., 2019) to cope with the plant metabolites, including primary and secondary metabolites. It is also accepted that herbivorous insects with different diet breadths have different capacities to discriminate these metabolites and extend to their decisions in host acceptance (Bernays et al., 2000b; Govind et al., 2010; Ahn et al., 2011; Liu et al., 2012; Kumar et al., 2014; Wang et al., 2017; Zhu et al., 2020). For example, the specialist herbivores were frequently reported to have more ability to metabolize or utilize the secondary metabolites than the generalists (Bernays et al., 2000b; Govind et al., 2010; Ahn et al., 2011; Liu et al., 2012; Kumar et al., 2014; Sun et al., 2019). Some specialists even detect the secondary metabolites as "token stimuli" for recognizing the specific host plant by using their chemoreceptors (Jermy, 1966; Schoonhoven, 1967; Renwick and Lopez, 1999; del Campo et al., 2001; Vickerman and de Boer, 2002; Miles et al., 2005). However, little attention has been paid in understanding whether the generalist herbivorous insects could recognize the plant metabolites from their hosts as "token' timuli."

The dietary acceptance and host range of caterpillars might relate to the spectrum of the sensitivity of gustatory receptor neurons (GRNs) in the galeal styloconic sensilla to the plant metabolites (Jermy, 1966; Thompson, 1991; Bernays et al., 2000b; Wada-Katsumata et al., 2013; Sollai and Crnjar, 2019). Therefore, comparing feeding behaviors and taste responses between closely related species with different host ranges could contribute to understanding the host acceptability, diet breadth, and evolution of host adaptation (Sheck and Gould, 1996; Bernays et al., 2000b; Renwick, 2001; Liu et al., 2012; Sollai et al., 2014). The cotton bollworm *Helicoverpa armigera* (Hübner) (Lepidoptera: Noctuidae) and the tobacco budworm *Helicoverpa assulta* (Guenée) (Lepidoptera: Noctuidae) are two sympatric closely related herbivorous species. The former is an extreme generalist feeding on at least 161 host plant species in 49 plant families, including cotton, tomato, and tobacco (Zalucki et al., 1986; Fitt, 1989), whereas the latter is a specialist insect species feeding on the Solanaceae and several *Physalis* species, tobacco, and hot pepper on the natural field (Mitter et al., 1993). The two species could be hybridized to produce viable offspring under laboratory conditions (Wang and Dong, 2001) and are good models to investigate the interaction between plants and herbivorous insects (Tang et al., 2006, 2014; Ahn et al., 2011; Liu et al., 2012; Yang et al., 2017; Zhu et al., 2020).

In this study, we investigated the feeding preferences and the gustatory responses of caterpillars of the two *Helicoverpa* species to three plant primary metabolites, including fructose, glucose, and proline, and four plant secondary metabolites including gossypol, tomatine, nicotine, and capsaicin (**Table 1**). Fructose, glucose, and proline have been well known to be the energy source and phagostimulants for herbivorous insects (Albert et al., 1982; Bernays and Chapman, 2001; Liscia et al., 2004; Jiang et al., 2015; Mang et al., 2016). Gossypol and tomatine are plant secondary metabolites of cotton (Oliver et al., 1970; Montandon et al., 1987) and tomato, respectively (Barbour and Kennedy, 1991). Nicotine and capsaicin are plant secondary metabolites of tobacco and pepper, respectively (Pearson et al., 2019). Finally, we attempt to understand whether behavioral responses of two *Helicoverpa* species toward these plant metabolites corresponded with the diet breadth or not.

TABLE 1 | The investigated plant metabolites and the corresponding host plants of the two Helicoverpa species.

Species	Host plant	Secondary metabolites
H. armigera	Cotton	Gossypol
	Tomato	Tomatine
	Tobacco	Nicotine
	Hot pepper	Capsaicin
H. assulta	Tobacco	Nicotine
	Hot pepper	Capsaicin

MATERIALS AND METHODS

Insect Culture

All colonies of the *Helicoverpa* caterpillars were maintained in the laboratory at 75% ± 5% relative humidity and temperature (27 ± 1°C) under a controlled photoperiod (L16:D8). Both larvae of *H. armigera* and *H. assulta* were obtained from established laboratory colonies, which were reared on an artificial diet prepared from the following ingredients: wheat bran (150 g), soybean powder (80 g), yeast powder (25 g), casein (40 g), sorbic acid (3 g), ascorbic acid (3 g), sucrose (10 g), agar (20 g), vitamin composite powders (8 g), acetic acid (4 ml), and distilled water (1,500 ml) (Wu et al., 1990; Wu and Gong, 1997; Jiang et al., 2010). Adults were supplied with a 10% v/v solution of sucrose in water.

Compounds

D-(-)-Fructose (Cas:57-48-7), D-(+)-glucose (Cas:50-99-7), L-proline (Cas:147-85-3), gossypol (Cas:303-45-7), capsaicin (Cas:2444-86-4), and tomatine (Cas:17406-45-0) were obtained from Beijing Solarbio Science & Technology Co., Ltd. Nicotine (Cas:54-11-5) was from Alfa Aesar. Ethanol absolute (Cas:64-17-5) and methanol (Cas:67-56-1) were from Tianjin De-En Chemical Reagent Co., Ltd. PVP (Cas:9003-39-8) was obtained from Tianjin Guangfu Fine Chemical Research Institute.

Feeding Choice Assay

The dual-choice plant leaf disc bioassay was used to test the feeding preference of 5th instar larvae of the two *Helicoverpa* species as described by Wang et al. (2017). In general, leaf discs (10 mm diameter, about 156 mm^2) were punched from fresh leaves of pepper *Capsicum frutescens* L., "Yu-Yi" (Solanaceae), which then were immersed in control or treatment solutions for 30 min. The plant primary metabolites D-fructose (1.0, 10, 30, 50 mM), D-glucose (1.0, 10, 30, 50 mM), and L-proline (0.1, 1.0, 10, 50 mM) were dissolved in water. The plant secondary metabolites gossypol, tomatine, and capsaicin were dissolved in solvent I (0.25% methanol, 5% ethanol, and 0.32% polyvinylpyrrolidone (PVP) in water) at 0.001, 0.01, 0.1, and 1.0 mM. Nicotine was dissolved in solvent II (0.16% PVP in

water) at the concentrations of 0.001 mM, 0.01 mM, 0.1 mM, and 1.0 mM. The solvents were used as control.

Before the test, the fifth-instar caterpillars had been starved for about 8 h. A single caterpillar was placed in the center of a Petri dish (12 cm diameter) with a moist filter paper (Φ11 cm, Jiaojie®, China). Four solvent-treated leaf discs and four plant metabolite-treated leaf discs were arranged in an ABABABAB fashion around the dish. All Petri dishes were put under evenly distributed LED strip lights (8,000 Lm) at a temperature of 27 ± 1°C. Areas of all remnants of leaf discs were measured by using a transparency film (PP2910, 3M Corp.) when two of the four disks of either plant (A or B) had been consumed. Each caterpillar was tested only once. For the feeding preference assays, at least 90 replicates were conducted.

The feeding preference index was calculated as follows:

Preference index for control leaves (Pc) = area of control-disc consumed/(area of control-disc consumed + area of treatment-disc consumed)

Preference index for treatment leaves (Pt) = area of treatment-disc consumed/(area of control-disc consumed + area of treatment-disc consumed)

Electrophysiological Recordings

The electrophysiological sensitivity of gustatory neurons in the styloconic sensilla on the maxillary galea of caterpillars to the plant metabolites was investigated using the single sensillum recording technique (van Loon, 1990; Roessingh et al., 1999). In

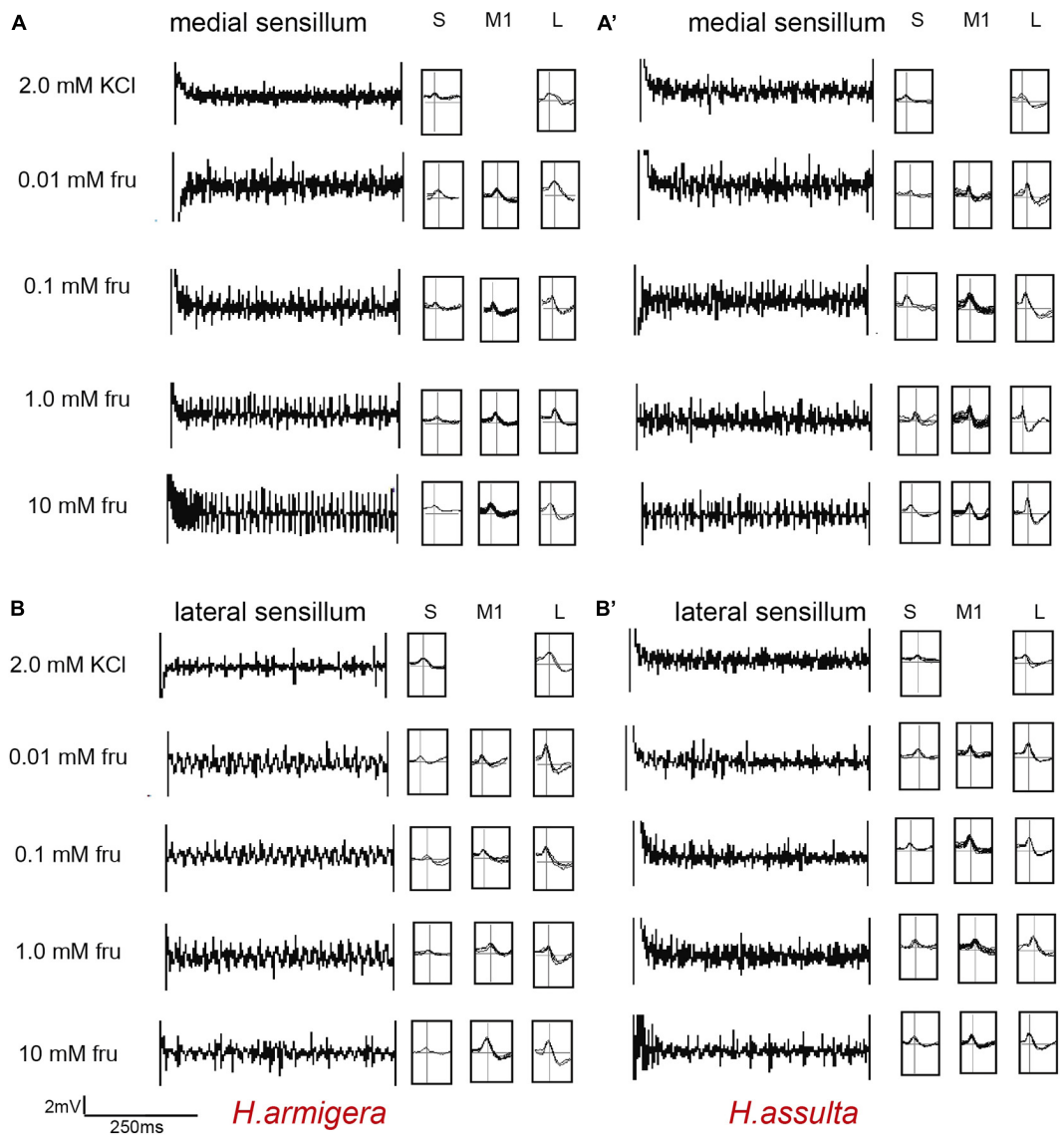

FIGURE 1 | Representative traces and indentified GRNs from responses of the medial and lateral sensilla of *Helicoverpa* caterpillars to fructose. "S," "M1," and "L" in *H. armigera* **(A,A')** and *H. assulta* **(B,B')** represent the identified GRNs from recording traces based on the analysis of AutoSpike software. The time duration of each trace is 500 ms.

brief, a head of an excised 5th instar caterpillar was mounted on a silver wire electrode which was connected to the input of a pre-amplifier (Syntech Taste Probe DTP-1, Hilversum, The Netherlands). The lateral or medial styloconic sensillum was recorded for the sensitivity to a stimulus at different concentrations. D-fructose, D-glucose, and L-proline were used as stimuli of primary metabolites with concentrations varying from 0.01, 0.1, 1.0 to 10 mM in 2 mM KCl. The previous work has shown that 2 mM KCl was an adequate electrolyte solvent for *Helicoverpa* caterpillars (Tang et al., 2015; Ma et al., 2016). The concentrations of gossypol, capsaicin, tomatine, and nicotine were from 0.001, 0.01, 0.1 to 1.0 mM. The first three stimuli were dissolved in solvent I, and nicotine was in solvent II. Both solvents for electrophysiological tests consist of 2 mM KCl. In case of synergistic interactions of mixed metabolites to GRNs, only a single sensillum in one caterpillar was tested for the responses to one kind of stimulus from low to high concentration. The electrolyte solvent was also tested as the control. For a single test, a glass microelectrode (tip diameter *ca.* 30 μm) filled with a stimulating solution was moved to contact with the tip of the lateral or medial sensillum with the aid of a micro-manipulator. The duration of a single stimulation was 2 s with a time interval of at least 3 min. Amplified signals were digitized by an A/D interface (IDAC-4, Syntech) and sampled into a personal

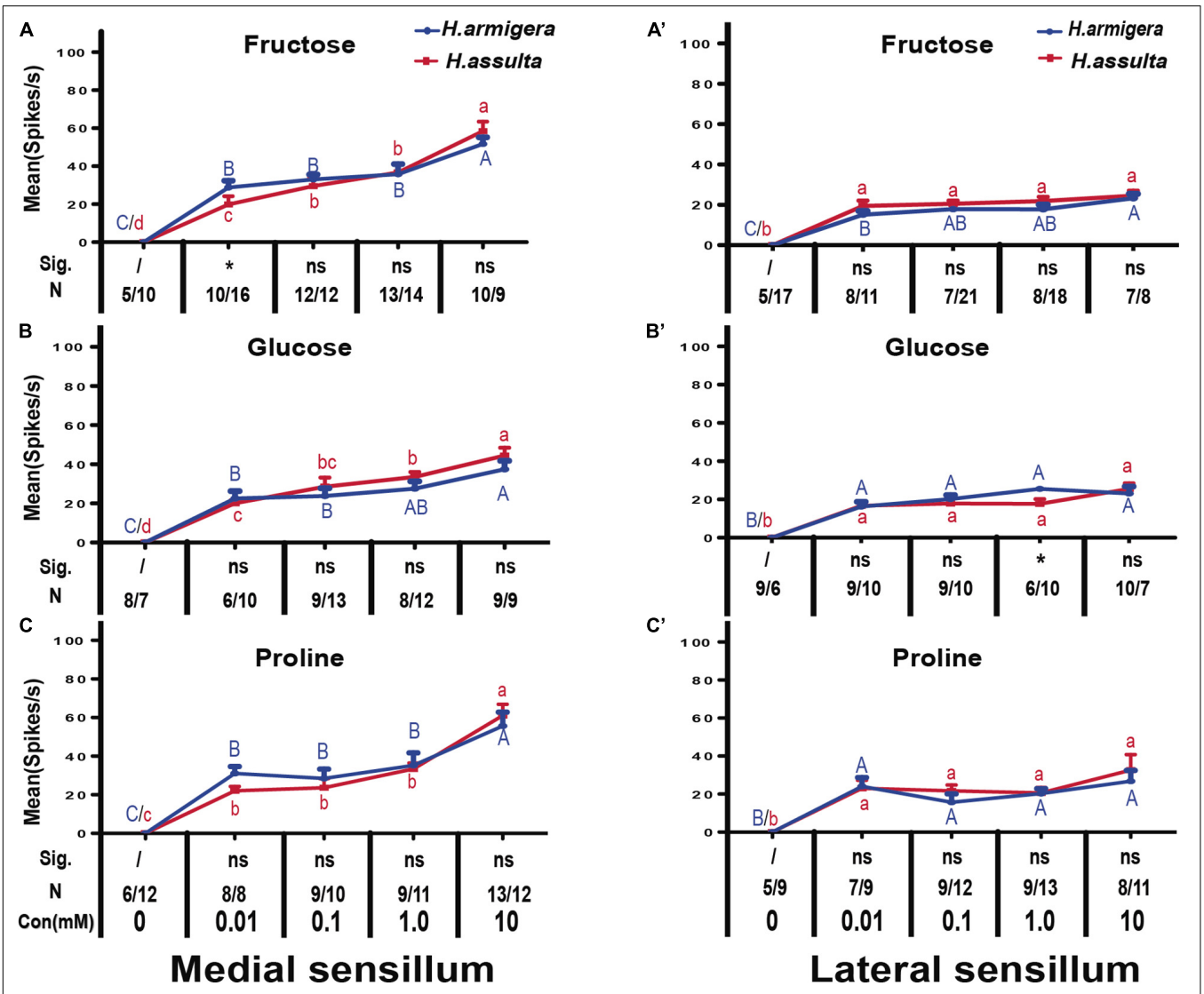

FIGURE 2 | Comparisons of gustatory responses of "M1" GNRs in styloconic sensilla of *Helicoverpa* caterpillars to plant primary metabolites. Curves show the mean responding frequency ± SE of "M1" GNRs in the medial sensillum **(A–C)** and in the lateral sensillum **(A'–C')** of *Helicoverpa* caterpillars to plant primary metabolites from 0.01 to 10 mM. Different capital letters and lowercase letters represent the mean responding frequencies of "M1" GNRs were significantly different in response to one primary metabolite at different concentrations in caterpillars of *H. armigera* and *H. assulta*, respectively (*post-hoc* SNK test of ANOVA: $P < 0.05$). Independent *t*-test was used to compare the difference of the mean responding frequency of "M1" GNRs to the same compound at the same concentration between the two *Helicoverpa* species. "Sig." represents the levels of difference. "ns": no significant different ($P > 0.05$); "*" represents the difference was significant at the 0.05 level. "N" represents the number of tested caterpillars of *H. armigera*/*H. assulta*.

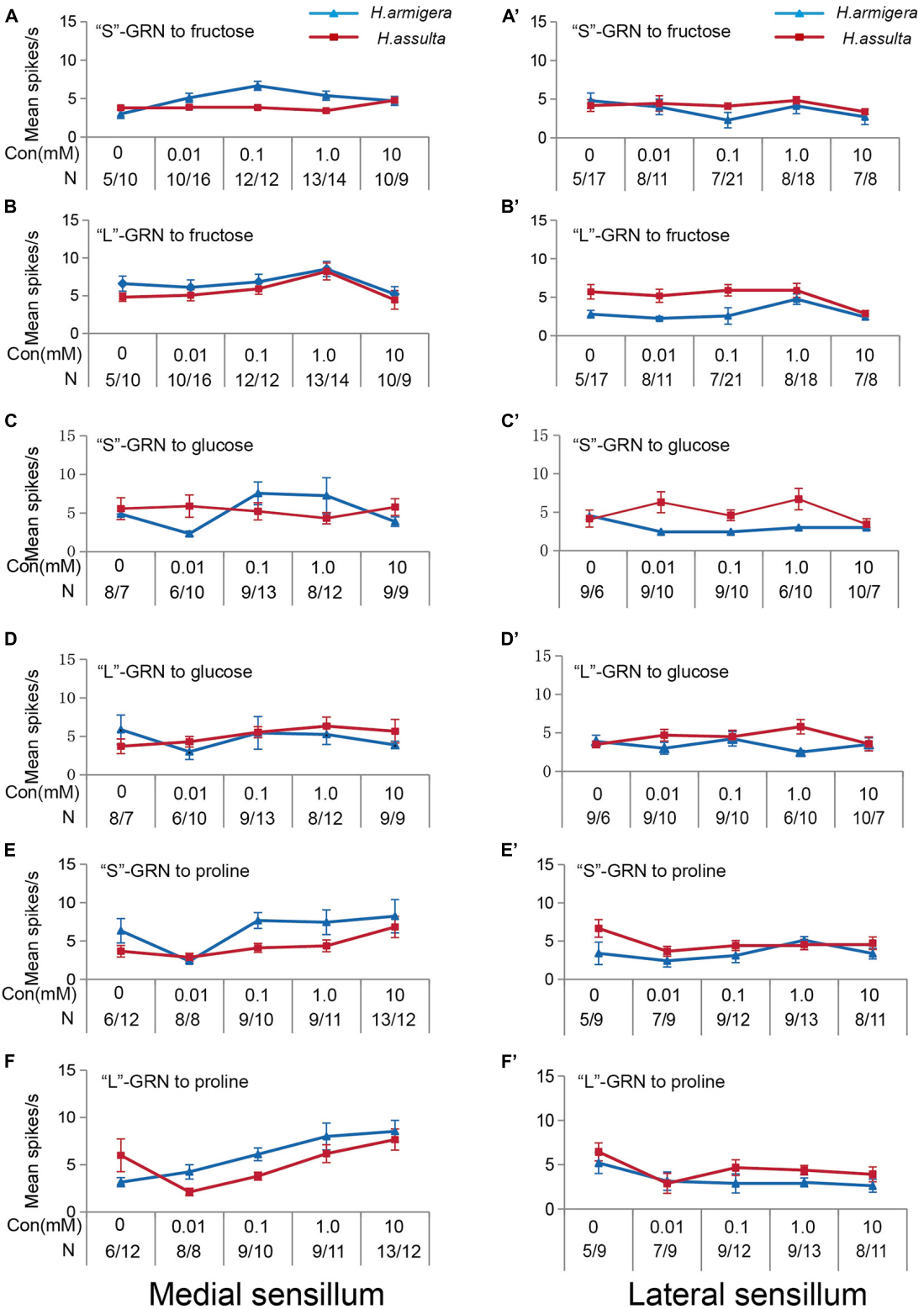

FIGURE 3 | Responses of "S" and "L" GRNs in the styloconic sensilla of *Helicoverpa* caterpillars to the three primary metabolites. **(A,C,E)**: responses of the indentified "S" GRNs from the medial sensillum to fructose, glucose, and proline, respectively; **(B,D,F)**: responses of the indentified "L" GRNs from the medial sensillum to fructose, glucose, and proline, respectively; **(A',C',E')**: responses of the indentified "S" GRNs from the lateral sensillum to fructose, glucose, and proline, respectively; **(B',D',F')**: responses of the indentified "L" GRNs in the lateral sensillum to fructose, glucose, and proline, respectively.

computer. For each given concentration of a stimulus, the electrophysiological responses of at least 10 larvae were recorded.

The analysis of electrophysiological responses of styloconic sensilla to different stimuli was performed with the aid of AutoSpike v. 3.7 software (Syntech, Hilversum, The Netherlands). Briefly, in the case of the identification of GRNs, by measuring the amplitude, shape, and phasic temporal pattern, three impulse spikes were generally identified and labeled as small (S), intermediate (M), and large (L), which best responded to water, metabolites, and salt, respectively (Sollai et al., 2014; Ma et al., 2016). For distinguishing M-type spikes induced by primary metabolites and secondary metabolites, the intermediate

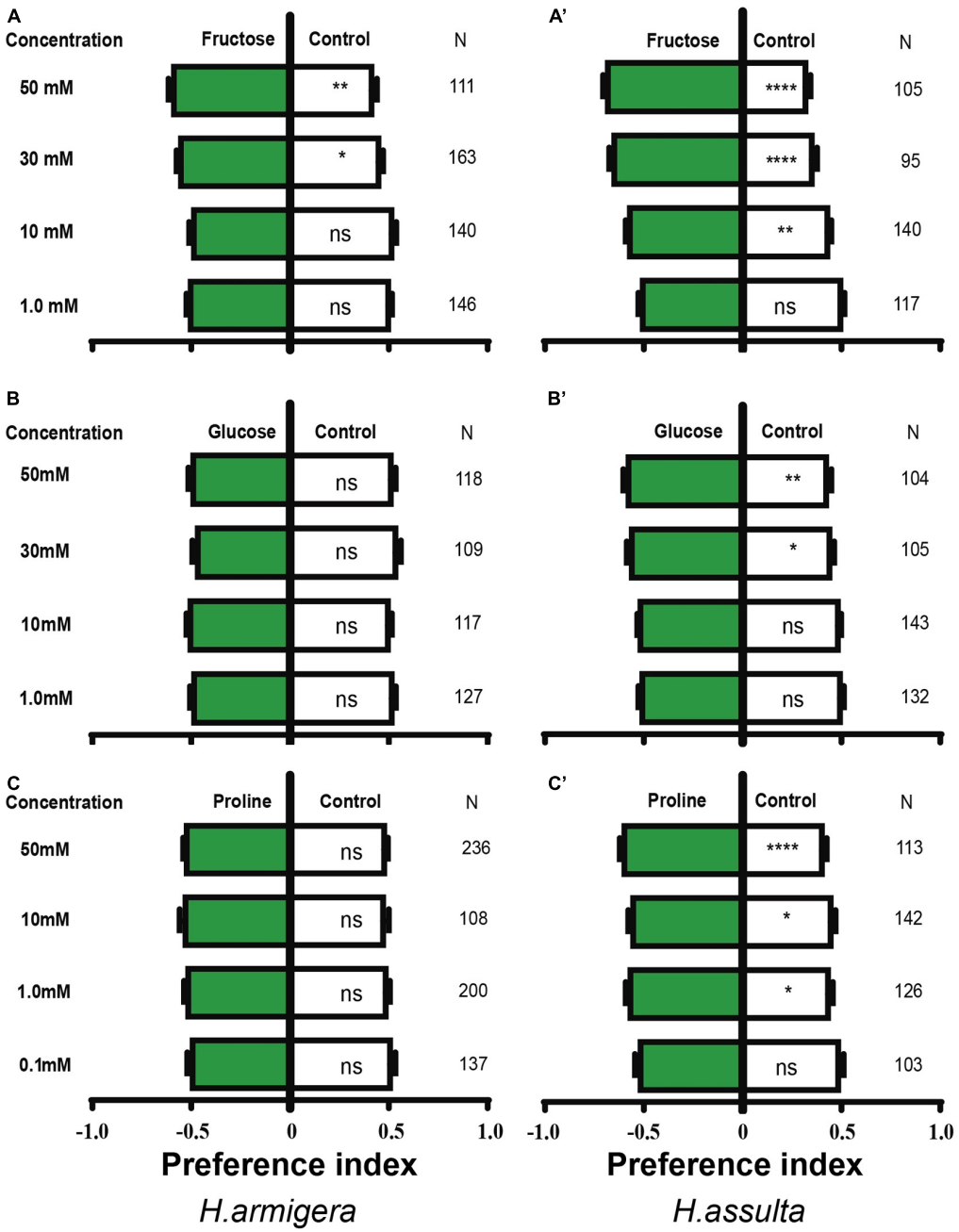

FIGURE 4 | Effects of three primary metabolites on the feeding preferences of *Helicoverpa* caterpillars. The preference indexes of caterpillars for primary metabolites (green bars) and for control leaves (white bar) were compared. The dual-choice assay was used to test the feeding preference for control and pepper leaves treated by primary metabolites and water, respectively. **(A–C)**: *H. armigera* caterpillars; **(A'–C')**: *H. assulta* caterpillars. A paired-sample *t*-test was used to compare the means of the preference indices between treatment and control. "*," "**," and "****" represent that the difference was significant at 0.05, 0.01, and 0.0001 levels, respectively. NS: non-significant difference. N: the number of tested caterpillars.

1 (M1) and intermediate 2 (M2) were assigned based on the spike amplitudes, correspondingly. The mean impulse frequency of each GRN in the first second (spk.s^{-1}) was calculated.

Statistical Analysis

For the comparison of feeding preferences of caterpillars between control and treatment, the value of the preference index was arcsine transformed and then subjected to the paired-sample *t*-test ($P < 0.05$).

All the values of the impulse frequency (spk.s^{-1}) were square-root transformed before analysis. One-way ANOVA followed by the Student–Newman–Keuls (SNK) *post-hoc* test ($P < 0.05$) was used to compare the difference of the firing frequency of one type of GNR to one stimulus at different concentrations. The independent *t*-test was used to compare the mean impulse frequency of the same type of GRN between species. Finally, the GLM-Univariate was used to analyze the order of the mean impulse frequency of one type of GRNs to different compounds within species followed by the SNK *post-hoc* test for multiple comparisons ($P < 0.05$). All data were analyzed using SPSS software version 16.0.

RESULTS

Electrophysiological Responses to Primary Metabolites

In most recordings, three types of GRNs were identified from both medial and lateral sensilla of two *Helicoverpa* species in response to three plant primary metabolites, labeled as the "S" GRNs, "M1" GRNs, and "L" GRNs which best responded to water, primary metabolites, and salt, respectively (e.g., see identified representative GRNs in **Figure 1**). In the medial sensillum, the responses of "M1" GRNs of *H. armigera* caterpillars to each

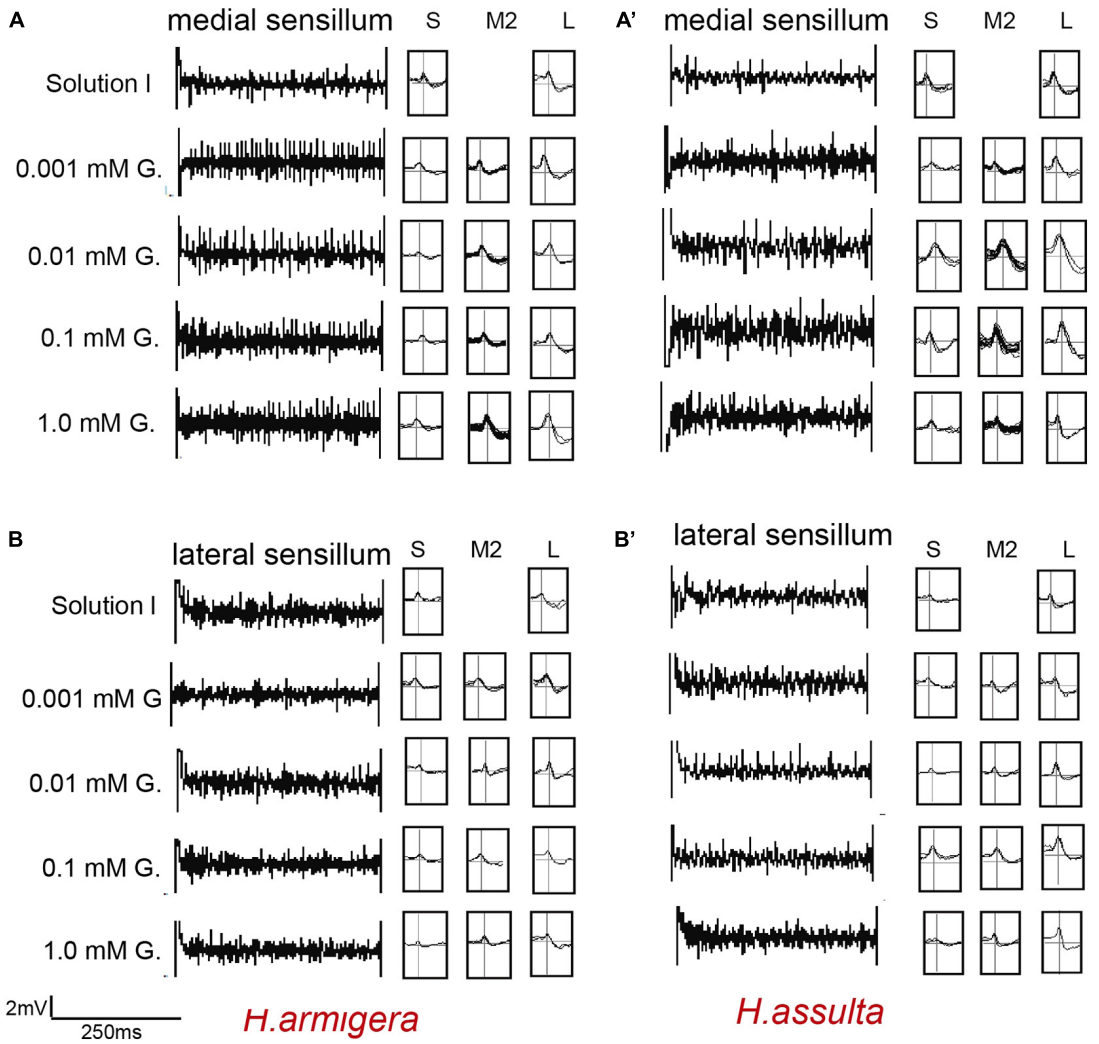

FIGURE 5 | Representative traces and indentified GRNs from the responses of the styloconic sensilla of *Helicoverpa* caterpillars to gossypol. "S," "M2," and "L" GRNs in *H. armigera* **(A,B)** and *H. assulta* **(A',B')** represent the identified GRNs from recording traces based on the analysis of AutoSpike software. G: gossypol. The time duration of each trace is 500 ms.

primary metabolite increased with the concentration increasing from 0, 0.01 mM, 0.1 mM, 1.0 mM to 10 mM [**Figure 2A**, one-way ANOVA of fructose: $F_{(4,45)} = 37.393$, $P < 0.0001$; **Figure 2B**, glucose: $F_{(4,35)} = 51.272$, $P < 0.0001$; **Figure 2C**, proline: $F_{(4,40)} = 29.965$, $P < 0.0001$]. The mean response frequencies of "M1" GRNs of *H. armigera* induced by 10 mM fructose, 10 mM glucose, and 10 mM proline were 51.70 ± 3.490 spk.s^{-1}, 37.44 ± 4.378 spk.s^{-1}, and 55.62 ± 7.161 spk.s^{-1}, respectively.

Similarly, "M1" GRNs in the medial sensillum of *H. assulta* also showed increasing responses to each primary metabolite with increasing concentrations [*H. assulta* in **Figure 2A'**; one-way ANOVA of fructose: $F_{(4,56)} = 99567$, $P < 0.0001$; **Figure 2B'**, glucose: $F_{(4,46)} = 55.164$, $P < 0.0001$; **Figure 2C'**, proline: $F_{(4,48)} = 93.889$, $P < 0.0001$]. The mean response frequency of "M1" GRNs in the medial sensillum of *H. assulta* to 10 mM fructose, 10 mM glucose, and 10 mM proline were 58.44 ± 5.430 spk.s^{-1}, 44.44 ± 4.045 spk.s^{-1}, and 61.0 ± 6.881 spk.s^{-1}, respectively. The responses of "M1" GRNs in the medial sensillum to one stimulus with the same concentration were always not significantly different between the two *Helicoverpa* species (**Figures 2A–C**, all comparisons: $P > 0.05$) except fructose at 0.01 mM which induced a significantly higher response of "M1" GRNs in *H. armigera* than that in *H. assulta* (**Figure 2A**, independent-sample *t*-test: df = 24, $t = 2.411$, $P = 0.024$). In the lateral sensillum, in contrast, the responses of "M1" GRNs to the three primary metabolites were low and the responses were similar between caterpillars of the two species (**Figures 2A'–C'**).

We also compared the general responding patterns of "M1" GRNs in one sensillum within the same species to the three primary metabolites using the GLM-Univariate with compounds and concentration as the fixed factors. It shows that the responses of "M1" GRNs in the medial sensillum of *H. armigera* caterpillars to the three compounds were significantly affected by both compounds and concentration (GLM-Univariate: compounds, df = 2, $F = 4.199$, $P = 0.017$; concentration, df = 4, $F = 107.877$, $P < 0.0001$). Analysis of the SNK *post-hoc* test showed that the responses of "M1" GRNs in the medial sensillum of *H. armigera* to glucose were significantly lower than those to fructose and proline (SNK *post-hoc* test: $P < 0.05$). However, for *H. assulta* caterpillars, the responses of "M1" GRNs in medial sensillum of *H. assulta* to the three compounds were not significantly affected by compound (GLM-Univariate: compounds, df = 2, $F = 1.040$, $P = 0.356$; concentration, df = 4, $F = 234.979$, $P < 0.0001$). Similarly, the responses of "M1" GRNs in lateral sensillum in both *Helicoverpa* species to the three compounds were also not significantly affected by compounds but affected significantly by concentrations (GLM-Univariate of *H. armigera*: compounds, df = 2, $F = 0.563$, $P = 0.571$; concentration, df = 4, $F = 88.709$, $P < 0.0001$; GLM-Univariate of *H. assulta*: compounds, df = 2, $F = 1.630$, $P = 0.199$; concentration, df = 4, $F = 22.90$, $P < 0.0001$).

The three primary metabolites also induced responses of "S" GRNs and "L" GRNs in both sensilla of the two *Helicoverpa* species. While the responses of the two types of GRNs to each compound were low with a non-significant change among different concentrations (SNK test after ANOVA for each compound: $P > 0.05$) (**Figure 3**).

Feeding Preferences for Primary Metabolites

The high concentration of fructose drove obvious appetitive feedings of both *H. armigera* caterpillars [**Figure 4A**; paired-sample *t*-test: 30 mM, $t(162) = -1.999$, $P = 0.047$; 50 mM, $t(110) = -2.88$, $P = 0.005$] and *H. assulta* caterpillars [**Figure 4A'**; paired-sample *t*-test: 10 mM, $t(139) = -3.329$, $P = 0.002$; 30 mM, $t(94) = -5.704$, $P < 0.0001$; 50 mM, $t(104) = -7.116$, $P < 0.0001$]. However, glucose showed no obvious effect on the feeding of *H. armigera* at the given concentrations [**Figure 4B**; paired-sample *t*-test: 1 mM, $t(126) = 0.700$, $P = 0.485$; 10 mM, $t(116) = -0.218$, $P = 0.828$; 30 mM, $t(108) = 1.358$, $P = 0.177$; 50 mM, $t(117) = 0.522$, $P = 0.602$], while it drove appetitive feedings of *H. assulta* caterpillars at high concentrations [**Figure 4B'**; paired-sample *t*-test: 30 mM, $t(104) = -2.308$, $P = 0.023$; 50 mM, $t(103) = -2.865$, $P = 0.004$].

Similarly, proline had no significant effect on the feeding of *H. armigera* caterpillars [**Figure 4C**; paired-sample *t*-test: 0.1 mM, $t(136) = 0.400$, $P = 0.690$; 1.0 mM, $t(199) = -0.803$,

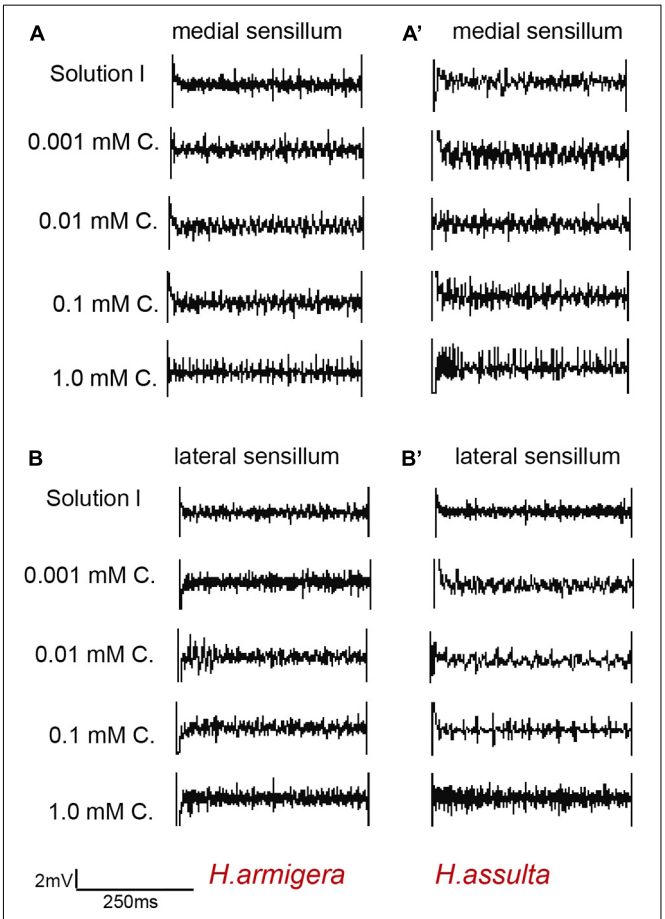

FIGURE 6 | Representative traces from responses of the styloconic sensillum of *Helicoverpa* caterpillars to capsaicin. **(A,A')**: medial sensillum of *H. armigera* and *H. assulta* to capsaicin, respectively; **(B,B')**: lateral sensillum of *H. armigera* and *H. assulta* to capsaicin, respectively. C: capsaicin. The time duration of each trace is 500 ms.

P = 0.423; 10 mM, $t(107)$ = −1.020, P = 0.310; 50 mM, $t(235)$ = −1.223, P = 0.223], while feeding preferences of *H. assulta* were significantly elicited at 1.0, 10, and 50 mM [**Figure 4C'**; paired-sample t-test: 1.0 mM, $t(125)$ = −2.541, P = 0.012; 10 mM, $t(141)$ = −2.252, P = 0.026; 50 mM, $t(112)$ = −4.276, $P < 0.0001$].

Electrophysiological Responses to Secondary Metabolites

The four investigated plant secondary metabolites induced high responses of the medial sensillum (e.g., see representative traces in **Figures 5A,A'**, **6A,A'**) compared to the relatively low responses of the lateral sensillum of the two *Helicoverpa* species (e.g., see traces in **Figures 5B,B'**, **6B,B'**). Three types of GRNs, in most traces, were identified in the responses of both sensilla to the four compounds, including the "S" GRNs, the "M2" GRNs, and the "L" GRNs, which best responded to water, the secondary metabolites, and salt, respectively (e.g., see representative identified GRNs in **Figure 5**).

In general, the responses of "M2" GRNs in both sensilla of the two *Helicoverpa* species induced by four secondary metabolites were high, while the responses of "S" GRNs and "L" GRNs in both sensilla induced by four secondary metabolites were relatively

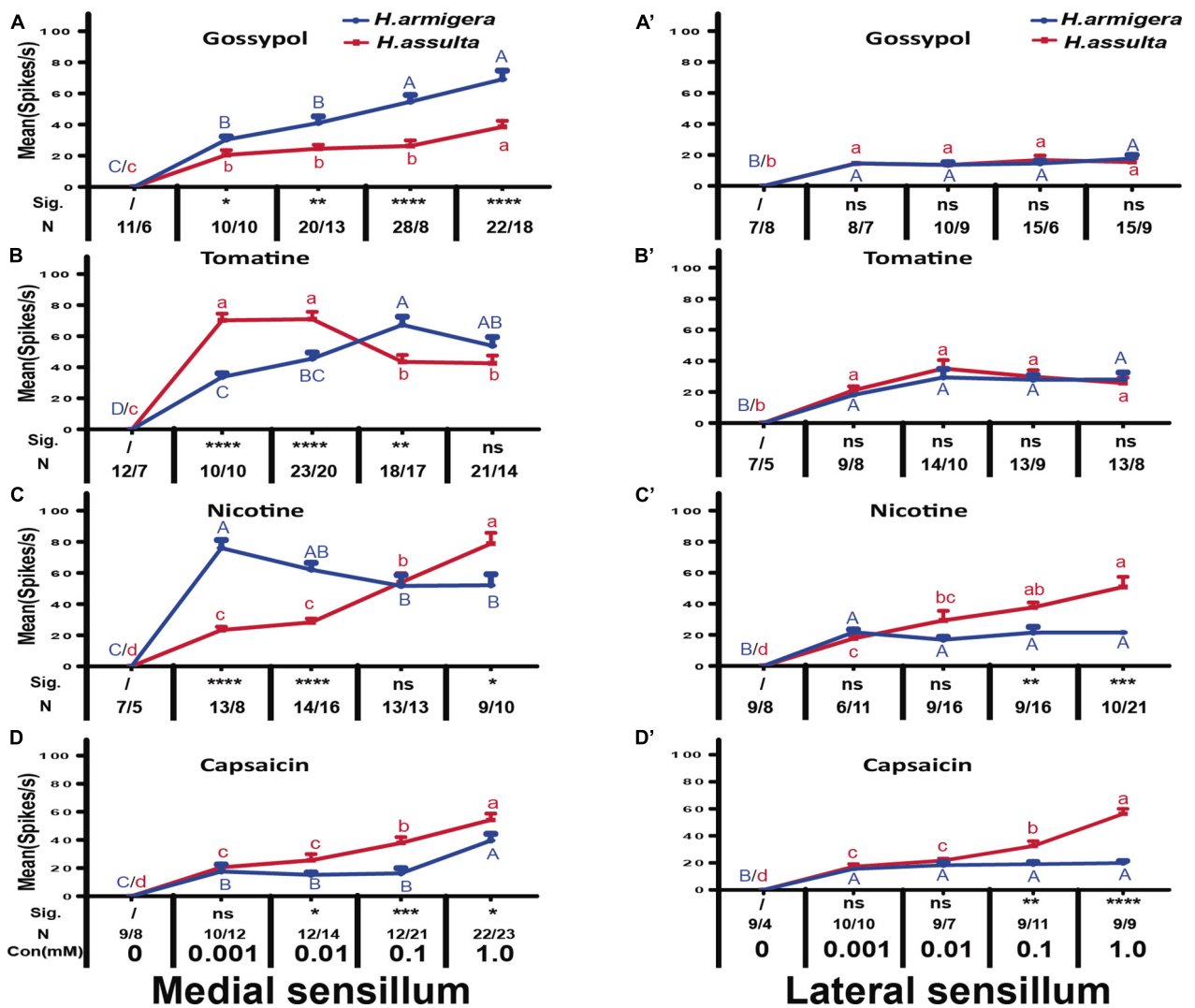

FIGURE 7 | Comparisons of gustatory responses of "M2" GNRs in styloconic sensilla of *Helicoverpa* caterpillars to different plant secondary metabolites. Curves show the mean responding frequency ± SE of "M2" GNRs in the medial sensillum **(A–D)** and in the lateral sensillum **(A'–D')** of *H. armigera* and *H. assulta* caterpillars to secondary metabolites from 0.001 to 1.0 mM. Different capital letters and lowercase letters represent the mean responding frequencies of "M2" GNRs which were significantly different in response to one compound at different concentrations in caterpillars of *H. armigera* and *H. assulta*, respectively (*post-hoc* SNK test of ANOVA: $P < 0.05$). Independent t-test was used to compare the difference of the mean responding frequency of "M2" GNRs to the same compound at the same concentration between the two Helicoverpa species. "Sig." represents the levels of difference. "ns": no significant different ($P > 0.05$); "*," "**," "***," and "****" represent that the difference was significant at the 0.05, 0.01, 0.001, and 0.0001 levels, respectively. "N" represents the number of tested caterpillars of *H. armigera*/*H. assulta*.

low. The responses of "M2" GRNs in the medial sensillum to each of the four plant secondary metabolites were different between the two species. Gossypol induced higher levels of response of "M2" GRNs in medial sensillum of *H. armigera* caterpillars than that of *H. assulta* (**Figure 7A**, independent-sample *t*-test of 0.001 mM: df = 18, $t = 2.79$, $P = 0.0121$; 0.01 mM: df = 31, $t = 3.19$, $P = 0.0033$; 0.1 mM: df = 34, $t = 3.70$, $P = 0.0001$; 1.0 mM: df = 38, $t = 4.45$, $P = 0.0001$). Tomatine at 0.001 mM and 0.01 mM induced lower responses of "M2" GRNs in *H. armigera* than those in *H. assulta* caterpillars (**Figure 7B**, independent-sample *t*-test of 0.001 mM: df = 18, $t = -7.65$, $P < 0.0001$; 0.01 mM: df = 41, $t = -4.06$, $P = 0.0002$) but elicited higher levels of response at high concentration in *H. armigera* than that of *H. assulta* (**Figure 7B**, independent-sample *t*-test of 0.1 mM: df = 33, $t = 3.36$, $P = 0.002$; 1.0 mM: df = 33, $t = 1.26$, $P = 0.2128$).

Different from tomatine, nicotine at 0.001 mM and 0.01 mM induced higher levels of responses of "M2" GRNs in the medial sensillum of *H. armigera* than those of *H. assulta* (**Figure 7C**, independent-sample *t*-test of 0.001 mM: df = 19, $t = 8.69$, $P < 0.0001$; 0.01 mM: df = 28, $t = 6.91$, $P < 0.0001$) but elicited lower levels of response at 1.0 mM in *H. armigera* than that of *H. assulta* caterpillars(**Figure 7C**, 1.0 mM: df = 17, $t = -2.88$, $P = 0.0105$). Capsaicin elicited relatively lower levels of responses of "M2" GRNs in the medial sensillum of *H. armigera* caterpillars than those of *H. assulta* caterpillars (**Figure 7D**, independent-sample *t*-test of 0.01 mM: df = 20, $t = -2.35$, $P = 0.0271$; 0.1 mM: df = 31, $t = -4.05$, $P = 0.0003$; 1.0 mM: df = 43, $t = -2.33$, $P = 0.0245$).

For responses of "M2" GRNs in the lateral sensillum, it showed that gossypol and tomatine induced low and similar responses of "M2" GRNs between the two *Helicoverpa* species (**Figure 7A'** 0.001 mM gossypol: df = 13, $t = 0.01$, $P = 0.99$; 0.01 mM gossypol: df = 17, $t = -0.02$, $P = 0.98$; 0.1 mM gossypol: df = 19, $t = -0.70$, $P = 0.49$; 1.0 mM gossypol: df = 22, $t = 0.54$, $P = 0.60$; **Figure 7B'**, 0.001 mM tomatine: df = 15, $t = -0.92$, $P = 0.37$; 0.01 mM tomatine: df = 22, $t = -0.92$, $P = 0.37$; 0.1 mM tomatine: df = 20,

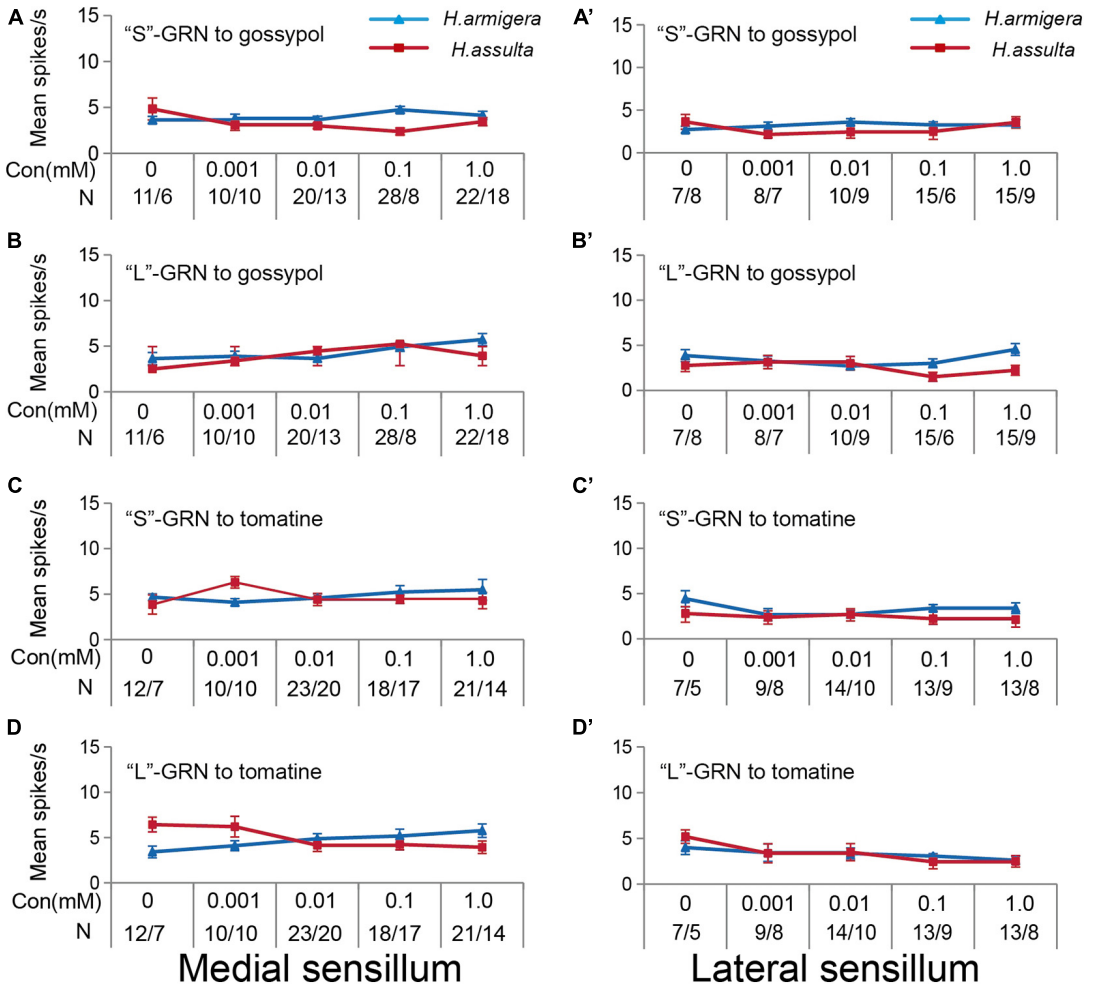

FIGURE 8 | Responses of "S" and "L" GRNs in the styloconic sensilla of *Helicoverpa* caterpillars to gossypol and tomatine. **(A,A')**: responses to gossypol of the indentified "S" GRNs from the medial and the lateral sensillum, respectively; **(B,B')**: responses to gossypol of the indentified "L" GRNs from the medial and the lateral sensillum, respectively; **(C,C')**: responses to tomatine of the indentified "S" GRNs from the medial and the lateral sensillum, respectively; **(D,D')**: responses to tomatine of the indentified "L" GRNs from the medial and the lateral sensillum, respectively.

$t = -0.40$, $P = 0.69$; 1.0 mM tomatine: df = 19, $t = 0.18$, $P = 0.86$). However, the responses of "M2" GRNs in the lateral sensillum to both nicotine and capsaicin at 0.1 mM and 1.0 mM were higher in *H. assulta* caterpillars than those of *H. armigera* (**Figure 7C'**, 0.1 mM nicotine: df = 23, $t = -3.30$, $P = 0.0031$; 1.0 mM nicotine: df = 29, $t = -4.13$, $P = 0.0004$; **Figure 7D'**, 0.1 mM capsaicin: df = 18, $t = -3.23$, $P = 0.0047$; 1.0 mM capsaicin: df = 16, $t = -9.27$, $P < 0.0001$).

Four plant secondary metabolites also induced responses of "S" GRNs and "L" GRNs in both sensilla of the two *Helicoverpa* species. While the responses of the two GRNs to each compound were low with non-significant change among different concentrations (SNK test after ANOVA for each compound: $P > 0.05$) (gossypol: **Figures 8A,A', B,B'**; tomatine: **Figures 8C,C', D,D'**; nicotine: **Figures 9A,A', B,B'**; capsaicin: **Figures 9C,C', D,D'**).

By comparing the responses of "M2" GRNs within one sensillum to the four secondary metabolites, it shows that the responses were significantly affected by both compounds and concentrations in either *Helicoverpa* species (GLM-univariate analysis of medial sensillum of *H. armigera*: compounds, df = 3, $F = 39.814$, $P < 0.0001$; concentrations, df = 4, $F = 188.576$, $P < 0.0001$; compounds × concentrations, df = 12, $F = 7.659$, $P < 0.0001$; medial sensillum of *H. assulta*: compounds, df = 3, $F = 19.4448$, $P < 0.0001$; concentrations, df = 4, $F = 151.172$, $P < 0.0001$; compounds × concentrations, df = 12, $F = 17.406$,

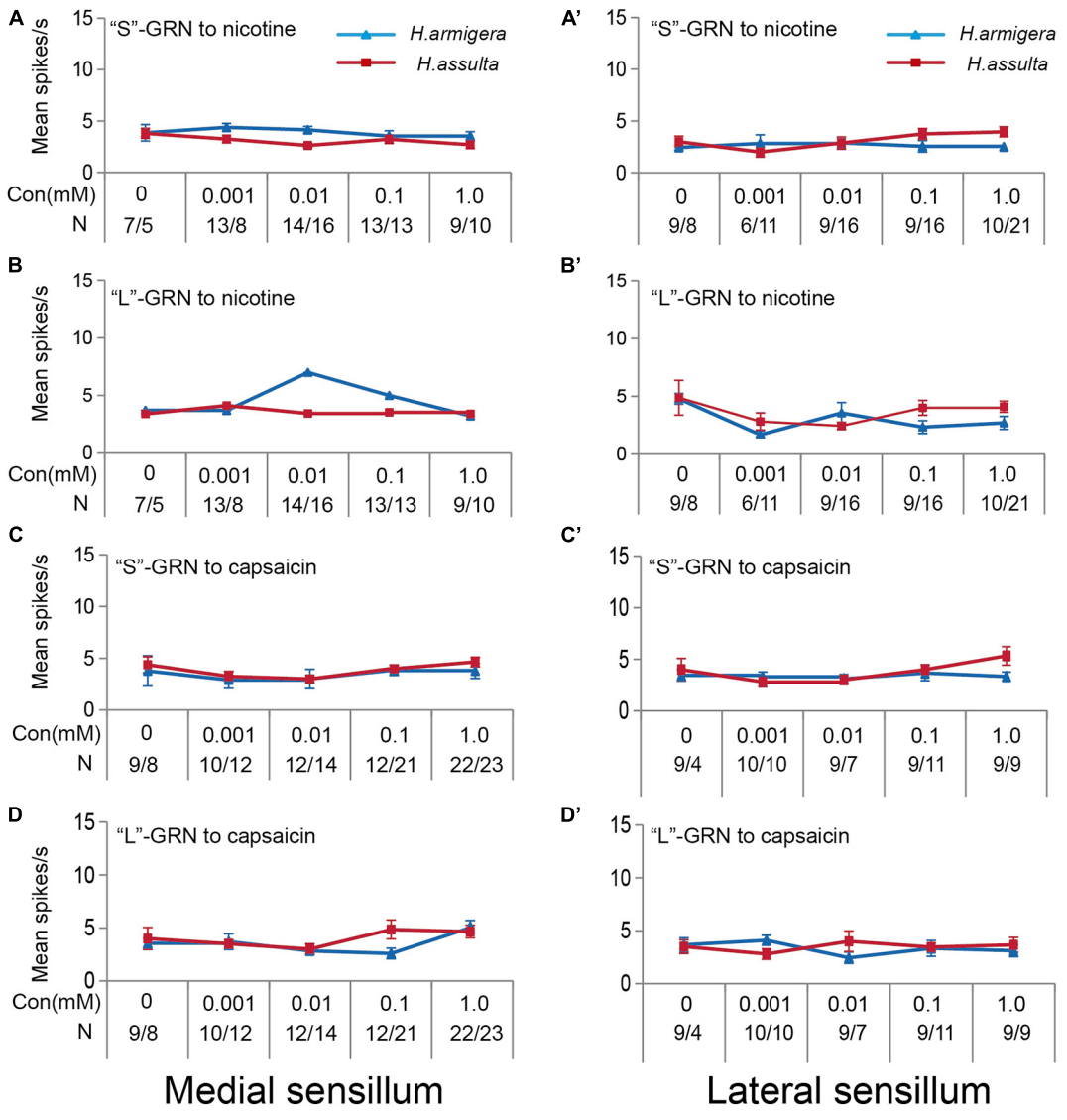

FIGURE 9 | Responses of "S" and "L" GRNs in the styloconic sensilla of Helicoverpa caterpillars to nicotine and capsaicin. **(A,A')**: responses to nicotine of the indentified "S" GRNs from the medial and lateral sensillum, respectively; **(B,B')**: responses to nicotine of the indentified "L" GRNs from the medial and lateral sensillum, respectively; **(C,C')**: responses to capsaicin of the indentified "S" GRNs from the medial and the lateral sensillum, respectively; **(D,D')**: responses to capsaicin of the indentified "L" GRNs from the medial and the lateral sensillum, respectively.

$P < 0.0001$) (**Table 2**). However, the ranks of the general responding frequency between the two species were different. The response of "M2" GRNs in medial sensillum of *H. armigera* was the strongest to nicotine, followed by gossypol and tomatine, then low response to capsaicin (**Table 3**). However, for *H. assulta*, tomatine induced the strongest response of "M2" GRNs in the medial sensillum, followed by nicotine, capsaicin, and gossypol (**Table 3**). For the "M2" GRNs in the lateral sensillum between the two species, tomatine induced relatively stronger responses than those induced by gossypol, nicotine, and capsaicin in *H. armigera*, whereas gossypol induced the lowest responses compared to those by other three compounds in *H. assulta* (**Table 3**).

Feeding Preferences for Plant Secondary Metabolites

Gossypol at 0.1 and 1.0 mM drove appetitive feedings in *H. armigera* caterpillars [**Figure 10A**; paired-sample *t*-test: 0.1 mM, $t(135) = -4.403$, $P < 0.0001$; 1.0 mM, $t(97) = -3.415$, $P = 0.001$], but 0.1 mM and 1.0 mM gossypol drove aversive feedings in *H. assulta* caterpillars [**Figure 10A'**; paired-sample *t*-test: 0.1 mM, $t(99) = 3.268$, $P = 0.001$; 1.0 mM, $t(137) = 2.179$, $P = 0.031$]. Tomatine at concentrations of 0.01 and 0.1 mM drove appetitive feedings in *H. armigera* caterpillars [**Figure 10B**; paired-sample *t*-test: 0.01 mM, $t(103) = -2.371$, $P = 0.02$; 0.1 mM, $t(114) = -3.324$, $P = 0.001$], while 0.1 mM and 1.0 mM tomatine significantly deterred feedings of *H. assulta* caterpillars [**Figure 10B'**; paired-sample *t*-test: 0.1 mM, $t(118) = 6.941$, $P < 0.0001$; 1.0 mM, $t(170) = 9.369$, $P < 0.0001$].

Nicotine at the concentration of 1.0 mM deterred feedings of *H. armigera* caterpillars [**Figure 10C**; paired-sample *t*-test: 1.0 mM, $t(98) = 6.471$, $P < 0.0001$] but drove appetitive feedings of *H. assulta* caterpillars at concentrations of 0.1 and 1.0 mM [**Figure 10C'**; paired-sample *t*-test: 0.1 mM, $t(101) = -7.569$, $P < 0.0001$; 1.0 mM, $t(110) = -2.916$, $P = 0.004$]. Capsaicin at the concentration of 1.0 mM significantly drove aversive feedings of *H. armigera* caterpillars [**Figure 10D**; one-sample *t*-test: 1.0 mM, $t(100) = 2.972$, $P = 0.004$), while 0.01 and 0.1 mM capsaicin significantly drove appetitive feedings of *H. assulta* caterpillars [**Figure 10D'**; one-sample *t*-test: 0.01 mM, $t(90) = -5.727$, $P < 0.0001$; 0.1 mM, $t(100) = -2.412$, $P = 0.018$].

DISCUSSION

Behavioral and Gustatory Response to the Primary Metabolites

Fructose, glucose, and proline have been widely reported to be phagostimulants for a variety of insect herbivores

TABLE 2 | Analysis of variance of the gustatory responses of "M2" GRNs in styloconic sensilla of *Helicoverpa* spp. partitioning effects of compounds and concentrations (GLM-Univariate analysis).

Source of variation	Medial sensillum				Lateral sensillum			
	df	MS	F	Sig.	df	MS	F	Sig.
(A) *H. armigera*								
Com.	3	73.636	39.814	< 0.0001	3	7.276	9.424	< 0.0001
Con.	4	348.751	188.576	< 0.0001	4	126.464	163.801	< 0.0001
Com. × Con.	12	14.166	7.659	< 0.0001	12	0.962	1.245	0.255
Error	276	1.849			180	0.772		
(B) *H. assulta*								
Com.	3	31.01	19.4448	< 0.0001	3	16.636	11.027	< 0.0001
Con.	4	241.048	151.172	< 0.0001	4	138.273	91.657	< 0.0001
Com. × Con.	12	17.406	10.916	< 0.0001	12	5.381	3.567	< 0.0001
Error	235	1.595			172	1.509		

Raw data of response frequencies were square-root transformed before analysis to meet the assumptions of GLM. Com.: compounds including gossypol, tomatine, nicotine, and capsaicin. Con.: concentrations.

TABLE 3 | Multiple comparisons of gustatory responses of "M2" GRNs in styloconic sensilla of *Helicoverpa* spp. to different plant secondary metabolites.

Compounds	Medial sensillum		Lateral sensillum	
	H. armigera	*H. assulta*	*H. armigera*	*H. assulta*
Gossypol	45.90 ± 29.09 b	28.07 ± 19.98 d	13.35 ± 8.36 b	11.87 ± 7.92 b
Tomatine	44.36 ± 28.21 b	50.81 ± 27.85 a	23.20 ± 16.76 a	24.83 ± 15.59 a
Nicotine	53.55 ± 29.18 a	40.94 ± 28.49 b	16.05 ± 10.42 b	32.44 ± 26.03 a
Capsaicin	21.92 ± 20.52 c	33.95 ± 23.84 c	14.57 ± 8.67 b	28.98 ± 19.28 a

Data are shown as general mean responding frequency ± SE (spk.s^{-1}) of "M2" GRNs to stimulus. Raw data of responding frequencies were square-root transformed before analysis. The SNK post-hoc test was used to the difference of response of "M2" GRNs in the same sensillum to different compounds ($P < 0.05$). Different lowcase letters in a vertical column represent the difference is significant ($P < 0.05$).

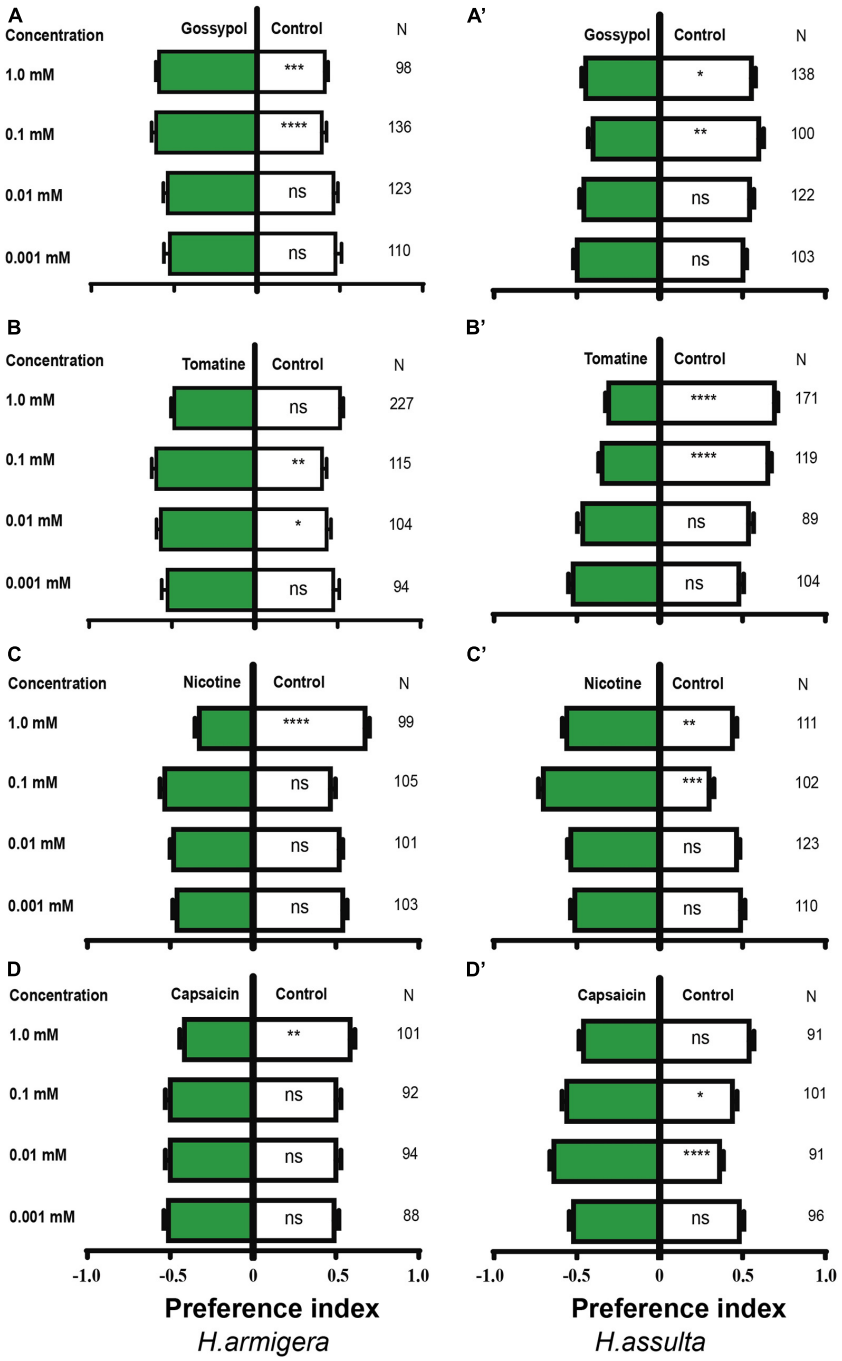

FIGURE 10 | Effects of secondary metabolites on the feeding preferences of *Helicoverpa* caterpillars. The preference indexes of caterpillars for control leaves (white bar) and for secondary metabolites treated leaves (green bars) were compared by using the paired-sample *t*-test. The dual-choice assay was used to test the feeding preference for pepper leaves treated by secondary metabolites at different concentrations and for control (electrolyte-treated) leaves. Electrolyte in **(A,A',B,B',C,C')** was solvent I (0.25% methanol, 5% ethanol, and 0.32% PVP in water). Electrolyte in **(D,D')** was solvent II (0.16% PVP in water). **(A–D)**: *H. armigera* caterpillars; **(A'–D')**: *H. assulta* caterpillars. "*," "**," "***," and "****" represent that the difference was significant at the 0.05, 0.01, 0.001, and 0.0001 level, respectively. ns: non-significant difference. N: the number of tested caterpillars.

(Albert et al., 1982; Bernays and Chapman, 2001; Liscia et al., 2004; Jiang et al., 2015; Mang et al., 2016). Our present study also shows that fructose could drive appetitive feedings of caterpillars in both *Helicoverpa* species. Glucose and proline at the given concentrations drove appetitive feedings of *H. assulta* caterpillars but had no significant effects on the generalist species *H. armigera*, suggesting that the generalist is less sensitive to the two compounds. This result is consistent with our previous

study that the feeding preference of *H. armigera* caterpillars is more flexible than that of *H. assulta* if caterpillars pre-exposed to different diets (Wang et al., 2017). The neural constraint hypothesis predicts that specialist herbivores always make more accurate decisions than generalists in the process of selection plants (Bernays, 1998). Our data provide further evidence that the specialist had better ability to perceive the sugars or essential nutrients than the generalist. However, our result indicated that the responding patterns of GRNs in galeal sensilla to each primary metabolite were similar between the two species, suggesting that the difference of feeding preferences should not be attributed to the firing rate of peripheral GRNs but might be from differences of the processing information within the central nervous system.

Behavioral and Gustatory Response to the Secondary Metabolites

Gossypol and tomatine are two major plant secondary metabolites from cotton and tomato, respectively, which are toxic or aversive on herbivorous insects (Vickerman and de Boer, 2002; Mulatu et al., 2006; Arnason and Bernards, 2010; Carriere et al., 2019). Our results also show that the two compounds drove aversive feedings of the specialist *H. assulta*, but caterpillars of the generalist *H. armigera* exhibited appetitive feedings for the two secondary metabolites. Such kind of secondary metabolites drove appetitive feedings of the generalist herbivores; to our knowledge, they have not been reported to date. We postulate that it should be attributed to the extraordinary adaptive capacity of caterpillars of *H. armigera* to the two compounds, for example, the tolerance and detoxifying metabolism (Mao et al., 2007; Zhou et al., 2010; Bretschneider et al., 2016; Krempl et al., 2016), while caterpillars of the specialist *H. assulta* do not feed on cotton and tomato plants in nature (Mitter et al., 1993) and exhibit aversive responses to the two secondary metabolites.

Nicotine (Szentesi and Bernays, 1984; Shields et al., 2008; Hori et al., 2011; Sollai et al., 2015) and capsaicin (Cowles et al., 1989; Hori et al., 2011; Li et al., 2020) have been generally reported as feeding deterrents for herbivorous insects. However, our results demonstrate that the two solanaceous alkaloids elicited appetitive feedings of the specialist *H. assulta*, while they drove aversive feedings of the generalist *H. armigera*. We also postulate that it could be attributed to the specialist *H. assulta* being more adaptive to the two alkaloids than the generalist *H. armigera*. Firstly, it is known that tobacco and hot pepper are two limited host plants of the specialist *H. assulta* (Mitter et al., 1993), while the generalists have to deal with lots of toxic plant metabolites based on the neural-constraint hypothesis (Levins and Macarthur, 1969; Bernays and Wcislo, 1994; Bernays and Funk, 1999). Secondly, the adaptations of specialists to nicotine and tobacco plants have been well reported on caterpillars of the tobacco cutworm *Manduca sexta* (Snyder et al., 1993; Glendinning, 2002; Wink and Theile, 2002; Govind et al., 2010; Kumar et al., 2014). For capsaicin, it has been found that the larval development of *H. assulta* could benefit from the dietary capsaicin compared to the negative effects on *H. armigera* (Ahn et al., 2011; Jia et al., 2012). At the level of metabolism, the capacity of degrading the capsaicinoids in *H. assulta* was overall higher than that in *H. armigera* (Zhu et al., 2020). Then, our data provide further evidence of adaptation of the specialist *H. assulta* to the toxic plant metabolites at the behavioral and chemosensory levels, which is similar to the attractive effects of "token stimuli," the specific secondary metabolites from host plants, on other investigated specialist herbivores (Renwick and Lopez, 1999; del Campo et al., 2001; Miles et al., 2005; Sollai et al., 2018).

For the response of galeal sensilla to the four secondary metabolites, it also indicates that each of the four secondary metabolites stimulated different responding patterns of GRNs between the two closely related species. Combining the differences of feeding preferences with the taste response of GRNs of the two species, it suggests that the activities of peripheral GRNs to the four alkaloids could contribute to the difference of feeding behaviors between the two *Helicoverpa* species. Therefore, it seems that the neural coding for behavioral decisions of the investigated secondary metabolites in the two *Helicoverpa* species is different from that for behavioral decisions of the primary metabolites. The present results suggest that the two *Helicoverpa* species evaluate the plant primary metabolites differently at the CNS level, while they evaluate the secondary metabolites differently at both peripheral and central levels.

CONCLUSION

In conclusion, our present results show that the difference of both behavioral feedings and electrophysiological responses to plant metabolites between the two *Helicoverpa* species could contribute to the difference of diet breadth in the two species. Especially, it indicates that caterpillars of the specialist *H. assulta* preferred more to glucose and proline than the generalist *H. armigera*, suggesting that specialist herbivores are more efficient in finding food sources than generalists. More interestingly, gossypol and tomatine, the two secondary metabolites from host plants of the generalist, could drive appetitive feedings of this insect species, suggesting that generalist insects adapt not only to toxic secondary metabolites at metabolism level but also at the behavioral and chemosensory levels.

We also found that nicotine and capsaicin, the secondary metabolites from two limited host plants of the specialist *H. assulta*, could drive appetitive feedings of this insect herbivore, suggesting that this specialist also has adapted to its host plants at behavioral and gustatory levels. However, it is not clear why the generalist *H. armigera* did not prefer nicotine and capsaicin since tobacco and hot pepper plants are also the host plants of this generalist species. We postulate that it may be related to the host plant shifts, host adaptations, fitness costs, and evolutionary pressures during the evolution between *Helicoverpa* species and their host plants. Regardless, our finding would give a new insight of underscoring the adaptation of generalist insects to its host plant. In addition, in future work, the ecological context of the evolution and the further adaptation mechanisms of *H. armigera* to these compounds should be addressed.

DATA AVAILABILITY STATEMENT

The original contributions presented in the study are included in the article/supplementary material, further inquiries can be directed to the corresponding author/s.

AUTHOR CONTRIBUTIONS

QT, WH, and YM conceived the experiment. LS, WH, and JZ conducted the experiment. QT, LS, and XZ wrote the manuscript. LS, QT, and WH analyzed the data. YM, YD, and QY edited the manuscript. All authors read and approved the final manuscript.

FUNDING

The work was supported by the National Natural Science Foundation of China (Grant Nos. 31672367 and 31861133019) and the Key Scientific and Technological Project of Henan Province (202102110072). The funders had no role in the study design, data collection and analysis, decision to publish, or preparation of the manuscript.

ACKNOWLEDGMENTS

We thank Mr. Zhongwei Sun for kindly helping in supplying the pepper seedlings.

REFERENCES

Ahn, S. J., Badenes-Perez, F. R., and Heckel, D. G. (2011). A host-plant specialist, *Helicoverpa assulta*, is more tolerant to capsaicin from Capsicum annuum than other noctuid species. *J. Insect Physiol.* 57, 1212–1219. doi: 10.1016/j.jinsphys.2011.05.015

Albert, P. J., Charley, C., Hanson, F., and Parisella, S. (1982). Feeding responses of eastern spruce budworm larvae to sucrose and other carbohydrates. *J. Chem. Ecol.* 8, 233–239. doi: 10.1007/BF00984019

Arnason, J. T., and Bernards, M. A. (2010). Impact of constitutive plant natural products on herbivores and pathogens. *Can. J. Zool.* 88, 615–627. doi: 10.1139/Z10-038

Barbour, J. D., and Kennedy, G. G. (1991). Role of steroidal glycoalkaloid alpha-tomatine in host-plant resistance of tomato to colorado potato beetle. *J. Chem. Ecol.* 17, 989–1005. doi: 10.1007/BF01395604

Behmer, S. T., Elias, D. O., and Bernays, E. A. (1999). Post-ingestive feedbacks and associative learning regulate the intake of unsuitable sterols in a generalist grasshopper. *J. Exp. Biol.* 202(Pt 6), 739–748. doi: 10.1080/106351599260508

Bernays, E. A. (1998). The value of being a resource specialist: behavioral support for a neural hypothesis. *Am. Nat.* 151, 451–464. doi: 10.1086/286132

Bernays, E. A., and Chapman, R. F. (2001). Taste cell responses in the polyphagous arctiid, Grammia geneura: towards a general pattern for caterpillars. *J. Insect Physiol.* 47, 1029–1043. doi: 10.1016/s0022-1910(01)00079-8

Bernays, E. A., Chapman, R. F., and Singer, M. S. (2000a). Sensitivity to chemically diverse phagostimulants in a single gustatory neuron of a polyphagous caterpillar. *J. Comp. Physiol. A* 186, 13–19. doi: 10.1007/s003590050002

Bernays, E. A., and Funk, D. J. (1999). Specialists make faster decisions than generalists: experiments with aphids. *Proc. R. Soc. Biol. Sci. Ser. B* 266:151. doi: 10.1098/rspb.1999.0615

Bernays, E. A., Oppenheim, S., Chapman, R. F., Kwon, H., and Gould, F. (2000b). Taste sensitivity of insect herbivores to deterrents is greater in specialists than in generalists: a behavioral test of the hypothesis with two closely related caterpillars. *J. Chem. Ecol.* 26, 547–563. doi: 10.1023/A:1005430010314

Bernays, E. A., and Wcislo, W. T. (1994). Sensory capabilities, information processing, and resource specialization. *Q. Rev. Biol.* 69, 187–204. doi: 10.1086/418539

Bretschneider, A., Heckel, D. G., and Vogel, H. (2016). Know your ABCs: characterization and gene expression dynamics of ABC transporters in the polyphagous herbivore *Helicoverpa armigera*. *Insect Biochem. Mol. Biol.* 72, 1–9. doi: 10.1016/j.ibmb.2016.03.001

Carriere, Y., Yelich, A. J., Degain, B., Harpold, V. S., Unnithan, G. C., Kim, J. H., et al. (2019). Gossypol in cottonseed increases the fitness cost of resistance to Bt cotton in pink bollworm. *Crop Prot.* 126:104914. doi: 10.1016/J.Cropro.2019.104914

Cowles, R. S., Keller, J. E., and Miller, J. R. (1989). Pungent spices, ground red pepper, and synthetic capsaicin as onion fly ovipositional deterrents. *J. Chem. Ecol.* 15, 719–730. doi: 10.1007/BF01014714

del Campo, M. L., Miles, C. I., Schroeder, F. C., Mueller, C., Booker, R., and Renwick, J. A. (2001). Host recognition by the tobacco hornworm is mediated by a host plant compound. *Nature* 411, 186–189. doi: 10.1038/35075559 35075559

Fitt, G. P. (1989). The ecology of Heliothis species in relation to agroecosystems. *Annu. Rev. Entomol.* 34, 17–52. doi: 10.1146/annurev.en.34.010189.000313

Glendinning, J. I. (2002). How do herbivorous insects cope with noxious secondary plant compounds in their diet? *Entomol. Exp. Appl.* 104, 15–25. doi: 10.1046/j.1570-7458.2002.00986.x

Govind, G., Mittapalli, O., Griebel, T., Allmann, S., Bocker, S., and Baldwin, I. T. (2010). Unbiased transcriptional comparisons of generalist and specialist herbivores feeding on progressively defenseless Nicotiana attenuata plants. *PLoS One* 5:e8735. doi: 10.1371/journal.pone.0008735

Hori, M., Nakamura, H., Fujii, Y., Suzuki, Y., and Matsuda, K. (2011). Chemicals affecting the feeding preference of the Solanaceae-feeding lady beetle Henosepilachna vigintioctomaculata (Coleoptera: Coccinellidae). *J. Appl. Entomol.* 135, 121–131. doi: 10.1111/j.1439-0418.2010.01519.x

Jermy, T. (1966). Feeding inhibitors and food preference in chewing phytophagous insects. *Entomol. Exp. Appl.* 9, 1–12. doi: 10.1111/j.1570-7458.1966.tb00973.x

Jia, Y., Cheng, X., Cai, Y., Luo, M., and Guo, X. (2012). Difference of the fitness of *Helicoverpa armigera* (Hübner) fed with different pepper varieties. *Acta Ecol. Sin.* 32, 159–167.

Jiang, J., Ding, S., Zhang, Y., and Wang, Y. (2010). Effects of artificial diet on the growth & development and fecundity of H. armigera. *J. Henan Agr. Univ.* 44, 78–82. doi: 10.16445/j.cnki.1000-2340.2010.01.007

Jiang, X., Ning, C., Guo, H., Jia, Y., Huang, L., Qu, M., et al. (2015). A gustatory receptor tuned to D-fructose in antennal sensilla chaetica of Helicoverpa armigera. *Insect Biochem. Mol. Biol.* 60, 39–46. doi: 10.1016/j.ibmb.2015.03.002

Krempl, C., Sporer, T., Reichelt, M., Ahn, S. J., Heidel-Fischer, H., Vogel, H., et al. (2016). Potential detoxification of gossypol by UDP-glycosyltransferases in the two Heliothine moth species *Helicoverpa armigera* and Heliothis virescens. *Insect Biochem. Mol. Biol.* 71, 49–57. doi: 10.1016/j.ibmb.2016.02.005

Kumar, P., Rathi, P., Schottner, M., Baldwin, I. T., and Pandit, S. (2014). Differences in ncotine metabolism of two Nicotiana attenuata herbivores render them differentially susceptible to a common native predator. *PLoS One* 9:e95982. doi: 10.1371/journal.pone.0095982

Levins, R., and Macarthur, R. (1969). An hypothesis to explain the incidence of monophagy. *Ecology* 50, 910–911. doi: 10.2307/1933709

Li, Y., Bai, P., Wei, L., Kang, R., Chen, L., Zhang, M., et al. (2020). Capsaicin functions as *Drosophila ovipositional* repellent and causes intestinal dysplasia. *Sci. Rep.* 10:9963. doi: 10.1038/s41598-020-66900-2

Liscia, A., Masala, C., Crnjar, R., Sollai, G., and Solari, P. (2004). Saccharin stimulates the "deterrent" cell in the blowfly: behavioral and electrophysiological evidence. *Physiol. Behav.* 80, 637–646. doi: 10.1016/j.physbeh.2003.11.002

Liu, Z., Scheirs, J., and Heckel, D. G. (2012). Trade-offs of host use between generalist and specialist Helicoverpa sibling species: adult oviposition and larval performance. *Oecologia* 168, 459–469. doi: 10.1007/s00442-011-2103-0

Ma, Y., Li, J. J., Tang, Q. B., Zhang, X. N., Zhao, X. C., Yan, F. M., et al. (2016). Trans-generational desensitization and within-generational resensitization of

a sucrose-best neuron in the polyphagous herbivore *Helicoverpa armigera* (Lepidoptera: Noctuidae). *Sci. Rep.* 6:39358. doi: 10.1038/srep39358

Mang, D., Shu, M., Tanaka, S., Nagata, S., Takada, T., Endo, H., et al. (2016). Expression of the fructose receptor BmGr9 and its involvement in the promotion of feeding, suggested by its co-expression with neuropeptide F1 in Bombyx mori. *Insect Biochem. Mol. Biol.* 75, 58–69. doi: 10.1016/j.ibmb.2016.06.001

Mao, Y. B., Cai, W. J., Wang, J. W., Hong, G. J., Tao, X. Y., Wang, L. J., et al. (2007). Silencing a cotton bollworm P450 monooxygenase gene by plant-mediated RNAi impairs larval tolerance of gossypol. *Nat. Biotechnol.* 25, 1307–1313. doi: 10.1038/nbt1352

Miles, C. I., del Campo, M. L., and Renwick, J. A. (2005). Behavioral and chemosensory responses to a host recognition cue by larvae of Pieris rapae. *J. Comp. Physiol. A* 191, 147–155. doi: 10.1007/s00359-004-0580-x

Mitter, C., Poole, R. W., and Matthews, M. (1993). Biosystematics of the *Heliothinae* (Lepidoptera: Noctuidae). *Annu. Rev. Entomol.* 38, 207–225. doi: 10.1146/annurev.en.38.010193.001231

Montandon, R., Stipanovic, R. D., Williams, H. J., Sterling, W. L., and Vinson, S. B. (1987). Nutritional indices and excretion of gossypol by Alabama argillacea (Hübner) and Heliothis virescens (F.) (Lepidoptera: Noctuidae) fed glanded and glandless cotyledonary cotton leaves. *J. Econ. Entomol.* 80, 32–36. doi: 10.1093/jee/80.1.32

Mulatu, B., Applebaum, S. W., Kerem, Z., and Coll, M. (2006). Tomato fruit size, maturity and alpha-tomatine content influence the performance of larvae of potato tuber moth *Phthorimaea operculella* (Lepidoptera: Gelechiidae). *Bull. Entomol. Res.* 96, 173–178. doi: 10.1079/ber2005412

Oliver, B. F., Maxwell, F. G., and Jenkins, J. N. (1970). Utilization of glanded and glandless cotton diets by the bollworm. *J. Econ. Entomol.* 63, 1965–1966. doi: 10.1093/jee/63.6.1965

Pearson, D. E., Valliant, M., Carlson, C., Thelen, G. C., Ortega, Y. K., Orrock, J. L., et al. (2019). Spicing up restoration: can chili peppers improve restoration seeding by reducing seed predation? *Restor. Ecol.* 27, 254–260. doi: 10.1111/rec.12862

Renwick, J. A. (2001). Variable diets and changing taste in plant-insect relationships. *J. Chem. Ecol.* 27, 1063–1076. doi: 10.1023/A:1010381509601

Renwick, J. A., and Lopez, K. (1999). "Experience-based food consumption by larvae of *Pieris rapae*: addiction to glucosinolates?," in *Proceedings of the 10th International Symposium on Insect-Plant Relationships*, Vol. 56, eds S. Simpson, A. J. Mordue, and J. Hardie (Dordrecht: Springer Netherlands), 51–58. doi: 10.1046/j.1570-7458.1999.00465.x

Roessingh, P., Hora, K. H., van Loon, J. J. A., and Menken, S. B. J. (1999). Evolution of gustatory sensitivity in Yponomeuta caterpillars: sensitivity to the stereoisomers dulcitol and sorbitol is localised in a single sensory cell. *J. Comp. Physiol. A* 184, 119–126. doi: 10.1007/s003590050311

Schoonhoven, L. M. (1967). Chemoreception of mustard oil glucosides in larvae of Pieris brassicae. *P. Koninkl. Nederl. Akad. Wetensehappen, Amsterdam. Series C* 70, 556–568.

Sheck, A. L., and Gould, F. (1996). The genetic basis of differences in growth and behavior of specialist and generalist herbivore species: selection on hybrids of *Heliothis virescens* and H. subflexa (Lepidoptera). *Evolution* 50, 831–841. doi: 10.1111/j.1558-5646.1996.tb03892.x

Shields, V. D., Smith, K. P., Arnold, N. S., Gordon, I. M., Shaw, T. E., and Waranch, D. (2008). The effect of varying alkaloid concentrations on the feeding behavior of gypsy moth larvae, *Lymantria dispar* (L.) (Lepidoptera: Lymantriidae). *Arthropod Plant Interact.* 2, 101–107. doi: 10.1007/s11829-008-9035-6

Simões, P. M. V., Ott, S. R., and Niven, J. E. (2012). A long-latency aversive learning mechanism enables locusts to avoid odours associated with the consequences of ingesting toxic food. *J. Exp. Biol.* 215(Pt 10), 1711–1719. doi: 10.1242/jeb.068106

Snyder, M., Hsu, E.-L., and Feyereisen, R. (1993). Induction of cytochrome P-450 activities by nicotine in the tobacco hornworm, Manduca sexta. *J. Chem. Ecol.* 19, 2903–2916. doi: 10.1007/BF00980591

Sollai, G., Biolchini, M., and Crnjar, R. (2018). Taste sensitivity and divergence in host plant acceptance between adult females and larvae of Papilio hospiton. *Insect Sci.* 25, 809–822. doi: 10.1111/1744-7917.12581

Sollai, G., and Crnjar, R. (2019). The contribution of gustatory input to larval acceptance and female oviposition choice of potential host plants in Papilio hospiton (Gene). *Arch. Insect Biochem. Physiol.* 100:e21521. doi: 10.1002/arch.21521

Sollai, G., Tomassini Barbarossa, I., Masala, C., Solari, P., and Crnjar, R. (2014). Gustatory sensitivity and food acceptance in two phylogenetically closely related papilionid species: Papilio hospiton and Papilio machaon. *PLoS One* 9:e100675. doi: 10.1371/journal.pone.0100675

Sollai, G., Tomassini Barbarossa, I., Solari, P., and Crnjar, R. (2015). Taste discriminating capability to different bitter compounds by the larval styloconic sensilla in the insect herbivore Papilio hospiton (Gene). *J. Insect Physiol.* 74, 45–55. doi: 10.1016/j.jinsphys.2015.02.004

Sun, Z. X., Shi, Q., Li, Q. L., Wang, R. M., Xu, C. C., Wang, H. H., et al. (2019). Identification of a cytochrome P450 CYP6AB60 gene associated with tolerance to multi-plant allelochemicals from a polyphagous caterpillar tobacco cutworm (Spodoptera litura). *Pestic. Biochem. Physiol.* 154, 60–66. doi: 10.1016/j.pestbp.2018.12.006

Szentesi, A., and Bernays, E. A. (1984). A study of behavioural habituation to a feeding deterrent in nymphs of Schistocerca gregaria. *Physiol. Entomol.* 9, 329–340. doi: 10.1111/j.1365-3032.1984.tb00714.x

Tang, Q., Hong, Z., Cao, H., Yan, F., and Zhao, X. (2015). Characteristics of morphology, electrophysiology, and central projections of two sensilla styloconica in Helicoverpa assulta larvae. *Neuroreport* 26, 703–711. doi: 10.1097/WNR.0000000000000413

Tang, Q., Huang, L., Wang, C., Zhan, H., and van Loon, J. J. A. (2014). Inheritance of electrophysiological responses to leaf saps of host- and nonhost plants in two *Helicoverpa* species and their hybrids. *Arch. Insect Biochem. Physiol.* 86, 19–32. doi: 10.1002/arch.21154

Tang, Q., Jiang, J., Yan, Y., van Loon, J. J. A., and Wang, C. (2006). Genetic analysis of larval host-plant preference in two sibling species of Helicoverpa. *Entomol. Exp. Appl.* 118, 221–228. doi: 10.1111/j.1570-7458.2006.00387.x

Tao, X., Xue, X., Huang, Y., Chen, X., and Mao, Y. (2012). Gossypol-enhanced P450 gene pool contributes to cotton bollworm tolerance to a pyrethroid insecticide. *Mol. Ecol.* 21, 4371–4385. doi: 10.1111/j.1365-294X.2012.05548.x

Thompson, J. D. (1991). Phenotypic plasticity as a component of evolutionary change. *Trends. Ecol. Evol.* 6, 246–249. doi: 10.1016/0169-5347(91)90070-E

Tian, K., Zhu, J., Li, M., and Qiu, X. H. (2019). Capsaicin is efficiently transformed by multiple cytochrome P450s from Capsicum fruit-feeding *Helicoverpa armigera*. *Pestic. Biochem. Physiol.* 156, 145–151. doi: 10.1016/j.pestbp.2019.02.015

van Loon, J. J. A. (1990). Chemoreception of phenolic acids and flavonoids in larvae of two species of Pieris. *J. Comp. Physiol. A* 166, 889–899. doi: 10.1007/bf00187336

Vickerman, D. B., and de Boer, G. (2002). Maintenance of narrow diet breadth in the monarch butterfly caterpillar: response to various plant species and chemicals. *Entomol. Exp. Appl.* 104, 255–269. doi: 10.1046/j.1570-7458.2002.01012.x

Wada-Katsumata, A., Silverman, J., and Schal, C. (2013). Changes in taste neurons support the emergence of an adaptive behavior in cockroaches. *Science* 340, 972–975. doi: 10.1126/science.1234854

Wang, C., and Dong, J. (2001). Interspecific hybridization of *Helicoverpa armigera* and H. assulta (Lepidoptera: Noctuide). *Chin. Sci. Bull.* 46, 489–491. doi: 10.1007/bf03187264

Wang, Y., Ma, Y., Zhou, D., Gao, S., Zhao, X., Tang, Q., et al. (2017). Higher plasticity in feeding preference of a generalist than a specialist: experiments with two closely related Helicoverpa species. *Sci. Rep.* 7:17876. doi: 10.1038/s41598-017-18244-7

Wink, M., and Theile, V. (2002). Alkaloid tolerance in Manduca sexta and phylogenetically related sphingids (Lepidoptera : Sphingidae). *Chemoecology* 12, 29–46. doi: 10.1007/s00049-002-8324-2

Wright, G. A., Mustard, J. A., Simcock, N. K., Ross-Taylor, A. A., McNicholas, L. D., Popescu, A., et al. (2010). Parallel reinforcement pathways for conditioned food aversions in the honeybee. *Curr. Biol.* 20, 2234–2240. doi: 10.1016/j.cub.2010.11.040

Wu, K., and Gong, P. (1997). A new and practical artificial diet for the cotton bollworm. *Insect Sci* 4, 277–282. doi: 10.1111/j.1744-7917.1997.tb00101.x

Wu, K., Gong, P., and Li, X. (1990). Studies on artificial diets for rearing the tobacco budworm *Heliothis assulta* (Guenée). *Acta Entomol. Sin.* 33, 301–308. doi: 10.16380/j.kcxb.1990.03.007

Yang, L., Wang, X., Bai, S., Li, X., Gu, S., Wang, C. Z., et al. (2017). Expressional divergence of insect GOX genes: from specialist to generalist glucose oxidase. *J. Insect Physiol.* 100, 21–27. doi: 10.1016/j.jinsphys.2017.05.003

Zalucki, M. P., Daglish, G., Firempong, S., and Twine, P. H. (1986). The biology and ecology of *Heliothis armigera* (Hübner) and H. punctigera Wallengren (Lepidoptera:Noctuidae) in Australia - What do we know? *Aust. J. Zool.* 34, 779–814. doi: 10.1071/ZO9860779

Zhou, X., Sheng, C., Li, M., Wan, H., Liu, D., and Qiu, X. (2010). Expression responses of nine cytochrome P450 genes to xenobiotics in the cotton bollworm Helicoverpa armigera. *Pestic. Biochem. Physiol.* 97, 209–213. doi: 10.1016/j.pestbp.2010.02.003

Zhu, J., Tian, K., Reilly, C. A., and Qiu, X. H. (2020). Capsaicinoid metabolism by the generalist *Helicoverpa armigera* and specialist H. *assulta*: species and tissue differences. *Pestic. Biochem. Physiol.* 163, 164–174. doi: 10.1016/j.pestbp.2019.11.013

Conflict of Interest: The authors declare that the research was conducted in the absence of any commercial or financial relationships that could be construed as a potential conflict of interest.

Copyright © 2021 Sun, Hou, Zhang, Dang, Yang, Zhao, Ma and Tang. This is an open-access article distributed under the terms of the Creative Commons Attribution License (CC BY). The use, distribution or reproduction in other forums is permitted, provided the original author(s) and the copyright owner(s) are credited and that the original publication in this journal is cited, in accordance with accepted academic practice. No use, distribution or reproduction is permitted which does not comply with these terms.

frontiers in Neuroanatomy

ORIGINAL RESEARCH
published: 28 April 2021
doi: 10.3389/fnana.2021.673420

Functional Characterization of Sex Pheromone Neurons and Receptors in the Armyworm, *Mythimna separata* (Walker)

Chan Wang[1], Bing Wang[1] and Guirong Wang[1,2]**

[1] State Key Laboratory for Biology of Plant Diseases and Insect Pests, Institute of Plant Protection, Chinese Academy of Agricultural Sciences, Beijing, China, [2] Guangdong Laboratory of Lingnan Modern Agriculture, Shenzhen, Genome Analysis Laboratory of the Ministry of Agriculture, Agricultural Genomics Institute at Shenzhen, Chinese Academy of Agricultural Sciences, Shenzhen, China

Pheromone receptors (PRs) of moths are expressed on the dendritic membrane of odorant receptor neurons (ORNs) housed in the long trichoid sensilla (TS) of antennae and are essential to sex pheromone reception. The function of peripheral neurons of *Mythimna separata* in recognizing sex pheromones is still unclear. In this study, electroantennogram recordings were performed from male and female antennae of *M. separata*, and showed that the major component of sex pheromones, (*Z*)-11-hexadecenal (Z11–16:Ald), evoked the strongest response of male antennae with significant differences between sexes. Single sensillum recording was used to record responses of neurons housed in TS of male *M. separata*. The results revealed four types of TS with three neurons housed in each type, based on profiles of responses to sex pheromone components and pheromone analogs. ORN-B of type-I TS was specifically tuned to the major sex pheromone component Z11–16:Ald; ORN-Bs in type-III and type-IV TSs were, respectively, activated by minor components (*Z*)-11-hexadecen-1-yl acetate (Z11–16:OAc) and hexadecenal (16:Ald); and ORNs in type-II TS were mainly activated by the sex pheromone analogs. We further cloned full-length sequences of six putative *PR* genes and an *Orco* gene. Functional characterization of PRs in the *Xenopus* oocyte system demonstrated that male antennae-biased MsepPR1 responded strongly to (*Z*)-9-tetradecenal (Z9-14:Ald), suggesting that *MsepPR1* may be expressed in type-II TS. MsepPR6 was exclusively tuned to (*Z*)-9-tetradecen-1-yl acetate (Z9–14:OAc). MsepPR2 and MsepPR4 showed no responses to any tested components. Female antennae-biased MespPR5 was broadly tuned to Z9–14:Ald, Z9–14:OAc, Z11–16:Ald, and (*Z*)-11-hexadecen-1-ol (Z11–16:OH). Our results further enriched the sex pheromone recognition mechanism in the peripheral nervous system of moth *M. separata*.

Keywords: *Mythimna separata*, pheromone receptors, odorant receptor neurons, single sensillum recording, *Xenopus* oocyte

OPEN ACCESS

Edited by:
Xin-Cheng Zhao,
Henan Agricultural University, China

Reviewed by:
Sylvia Anton,
Institut National de la Recherche Agronomique (INRA), France
XiangBo Kong,
Chinese Academy of Forestry, China

****Correspondence:***
Guirong Wang
grwang@ippcaas.cn
Bing Wang
wangbing02@caas.cn

Received: *27 February 2021*
Accepted: *30 March 2021*
Published: *28 April 2021*

Citation:
Wang C, Wang B and Wang G (2021) Functional Characterization of Sex Pheromone Neurons and Receptors in the Armyworm, Mythimna separata (Walker). Front. Neuroanat. 15:673420. doi: 10.3389/fnana.2021.673420

INTRODUCTION

Pheromone-based sexual communication in moths has become an excellent model system for investigating the molecular mechanism of sensory perception because of the surprisingly high specificity in insect olfaction (Gould et al., 2010; Leal, 2013; Liu et al., 2013). Peripheral reception of pheromones in moths involves multiple proteins in male antennae, including pheromone binding proteins (PBPs), pheromone receptors (PRs), pheromone degrading enzymes, and sensory neuron membrane proteins (SNMPs; Leal, 2005; Rutzler and Zwiebel, 2005; Touhara and Vosshall, 2009).

In Lepidoptera, females release pheromone molecules that are specific and attractive to conspecific males at incredibly low concentrations over long distances (Ando et al., 2004). The species-specificity of pheromone production and recognition limits hetero-specific mating behaviors (Linn and Roelofs, 1995). Moth sex pheromones are generally a blend of pheromone components detected by odorant receptor neurons (ORNs) housed in trichoid sensilla (TS) of male antennae (Kaissling, 1986; Heinbockel and Kaissling, 1996; Hallem et al., 2004; Hansson and Stensmyr, 2011). In general, PRs expressed on the dendrite membrane of ORNs in the peripheral olfactory system of male antennae play a significant role in detecting conspecific sex pheromones (Vogt, 2005; Tanaka et al., 2009).

In early studies, two PRs of *Bombyx mori*, BmorOR1, and BmorOR3, were deorphanized (Sakurai et al., 2004; Nakagawa et al., 2005). Later, many PRs from moth species were characterized by homologous cloning technology, including *Heliothis virescens*, *Manduca sexta*, *Helicoverpa armigera*, *Spodoptera exigua*, *Sesamia inferens*, *Spodoptera litura*, *Helicoverpa assulta*, *Grapholita molesta*, *Operophtera brumata*, *Cydia pomonella*, *Ostrinia furnacalis*, *Lampronia capitella*, *Athetis lepigone*, and *Spodoptera frugiperda* (Zhang and Löfstedt, 2015). A phylogenetic analysis showed that PR clades were highly conserved and divided into different groups in Lepidoptera species (Zhang et al., 2017). In a recent study, a novel lineage of PRs clade that was part of a distinct early diverging lineage for detecting sex pheromones was characterized in *Spodoptera littoralis* and *Dendrolimus punctatus*, providing new insights into sex communication in moths (Bastin-Héline et al., 2019; Shen et al., 2020). These receptors have a potentially critical function in maintaining the integrity of species as well as in adaptation and evolution.

The oriental armyworm, *Mythimna separata* (Lepidoptera: Noctuidae) is a serious pest in many parts of the world. It distributed widely in eastern Asia and Australia, and there have been recent outbreaks in north China (Jiang et al., 2014a). The gluttonous and omnivorous characteristics of *M. separata* larvae cause huge damage to cereal crops annually, including maize, cotton, wheat, and corn (Jiang et al., 2014b). In addition, it is a migratory pest that can migrate about 1,000 km per season (Liu et al., 2017). In general, sex pheromones can be used as an efficient and environmentally friendly way of studying behavioral regulation and monitoring populations in pest control (Witzgall et al., 2010; Jiang et al., 2011). Different geographical populations of *M. separata* have different compositions and proportions in the sex pheromone gland (Takahashi et al., 1979; Zhu et al., 1987; Kou et al., 1992; Wang and Liu, 1997; Lebedeva et al., 2000; Fónagy et al., 2011; Song et al., 2017). The sex pheromone component of female *M. separata* in north China is a blend of (*Z*)-11-hexadecen-1-ol (Z11–16:Ald), (*Z*)-11-hexadecen-1-ol (Z11–16:OH), (*Z*)-11-hexadecenyl acetate (Z11–16:OAc), and hexadecenal (16:Ald; Jiang et al., 2019). Field trapping experiments showed that Z11–16:Ald alone resulted in high male moth captures (Wei and Pan, 1985; Zhu et al., 1987; Jung et al., 2013; Chen et al., 2018). A subsequent wind tunnel experiment indicated that single component Z11–16:Ald could sufficiently induce male sexual behaviors and elicit electrophysiological activity of male antennae in the gas chromatography-electroantennographic detection analyses (Jiang et al., 2019). This result revealed that Z11–16:Ald was the major component while the other three were minor components of sex pheromones in geographical populations of *M. separata* in north China.

Sex pheromone components are usually detected in TS of male moth (Kaissling, 2004). The ultrastructure of antennal sensilla of *M. separata* has been studied by scanning electron microscopy (SEM). And three dendrites were observed in the TS by the transmission electron microscopy (TEM), indicated three neurons housed in TS (Chang X. Q. et al., 2015). Recently, several studies have identified multiple chemosensory genes in the *M. separata* antennal transcriptome (Chang et al., 2017; He et al., 2017; Du et al., 2018; Jiang et al., 2019). In the geographic population of Kyoto, two PRs were deorphanized and one of them, MsOR1, was mainly tuned to sex pheromone component Z11–16:OAc (Mitsuno et al., 2008). In the geographic population of northern China, a previous analysis of antennae transcriptome identified *Orco* and six putative *PR* genes according to tissue expression and phylogenetic relationships. These genes were named *MsepPRs*, of which *MsepPR1*, *MsepPR3,* and *MsepPR4* appear to be specifically expressed in male antennae, while *MsepPR5* was highly expressed in female antennae (Du et al., 2018). Recent work published by Jiang et al. (2019) indicated that the major sex pheromone component Z11–16:Ald activated MsepOR3 and the cumulus of the macroglomerular complex (MGC) in the central nervous system, also studied olfactory coding of sex pheromones in the males *M. separata*. However, the function of peripheral neurons in discriminating minor sex pheromone components and pheromone analogs is still unclear.

In this study, we selected four sex pheromone components Z11–16:Ald, Z11–16:OAc, Z11–16:OH, and 16:Ald, consistent with the sex pheromone blend of *M. separata* identified by Jiang et al. (2019) and four pheromone analogs Z9–14:OAc, Z9–16:Ald, Z9–14:Ald, and Z9–14:OH, to focus on the sex pheromone recognition mechanism in the peripheral neuron system of *M. separata*. Firstly, we measured electroantennography (EAG) responses of male and female *M. separata* antennae to sex pheromone components. Secondly, we recorded multiple ORNs housed in TS of male moth using single sensillum recording (SSR). Different types of TS were sorted according to functional profiles. Thirdly, we cloned six full-length *PR* genes and an *Orco* gene identified from published antennae transcriptomes using rapid amplification of cDNA ends (RACE) technology.

Finally, we identified the functions of MsepPRs using the *Xenopus* oocyte heterologous expression system and two-electrode voltage clamp. Our results enriched the mechanism of sex pheromone recognition in the peripheral nervous system of *M. separata*.

MATERIALS AND METHODS

Insects

Mythimna *separata* adults were caught in the field in Xinxiang, Henan Province, China (35°18′ N, 113°55′ E). The larvae were reared on an artificial diet at a temperature of 25 ± 1°C, humidity of 75 ± 10% and photoperiod of 14:10 h (light:dark) in the Institute of Plant Protection, Chinese Academy of Agricultural Sciences. Pupae were distinguished based on sex and placed in separate cages before eclosion. The adults were fed with fresh 10% glucose water.

Chemical Compounds

Four sex pheromone components Z11–16:Ald (CAS:53939-28-9), Z11–16:OH (CAS:56683-54-6), Z11–16:OAc (CAS:34010-21-4), 16:Ald (CAS:629-80-1), and four pheromone analogs (*Z*)-9-hexadecenal (Z9-16:Ald; CAS:56219-04-6), Z9–14:Ald (CAS:53939-27-8), (*Z*)-9-tetradecen-1-ol (Z9-14:OH; CAS:35153-15-2), Z9–14:OAc (CAS:16725-53-4) used in this study were purchased from Nimrod Inc. (Changzhou, China; purity ≥ 96%).

Electroantennogram Recordings

The electrophysiological recordings of whole male and female antennae in response to four sex pheromone components and pheromone analogs were performed according to the standard technique (Cao et al., 2016). The components used in the EAG assay were dissolved in paraffin oil and diluted to 10 μg/μL. A piece of filter paper (0.5 × 5 cm) loaded with 10 μL pheromones was used as a stimulus, and paraffin oil was used as a control. 3-day-old moths were tested and signals from antennae were amplified with a 10 × AC/DC headstage preamplifier (Syntech, Kirchzarten, Germany) and further acquired with an Intelligent Data Acquisition Controller (IDAC-4-USB; Syntech, Kirchzarten, Germany). Signals were recorded with Syntech EAG-software (EAGPro 2.0). After subtracting the responses of the control, data were analyzed using the Student's *t*-test (El-Sayed et al., 2009).

Single Sensillum Recordings

Trichoid sensilla of antennae of 3-day-old male adults were used for recordings. TS in the basal, middle, and proximal parts of the antennae were recorded for each antenna. Individuals were restrained in a remodeled 1 mL plastic pipette tip with an exposed head fixed by dental wax, and the antenna from one side was attached to a coverslip with double-sided tape. A tungsten wire was inserted into one compound eye of the moth as a reference electrode, and a recording electrode was inserted into the base of each TS after sharpening the tip with 40% KNO_2 solution. The recording electrode was attached to an olfactory probe (Syntech) under a Leica Z16 APO microscope at 920 × magnification, and action potentials were amplified by a 10 × AC/DC preamplifier (Syntech).

The sex pheromone components were dissolved in paraffin oil at a concentration of 100 μg/μL and were stored at −20°C. The working concentrations were prepared by a serial dilution from 200 to 0.01 μg/μL (200, 100, 10, 1, 0.1, 0.01 μg/μL). Paraffin oil was used as a negative control. The chemicals were dripped on a filter paper strip (0.5 × 5 cm) inserted into a pasteur pipette (15 cm long). Purified and humidified air flow set at 1.2 L/min continuously blew toward the antenna through a 14 cm-long metal tube controller (Syntech, Kirchzarten, Germany). The fixed antennae were exposed to a 300 ms stimulus air pulse controlled by a Syntech stimulus controller (CS-55, Syntech, Kirchzarten, Germany). AC signals were recorded for 10 s using a data acquisition controller (IDAC-4, Syntech, Kirchzarten, Germany). Action potentials were digitized and displayed on a computer screen using Autospike software (Syntech). Responses were calculated as the difference of spike-number between the 1 s before the stimulus delivery point and 1 s after (Chang et al., 2016).

RNA Extraction and cDNA Synthesis

Total RNAs were extracted using Trizol reagent (Invitrogen, Carlsbad, CA, United States) following the manufacturer's instructions from male' and female' antennae. The quantity and quality of RNA were, respectively, detected using a Nanodrop ND-1000 spectrophotometer (NanoDrop Products, Wilmington, DE, United States) and gel electrophoresis. Single first strand cDNAs were synthesized using RevertAid First Strand cDNA Synthesis Kit (Thermo Scientific, United States).

Phylogenetic Analysis and Cloning of Pheromone Receptors

The sequences of *MsepOrco* and six *MsepPR* genes were identified by antennal transcriptomic analysis in our previous study (Du et al., 2018). For the phylogeny, we aligned six MsepPRs with previously identified PRs in *M. separata* (Mitsuno et al., 2008; Jiang et al., 2019) and four other closely related species in Lepidoptera, including *H. virescens* (Wang et al., 2010), *H. armigera* (Liu et al., 2013), *H. assulta* (Jiang et al., 2014c), and *S. litura* (Zhang and Löfstedt, 2015). Sequences were aligned using DNAMAN 7.0 (Lynnon Bioisoft, United States). Phylogenetic and molecular evolutionary analyses were conducted using MEGA 6.0 (Tamura et al., 2013).

To get the full-length open reading frame sequences of the candidate *MsepPRs*, 3' and 5' RACE were performed using a SMARTer RACE cDNA Amplification kit (Clontech, Mountain View, CA, United States). Specific primers were designed using Primer Premier 5.0 software (PREMIER Biosoft International, CA, United States) and were listed in **Supplementary Table 1**. The polymerase chain reactions were carried out under the following conditions: 95°C for 3 min; 35 cycles of 98°C for 10 s, 55°C for 30 s, 72°C for 1.5 min; 72°C for 10 min. PCR products were run on a 1.0% agarose gel, and sequences were verified by DNA sequencing after ligation into the cloning vector pEASY-Blunt (TransGen Biotech, China).

PR Expression in *Xenopus* Oocytes and Two-Electrode Voltage-Clamp Recordings

Open reading frames of *PR* genes were subcloned into the pT_7Ts vector based on the specific restriction enzyme digestion sites (**Supplementary Table 1**). Plasmids were fully linearized with corresponding restriction enzymes. cRNAs were synthesized using mMESSAGE mMACHINE SP6 kit (Thermo Scientific, United States). Purified cRNAs were diluted at a concentration of 2 μg/μL and stored at −80°C. Mature healthy oocytes were treated with 2 mg/mL collagenase type I in washing buffer for 1-2 h at room temperature (Liu et al., 2013). A mixture of 27.6 ng of *MsepPR* cRNA and *MsepOrco* cRNA was microinjected into oocytes. After 3–5 days of incubation at 18°C in 1 × Ringer's buffer (96 mM NaCl, 2 mM KCl, 5 mM $MgCl_2$, 0.8 mM $GaCl_2$, and 5 mM HEPES; pH 7.6 adjusted by NaOH) supplemented with 5% dialyzed horse serum, 50 μg/mL tetracycline, 100 μg/mL streptomycin, and 550 μg/mL sodium pyruvate, the injected oocytes were recorded with a two-electrode voltage clamp.

Four sex pheromone components and four pheromone analogs were dissolved in dimethyl sulfoxide (DMSO) to form the stock solutions (1 M) and stored at −20°C. Stock solutions were diluted in 1 × Ringer's buffer up to work concentration of 10^{-4} M. The negative control was 1 × Ringer's buffer. Currents induced by sex pheromone components were recorded using an OC-725C oocyte clamp (Warner Instruments, Hamden, CT, United States) at a holding potential of −80 mV. Between each stimulus, the oocytes were washed with 1 × Ringer's buffer to return to a stable baseline (Wang et al., 2010). Data were acquired and analyzed with Digidata 1440A and pCLAMP 10.0 software (Axon Instruments Inc., Union City, CA, United States).

Statistics and Data Analysis

Statistics were mainly analyzed using SPSS 22.0 (IBM Inc., Chicago, IL, United States) and bar-graphs were created with GraphPad Prism 5 (GraphPad Software, Inc., CA, United States). Data of EAG responses were analyzed using Student's *t*-test ($P < 0.05$ or $P < 0.01$). Odor responses were normalized using linear model for each neuron and clustered using the agglomerative hierarchical clustering method with HemI 1.0 (Deng et al., 2014). Data of two-electrode voltage-clamp recordings were analyzed using one-way ANOVA followed by LSD test ($P < 0.05$). Dose-response data were analyzed using GraphPad Prism 5 (GraphPad Software, Inc., CA, United States). Amino acid sequence alignment was performed using DNAMAN 7.0 (Lynnon Bioisoft, United States) and the phylogenetic tree was constructed using MEGA 6.0 (Tamura et al., 2013) and visualized and modified using FigTree 1.4.4 (Institute of Evolutionary Biology, University of Edinburgh, United Kingdom).

RESULTS

Electroantennogram Responses

In this study, four sex pheromone components and four pheromone analogs were chosen to evaluate the antennal EAG responses of male and female *M. separata*. The results showed that all tested compounds elicited EAG responses of male antennae at the dose of 100 μg (**Figure 1**). Major sex pheromone component Z11–16:Ald evoked the strongest EAG responses from antennae of male moths and showed highly significant differences between sexes ($P < 0.01$). The responses

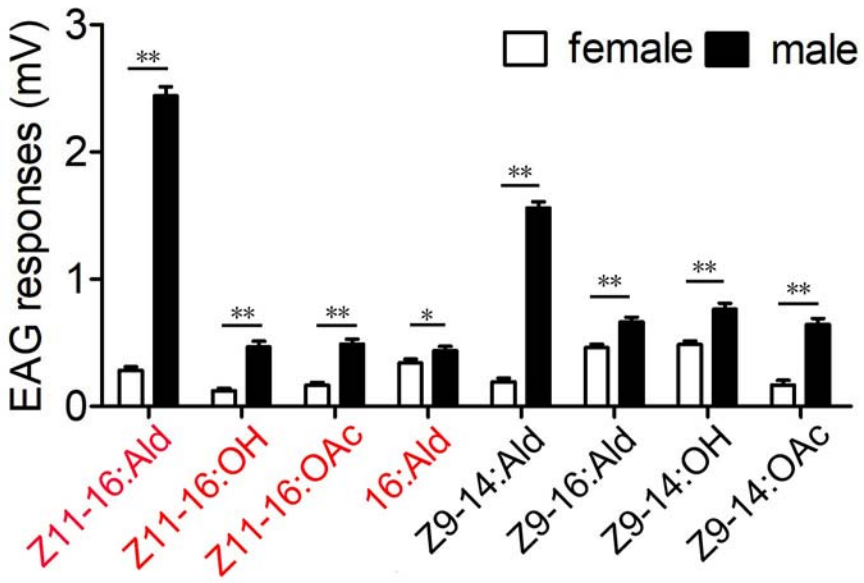

FIGURE 1 | Electroantennography (EAG) responses from antennae of male and female *M. separata* to four sex pheromone components (red) and four pheromone analogs (black). The EAG response values marked with asterisks represent significant differences between sexes (*, **, respectively, indicate significant differences under 0.05 and 0.01 levels, determined by a Student's *t*-test). Error bars indicate SEM ($n = 13$).

of male antennae were also significantly evoked by analog Z9–14:Ald. Minor pheromone components Z11–16:OH, Z11–16:OAc, 16:Ald and other analogs induced weak EAG responses. The EAG responses showed significant differences between male and female antennae for all tested compounds ($^{*}P < 0.05$ or $^{**}P < 0.01$; **Figure 1**).

Responses of ORNs to Sex Pheromones

Single sensillum recordings were extensively performed on the TS of male moths to test neuronal responses to four sex pheromone components and four pheromone analogs at the dose of 1 mg. In total, ORNs housed in 466 TS at different positions from all segments of male antennae were recorded. The functional patterns were clustered into four distinct types (named I, II, III, and IV) of TS (**Figure 2**), and each of them housed three neurons, named A, B and C based on the amplitude size of the spike (**Figures 3-A1, -B1, -C1, -D1**). Neuron A had the smallest action potential, followed by neuron B, while neuron C had the largest amplitude. We found that neurons housed in 403 TS were activated (**Figure 2**), and a great majority of those were type-I ($n = 293$), followed by type-II ($n = 70$), and type-IV ($n = 27$). Much less abundant responses were recorded with type-III ($n = 13$).

The activities of ORNs housed in different sensilla types revealed peripheral coding of sex pheromone components of male *M. separata*. ORN-B of type-I TS exhibited highly specific responses to the major component Z11–16:Ald and slight responses to analog Z9–14:Ald, while no responses of ORN-A and -C were activated to tested pheromone components (**Figure 3-A2** and **Supplementary Figure 1-A1**). We next measured dose-response curves of neurons housed in type-I TS to their active compounds across a dose range from 10^{-7} *g* to 2×10^{-3} *g*, showing that ORN-B in type-I TS are more sensitive to the major component Z11-16:Ald with an EC_{50} value of 2.58×10^{-4} *g* and low sensitivity to analog Z9-14:Ald with an EC_{50} value of 1.04×10^{-3} *g* (**Figure 3-A3** and **Supplementary Figures 1-A2, -A3**).

Type-II TS were divided into two sub-groups based on responses of ORN-B to analog Z9–14:OAc. In sub-group 1, there was no response of ORN activated by Z9–14:OAc, showing that ORN-A and -B of type-II TS mainly responded to minor pheromone components and their analogs. ORN-A in type-II TS were strongly activated by analog Z9–14:Ald, followed by minor components Z11–16:OAc and Z11–16:OH. ORN-B were activated by analog Z9–16:Ald (**Figure 3-B2** and **Supplementary Figure 1-B1**). The dose-response curves of ORN-A and -B are, respectively, shown in **Figures 3-B3,-B4**. ORN-A was more sensitive to analog Z9–14:Ald ($EC_{50} = 1.25 \times 10^{-4}$ *g*) than minor components Z11–16:OH ($EC_{50} = 3.23 \times 10^{-4}$ *g*) and Z11–16:OAc ($EC_{50} = 3.45 \times 10^{-4}$ *g*; **Supplementary Figures 1-B2, -B3, -B4, 3-B3**), while ORN-B was less sensitive to analog Z9–16:Ald with an EC_{50} value of 1.55×10^{-3} *g* (**Supplementary Figures 1-B5**, **3-B4**). The sub-group 2 (in a few cases) showed that ORN-A was activated by Z9–14:Ald, Z11–16:OH, Z9–14:OAc and Z9–14:OH (**Figure 2** and **Supplementary Figure 2**); ORN-B was also activated by analog Z9–16:Ald (**Supplementary Figures 2-A, -B**). Dose-response curves of ORN-A showed sensitivity to analog Z9–14:OAc with an EC_{50} value of 1.31×10^{-3} *g* (**Supplementary Figures 2-C, -D**).

ORN-B of type-III TS responded to minor component Z11–16:OAc and analog Z9–14:OAc (**Figure 3-C2** and **Supplementary Figure 1-C1**). ORN-B of type-IV TS mainly responded to minor component 16:Ald and had a small response to the major component Z11–16:Ald (**Figure 3-D2** and **Supplementary Figure 1-D1**). In type-III and -IV TS, there were neuronal responses to several concentrations of minor components Z11–16:OAc ($EC_{50} = 1.71 \times 10^{-4}$ *g*; **Figure 3-C3** and **Supplementary Figure 1-C2**) and 16:Ald ($EC_{50} = 2.76 \times 10^{-4}$ *g*; **Figure 3-D3** and **Supplementary Figure 1-D2**), respectively, suggesting increasing firing rate in a dose-related manner.

Gene Cloning and Sequence Analysis of *M. separata* PRs

We cloned the full-length of *MsepOrco* and six *MsepPR* genes (*MsepPR1*, *MsepPR2*, *MsepPR3*, *MsepPR4*, *MsepPR5*, *MsepPR6*) from published *M. separata* antennal transcriptome, which separately encode 473, 432, 435, 424, 445, 431, and 434 amino acids (Du et al., 2018). The amino acid sequences of MsepOrco and six MsepPRs from this study were used to construct a phylogenetic tree with two previously identified PRs from *M. separata* of the Kyoto geographic population (Mitsuno et al., 2008), seven PRs from *H. armigera*, six PRs from *H. assulta*, four PRs from *S. litura* and six PRs from *H. virescens*, and their Orco sequences, clearly showing a highly conserved Orco group and another PR clade (**Figure 4**). The PRs in this study clustered in different clades as follows: MsepPR1 and OR16; MsepPR2 and OR11; MsepPR3 and OR13; MsepPR4 and OR15; in addition to MsepPR5 and MsepPR6 (**Figure 4**). The identities of amino acid sequences in OR11, OR13, OR15, and OR16 clades were quite different (**Supplementary Figure 3**). The OR11 sequences from five closely related species were conserved with 80.59–81.96% similarity (**Supplementary Figure 3-B**), while other clades were relatively divergent (**Supplementary Figures 3-A, -C, -D**). We also compared the identities of amino acid sequence of MsepPR3 with two geographic populations in north China (MespOR3, Jiang et al., 2019), which showed 99.76% similarity with only one amino acid varying (**Supplementary Figure 4**). The amino acid sequences of MsepOrco between the two geographic populations were exactly the same (**Supplementary Figure 4**). All of the *PR* genes identified from *M. separata* in different geographic populations are listed in **Supplementary Table 2**.

Functional Characterization of *M. separata* PRs in the *Xenopus* Oocyte Expression System

In this study, responses of five PRs to sex pheromone components were recorded using a two-electrode voltage clamp. In total, four sex pheromone components and four pheromone analogs at the concentration of 10^{-4} M were tested. The responses of MsepPR1 with a high expression level in male antenna were mainly tuned to analog Z9–14:Ald (787 ± 71 nA), followed by minor sex pheromone component Z11–16:OH and analog

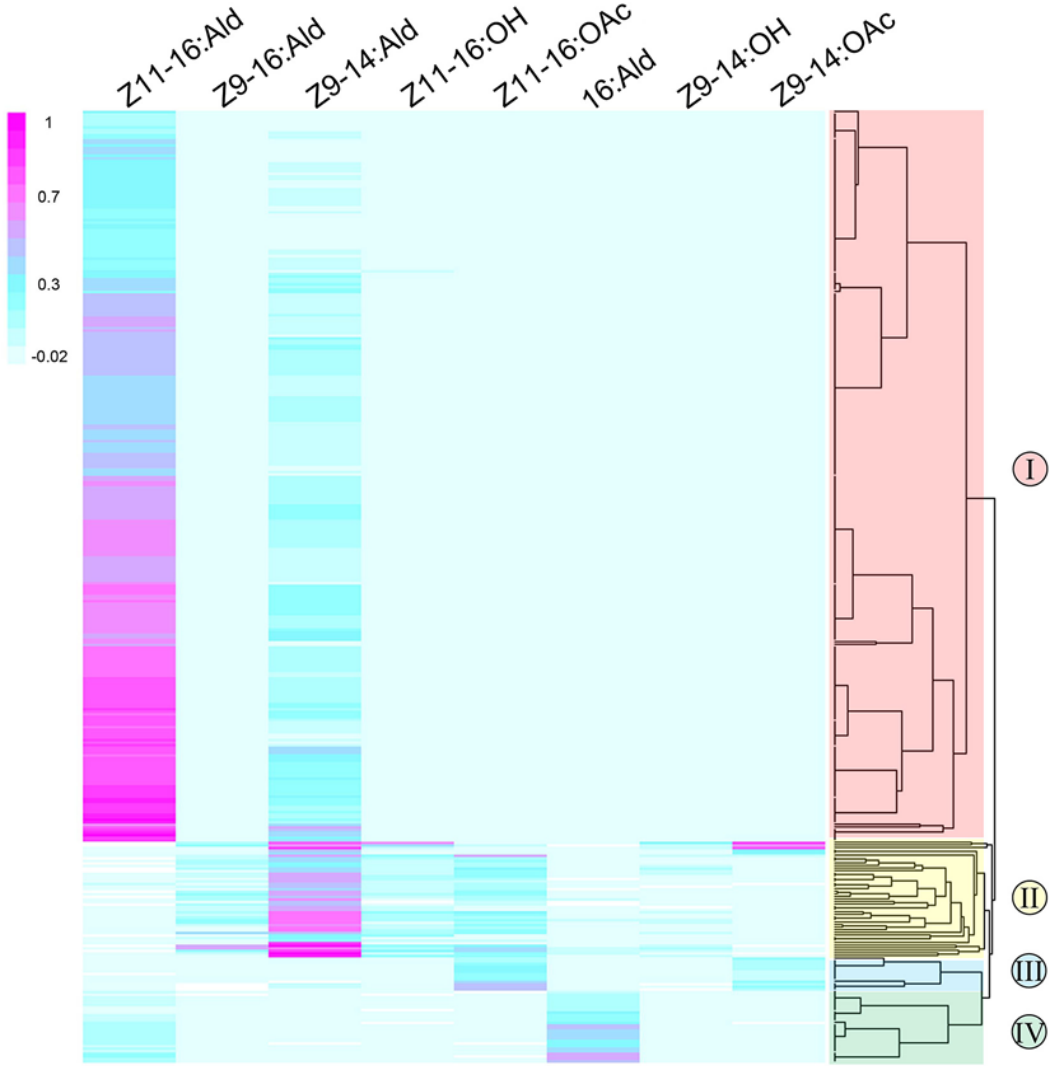

FIGURE 2 | Response profiles of functional ORNs housed in 403 TS in the antennae of male *M. separata* (*y*-axis) in response to four sex pheromone components and four pheromone analogs (*x*-axis). The classification dendrogram was generated using the agglomerative hierarchical clustering method, leading to four functional TS types (I, II, III, and IV). Responses are normalized using linear model and color coded for each neuron. Magenta indicates a strong response of ORNs to odorants; blue, weak excitation; light blue, no response; white indicates that spontaneous spiking activity was reduced compared to baseline.

Z9–14:OAc with current values of 460 ± 56 and 151 ± 47 nA, respectively, (**Figure 5A** and **Supplementary Figure 5-A1**). In a dose-response experiment, MsepPR1/MsepOrco was sensitive to Z9–14:Ald at concentrations as low as 10^{-6} M with an EC_{50} value of 4.90×10^{-5} M (**Figure 5B** and **Supplementary Figure 5-A2**). MsepPR5 had a high expression level in female antennae and was tuned to analogs Z9–14:Ald (254 ± 26 nA) and Z9–14:OAc (268 ± 18 nA), and was also slightly activated by the major sex pheromone component Z11–16:Ald and minor component Z11–16:OH with the current values of 125 ± 32 and 54 ± 11 nA, respectively, (**Figure 5C** and **Supplementary Figure 5-B1**). Dose-response study showed MsepPR5/MsepOrco was sensitive to Z9–14:Ald at concentrations as low as 10^{-6} M with an EC_{50} value of 3.04×10^{-5} M (**Figure 5D** and **Supplementary Figure 5-B2**). MsepPR6 expressed in male antenna was specifically tuned to analog Z9–14:OAc with a large current value of 2764 ± 285 nA (**Figure 5E** and **Supplementary Figure 5-C1**). Dose-response study showed MsepPR6/MsepOrco was sensitive to Z9–14:OAc at concentrations as low as 10^{-7} M with an EC_{50} value of 7.46×10^{-7} M (**Figure 5F** and **Supplementary Figure 5-C2**). MsepPR2 and MsepPR4 showed no response to any tested compounds (**Supplementary Figure 6**).

DISCUSSION

Courtship and mating behaviors in moths largely rely on sex pheromones released from females, which are artificially applied to lure males and for population monitoring in pest control. Male moths could recognize intra- and inter-specific sex

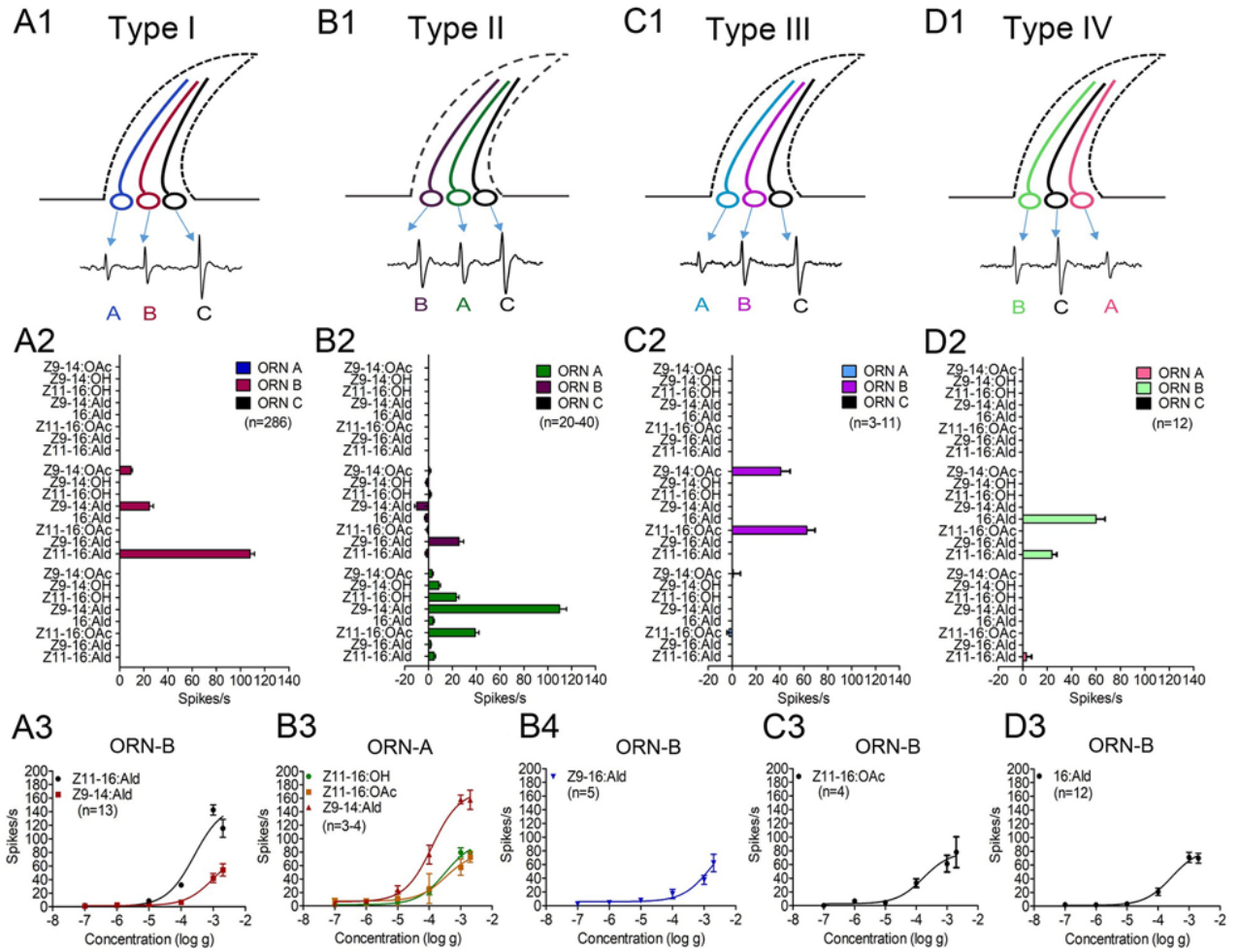

FIGURE 3 | Response profiles of three distinct ORNs (-A, -B, -C) and dose-response curves of functional ORNs housed in four types of TS (type I, II, III, and IV) on the antennae of male *M. separata* in response to four sex pheromone components and four pheromone analogues. **(A1,B1,C1,D1)** Distinct ORNs housed in four types of TS. **(A2,B2,C2,D2)** Response profiles of distinct ORNs housed in four types of TS. The amount of each stimulus was 1 mg. The responses of ORN-B of type-I TS were 101 ± 2 spikes/s (n = 286) for Z11–16:Ald and 27 ± 1 spikes/s (n = 286) for Z9–14:Ald. The ORN-A of type-II TS was activated by Z9–14:Ald, Z11–16:OAc, Z11–16:OH, with responses of 110 ± 6 spikes/s (n = 40), 39 ± 3 spikes/s (n = 40), and 23 ± 2 spikes/s (n = 40), respectively. Responses of ORN-B were 26 ± 4 spikes/s (n = 40) for Z9–16:Ald. The ORN-B of type-III TS was activated by Z11–16:OAc and Z9–14:OAc with responses of 63 ± 7 spikes/s (n = 11) and 41 ± 8 spikes/s (n = 3), respectively. The ORN-B of type-IV TS was activated by 16:Ald and Z11–16:Ald with responses of 60 ± 7 spikes/s (n = 12) and 24 ± 4 spikes/s (n = 12). **(A3,B3,B4,C3,D3)** Dose-response curves of functional ORNs. The order of the neurons among sensilla types and color code were random. Error bars indicate mean ± SEM.

pheromones to multiply and keep species isolation. In this study, four functional types of TS were characterized. Type-I TS was responsible for the major pheromone component Z11–16:Ald, type-II TS was responsible for the minor pheromone component Z11–16:OH, behavioral antagonist Z9–14:Ald and some inter-specific pheromones. Type-III and -IV TS recognized minor pheromone components Z11–16:OAc and 16:Ald, respectively. Subsequently, putative PRs were functionally characterized. Our results help to improve the olfactory coding of sex pheromones and inter-specific pheromones in the peripheral neuron system.

Functions of ORNs housed in each type of TS were characterized using the SSR technique. Unlike the results of two types of TS identified by Jiang et al. (2020), we characterized four functional types of TS housed 12 ORNs in *M. separata*, implying that peripheral coding in olfaction of *M. separata* was more complicated than in other Lepidoptera moths such as *H. armigera* and closely related species (Wu et al., 2013; Zhang et al., 2013; Sakurai et al., 2014; Chang et al., 2016; Liu et al., 2018). Our results show that five ORNs are separately activated by major and minor sex pheromone components and their analogs (**Figure 3**). Of those, ORN-B housed in type-I TS is considered the neuron type detecting the major pheromone component and represents the most frequently occuring neuron type in our recordings. This result is consistent with a recent study by Jiang et al. (2020). Otherwise, their previous work indicated that MsepOR3 (equal to MsepPR3 in this study, see **Supplementary Figure 4**) was tuned to the major component Z11–16:Ald and analog Z9–14:Ald from *M. separata*, inferring that an *MsepOR3*-expressing neuron may

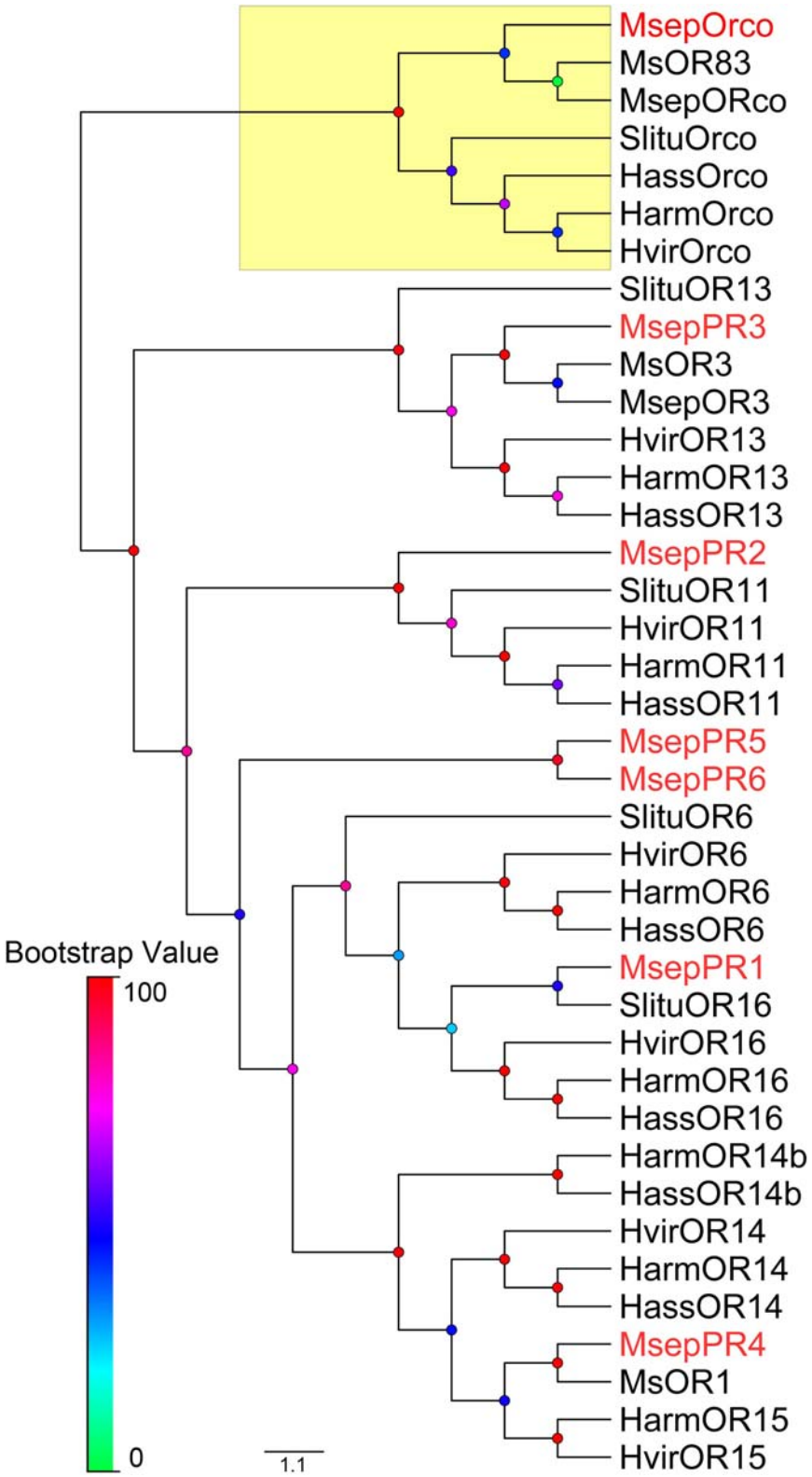

FIGURE 4 | Phylogenetic tree of PRs from *M. separata* and four other Lepidoptera species. Msep: *M. separata* (red), Msep: *M. separata* (black, Jiang et al., 2019, 2020), Ms: *M. separata* (black, Mitsuno et al., 2008), Harm: *Helicoverpa armigera*, Hass: *H. assulta*, Hvir: *Heliothis virescens*, and Slitu: *Spodoptera litura*. The Orco clade is marked with yellow. This tree was inferred using the neighbor-joining method. Node support was assessed with 1,000 bootstrap replicates.

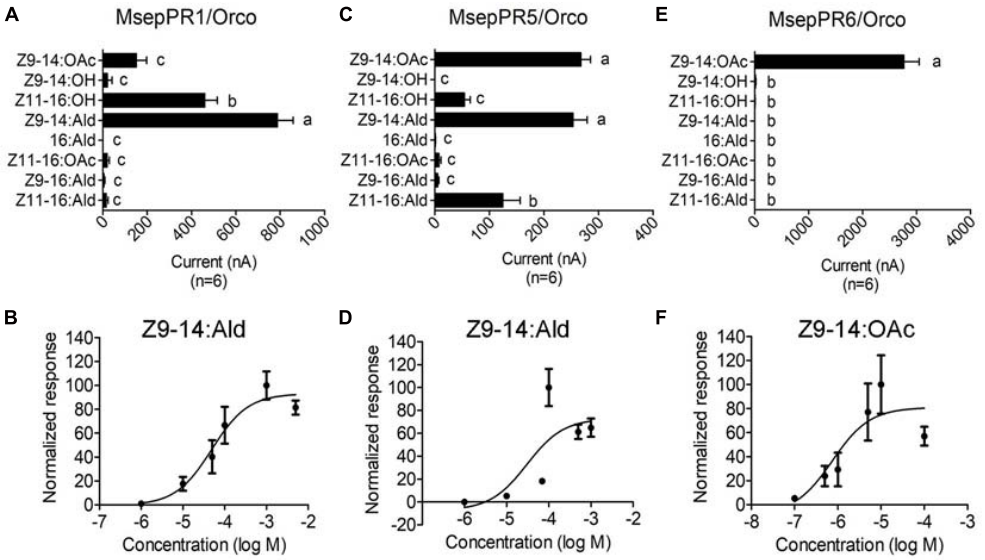

FIGURE 5 | Response profiles of MsepPR1/Orco, MsepPR5/Orco, and MsepPR6/Orco to four sex pheromone components and four pheromone analogs in *Xenopus* oocyte system. **(A,C,E)** Response profiles of MsepPR1/Orco, MsepPR5/Orco, and MsepPR6/Orco in response to 10^{-4} M solution of stimuli. Error bars indicate mean ± SEM (n = 6). Comparisons between groups were made using ANOVA followed by LSD's test. Different letters above the error bars indicated significant difference at the 0.05 level. **(B)** Dose-response curves of MsepPR1/Orco expressed in *Xenopus* oocyte to Z9–14:Ald. EC_{50} = 4.90 × 10^{-5} M. Error bars indicate mean ± SEM (n = 10). **(D)** Dose-response curves of MsepPR5/Orco to Z9–14:Ald. EC_{50} = 3.04 × 10^{-5} M. Error bars indicate mean ± SEM (n = 5). **(F)** Dose-response curves of MsepPR6/Orco to Z9–14:OAc. EC_{50} = 7.46 × 10^{-7} M. Error bars indicate mean ± SEM (n = 8). Responses are normalized by defining the average response as 100.

be ORN-B of type-I TS based on identical function and the axons from this neuron projects to the cumulus (CU) of the MGC in male antennal lobes (ALs; **Figure 6**). Moreover, since a majority of ORN-B of type-I TS are recorded in response to the major component Z11–16:Ald, it might explain why the largest EAG activities are observed from male antennae (**Figure 1**).

In our study, the response profiles of neurons of type-II TS are quite similar with those in B type sensilla reported by Jiang et al. (2020). However, the number of active neurons between these two studies is different. The results by Jiang et al. (2020) showed that three neurons and three different subunits of MGC were activated by Z9–16:Ald, Z11–16:OAc, Z9–14:Ald and Z11–16:OH, respectively, according to the evidence provided by SSR technology and *in vivo* optical imaging methods, while our study had its limitation for characterizations of active neurons at peripheral neuron system based on the amplitude size of the spike. We preliminarily identified two active neurons, one (ORN-A) was activated by Z9–14:Ald, Z11–16:OH and Z11–16:OAc, another (ORN-B) was activated by Z9–16:Ald. In fact, neurons activated by Z11–16:OAc and Z11–16:OH in our study were hard to distinguish according to the shape and size of the spike. Therefore, we integrated the results in our studies and in reported studies by Jiang et al. (2019, 2020), and divided neurons of type-II TS into four ORNs. We drew a schematic diagram in **Figure 6**, showing that Z11–16:OAc activated ORN-A, Z9–14:Ald and Z11–16:OH activated ORN-B, Z9–16:Ald activated ORN-C of type-II TS, respectively.

In *H. armigera*, Z9–14:Ald is an agonist at low concentrations and becomes an antagonist at high concentrations when in combination with other compounds (Gothilf et al., 1978; Kehat and Dunkelblum, 1990; Zhang et al., 2012; Wu et al., 2015). Further functional characterization showed that Z9–14:Ald was recognized by HarmOR14b, HarmOR16, and HarmOR6 expressed in Type B or Type C TS (Liu et al., 2013; Chang et al., 2016; Wang et al., 2018). In this study, we found that analog Z9–14:Ald could strongly elicit the ORN-B of type-II TS of *M. separata*, and also ORN-B of type-I TS with mild sensitivity (**Figure 6**), corresponding to a recent study that Z9–14:Ald activated the CU and the dorso-anterior (DA) of the MGC in ALs of male *M. separata* (Jiang et al., 2020). Wind tunnel assay further indicated that addition of Z9–14:Ald at the ratio of 1:1, 1:10, and 1:100 greatly reduced the attractiveness of *M. separata* to Z11–16:Ald (Jiang et al., 2020), suggesting that Z9–14:Ald plays vital roles in species isolation of *M. separata* and its function as antagonist within noctuid moths is conserved in the evolution. We also found that MsepPR1 was homologous with OR16 from *H. virescens*, *H. armigera*, *H. assulta,* and *S. litura*, and shared 70.02–73.61% identities of conserved amino acid sequences (Wang et al., 2011; Liu et al., 2013; Jiang et al., 2014c; Zhang and Löfstedt, 2015), indicating that they may have the same function. The *Xenopus* oocyte *in vitro* study showed that MsepPR1 was a PR for detecting Z9–14:Ald, Z11–16:OH and Z9–14:OAc, which was consistent with the SSR recording from the ORN-B of type-II TS, especially in sub-group 2, suggesting that MsepPR1 may be expressed in this neuron with its axon projecting to the DA of MGC (**Figure 6**).

In our experiments, MsepPR6-expressing oocytes responded highly to analog Z9–14:OAc, also known as the interspecific

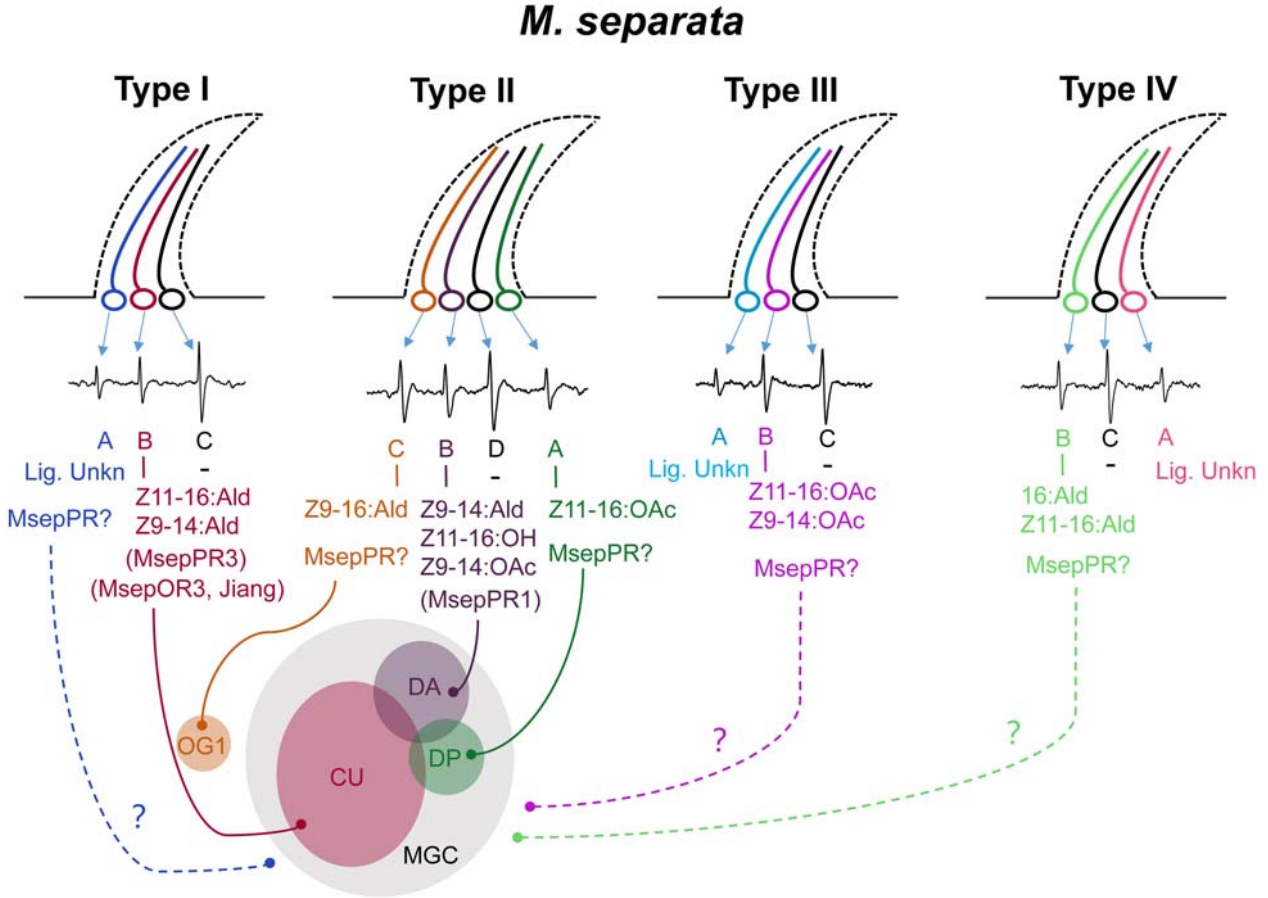

FIGURE 6 | A schematic diagram of olfactory coding of sex pheromones and analogs in male *M. separata* at the peripheral and central nervous system. Four functional types of TS were characterized. The classification of neurons housed in type-II TS is modified by our SSR recording and the reported results by Jiang et al. (2020). Neuron of type-II TS activated by Z11–16:OAc is divided as a active one. In total, six ORNs are separately activated by major and minor sex pheromone components and their analogs. "–" indicates the largest spontaneous action potential without ligands identified. "Lig. Unkn" indicates no ligand has been characterized for a specific neuron by SSR recording. The curves with solid lines indicate candidate project pathways. The curves with dotted lines indicate unknown project pathways. MGC, macroglomerular complex; CU, cumulus; DA, dorso-anterior; DP, dorso-posterior; and OG1, ordinary glomerulus 1.

pheromones of *S. frugiperda* (Groot et al., 2008), *Agrotis segetum* (Zhang and Löfstedt, 2013), *S. exigua* (Liu et al., 2013), *S. litura* (Zhang and Löfstedt, 2015), and *A. lepigone* (Zhang et al., 2019). Thus, MsepPR6 may be involved in reproductive isolation of *M. separata*. However, we did not find potential neurons elicited by Z9–14:OAc alone. In addition, the expression level of *MsepPR6* gene was low in male antennae (Du et al., 2018). We therefore speculate that the *MsepPR6*-expressing neuron is not characterized in our experiments. However, identifying more functions needs support from experiments such as *in situ* hybridization and CRISPR-Cas9 technology.

In a previous study, Z11–16:OAc and Z11–16:OH were isolated at a ratio of 8:1 from female abdominal tips of *Leucania separata* Walker, a geographic population of Japan (Takahashi et al., 1979). Later, MsOR1 was identified and characterized as a major PR responding to Z11–16:OAc (Mitsuno et al., 2008). The phylogenetic analysis in this study revealed that MsOR1 (geographic population of Kyoto) and MsepPR4 (geographic population of north China) were homologous to HvirOR15 and HarmOR15 in the PR15 clade, which had no ligands based on previous studies (Wang et al., 2011; Liu et al., 2013). In our experiments, MsepPR4 did not respond to any sex pheromone components or their analogs but shared 91.24% identity of amino acid sequences with MsOR1. The functional differentiation of PRs in different geographic populations could be explained by variation of key sites of amino acid sequences. Besides, responses in ORN-A of type-II TS, ORN-B of type-III TS and ORN-B of type-IV TS were elicited by the minor sex pheromones Z11–16:OAc and 16:Ald, respectively. However, the PRs expressed in these types of TS and subunits of the MGC in ALs are still unknown (**Figure 6**). This phenomenon may be explained by limiting conditions such as the lack of other co-factor PBPs and SNMPs in the *Xenopus* oocyte system or unidentified PRs in a novel lineage of the PR clade (Große-Wilde et al., 2006; Benton et al., 2007; Sun et al., 2013; Chang H. et al., 2015; Wang et al., 2016; Bastin-Héline et al., 2019; Shen et al., 2020).

In this study, we found that the number of ORNs, which had the largest spontaneous action potential recorded by a tungsten

wire electrode (ORN-C of type-I, -III, -IV TS, and ORN-D of type-II TS, see **Figure 6**), housed in each type of TS is quite low. Similar action potentials were also recorded in coeloconic sensilla of *M. separata* (Tang et al., 2020), *Manduca sexta* (Zhang et al., 2019), and *Drosophila melanogaster* (Benton et al., 2009). We speculate that non-responding neurons in TS to express for example IRs and to respond to other odor classed than pheromones. Further study is needed to confirm it.

It is worth mentioning that female moths could also detect sex pheromones emitted from inter- and intra-specific females. Several behavioral assays revealed that female moths detected such sex pheromones to repel conspecific females, reduce mating, increase movements and flight activity to a significant degree, and improve chances of progeny survival (Ellis et al., 1980; Saad and Scott, 1981; Stelinski et al., 2014; Holdcraft et al., 2016). In this study, we tested the function of MsepPR5, which was specifically highly expressed in female antennae (Du et al., 2018), showing that it could be activated by the major sex pheromone component Z11–16:Ald, antagonist Z9–14:Ald and interspecific pheromone component Z9–14:OAc, espeacially from the genus *Spodoptera* (Tamaki et al., 1973; Teal et al., 1985; Fumiaki et al., 1993). MsepPR5 is hypothesized to play an important role in sex pheromone detection of female moths, and to be involved in repellent behavior through perception of high population density in order to reduce resource competition among progeny (Pearson et al., 2004). However, the molecular mechanism of olfactory recognition of sex pheromones in female *M. separata*, is still unknown and requires follow-up experiments.

DATA AVAILABILITY STATEMENT

The datasets presented in this study can be found in online repositories. The names of the repository/repositories and accession number(s) can be found in the article/ **Supplementary Material**.

AUTHOR CONTRIBUTIONS

CW, BW, and GW designed the experiments. CW performed the experiments and analyzed the data. BW and GW contributed reagents and materials. CW, BW, and GW wrote and revised the manuscript. All authors contributed to the article and approved the submitted version.

FUNDING

This project was supported by the National Natural Science Foundation of China (31725023 and 31911530234) and the Shenzhen Science and Technology Program (KQTD20180411143628272).

ACKNOWLEDGMENTS

We thank master student Yang Jing for supplying the *Mythimna separata* moths.

SUPPLEMENTARY MATERIAL

The Supplementary Material for this article can be found online at: https://www.frontiersin.org/articles/10.3389/fnana.2021.673420/full#supplementary-material

REFERENCES

Ando, T., Inomata, S., and Yamamoto, M. (2004). Lepidopteran sex pheromones. *Top. Curr. Chem.* 239, 51–96. doi: 10.1007/b95449

Bastin-Héline, L., Fouchier, A. D., Cao, S., Koutroumpa, F., Caballero-Vidal, G., Robakiewicz, S., et al. (2019). A novel lineage of candidate pheromone receptors for sex communication in moths. *eLife* 8:e49826.

Benton, R., Vannice, K. S., Gomez-Diaz, C., and Vosshall, L. B. (2009). Variant ionotropic glutamate receptors as chemosensory receptors in *Drosophila*. *Cell* 136, 149–162. doi: 10.1016/j.cell.2008.12.001

Benton, R., Vannice, K. S., and Vosshall, L. B. (2007). An essential role for a CD36-related receptor in pheromone detection in *Drosophila*. *Nature* 450, 289–293. doi: 10.1038/nature06328

Cao, S., Liu, Y., Guo, M., and Wang, G. (2016). A conserved odorant receptor tuned to floral volatiles in three Heliothinae species. *PLoS One* 11:e0155029. doi: 10.1371/journal.pone.0155029

Chang, H., Guo, M., Wang, B., Liu, Y., Dong, S., and Wang, G. (2016). Sensillar expression and responses of olfactory receptors reveal different peripheral coding in two *Helicoverpa* species using the same pheromone components. *Sci. Rep.* 6:18742.

Chang, H., Liu, Y., Yang, T., Pelosi, P., Dong, S., and Wang, G. (2015). Pheromone binding proteins enhance the sensitivity of olfactory receptors to sex pheromones in *Chilo suppressalis*. *Sci. Rep.* 5:13093.

Chang, X. Q., Nie, X. P., Zhang, Z., Zeng, F. F., Lv, L., Zhang, S., et al. (2017). *De novo* analysis of the oriental armyworm *Mythimna separata* antennal transcriptome and expression patterns of odorant-binding proteins. *Comp. Biochem. Physiol. D Genomics Proteomics* 22, 120–130. doi: 10.1016/j.cbd.2017.03.001

Chang, X. Q., Zhang, S., Lv, L., and Wang, M. Q. (2015). Insight into the ultrastructure of antennal sensilla of *Mythimna separata* (Lepidoptera: Noctuidae). *J. Insect. Sci.* 15:124. doi: 10.1093/jisesa/iev103

Chen, Q. H., Zhu, F., Tian, Z. H., Zhang, W. M., Guo, R., Liu, W. C., et al. (2018). Minor components play an important role in interspecific recognition of insects: a basis to pheromone based electronic monitoring tools for rice pests. *Insects* 9:192. doi: 10.3390/insects9040192

Deng, W., Wang, Y., Liu, Z., Cheng, H., and Xue, Y. (2014). HemI: a toolkit for illustrating heatmaps. *PLoS One* 9:e111988. doi: 10.1371/journal.pone.0111988

Du, L., Zhao, X., Liang, X., Gao, X., Liu, Y., and Wang, G. (2018). Identification of candidate chemosensory genes in *Mythimna separata* by transcriptomic analysis. *BMC Genomics* 19:518. doi: 10.1186/s12864-018-4898-0

Ellis, P. E., Brimacombe, L. C., Mcveigh, L. J., and Dignan, A. (1980). Laboratory experiments on the disruption of mating in the Egyptian cotton leafworm *Spodoptera littoralis* (Boisduval) (Lepidoptera: Noctuidae) by excesses of female pheromones. *Bull. Entomol. Res.* 70, 673–684. doi: 10.1017/s0007485300007963

El-Sayed, A. M., Manning, L. A., Unelius, C. R., Park, K. C., Stringer, L. D., White, N., et al. (2009). Attraction and antennal response of the common wasp, *Vespula Vulgaris* (L.), to selected synthetic chemicals in New Zeal and beech forests. *Pest Manage. Sci.* 65, 975–981. doi: 10.1002/ps.1782

Fónagy, A., Moto, K., Ohnishi, A., Kurihara, M., Kis, J., and Matsumoto, S. (2011). Studies of sex pheromone production under neuroendocrine control

by analytical and morphological means in the oriental armyworm, *Pseudaletia separata*, Walker (Lepidoptera: Noctuidae). *Gen. Comp. Endocrinol.* 172, 62–76. doi: 10.1016/j.ygcen.2011.02.018

Fumiaki, M., Tatsuaki, S., Toshiaki, I., and Sadao, W. (1993). Electrophysiological responses of the male antenna to compounds found in the female sex pheromone gland of *Spodoptera exigua*, (Hubner) (Lepidoptera:Noctuidae). *Appl. Entomol. Zool.* 28, 489–496. doi: 10.1303/aez.28.489

Gothilf, S., Kehat, M., Jacobson, M., and Galun, R. (1978). Sex attractants for male *Heliothis armigera* (Hbn.). *Experientia* 34, 853–854. doi: 10.1007/bf01939662

Gould, F., Estock, M., Hillier, N. K., Powell, B., Groot, A. T., Ward, C. M., et al. (2010). Sexual isolation of male moths explained by a single pheromone response QTL containing four receptor genes. *Proc. Natl. Acad. Sci. U.S.A.* 107, 8660–8665. doi: 10.1073/pnas.0910945107

Groot, A. T., Marr, M., Schöfl, G., Lorenz, S., Svatos, A., and Heckel, D. G. (2008). Host strain specific sex pheromone variation in *Spodoptera frugiperda*. *Front. Zool.* 5:20. doi: 10.1186/1742-9994-5-20

Große-Wilde, E., Svatos, A., and Krieger, J. (2006). A pheromone-binding protein mediates the bombykol-induced activation of a pheromone receptor *in vitro*. *Chem. Senses* 31, 547–555. doi: 10.1093/chemse/bjj059

Hallem, E. A., Ho, M. G., and Carlson, J. R. (2004). The Molecular basis of odor coding in the *Drosophila* antenna. *Cell* 117, 965–979. doi: 10.1016/j.cell.2004.05.012

Hansson, B. S., and Stensmyr, M. C. (2011). Evolution of insect olfaction. *Neuron* 72, 698–711. doi: 10.1016/j.neuron.2011.11.003

He, Y. Q., Feng, B., Guo, Q. S., and Du, Y. (2017). Age influences the olfactory profiles of the migratory oriental armyworm *Mythimna separate* at the molecular level. *BMC Genomics* 18:32. doi: 10.1186/s12864-016-3427-2

Heinbockel, T., and Kaissling, K. E. (1996). Variability of olfactory receptor neuron responses of female silkmoths (*Bombyx mori* L.) to benzoic acid and (±)-linalool. *J. Insect Physiol.* 42, 565–578. doi: 10.1016/0022-1910(95)00133-6

Holdcraft, R., Rodriguez-Saona, C., and Stelinski, L. L. (2016). Pheromone autodetection: evidence and implications. *Insects* 7:17. doi: 10.3390/insects7020017

Jiang, N. J., Tang, R., Guo, H., Ning, C., Li, J. C., Wu, H., et al. (2020). Olfactory coding of intra- and interspecific pheromonal messages by the male *Mythimna separata* in North China. *Insect Biochem. Mol. Biol.* 125:103439. doi: 10.1016/j.ibmb.2020.103439

Jiang, N. J., Tang, R., Wu, H., Xu, M., Ning, C., Huang, L. Q., et al. (2019). Dissecting sex pheromone communication of *Mythimna separata* (Walker) in North China from receptor molecules and antennal lobes to behavior. *Insect Biochem. Mol. Biol.* 111:103176. doi: 10.1016/j.ibmb.2019.103176

Jiang, X., Luo, L., Zhang, L., Sappington, T. W., and Hu, Y. (2011). Regulation of migration in *Mythimna separata* (Walker) in China: a review integrating environmental, physiological, hormonal, genetic, and molecular factors. *Environ. Entomol.* 40, 516–533. doi: 10.1603/en10199

Jiang, X. F., Zhang, L., Cheng, Y. X., and Luo, L. Z. (2014a). Novel features, occurrence trends and economic impact of the oriental armyworm, *Mythimna separata* (Walker) in China. *CHS J. Appl. Entomol.* 51, 1444–1449.

Jiang, X. F., Zhang, L., Cheng, Y. X., and Luo, L. Z. (2014b). Current status and trends in research on the oriental armyworm, *Mythimna separata* (Walker) in China. *CHS J. Appl. Entomol.* 51, 881–889.

Jiang, X. J., Guo, H., Di, C., Yu, S., Zhu, L., Huang, L. Q., et al. (2014c). Sequence similarity and functional comparisons of pheromone receptor orthologs in two closely related *Helicoverpa* species. *Insect Biochem. Mol. Biol.* 48, 63–74. doi: 10.1016/j.ibmb.2014.02.010

Jung, J. K., Seo, B. Y., Cho, J. R., and Kim, Y. (2013). Monitoring of Mythimna separata adults by using a remote-sensing sex pheromone trap. *Korean J. Appl. Entomol.* 52, 341–348. doi: 10.5656/ksae.2013.10.0.058

Kaissling, K. E. (1986). Chemo-electrical transduction in insect olfactory receptors. *Annu. Rev. Neurosci.* 9, 121–145. doi: 10.1146/annurev.ne.09.030186.001005

Kaissling, K. E. (2004). Physiology of pheromone reception in insects (an example of moths). *ANIR* 6, 73–91.

Kehat, M., and Dunkelblum, E. (1990). Behavioral responses of male *Heliothis armigera* (Lepidoptera: Noctuidae) moths in a flight tunnel to combinations of components identified from female sex pheromone glands. *J. Insect Behav.* 3, 75–83. doi: 10.1007/bf01049196

Kou, R., Chow, Y. S., and Ho, H. Y. (1992). Chemical composition of sex pheromone gland extract in female oriental armyworm *Pseudaletia separata* Walker (Lepidoptera, Noctuidae) in Taiwan. *Bull. Zool. Acad. Sin.* 31, 246–250.

Leal, W. S. (2005). "*Pheromone reception*," in *The Chemistry of Pheromones and Other Semiochemicals II*, Vol. 240, ed. S. Schulz (Berlin: Springer), 1–36.

Leal, W. S. (2013). Odorant reception in insects: roles of receptors, binding proteins and degrading enzymes. *Annu. Rev. Entomol.* 58, 373–391. doi: 10.1146/annurev-ento-120811-153635

Lebedeva, K. V., Vendilo, N. V., Kurbatov, S. A., Pletnev, V. A., Ponomarev, V. L., Pyatnova, Y. B., et al. (2000). Identification of the pheromone of eastern-meadow cutworm *Mythimna separata* (Lepidoptera: Noctuidae). *Agrokhimiya* 5, 57–69.

Linn, C. E., and Roelofs, W. L. (1995). "Pheromone communication in moths and its role in the speciation process," in *Speciation and the Recognition Concept: Theory and Application*, eds D. M. Lambert and H. G. Spencer (London: John Hopkins University), 263–300.

Liu, W., Jiang, X.-C., Cao, S., Yang, B., and Wang, G. R. (2018). Functional studies of sex pheromone receptors in asian corn borer *ostrinia furnacalis*. *Front. Physiol.* 9:591. doi: 10.3389/fphys.2018.00591

Liu, Y., Liu, C., Lin, K., and Wang, G. (2013). Functional specificity of sex pheromone receptors in the cotton bollworm *Helicoverpa armigera*. *PLoS One* 8:e62094. doi: 10.1371/journal.pone.0062094

Liu, Z., Wang, X., Lei, C., and Zhu, F. (2017). Sensory genes identification with head transcriptome of the migratory armyworm, *Mythimna separata*. *Sci. Rep.* 7:46033.

Mitsuno, H., Sakurai, T., Murai, M., Yasuda, T., Kugimiya, S., Ozawa, R., et al. (2008). Identification of receptors of main sex-pheromone components of three *Lepidopteran* species. *Eur. J. Neurosci.* 28, 893–902. doi: 10.1111/j.1460-9568.2008.06429.x

Nakagawa, T., Sakurai, T., Nishioka, T., and Touhara, K. (2005). Insect sex-pheromone signals mediated by specific combinations of olfactory receptors. *Science* 307, 1638–1642. doi: 10.1126/science.1106267

Pearson, G. A., Dillery, S., and Meyer, J. R. (2004). Modeling intra-sexual competition in a sex pheromone system: How much can female movement affect female mating success? *J. Theor. Biol.* 231, 549–555. doi: 10.1016/j.jtbi.2004.07.010

Rutzler, M., and Zwiebel, L. J. (2005). Molecular biology of insect olfaction: recent progress and conceptual models. *J. Comp. Physiol. A Neuroethol. Sens. Neural Behav. Physiol.* 191, 777–790. doi: 10.1007/s00359-005-0044-y

Saad, A. D., and Scott, D. R. (1981). Repellency of pheromones released by females of *Heliothis armigera* and *H. zea* to females of both species. *Entolmol. Exp. Appl.* 30, 123–127. doi: 10.1111/j.1570-7458.1981.tb03085.x

Sakurai, T., Nakagawa, T., Mitsuno, H., Mori, H., Endo, Y., Tanoue, S., et al. (2004). Identification and functional characterization of a sex pheromone receptor in the silkmoth *Bombyx mori*. *Proc. Natl. Acad. Sci. U.S.A.* 101, 16653–16658. doi: 10.1073/pnas.0407596101

Sakurai, T., Namiki, S., and Kanzaki, R. (2014). Molecular and neural mechanisms of sex pheromone reception and processing in the silkmoth *Bombyx mori*. *Front. Physiol.* 5:125. doi: 10.3389/fphys.2014.00125

Shen, S., Cao, S., Zhang, Z., Kong, X., Liu, F., Wang, G., et al. (2020). Evolution of sex pheromone receptors in *Dendrolimus punctatus* Walker (Lepidoptera: Lasiocampidae) is divergent from other moth species. *Insect Biochem. Mol. Biol.* 122:103375. doi: 10.1016/j.ibmb.2020.103375

Song, Y., Zhang, L., Cheng, Y., Luo, L., Jiang, X., and Li, K. (2017). Identification of the characteristic components of female sex pheromone of the oriental armyworm *Mythimna separata* and attractive effects of them in different ratios indoors. *J. Plant Protect.* 44, 393–399.

Stelinski, L., Holdcraft, R., and Rodriguez-Saona, C. (2014). Female moth calling and flight behavior are altered hours following pheromone autodetection: possible implications for practical management with mating disruption. *Insects* 5, 459–473. doi: 10.3390/insects5020459

Sun, M., Liu, Y., Walker, W. B., Liu, C., Lin, K., Gu, S., et al. (2013). Identification and characterization of pheromone receptors and interplay between receptors and pheromone binding proteins in the diamondback moth, *Plutella xyllostella*. *PLoS One* 8:e62098. doi: 10.1371/journal.pone.0062098

Takahashi, S., Kawaradani, M., Sato, Y., and Sakai, M. (1979). Sex pheromone components of *Leucania separta* Walker and *Leucania loreyi* Duponchel. *Jpn. J. Appl. Entomol. Zool.* 23, 78–81. doi: 10.1303/jjaez.23.78

Tamaki, Y., Noguchi, H., and Yushima, T. (1973). Sex pheromone of *Spodoptera litura* (F.) (Lepidoptera: Noctuidae): isolation, identification, and synthesis. *Appl. Entomol. Zool.* 8, 200–203. doi: 10.1303/aez.8.200

Tamura, K., Stecher, G., Peterson, D., Filipski, A., and Kumar, S. (2013). MEGA6: molecular evolutionary genetics analysis version 6.0. *Mol. Biol. Evol.* 30, 2725–2729. doi: 10.1093/molbev/mst197

Tanaka, K., Uda, Y., Ono, Y., Nakagawa, T., Suwa, M., Yamaoka, R., et al. (2009). Highly selective tuning of a silkworm olfactory receptor to a key mulberry leaf volatile. *Curr. Biol.* 19, 881–890. doi: 10.1016/j.cub.2009.04.035

Tang, R., Jiang, N. J., Ning, C., Li, G. C., Huang, L. Q., and Wang, C. Z. (2020). The olfactory reception of acetic acid and ionotropic receptors in the Oriental armyworm, *Mythimna separata* Walker. *Insect Biochem. Mol. Biol.* 118, 103312. doi: 10.1016/j.ibmb.2019.103312

Teal, P. E. A., Mitchell, E. R., Tumlinson, J. H., Heath, R. R., and Sugie, H. (1985). Identification of volatile sex pheromone components released by the southern armyworm, *Spodoptera eridania* (Cramer). *J. Chem. Ecol.* 11, 717–725. doi: 10.1007/bf00988301

Touhara, K., and Vosshall, L. B. (2009). Sensing odorants and pheromones with chemosensory receptors. *Annu. Rev. Physiol.* 71, 307–332. doi: 10.1146/annurev.physiol.010908.163209

Vogt, R. G. (2005). "Molecular basis of pheromone detection in insects," in *Comprehensive Insect Physiology, Biochemistry, Pharmacology and Molecular Biology*, Vol. 3, *Endocrinology*, (London: Elsevier), 753–804. doi: 10.1016/b0-44-451924-6/00047-8

Wang, B., Liu, Y., He, K., and Wang, G. (2016). Comparison of research methods for functional characterization of insect olfactory receptors. *Sci. Rep.* 6: 32806.

Wang, B., Liu, Y., and Wang, G. R. (2018). Proceeding from *in vivo* functions of pheromone receptors: peripheral-coding perception of pheromones from three closely related species, *Helicoverpa armigera*, *H. assulta*, and *Heliothis virescens*. *Front. Physiol.* 9:1188. doi: 10.3389/fphys.2018.01188

Wang, G., Carey, A. F., Carlson, J. R., and Zwiebel, L. J. (2010). Molecular basis of odor coding in the malaria vector mosquito Anopheles gambiae. *Proc. Natl. Acad. Sci. U.S.A.* 107, 4418–4423. doi: 10.1073/pnas.0913392107

Wang, G., Vásquez, G. M., Schal, C., Zwiebel, L. J., and Gould, F. (2011). Functional characterization of pheromone receptors in the tobacco budworm *Heliothis virescens*. *Insect Mol. Biol.* 20, 125–133. doi: 10.1111/j.1365-2583.2010.01045.x

Wang, X. W., and Liu, M. Y. (1997). Extract components of single sex pheromone gland of oriental armyworm *Mythimna separata* walker with trace analytical techniques. *Acta Entomol. Sin.* 40, 158–165.

Wei, Z. H., and Pan, F. M. (1985). Preliminary report on the sex pheromone of the armyworm *Mythimna separata*. *Acta Entomol. Sin.* 28, 348–350.

Witzgall, P., Kirsch, P., and Cork, A. (2010). Sex pheromones and their impact on pest management. *J. Chem. Ecol.* 36, 80–100. doi: 10.1007/s10886-009-9737-y

Wu, H., Hou, C., Huang, L. Q., Yan, F. S., and Wang, C. Z. (2013). Peripheral coding of sex pheromone blends with reverse rations in two *Helicoverpa* species. *PLoS One* 8:e70078. doi: 10.1371/journal.pone.0070078

Wu, H., Xu, M., Hou, C., Huang, L. Q., Dong, J. F., and Wang, C. Z. (2015). Specific olfactory neurons and glomeruli are associated to differences in behavioral responses to pheromone components between two *Helicoverpa* species. *Front. Behav. Neurosci.* 9:206. doi: 10.3389/fnbeh.2015.00206

Zhang, D. D., and Löfstedt, C. (2013). Functional evolution of a multigene family: orthologous and paralogous pheromone receptor genes in the turnip moth, *Agrotis segetum*. *PLoS One* 8:e77345. doi: 10.1371/journal.pone.0077345

Zhang, D. D., and Löfstedt, C. (2015). Moth pheromone receptors: gene sequences, function, and evolution. *Front. Ecol. Evol.* 3:105. doi: 10.3389/fevo.2015.00105

Zhang, J., Bisch-Knaden, S., Fandino, R. A., Yan, S., Obiero, G. F., Grosse-Wilde, E., et al. (2019). The olfactory coreceptor IR8a governs larval feces-mediated competition avoidance in a hawkmoth. *Proc. Natl. Acad. Sci. U.S.A.* 116, 21828–21833. doi: 10.1073/pnas.1913485116

Zhang, J., Liu, C., Yan, S., Liu, Y., Guo, M., Dong, S., et al. (2013). An odorant receptor from the common cutworm (*Spodoptera litura*) exclusively tuned to the important plant volatile cis-3-hexenyl acetate. *Insect Mol. Biol.* 22, 424–432. doi: 10.1111/imb.12033

Zhang, J. P., Salcedo, C., Fang, Y. L., Zhang, R. J., and Zhang, Z. N. (2012). An overlooked component: (Z)-9-tetradecenal as a sex pheromone in *Helicoverpa armigera*. *J. Insect Physiol.* 58, 1209–1216. doi: 10.1016/j.jinsphys.2012.05.018

Zhang, Q. H., Wu, Z. N., Zhou, J. J., and Du, Y. J. (2017). Molecular and functional characterization of a candidate sex pheromone receptor OR1 in *Spodoptera litura*. *Insect Sci.* 24, 543–558. doi: 10.1111/1744-7917.12294

Zhu, P. C., Kong, F. L., and Yu, Y. Q. (1987). Sex pheromone of oriental armyworm *Mythimna separata* Walker. *J. Chem. Ecol.* 13, 977–981.

Conflict of Interest: The authors declare that the research was conducted in the absence of any commercial or financial relationships that could be construed as a potential conflict of interest.

The handling editor declared a past co-authorship with one of the authors, GW.

Copyright © 2021 Wang, Wang and Wang. This is an open-access article distributed under the terms of the Creative Commons Attribution License (CC BY). The use, distribution or reproduction in other forums is permitted, provided the original author(s) and the copyright owner(s) are credited and that the original publication in this journal is cited, in accordance with accepted academic practice. No use, distribution or reproduction is permitted which does not comply with these terms.

frontiers in Physiology

ORIGINAL RESEARCH
published: 07 July 2021
doi: 10.3389/fphys.2021.690185

Comparative Genomics Provide Insights Into Function and Evolution of Odorant Binding Proteins in *Cydia pomonella*

Cong Huang[1†], Xue Zhang[1,2†], Dongfeng He[1,3], Qiang Wu[1], Rui Tang[4], Longsheng Xing[1], Wanxue Liu[5], Wenkai Wang[3], Bo Liu[1], Yu Xi[1], Nianwan Yang[5], Fanghao Wan[1,2,5]* and Wanqiang Qian[1]**

[1] Shenzhen Branch, Guangdong Laboratory for Lingnan Modern Agriculture, Genome Analysis Laboratory of the Ministry of Agriculture and Rural Affairs, Agricultural Genomics Institute at Shenzhen, Chinese Academy of Agricultural Sciences, Shenzhen, China, [2] College of Plant Health and Medicine, Qingdao Agricultural University, Qingdao, China, [3] Hubei Engineering Research Center for Pest Forewarning and Management, Yangtze University, Jingzhou, China, [4] Guangdong Key Laboratory of Animal Conservation and Resource Utilization, Guangdong Public Laboratory of Wild Animal Conservation and Utilization, Institute of Zoology, Guangdong Academy of Sciences, Guangzhou, China, [5] Institute of Plant Protection, Chinese Academy of Agricultural Sciences, Beijing, China

Insect olfaction is vital for foraging, mating, host-seeking, and avoidance of predators/pathogens. In insects, odorant binding proteins (OBPs) are involved in transporting hydrophobic odor molecules from the external environment to receptor neurons. The codling moth, *Cydia pomonella*, one of the most destructive insect fruit pests, causes enormous economic losses. However, little is known about the number, variety, gains and losses, and evolution of *OBP* genes in *C. pomonella*. Here we report the identification of 40 *OBPs* in *C. pomonella*, most (75%) of which are classic *OBPs*, using genomic and transcriptomic analyses. Two *OBP* genes were lost in *C. pomonella* relative to possible distant ancestor in Lepidoptera lineage based on an analysis of gene gains and losses. The phylogenetic tree and chromosome location showed that the expansion of *OBP* genes mainly resulted from tandem duplications, as the *CpomGOBP2* gene was duplicated twice along with loss of *CpomPBPB*. Two positive selection sites of the *CpomGOBP1* gene were identified while other *OBP* genes evolved under purifying selection. Our results provide fundamental knowledge of *OBP* genes allowing further study of their function in *C. pomonella*.

Keywords: odorant binding proteins, codling moth, *Cydia pomonella*, positive selection, comparative genomics, gene gains and losses

OPEN ACCESS

Edited by:
Paivi H. Torkkeli, Dalhousie University, Canada

Reviewed by:
William Benjamin Walker III, United States Department of Agriculture (USDA-ARS), United States
Ana Claudia A. Melo, Federal University of Rio de Janeiro, Brazil

***Correspondence:**
Nianwan Yang
yangnianwan@caas.cn
Fanghao Wan
wanfanghao@caas.cn
Wanqiang Qian
qianwanqiang@caas.cn

[†] These authors have contributed equally to this work

Specialty section:
This article was submitted to Invertebrate Physiology, a section of the journal Frontiers in Physiology

Received: *02 April 2021*
Accepted: *15 June 2021*
Published: *07 July 2021*

Citation:
Huang C, Zhang X, He D, Wu Q, Tang R, Xing L, Liu W, Wang W, Liu B, Xi Y, Yang N, Wan F and Qian W (2021) Comparative Genomics Provide Insights Into Function and Evolution of Odorant Binding Proteins in Cydia pomonella. Front. Physiol. 12:690185. doi: 10.3389/fphys.2021.690185

INTRODUCTION

Insects rely on their olfactory system to sense environmental odors related to behaviors such as foraging, host-seeking, mating, and oviposition, as well as avoiding predators and pathogens (Andersson et al., 2015). Odorant binding proteins (OBPs) are small water-soluble globular proteins with molecular masses of 10–30 kDa (Sun et al., 2018). *OBPs* are highly expressed in the hydrophilic

lymph of insect olfactory sensilla (Pelosi et al., 2014). When lipophilic semiochemicals from the environment enter the lymph through micropores on the surface of olfactory sensilla, the *OBPs* bind, solubilize, and deliver the semiochemicals to the receptor proteins, e.g., odorant receptors (ORs) or ionotropic receptors (IRs), which are located on the membranes of olfactory sensory neurons. This delivery activates a series of downstream olfactory signal transductions accompanied by corresponding behavioral movements in insects (Zhang et al., 2020). *OBPs* are clearly essential in communications between insects and environmental semiochemicals including both pheromones and host volatiles.

OBPs are involved in the initial step of recognizing host volatiles or sex pheromones, suggesting that the functional divergence of *OBPs* is associated with speciation or host diversity. Considering the low sequence identities between orthologous/paralogous *OBP* genes, *OBP* genes have likely been evolving at a rapid rate through gene gains or losses (McKenzie et al., 2014) and positive selection (Campanini and de Brito, 2016). Most *OBP* genes are tandemly arranged in chromosomes, indicating that the occurrence of these genes arose from tandem duplication (Hekmat-Scafe et al., 2002; Gong D. P. et al., 2009; Manoharan et al., 2013; Dippel et al., 2014). The duplicate genes then gradually diverge in function through mutation or pseudogenization (Nei and Rooney, 2005; Vieira et al., 2007).

Studies on the origin, evolution, and structural variation of *OBP* genes provide insight into the functional differentiation of *OBPs* and host preference in insects. However, there is little knowledge of the numbers, structures, and evolution of the *OBP* gene family in important insect crop pests such as the codling moth, *Cydia pomonella* (L.) (Lepidoptera: Tortricidae). *C. pomonella* is an economically threatening pest worldwide (Witzgall et al., 2008; Kumar et al., 2015; Zhu et al., 2017). It mainly destroys apples and pears as well as other seed and stone fruits. Some studies focused on the structures and functions of pheromone binding proteins (PBPs) (Liu et al., 2016; Tian et al., 2016a,b; Tian and Zhang, 2016) and identification of general odorant binding proteins (GOBPs) (Garczynski et al., 2013). In contrast, studies on *OBPs* are lacking in *C. pomonella*, with little information of their roles in recognizing hosts or locating mates.

To understand the evolution and function of *OBPs* in *C. pomonella*, we identified and annotated its *OBP* genes by combining transcriptome data with the high quality genome we released previously (Wan et al., 2019). The gene gains and losses of *OBPs* were estimated by CAFÉ 3.0 (Han et al., 2013) for seven moth species. Subsequently, a phylogenetic tree of *OBP* genes from three lepidopteran insects (*C. pomonella*, *Bombyx mori*, and *Manduca sexta*) was constructed to explore their evolutionary relationships. The collinearity and chromosome locations were used to compare the divergence of *OBP* genes between *C. pomonella* and *B. mori*. Finally, the positive selection of genes and structural homology model were analyzed to predict the functional divergence of selected *OBPs*. Our results provide insights into the evolution of *OBP* genes in *C. pomonella*, which will facilitate future functional studies.

MATERIALS AND METHODS

Identification of *OBP* Genes in the *C. pomonella* Genome

The protein sequences of seven lepidopteran insect *OBPs* were collected from deposited data of published articles, which have been identified from their genomes, and these species included *B. mori* (Gong D. P. et al., 2009), *M. sexta* (Vogt et al., 2015), *Plutella xylostella* (Cai et al., 2020), *Spodoptera litura* (Cheng et al., 2017), *Spodoptera frugiperda* (Gouin et al., 2017), *Helicoverpa armigera* (Pearce et al., 2017), and *Danaus plexippus* (Zhan et al., 2011). These protein sequences were then used as queries in iterative BLASTP searches with parameter "-*e*-value 1e–5" against the *C. pomonella* genome (Wan et al., 2019) to find candidate *OBP* genes. A local command line HMMER (version 3.1b2) search was conducted for these candidate *OBP* genes against the Pfam-A database (El-Gebali et al., 2019) to find the PBP_GOBP (PF01395) HMM profile. The identified *OBP* genes were subsequently used as queries to align the *C. pomonella* genome using tBLASTn search with parameter "-*e*-value 1e-5" to identify the missing *OBP* genes during gene prediction for the genome. We used an in-house Perl script to extract DNA sequences of novel genes from the genome, followed by predicting the CDS using the online website FGENESH (Solovyev et al., 2006). Gene prediction was verified by comparing with the transcriptome data that we used in the *C. pomonella* genome paper to confirm the complete gene structure (Wan et al., 2019). Finally, we used GMAP (Wu and Watanabe, 2005) to rebuild gene structures of all *OBP* genes. For *B. mori*, we used the 44 *OBPs* of *B. mori* which were identified by Gong (Gong D. P. et al., 2009), to perform tBLASTn search against the newest version of the *B. mori* genome (Kawamoto et al., 2019) and rebuilt their gene structures by GMAP (Wu and Watanabe, 2005).

To check the conserved cysteine pattern, which is the predominant feature of *OBP* genes, we first performed multiple sequence alignment of *OBP* sequences using MAFFT v7 (Katoh et al., 2002) with default parameters. Then, the aligned sequences were trimmed by trimAl v1.2 (Capella-Gutierrez et al., 2009) to remove gaps and low-quality regions with the parameter "-automated1." The trimmed sequences were subsequently submitted to ESPript 3.0 Server[1] for visualization.

Estimation of Gene Gains and Losses

To explore gene gains and losses of *OBPs* in moths, seven moth species with available genomes and past investigations of the *OBP* gene family were selected, including *S. litura*, *S. frugiperda*, *H. armigera*, *B. mori*, *M. sexta*, *C. pomonella*, and *P. xylostella*. Orthologous and paralogous groups of these species were inferred by OrthoFinder v2.3.1 (Emms and Kelly, 2015) with default parameters. Orthologous groups including only single copy genes for each species were selected to construct the species tree. Protein sequences of each orthologous group were independently aligned using MAFFT v7 (Katoh et al., 2002), trimmed by trimAl v1.2 (Capella-Gutierrez et al., 2009), and

[1] http://espript.ibcp.fr/ESPript/cgi-bin/ESPript.cgi

then concatenated into one super-sequence. The phylogenetic tree was inferred using maximum likelihood (ML) in RAxML with the best-fit model (JTT + I + F) estimated by ProtTest3 v3.4.2 (Darriba et al., 2011). The Bayesian Relaxed Molecular Clock (BRMC) approach was adopted to estimate the neutral evolutionary rate and species divergence time using the program MCMCTree, implemented in PAML v4.9b package (Yang, 2007). The tree was calibrated with the following time frames adopted from TimeTree (Kumar et al., 2017) to constrain the age of the nodes between the species: 99–121 million years ago (Mya) for *B. mori* and *H. armigera*, and 80–243 Mya for *C. pomonella* and *P. xylostella*.

The *OBP* gene gains and losses were estimated by CAFÉ v3.0 (Han et al., 2013). Gene numbers of the *OBP* gene family in each insect were collected from published articles for *S. litura* (Cheng et al., 2017), *S. frugiperda* (Gouin et al., 2017), *H. armigera* (Pearce et al., 2017), *M. sexta* (Vogt et al., 2015), and *P. xylostella* (Cai et al., 2020), while the numbers of *OBP* genes in *B. mori* and *C. pomonella* were identified in this study (see section "Materials and Methods"). This gene number matrix together with the phylogenetic tree corrected by MCMCTree were used as input files for CAFÉ 3.0 (Han et al., 2013).

Phylogenetic Analysis

A total of 133 *OBP* genes from three species (*C. pomonella*, *B. mori*, and *M. sexta*) were used in the phylogenetic analysis. These gene sequences were aligned using MAFFT v7 (Katoh et al., 2002) with default parameters, then the alignments were trimmed by trimAl v1.2 (Capella-Gutierrez et al., 2009) with the parameter "-automated1." RAxML (Stamatakis, 2014) was used to construct a maximum likelihood evolutionary tree with the best-fit model (LG) estimated by ProtTest3 v3.4.2 (Darriba et al., 2011). FigTree v1.4.3[2] and Adobe Illustrator CC 2017 were used to visualize and annotate the phylogenetic tree.

Collinearity and Chromosomal Distribution of *OBP* Genes

We mapped the 44 *OBP* genes of *B. mori* (Gong D. P. et al., 2009) to the chromosomes in the newest version of the *B. mori* genome (Kawamoto et al., 2019) and rebuilt their gene structure by GMAP (Wu and Watanabe, 2005). However, only 43 *OBP* genes were successfully mapped: *BmorOBP24* is a pseudogene that was discarded. Subsequently, the best reciprocal BLAST hit was used to identify the orthologous *OBP* gene pairs in *C. pomonella* and *B. mori* genomes. MapGene2Chrom web v2[3] was used to draw the distribution map of *OBP* genes on the chromosomes of both species. Orthologous gene pairs or blocks were linked by lines.

Molecular Evolutionary Analysis

To estimate whether natural selection acted on the evolution of *OBP* genes in *C. pomonella*, we inferred the ratio of the normalized non-synonymous rate (d_N) to the synonymous rate (d_S) of nucleotide substitutions ($\omega = d_N/d_S$) by a maximum likelihood method using the Codeml program in PAML v4.9b (Yang, 2007), with $\omega > 1$, $\omega = 1$, $\omega < 1$ indicating positive selection, neutral evolution, and purifying selection, respectively. We first aligned the protein sequences for each analysis in MAFFT v7 (Katoh et al., 2002), then these protein alignments were converted to CDS alignments by the PAL2NAL program[4]. Subsequently, the protein alignments were trimmed by trimAl v1.2 (Capella-Gutierrez et al., 2009) and were used in MEGA6 (Tamura et al., 2013) to build Neighbor-Joining (NJ) trees with the Jones-Taylor-Thornton (JTT) model and 1,000 bootstrap replications.

We used the site model for each group of *OBP* orthologous/paralogous genes clustered by the phylogenetic tree to test which genes or sites might have evolved under positive selection. In this site model, we performed a test of heterogeneity across sites by comparing the M0 and M3 models with $K = 3$ categories. Another test of positive selection on sites involved fitting a beta distribution of ω values across sites by comparing M7 and M8 models. Considering the evolutionary specificity of *GOBP* and *PBP* genes in lepidopteran insects (Yasukochi et al., 2018), we used the branch-site model to test the genes as well as their amino acid sites that evolved under positive selection in nine lepidopteran insects including *B. mori*, *C. pomonella*, *D. plexippus*, *Heliconius melpomene*, *M. sexta*, *Operophtera brumata*, *Papilio xuthus*, *P. xylostella*, and *S. litura*. In the phylogenetic tree of each gene (*GOBP1*, *GOBP2*, *PBPA*, *PBPC*, and *PBPD*, but not *PBPB* due to lack of gene numbers), we labeled the branch composed of genes from *C. pomonella* as the foreground branch and the remaining branches as background branches to test positive selection in *C. pomonella* *GOBP* and *PBP* genes. We compared model A (the alternative model), in which some sites on the foreground branch were allowed to change to a value of $\omega > 1$, with the null model of neutral evolution.

The likelihood ratio tests (LRTs) statistic ($2\Delta L$), which approximates a χ^2 distribution, was used for comparisons between models, and significant results were determined using χ^2-tests. If the LRT was significant, Bayes empirical Bayes (BEB) was used to identify sites of positive selection. The sites with posterior probabilities (PPs) of ≥ 0.95 were considered positively selected, thus they were defined as positively selected sites (PSS).

Homology Modeling and Molecular Docking

To further understand the functional significance of the identified positively selected sites, we labeled them on protein sequences and tertiary structures. The amino acid sequences of *CpomGOBP1* gene which evolved under positive selection in *C. pomonella* were submitted to the SWWISS-MODEL Server[5] to predict and refine 3D structures. The best template was BmorGOBP2 (PDB ID: 2WCK), which has 53.57% identity with *CpomGOBP1*. Subsequently, we used the SAVES server[6] and RAMPAGE server to estimate the quality of the predicted 3D structure. SAVES assesses the quality of protein 3D structure

[2]http://tree.bio.ed.ac.uk/software/figtree/

[3]http://mg2c.iask.in/mg2c_v2.1/

[4]http://www.bork.embl.de/pal2nal/

[5]https://swissmodel.expasy.org/

[6]https://servicesn.mbi.ucla.edu/SAVES/

based on the PROCHECK (Laskowski et al., 1993), ERRAT (Colovos and Yeates, 1993), and VERIFY 3D (Lüthy et al., 1992) program. RAMPAGE assesses the quality based on the Ramachandran plot (Wang et al., 2016). The generated model structures were rendered and visualized using Visual Molecular Dynamics (VMD) v1.9.3 (Humphrey et al., 1996).

We collected 48 odorant molecules including pheromones and host plant volatiles by mining literatures (Bengtsson et al., 2001; Ansebo et al., 2004; Bengtsson et al., 2014; Knight et al., 2019). Then, docking was carried out by AutoDock Vina (Trott and Olson, 2010). The binding patterns between *CpomGOBP1* and the odorant molecule was visualized using VMD (Humphrey et al., 1996). The key binding site analysis was performed using LigPlus (Wallace et al., 1995).

Expression Profiling of 40 *CpomOBPs*

We calculated the expression levels of 40 *CpomOBPs* in several sensory tissues based on transcriptome data. The sensory tissues were collected from female and male adults, including the antennae, head, leg, wing, labial palp, each sample with three biological replicates. The paired-end clean reads were mapped to the *C. pomonella* genome using HISAT2 (Kim et al., 2015). The FPKM (Fragments Per Kilobase of transcript per Million mapped reads) was calculated by StringTie software (Pertea et al., 2016). The heatmap.2 function of R package "gplots" to draw the heatmap of expression profiling based on the FPKM values.

RESULTS

Identification of *OBP* Genes in *C. pomonella*

A total of 40 *OBP* genes were identified in the *C. pomonella* genome. Complete CDS were determined by cross-checking with transcriptome assemblies. All gene information including gene names, CDS, amino acid sequences, chromosomes, and gene lengths and classification are provided in **Supplementary Table 1**. We compared the 40 *CpomOBPs* with those previous reported (Garczynski et al., 2013) and renamed them, and those that were not well matched were renamed by the sequence length. The amino acid sequences range from 133 to 339 amino acids (**Supplementary Table 1**). Multiple sequence alignments show that most have six typical conserved cysteine residues (**Figure 1** and **Supplementary Table 1**). Based on the number and location of the conserved cysteines, the 40 *CpomOBPs* were classified into four subfamilies, including classic, minus-C, plus-C, and atypical. In total, 30 *CpomOBPs* belong to the classic subfamily, which had six typical conserved cysteine residues. Four *CpomOBPs* contained more cysteines than the classic *OBPs*, and were classified into the plus-C subfamily. Four *CpomOBPs* belong to the minus-C subfamily, which had fewer than six cysteines. The remaining two *CpomOBPs*, which exhibited none of the above characteristics, were classified into the atypical subfamily.

Estimation of Gene Gains and Losses

A statistical gene birth and death analysis for *OBP* genes from seven moth species (*S. litura*, *S. frugiperda*, *H. armigera*, *B. mori*, *M. sexta*, *C. pomonella*, and *P. xylostella*) was performed by CAFÉ (**Figure 2**). Forty-two *OBP* genes were inferred in the common ancestor node of moth species considered in this study at 162 Mya. The gene gains and losses range from -1 (lost one gene) to + 1 (gained one gene) between the adjacent ancestor nodes. However, different species have various gene gains or losses ranging from 1 to 7 compared with their adjacent ancestors. For example, gene gains occurred in *S. frugiperda* (+ 7) and *M. sexta* (+ 6), while gene losses occurred in *S. litura* (-7), *H. armigera* (-2), *B. mori* (-1), *C. pomonella* (-2), and *P. xylostella* (-3) compared with their adjacent ancestors. Our results suggested that the gains and losses of *OBP* genes may be associated with functional divergence which results from adaptation.

Phylogenetic Analysis of *OBP* Genes

The phylogenetic tree was inferred using a total of 133 amino acid sequences of *OBP* genes, including 40 *OBPs* from *C. pomonella*,

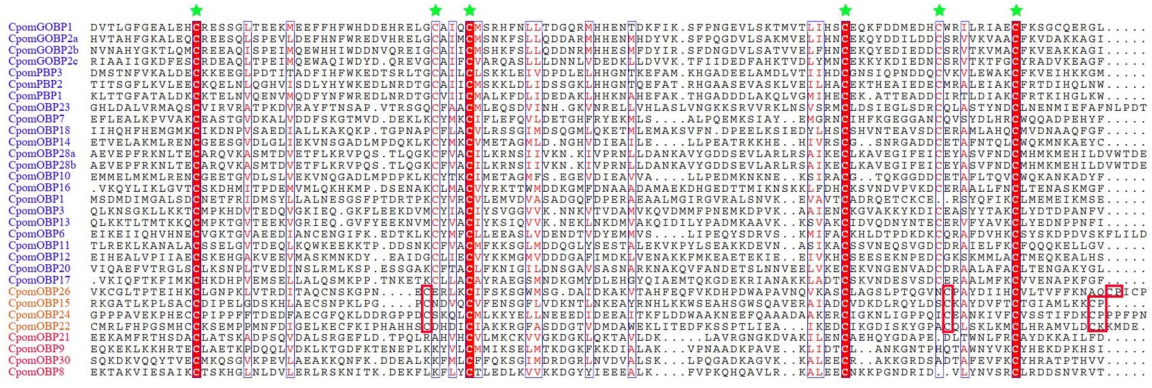

FIGURE 1 | Amino acid alignment of various *C. pomonella OBP* family members. The alignment was performed by MAFFT v7, aligned sequences were depicted with ESPript 3.0 server (http://espript.ibcp.fr/ESPript/cgi-bin/ESPript.cgi). Highly conserved cysteine residues are marked by green stars. The gene IDs of classic, plus-C, and minus-C *OBPs* are shown in blue, orange and red color, respectively. Only the cysteines which are conserved in all of alignment sequences are highlighted in red block. Seven classic and two atypical *OBPs* are not shown in this figure.

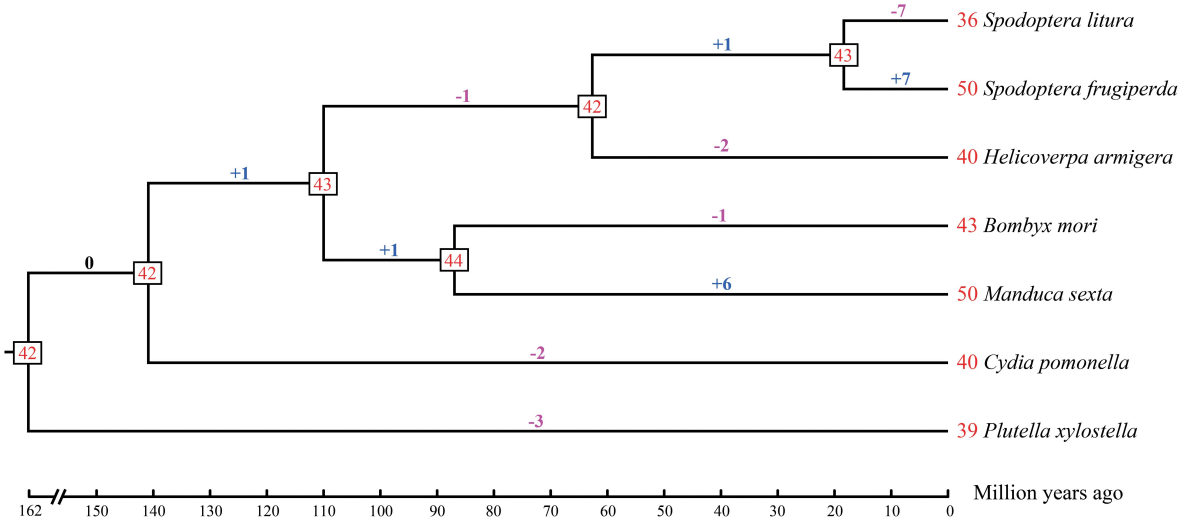

FIGURE 2 | Estimation of *OBP* gene gains and losses during the evolution of seven moth species. The phylogenetic tree with estimated divergence times (million year ago) was inferred by MCMCTree in PAML v4.9b. The numbers at the tree termini are the numbers of genes in each species, which we found in the literature: *Spodoptera litura*, *Spodoptera frugiperda*, *Helicoverpa armigera*, *Manduca sexta*, and *Plutella xylostella*, the numbers of *OBP* genes in *Cydia pomonella* were identified in this study, while the number of *OBP* genes in *Bombyx mori* was corrected by this study (see section "Materials and Methods"). The numbers at the tree nodes are the numbers of genes in their most recent common ancestors. The numbers of gene gains and losses are shown above the branches, where the symbol "+" represents gene gains while "-" represents gene losses. The numbers before each species represent the *OBP* genes of the specific moth.

43 *OBPs* from *B. mori*, and 50 *OBPs* from *M. sexta* (**Figure 3**). We classified these *OBP* genes into 12 groups (Groups 1–12) according to the clusters in the phylogenetic tree. Eleven of them were orthologous groups shared among these three species with nearly 1:1 orthologous genes in each group from each species, except that Group 2 has a lineage-specific expansion in *M. sexta*. The GOBP/PBP subfamily is a specific cluster in lepidopteran species (Vogt et al., 2015; Yasukochi et al., 2018), consisting of six typical tandem genes including *GOBP1*, *GOBP2*, and *PBPA-PBPD*. In our study, Group 1 was the conserved GOBP/PBP cluster, including six genes from *B. mori* (*GOBP1*, *GOBP2*, *PBPA-1*, *PBPA-2*, *PBPC*, and *PBPD*), six genes from *M. sexta* (*GOBP1*, *GOBP2*, *PBPA*, *PBPB*, *PBPC*, and *PBPD*), and seven genes from *C. pomonella* (*GOBP1*, *GOBP2a*, *GOBP2b*, *GOBP2c*, *PBP3*, *PBP2*, and *PBP1*). The *PBPB* gene was lost in *C. pomonella*, while the *GOBP2* gene is duplicated twice, which suggested that *GOBP2* may be under positive selection. In general, the *OBP* gene family is evolutionarily conserved in Lepidoptera insects.

Collinearity and Chromosomal Distribution of *OBP* Genes

All 40 *OBP* genes were located on 11 *C. pomonella* chromosomes (**Figure 4**). These genes are organized into two major clusters on chromosomes 18 and 8, while the other chromosomes contain scattered and few *OBP* genes. The largest cluster contains 11 tandem *OBP* genes on chromosome 18, accounting for 27.5% of the total number of *OBP* genes. These genes have a collinearity block in chromosome 18 of *B. mori* that contains 12 tandem *OBP* genes. Furthermore, this collinearity block of *OBP* genes was clustered into Groups 5, 7, and 11 in the phylogenetic tree, which belong to antennal binding protein I (ABPI) and antennal binding protein II (ABPII) (**Figure 3**) (Gong D. P. et al., 2009). Another big cluster on chromosome 8 contains seven *OBP* genes, which account for 17.5% of the total number of *OBP* genes. Six of them were in a tandem *GOBP/PBP* gene cluster, including *GOBP1*, *GOBP2a*, *PBP3*, *PBP2*, and *PBP1*. There was also a tandem *GOBP/PBP* gene cluster on chromosome 19 in *B. mori*. There was a collinearity block of the *GOBP/PBP* gene cluster between *C. pomonella* and *B. mori*, and they were clustered into Group 1 in the phylogenetic tree (**Figure 3**). Seven *OBP* genes in *C. pomonella* have no collinearity compared with *B. mori*.

Tests of Selective Pressures on Lepidopteran *OBP* Genes

We selected eight clades (groups) from the phylogeny to test whether some orthologous/paralogous *OBP* genes of three moths (including *B. mori*, *C. pomonella*, and *M. sexta*) evolved under positive selection. Selected groups included Groups 2–6, 9, 11, and 12 (**Table 1**). Groups 7–8 and 10 were excluded since they had too few genes. Group 1 was later tested independently using the branch-site model.

According to tests of the one-ratio model (M0), which assumes a single ω for all amino acid sites, the ω values of eight clades ranged from 0.00547 to 0.15846 (**Table 1**), suggesting the existence of strong purifying selection. However, the comparison between models M0 and M3 (discrete) provided strong evidence of variation in selective pressures at different amino acid sites in Groups 2–3, 5, 9, and 11 ($P < 0.01$, **Table 1**), indicating that purifying selection has been relaxed at some amino acid sites. We further compared models M7 and M8 for clades showing $0.5 < d_S < 1$ to investigate whether some amino acid

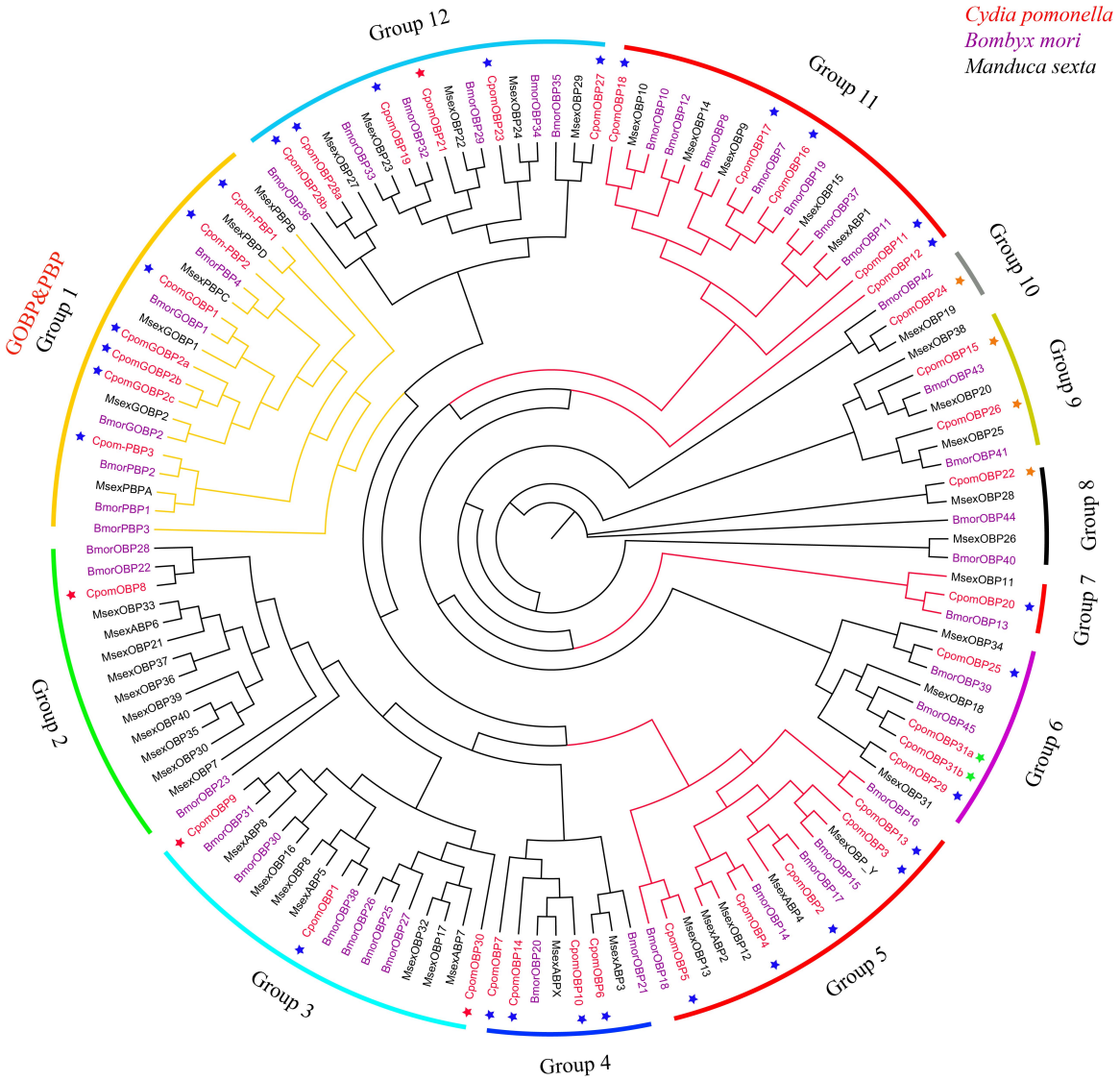

FIGURE 3 | The phylogenetic tree of the *OBP* gene family in lepidopteran insects. *C. pomonella OBPs* are classified as Classic, Minus-C, Plus-C, and Atypical, which are represented by blue, red, orange, and green stars, respectively. The GOBP/PBP genes are shown in orange.

sites actually evolved under positive selection. Only Group 2 presented evidence of positive selection (P = 0.0008) with one positively selected site (PSS). However, the Bayes empirical Bayes (BEB) analysis showed that the PSS only had a 93.4% posterior probabilities (PPs), which is not statistically significant.

We used the branch-site model to test the positive selection in each codon for different gene clades of GOBPs and PBPs from nine species (*B. mori*, *C. pomonella*, *D. plexippus*, *Heliconius melpomene*, *M. sexta*, *Operophtera brumata*, *Papilio xuthus*, *P. xylostella*, and *S. litura*) (**Figure 5**). Only GOBP1 was identified as being under positive selection for *C. pomonella* after the likelihood ratio test (P = 0.0318). We further used the BEB approach to detect the positive sites in GOBP1, which showed that sites 41S and 43G were significant signs of positive selection with PPs of 0.994 and 0.972, respectively (**Table 2**).

Structural Links to Protein Function

To get additional insight into the functional significance of PSSs, we mapped the PSSs to the multiple sequence alignments of GOBP1 protein sequences from nine species, and labeled them on the structural homology model of *C. pomonella* GOBP1 (**Figure 6A**). Compared to the other eight species, the 41st amino acid Glutamic acid (E) was substituted by Serine (S), while the 43rd amino acid Glutamine (Q) was substituted by Glycine (G) (**Figure 6B**). The structural homology model of *C. pomonella* GOBP1 showed that both the 41st and 43rd amino acids were located in the loop near the first helix (**Figure 6A**).

The binding energies that *CpomGOBP1* bind with 48 odorant molecules were assessed by AutoDock Vina (Trott and Olson, 2010). Among them, β-bourbonene had the lowest binding energy (-9.3 KJ/mol) with *CpomGOBP1*

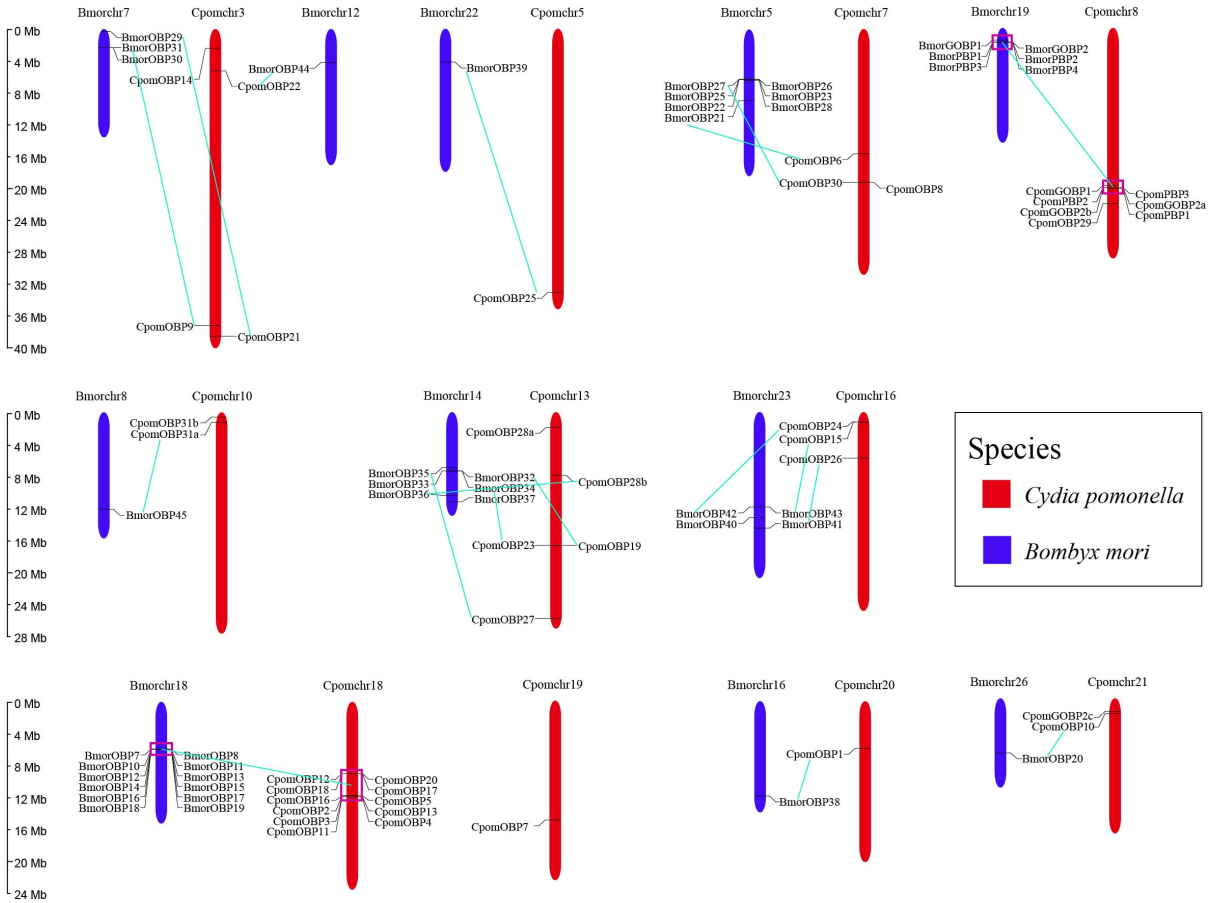

FIGURE 4 | Chromosomal distribution of *OBP* genes in *C. pomonella* (red) and *B. mori* (blue). Cyan solid lines represent the correspondence between *C. pomonella* and *B. mori OBP* genes.

TABLE 1 | Tests of positive selection on the orthologous/paralogous *OBP* genes of moths by site model.

Clade	n	d_N/d_S	2△l	
		M0 vs. M3	**M7 vs. M8**	
Group2	14	0.15846	55.305518** (*P* = 0)	14.265552 (*P* = 0.0008)**
Group3	16	0.11555	52.788572** (*P* = 0)	0.001414 (*P* = 0.9993)
Group4	8	0.04517	0 (*P* = 1)	7.520000 (*P* = 0.9996)
Group5	15	0.00687	135.091616** (*P* = 0)	0.001886 (*P* = 0.9991)
Group6	9	0.01691	0 (*P* = 1)	0.001218 (*P* = 0.9994)
Group9	7	0.00547	16.037306** (*P* = 0.0030)	3.500000 (*P* = 0.9998)
Group11	17	0.02222	13.897966** (*P* = 0.0076)	7.020000 (*P* = 0.9996)
Group12	17	0.01384	0 (*P* = 1)	0.001418 (*P* = 0.9993)
Clade	**Parameter estimated under M8 model**			**Positively selected sites (PSSs) from Bayes empirical Bayes (BEB) analysis**
Group2	p0 = 0.98223, *p* = 3.14309, *q* = 15.84241, p1 = 0.01777, ω = 3.42058			5T (0.934)

n, Number of genes tested; d_N/d_S, Estimated under M0; 2△l, Likelihood ratio test.
***Significant within the 1% interval after Bonferroni correction.*

(**Supplementary Table 2**). β-bourbonene was located in the binding cavity composed of 11 hydrophobic amino acid residues, including Phe12, Phe33, Phe36, Phe76, Phe118, Ile52, Ile94, Val8, Trp37, Met5, and Leu61 (**Figures 7A,B**).

Expression Profiling of 40 *CpomOBPs*

The expression profiling of all 40 *CpomOBPs* were assessed using FPKM values based on transcriptome data (**Figure 8**). The result showed that 31 *CpomOBPs* expressed (FPKM ≥ 10) in the

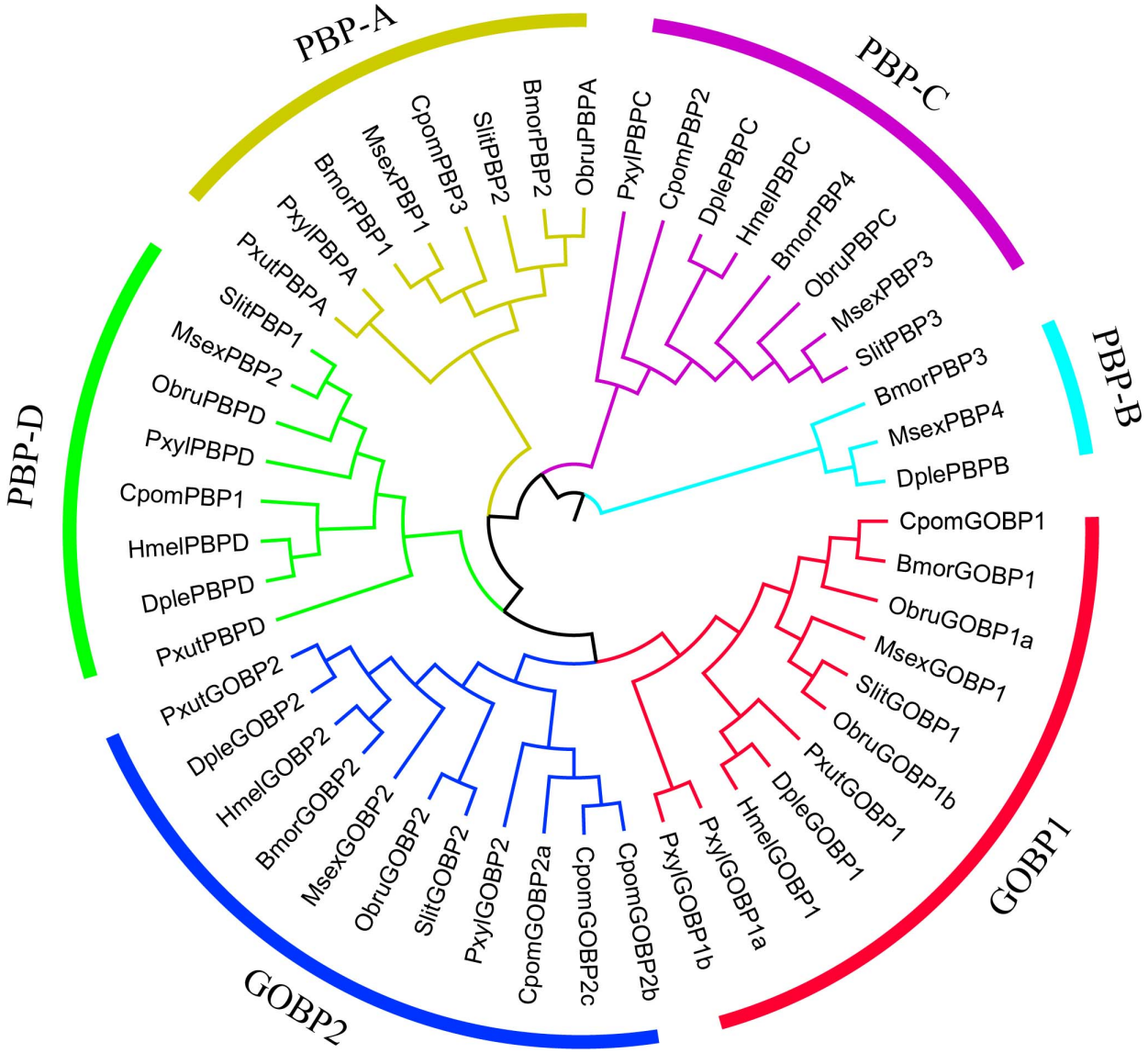

FIGURE 5 | Phylogenetic relationships of *GOBP* and *PBP* genes in lepidopteran insects. The maximum likelihood tree was constructed based on the 49 *GOBP* and *PBP* genes from nine lepidopteran species. The amino acid sequences were aligned by MAFFT v7 with default parameters, and then the alignments were trimmed by trimAl with the parameter "-automated1." (Bmor: *Bombyx mori*, Cpom: *Cydia pomonella*, Dple: *Danaus plexippus*, Hmel: *Heliconius melpomene*, Msex: *Manduca sexta*, Obru: *Operophtera brumata*, Pxut: *Papilio xuthus*, Pxyl: *Plutella xylostella*, Slit: *Spodoptera litura*). MEGA v6 was used to construct a Neighbor-Joining tree with the Jones-Taylor-Thornton (JTT) model and 1,000 bootstrap replications. FigTree v1.4.3 (http://tree.bio.ed.ac.uk/software/figtree/) and Adobe Illustrator CC 2017 were used to visualize and annotate the phylogenetic tree.

antennae, head, leg, wing, and labial palp, except *CpomOBP23*, *CpomOBP2*, *CpomOBP18*, *CpomOBP28a*, *CpomOBP28b*, *CpomOBP19*, *CpomOBP21*, *CpomOBP27*, and *CpomOBP17*. There were 25 and 26 *CpomOBPs* that are expressed in the antennae of female and male adults, respectively, 22 of them were classic *OBPs*. The other enriched expression tissue is the labial palp, in which there are 27 and 25 *CpomOBPs* expressed in female and male adults. Three *CpomPBPs*, *CpomGOBP1*, *CpomGOBP2a*, and *CpomGOBP2b*, were mainly expressed in the antennae and labial palp. It is interesting to note that *CpomGOBP2c* was specifically expressed in wing.

DISCUSSION

In this study, we identified 40 *OBP* genes in *C. pomonella*, which is similar to several lepidopteran moth species e.g., 43 *OBPs* in *B. mori* (Gong D. P. et al., 2009), 39 *OBPs* in *P. xylostella* (Cai et al., 2020), 40 *OBPs* in *H. armigera* (Pearce et al., 2017), and 36 *OBPs* in *S. litura* (Cheng et al., 2017). However, *C. pomonella* has fewer *OBPs* than *M. sexta* and *S. frugiperda*, both of which have 50 *OBP* genes (Gouin et al., 2017). Variation in the numbers of *OBP* genes among moth species suggests that the evolution of *OBP* genes occurred during the speciation adaptation process

TABLE 2 | Tests of positive selection on Lepidopteran *GOBP* and *PBP* genes by branch-site model (Branch labels referring to **Figure 5**).

Branch-site model	H0 lnL Vs. H1 lnL	df	2△l and *P*-value	Parameter Estimated under H1	Positively Selected Sites (PSSs)
GOBP1	–3159.24	1	4.61	p_0 = 0.809, p_1 = 0.140	**41S** 43G
	–3156.94		*P* = 0.0318*	p_{2a} = 0.043, p_{2b} = 0.007	
				ω_1 = 1.000, ω_2 = 533.665	
GOBP2	–3897.96	1	2.89	p_0 = 0.861, p_1 = 0.107	N/A
	–3896.51		*P* = 0.0890	p_{2a} = 0.028, p_{2b} = 0.004	
				ω_1 = 1.000, ω_2 = 999.000	
PBP3	–3313.48	1	0.18	p_0 = 0.639, p_1 = 0.104	26Q 46E 112D 115T **148K** 149G 150M 153S
	–3313.39		*P* = 0.6755	p_{2a} = 0.221, p_{2b} = 0.036	
				ω_1 = 1.000, ω_2 = 1.269	
PBP2	–3414.50	1	0	p_0 = 0.759, p_1 = 0.191	N/A
	–3414.50		*P* = 1.0000	p_{2a} = 0.040, p_{2b} = 0.010	
				ω_1 = 1.000, ω_2 = 1.000	
PBP1	–3254.95	1	0.41	p_0 = 0.769, p_1 = 0.197	N/A
	–3254.75		*P* = 0.5212	p_{2a} = 0.027, p_{2b} = 0.007	
				ω_1 = 1.000, ω_2 = 2.733	

**Significant within the 5% interval after Bonferroni correction.*
***Significant within the 1% interval after Bonferroni correction.*
PSSs in bold show 99% posterior probability confidence.
N/A: No positively selected sites were detected.

FIGURE 6 | Structural homology model and positively selected sites of *C. Pomonella* GOBP1. **(A)** Structural homology model of *C. pomonella* GOBP1, positively selected sites are marked in red. **(B)** Multiple sequence alignments of GOBP1 genes from ten moth species.

and functional requirements for each species. A study in *B. mori* found that classic *OBPs* were dominant in the *OBP* gene family: *B. mori* has 29 classic *OBPs*, five plus-C *OBPs*, and eight minus-C *OBPs* (Gong D. P. et al., 2009). Similarly, in our study the 40 *OBP* genes of *C. pomonella* were classified as 30 classic *OBPs*, four plus-C *OBPs*, four minus-C *OBPs*, and two atypical *OBPs*. A previous study suggested that most of the classic *OBPs* and all ABPIIs are likely involved in chemoreception, since they show increased chemosensory tissue expression (Dippel et al., 2014). The fact that 75% of *OBPs* in *C. pomonella* are classic *OBPs* indicated that these genes are essential in recognizing host plants or pheromones such as sex pheromones. The result of expression profiling indicates that 22 classic *OBPs* were expressed in the antennae, which is similar to the finding in *Tribolium castaneum* (Dippel et al., 2014).

We used the CAFÉ software to estimate gene gains and losses, rather than directly comparing the number of *OBP* genes, because it considers a birth-and-death model in the evolutionary process (Han et al., 2013). In the most recent common ancestor of moths considered in this study, approximately 162 Mya inferred by two time frames adopted from TimeTree (see section "Materials and Methods"), 42 *OBP* genes were shared. There were no more than two expanded and contracted genes in each ancestor node, which indicated that speciation may not be driven by the evolution of *OBP* genes. The gene gains or losses of each species compared to their distant ancestors range from 1 to 7. According to this result, we suggest that the functional divergence of *OBP* genes occurred mainly after speciation, as a result of adapting to a new diversity of environments such as new host plants or pheromones. As a result, the *OBP* genes may be under positive selection. However, the variation of *OBPs* in moths is smaller than the odorant receptors (ORs) or gustatory receptors (GRs): the expanded or contracted genes of these two gene families is as high as 54 (Engsontia et al., 2014). In general, we found that *C. pomonella* lost two *OBP* genes compared to its closest ancestor.

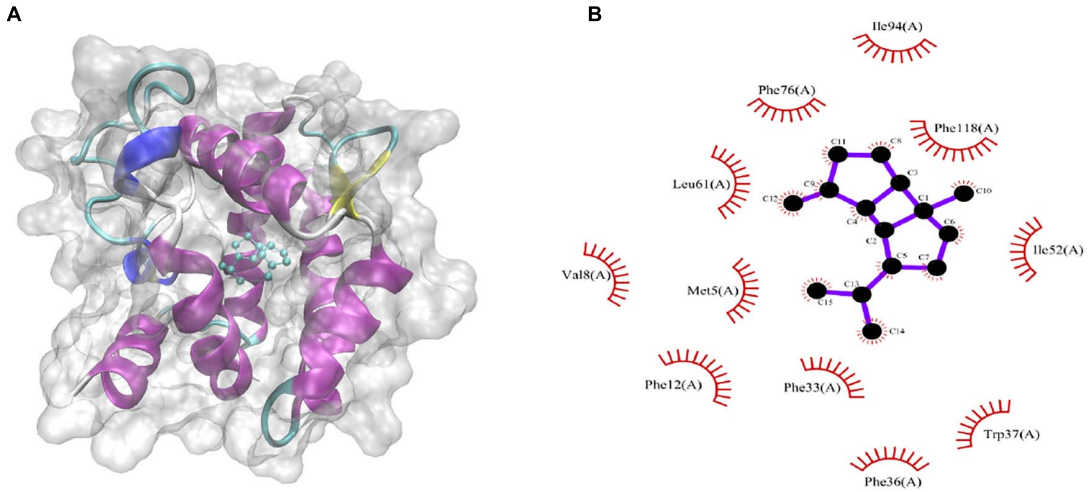

FIGURE 7 | Molecular docking of *CpomGOBP1* with β-bourbonene. **(A)** β-bourbonene located in the binding cavity of *CpomGOBP1*. **(B)** Key amino acid residues that interact with β-bourbonene.

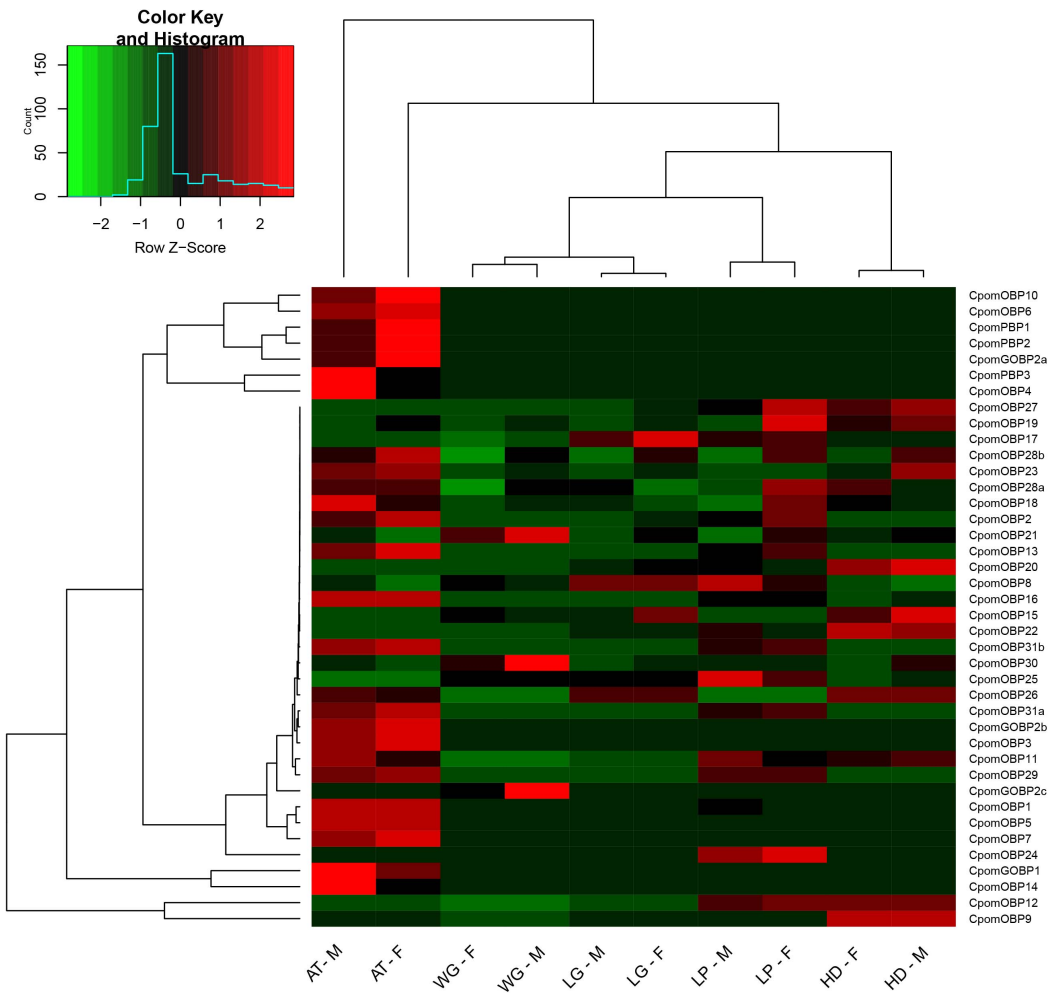

FIGURE 8 | Expression profiling of 40 *CpomOBPs* in different tissues. F, female; M, male; AT, antenna; HD, head (antennae removed); WG, wing; LG, leg; LP, labial palp.

To further explore which *OBP* genes have expanded or contracted in *C. pomonella*, we built a phylogenetic tree and performed collinearity analysis in chromosome location by comparing with related moth species. The results showed that *OBP* genes were conserved except the genes in Group 2, which contains many expanded genes in *M. sexta*. We also noticed some gene gains and losses in the conserved clade Group 1, composed of *GOBP* and *PBP* genes. The *GOBPs* and *PBPs* were a specific conserved subfamily in butterflies and moths, including GOBP1-2 and PBPA-D, which are in a tandem array with a fixed order in the same chromosome. These genes were thought to be involved in the recognition of volatile organic compounds (VOC) and sex pheromones of insects (Liu et al., 2020). However, recent studies showed some variations in this subfamily, including gene gains, losses, inversions, and translocations (Yasukochi et al., 2018). Although *GOBP1* and *GOBP2* were regarded as conserved in lepidopteran species (Vogt et al., 2015), some studies found that gene gains occurred in the *GOBP1* genes, such as duplication events of *GOBP1* in *P. xylostella* (Yasukochi et al., 2018) and *Operophtera brumata* (Yasukochi et al., 2018). In our study, we found a duplication event of a *GOBP2* gene that generated three *GOBP2* (*GOBP2a*, *GOBP2b*, and *GOBP2c*), two of which have been reported by Garczynski (Garczynski et al., 2013). *PBP* gene gains and losses occurred more commonly; most Lepidoptera have lost the *PBPB* gene (Yasukochi et al., 2018), while *PBPA* was expanded in *B. mori* (Gong D. P. et al., 2009). Similarly, we found that the *PBPB* gene was also lost in *C. pomonella*, which suggests that this gene may be undergoing a gene fusion event (Yasukochi et al., 2018).

Most *OBP* genes result from tandem duplications in insects, such as *Drosophila melanogaster* (Hekmat-Scafe et al., 2002) and *Anopheles gambiae* (Xu et al., 2003) in Diptera; *Tribolium castaneum* (Dippel et al., 2014) in Coleoptera; and *B. mori* (Gong D. P. et al., 2009) and *C. pomonella* (this study) in Lepidoptera. However, in earlier diverging ancestor orders including Hemiptera and Hymenoptera, there are fewer *OBP* genes without large tandem duplications (Vieira and Rozas, 2011), as in *Acyrthosiphon pisum* (Zhou et al., 2010) and *Bemisia tabaci* (Zeng et al., 2019) in Hemiptera; and *Apis mellifera* (Foret and Maleszka, 2006) and *Solenopsis invicta* (Pracana et al., 2017) in Hymenoptera. We also found a very consistent collinearity between *B. mori* and *C. pomonella*. These findings strongly suggest that the expansion of most *OBP* genes is caused by tandem duplications, and the tandem duplications of *OBP* genes in Lepidoptera occurred before speciation, indicating the existence of mainly purifying selection in moth *OBP* genes. In addition, the duplicated *CpomGOBP2c* gene is located in chromosome 21, instead of the GOBP/PBP gene cluster in chromosome 8, which indicates functional differentiation.

Some studies showed that single-point mutation of an amino acid could cause functional differentiation (Leary et al., 2012; Yang et al., 2017). Therefore, we further tested whether there are some positive sites in the *OBP* genes in *C. pomonella*. The results of evolutionary analysis by site model showed that most *OBP* genes evolved under purifying selection with ω ranging from 0.00547 to 0.15846 estimated by the M0 model. Similarly, most *OBP* genes in *B. mori* also evolved under purifying selection (Gong D. P. et al., 2009). The purifying selection of *OBP* genes is potentially due to functional constraints (Gong D. P. et al., 2009). However, among the *OBP* genes of lepidopteran species, the major function of *PBP*s is mainly to sense pheromones (Gong Y. et al., 2009), while *GOBP*s mainly sense the volatiles of host plants (Vogt et al., 2002). We assumed that *GOBP/PBP* genes may evolve under positive selection due to the vast diversity of sex pheromones and host volatiles. The results of the branch-site model on *GOBP/PBP* genes suggested that the *GOBP1* gene in *C. pomonella* evolved under positive selection. We detected two positively selected sites (41 S and 43 G) in *CpomGOBP1*, both located in the loop, close to the first disulfide bridge on helix 1. The mutations of these two amino acid residues may influence the fold shape of the binding cavity by modifying the disulfide bridge, which will cause functional differentiation (Sanchez-Gracia and Rozas, 2008). The docking result suggests that *CpomGOBP1* may have the ability to bind with β-bourbonene, however this must be functionally validated.

DATA AVAILABILITY STATEMENT

The original contributions presented in the study are included in the article/ **Supplementary Material**, further inquiries can be directed to the corresponding author/s.

AUTHOR CONTRIBUTIONS

FW, WQ, and NY conceived, designed this study, and revised the manuscript. CH, XZ, DH, QW, RT, LX, WL, WW, BL, and YX collected the data and completed bioinformatics analysis. CH and XZ drafted the manuscript. All authors read and approved the final manuscript.

FUNDING

This research was supported by Shenzhen Science and Technology Program (KQTD20180411143628272), China Postdoctoral Science Foundation (2020M683001), the Science and Technology Innovation Program of Chinese Academy of Agricultural Sciences (caascx-2017-2022-IAS), the Youth Program of National Natural Science Foundation of China (31901949 and 31801803), and the Special Fund for Science Technology Innovation and Industrial Development of Shenzhen Dapeng New District (PT202001-05).

SUPPLEMENTARY MATERIAL

The Supplementary Material for this article can be found online at: https://www.frontiersin.org/articles/10.3389/fphys.2021.690185/full#supplementary-material

REFERENCES

Andersson, M. N., Löfstedt, C., and Newcomb, R. D. (2015). Insect olfaction and the evolution of receptor tuning. *Front. Ecol. Evol.* 3:53. doi: 10.3389/fevo.2015.00053

Ansebo, L., Coracini, M. D. A., Bengtsson, M., Liblikas, I., Ramírez, M., Borg-Karlson, A. K., et al. (2004). Antennal and behavioural response of codling moth *Cydia pomonella* to plant volatiles. *J. Appl. Entomol.* 128, 488–493. doi: 10.1111/j.1439-0418.2004.00878.x

Bengtsson, J. M., Gonzalez, F., Cattaneo, A. M., Montagne, N., Walker, W. B., Bengtsson, M., et al. (2014). A predicted sex pheromone receptor of codling moth *Cydia pomonella* detects the plant volatile pear ester. *Front. Ecol. Evol.* 2:33. doi: 10.3389/fevo.2014.00033

Bengtsson, M., Bäckman, A. C., Liblikas, I., Ramirez, M. I., Borg-Karlson, A. K., Ansebo, L., et al. (2001). Plant odor analysis of apple: antennal response of codling moth females to apple volatiles during phenological development. *J. Agri. Food Chem.* 49, 3736–3741. doi: 10.1021/jf0100548

Cai, L. J., Zheng, L. S., Huang, Y. P., Xu, W., and You, M. S. (2020). Identification and characterization of odorant binding proteins in the diamondback moth, *Plutella xylostella*. *Insect Sci.* 29, 531–544. doi: 10.1111/imb.12664

Campanini, E. B., and de Brito, R. A. (2016). Molecular evolution of odorant-binding proteins gene family in two closely related *Anastrepha* fruit flies. *BMC Evol. Biol.* 16:198. doi: 10.1186/s12862-016-0775-0

Capella-Gutierrez, S., Silla-Martinez, J. M., and Gabaldon, T. (2009). trimAl: a tool for automated alignment trimming in large-scale phylogenetic analyses. *Bioinformatics* 25, 1972–1973. doi: 10.1093/bioinformatics/btp348

Cheng, T. C., Wu, J. Q., Wu, Y. Q., Chilukuri, R. V., Huang, L. H., Yamamoto, K., et al. (2017). Genomic adaptation to polyphagy and insecticides in a major East Asian noctuid pest. *Nat. Ecol. Evol.* 1, 1747–1756. doi: 10.1038/s41559-017-0314-4

Colovos, C., and Yeates, T. O. (1993). Verification of protein structures: patterns of nonbonded atomic interactions. *Protein Sci.* 2, 1511–1519. doi: 10.1002/pro.5560020916

Darriba, D., Taboada, G. L., Doallo, R., and Posada, D. (2011). ProtTest-HPC: fast selection of best-fit models of protein evolution. *Lect. Notes Comput. Sci.* 6586, 177–184. doi: 10.1007/978-3-642-21878-1_22

Dippel, S., Oberhofer, G., Kahnt, J., Gerischer, L., Opitz, L., Schachtner, J., et al. (2014). Tissue-specific transcriptomics, chromosomal localization, and phylogeny of chemosensory and odorant binding proteins from the red flour beetle *Tribolium castaneum* reveal subgroup specificities for olfaction or more general functions. *BMC Genomics* 15:1141. doi: 10.1186/1471-2164-15-1141

El-Gebali, S., Mistry, J., Bateman, A., Eddy, S. R., Luciani, A., Potter, S. C., et al. (2019). The Pfam protein families database in 2019. *Nucleic Acids Res.* 47, D427–D432.

Emms, D. M., and Kelly, S. (2015). OrthoFinder: solving fundamental biases in whole genome comparisons dramatically improves orthogroup inference accuracy. *Genome Biol.* 16:157.

Engsontia, P., Sangket, U., Chotigeat, W., and Satasook, C. (2014). Molecular evolution of the odorant and gustatory receptor genes in *Lepidopteran* insects: implications for their adaptation and speciation. *J. Mol. Evol.* 79, 21–39. doi: 10.1007/s00239-014-9633-0

Foret, S., and Maleszka, R. (2006). Function and evolution of a gene family encoding odorant binding-like proteins in a social insect, the honey bee (*Apis mellifera*). *Genome Res.* 16, 1404–1413. doi: 10.1101/gr.5075706

Garczynski, S. F., Coates, B. S., Unruh, T. R., Schaeffer, S., Jiwan, D., Koepke, T., et al. (2013). Application of *Cydia pomonella* expressed sequence tags: identification and expression of three general odorant binding proteins in codling moth. *Insect Sci.* 20, 559–574. doi: 10.1111/j.1744-7917.2012.01560.x

Gong, D. P., Zhang, H. J., Zhao, P., Xia, Q. Y., and Xiang, Z. H. (2009). The odorant binding protein gene family from the genome of silkworm, *Bombyx mori*. *BMC Genomics* 10:332. doi: 10.1186/1471-2164-10-332

Gong, Y., Pace, T. C., Castillo, C., Bohne, C., O'Neill, M. A., and Plettner, E. (2009). Ligand-interaction kinetics of the pheromone- binding protein from the gypsy moth. *L. dispar*: insights into the mechanism of binding and release. *Chem. Biol.* 16, 162–172. doi: 10.1016/j.chembiol.2009.01.005

Gouin, A., Bretaudeau, A., Nam, K., Gimenez, S., Aury, J.-M., Duvic, B., et al. (2017). Two genomes of highly polyphagous lepidopteran pests (*Spodoptera frugiperda*, Noctuidae) with different host-plant ranges. *Sci. Rep.* 7:11816.

Han, M. V., Thomas, G. W. C., Lugo-Martinez, J., and Hahn, M. W. (2013). Estimating gene gain and loss rates in the presence of error in genome assembly and annotation using CAFE 3. *Mol. Biol. Evol.* 30, 1987–1997. doi: 10.1093/molbev/mst100

Hekmat-Scafe, D. S., Scafe, C. R., McKinney, A. J., and Tanouye, M. A. (2002). Genome-wide analysis of the odorant-binding protein gene family in *Drosophila melanogaster*. *Genome Res.* 12, 1357–1369. doi: 10.1101/gr.239402

Humphrey, W., Dalke, A., and Schulten, K. (1996). VMD: visual molecular dynamics. *J. Mol. Graph.* 14, 33–38. doi: 10.1016/0263-7855(96)00018-5

Katoh, K., Misawa, K., Kuma , K-i., and Miyata, T. (2002). MAFFT: a novel method for rapid multiple sequence alignment based on fast Fourier transform. *Nucleic Acids Res.* 30, 3059–3066. doi: 10.1093/nar/gkf436

Kawamoto, M., Jouraku, A., Toyoda, A., Yokoi, K., Minakuchi, Y., Katsuma, S., et al. (2019). High-quality genome assembly of the silkworm, *Bombyx mori*. *Insect Biochem. Mole. Biol.* 107, 53–62. doi: 10.1016/j.ibmb.2019.02.002

Kim, D., Langmead, B., and Salzberg, S. L. (2015). HISAT: a fast spliced aligner with low memory requirements. *Nat. Methods* 12, 357–360. doi: 10.1038/nmeth.3317

Knight, A. L., Mujica, V., Herrera, S. L., and Tasin, M. (2019). Addition of terpenoids to pear ester plus acetic acid increases catches of codling moth (Lepidoptera: Tortricidae). *J. Appl. Entomol.* 143, 813–821. doi: 10.1111/jen.12646

Kumar, S., Neven, L. G., Zhu, H., and Zhang, R. (2015). Assessing the global risk of establishment of *Cydia pomonella* (Lepidoptera: Tortricidae) using CLIMEX and MaxEnt niche models. *J. Econ. Entomol.* 108, 1708–1719. doi: 10.1093/jee/tov166

Kumar, S., Stecher, G., Suleski, M., and Hedges, S. B. (2017). TimeTree: a resource for timelines, timetrees, and divergence times. *Mol. Biol. Evol.* 34, 1812–1819. doi: 10.1093/molbev/msx116

Laskowski, R. A., MacArthur, M. W., Moss, D. S., and Thornton, J. M. (1993). PROCHECK: a program to check the stereochemical quality of protein structures. *J. Appl. Cryst.* 26, 283–291. doi: 10.1107/s0021889892009944

Leary, G. P., Allen, J. E., Bunger, P. L., Luginbill, J. B., Linn, C. E., Macallister, I. E., et al. (2012). Single mutation to a sex pheromone receptor provides adaptive specificity between closely related moth species. *Proc. Natl. Acad. Sci. U.S.A.* 109, 14081–14086. doi: 10.1073/pnas.1204661109

Liu, J. Y., Tian, Z., and Zhang, Y. L. (2016). Structure-based discovery of potentially active semiochemicals for *Cydia pomonella* (L.). *Sci. Rep.* 6:34600.

Liu, Y., Hu, Y., Bi, J., Kong, X., Long, G., Zheng, Y., et al. (2020). Odorant-binding proteins involved in sex pheromone and host-plant recognition of the sugarcane borer *Chilo infuscatellus* (Lepidoptera: Crambidae). *Pest Manag. Sci.* 76, 4064–4076. doi: 10.1002/ps.5961

Lüthy, R., Bowie, J. U., and Eisenberg, D. (1992). Assessment of protein models with three-dimensional profiles. *Nature* 356, 83–85. doi: 10.1038/356083a0

Manoharan, M., Ng Fuk Chong, M., Vaïtinadapoulé, A., Frumence, E., Sowdhamini, R., and Offmann, B. (2013). Comparative genomics of odorant binding proteins in *Anopheles gambiae*, *Aedes aegypti*, and *Culex quinquefasciatus*. *Genome Biol. Evol.* 5, 163–180. doi: 10.1093/gbe/evs131

McKenzie, S. K., Oxley, P. R., and Kronauer, D. J. C. (2014). Comparative genomics and transcriptomics in ants provide new insights into the evolution and function of odorant binding and chemosensory proteins. *BMC Genomics* 15:718. doi: 10.1186/1471-2164-15-718

Nei, M., and Rooney, A. P. (2005). Concerted and birth-and-death evolution of multigene families. *Annu. Rev. Genet.* 39, 121–152. doi: 10.1146/annurev.genet.39.073003.112240

Pearce, S. L., Clarke, D. F., East, P. D., Elfekih, S., Gordon, K. H. J., Jermiin, L. S., et al. (2017). Genomic innovations, transcriptional plasticity and gene loss underlying the evolution and divergence of two highly polyphagous and invasive *Helicoverpa* pest species. *BMC Biol.* 15:63. doi: 10.1186/s12915-017-0402-6

Pelosi, P., Iovinella, I., Felicioli, A., and Dani, F. R. (2014). Soluble proteins of chemical communication: an overview across arthropods. *Front. Physiol.* 5:320. doi: 10.3389/fphys.2014.00320

Pertea, M., Kim, D., Pertea, G. M., Leek, J. T., and Salzberg, S. L. (2016). Transcript-level expression analysis of RNA-seq experiments with HISAT, StringTie and Ballgown. *Nat. Protoc.* 11:1650. doi: 10.1038/nprot.2016.095

Pracana, R., Levantis, I., Martinez-Ruiz, C., Stolle, E., Priyam, A., and Wurm, Y. (2017). Fire ant social chromosomes: differences in number, sequence and

expression of odorant binding proteins. *Evol. Lett.* 1, 199–210. doi: 10.1002/evl3.22

Sanchez-Gracia, A., and Rozas, J. (2008). Divergent evolution and molecular adaptation in the *Drosophila* odorant-binding protein family: inferences from sequence variation at the *OS-E* and *OS-F* genes. *BMC Evol. Biol.* 8:323. doi: 10.1186/1471-2148-8-323

Solovyev, V., Kosarev, P., Seledsov, I., and Vorobyev, D. (2006). Automatic annotation of eukaryotic genes, pseudogenes and promoters. *Genome Biol.* 7:S10.

Stamatakis, A. (2014). RAxML version 8: a tool for phylogenetic analysis and post-analysis of large phylogenies. *Bioinformatics* 30, 1312–1313. doi: 10.1093/bioinformatics/btu033

Sun, J. S., Xiao, S., and Carlson, J. R. (2018). The diverse small proteins called odorant-binding proteins. *Open Biol.* 8:180208. doi: 10.1098/rsob.180208

Tamura, K., Stecher, G., Peterson, D., Filipski, A., and Kumar, S. (2013). MEGA6: molecular evolutionary genetics analysis version 6.0. *Mol. Biol. Evol.* 30, 2725–2729. doi: 10.1093/molbev/mst197

Tian, Z., Liu, J. Y., and Zhang, Y. L. (2016a). Key residues involved in the interaction between *Cydia pomonella* pheromone binding protein 1 (CpomPBP1) and codlemone. *J. Agric. Food Chem.* 64, 7994–8001. doi: 10.1021/acs.jafc.6b02843

Tian, Z., Liu, J. Y., and Zhang, Y. L. (2016b). Structural insights into *Cydia pomonella* pheromone binding protein 2 mediated prediction of potentially active semiochemicals. *Sci. Rep.* 6:22336.

Tian, Z., and Zhang, Y. (2016). Molecular characterization and functional analysis of pheromone binding protein 1 from *Cydia pomonella* (L.). *Insect Mol. Biol.* 25, 769–777. doi: 10.1111/imb.12261

Trott, O., and Olson, A. J. (2010). AutoDock Vina: improving the speed and accuracy of docking with a new scoring function, efficient optimization, and multithreading. *J. Comput. Chem.* 31, 455–461.

Vieira, F. G., and Rozas, J. (2011). Comparative genomics of the odorant-binding and chemosensory protein gene families across the arthropoda: origin and evolutionary history of the chemosensory system. *Genome Biol. Evol.* 3, 476–490. doi: 10.1093/gbe/evr033

Vieira, F. G., Sanchez-Gracia, A., and Rozas, J. (2007). Comparative genomic analysis of the odorant-binding protein family in 12 *Drosophila* genomes: purifying selection and birth-and-death evolution. *Genome Biol.* 8:R235.

Vogt, R. G., Grosse-Wilde, E., and Zhou, J. J. (2015). The Lepidoptera odorant binding protein gene family: gene gain and loss within the GOBP/PBP complex of moths and butterflies. *Insect Biochem. Mol. Biol.* 62, 142–153. doi: 10.1016/j.ibmb.2015.03.003

Vogt, R. G., Rogers, M. E., Franco, M. D., and Sun, M. (2002). A comparative study of odorant binding protein genes: differential expression of the PBP1-GOBP2 gene cluster in *Manduca sexta* (Lepidoptera) and the organization of OBP genes in *Drosophila melanogaster* (Diptera). *J. Exp. Biol.* 205, 719–744. doi: 10.1242/jeb.205.6.719

Wallace, A. C., Laskowski, R. A., and Thornton, J. M. (1995). LIGPLOT: a program to generate schematic diagrams of protein-ligand interactions. *Protein Eng.* 8, 127–134. doi: 10.1093/protein/8.2.127

Wan, F., Yin, C., Tang, R., Chen, M., Wu, Q., Huang, C., et al. (2019). A chromosome-level genome assembly of *Cydia pomonella* provides insights into chemical ecology and insecticide resistance. *Nat. Commun.* 10:4237.

Wang, W., Xia, M., Chen, J., Deng, F. N., Yuan, R., Zhang, X. P., et al. (2016). Data set for phylogenetic tree and RAMPAGE Ramachandran plot analysis of SODs in *Gossypium raimondii* and *G. arboreum*. *Data. Brief* 9, 345–348. doi: 10.1016/j.dib.2016.05.025

Witzgall, P., Stelinski, L., Gut, L., and Thomson, D. (2008). Codling moth management and chemical ecology. *Annu. Rev. Entomol* 53, 503–522. doi: 10.1146/annurev.ento.53.103106.093323

Wu, T. D., and Watanabe, C. K. (2005). GMAP: a genomic mapping and alignment program for mRNA and EST sequences. *Bioinformatics* 21, 1859–1875. doi: 10.1093/bioinformatics/bti310

Xu, P. X., Zwiebel, L. J., and Smith, D. P. (2003). Identification of a distinct family of genes encoding atypical odorant-binding proteins in the malaria vector mosquito, *Anopheles gambiae*. *Insect Mol. Biol.* 12, 549–560. doi: 10.1046/j.1365-2583.2003.00440.x

Yang, K., Huang, L. Q., Ning, C., and Wang, C. Z. (2017). Two single-point mutations shift the ligand selectivity of a pheromone receptor between two closely related moth species. *Elife* 6:e29100.

Yang, Z. (2007). PAML 4: phylogenetic analysis by maximum likelihood. *Mol. Biol. Evol.* 24, 1586–1591. doi: 10.1093/molbev/msm088

Yasukochi, Y., Yang, B., Fujimoto, T., Sahara, K., Matsuo, T., and Ishikawa, Y. (2018). Conservation and lineage-specific rearrangements in the GOBP/PBP gene complex of distantly related ditrysian Lepidoptera. *PLoS One* 13:e0192762. doi: 10.1371/journal.pone.0192762

Zeng, Y., Yang, Y. T., Wu, Q. J., Wang, S. L., Xie, W., and Zhang, Y. J. (2019). Genome-wide analysis of odorant-binding proteins and chemosensory proteins in the sweet potato whitefly, *Bemisia tabaci*. *Insect Sci.* 26, 620–634. doi: 10.1111/1744-7917.12576

Zhan, S., Merlin, C., Boore, J. L., and Reppert, S. M. (2011). The monarch butterfly genome yields insights into long-distance migration. *Cell* 147, 1171–1185. doi: 10.1016/j.cell.2011.09.052

Zhang, H., Chen, J. L., Lin, J. H., Lin, J. T., and Wu, Z. Z. (2020). Odorant-binding proteins and chemosensory proteins potentially involved in host plant recognition in the Asian citrus psyllid, *Diaphorina citri*. *Pest Manag. Sci.* 76, 2609–2618. doi: 10.1002/ps.5799

Zhou, J. J., Vieira, F. G., He, X. L., Smadja, C., Liu, R., Rozas, J., et al. (2010). Genome annotation and comparative analyses of the odorant-binding proteins and chemosensory proteins in the pea aphid *Acyrthosiphon pisum*. *Insect Mol. Biol.* 19, 113–122. doi: 10.1111/j.1365-2583.2009.00919.x

Zhu, H., Kumar, S., and Neven, L. G. (2017). Codling moth (Lepidoptera: Tortricidae) establishment in China: stages of invasion and potential future distribution. *J. Insect Sci.* 17:85.

Conflict of Interest: The authors declare that the research was conducted in the absence of any commercial or financial relationships that could be construed as a potential conflict of interest.

Copyright © 2021 Huang, Zhang, He, Wu, Tang, Xing, Liu, Wang, Liu, Xi, Yang, Wan and Qian. This is an open-access article distributed under the terms of the Creative Commons Attribution License (CC BY). The use, distribution or reproduction in other forums is permitted, provided the original author(s) and the copyright owner(s) are credited and that the original publication in this journal is cited, in accordance with accepted academic practice. No use, distribution or reproduction is permitted which does not comply with these terms.

frontiers in Ecology and Evolution

ORIGINAL RESEARCH
published: 25 October 2021
doi: 10.3389/fevo.2021.759778

Detection of Volatile Organic Compounds by Antennal Lamellae of a Scarab Beetle

Ya-Ya Li[1,2,3], Deguang Liu[2,3], Ping Wen[4] and Li Chen[1]**

[1] School of Life Sciences, Institute of Life Science and Green Development, Hebei University, Baoding, China, [2] College of Plant Protection, Northwest A&F University, Xianyang, China, [3] State Key Laboratory of Crop Stress Biology for Arid Areas, Northwest A&F University, Xianyang, China, [4] Key Laboratory of Tropical Forest Ecology, Xishuangbanna Tropical Botanical Garden, Chinese Academy of Science (CAS), Kunming, China

Chemoreceptive sensilla are abundantly distributed on antennal lamellae of scarab beetles. Olfactory reception by these sensory lamellae plays a major role in feeding behaviors and sexual communication of these beetles. A new electroantennogram (EAG) recording technique is here described for evaluation of electrophysiological responses of antennal lamellae of *Pseudosymmachia flavescens* to sex pheromones and host plant-related compounds. EAG responses were recorded simultaneously from each lamella and the closed antennal club. All test stimuli elicited similar EAG depolarization profiles in all the three lamellae and the closed club although EAG amplitudes from the same lamella or the club varied widely among different chemical stimuli. The mid lamella tended to produce significantly greater EAG responses. EAG responses evoked by a sex pheromone component, anisole, showed a significant correlation with the density of sensilla placodea subtype 1 (SP1). However, no general patterns were obtained for correlations between the density of any test sensilla type and EAG amplitudes evoked by all the six plant volatiles. Single sensillum recordings are needed to elucidate the specific roles of these sensilla in intraspecific sexual communication and perception of host plant volatiles.

Keywords: Scarabaeidae, electroantennogram, *Pseudosymmachia flavescens*, sex pheromone, host plant volatiles

OPEN ACCESS

Edited by:
Xin-Cheng Zhao,
Henan Agricultural University, China

Reviewed by:
Qi Yan,
Nanjing Agricultural University, China
Stefan Dötterl,
University of Salzburg, Austria

****Correspondence:***
Ping Wen
wenping@xtbg.ac.cn
Li Chen
chenli1@hbu.edu.cn
orcid.org/0000-0002-0394-4387

Specialty section:
This article was submitted to Chemical Ecology, a section of the journal Frontiers in Ecology and Evolution

Received: *17 August 2021*
Accepted: *28 September 2021*
Published: *25 October 2021*

Citation:
Li Y-Y, Liu D, Wen P and Chen L (2021) Detection of Volatile Organic Compounds by Antennal Lamellae of a Scarab Beetle. Front. Ecol. Evol. 9:759778. doi: 10.3389/fevo.2021.759778

INTRODUCTION

As an important feature of living organisms, olfaction plays a key role in regulating essential behaviors. In insects, the location of mates, food sources, and oviposition sites, as well as avoidance of predators and other threats, primarily relies on olfactory perception of environmental chemical signals. The main olfactory organs in insects include antennae, maxillary palps, labial palps, ovipositor, and feet. Among them, the antennae are the most important sensory organ and their function in olfaction in insects has been commonly recognized. A variety of sensilla are distributed on the surface of the antennae, and mainly tuned to detect odorants in the environment (Altner and Prillinger, 1980; Zacharuk, 1985; Steinbrecht, 1997).

The antennae of scarab beetles (Coleoptera: Scarabaeidae) are usually 10-segmented with the last 3–7 segments forming a lamellate club (Meinecke, 1975). The lamellar segments are always folded together to protect their inner surfaces when resting or crawling in soil, but wide-open during

olfaction in mate finding and host plant location. As most olfactory sensilla are present on the surfaces of lamellae, it is crucial to allow lamellae to stay open when recording EAG response to odorants. However, such antennal structures and the closing feature of the antennal club in the resting position have made the antennal preparation for an electrophysiological study difficult. Several different techniques have been used to manually maneuver the antennal club for EAG recordings from scarab beetles [reviewed by Chen et al. (2019)]. With these techniques, electrical conductivity between antenna and the recording electrode may be insufficient, resulting in non-negligible background noises. Recently, we have developed a practical technique for recording EAG responses from one of the three lamellae of a scarab beetle, *Pseudosymmachia flavescens* (Brenske) (Coleoptera: Scarabaeidae: Melolonthinae). A key step of this antennal preparation technique is to make glass electrodes with appropriate size at opening to rightly fit the base or the tip of an excised antenna. One lamella was held apart from the other two on the antenna with a minuten pin and a disposable syringe needle, and directly connected to the recording electrode. The Beadle-Ephrussi Ringer solution modified with Tween® 80 (0.05%, *W*/*V*) was used to improve the signal-to-noise ratio. This technique is very useful even when testing EAG responses from very tiny antennae of small-sized scarab beetles (Chen et al., 2019).

In the present study, we developed a new technique to record EAG responses from three lamellae of one antenna and the closed club of the other one at same time to sex and host plant-related compounds. This approach allows to test whether the three lamellae on an antenna respond the same or differently to the same compounds, and whether the amplitudes of the EAG responses are comparable among the three lamellae and the closed club. In a previous study, four different types of sensilla on the antennal club of *P. flavescens* were observed, including sensilla basiconica, coeloconica, placodea, and trichodea (Li et al., under review). Porous sensilla placodea are predominant on lamellar surfaces (Bohacz et al., 2020), which have been demonstrated to detect sex pheromones and host plant-related volatiles in melolonthids (subfamilies Melolonthinae, Rutelinae, and Dynastinae) (Hansson et al., 1999; Nikonov et al., 2001; Ochieng et al., 2002). The presence of cuticular wall pores on sensilla basiconica intermingled with sensilla placodea all over the lamellar surface suggests an olfactory role for them. A comparison of the electrophysiological data with previous morphological data is aimed at demonstrating likely correlations between the number of any specific olfactory sensilla and the strength of EAG responses to certain compounds.

MATERIALS AND METHODS

Insects

Adult beetles were collected from clove [*Syzygium aromaticum* (L.) Merr. and L. M. Perry] tree leaves on the campus of Institute of Zoology, Chinese Academy of Sciences, Beijing, China (116.39° E, 40.01° N). The beetles were sexed and the two sexes were held separately in clear plastic boxes (30 cm × 12 cm × 22 cm) containing moisturized soil at 25°C, 80% RH, and under a 16L:8D photoperiod. Fresh clove leaves were supplied daily to the beetles. Both female and male beetles were used for electrophysiological recordings.

Chemicals

HPLC grade hexane was purchased from CNW Technologies GmbH (Düsseldorf, Germany). Anisole (99%), *Z*-3-hexenal (50% in triacetin, stabilized), eucalyptol (99%), 6-methyl-5-hepten-2-one (99%), 1-hexanol (98%), (-)-*E*-pinocarveol (96%), and 4-ethyl-phenol (99%) were all purchased from Sigma-Aldrich (St. Louis, MO, United States). Anisole is a major component identified from the sex gland of female *P. flavescens* (unpublished data). The other compounds are electrophysiologically active, derived from leaves of walnut (*Juglans regia* L.), a preferred host plant of *P. flavescens* (Chen et al., 2019). Anisole was prepared in hexane and diluted to 0.1 and 0.01 μg/μL while all other synthetic plant volatiles were diluted with hexane to 10 and 1 μg/μL.

Electroantennographic Recordings

Olfactory responses of antennal lamellae of *P. flavescens* adults to volatile organic compounds were measured by the conventional EAG technique. The protocol for antennal preparation was similar to Chen et al. (2019). Glass capillary tubes (O.D. 1.5 mm, I.D. 0.84 mm, VitalSense Scientific Instruments Co., Ltd., Chengdu, China) were manually pulled over the flame of an alcohol lamp, and then cut with a column cutter, having tip openings with an internal diameter of 20 μm. Some heated capillary tubes were bent to 120–150° by further heating the point about 1 cm away from their tips (**Figure 1A**). All these capillary tubes were filled with the Tween® 80-modified Beadle-Ephrussi Ringer solution (Chen et al., 2019), serving as reference and recording electrodes. The head of a beetle was excised with a microknife, and fixed on a holding stage with dental wax in a downright position (**Figure 1B**). The reference electrode was connected to the neck of the isolated head. The three lamellae of one antennal club were carefully separated with a minuten pin and connected to three recording electrodes. The mid-lamella (L2 in **Figure 1B**) was allowed to connect to the second recording electrode (2 in **Figure 1A**) followed by the proximal (L1 in **Figure 1B**) and distal lamellae (L3 in **Figure 1B**) connecting to the first (1 in **Figure 1A**) and third recording electrodes (3 in **Figure 1A**), respectively. The other antennal club (**Figure 1B**) was directly connected to the fourth recording electrode (4 in **Figure 1A**). This connecting procedure ensured a high success rate of antennal preparation. Platinum wire (D. 0.4 mm) was used to establish an electrical connection between the electrode and the customized EAG probe (Wen et al., 2017).

A 10-μL aliquot of each solution was loaded on a filter paper strip (4 mm × 40 mm), which was then inserted into a glass Pasteur pipette to constitute an odor cartridge. The odor cartridge was connected to an air stimulus controller CS-55 (Syntech, Kirchzarten, Germany) to deliver odor stimuli through a small hole in the wall of a PTFE tube (I.D. 6 mm) as 0.2-s puffs. The antennae were flushed continuously by a charcoal-filtered and humidified air stream at 800 mL/min in the PTFE tube that

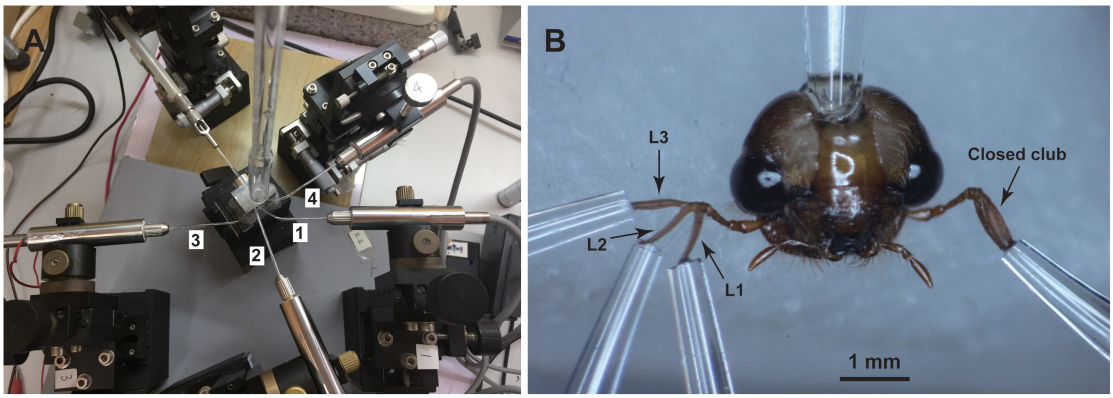

FIGURE 1 | Experimental set-up **(A)** and antennal preparation **(B)** for EAG recordings. The isolated head of a beetle was mounted on a dental wax stage. The reference electrode was connected to the neck while the recording electrodes were connected to the three separated lamellae, L1, L2, and L3, of one antennal club and the other closed club. The numbers 1, 2, 3, and 4 of the recording electrodes correspond to the lamellae L1, L2, L3, and one antennal club, respectively.

ended directly at the antennal preparation. A single antennal preparation was used for a series of measurements of various compounds at the same concentration. A blank stimulus (solvent control) was presented before testing the compounds, and the testing sequence of these compounds was randomized. Intervals of 2 min between successive stimulations were used to ensure antennal recovery. For strict signal separation, signals captured by the four individual battery powered EAG probes were output to four independent HP-34465A digital multimeters (Keysight, United States) controlled by a BenchVue software (Keysight, United States) running on a PC (Wen et al., 2017). There were two dose groups, designated as low (0.1 μg anisole and 10 μg plant volatile compounds) and high (1 μg anisole and 100 μg plant volatile compounds). EAG recordings were obtained from 10 antennal preparations for each dose group. To minimize any variation among antennae, EAG responses in a lamella or the closed antennal club were corrected by deducting the EAG amplitude to the solvent control from the EAG amplitude elicited by the test compound.

Statistical Analyses

All values reported were mean ± standard error. One-way analysis of variance with Tukey's HSD multiple comparisons was used to investigate significant differences in the EAG responses of different lamellae and the closed club to the same odor. The effects of sex, compound, dose, and lamella, as well as two-way, three-way, and four-way interactions (a total of 11 possible interactions) among these four variables on the EAG amplitudes were analyzed using a four-way mixed ANOVA. Data on the abundance of sensilla placodea (SP) and sensilla basiconica (SB) published in a previous study (Li et al., under review) were used for correlational analyses. The correlation between sensillar abundance and EAG responses of male beetles to high-dose sex pheromone or EAG responses of female beetles to high-dose host plant-related compounds was analyzed using the PROC REG procedure. Statistical significance was set at the α level of 0.05. All analyses were performed using the SAS statistical software (SAS Institute, 2004).

RESULTS

All the tested stimuli evoked EAG responses of a fairly constant and reproducible time course and a characteristic shape (**Figure 2**). These responses were similar in the shape across all individual lamellae and the closed antennal club on antennae of *P. flavescens*.

Multifactorial ANOVA revealed significant effects of sex, compound, dose, and lamella on EAG responses of *P. flavescens*. Various interactions among these factors were also significant (**Table 1**). For each sex and dose, all tested compounds triggered apparent antennal responses in all lamellae and the closed club (**Figure 3**). In both sexes, the mid-lamella L2 appeared to show higher EAG response than the other two lamellae and the closed club, but the differences were not always significant. Anisole elicited significantly stronger responses in males, with 1.77–2.83 mV from 0.1 μg and 3.21–4.27 mV from 1.0 μg, showing a sex-specific response pattern. Generally, male lamellae tended to show significantly higher responses to most plant-related compounds (except 4-ethyphenol), especially at high doses, than female counterparts (**Supplementary Table 1**). The EAG responses to all compounds except for 6-methyl-5-hepten-2-one and eucalyptol significantly increased with dose in females (significant dose effect, **Figure 3** and **Supplementary Table 2**). Among the six plant-related compounds, 1-hexanol generally elicited the highest EAG responses in females at low dose and in males at both doses, followed by 6-methyl-5-hepten-2-one, (-)-*E*-pinocarveol, and eucalyptol. *Z*-3-Hexenal and 4-ethylphenol were the least active in most cases (**Supplementary Figure 1**). The EAG amplitude patterns to these volatiles across all lamellae were similar. In the case of low dose, however, there were no significant differences in EAG responses of female lamellae to 1-hexanol and 6-methyl-5-hepten-2-one.

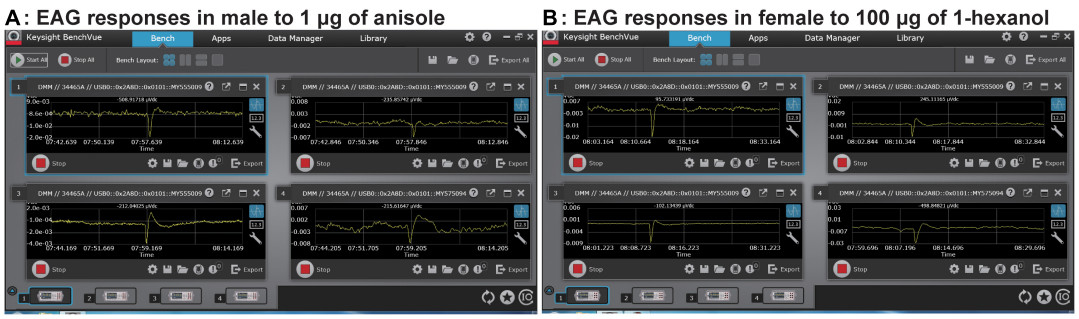

FIGURE 2 | Simultaneous EAG recordings from three lamellae of one antennal club and the closed club of the second antenna in response to anisole **(A)** and 1-hexanol **(B)**. The amplitudes in each small window were instantaneous reads recorded by a customized probe. The windows 1, 2, 3, and 4 display EAG traces captured by the recording electrodes 1, 2, 3, and 4 in **Figure 1**, respectively.

TABLE 1 | The effects of sex, compound, dose, lamella, and interactions of these variables on absolute EAG responses.

Source of variation	d.f.	*F*	*P*
Sex	1	876.19	<0.0001
Compound	6	792.89	<0.0001
Dose	1	1,120.11	<0.0001
Lamella	3	105.91	<0.0001
Sex × Compound	6	351.70	<0.0001
Sex × Dose	1	205.33	<0.0001
Sex × Lamella	3	20.16	<0.0001
Compound × Dose	6	106.64	<0.0001
Compound × Lamella	18	8.17	<0.0001
Dose × Lamella	3	5.34	0.0012
Sex × Compound × Dose	6	26.36	<0.0001
Sex × Compound × Lamella	18	2.36	0.0012
Sex × Dose × Lamella	3	1.14	0.3304
Compound × Dose × Lamella	18	0.89	0.5882
Sex × Compound × Dose × Lamella	18	0.34	0.9957

By means of the linear regression analysis, a significant correlation between the sensillar abundance and EAG responses of males to high dose of anisole was obtained for sensilla placodea subtype 1 (SP1) (P = 0.0373) (**Table 2**). This thus suggests that olfactory neurons in SP1 in males is tuned to anisole. EAG values for *Z*-3-hexenal, 6-methyl-5-hepten-2-one, and 1-hexanol were correlated with the population density values of SP1 or SP2 (sensilla placodea subtype 2). The EAG responses to eucalyptol was likely to correlate with the population density of SP2 (P = 0.0717). However, there was no correlational relationship between the sensilla abundance and EAG responses to (-)-*E*-pinocarveol and 4-ethyl-phenol. The EAG values of all stimuli were not correlated with the density of SB at all (**Table 2**).

DISCUSSION

The antennae of scarab beetles show a characteristic lamellicorn shape, on which olfactory sensilla are concentrated (Meinecke, 1975). All lamellar segments of the antennal club are involved in sexual chemical communication and perception of plant volatiles (Leal, 1998). For the first time, we presented differences in EAG amplitudes among the three lamellae of a scarab beetle. The mid lamella of *P. flavescens* tended to show greater EAG responses as compared to the first and third ones and the whole club to the host plant-related compounds, eucalyptol, 6-methyl-5-hepten-2-one, 1-hexanol, and (-)-*E*-pinocarveol. This tendency correlated well to a greater number of sensilla placodea on the mid lamella (Li et al., under review). It is therefore reasonable to estimate the electrical contribution provided to the EAG by such sensilla distributed on the lamellar surface. If the sensitivities of same-type sensilla on different lamellae to the same odor stimulation are quite similar, the contributions by the receptors in each sensilla would be directly related to its density on the individual lamella. Therefore, the distribution of specialized sensilla tuned to sex pheromones or host plant-related compounds determines the EAG amplitudes. The position of the recording electrode on an insect antenna affects conclusions on the detection of odorants (Biasazin et al., 2014; Jacob et al., 2017; Jacob, 2018). Our data showed that the three lamellae detected the same odorants, however, the sensitivities to different compounds varied with lamella position although the difference were not always significant (**Figure 3**). The receptors housed in sensilla placodea have proven to

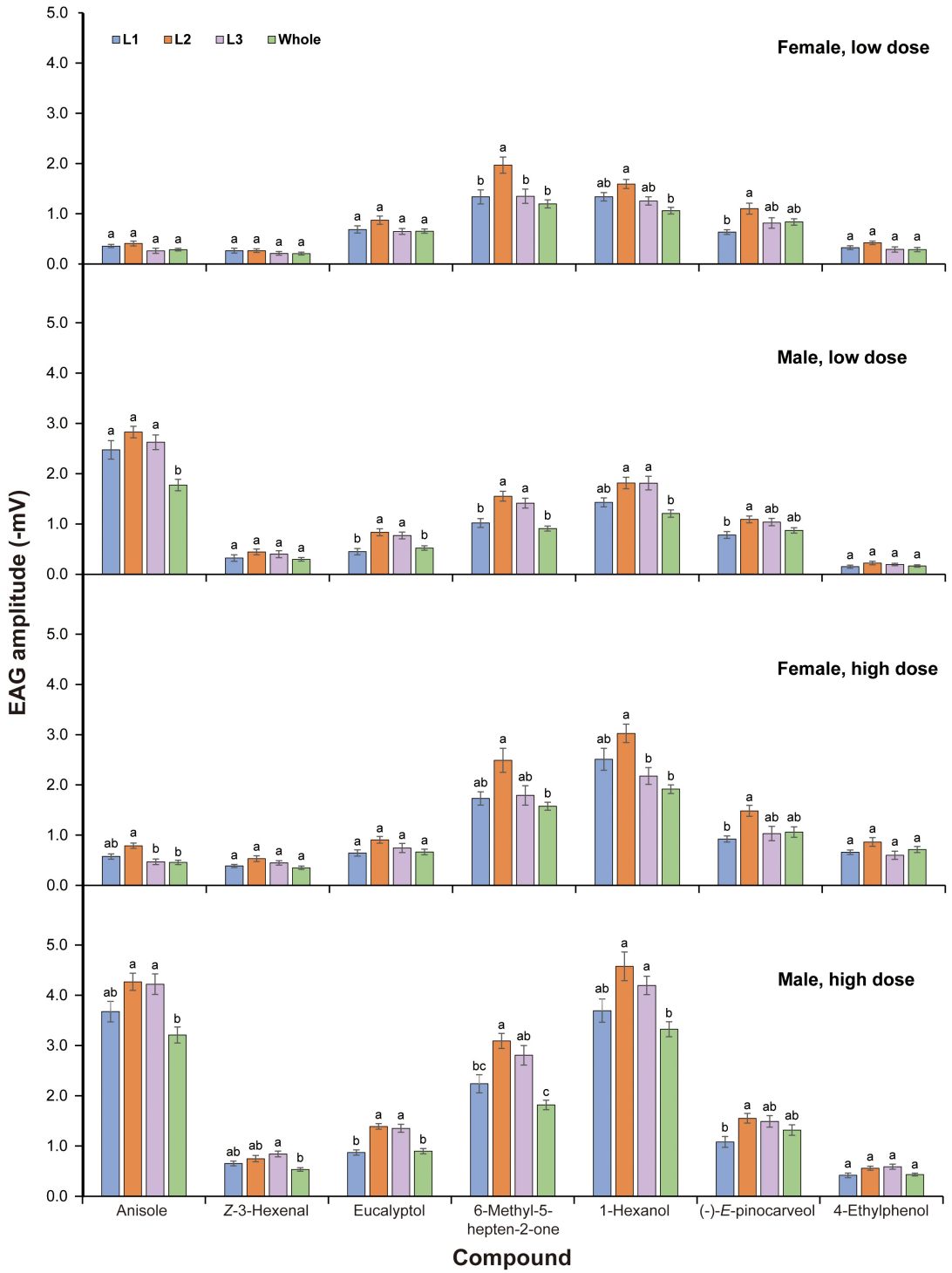

FIGURE 3 | EAG responses of antennae of *Pseudosymmachia flavescens* to synthetic volatile compounds. L1: proximal lamella; L2: mid lamella; L3: distal lamella; Whole: the closed club. Low dose: 0.1 μg for anisole and 10 μg for all plant volatile compounds; High dose: 1 μg for anisole and 100 μg for all plant volatile compounds. Columns with different lowercase letters are significantly different at $P < 0.05$ ($N = 10$, Tukey tests after significant ANOVA).

respond to sex pheromones and host plant-related volatiles in melolonthids (Hansson et al., 1999; Nikonov et al., 2001; Ochieng et al., 2002). Significant correlations found between population density of sensilla placodea (SP1 and/or SP2) and EAG responses evoked by anisole, *Z*-3-hexenal, 6-methyl-5-hepten-2-one, and 1-hexanol (**Table 2**) indicate that sensilla

TABLE 2 | Correlations between sensillar abundance and EAG responses.

Compound	Sex	Sensilla	*P*
Anisole	Male	SP1	**0.0373**
		SP2	0.1351
		SP	0.0596
		SB	0.7986
Z-3-Hexenal	Female	SP1	0.2122
		SP2	**0.0044**
		SP	0.0880
		SB	0.9842
Eucalyptol	Female	SP1	0.2686
		SP2	0.0717
		SP	0.1517
		SB	0.7498
6-Methyl-5-hepten-2-one	Female	SP1	0.0963
		SP2	0.0832
		SP	**0.0393**
		SB	0.9736
1-Hexanol	Female	SP1	**0.0029**
		SP2	0.1918
		SP	**0.0170**
		SB	0.6570
(-)-*E*-Pinocarveol	Female	SP1	0.2772
		SP2	0.2244
		SP	0.2155
		SB	0.5993
4-Ethyl-phenol	Female	SP1	0.2652
		SP2	0.4953
		SP	0.3101
		SB	0.6534

SP, sensilla placodea; SP1, sensilla placodea subtype 1; SP2, sensilla placodea subtype 2; SB, sensilla basiconica. Significant correlations are highlighted in bold.

placodea are responsible for perception to the above test stimuli. However, no satisfactory correlations were obtained for (-)-*E*-pinocarveol and 4-ethyl-phenol (**Table 2**). These results suggested that morphological features could be somewhat insufficient to distinguish between sensillar types responsible for the EAG responses to odorant stimuli.

In Rutelinae, sensilla placodea without pits in the smooth area of the lamella surface respond to sex pheromones (Leal and Mochizuki, 1993; Larsson et al., 1999, 2001; Kim and Leal, 2000), whilst sensilla placodea with pits in the longitudinal heterogeneous area respond to host plant-related compounds (Hansson et al., 1999; Larsson et al., 2001; Bengtsson et al., 2011). Similar spatial division of the lamellar surface occurs in Cetoniinae (Stensmyr et al., 2001). Sensilla placodea in smooth areas in both grooved and smooth areas are capable of detecting host plant-related compounds (Stensmyr et al., 2001; Bengtsson et al., 2011). In Melolonthinae, there is no spatial separation of the lamellar surface, and sensilla involved in the reception of sex pheromones and plant-associated volatiles are uniformly distributed (Ochieng et al., 2002; Romero-López et al., 2004). As EAG responses to anisole significantly correlated with the density of SP1, it is very likely that SP1 in male *P. flavescens* generates responses to sex pheromones. Provided that SP1 is pheromone-sensitive, the percentage of SP1 in total SP is 69% in males (Li et al., under review) is consistent with the percentage of the pheromone-sensitive sensilla placodea (68%) in male Japanese beetle (Kim and Leal, 2000; Nikonov and Leal, 2002). In *P. flavescens*, sensilla placodea are significantly more abundant in males than in females (Li et al., under review). It has been previously demonstrated that both female and male scarabs can detect their own pheromones, and the response properties of pheromone-sensitive receptor neurons are similar in female and male scarabs, but with a lower sensitivity in females (Larsson et al., 1999; Nikonov et al., 2001, 2002). The sexual differences in the number of pheromone-sensitive sensilla (SP1, in the case of *P. flavescens*) and pheromone sensitivity may account for significantly greater EAG responses to anisole in males than in females. Because there is no general pattern of correlation between abundance of a specific sensilla placodea subtype with EAG responses, it is unlikely to determine which sensilla subtype responds to plant volatiles.

In comparison with sensilla placodea, sensilla basiconica on each lamella was at least 10 times less abundant (Li et al., under review). A significant correlation has been previously found between EAG amplitude and population density of long sensilla basiconica in *Bactrocera oleae*, which specifically responds to host plant-related compounds (Crnjar et al., 1989). However, no satisfactory correlations between EAG amplitude and population density of sensilla basiconica in *P. flavescens* were found for any test stimuli (**Table 2**). Although the multiporous feature of sensilla basiconica suggests an olfactory role for them (Zacharuk, 1980; Keil and Steinbrecht, 1984), it might be difficult to obtain EAG responses due to the very low-density distribution. Their contributions to EAG responses cannot be determined in the present study. Further electrophysiological recordings from single sensilla are desperately needed to better differentiate sensilla types, and assess the specific sensitivity spectra of a specific sensillar type in *P. flavescens*.

Scarab beetles usually fold their lamellae forming a compact club at rest to protect sensorial areas located in the inner lamella surfaces. The closed club showed evident EAG responses to sex pheromone and plant volatiles, suggesting that scarabs are responsive to chemical stimuli at rest with functioning sensilla placodea on the outer surfaces of L1 and L3. However, we cannot rule out the possibility that air may be able to enter in between the lamellae even when the club is closed. The capability of detecting environmental and chemical cues at rest appears to be related to the synchronized behavior in both female and male *P. flavescens* emerging simultaneously from belowground in search for food and mate. The significant olfactory responses to the six host plant-related compounds are consistent with findings in Chen et al. (2019) (**Figure 3** and **Supplementary Figure 1**). In general, lamellae in males showed significantly greater EAG responses to these plant volatiles than those in females. Significantly longer lamellae and higher number of sensilla placodea on males than females (Li et al., under review) may account for the higher EAG responses in males. The higher

sensitivity in males is likely related to the male's ability to find a conspecific mate on a host plant, which may be linked to strong competition for mates among males. The biological significance of higher electrophysiological sensitivity in males requires further investigation.

DATA AVAILABILITY STATEMENT

The raw data supporting the conclusions of this article will be made available by the authors, without undue reservation.

AUTHOR CONTRIBUTIONS

LC and PW conceived and designed the experiments. Y-YL, LC, and PW carried out the experiments. Y-YL, LC, PW, and DL analyzed the data and wrote the manuscript. All authors agreed to publish this manuscript.

FUNDING

This research was supported by the National Natural Science Foundation of China (Grant Nos. 31171847 and 31460474) and the High-level Talents Research Start-up Project of Hebei University (Grant No. 521000981387).

SUPPLEMENTARY MATERIAL

The Supplementary Material for this article can be found online at: https://www.frontiersin.org/articles/10.3389/fevo.2021.759778/full#supplementary-material

REFERENCES

Altner, H., and Prillinger, L. (1980). Ultrastructure of invertebrate chemo-, thermo-, and hygroreceptors and its functional significance. *Int. Rev. Cytol.* 67, 69–139. doi: 10.1016/S0074-7696(08)62427-4

Bengtsson, J. M., Khbaish, H., Reinecke, A., Wolde-Hawariat, Y., Negash, M., Seyoum, E., et al. (2011). Conserved, highly specialized olfactory receptor neurons for food compounds in 2 congeneric scarab beetles, *Pachnoda interrupta* and *Pachnoda marginata*. *Chem Senses* 36, 499–513. doi: 10.1093/chemse/bjr002

Biasazin, T. D., Karlsson, M. F., Hillbur, Y., Seyoum, E., and Dekker, T. (2014). Identification of host blends that attract the african invasive fruit fly, *Bactrocera invadens*. *J. Chem. Ecol.* 40, 966–976. doi: 10.1007/s10886-014-0501-6

Bohacz, C., du G. Harrison, J., and Ahrens, D. (2020). Comparative morphology of antennal surface structures in pleurostict scarab beetles (Coleoptera). *Zoomorphology* 139, 327–346. doi: 10.1007/s00435-020-00495-0

Chen, L., Li, Y.-Y., and Shao, K.-M. (2019). A practical technique for electrophysiologically recording from lamellated antenna of scarab beetle. *J. Chem. Ecol.* 45, 392–401. doi: 10.1007/s10886-019-01059-3

Crnjar, R., Scalera, G., Liscia, A., Angioy, A. M., Bigiani, A., Pietra, P., et al. (1989). Morphology and EAG mapping of the antennal olfactory receptors in *Dacus oleae*. *Entomol. Exp. Appl.* 51, 77–85. doi: 10.1111/j.1570-7458.1989.tb01216.x

Hansson, B. S., Larsson, M. C., and Leal, W. S. (1999). Green leaf volatile-detecting olfactory receptor neurones display very high sensitivity and specificity in a scarab beetle. *Physiol. Entomol.* 24, 121–126. doi: 10.1046/j.1365-3032.1999.00121.x

SAS Institute (2004). *SAS User Guide*. Cary: SAS Institute.

Jacob, V., Scolari, F., Delatte, H., Gasperi, G., Jacquin-Joly, E., Malacrida, A. R., et al. (2017). Current source density mapping of antennal sensory selectivity reveals conserved olfactory systems between tephritids and *Drosophila*. *Sci. Rep.* 7:15304. doi: 10.1038/s41598-017-15431-4

Jacob, V. E. J. M. (2018). Current source density analysis of electroantennogram recordings: a tool for mapping the olfactory response in an insect antenna. *Front. Cell. Neurosci.* 12:287. doi: 10.3389/fncel.2018.00287

Keil, T. A., and Steinbrecht, R. A. (1984). "Mechanosensitive and olfactory sensilla of insects," in *Insect Ultrastructure*, eds R. C. King and H. Akai (Boston: Springer).

Kim, J. Y., and Leal, W. S. (2000). Ultrastructure of pheromone-detecting sensillum placodeum of the Japanese beetle, *Popillia japonica* newmann (Coleoptera: Scarabaeidae). *Arthropod Struct. Dev.* 29, 121–128. doi: 10.1016/s1467-8039(00)00022-0

Larsson, M. C., Leal, W. S., and Hansson, B. S. (1999). Olfactory receptor neurons specific to chiral sex pheromone components in male and female *Anomala cuprea* beetles (Coleoptera: Scarabaeidae). *J. Comp. Physiol. A Neuroethol. Sens. Neural Behav. Physiol.* 184, 353–359. doi: 10.1007/s003590050334

Larsson, M. C., Leal, W. S., and Hansson, B. S. (2001). Olfactory receptor neurons detecting plant odours and male volatiles in *Anomala cuprea* beetles (Coleoptera: Scarabaeidae). *J. Insect Physiol.* 47, 1065–1076. doi: 10.1016/S0022-1910(01)00087-7

Leal, W. S. (1998). Chemical ecology of phytophagous scarab beetles. *Annu. Rev. Entomol.* 43, 39–61. doi: 10.1146/annurev.ento.43.1.39

Leal, W. S., and Mochizuki, F. (1993). Sex pheromone reception in the scarab beetle *Anomala cuprea*: enantiomeric discrimination by sensilla placodea. *Naturwissenschaften* 80, 278–281. doi: 10.1007/bf01135914

Meinecke, C.-C. (1975). Riechsensillen und systematik der lamellicornia (insecta, Coleoptera). *Zoomorphologie* 82, 1–42. doi: 10.1007/bf00995905

Nikonov, A. A., and Leal, W. S. (2002). Peripheral coding of sex pheromone and a behavioral antagonist in the Japanese beetle, *Popillia japonica*. *J. Chem. Ecol.* 28, 1075–1089.

Nikonov, A. A., Peng, G., Tsurupa, G., and Leal, W. S. (2002). Unisex pheromone detectors and pheromone-binding proteins in scarab beetles. *Chem. Senses* 27, 495–504. doi: 10.1093/chemse/27.6.495

Nikonov, A. A., Valiyaveettil, J. T., and Leal, W. S. (2001). A photoaffinity-labeled green leaf volatile compound 'tricks' highly selective and sensitive insect olfactory receptor neurons. *Chem. Senses* 26, 49–54. doi: 10.1093/chemse/26.1.49

Ochieng, S. A., Robbins, P. S., Roelofs, W. L., and Baker, T. C. (2002). Sex pheromone reception in the scarab beetle *Phyllophaga anxia* (Coleoptera: Scarabaeidae). *Ann. Entomol. Soc. Am.* 95, 97–102. doi: 10.1603/0013-8746(2002)095[0097:sprits]2.0.co;2

Romero-López, A. A., Arzuffi, R., Valdez, J., Morón, M. A., Castrejón-Gómez, V., and Villalobos, F. J. (2004). Sensory organs in the antennae of *Phyllophaga obsoleta* (Coleoptera: Melolonthidae). *Ann. Entomol. Soc. Am.* 97, 1306–1312. doi: 10.1603/0013-8746(2004)097[1306:soitao]2.0.co;2

Steinbrecht, R. A. (1997). Pore structures in insect olfactory sensilla: A review of data and concepts. *Int. J. Insect Morphol. Embryol.* 26, 229–245. doi: 10.1016/S0020-7322(97)00024-X

Stensmyr, M. C., Larsson, M. C., Bice, S., and Hansson, B. S. (2001). Detection of fruit-and flower-emitted volatiles by olfactory receptor neurons in the polyphagous fruit chafer *Pachnoda marginata* (coleoptera: Cetoniinae). *J. Comp. Physiol. A Sens. Neural Behav. Physiol.* 187, 509–519. doi: 10.1007/s003590100222

Wen, P., Cheng, Y., Qu, Y., Zhang, H., Li, J., Bell, H., et al. (2017). Foragers of sympatric asian honey bee species intercept competitor signals by avoiding

benzyl acetate from *Apis cerana* alarm pheromone. *Sci. Rep.* 7:6721. doi: 10.1038/s41598-017-03806-6

Zacharuk, R. Y. (1980). Ultrastructure and function of insect chemosensilla. *Annu. Rev. Entomol.* 25, 27–47. doi: 10.1146/annurev.en.25.010180.000331

Zacharuk, R. Y. (1985). "Antennal sensilla," in *Comparative Insect Physiology, Biochemistry and Pharmacology*, eds G. A. Kerkut and L. I. Gilbert (Oxford: Pergamon Press).

Conflict of Interest: The authors declare that the research was conducted in the absence of any commercial or financial relationships that could be construed as a potential conflict of interest.

Publisher's Note: All claims expressed in this article are solely those of the authors and do not necessarily represent those of their affiliated organizations, or those of the publisher, the editors and the reviewers. Any product that may be evaluated in this article, or claim that may be made by its manufacturer, is not guaranteed or endorsed by the publisher.

Copyright © 2021 Li, Liu, Wen and Chen. This is an open-access article distributed under the terms of the Creative Commons Attribution License (CC BY). The use, distribution or reproduction in other forums is permitted, provided the original author(s) and the copyright owner(s) are credited and that the original publication in this journal is cited, in accordance with accepted academic practice. No use, distribution or reproduction is permitted which does not comply with these terms.

frontiers in Ecology and Evolution

ORIGINAL RESEARCH
published: 03 December 2021
doi: 10.3389/fevo.2021.773915

The Chemosensory Transcriptome of a Diving Beetle

Nicolas Montagné[1]†, Muriel Jager[2†], Thomas Chertemps[1], Emma Persyn[2], Yan Jaszczyszyn[3], Camille Meslin[1], Emmanuelle Jacquin-Joly[1] and Michaël Manuel[2]**

[1] Sorbonne Université, INRAE, CNRS, IRD, UPEC, Université de Paris, Institute of Ecology and Environmental Sciences of Paris (iEES-Paris), Paris, France, [2] Sorbonne Université, MNHN, CNRS, EPHE, Institut de Systématique, Evolution, Biodiversité (ISYEB UMR 7205), Paris, France, [3] Université Paris-Saclay, CEA, CNRS, Institute for Integrative Biology of the Cell (I2BC), Gif-sur-Yvette, France

OPEN ACCESS

Edited by:
Rui Tang,
Institute of Zoology, Guangdong Academy of Science, Chinese Academy of Sciences (CAS), China

Reviewed by:
Hao Guo,
Chinese Academy of Sciences (CAS), China
Zhongzhen Wu,
Zhongkai University of Agriculture and Engineering, China

***Correspondence:**
Nicolas Montagné
nicolas.montagne@sorbonne-universite.fr
Michaël Manuel
michael.manuel@upmc.fr

† These authors have contributed equally to this work and share first authorship

Specialty section:
This article was submitted to Chemical Ecology, a section of the journal Frontiers in Ecology and Evolution

Received: *10 September 2021*
Accepted: *17 November 2021*
Published: *03 December 2021*

Citation:
Montagné N, Jager M, Chertemps T, Persyn E, Jaszczyszyn Y, Meslin C, Jacquin-Joly E and Manuel M (2021) The Chemosensory Transcriptome of a Diving Beetle. Front. Ecol. Evol. 9:773915. doi: 10.3389/fevo.2021.773915

Insects astoundingly dominate Earth's land ecosystems and have a huge impact on human life. Almost every aspect of their life relies upon their highly efficient and adaptable chemosensory system. In the air, most chemical signals that are detected at long range are hydrophobic molecules, which insects detect using proteins encoded by multigenic families that emerged following land colonization by insect ancestors, namely the odorant-binding proteins (OBPs) and the odorant receptors (ORs). However, land-to-freshwater transitions occurred in many lineages within the insect tree of life. Whether chemosensory gene repertoires of aquatic insects remained essentially unchanged or underwent more or less drastic modifications to cope with physico-chemical constraints associated with life underwater remains virtually unknown. To address this issue, we sequenced and analyzed the transcriptome of chemosensory organs of the diving beetle *Rhantus suturalis* (Coleoptera, Dytiscidae). A reference transcriptome was assembled *de novo* using reads from five RNA-seq libraries (male and female antennae, male and female palps, and wing muscle). It contained 47,570 non-redundant unigenes encoding proteins of more than 50 amino acids. Within this reference transcriptome, we annotated sequences coding 53 OBPs, 48 ORs, 73 gustatory receptors (GRs), and 53 ionotropic receptors (IRs). Phylogenetic analyses notably revealed a large OBP gene expansion (35 paralogs in *R. suturalis*) as well as a more modest OR gene expansion (9 paralogs in *R. suturalis*) that may be specific to diving beetles. Interestingly, these duplicated genes tend to be expressed in palps rather than in antennae, suggesting a possible adaptation with respect to the land-to-water transition. This work provides a strong basis for further evolutionary and functional studies that will elucidate how insect chemosensory systems adapted to life underwater.

Keywords: ecological transitions, freshwater insects, Dytiscidae, chemical ecology, chemosensory receptors, odorant-binding proteins

INTRODUCTION

Chemical senses are at the crossroad between an animal and its environment, and thus play a key role in species adaptation (Yohe and Brand, 2018). Over hundreds of millions of years, insects have remained tremendously diverse and ecologically successful in every kind of continental ecosystem on Earth. This owes a great deal to the characteristics and evolvability of their chemosensory system,

finely tuned to detect chemical cues in an aerial environment. Although the vast majority of insect species are terrestrial, there are also many insects that live in freshwater habitats, where they are abundant and diversified worldwide (Dijkstra et al., 2014). All are members of lineages derived from terrestrial ancestors, which have secondarily adapted to life in water. This raises the question of how the fundamentally aerial chemosensory equipment of insects has been remodeled in these lineages, to cope with the drastically different physico-chemical constraints associated with an aquatic environment. Indeed, the compounds most readily displaced over long distances in water are predominantly hydrophilic whereas those displaced in the air are mainly hydrophobic (Mollo et al., 2014). Until recently, it was thought that aquatic animals were only able to detect hydrophilic molecules. However, hydrophobic compounds are also prevalent in aquatic ecosystems, and it has recently been shown that marine shrimps and freshwater fish can perceive hydrophobic molecules, either by contact or at short-range (Giordano et al., 2017).

In aerial insects, olfactory sensory neurons—involved in long-range chemodetection—are mainly localized on antennae but can also be found on other body parts, including maxillary and labial palps, depending on the taxa (Hansson and Stensmyr, 2011). Gustatory sensory neurons—involved in short-range or contact chemodetection—are found on palps and legs, as well as antennae, wings and ovipositors (Montell, 2009). Detection of odorants and tastants by these peripheral neurons is mediated by different families of chemoreceptor proteins localized in their dendritic membrane. Among these, an insect-specific family of chemoreceptors called odorant receptors (ORs) arose after water-to-land transition (ca. 410 My ago), in a common ancestor of Ectognatha (Brand et al., 2018). ORs are expressed in olfactory neurons and bind airborne hydrophobic molecules (e.g., terpenoids, benzenoids, fatty acid derivatives, . . .). They are transmembrane proteins associated in heteromers with a unique co-receptor named Orco, forming a non-selective cation channel that opens upon ligand binding (Wicher and Miazzi, 2021). In addition to ORs, two major chemoreceptor families have been characterized through genomic and functional studies in aerial insects. The gustatory receptors (GRs) belong to the same superfamily as ORs, though they are not specific to insects (Eyun et al., 2017; Robertson, 2019). They are expressed in gustatory sensory neurons and some have been shown to bind CO_2, sugars or bitter molecules (Isono and Morita, 2010; Robertson, 2019; Xu, 2020). The third family of chemosensory receptors in insects are the ionotropic receptors (IRs), also found in other protostomes (Croset et al., 2010). To date, the function of IRs has been studied mainly in *Drosophila*, where they are expressed in olfactory, gustatory and other sensory neurons and form complexes with several co-receptors (Silbering et al., 2011; Sanchez-Alcaniz et al., 2018). Antennal IRs are primarily responsible for the detection of volatile hydrophilic molecules such as acids and amines, but some are also involved in temperature or humidity sensing (van Giesen and Garrity, 2017; Rimal and Lee, 2018). Outside of *Drosophila*, involvement of antennal IRs in odorant detection has also been demonstrated in Hymenoptera and Lepidoptera (Shan et al., 2019; Zhang et al., 2019, 2021). Whatever the family considered, the size of chemoreceptor repertoires varies widely among insects, from ten to several hundreds of genes per species. This variability reflects their rapid evolution following a birth-and-death process, characterized by numerous gene duplications and losses (Robertson, 2019).

In addition to receptors, other chemosensory gene families are involved in the detection of chemical cues in insects. This is notably the case of odorant-binding proteins (OBPs), secreted in high concentration in the lymph of olfactory sensilla, where they solubilize hydrophobic molecules to facilitate their transport to the chemoreceptors. These proteins thus contribute to the sensitivity of the olfactory system in aerial insects (Brito et al., 2016; Rihani et al., 2021). In addition to OBPs, which are insect-specific, other soluble proteins such as chemosensory proteins (CSPs) and Niemann-Pick C2 (NPC2) proteins are suspected to play a role in chemical senses (Pelosi et al., 2014). The lymph of olfactory sensilla also contains large amounts of odorant-degrading enzymes, belonging to various enzymatic families, important for rapid signal termination following receptor activation (Leal, 2013; Chertemps and Maïbèche, 2021).

The evolution of chemosensory genes has likely played a major role in adaptation of insects to freshwater habitats. However, we know virtually nothing about chemosensory genes in aquatic insects besides pioneering works in mosquito larvae (Xia et al., 2008; Liu et al., 2010; Ruel et al., 2018). In this study, we aimed to gain insights into evolutionary changes that affected chemosensory gene repertoires after land-to-water transition, through transcriptome analysis of chemosensory organs of a diving beetle (Coleoptera, Dytiscidae). Among the many Coleoptera lineages in which such transitions occurred (Short, 2018), Dytiscidae exhibit the highest degree of adaptation to an aquatic life. Adult diving beetles are capable of flying from one water body to another, but they spend most of their life in water and notably feed and reproduce only underwater. They are predaceous animals, like most other members of the Coleoptera suborder Adephaga, and chemical senses may play a prominent role in prey detection (Culler et al., 2014). Morphological studies have indicated that porous sensilla at the surface of antennae and palps of Dytiscidae differ from those of their closest terrestrial cousins, the Carabidae (Baker, 2001). In diving beetles, there is experimental evidence suggesting that the antennae play a role in chemoreception both underwater and in the air, whereas the palps detect chemical stimuli in the liquid medium only (Hodgson, 1953). Furthermore, active movements of the maxillary palps occur at rest in response to exposure to food odors, during subsequent swimming when attempting to locate preys, and upon feeding (M. Manuel, personal observations). However, very little is known concerning the physiology of these chemosensory structures in diving beetles.

Here we have sequenced, assembled and analyzed the transcriptomes of antennae and palps from adult males and females of the diving beetle species *Rhantus suturalis* Macleay, 1825. This species is of moderate size (10.5–12.5 mm), is common and widespread from western Europe and North Africa through Asia to northern Australia, and lives in a wide variety

of freshwater lentic habitats, with a preference for more or less temporary ponds in open environments. Species of the genus *Rhantus* are prominent predators of mosquito larvae (Culler et al., 2014). Furthermore, it was recently demonstrated that *R. suturalis* males are attracted underwater by a sex pheromone of unknown composition emitted by females (Herbst et al., 2011). The *R. suturalis* transcriptome was used to annotate genes belonging to major families of soluble proteins and transmembrane receptors responsible for semiochemical detection in insects, and to estimate their expression levels in antennae and palps. In parallel to this candidate gene approach, we also searched genes specifically expressed in these chemosensory tissues relative to wing muscle, and genes specifically expressed in one sex vs. the other. By doing so, our main goal was to identify features of the diving beetle chemosensory gene toolkit that may reflect specificities associated with an aquatic life, notably expansions or contractions of gene repertoires and unusual expression patterns in antennae and palps when compared to terrestrial insects.

MATERIALS AND METHODS

Sample Preparation and RNA Extraction

Adult males and females of *R. suturalis* were collected in several ponds in the Fontainebleau forest (Bois-le-Roi, ca. 48°28′N 2°39′E, France) and kept alive in the laboratory in small water tanks. Ablations of antennae and palps were performed under a Leica MZ16 stereomicroscope, with the specimen placed upside down and immobilized in a custom device. Appendages were removed by grasping with forceps at the most basal article (antennomere or palpomere I). Samples and numbers of individuals used for each sample (in brackets) were as follows: female antennae (50), male antennae (45), female palps (maxillary and labial palps mixed in the same sample, 79), male palps (69) and wing muscle (one male individual), leading to a total of five samples. Each specimen was killed in liquid nitrogen immediately after appendage ablations. Each appendage was rinsed in RNAse free water, then immediately transferred into a 2 ml tube on ice containing 500 μl TRIzol™ Reagent (Thermo Fisher Scientific, Waltham, MA) and a mixture of micro-ceramic beads. Tubes were frozen during at least one night at –20°C.

For RNA extraction, 300 μl of TRIzol™ Reagent was added to the tubes prior to grinding, lysis and homogenization (3 × 30 s, then 5 min on ice, then 3 × 30 s all cycles at 5,000 rpm) in a Minilys homogenizer (Bertin technologies SAS, Montigny Le Bretonneux, France). The liquid phase was then separated from the beads and total RNA was extracted using the phenol/chloroform method as described in the TRIzol™ Reagent user guide. Total RNA was treated with TURBO DNase (Thermo Fischer Scientific) according to manufacturer's instructions, then purified and concentrated using the RNeasy® MinElute™ Cleanup Kit (Qiagen, Hilden, Germany). RNA quality and quantity were measured using a ND-1,000 NanoDrop spectrophotometer (Thermo Fisher Scientific). All RNA samples were also analyzed on a Bioanalyzer 2100 (Agilent Technologies, Santa Clara, CA) to determine their RNA Integrity Numbers (RIN). All measured RIN were > 7.

RNA Sequencing and *de novo* Transcriptome Assembly

cDNA library construction and sequencing were carried out at the high-throughput sequencing facility of the Institute for Integrative Biology of the Cell (Gif-sur-Yvette, France). Libraries have been prepared using the Illumina TruSeq mRNA Stranded kit, with minor modifications allowing to obtain long cDNA inserts. Sequencing (150-bp paired-end reads) was performed using a NextSeq500 instrument. Data processing and analysis (summarized in **Supplementary Figure 1**) was performed on the Galaxy server hosted by the BioInformatics Platform for Agro-ecosystems Arthropods (Rennes, France). Quality check was done with FastQC 0.69 and reads were trimmed with Trimmomatic 0.32 (Bolger et al., 2014). Parameters were as follow: Sliding window = 4 bases; average quality = 20; minlen = 30 bases; headcrop = 10 bases; trailing min. quality = 20. Clean reads from the five samples were assembled using Trinity 2.4 (Grabherr et al., 2011), with the following parameters: min contig length = 200, min count for k-mers to be assembled = 1. Coding sequences were extracted from the reference transcriptome using Transdecoder 3.0 (Haas et al., 2013) with a minimum protein length of 50 amino acids. Redundant sequences were then clustered using CD-HIT-EST 1.3 (Fu et al., 2012) with a similarity threshold of 0.9 and a word size of 8.

Transcriptome Analysis

Transcriptome quality was estimated using BUSCO 3.0 (Simao et al., 2015) with the insecta_odb9 dataset. For transcript annotation, coding sequences were first translated with Transeq 5.0 (Rice et al., 2000). Then, an alignment search was performed using DIAMOND (Buchfink et al., 2015) on the NCBI non-redundant (nr) protein sequence database (access March 2020) with the "more sensitive" mode, a BLOSUM62 scoring matrix and a maximum *e*-value of 1e-05. In parallel with the alignment search strategy, a protein domain analysis was performed with hmmscan 3.2 (Finn et al., 2011) using the Pfam-A hidden Markov model database (access May 2020; El-Gebali et al., 2019) and default parameters.

To measure expression levels, reads generated for each of the five libraries were aligned on the reference transcriptome with HISAT 2.1.0 (Kim et al., 2015). Transcript abundance was then measured in each sample as FPKM (fragments per kilobase of exon per million fragments mapped) with the Cufflinks 2.2.1 suite (Trapnell et al., 2012), with default parameters. Heatmaps were built using $\log_2$(FPKM + 1) values. Transcripts specifically expressed in chemosensory organs (antennae or palps) vs. wing muscle and transcripts specifically expressed in chemosensory organs of one sex vs. the other were identified using the Cuffdiff tool, with a False Discovery Rate of 0.05. Amino acid sequences translated from these transcripts were used as queries to search the UniProt database (access May 2020) using BLASTp (Johnson et al., 2008), with a *e*-value cutoff of 1e-03.

For the comparison of chemosensory gene expression bias in antennae and palps of *R. suturalis* and *Tribolium castaneum*, data used for *T. castaneum* were RPKM values provided in previously published transcriptomic analyses (Dippel et al., 2014, 2016). For each family (OBP, OR, GR, IR), orthologous relationships between *R. suturalis* and *T. castaneum* genes were determined using neighbor-joining phylogenies built with Seaview 4.7 (Gouy et al., 2010). Genes with FPKM or RPKM values < 1 in both tissues and genes with no orthologous relationship identified were discarded.

Annotation of Chemosensory Genes

For each gene family to be annotated, datasets containing amino acid sequences manually annotated in other coleopteran species were first created. The OR dataset consisted in sequences previously annotated (Mitchell et al., 2020) in the genomes of *Calosoma scrutator* (Carabidae), *Nicrophorus vespilloides* (Silphidae), *Agrilus planipennis* (Buprestidae), *Anoplophora glabripennis* (Cerambycidae), and *Dendroctonus ponderosae* (Curculionidae). The GR, IR, OBP, and CSP datasets contained sequences from *A. glabripennis* (McKenna et al., 2016), *A. planipennis*, and *D. ponderosae* (Andersson et al., 2019). The NPC2 dataset contained sequences from *T. castaneum* (Pelosi et al., 2014). These amino acid sequences were used as queries to search the *R. suturalis* reference transcriptome using tBLASTn 2.5 (Cock et al., 2015) with an *e*-value cutoff set at 1e-10. In parallel, results of the hmmscan analysis were mined for the following domains: pfam03392, OS-D Insect pheromone-binding family (CSPs); pfam01395, PBP/GOBP family (OBPs); pfam02949, 7tm_6 Odorant receptor (ORs); pfam08395, 7tm_7 Chemosensory receptor (GRs); pfam00060, Ligand-gated ion channel (IRs). To verify annotations and eliminate false positive hits, amino acid translations of the unigenes were searched against the NCBI nr database using BLASTp (Johnson et al., 2008). In some cases, redundant unigenes encoding the same protein but not clustered by CD-HIT-EST were manually clustered to rebuild a longer sequence. The presence of signal peptides within sequences of soluble protein precursors was predicted with SignalP 4.1 (Nielsen, 2017) and the presence of transmembrane domains within sequences of candidate chemoreceptors was predicted with TMHMM 2.0 (Krogh et al., 2001).

Phylogenetic Analyses

To rebuild the phylogenies of the CSP, OBP, OR, GR, and IR families, amino acid sequences from *R. suturalis* were aligned with the coleopteran sequences described above. Datasets were purged of predicted pseudogenes and isoforms resulting from alternative splicing. CSP, OBP, and IR alignments were performed with MAFFT 7 (Katoh et al., 2019) and OR and GR alignments were performed with Muscle (Edgar, 2004) as implemented in Seaview 4.7 (Gouy et al., 2010), then manually curated. The best model of amino acid substitution was determined by SMS (Lefort et al., 2017) and trees were calculated with the maximum-likelihood method using PhyML 3.0 (Guindon et al., 2010), with a mix of SPR and NNI algorithms. Node support was assessed with the SH-like approximate likelihood-ratio test (aLRT) as implemented in PhyML (Anisimova and Gascuel, 2006).

Quantitative Real-Time PCR

Relative gene expression levels were estimated by quantitative real-time PCR (qPCR) for 12 selected genes (3 genes for each of the OBP, OR, IR, and GR families) showing contrasted expression profiles in RNAseq results, in order to validate gene expression data derived from RNAseq. qPCR estimates were performed on RNA preparations independent from those used for RNAseq, and with maxillary and labial palps treated as two distinct samples. Twenty-five *R. suturalis* adults (11 males and 14 females) were collected in a pond in Rue (Somme, France) in October 2020 and kept alive in the lab for a few weeks before sample preparation. Dissections and RNA extractions were performed as described above, except that maxillary and labial palps were separated and that male and female tissues were mixed. First-strand cDNAs were synthesized using 500 ng of total RNA, oligo-dT primer and SuperScript™ II Reverse Transcriptase (Thermo Fischer Scientific). The pooled cDNA used to build standard curves for calculating PCR efficiencies was synthesized from a mix of 200 ng of RNA from antennae, 100 ng of RNA from each palp and 100 ng of RNA from wing muscle. Specific primer pairs were designed with OligoAnalyzer™ (Integrated DNA Technologies, Coralville, IA) to amplify fragments between 150 and 230 bp (primer sequences are given in **Supplementary Table 3**). These genes were selected based on the RNAseq data in order to have—for each family—one gene expressed in both antennae and palps, one antenna-biased gene and one palp-biased gene. The gene encoding the ribosomal protein RsutRPL13 was used as the reference gene.

qPCR assays were performed in technical duplicates on the pooled cDNA dilutions (undiluted, 1/5, 1/25, 1/50, 1/100, 1/200, 1/400), and in technical triplicates on the four cDNA samples (antennae, maxillary palps, labial palps, wing muscle). The qPCR mix contained 2 µl of cDNA (or water for the negative controls), 8 µl of SsoAdvanced™ universal SYBR® Green Supermix (Bio-Rad, Hercules, CA), and 500 nM of both gene-specific primers, in a final volume of 10 µl. PCR reactions were run in 96-well plates, in a CFX96 Touch™ Real-Time PCR detection system (Bio-Rad) with the following thermal cycling conditions: 98°C for 4 min; 40 amplification cycles at 98°C for 15 s, 60°C for 1 min. After amplification, melt curve analyses were performed by gradual heating from 65 to 95°C at 0.5°C.s^{-1}. Only one peak was detected for each sample. The slopes of the standard curves were calculated and the amplification efficiency was estimated as $E = (10^{-1/slope})$. Mean normalized expression of the target genes were calculated with Q-Gene (Simon, 2003).

RESULTS

The *Rhantus suturalis* Reference Transcriptome

Illumina sequencing of the five libraries generated a total of 526 million pairs of raw reads. After trimming, we finally obtained 72,793,754 pairs of clean reads for female antennae, 104,087,147

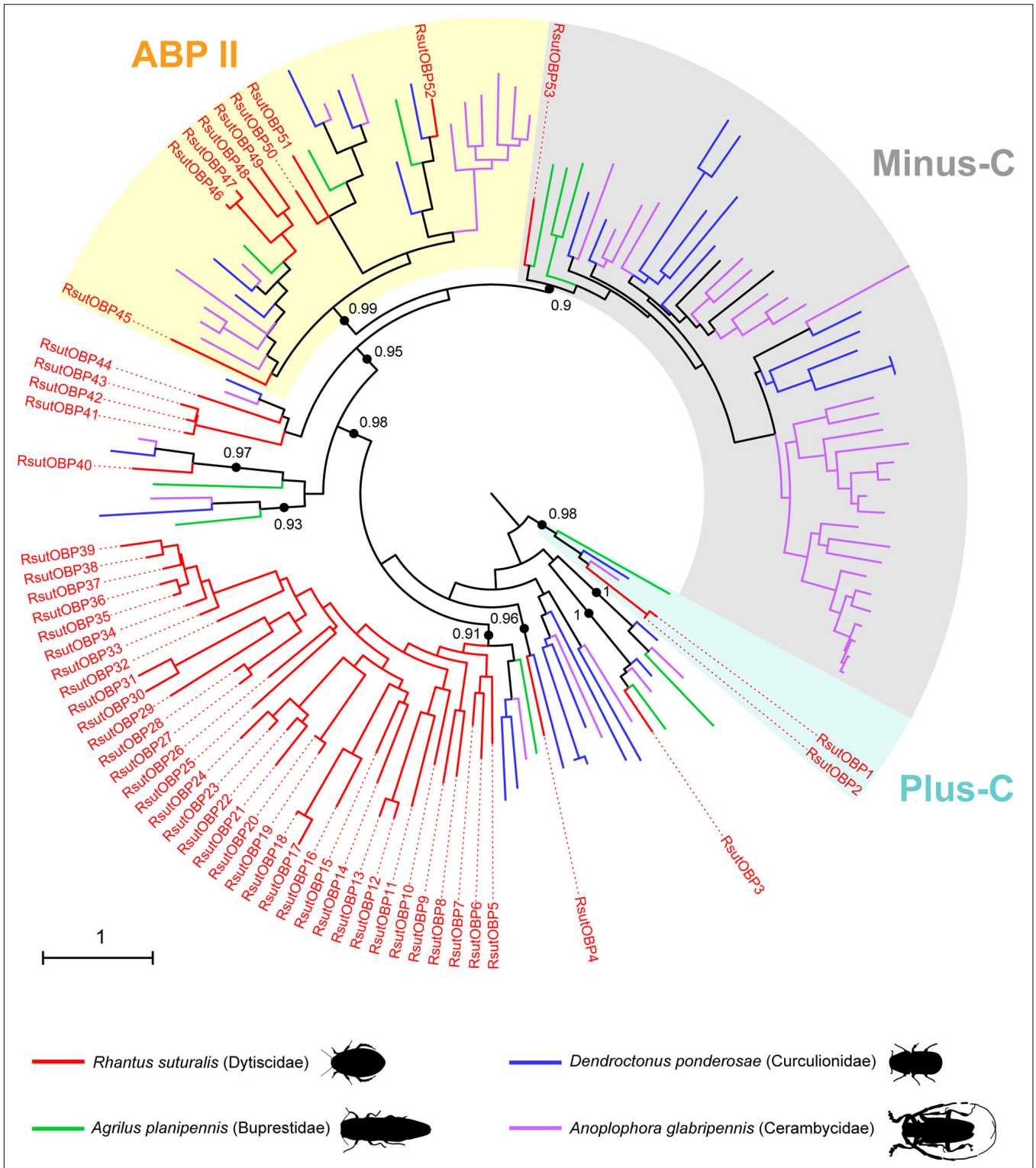

FIGURE 1 | Maximum-likelihood phylogeny of coleopteran OBPs. The tree was built from an alignment of amino acid sequences of *R. suturalis* OBPs (RsutOBP, available in **Supplementary Table 1**) with sequences annotated from the genomes of three coleopteran species belonging to distinct superfamilies. The Plus-C, Minus-C and Antennal Binding Protein II (ABPII) clades were defined as in Andersson et al. (2019). Black dots indicate deep nodes highly supported by the likelihood-ratio test (aLRT > 0.9), with the corresponding value. The tree was rooted using the Plus-C clade as an outgroup. The scale bar indicates the expected number of amino acid substitutions per site.

pairs for female maxillary and labial palps, 85,494,452 pairs for male antennae, 94,355,486 pairs for male palps and 86,825,522 pairs for the male wing muscle sample. These clean reads were pooled and assembled into ∼300,000 contigs, which led to a reference transcriptome of 47,570 unigenes encoding proteins of more than 50 amino acids (**Supplementary Figure 1**). The BUSCO analysis revealed a good completeness of this reference transcriptome (only 4.1% of missing genes) as well as a very low level of redundancy (2.7% of duplicated sequences). We found corresponding hits in the NCBI nr protein sequence database for 26,403 of the 47,750 unigenes, and identified conserved protein domains (from the Pfam database) for 27,553 unigenes.

Soluble Proteins Potentially Involved in Chemical Sensing

We annotated 53 transcripts encoding candidate OBPs (including 17 full-length coding sequences) in the reference transcriptome (**Supplementary Table 1**). Among these 53 RsutOBPs, we identified two members of the Plus-C clade (RsutOBP1-2), an OBP sub-family characterized by a number of cysteine residues above six (the number usually observed in OBPs), eight members of the Antennal Binding Protein II clade (RsutOBP45-52) and a single member of the Minus-C clade (RsutOBP53), characterized by the presence of only four cysteine residues instead of six (**Figure 1**). The other RsutOBPs clustered in clades generally referred to as "classical OBPs" (Dippel et al., 2014; Andersson et al., 2019). Among them, we identified a remarkable lineage-specific expansion, with RsutOBP5-39 (i.e., 35 out of the 53 OBPs) belonging to a single clade, which contained only two OBPs from *D. ponderosae* and one OBP from both *A. planipennis* and *A. glabripennis*.

Although the lack of biological replicates did not allow to unambiguously demonstrate differential gene expressions between tissues, we used FPKM values to estimate transcript abundance in each tissue. Moreover, quantitative real-time PCR on selected genes exhibiting contrasted expression patterns further confirmed the results obtained by RNAseq (**Supplementary Figure 2**). Reliable expression in chemosensory organs (i.e., antennae and palps) was observed for 48 of the 53 RsutOBP unigenes annotated, with no visible sexual dimorphism (**Figure 2** and **Supplementary Table 1**). Among these, we found 17 RsutOBPs exhibiting similar FPKM values in antennae and palps. This was notably the case for members of the Plus-C (RsutOBP1 and 2) and Minus-C (RsutOBP53) clades. Eight RsutOBPs appeared more expressed in antennae than palps (ratio of FPKM values above 4), all but one (RsutOBP45-52) belonging to the ABPII clade. Finally, 23 RsutOBPs seemed more expressed in palps than in antennae and most of these OBPs belong to the large RsutOBP expansion (RsutOBP5-39).

In addition to OBPs, we annotated four *R. suturalis* transcripts encoding CSPs and three transcripts encoding NPC2 proteins (**Supplementary Table 1**). RsutCSPs belonged to conserved lineages in the coleopteran CSP phylogeny (**Supplementary Figure 3**). Among the four candidate CSPs, two were highly expressed in chemosensory organs and therefore likely to be involved in chemical sensing: RsutCSP3 was expressed in antennae of both sexes whereas RsutCSP4 exhibited extremely high expression levels in both antennae and palps, as well as faint expression in muscle. None of the NPC2 proteins identified

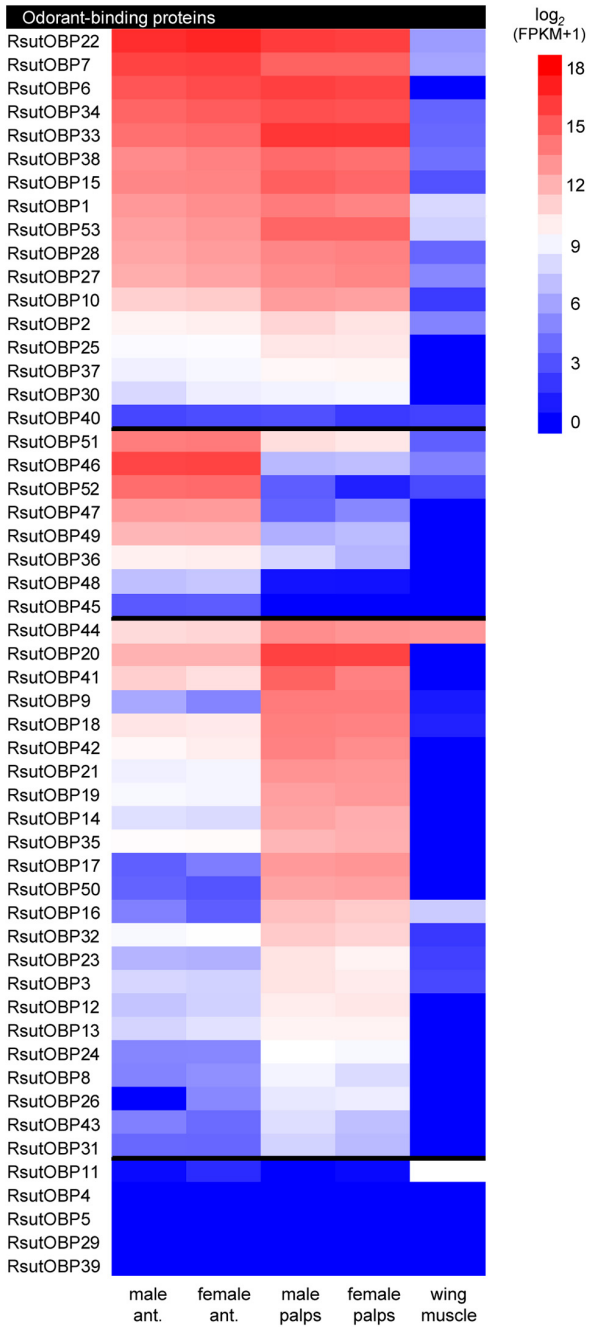

FIGURE 2 | Heatmap showing expression levels of *R. suturalis* transcripts encoding OBPs. Color coding is based on $\log_2$(FPKM + 1) values; raw FPKM values are available in **Supplementary Table 1**. Transcripts were classified in three categories, from top to bottom: equally expressed in antennae and palps; more expressed in antennae; more expressed in palps. A transcript was classified as more expressed in a specific tissue when the ratio of FPKM values was at least four-fold. Transcripts with FPKM values lower than 1 in all tissues are not shown.

was specific to chemosensory organs, with RsutNCP2_2 and 3 being moderately expressed in all tissues investigated (**Supplementary Table 1**).

Candidate Chemosensory Receptors

Altogether, we annotated transcripts encoding 48 ORs (30 full-length), 73 GRs (47 full-length) and 53 IRs (24 full-length) in the reference transcriptome (**Supplementary Table 1**). The *R. suturalis* ORs were distributed among six of the eight clades of the coleopteran OR phylogeny (**Figure 3**). Within each clade, RsutORs clustered with ORs annotated in the ground beetle *C. scrutator* (Carabidae), also belonging to the sub-order Adephaga. We found no RsutOR belonging to clades 5 and 6, but RsutOR9 and four *C. scrutator* ORs formed a clade that could be specific to Adephaga, with no Polyphaga representative. As ORs are the only chemosensory genes that have been annotated in *C. scrutator*, the OR tree is the only one in which duplications more recent than the divergence of the dytiscid lineage with respect to that of the terrestrial carabids can be identified. In addition to a few instances of such duplications that involve only two or three *R. suturalis* genes (e.g., RsutOR1–3 and RsutOR6 and 7, within clade 1), a significant OR expansion was apparent within clade 3, which gave rise to 9 *R. suturalis* paralogs (RsutOR26–34). As expected, the OR family member with the highest expression level was the obligate co-receptor RsutOrco, expressed at high levels in both antennae and palps (**Figure 4** and **Supplementary Table 1**). Most RsutORs (31 out of 48) were found reliably expressed only in male and female antennae, some with high expression levels. However, eight RsutORs appeared expressed in palps and not in antennae. All but one (RsutOR1) belong to the RsutOR expansion within clade 3 (RsutOR26–34). Interestingly, the two palpal RsutOR genes studied by qRT-PCR were found expressed in maxillary palps but not labial palps (**Supplementary Figure 2**).

In the GR phylogeny, RsutGR1–3 belong to the candidate CO_2 receptor clade, RsutGR4 and 5 to the candidate sugar receptor clade, and RsutGR10 to the candidate fructose receptor clade (**Figure 5**). The vast majority of GRs identified in *R. suturalis* (RsutGR15–70) belong to a single clade of the GR phylogeny without reported putative function. This clade contained only a few representatives from Polyphaga species and several occurrences of massive expansions of *R. suturalis* GRs. The vast majority of RsutGRs were either found expressed only in palps or more expressed in palps than in antennae (**Figure 4** and **Supplementary Table 1**). They generally exhibited low FPKM values, with the exception of the candidate CO_2 receptors RsutGR1–3 and a few others (RsutGR9, 36, 37, 72, and 73). The GR gene with the highest FPKM value—RsutGR9—was found specifically expressed in labial palps by qRT-PCR (**Supplementary Figure 2**).

Based on the IR phylogeny (**Figure 6**), we identified unigenes encoding each of the eight following "antennal" IRs, whose putative functions have been assigned based on previous work on the fruit fly (van Giesen and Garrity, 2017; Rimal and Lee, 2018): the four IR co-receptors IR25a, 8a, 93a, and 76b, the two humidity-sensing IR40a and 68a, the temperature-sensing IR21a and the olfactory IR41a. We also identified six RsutIRs within the IR75 clade (RsutIR75a-f), supposedly involved in the detection of water-soluble semiochemicals carrying a carboxylic acid or an amine function (Silbering et al., 2011; Prieto-Godino et al., 2017). The other 39 IRs found in the *R. suturalis* transcriptome belong to the divergent IR clade, involved in taste in *Drosophila* (Koh et al., 2014; Sanchez-Alcaniz et al., 2018). Several independent RsutIR expansions were found within this clade, including two large groups of 12 and 13 *R. suturalis* paralogs, respectively. RsutIR25a (candidate universal IR co-receptor) was the most highly expressed coreceptor, in both antennae and palps (**Figure 4** and **Supplementary Table 1**). RsutIR76b (candidate gustatory IR coreceptor) exhibited a high expression in palps, whereas RsutIR8a (candidate IR olfactory coreceptor) and RsutIR93a were highly expressed in antennae, like the four conserved antennal IRs (IR21a, 40a, 41a, 68a). Two RsutIRs belonging to the IR75 clade were also highly expressed in antennae, and three others exhibited similar FPKM values for both antennae and palps. Among these, RsutIR75f exhibited an exceptionally high expression level in both tissues (**Figure 4** and **Supplementary Figure 2**). The 39 divergent RsutIRs were globally expressed at low levels in palps, although a few of them were also expressed in antennae, sometimes specifically (e.g., RsutIR130). As observed for the soluble proteins, none of the candidate chemosensory receptors annotated here exhibited a sexually dimorphic expression.

Representatives of Other Protein Families Expressed in Chemosensory Organs

Complementary to the detailed analysis of gene families described above, we searched for unigenes from other families that would be specifically expressed in the chemosensory organs relative to the wing muscle. By doing so, we found more than 700 unigenes with hits in UniProt or Pfam databases (**Supplementary Table 2**). We notably identified more than 40 sequences encoding enzymes that may play a role in metabolism of semiochemicals, such as cytochrome P450 enzymes, carboxylesterases, lipases, short-chain dehydrogenases and UDP-glucuronosyl transferases (Chertemps and Maïbèche, 2021). Some of these unigenes exhibited high FPKM values (**Figure 7**). We also found six unigenes encoding CD36 proteins, a family to which Sensory Neuron Membrane Proteins (SNMP) belong (Zhao et al., 2020), and three unigenes encoding candidate pickpocket channels (amiloride-sensitive sodium channels), some of which are involved in olfaction and taste in *Drosophila* and mosquitoes (Chen et al., 2010; Matthews et al., 2019; Ng et al., 2019; Liu et al., 2020). We also searched for unigenes that would be expressed in chemosensory organs of a single sex (either male or female) and found only a dozen of such unigenes, i.e., five expressed in antennae and 10 in palps. None of these corresponded to gene families with a known direct or indirect role in chemical senses (**Supplementary Table 2**). This confirmed our initial observation that no chemosensory gene seemed differentially

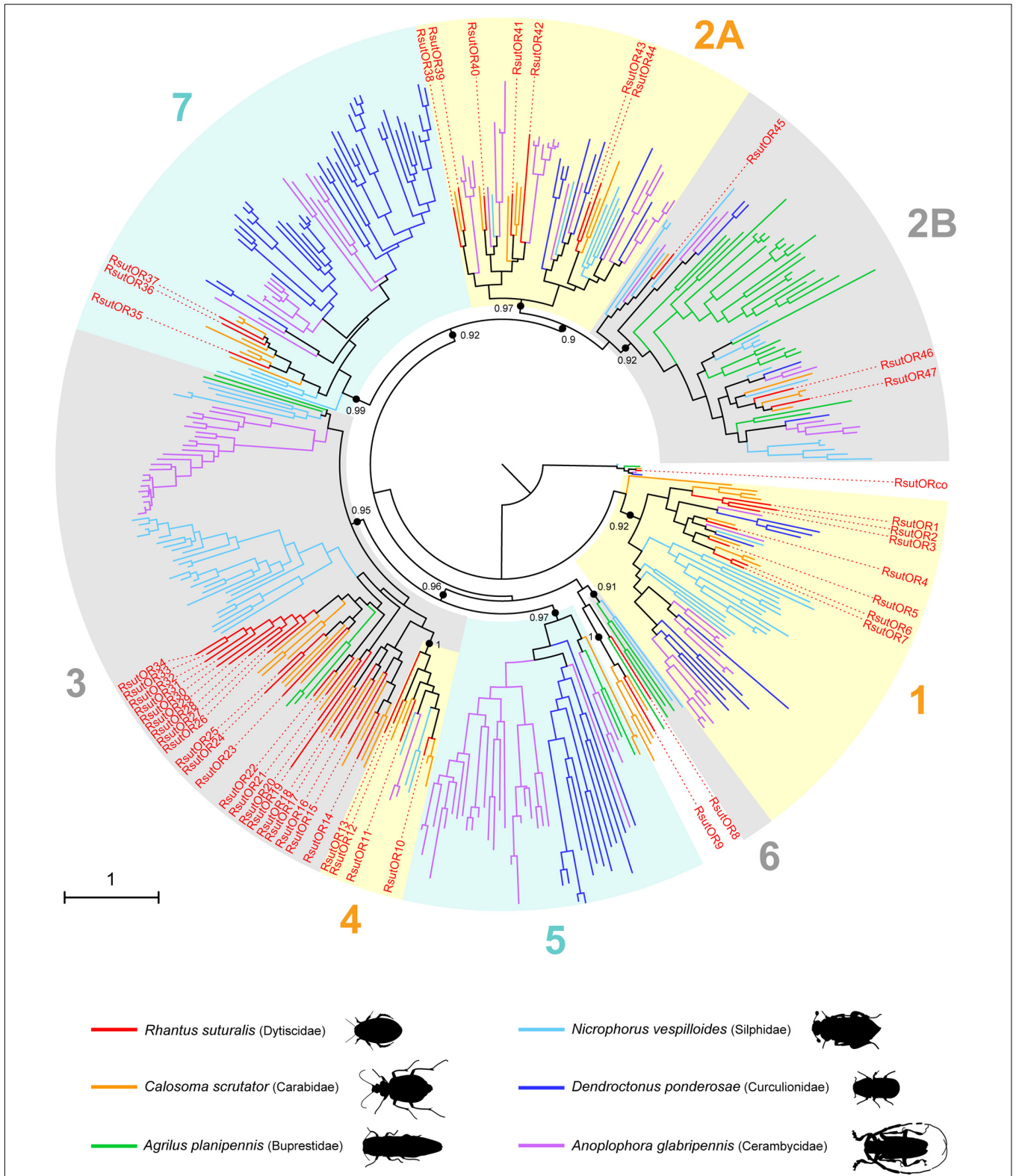

FIGURE 3 | Maximum-likelihood phylogeny of coleopteran ORs. The tree was built from an alignment of amino acid sequences of *R. suturalis* ORs (RsutOR, available in **Supplementary Table 1**) with sequences annotated from the genomes of five coleopteran species belonging to distinct superfamilies. The OR clades 1–7 were defined as in Mitchell et al. (2020). Black dots indicate deep nodes highly supported by the likelihood-ratio test (aLRT > 0.9), with the corresponding value. The tree was rooted using the Orco clade as an outgroup. The scale bar indicates the expected number of amino acid substitutions per site.

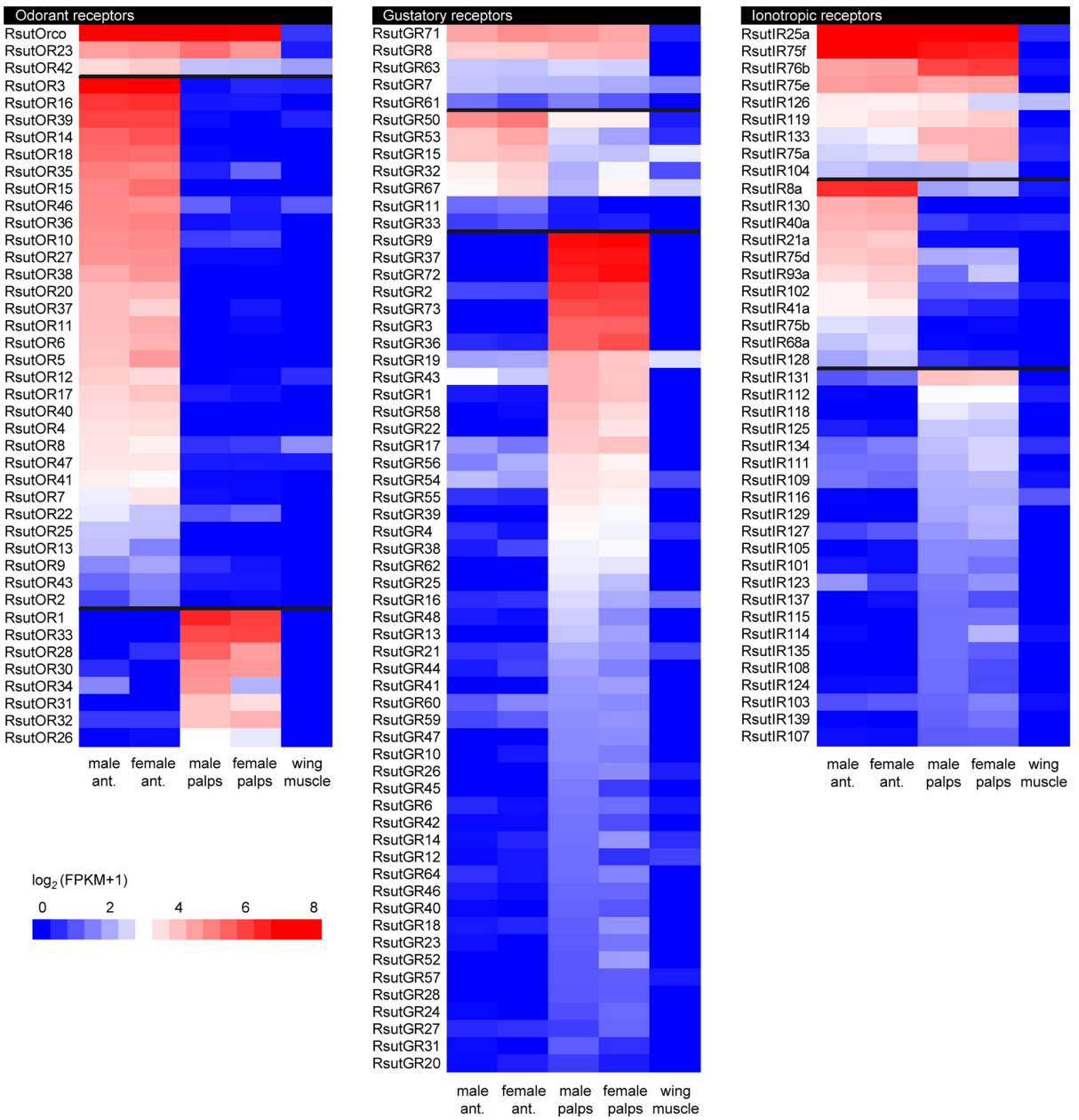

FIGURE 4 | Heatmaps showing expression levels of *R. suturalis* transcripts encoding candidate chemosensory transmembrane receptors. Color coding is based on $\log_2$(FPKM + 1) values; raw FPKM values are available in **Supplementary Table 1**. Transcripts were classified in three categories, from top to bottom: equally expressed in antennae and palps; more expressed in antennae; more expressed in palps. A transcript was classified as more expressed in a specific tissue when the ratio of FPKM values was at least four-fold. Transcripts with FPKM values lower than 1 in all tissues are not shown.

expressed between male and female chemosensory appendages in *R. suturalis*.

DISCUSSION

In this study, we have identified the first chemosensory genes of an aquatic member of the megadiverse order Coleoptera, the diving beetle *Rhantus suturalis*. Members of six chemosensory gene families (OBPs, CSPs, NPC2 proteins, and receptors of the OR, GR, and IR families) were annotated, incorporated into phylogenetic analyses, and their relative expression levels were estimated, based on RNA-seq data from antennae and palps of adult males and females as well as wing muscle (i.e., in total, 5 samples). The gene repertoires recovered from these transcriptomic data are necessarily partial in the absence of a reference genome for *R. suturalis*, and because only the main cephalic sensory organs at a single life stage were processed. This

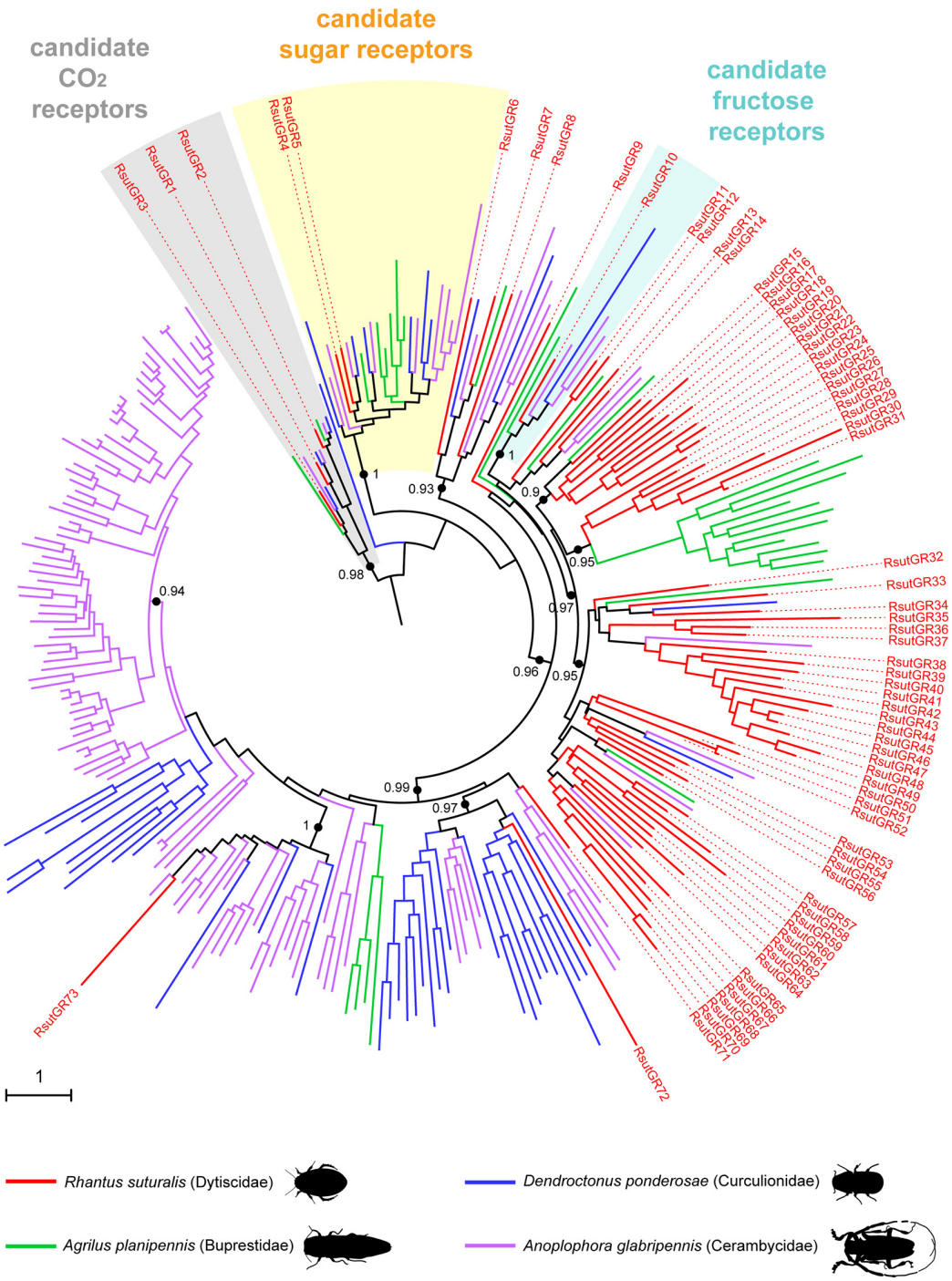

FIGURE 5 | Maximum-likelihood phylogeny of coleopteran GRs. The tree was built from an alignment of amino acid sequences of *R. suturalis* GRs (RsutGR, available in **Supplementary Table 1**) with sequences annotated from the genomes of three coleopteran species belonging to distinct superfamilies. Putative functions were assigned to several clades as in Andersson et al. (2019). Black dots indicate deep nodes highly supported by the likelihood-ratio test (aLRT > 0.9), with the corresponding value. The tree was rooted using the CO_2 receptor clade as an outgroup. The scale bar indicates the expected number of amino acid substitutions per site.

limitation has to be kept in mind, especially for comparisons of gene family sizes with respect to other Coleoptera or insect species for which genes have been annotated based on complete genomes. However, given our relatively deep sequencing strategy, and results from the BUSCO analysis (only 4.1% of genes missing), we can surmise that the contents obtained here

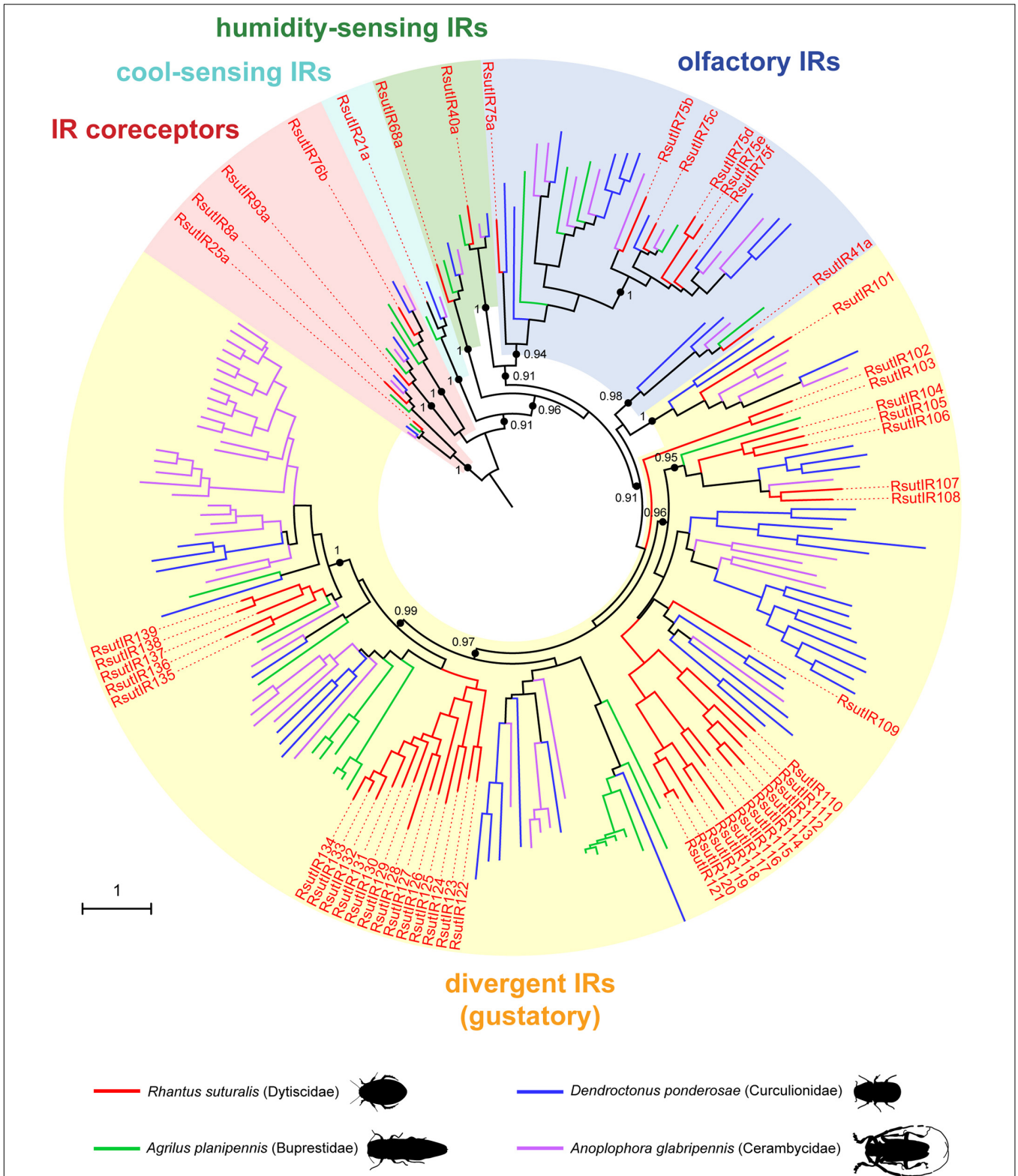

FIGURE 6 | Maximum-likelihood phylogeny of coleopteran IRs. The tree was built from an alignment of amino acid sequences of *R. suturalis* IRs (RsutIR, available in **Supplementary Table 1**) with sequences annotated from the genomes of three coleopteran species belonging to distinct superfamilies. Putative functions were assigned to the different IR clades based on previous works on *Drosophila*. Black dots indicate deep nodes highly supported by the likelihood-ratio test (aLRT > 0.9), with the corresponding value. The tree was rooted using the IR25a/IR8a clade as an outgroup. The scale bar indicates the expected number of amino acid substitutions per site.

unigene	BlastP UniProt best hit	Species	UniProt ID	E-value	male ant.	female ant.	male palps	female palps	wing muscle
cytochrome P450									
contig_108714	Uncharacterized protein	*Cryptotermes secundus*	A0A2J7R4Q4	9.67e-25					
contig_108707	Cytochrome P450 CYP6BQ22	*Dastarcus helophoroides*	M9TLT7	1.80e-28					
contig_160300	Uncharacterized protein	*Photinus pyralis*	A0A1Y1K8X2	2.18e-21					
contig_159068	Cytochrome P450 12H1	*Tribolium castaneum*	D6WP99	4.51e-32					
contig_48897	Putative cytochrome P450 6a14	*Cryptotermes secundus*	A0A2J7R4Q0	3.09e-114					
contig_160295	Cytochrome P450 monooxygenase CYP6BQ35	*Tenebrio molitor*	A0A0K1YWE6	2.08e-134					
contig_114244	Cytochrome P450 301B1	*Tribolium castaneum*	D2A103	0.0					
contig_72829	Uncharacterized protein	*Photinus pyralis*	A0A1Y1K2A7	2.42e-156					
contig_156394	Uncharacterized protein	*Glossina brevipalpis*	A0A1A9W296	5.75e-105					
contig_187886	Putative cytochrome P450 6a14	*Cryptotermes secundus*	A0A2J7R4P8	1.18e-166					
contig_243870	Putative cytochrome P450 6a13	*Zootermopsis nevadensis*	A0A067RK29	5.69e-45					
contig_162369	Cytochrome P450 6BQ13	*Tribolium castaneum*	D6WB59	5.68e-151					
contig_64438	Uncharacterized protein	*Photinus pyralis*	A0A1Y1KCR3	7.02e-141					
carboxylesterase family									
contig_356304	Carboxylic ester hydrolase	*Harmonia axyridis*	E2QC35	9.83e-26					
contig_317173	Carboxylic ester hydrolase	*Liposcelis bostrychophila*	B6D7H0	2.95e-77					
contig_317168	Carboxylic ester hydrolase	*Harmonia axyridis*	E2QC35	4.75e-26					
contig_263675	Carboxylic ester hydrolase	*Tenebrio molitor*	A0A0K1YW40	4.65e-61					
contig_263672	Carboxylic ester hydrolase	*Leptinotarsa decemlineata*	A0A0A7ENL4	1.51e-12					
contig_333714	Carboxylic ester hydrolase	*Leptinotarsa decemlineata*	A0A0A7EQM9	2.28e-114					
contig_333705	Carboxylic ester hydrolase	*Dendroctonus ponderosae*	U4UFS6	2.76e-39					
lipase									
contig_129485	Ves G 1 allergen precursor, putative	*Pediculus humanus*	E0VE21	5.32e-22					
contig_284122	PNLIPRP2_0 protein	*Fopius arisanus*	A0A0C9RCJ3	1.76e-37					
contig_329878	Uncharacterized protein	*Apis mellifera*	A0A088AM94	9.99e-30					
short chain dehydrogenase									
contig_346543	Dehydrogenase/reductase SDR family	*Zootermopsis nevadensis*	A0A067QVP7	3.33e-23					
contig_346530	farnesol dehydrogenase-like	*Agrilus planipennis*	A0A1W4WN42	3.02e-18					
contig_275110	Uncharacterized protein	*Apis mellifera*	H9K5X4	7.48e-24					
contig_60810	Uncharacterized protein	*Graphocephala atropunctata*	A0A1B6M980	7.65e-15					
contig_275114	Uncharacterized protein	*Musca domestica*	A0A1I8MBG2	3.00e-16					
contig_275113	Dehydrogenase/reductase SDR family	*Blattella germanica*	A0A2P8XJR8	5.23e-31					
contig_216873	Uncharacterized protein	*Tribolium castaneum*	D7ELE5	4.37e-77					
contig_111444	Zgc:56585	*Astyanax mexicanus*	W5JZW2	9.34e-46					
contig_319907	Uncharacterized protein	*Glossina pallidipes*	A0A1A9Z224	5.35e-16					
contig_335408	Dehydrogenase	*Oryctes borbonicus*	A0A0T6B086	1.19e-66					
contig_102214	15-hydroxyprostaglandin dehydrogenase	*Blattella germanica*	A0A140KPR8	3.49e-62					
contig_111449	15-hydroxyprostaglandin dehydrogenase	*Lingula unguis*	A0A1S3IUI5	4.49e-15					
contig_281499	farnesol dehydrogenase-like	*Agrilus planipennis*	A0A1W4WZ38	1.04e-74					
contig_281511	Dehydrogenase/reductase SDR family	*Zootermopsis nevadensis*	A0A067QVP7	2.76e-29					
contig_62298	Uncharacterized protein	*Tribolium castaneum*	D7ELE5	3.48e-74					
contig_33141	Uncharacterized protein	*Photinus pyralis*	A0A1Y1LK58	1.20e-102					
contig_235599	Uncharacterized protein	*Photinus pyralis*	A0A1Y1N8N2	3.94e-85					
UDP-glucuronosyl and UDP-glucosyl transferase									
contig_114450	UDP-glucuronosyltransferase	*Agrilus planipennis*	A0A1W4XHV4	2.35e-106					
contig_47820	UDP-glucuronosyltransferase	*Photinus pyralis*	A0A1Y1N2G3	2.21e-99					
contig_81795	UDP-glucuronosyltransferase	*Pediculus humanus*	E0VMM1	2.05e-75					
CD36 family									
contig_93159	scavenger receptor class B member 1-like	*Agrilus planipennis*	A0A1W4WGT2	7.27e-38					
contig_93152	scavenger receptor class B member 1-like	*Agrilus planipennis*	A0A1W4WGT2	1.22e-78					
contig_21684	sensory neuron membrane protein 1-like	*Agrilus planipennis*	A0A1W4WII7	4.60e-35					
contig_200289	Sensory neuron membrane protein 2	*Holotrichia parallela*	A0A2P1ERQ2	9.63e-130					
contig_161176	Sensory neuron membrane protein SNMP-1	*Tenebrio molitor*	A0A0C5DMP8	1.21e-168					
contig_284635	scavenger receptor class B member 1-like	*Agrilus planipennis*	A0A1W4WTV9	0.0					
amiloride-sensitive sodium channel									
contig_162809	Sodium channel protein Nach	*Zootermopsis nevadensis*	A0A067QUS0	1.70e-46					
contig_349482	Pickpocket protein 11-like Protein	*Tribolium castaneum*	D7EHU3	7.98e-69					
contig_37680	Sodium channel protein Nach-like Protein	*Tribolium castaneum*	A0A139WEM9	2.70e-121					

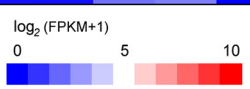

FIGURE 7 | List of *R. suturalis* unigenes specifically expressed in antennae and palps and potentially involved in chemical senses. Protein families were defined following Pfam protein domains found by hmmscan (see detail in section "Materials and Methods"). Color coding in the heatmap is based on $\log_2$(FPKM + 1) values; raw FPKM values are available in **Supplementary Table 2**.

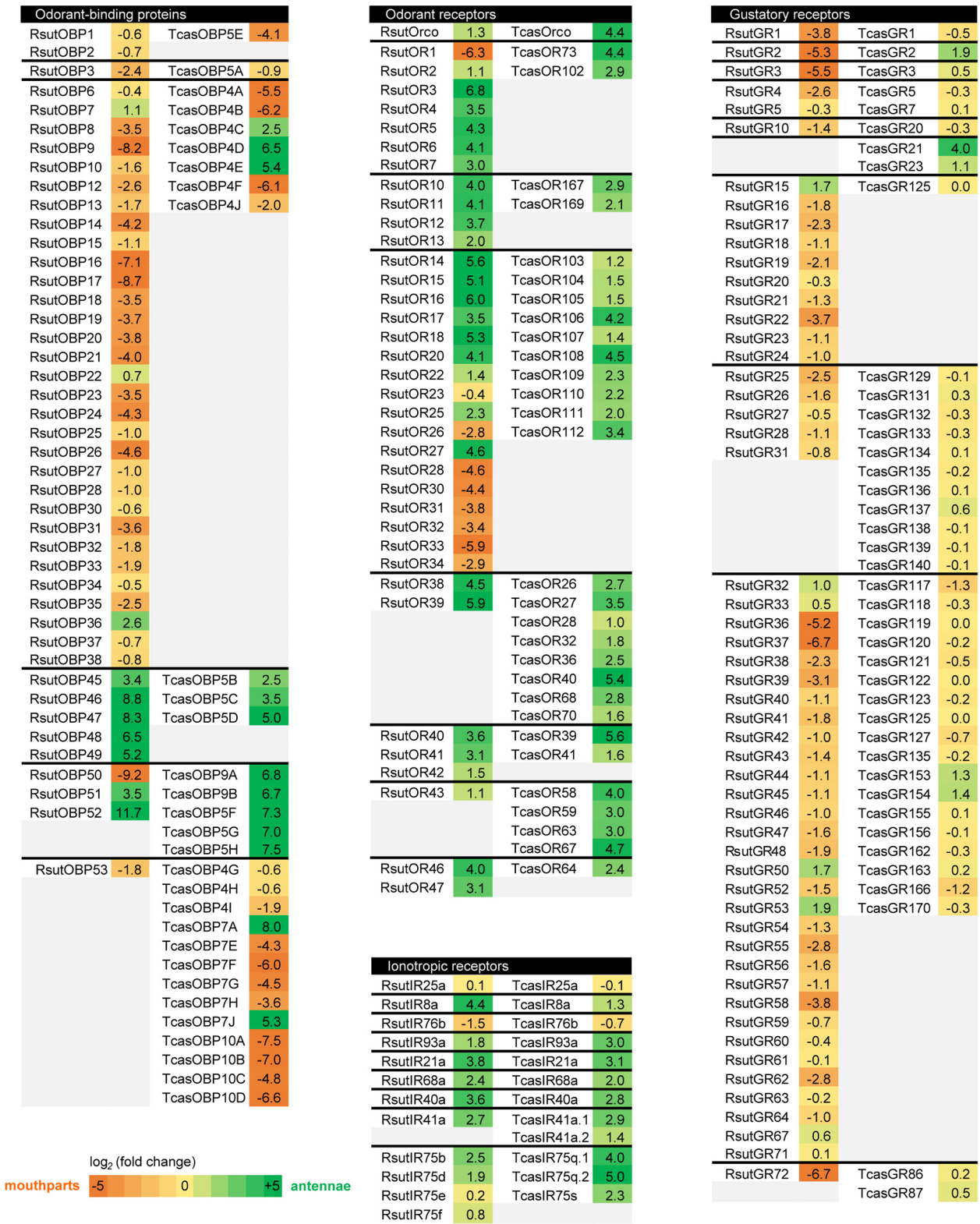

FIGURE 8 | Heatmaps comparing chemosensory gene expression bias in antennae vs. maxillary and labial palps (or entire mouthparts) in *R. suturalis* and *T. castaneum*. Fold changes were calculated based on FPKM values (*R. suturalis*) or RPKM values (*T. castaneum*, Dippel et al., 2014, 2016), and color coding shows $\log_2$(fold change). For each family, genes are separated by groups of orthology.

for the different gene families should not be considerably far from exhaustiveness.

Our *R. suturalis* transcriptome yielded chemosensory gene repertoires whose sizes are generally within the range of what has been previously obtained for terrestrial Coleoptera species, but in the lower, middle or upper range depending of the gene families. *R. suturalis* has more OBPs (53 retrieved in this study) than the Curculionidae *D. ponderosae* and the Buprestidae *A. planipennis* but this number is of the same order of magnitude as in genomes of the Tenebrionidae *T. castaneum*, the Chrysomelidae *Leptinotarsa decemlineata* and the Cerambycidae *A. glabripennis* (Andersson et al., 2019). Among other roles, OBPs are thought to mediate transport of hydrophobic odorants through the sensillar lymph to the olfactory neuron dendrites (Brito et al., 2016; Rihani et al., 2021). Numerous functional studies carried out on Coleoptera (mainly in Scarabaeidae and Chrysomelidae) have identified OBPs capable of binding hydrophobic molecules, whether they are aggregation pheromones or plant volatiles (see Mitchell and Andersson, 2021 for a review). Interestingly, this holds true for the Dytiscidae *Cybister japonicus*, where a classical OBP and a Minus-C OBP have shown a good affinity for a monoterpene (citral) and for a phenypropanoid (coniferyl aldehayde), respectively (Song et al., 2016). The fact that *R. suturalis* has a rich complement of OBPs suggests that detection of hydrophobic odorants is important in the chemical ecology of this aquatic beetle. Moreover, the OBP phylogeny revealed an impressive gene expansion in the lineage leading to the Dytiscidae, with a clade of classical OBPs exclusively containing 35 *R. suturalis* paralogs (**Figure 1**). In its breadth, this expansion is unparalleled in any other beetle species investigated. This may reflect peculiar functional requirements on OBPs in aquatic Adephaga, perhaps due to the low concentration of hydrophobic molecules in water. However, no OBP has been described yet in terrestrial Adephaga and it remains to be determined whether this large OBP expansion is linked with the transition to an aquatic lifestyle or not.

Contrary to OBPs, the *R. suturalis* transcriptome contained a low number of NPC2 proteins and CSPs, which are other soluble proteins potentially involved in chemical senses in insects. Whereas the low number of NPC2 proteins is on a par with previous observations in Coleoptera (Pelosi et al., 2014), the number of four CSPs identified in *R. suturalis* is far below what has been found in beetle genomes (11–20; Andersson et al., 2019). Together with the fact that their expression was generally not restricted to antennae and palps, this suggests that these two protein families may not play a major role in chemoreception in *R. suturalis* and aquatic Adephaga. Potential roles of CSPs in detoxification, immunity or secretion of defensive compounds have already been proposed in *T. castaneum* (Contreras et al., 2013; Li et al., 2013).

For chemoreceptors, the number of 48 ORs identified in *R. suturalis* stands in the lower range for Coleoptera (32–258; Mitchell et al., 2020). Like OBPs, ORs are supposed to be functionally involved in the detection of hydrophobic odorants. It is interesting to observe that this diving beetle species does not present an impoverished complement of ORs with respect to the terrestrial Adephaga beetle *C. scrutator* (51 ORs). Of the Coleoptera species whose OR genes have been annotated from complete genomes, only the Hydroscaphidae *Hydroscapha redfordi* has less ORs than *R. suturalis* (32). Hydroscaphidae are aquatic members of suborder Myxophaga, feeding on algae. The OR phylogeny revealed a possible Dytiscidae-specific OR gene expansion within clade 3, harboring 9 *R. suturalis* paralogs. Lineage-specific expansions have previously been found in this OR clade of unknown function for species with different lifestyles and feeding habits, namely the carnivorous burying beetle *N. vespilloides* and the phytophagous long-horned beetle *A. glabripennis*. Nevertheless, *R. suturalis* together with its terrestrial Adephaga cousin *C. scrutator* underwent much less massive gene expansions in the whole OR phylogeny than observed in Polyphaga species for which data are available (Mitchell et al., 2020).

We identified 73 GRs from the *R. suturalis* transcriptome, mostly expressed in palps. This number is higher than the GR gene repertoire of specialized phytophagous Polyphaga but much lower than in polyphagous species of Polyphaga (e.g., *T. castaneum*: 219; *A. glabripennis*: 190; Andersson et al., 2019). Our phylogenetic analysis showed that GR expansions identified in *R. suturalis* did not occur in the same lineages as those observed in *A. glabripennis* and *D. ponderosae*. However, the current lack of GR functional characterization in Coleoptera hampers any discussion on the potential role of these expansions. As insect GRs are mostly known for their ability to bind water-soluble non-volatile semiochemicals, it is tempting to speculate that a larger GR complement would increase underwater chemodetection capabilities but this has yet to be demonstrated. Moreover, the lack of GR gene identification in any other Adephaga makes it impossible to determine which of these GR expansions observed in *R. suturalis* are possibly specific to water beetles. The same is true for lineage-specific expansions involving *R. suturalis* divergent IR genes mostly expressed in palps.

In the absence of biological replicates, we could not carry out a differential expression analysis able to capture subtle differences of expression between samples, notably between males and females. Anyway, no *R. suturalis* chemosensory gene showed any hint of sex-biased expression, a quite puzzling result in light of the recent experimental demonstration that in this species, males are attracted underwater by a sex pheromone (of unknown composition) emitted by females (Herbst et al., 2011). With the exception of *D. melanogaster*, all pheromone receptors identified so far in insects belong to the OR family (see Fleischer and Krieger, 2021 for a comprehensive review). Even though receptors to aggregation pheromone components (such as those identified in Coleoptera) can be expressed at similar levels in both sexes, sex pheromone receptors generally present a strong sex-biased expression, as commonly observed in male moths (Bastin-Heline et al., 2019). It is of course conceivable that in diving beetles, receptors allowing males to detect the female pheromone belong to a receptor family other than those examined in this study. Other possible explanations could be that a pheromone receptor is indeed present among the candidate receptors that we characterized but is not differentially expressed between the sexes, or that expression of the pheromone receptor is seasonal and was not different between sexes at the period of

the year in which we sampled the specimens used in this study (between April and October 2017).

One of the most interesting features of the *R. suturalis* chemosensory gene repertoires in the face of the terrestrial-aquatic ecological transition is that possible dytiscid-specific gene expansions were systematically associated with expression in palps. The comparison of chemosensory gene expression levels in antennae vs. palps (or entire mouthparts) in *R. suturalis* and *T. castaneum* (the only terrestrial beetle for which comparable data are available; Dippel et al., 2014, 2016) reveals that preferential expression sites clearly differ for several orthologous genes or gene groups, with a striking recurrent tendency across chemosensory gene families: expression tends to be shifted to the palps in *R. suturalis* (**Figure 8**). Amongst ORs, *R. suturalis* has several palp-specific ORs whose *T. castaneum* orthologs are antennae-specific: RsutOR1 (member of clade 1) and all but one members of the *R. suturalis*-specific expansion in clade 3 (RsutOR26–34). Concerning GRs, most *T. castaneum* genes are expressed similarly in antennae and mouthparts and some are antennae-biased, whereas the vast majority of RsutGRs seem to be more expressed in palps, notably the highly expressed RsutGR36, 37 and 72, as well as the candidate CO_2 receptors RsutGR1-3. Contrary to the other two chemoreceptor families, expression of IRs is highly similar in *T. castaneum* and *R. suturalis*, yet this comparison does not include divergent IRs, which have not been analyzed in *T. castaneum* (Dippel et al., 2016). Finally, several *T. castaneum* orthologs of the large *R. suturalis* OBP expansion (RsutOBP5–39) are also expressed at a higher level in palps, but RsutOBP50 (belonging to the ABP II clade) is highly expressed in palps whereas its *T. castaneum* orthologs are all antenna-specific.

CONCLUSION

In conclusion, our transcriptome analysis of chemosensory organs in a diving beetle has revealed chemosensory gene repertoires that are rather similar to those of terrestrial Coleoptera. This seems at odds with prevailing views on the impact of physical constraints on chemical communication underwater. However, we did identify several occurrences of genes highly diversified in *R. suturalis*, notably in the OBP and OR families, which are associated to the detection of hydrophobic odorants in insects. Moreover, these diversified genes were generally highly expressed in palps. A shift of expression of OBPs and ORs from the antennae to the palps may have significant implication with respect to the ecological transition from terrestrial to aquatic life. Indeed, hydrophobic molecules are much less diffusive in water than in the air, leading to the idea that the same proteins that mediate long-range chemodetection (i.e., olfaction in the classic sense) in aerial animals may be involved in short-range or contact chemodetection (gustation, or taste, in the classic sense) in aquatic animals (Mollo et al., 2014). Further expression analyses in Adephaga with various lifestyles associated with functional studies of their chemosensory genes will be necessary to verify whether part of the molecular toolkit functioning in the antennae of terrestrial beetles has indeed diversified and has been re-allocated to the palps in aquatic beetles, to allow short-range perception of hydrophobic molecules.

DATA AVAILABILITY STATEMENT

The datasets presented in this study can be found in online repositories. The names of the repository/repositories and accession number(s) can be found below: NCBI (accession: PRJNA762278).

AUTHOR CONTRIBUTIONS

NM, MJ, TC, and MM conceived the study. MJ and MM performed insect collection and sample preparation. YJ prepared RNA-seq libraries and performed sequencing. NM, TC, EP, CM, and EJ-J performed transcriptome assembly, data analysis, and phylogenetic reconstructions. NM and MM drafted the manuscript, with input from all authors. All authors contributed to the article and approved the submitted version.

FUNDING

This work was funded by the Alliance Sorbonne Université (EMERGENCE project Beetle-EvoChem) and the French National Research Agency (ANR-19-CE02-003-01 grant). This work has benefited from the expertise of the High-throughput Sequencing Platform of I2BC.

ACKNOWLEDGMENTS

We thank Paula Graça and Latifa Belkessa (ISYEB, Sorbonne Université) for technical help and Thierry Jaffredo (IBPS, Sorbonne Université) for laboratory facilities.

SUPPLEMENTARY MATERIAL

The Supplementary Material for this article can be found online at: https://www.frontiersin.org/articles/10.3389/fevo.2021.773915/full#supplementary-material

REFERENCES

Andersson, M. N., Keeling, C. I., and Mitchell, R. F. (2019). Genomic content of chemosensory genes correlates with host range in wood-boring beetles (*Dendroctonus ponderosae*, *Agrilus planipennis*, and *Anoplophora glabripennis*). *BMC Genomics* 20:690. doi: 10.1186/s12864-019-6054-x

Anisimova, M., and Gascuel, O. (2006). Approximate likelihood-ratio test for branches: a fast, accurate, and powerful alternative. *Syst. Biol.* 55, 539–552. doi: 10.1080/10635150600755453

Baker, G. T. (2001). Distribution patterns and morphology of sensilla on the apical segment of the antennae and palpi of Hydradephaga (*Coleoptera: adephaga*). *Microsc. Res. Tech.* 55, 330–338. doi: 10.1002/jemt.1181

Bastin-Heline, L., de Fouchier, A., Cao, S., Koutroumpa, F., Caballero-Vidal, G., Robakiewicz, S., et al. (2019). A novel lineage of candidate pheromone receptors for sex communication in moths. *ELife* 8:e49826. doi: 10.7554/eLife.49826

Bolger, A. M., Lohse, M., and Usadel, B. (2014). Trimmomatic: a flexible trimmer for Illumina sequence data. *Bioinformatics* 30, 2114–2120. doi: 10.1093/bioinformatics/btu170

Brand, P., Robertson, H. M., Lin, W., Pothula, R., Klingeman, W. E., Jurat-Fuentes, J. L., et al. (2018). The origin of the odorant receptor gene family in insects. *ELife* 7:e38340. doi: 10.7554/eLife.38340

Brito, N. F., Moreira, M. F., and Melo, A. C. (2016). A look inside odorant-binding proteins in insect chemoreception. *J. Insect Physiol.* 95, 51–65. doi: 10.1016/j.jinsphys.2016.09.008

Buchfink, B., Xie, C., and Huson, D. H. (2015). Fast and sensitive protein alignment using DIAMOND. *Nat. Methods* 12, 59–60. doi: 10.1038/nmeth.3176

Chen, Z., Wang, Q., and Wang, Z. (2010). The amiloride-sensitive epithelial Na^+ channel PPK28 is essential for drosophila gustatory water reception. *J. Neurosci.* 30, 6247–6252. doi: 10.1523/JNEUROSCI.0627-10.2010

Chertemps, T., and Maïbèche, M. (2021). "Odor degrading enzymes and signal termination," in *Insect Pheromone Biochemistry and Molecular Biology*, 2nd Edn, eds G. J. Blomqvist and R. G. Vogt (Amsterdam: Elsevier), 619–644. doi: 10.1016/B978-0-12-819628-1.00019-5

Cock, P. J., Chilton, J. M., Gruning, B., Johnson, J. E., and Soranzo, N. (2015). NCBI BLAST+ integrated into Galaxy. *Gigascience* 4:39. doi: 10.1186/s13742-015-0080-7

Contreras, E., Rausell, C., and Real, M. D. (2013). Proteome response of *Tribolium castaneum* larvae to *Bacillus thuringiensis* toxin producing strains. *PLoS One* 8:e55330. doi: 10.1371/journal.pone.0055330

Croset, V., Rytz, R., Cummins, S. F., Budd, A., Brawand, D., Kaessmann, H., et al. (2010). Ancient protostome origin of chemosensory ionotropic glutamate receptors and the evolution of insect taste and olfaction. *PLoS Genet.* 6:e1001064. doi: 10.1371/journal.pgen.1001064

Culler, L. E., Ohba, S., and Crumrine, P. (2014). "Predator-Prey Interactions of Dytiscids," in *Ecology, Systematics, and the Natural History of Predaceous Diving Beetles (Coleoptera: Dytiscidae)*, ed. D. Yee (Dordrecht: Springer), 363–386. doi: 10.1007/978-94-017-9109-0_8

Dijkstra, K. D., Monaghan, M. T., and Pauls, S. U. (2014). Freshwater biodiversity and aquatic insect diversification. *Annu. Rev. Entomol.* 59, 143–163. doi: 10.1146/annurev-ento-011613-161958

Dippel, S., Kollmann, M., Oberhofer, G., Montino, A., Knoll, C., Krala, M., et al. (2016). Morphological and transcriptomic analysis of a beetle chemosensory system reveals a gnathal olfactory center. *BMC Biol.* 14:90. doi: 10.1186/s12915-016-0304-z

Dippel, S., Oberhofer, G., Kahnt, J., Gerischer, L., Opitz, L., Schachtner, J., et al. (2014). Tissue-specific transcriptomics, chromosomal localization, and phylogeny of chemosensory and odorant binding proteins from the red flour beetle *Tribolium castaneum* reveal subgroup specificities for olfaction or more general functions. *BMC Genomics* 15:1141. doi: 10.1186/1471-2164-15-1141

Edgar, R. C. (2004). MUSCLE: a multiple sequence alignment method with reduced time and space complexity. *BMC Bioinformatics* 5:113. doi: 10.1186/1471-2105-5-113

El-Gebali, S., Mistry, J., Bateman, A., Eddy, S. R., Luciani, A., Potter, S. C., et al. (2019). The Pfam protein families database in 2019. *Nucleic Acids Res.* 47, D427–D432. doi: 10.1093/nar/gky995

Eyun, S. I., Soh, H. Y., Posavi, M., Munro, J. B., Hughes, D. S. T., Murali, S. C., et al. (2017). Evolutionary history of chemosensory-related gene families across the arthropoda. *Mol. Biol. Evol.* 34, 1838–1862. doi: 10.1093/molbev/msx147

Finn, R. D., Clements, J., and Eddy, S. R. (2011). HMMER web server: interactive sequence similarity searching. *Nucleic Acids Res.* 39(Web Server issue), W29–W37. doi: 10.1093/nar/gkr367

Fleischer, J., and Krieger, J. (2021). "Molecular mechanisms of pheromone detection," in *Insect Pheromone Biochemistry and Molecular Biology* -, 2nd Edn, eds G. J. Blomqvist and R. G. Vogt (Amsterdam: Elsevier), 355–413. doi: 10.1016/B978-0-12-819628-1.00012-2

Fu, L., Niu, B., Zhu, Z., Wu, S., and Li, W. (2012). CD-HIT: accelerated for clustering the next-generation sequencing data. *Bioinformatics* 28, 3150–3152. doi: 10.1093/bioinformatics/bts565

Giordano, G., Carbone, M., Ciavatta, M. L., Silvano, E., Gavagnin, M., Garson, M. J., et al. (2017). Volatile secondary metabolites as aposematic olfactory signals and defensive weapons in aquatic environments. *Proc. Natl. Acad Sci. U.S.A.* 114, 3451–3456. doi: 10.1073/pnas.1614655114

Gouy, M., Guindon, S., and Gascuel, O. (2010). SeaView version 4: a multiplatform graphical user interface for sequence alignment and phylogenetic tree building. *Mol. Biol. Evol.* 27, 221–224. doi: 10.1093/molbev/msp259

Grabherr, M. G., Haas, B. J., Yassour, M., Levin, J. Z., Thompson, D. A., Amit, I., et al. (2011). Full-length transcriptome assembly from RNA-Seq data without a reference genome. *Nat. Biotechnol.* 29, 644–652. doi: 10.1038/nbt.1883

Guindon, S., Dufayard, J. F., Lefort, V., Anisimova, M., Hordijk, W., and Gascuel, O. (2010). New algorithms and methods to estimate maximum-likelihood phylogenies: assessing the performance of PhyML 3.0. *Syst. Biol.* 59, 307–321. doi: 10.1093/sysbio/syq010

Haas, B. J., Papanicolaou, A., Yassour, M., Grabherr, M., Blood, P. D., Bowden, J., et al. (2013). De novo transcript sequence reconstruction from RNA-seq using the Trinity platform for reference generation and analysis. *Nat. Protoc.* 8, 1494–1512. doi: 10.1038/nprot.2013.084

Hansson, B. S., and Stensmyr, M. C. (2011). Evolution of insect olfaction. *Neuron* 72, 698–711. doi: 10.1016/j.neuron.2011.11.003

Herbst, C., Baier, B., Tolasch, T., and Steidle, J. L. M. (2011). Demonstration of sex pheromones in the predaceous diving beetle *Rhantus suturalis* (MacLeay 1825) (Dytiscidae). *Chemoecology* 21, 19–23. doi: 10.1007/s00049-010-0061-3

Hodgson, E. S. (1953). A study of chemoreception in aqueous and gas phases. *Biol. Bull.* 105, 115–127. doi: 10.2307/1538560

Isono, K., and Morita, H. (2010). Molecular and cellular designs of insect taste receptor system. *Front. Cell Neurosci.* 4:20. doi: 10.3389/fncel.2010.00020

Johnson, M., Zaretskaya, I., Raytselis, Y., Merezhuk, Y., McGinnis, S., and Madden, T. L. (2008). NCBI BLAST: a better web interface. *Nucleic Acids Res.* 36(Web Server issue), W5–W9. doi: 10.1093/nar/gkn201

Katoh, K., Rozewicki, J., and Yamada, K. D. (2019). MAFFT online service: multiple sequence alignment, interactive sequence choice and visualization. *Brief. Bioinform.* 20, 1160–1166. doi: 10.1093/bib/bbx108

Kim, D., Langmead, B., and Salzberg, S. L. (2015). HISAT: a fast spliced aligner with low memory requirements. *Nat. Methods* 12, 357–360. doi: 10.1038/nmeth.3317

Koh, T. W., He, Z., Gorur-Shandilya, S., Menuz, K., Larter, N. K., Stewart, S., et al. (2014). The Drosophila IR20a clade of ionotropic receptors are candidate taste and pheromone receptors. *Neuron* 83, 850–865. doi: 10.1016/j.neuron.2014.07.012

Krogh, A., Larsson, B., von Heijne, G., and Sonnhammer, E. L. (2001). Predicting transmembrane protein topology with a hidden Markov model: application to complete genomes. *J Mol. Biol.* 305, 567–580. doi: 10.1006/jmbi.2000.4315

Leal, W. S. (2013). Odorant reception in insects: roles of receptors, binding proteins, and degrading enzymes. *Annu. Rev. Entomol.* 58, 373–391. doi: 10.1146/annurev-ento-120811-153635

Lefort, V., Longueville, J. E., and Gascuel, O. (2017). SMS: Smart Model Selection in PhyML. *Mol. Biol. Evol.* 34, 2422–2424. doi: 10.1093/molbev/msx149

Li, J., Lehmann, S., Weissbecker, B., Ojeda Naharros, I., Schutz, S., Joop, G., et al. (2013). Odoriferous defensive stink gland transcriptome to identify novel genes necessary for quinone synthesis in the red flour beetle, *Tribolium castaneum*. *PLoS Genet.* 9:e1003596. doi: 10.1371/journal.pgen.1003596

Liu, C., Pitts, R. J., Bohbot, J. D., Jones, P. L., Wang, G., and Zwiebel, L. J. (2010). Distinct olfactory signaling mechanisms in the malaria vector mosquito *Anopheles gambiae*. *PLoS Biol.* 8:467. doi: 10.1371/journal.pbio.1000467

Liu, T., Wang, Y., Tian, Y., Zhang, J., Zhao, J., and Guo, A. (2020). The receptor channel formed by ppk25, ppk29 and ppk23 can sense the *Drosophila* female pheromone 7,11-heptacosadiene. *Genes Brain Behav.* 19:e12529. doi: 10.1111/gbb.12529

Matthews, B. J., Younger, M. A., and Vosshall, L. B. (2019). The ion channel ppk301 controls freshwater egg-laying in the mosquito *Aedes aegypti*. *ELife* 8:e43963. doi: 10.7554/eLife.43963.001

McKenna, D. D., Scully, E. D., Pauchet, Y., Hoover, K., Kirsch, R., Geib, S. M., et al. (2016). Genome of the Asian longhorned beetle (*Anoplophora glabripennis*), a globally significant invasive species, reveals key functional and evolutionary

innovations at the beetle-plant interface. *Genome Biol.* 17:227. doi: 10.1186/s13059-016-1088-8

Mitchell, R. F., and Andersson, M. N. (2021). "Olfactory genomics of the Coleoptera," in *Insect Pheromone Biochemistry and Molecular Biology*-, 2nd Edn, eds G. J. Blomqvist and R. G. Vogt (Amsterdam: Elsevier), 547–589. doi: 10.1016/B978-0-12-819628-1.00017-1

Mitchell, R. F., Schneider, T. M., Schwartz, A. M., Andersson, M. N., and McKenna, D. D. (2020). The diversity and evolution of odorant receptors in beetles (*Coleoptera*). *Insect Mol. Biol.* 29, 77–91. doi: 10.1111/imb.12611

Mollo, E., Fontana, A., Roussis, V., Polese, G., Amodeo, P., and Ghiselin, M. T. (2014). Sensing marine biomolecules: smell, taste, and the evolutionary transition from aquatic to terrestrial life. *Front. Chem.* 2:92. doi: 10.3389/fchem.2014.00092

Montell, C. (2009). A taste of the *Drosophila* gustatory receptors. *Curr. Opin. Neurobiol.* 19, 345–353. doi: 10.1016/j.conb.2009.07.001

Ng, R., Salem, S. S., Wu, S. T., Wu, M., Lin, H. H., Shepherd, A. K., et al. (2019). Amplification of *Drosophila* olfactory responses by a DEG/ENaC channel. *Neuron* 104, 947–959. doi: 10.1016/j.neuron.2019.08.041

Nielsen, H. (2017). Predicting secretory proteins with SignalP. *Methods Mol. Biol.* 1611, 59–73. doi: 10.1007/978-1-4939-7015-5_6

Pelosi, P., Iovinella, I., Felicioli, A., and Dani, F. R. (2014). Soluble proteins of chemical communication: an overview across arthropods. *Front. Physiol.* 5:320. doi: 10.3389/fphys.2014.00320

Prieto-Godino, L. L., Rytz, R., Cruchet, S., Bargeton, B., Abuin, L., Silbering, A. F., et al. (2017). Evolution of Acid-Sensing Olfactory Circuits in Drosophilids. *Neuron* 93, 661–666. doi: 10.1016/j.neuron.2016.12.024

Rice, P., Longden, I., and Bleasby, A. (2000). EMBOSS: the european molecular biology open software suite. *Trends Genet.* 16, 276–277. doi: 10.1016/s0168-9525(00)02024-2

Rihani, K., Ferveur, J. F., and Briand, L. (2021). The 40-year mystery of insect odorant-binding proteins. *Biomolecules* 11:509. doi: 10.3390/biom11040509

Rimal, S., and Lee, Y. (2018). The multidimensional ionotropic receptors of *Drosophila melanogaster*. *Insect Mol. Biol.* 27, 1–7. doi: 10.1111/imb.12347

Robertson, H. M. (2019). Molecular evolution of the major arthropod chemoreceptor gene families. *Annu. Rev. Entomol.* 64, 227–242. doi: 10.1146/annurev-ento-020117-043322

Ruel, D. M., Yakir, E., and Bohbot, J. D. (2018). Supersensitive odorant receptor underscores pleiotropic roles of indoles in mosquito ecology. *Front. Cell Neurosci.* 12:533. doi: 10.3389/fncel.2018.00533

Sanchez-Alcaniz, J. A., Silbering, A. F., Croset, V., Zappia, G., Sivasubramaniam, A. K., Abuin, L., et al. (2018). An expression atlas of variant ionotropic glutamate receptors identifies a molecular basis of carbonation sensing. *Nat. Commun.* 9:4252. doi: 10.1038/s41467-018-06453-1

Shan, S., Wang, S. N., Song, X., Khashaveh, A., Lu, Z. Y., Dhiloo, K. H., et al. (2019). Antennal ionotropic receptors IR64a1 and IR64a2 of the parasitoid wasp *Microplitis mediator* (*Hymenoptera: Braconidate*) collaboratively perceive habitat and host cues. *Insect Biochem. Mol. Biol.* 114:103204. doi: 10.1016/j.ibmb.2019.103204

Short, A. E. Z. (2018). Systematics of aquatic beetles (*Coleoptera*): current state and future directions. *Syst. Entomol.* 43, 1–18. doi: 10.1111/syen.12270

Silbering, A. F., Rytz, R., Grosjean, Y., Abuin, L., Ramdya, P., Jefferis, G. S., et al. (2011). Complementary function and integrated wiring of the evolutionarily distinct *Drosophila* olfactory subsystems. *J. Neurosci.* 31, 13357–13375. doi: 10.1523/JNEUROSCI.2360-11.2011

Simao, F. A., Waterhouse, R. M., Ioannidis, P., Kriventseva, E. V., and Zdobnov, E. M. (2015). BUSCO: assessing genome assembly and annotation completeness with single-copy orthologs. *Bioinformatics* 31, 3210–3212. doi: 10.1093/bioinformatics/btv351

Simon, P. (2003). Q-Gene: processing quantitative real-time RT-PCR data. *Bioinformatics* 19, 1439–1440. doi: 10.1093/bioinformatics/btg157

Song, L. M., Jiang, X., Wang, X. M., Li, J. D., Zhu, F., Tu, X. B., et al. (2016). Male tarsi specific odorant-binding proteins in the diving beetle *Cybister japonicus* Sharp. *Sci. Rep.* 6:31848. doi: 10.1038/srep31848

Trapnell, C., Roberts, A., Goff, L., Pertea, G., Kim, D., Kelley, D. R., et al. (2012). Differential gene and transcript expression analysis of RNA-seq experiments with TopHat and Cufflinks. *Nat. Protoc.* 7, 562–578. doi: 10.1038/nprot.2012.016

van Giesen, L., and Garrity, P. A. (2017). More than meets the IR: the expanding roles of variant Ionotropic Glutamate Receptors in sensing odor, taste, temperature and moisture. *F1000Res* 6:1753. doi: 10.12688/f1000research.12013.1

Wicher, D., and Miazzi, F. (2021). "Insect odorant receptors: Function and regulation," in *Insect Pheromone Biochemistry and Molecular Biology*, 2nd Edn, eds G. J. Blomqvist and R. G. Vogt (Amsterdam: Elsevier), 415–433. doi: 10.1016/B978-0-12-819628-1.00013-4

Xia, Y., Wang, G., Buscariollo, D., Pitts, R. J., Wenger, H., and Zwiebel, L. J. (2008). The molecular and cellular basis of olfactory-driven behavior in *Anopheles gambiae* larvae. *Proc. Natl. Acad. Sci. U.S.A.* 105, 6433–6438. doi: 10.1073/pnas.0801007105

Xu, W. (2020). How do moth and butterfly taste? Molecular basis of gustatory receptors in *Lepidoptera*. *Insect Sci.* 27, 1148–1157. doi: 10.1111/1744-7917.12718

Yohe, L. R., and Brand, P. (2018). Evolutionary ecology of chemosensation and its role in sensory drive. *Curr. Zool.* 64, 525–533. doi: 10.1093/cz/zoy048

Zhang, J., Bisch-Knaden, S., Fandino, R. A., Yan, S., Obiero, G. F., Grosse-Wilde, E., et al. (2019). The olfactory coreceptor IR8a governs larval feces-mediated competition avoidance in a hawkmoth. *Proc. Natl. Acad. Sci U.S.A.* 116, 21828–21833. doi: 10.1073/pnas.1913485116

Zhang, X. X., Yang, B., Sun, D. D., Guo, M. B., Zhang, J., and Wang, G. R. (2021). Ionotropic receptor 8a is involved in the attraction of *Helicoverpa armigera* to acetic acid. *Insect Sci.* doi: 10.1111/1744-7917.12962 [Epub ahead of print].

Zhao, Y. J., Li, G. C., Zhu, J. Y., and Liu, N. Y. (2020). Genome-based analysis reveals a novel SNMP group of the Coleoptera and chemosensory receptors in *Rhaphuma horsfieldi*. *Genomics* 112, 2713–2728. doi: 10.1016/j.ygeno.2020.03.005

Conflict of Interest: The authors declare that the research was conducted in the absence of any commercial or financial relationships that could be construed as a potential conflict of interest.

Publisher's Note: All claims expressed in this article are solely those of the authors and do not necessarily represent those of their affiliated organizations, or those of the publisher, the editors and the reviewers. Any product that may be evaluated in this article, or claim that may be made by its manufacturer, is not guaranteed or endorsed by the publisher.

Copyright © 2021 Montagné, Jager, Chertemps, Persyn, Jaszczyszyn, Meslin, Jacquin-Joly and Manuel. This is an open-access article distributed under the terms of the Creative Commons Attribution License (CC BY). The use, distribution or reproduction in other forums is permitted, provided the original author(s) and the copyright owner(s) are credited and that the original publication in this journal is cited, in accordance with accepted academic practice. No use, distribution or reproduction is permitted which does not comply with these terms.

frontiers in Neuroanatomy

ORIGINAL RESEARCH
published: 16 December 2021
doi: 10.3389/fnana.2021.791900

Morphological and Ultrastructural Characterization of Antennal Sensilla and the Detection of Floral Scent Volatiles in *Eupeodes corollae* (Diptera: Syrphidae)

Wan-Ying Dong[1], Bing Wang[1] and Gui-Rong Wang[1,2]**

[1] State Key Laboratory for Biology of Plant Diseases and Insect Pests, Institute of Plant Protection, Chinese Academy of Agricultural Sciences, Beijing, China, [2] Shenzhen Branch, Guangdong Laboratory for Lingnan Modern Agriculture, Genome Analysis Laboratory of the Ministry of Agriculture, Agricultural Genomics Institute at Shenzhen, Chinese Academy of Agricultural Sciences, Shenzhen, China

OPEN ACCESS

Edited by:
Rui Tang,
Institute of Zoology, Guangdong Academy of Science, Chinese Academy of Sciences (CAS), China

Reviewed by:
Hao Guo,
Chinese Academy of Sciences (CAS), China
Peng He,
Guizhou University, China

***Correspondence:**
Bing Wang
wangbing02@caas.cn
Gui-Rong Wang
wangguirong@caas.cn

Received: *09 October 2021*
Accepted: *15 November 2021*
Published: *16 December 2021*

Citation:
Dong W-Y, Wang B and Wang G-R (2021) Morphological and Ultrastructural Characterization of Antennal Sensilla and the Detection of Floral Scent Volatiles in Eupeodes corollae (Diptera: Syrphidae). Front. Neuroanat. 15:791900. doi: 10.3389/fnana.2021.791900

The olfactory sensing system of the syrphid fly *Eupeodes corollae* is essential in pollination and prey localization, but little is known about the ultrastructural organization of their olfactory organs. In this study, the morphology, distribution, and ultrastructural organization of antennal sensilla of *E. corollae* in both sexes were observed by scanning electron microscopy (SEM) and transmission electron microscopy (TEM). Neuronal responses of a subtype of sensilla basiconica to floral scent compounds were recorded by single sensillum recording (SSR). Ten morphological types, including Böhm bristles, sensilla chaetica, microtrichiae, sensilla trichodea, sensilla basiconica, sensilla clavate, sensilla coeloconica, sensilla styloconica, sensilla placodea, and sensory pit, were identified. Except for Böhm bristles and sensilla chaetica, which were distributed on the scape and pedicel of *E. corollae* antennae, innervated sensilla were densely distributed on the flagellum, a vital sensory organ. Further, observing ultrastructural organization showed that the sensilla trichodea, basiconica, and clavate are single-walled with multiple nanoscale pores perforating the cuticle. Sensilla coeloconica are double-walled and have no wall pores, but instead, have longitudinal grooves along with the pegs. Sensilla chaetica, Böhm bristles, and microtrichiae did not have wall pores on the cuticle or sensory cells at the base. The SSR results indicated that neuron B housed in the subtype of sensilla basiconica I (SBI) mainly responded to methyl eugenol and other aromatic compounds. Overall, our results provide valuable information to understand the morphology and ultrastructure of antennal sensilla from *E. corollae*. These findings are beneficial for the studies of the neuronal function map of olfactory sensilla and for determining evolutionary relationships in Diptera.

Keywords: antenna, sensilla, odorant receptor neuron, scanning electron microscopy, transmission electron microscopy, single sensillum recording, methyl eugenol

INTRODUCTION

The insect olfactory system allows sensitive detection and precise discrimination of relevant odor cues from natural surroundings (Bruce et al., 2005; Renou and Anton, 2020). These cues include semiochemicals released by food sources, oviposition sites, predators, or competitors and also pheromones emitted from conspecifics (Fleischer et al., 2018; Renou and Anton, 2020). Various volatile organic compounds are detected by odorant receptor neurons (ORNs) housed in the sensilla, hair-like structures that extend from the insect cuticle with multiple cuticular pores on the antennae and maxillary palps (Steinbrecht, 1997; Keil, 1999). Odorants are thought to penetrate through the pores of the sensilla walls into the sensillum lymph and are transferred by odorant-binding proteins (OBPs) toward the dendrites of ORNs and then activate the odorant receptors (ORs) to generate action potentials (Leal, 2013). Subsequently, electrical signals are transmitted through the axons of ORNs and converge to the central nervous system (Wilson, 2013). The higher olfactory center reintegrates and processes this information and finally causes the insect to produce corresponding behavioral responses (Bates et al., 2020).

Odorants are initially discriminated by dedicated olfactory sensilla located on insect antennae (Ghaninia et al., 2014; Keesey et al., 2015). Generally, sensilla involved in olfaction occur in three major morphological types, trichoid, basiconic, and coeloconic (Venkatesh and Singh, 1984). The sensilla types, however, differ not only in micromorphological and anatomical structure but also in their functional responses to the activation of receptors and neurons. Sensilla trichodea in many insects, such as flies and moths, are mainly tuned to detect pheromone components (Wang et al., 2016; Chang et al., 2017; Liu S. et al., 2020; Khallaf et al., 2021). However, some sensilla trichodea detect other chemicals (Soni et al., 2019). For example, in the tsetse fly *Glossina morsitans* (Diptera: Glossinidae), ORNs housed in trichoid sensilla respond to a wide diversity of chemicals, such as 1-octen-3-ol, 2-heptanone, isoamyl acetate, and methyl laurate. Sensilla basiconica usually responds to plant volatiles, including many alcohols, aldehydes, esters, ketones, and carbon dioxide (de Bruyne et al., 2001; Keesey et al., 2015; Cui et al., 2018; Mansourian et al., 2018). ORNs in coeloconic sensilla are tuned to specific chemosensory stimuli, including acids, aldehydes, ammonia, putrescine, and water vapor (Yao, 2005; Prieto-Godino et al., 2016, 2017). Some sensilla coeloconica also respond to a range of temperatures and humidity (Ruchty et al., 2010; Schneider et al., 2018).

In addition to these common sensilla, other types of sensilla are found on Dipteran insect antennae. Sensilla styloconica are distributed on the antennal pedicel of Anthomyiidae (Ross, 1992) and Calliphoridae (Sukontason et al., 2004; Hassan et al., 2013) and the antennal flagellum of Tephritidae (Arzuffi et al., 2008; Bisotto-De-Oliveira et al., 2011), the function of which is supposed to hygro- and thermoreception. Sensilla auricillica was observed on the antennal flagellum of four species of Oestridae (Zhang et al., 2016). Moreover, Shanbhag et al. (1995) found sensory sacculus on the antennal flagellum of *Drosophila melanogaster*. The same structures were also found on the antennal flagellum of *Triceratopyga calliphoroides* (Zhang et al., 2014), *Fannia canicularis*, and *F. scalaris* and were defined as a multichambered invagination stretching into the cavity of the antennal funiculus containing different types of sensilla (Zhang et al., 2013a).

Similarly, sensory pits, single-chambered invaginations containing a cluster of sensilla with a fringe of microtrichiae around the edge, have been found on the antennae of flies from Fanniidae (Wang et al., 2012; Zhang et al., 2013a), Anthomyiidae (Honda et al., 1983; Ross, 1992), Muscidae (Sukontason et al., 2004; Smallegange et al., 2008; Tangtrakulwanich et al., 2011), Sarcophagidae (Liu et al., 2016; Pezzi et al., 2016), Oestridae (Zhang et al., 2012a, 2016; Liu et al., 2015), Calliphoridae (Setzu et al., 2011; Zhang et al., 2013b, 2014), Syrphidae (Henderson and Wellington, 1982; Jia et al., 2019), and Glossinidae (Isaac et al., 2015). Numerous sensilla gathered in the sensory sacculus and sensory pits can increase the contact area between the sensilla and the odor, improve the efficiency of the sensilla to capture the odor, and enhance the olfactory sensitivity of the antennae (Hunter and Adserballe, 1996; de Bruyne et al., 2001; Zhang et al., 2013b). The morphology and function of these different types of sensilla may be the result of the long adaptation of insects to the surrounding environment. Therefore, determining external morphology and fine structure of the sensilla will help in studies of comparative morphology and reveal mechanisms of olfactory recognition and evolution and adaptation in insects.

Larval hoverflies are a natural enemy of aphids that can significantly suppress aphid populations (Wotton et al., 2019). As adults, hoverflies are important pollinators (Baldock et al., 2019; Rader et al., 2020). In flowering plants, the aromatic compounds aldehydes, alcohols, ethers, and esters alone or in combination with some monoterpenes alcohols are often identified as floral volatiles perceived by and attractive to flower visitors or pollinators, such as bees, syrphid flies, butterflies, and moths (Dobson, 2006; Dötterl and Vereecken, 2010; Primante and Dötterl, 2010; Zito et al., 2019). Representative floral volatiles includes 2-phenylethanol, methyl salicylate, limonene, eugenol, and methyl eugenol, all reported to be detected by and an attractant for syrphid flies (Zhu and Park, 2005; Benelli et al., 2017; Li et al., 2020). In addition, inflorescence scents involving phenylacetaldehyde, pyranoid linalool oxide, methyl salicylate, dimethyl salicylate, linalool, and octyl acetate were recently reported as electrophysiologically active compounds for Syrphidae (Primante and Dötterl, 2010; Braunschmid et al., 2017). These findings emphasize that floral volatiles, especially aromatic compounds, are essential for attracting pollinating hoverflies. But the olfactory tools used by hoverflies to detect complicated floral cues have not been investigated (Braunschmid et al., 2017).

The hoverflies, *E. corollae* (Diptera, Syrphidae), are a dual service provider and a widely distributed species in the agricultural ecosystem of north-eastern China (Pekas et al., 2020). In this study, we describe the antennal sensilla morphology and distribution in *E. corollae* using SEM. The antennal sensilla in male and female *E. corollae* were classified into ten types according to their shape and morphological features. The ultrastructural organization and the neuronal numbers of seven

types of sensilla were further investigated by TEM. Then, we recorded responses of a single neuron in the subtype of sensilla basiconica I (SBI) to ten floral compounds on the antennae of male and female *E. corollae* using single sensillum recording (SSR) technology. Our study provides useful information in the aspect of the morphological types and ultrastructure of the antennal sensilla and helps to understand the molecular mechanisms of olfactory perception at the peripheral nervous system in *E. corollae*.

MATERIALS AND METHODS

Insect Rearing

Adults *E. corollae* were collected from the Langfang Experiment Station of the Institute of Plant Protection, Chinese Academy of Agricultural Sciences (CAAS), Langfang, Hebei province, China (116.60°E′, 39.50°N′). *E. corollae* was reared in our laboratory with *Acyrthosiphon pisum* (Hemiptera: Aphididae) at the larval stage and pollen and 10% honey solution at the adult stage at 25 ± 1°C, 60 ± 5% relative humidity and under a photoperiod of 14 h light: 10 h dark. After eclosion, females and males were processed for observation with SEM and TEM. Three- to four-day-old virgin females and males were used for electrophysiological recordings.

Scanning Electron Microscopy

Antennae of male and female adult hoverflies were excised from the base under a stereomicroscope and sonicated in 70% ethanol in 1.5 ml centrifuge tubes for 10 s in an ultrasonic bath (250W) to wash away impurities on the surface of the antennae. Subsequently, the specimens were dehydrated in ethanol solutions (80, 90, and 100%) for 5 min each. After drying in a carbon dioxide critical point drier (LEICA EM CPD030), the specimens were mounted on aluminum stubs with double-sided conductive adhesive, coated with gold in an ion sputtering device (HITACHI MC 1000), and stored in a desiccator until use. The preparations were examined with a HITACHI SU8010 scanning electron microscope (Hitachi, Tokyo, Japan) at the Electronic Microscopy Centre of the Institute of Food Science and Technology, CAAS (Beijing, China). Sensilla types in this study were classified according to the previous references (Bisotto-De-Oliveira et al., 2011; Pezzi et al., 2016; Hore et al., 2017).

Transmission Electron Microscopy

Antennae were dissected from newly emerged male and female hoverflies and transferred to 3.5% glutaraldehyde (prepared with a phosphate buffer solution at pH 7.4) containing 0.6% (v/v) TWEEN-20 and 0.09% (w/v) NaCl. Antennae were prefixed for 2 days at 4°C and then washed ten times in phosphate buffer (0.1 mol/L, pH 7.4) for 15 min each time. Next, postfixation antennae were incubated at room temperature for 2 h in a solution of 1% osmium tetroxide mixed with a phosphate buffer solution at a pH of 7.4. After four washes with phosphate buffer, specimens were dehydrated in ethanol solutions (30, 50, 60, 70, 80, and 90%) for 15 min each, followed by two washes in 100% ethanol for 20 min. The specimens were rinsed again and dehydrated with 100% acetone six or seven times for 10 min each, then embedded in a mixture of anhydrous acetone and Spurr's resin (a ratio of 3:1 for 4 h, 1:1 overnight, 1:3 for 8 h, and in pure resin for 12 h), and polymerized for 72 h at 60°C. Sections (50–80 nm thick) were cut with a LEICA EM UC6 ultramicrotome, transferred onto a copper grid, and stained in saturated uranyl acetate and 1% lead citrate for 10 min each, followed by air-drying. Finally, specimens were observed using a HITACHI H-7,500 (Hitachi, Tokyo, Japan) transmission electron microscope at the Electronic Microscopy Centre of the Institute of Food Science and Technology, CAAS (Beijing, China) operated at 80 kV. The terminology of the antennal segments follows *D. melanogaster* (Shanbhag et al., 1999), whereas sensilla types were classified according to the previous references (Lewis, 1971; Honda et al., 1983; Smallegange et al., 2008; Oh et al., 2019).

Single Sensillum Recording

A single hoverfly was restrained in a 200 μl plastic pipette tip with the narrow end cutoff. The hoverfly was gently pushed until its head protruded from the cut end and fixed to the rim of the pipette tip with dental wax. Then, one of the exposed antennae was stuck to a coverslip with a double-face adhesive tape. Before recording, tungsten wire electrodes were electrolytically sharpened by repeatedly immersing the tip into 40% KNO_2 solution. The reference electrode was placed in the hoverfly eye, and the recording electrode was gently inserted into the base of the basiconic sensillum. The recordings were performed under a LEICA Z16 APO microscope at × 920 magnification. A continuous stream of purified and humidified air was directed onto the antenna through a 14 cm-long steel tube controller (Syntech, Hilversum, the Netherlands). Tested odorants were injected into the air stream by a Syntech Stimulus controller (CS-55 model, Syntech), which generated 300 ms air pulses with an airflow of 20 ml/s delivered through a Pasteur pipette. Compensating airflow was provided to keep a constant air stream, but the compensatory flow was switched off during stimulation. Signals of the action potentials were amplified 10 × by a preamplifier (IDAC-4 USB System, Syntech, Kirchzarten, Germany) and then sent to a computer *via* an analog-to-digital converter. Software package Autospike 32 (Syntech) was used to amplify, digitize, and visualize the action potentials. The number of ORNs housed in a single sensillum could be deduced based on the differences in their spike amplitudes. Responses were calculated by the difference between the spike number counted 1 s before and 1 s after delivery of the stimulus. The data were shown as mean ± SEM. GraphPad PRISM version 6.0 software (San Diego, California, United States) was used to make the graphics.

Odor Stimulation

Ten representative floral scent compounds (98–99% minimum purity) were purchased from Sigma-Aldrich Co. (St. Louis, MO, United States) and used for electrophysiological recordings (**Table 1**). All odorants were diluted to a final concentration of 100 μg/μl in dimethyl sulfoxide (DMSO). For stimulus delivery, 10 μl of each solution was dripped on a filter paper strip

TABLE 1 | Ten floral scent compounds used for electrophysiological recordings.

Stimulus compounds	CAS number	Purity (%)	Company	References
Aromatics				
p-anisaldehyde	123-11-5	98	Sigma	Zito et al., 2019
4-methoxybenzyl alcohol	105-13-5	98	Sigma	Ervik et al., 1999
Methyl eugenol	93-15-2	98	Sigma	Solís-Montero et al., 2018
Eugenol	97-53-0	99	Sigma	Solís-Montero et al., 2018
2-phenylethanol	60-12-8	99	Sigma	Braunschmid et al., 2017
Methyl salicylate	119-36-8	99	Sigma	Solís-Montero et al., 2018
Terpenoids				
Linalool	78-70-6	97	Sigma	Zito et al., 2019
Geranyl acetate	105-87-3	97	Sigma	Braunschmid et al., 2017
Trans-β-farnesene	18794-84-8	90	Sigma	Braunschmid et al., 2017
Heterocyclic derivatives				
Indole	120-72-9	99	Sigma	Braunschmid et al., 2017

(0.5 × 4 cm) inserted in a Pasteur pipette (15 cm long). DMSO alone was tested as a negative control.

RESULTS

Gross Morphology of Antennae, Sensilla Types, and Distribution

Scanning electron microscopy observation revealed that the antennae of both sexes of *E. corollae* were composed of three segments, scape (Sc), pedicel (Pe), and flagellum (Fl). The Fl had a typical structure similar to that of the *Drosophila* counterpart and bore a long arista (Ar) arising from the proximal dorsal ridge (**Figure 1A**). Short and long hairs and numerous sensilla were present on the aristate Fl. No clear differences in the gross morphology of the antennae were found between male and female *E. corollae*. In total, ten morphologically distinct types of sensilla were observed externally on the antennae of female and male *E. corollae* and included Böhm bristles (BB), sensilla chaetica (SC), microtrichiae (Mt), sensilla trichodea (ST), sensilla basiconica (SB), sensilla clavate (SCl), sensilla coeloconica (SCo), sensilla styloconica (SSt), sensilla placodea (SP), and sensory pit.

Generally, BB spread over the surface of the antennal Sc and Pe segments, and the entire Ar. They displayed a small needle-like structure with a pointed tip, a smooth surface, and stood at an acute angle to the antennal surface. BB did not contain pores, longitudinal grooves, or a flexible socket (**Figure 1B**). SC was the longest sensilla found on the antennae of both sexes of *E. corollae*. Based on sensillum size, the SC was classified into two subtypes: long SC (LSC) and short SC (SSC) (**Figure 1C**). LSC was observed in the distal region of the Sc and Pe interspersed by numerous bristles, whereas SSC was only found on the Pe. These sensilla were characterized by thorn-shaped straight hairs incised with longitudinally arranged furrows. The base of the sensillum was inserted into a round socket that stands above the surface of the antenna. The tips of the stout sensilla were apiculiform and did not have pores in the wall (**Figure 1D**).

Microtrichiae densely covered the entire flagellum and were interspersed around some types of sensilla with no differences between sexes. These sensilla were slender, curved, hair-like structures with longitudinal grooves from base to tip. There was no distinct cuticular socket at the base (**Figure 1E**). ST was numerous and widely distributed on the surface of the antennal Fl, with the longest one towering over the layer of Mt. ST were present around the distal part of the Fl with fewer toward proximal and ventral regions. Their base arose from a small cuticular pit and tapered to a fine tip, showing a long, hair shape (**Figure 1E**). SB covered every region of the surface of the Fl. According to their external characteristics, SB can be classified into four subtypes. The subtype of SBI was finger shaped with a rounded tip and slightly curved under the tip (**Figure 1F**). The subtype of sensilla basiconica II (SBII) was the shortest, in the shape of sturdy pegs tapering from the base to the apex (**Figure 1G**). The subtype of sensilla basiconica III (SBIII) was relatively slender and somewhat curved (**Figures 1G,H**). The subtype of sensilla basiconica IV (SBIV) was similar to SBII in shape but much longer (**Figure 1G**).

Sensilla clavate had a club-like shape and were less widespread on the surface of the flagellum. SCl occurred in two subtypes, large (LSCl) and small (SSCl). SSCl was shorter and stouter than the LSCl. They were morphologically similar to the SB, but have a distal swelling (**Figures 1F,I**). SCo was quite short and generally located near the proximal region of the Fl on its dorsal and ventral sides. These sensilla arise from a shallow socket. The base of the hair shaft was slightly inflated and gradually tapered to a conical tip. The top two-thirds of SCo had deep longitudinal surface grooves, while the bottom one-third of the sensilla base was smooth, with no grooves or pores (**Figure 1I**). SSt were generally located on the anterior and posterior surface of the flagellum irregularly at low density. These sensilla were characterized by longitudinally grooved pegs protruding from the antennal surface that tapered into a rounded tip. The base of the SSt was smooth, with no grooves or pores. The top half of the SSt had about nine closely apposed finger-like ridges along with the peg. Some of them terminated below the tip so that the tip may have eight fingers or less (**Figure 1J**).

Sensilla placodea were scattered irregularly on the surface of the flagellum, like a small button. The shape of SP was like a smooth plate with a small ring around it. There was no pore or distinct socket on the surface of SP (**Figure 1K**). Only one type of SP was identified in each Fl of both male and female *E. corollae*. These pits have a roundish opening and are surrounded by Mt near the central region of the Fl on its dorsal and ventral sides. The SP appears as hemispherical invaginations and their inner surface was covered by basiconic-like sensilla (**Figure 1L**). These sensilla resemble the SB on the external surface of the antennal Fl but were slightly curved and smaller than SBII.

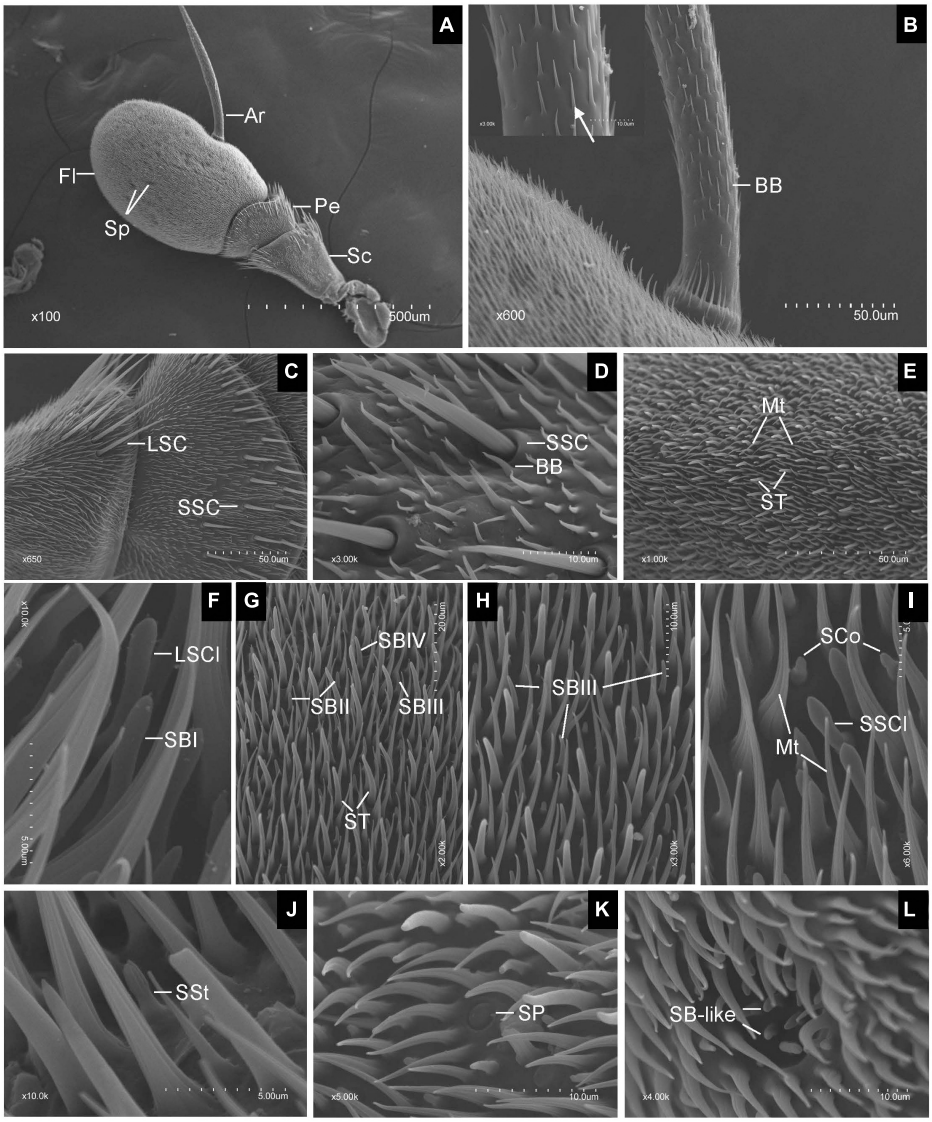

FIGURE 1 | Scanning electron micrographs of *Eupeodes corollae* antenna. **(A)** General view of the antenna from *E. corollae*, showing the scape, the pedicel, the flagellum, the arista, and the sensory pit. **(B)** Böhm bristles spread over the entire arista. Inlay: enlarged view of Böhm bristles (arrows). **(C)** Long sensilla chaetica and short sensilla chaetica in the distal region of the scape and pedicel. **(D)** Short sensilla chaetica with longitudinal furrows interspersed by Böhm bristles in the distal region of the pedicel. **(E)** Sensilla trichodea are long and tower over the layer of microtrichiae on the surface of the flagellum. **(F)** Large sensilla clavate with distal swelling and subtype of SBI with round tip on the surface of the flagellum. **(G)** Funicular subtype of SBII, SBIII, and SBIV. **(H)** Funicular subtype of SBIII with a relatively slender curved tip. **(I)** Small sensilla clavate and sensilla coeloconica. **(J)** Sensilla styloconica with closely apposed finger-like ridges along with the peg. **(K)** Sensilla placodea are like a button with smooth surface. **(L)** Sensory pit with basiconic-like sensilla. Sc, scape; Pe, pedicel; Fl, flagellum; Ar, arista; Sp, sensory pit; BB, Böhm bristle; LSC, long sensilla chaetica; SSC, short sensilla chaetica; ST, sensilla trichodea; Mt, microtrichiae; LSCl, large sensilla clavate; SBI, sensilla basiconica I; SBII, sensilla basiconica II; SBIII, sensilla basiconica III; SBIV, sensilla basiconica IV; SSCl, small sensilla clavate; SCo, sensilla coeloconica; SSt, sensilla styloconica; SP, sensilla placodea. Scale bars in **(F,I,J)** 5 μm; **(D,H,K,L)** 10 μm; **(G)** 20 μm; **(B,C,E)** 50 μm; **(A)**, 500 μm.

Fine Structure of Antennal Sensilla

Sensilla Trichodea

Transmission electron microscopy observations showed that ST was thick-walled and perforated by numerous pores. The wall pores widen into a relatively small pore kettle, which is connected to the sensillum lumen. Two dendrites at the basal region of the ST were bordered by thecogen, trichogen, and tormogen cells (**Figures 2A–C**). Cross-sections at the base of the sensilla showed one, two, or three dendrites in the lymph of the sensillum lumen (**Figures 2D–F**). Up to 17 cross-sections of dendrites were seen at the tip of the sensilla (**Figure 2G**).

Sensilla Basiconica

Longitudinal sections of SB showed a thin, homogeneous cuticle through the hair shaft that was pierced by numerous, visible pores. Sections through the base of SBI showed three

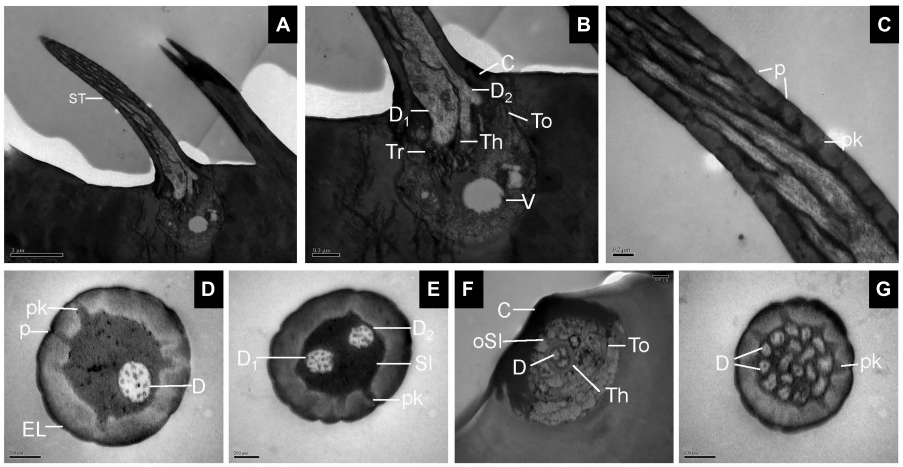

FIGURE 2 | Sensilla trichodea on the antennal surface of *E. corollae* in longitudinal and cross-sections. **(A)** Longitudinal section through the entire ST showing a long, hair-like shape. **(B)** Longitudinal section through the base of the ST, with two outer dendritic segments surrounded by thecogen, trichogen, and tormogen cells. The outer sensillum-lymph cavity contains a clear vesicle, possibly representing extracted lipid droplets. **(C)** Longitudinal section through the hair shaft of the ST at about half-length. The ST were thick-walled and perforated by pores widening into a relatively small pore kettle. **(D–F)** Cross-sections through the basal part of the ST, showing one, two, or three dendrites in the lymph of the sensillum lumen. **(G)** Cross-section through the tip of the ST, showing up to 17 branched dendrites. D, dendrite; Th, thecogen cell; Tr, trichogen cell; To, tormogen cell; V, vesicle; p, pore; pk, pore kettle; EL, epicuticular layers; C, cuticle; Sl, sensillum lymph; oSl, outer sensillum lymph. Scale bars in **(C–G)** 0.2 μm; **(B)** 0.5 μm; and **(A)** 2 μm.

dendrites branching profusely when entering the sensillum lumen (**Figures 3A,B**). The wall pores were distributed all around the sensilla, and typical pore tubules extended into the lumen (**Figure 3C**). Near the SBII base, an outer dendritic segment splits into abundant dendritic branches. This branching was restricted to a small region, resulting in a brush-like structure. The inner dendritic segment was tightly surrounded by thecogen and trichogen cells (**Figures 3D,E**). There were many fewer wall pores compared with SBI (**Figure 3F**). At the base of SBIII, the thecogen cells closely contacted two dendrites that extended either in longitudinal or in angled directions in the sensillum lumen (**Figures 3G,H**). The pore density gradually increased toward the sensilla tip (**Figure 3I**). Cross-sections through various subtypes of SB showed numerous nanoscale pores and pore tubules that perforated the comparatively thin cuticular wall. The outer dendritic segments in different subtypes of SB may branch at somewhat different levels (**Figures 3J–L**).

Sensilla Clavate

The longitudinal sections of LSC exhibited two dendrites varying in size that sends out numerous branches in the sensillum lumen (**Figures 4A,B**). The sensilla wall had many pores with pore tubules and their densities were comparable to those of the SB. The pore density at the proximal base gradually decreased (**Figure 4C**). Dendrites in the sensilla lumen were highly lamellated different from those of the SB (**Figure 4D**). No ultrastructure of SSC was observed in this experiment.

Sensilla Coeloconica, Sensilla Chaetica, Microtrichiae, and Böhm Bristles

The longitudinal section of SCo showed two outer dendritic segments tightly surrounded by a dendrite sheath and which extended unbranched into the sensilla lumen (**Figure 5A**). The distal cross-section of the sensillum had a rosette-shaped structure. The inner walls appeared to be fused. The outer walls of neighboring cuticular fingers are separated by grooves (**Figure 5B**). Therefore, pores may be present between the grooves. Basal cross-section exhibited the double-walled structure of the SCo. The lumen of the inner cuticle contained dendrite segments surrounded by electron-dense sensillum lymph. The space between the inner and outer cuticular walls was full of filament-like electron-dense structures (**Figure 5C**). The ultrastructure of the SC showed an obvious thick and aporous cuticular wall. There was no neuronal dendrite but narrow tubular space was observed in the sensilla lumen. The cuticular wall was bordered by visible ridges due to the external furrows (**Figure 5D**). The cross-section of Mt showed that the sensilla were not innervated (**Figure 5E**). The ultrastructure of BB showed that the cuticle was much thicker than that of the olfactory sensilla, and the neuronal dendrites were absent (**Figure 5F**).

Responses of Neurons Housed in SBI to Floral Scent Compounds

To evaluate the olfactory neuron responses of sensilla of *E. corollae* to floral volatiles, we performed SSR in SB and ST from antennae in both sexes using ten representative floral scent compounds (**Table 1**). Fortunately, the neurons housed in SBI were found activated by these chemicals. Spontaneous activity of neurons housed in the SBI revealed that three neurons were distinguishable as A, B, and C, based on the spike amplitudes (**Figure 6A**). The result further confirmed that three dendrites were observed in the SBI. Neuron B in the SBI was strongly activated by methyl eugenol and eugenol at doses of 1 mg. The

FIGURE 3 | Sensilla basiconica on the antennal surface of *E. corollae* in longitudinal and cross-sections. **(A–C)** Longitudinal section of subtype of SBI. Close to the base of SBI, three dendrites have different diameters and start branching at different levels. The outer dendritic segments are surrounded by thecogen cells. Many pores with pore tubules perforate the thin wall. **(D–F)** Longitudinal section of subtype of SBII. Close to the sensillar base, an outer dendritic segment sends out many dendrites, like a brush. Thecogen and trichogen cells tightly surround the inner dendritic segments at the base of SBII. The hair shaft is pierced by numerous pores. **(G–I)** Longitudinal section of subtype of SBIII. The hair shaft is a little longer and slenderer than SBII. The two dendrites are surrounded by thecogen and trichogen cells, and branch at different levels. The thin cuticular wall is perforated by narrow pore openings. **(J–L)** Cross-sections through various subtypes of sensilla basiconica on the antenna of *E. corollae*. The cuticular wall of sensilla basiconica is relatively thin and has numerous nanoscale wall pores. The outer pore widens into a visible pore tubule and contacts the sensillum lymph in the sensilla lumen. The shape and number of dendritic branches appeared to be different in different subtypes of sensilla basiconica. iD, inner dendritic segment; oD, outer dendritic segment; pt, pore tubule. Other abbreviations followed **Figures 1**, **2**. Scale bars in **(C,F,I–L)** 0.2 μm; **(B,E,H)** 0.5 μm; **(A,D,G)** 2 μm.

strongest response to methyl eugenol was 50 ± 7.57 spikes/s. *p*-Anisaldehyde, linalool, and methyl salicylate also elicited moderate responses of neuron B. By contrast, neurons A and C did not respond to any of these odorants (**Figures 6B,C**).

DISCUSSION

Syrphids represent a diverse and economically important family in Diptera, comprising about 6,697 described species in 283

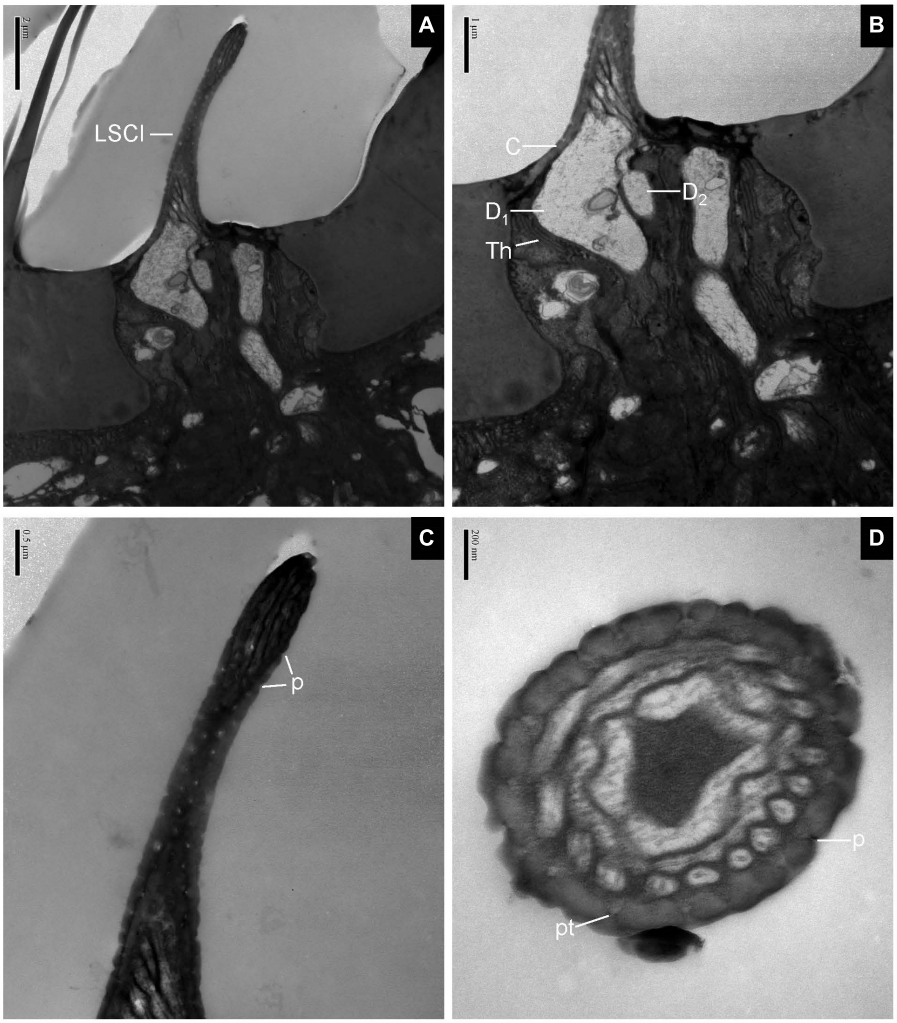

FIGURE 4 | Large sensilla clavate in longitudinal and cross-sections on the antennal surface of *E. corollae*. **(A–C)** Large sensilla clavate in longitudinal section. The distal swelling of the sensilla is conspicuous, like a wooden club. The two dendrites varying in sizes are split into many dendritic branches in the sensilla lumen. The pore density is somewhat higher on the relatively thin cuticular wall. **(D)** Large sensilla clavate in cross-section. The lumen of the sensilla contains highly lamellated dendrites. Abbreviations as in **Figures 1**, **2**. Scale bars in **(D)** 0.2 μm; **(C)** 0.5 μm; **(B)** 1 μm; and **(A)** 2 μm.

genera, with most species distributed in the Neotropical, Nearctic, and Palaeotropical regions.[1] Despite their significant roles as pollinators and predators in chemoreception (Dunn et al., 2020), there are few studies regarding the ultrastructural organization of their sensory organs (Henderson and Wellington, 1982; Skevington and Dang, 2002; Larson et al., 2012; Jia et al., 2019). In this study, based on SEM observations, we identified ten morphologically distinct types of sensilla on antennae of female and male *E. corollae*, including Böhm bristles, sensilla chaetica, microtrichiae, sensilla trichodea, sensilla basiconica, sensilla clavate, sensilla coeloconica, sensilla styloconica, sensilla placodea, and sensory pit. Böhm bristles and sensilla chaetica were distributed on the scape and pedicel of *E. corollae* antenna, while other innervated sensilla were densely distributed on the flagellum, indicating the predominant sensory function of this segment.

The morphological traits and different types of sensilla are similar to those of other Dipteran Cyclorrhapha species (**Supplementary Table 1**). But two traits in *E. corollae* make the antennae different from those of other Diptera species. First, the sensilla styloconica was short and had grooved pegs on the flagellum of hoverflies. However, as in *Hydrotaea irritans* (Muscidae) (Been et al., 1988), *Toxotrypana curvicauda* (Arzuffi et al., 2008), and *Anastrepha fraterculus* (Tephritidae) (Bisotto-De-Oliveira et al., 2011), they are mainly present on the antennal pedicel among most calyptrate families (**Supplementary Table 1**), including Fanniidae, Anthomyiidae, Muscidae, Sarcophagidae, and Calliphoridae. Furthermore, these SSt have two primary morphologic types. These sensilla with longitudinal grooves along with the pegs are gradually tapered

[1]https://doi.org/10.15468/39omei

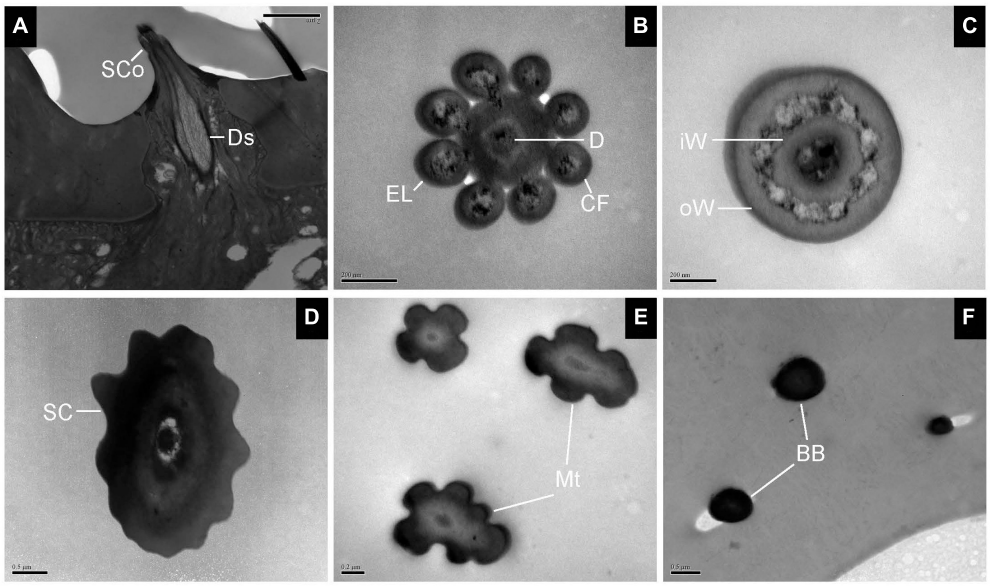

FIGURE 5 | Transmission electron micrographs of sensilla coeloconica, sensilla chaetica, microtrichiae, and Böhm bristles on the antennal surface of *E. corollae*. **(A–C)** TEM micrographs of sensilla coeloconica. **(A)** The longitudinal section through the peg shows a smooth shaft at the base and a deep groove at the distal end. The internal lumen is filled with two unbranched dendrites in a visible dendrite sheath. **(B)** Cross-section through the tip of sensilla coeloconica shows eight cuticular fingers surrounding the central lumen, where only one dendrite is visible. **(C)** Cross-section through the base of the sensilla coeloconica, showing the double-walled structure of the sensillum. **(D)** Cross-section through sensilla chaetica, showing a thick non-porous cuticular wall. No neuronal dendrite is present, but there is a narrow tubular space near the center lumen. **(E)** Cross-section through the microtrichiae, showing no dendrite in the sensilla central lumen. **(F)** Cross-section through the cuticular peg of a Böhm bristle, showing a thick aporous cuticular wall, and no sensory neurons. Ds, dendrite sheath; CF, cuticular finger; EL, epicuticular layers; iW, inner wall; oW, outer wall. Other abbreviations as in **Figures 1**, **2**. Scale bars in **(B,C,E)** 0.2 μm; **(D,F)** 0.5 μm; **(A)** 2 μm.

in Tephritidae and Syrphidae (Arzuffi et al., 2008; Bisotto-De-Oliveira et al., 2011). Throughout evolutionary history, this state has changed in most calyptrate families: the pegs have been transformed into setae that are bulbous at the base, and acute or obtuse at the distal end (Sukontason et al., 2004; Hore et al., 2017). Therefore, the distribution and morphology of SSt offer important information about the evolutionary history of Cyclorrhapha taxa, suggesting valuable potential in the phylogenetic signal of this structure. Second, the presence of sensilla placodea, already described on Hymenopteran (Xi et al., 2011; Silva et al., 2016) and Coleopteran antennae (Liu et al., 2012), was shown in a Dipteran species for the first time. Further electrophysiological studies are needed to verify the actual functions of those sensilla in *E. corollae*.

In addition, ultrastructural organization of sensilla trichodea, sensilla basiconica, large sensilla clavate, sensilla coeloconica, sensilla chaetica, Böhm bristles, and microtrichiae were obtained under TEM, providing fine morphological evidence of their possible sensory functions. The common morphological feature for olfactory sensilla is the multiple nanoscale wall pores on the surface of the hair shaft (Steinbrecht, 1997; Shanbhag et al., 1999). Our study showed that sensilla trichodea and all subtypes of sensilla basiconica from *E. corollae* antennae contain multiple nanoscale wall pores, suggesting that their major function is olfaction. Additionally, some basiconic-like sensilla are detected in the sensory pit near the central region of the flagellum, which are consistent with most previous morphological studies in *Delia radicum*, *D. floralis*, *D. antiqua*, *D. platura*, *Hypoderma bovis*, *Protophormia terraenovae*, *Fannia scalaris*, and *F. canicularis* (Ross, 1992; Hunter and Adserballe, 1996; Setzu et al., 2011; Zhang et al., 2013a). The convergence of sensilla in pits could expose a larger surface to receive odorants efficiently, increase sensitivity, and also protect the delicate sensilla from mechanical deformation (Ross, 1992; Hunter and Adserballe, 1996; de Bruyne et al., 2001; Zhang et al., 2012a,b, 2013a,b).

Moreover, we classified the LSC as an independent sensilla type due to the swelling in the distal region and the highly lamellated dendrites even though it has multiple walls pores on the surface like SB. LSCs have been observed and defined in *Hylemya antiqua* (Honda et al., 1983) and *Musca domestica* (Smallegange et al., 2008). The LSCs are widespread on the antennal flagellum, implying that they may have an important chemosensory function in detecting various chemical compounds related to certain behavior in *E. corollae*. An exception is sensilla coeloconica, which has deep longitudinal grooves along with the central peg instead of wall pores, also suggesting an olfactory function. TEM observation in the tobacco hornworm *Manduca sexta* (Shields and Hildebrand, 1999) and *D. melanogaster* (Yao, 2005) indicated that the intergroove region of sensilla coeloconica may be the entry point of odorants. Furthermore, cross-sections of the sensilla chaetica, Böhm bristles, and microtrichiae did not exhibit any wall pores on the cuticular surface nor any sensory cells at their base. The sensilla observed in this study are common to other Diptera families

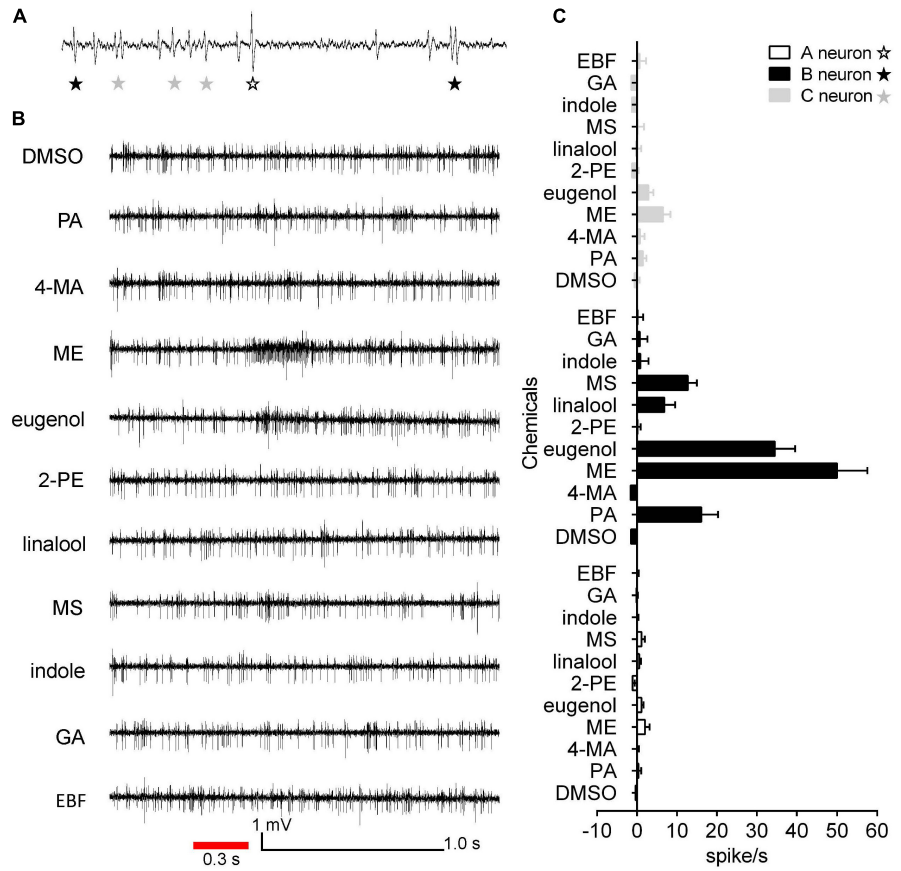

FIGURE 6 | Single sensillum recordings from subtype of SBI of female and male *E. corollae* responding to ten floral scent compounds. **(A)** Spontaneous activity (1 s) of subtype of SBI. Individual action potentials (spikes) were labeled A, B, or C according to their spike amplitude. **(B)** Representative traces of neurons in SBI stimulated by *p*-anisaldehyde, 4-methoxybenzyl alcohol, methyl eugenol, eugenol, 2-phenylethanol, linalool, methyl salicylate, indole, geranyl acetate, and (*E*)-β-farnesene; stimulus 1 mg (100 μg/μl). The red line represents the 0.3 s odorant stimulation. **(C)** Mean SSR responses of A, B, and C neurons from SBI stimulated by ten representative floral scent compounds. Neuron B in SBI was strongly activated by two odorants, eugenol, and methyl eugenol. Neurons A and C, by contrast, had no responses to any of the tested odorants. Responses were calculated by the difference between the spike number counted 1 s before and 1 s after delivery of the stimulus. $n = 8$. DMSO, dimethyl sulfoxide; PA, *p*-anisaldehyde; 4-MA, 4-methoxybenzyl alcohol; ME, methyl eugenol; 2-PE, 2-phenylethanol; MS, methyl salicylate; GA, geranyl acetate; EBF, (*E*)-β-farnesene.

such as Muscidae (Been et al., 1988; Smallegange et al., 2008), Tephritidae (Hu et al., 2010; Liu Y. et al., 2020), Sarcophagidae (Liu et al., 2016; Pezzi et al., 2016), and Drosophilidae (Gao et al., 2019), and are considered to have a mechanosensory function.

Odorant receptor neurons housed in the olfactory sensilla with multiple walls pores on the antennae are the first relay center between external odor stimuli and second-order neurons in the brain where the information is further processed (Wang et al., 2003; Wilson, 2004; de Bruyne and Baker, 2008). ORNs can be divided into distinct functional classes based on their odorant response spectra (de Bruyne et al., 2001; Yao, 2005; Soni et al., 2019). In this study, first, we evaluated the olfactory neuron responses in the subtype of SBI on the antennae of female and male *E. corollae* to ten floral scent compounds by SSR. We identified three ORNs housed within a subtype of SBI based on the different spike amplitudes, corresponding to the numbers of neuronal dendrites observed under TEM (**Figure 3B**). Our results showed that neuron B in the subtype of SBI is mainly responsible for detecting floral scent compounds, especially aromatic compounds. Similar findings in other species were reported in terms of the response of ORNs in the sensilla basiconica to aromatics. For example, in model insect *D. melanogaster*, sensilla basiconica usually houses two to four neurons, in which ab1D responded with a high degree of specificity to methyl salicylate (de Bruyne et al., 2001). In *Anoplophora glabripennis* (Coleoptera: Cerambycidae), ORNs in blunt-tipped sensilla basiconica were responsive to eugenol and some terpenoids (Wei et al., 2018). Moreover, the action potentials of ORNs lead to the activation of the second-order neurons in the brain to produce behavioral changes (Wei et al., 2018). A recent study showed that an odorant receptor EcorOR25 was narrowly tuned to aromatic compounds, particularly eugenol and methyl eugenol, which can strongly attract *E. corollae* adults of both sexes (Li et al., 2020). However, whether EcorOR25 is expressed in the ORNs of subtype of SBI or other sensilla remains unknown because not all types of SB were recorded due to the dense sensilla and microtrichiae

growing on the antenna. Hence, the receptor-to-neuron map of the olfactory sensilla in the peripheral nervous system of the *E. corollae* antenna is required for further studies.

CONCLUSION

In conclusion, ten types of sensilla on the antennae of male and female *E. corollae* were identified based on morphology, and the fine structure was characterized using SEM and TEM techniques. Our study also indicates that neuron B in the SBI primarily responds to aromatic compounds. These results provide a basis for functional studies of the ORNs in *E. corollae*. The detailed ultrastructural descriptions of antennal sensilla may provide critical data for taxonomic and phylogenetic studies of Diptera.

DATA AVAILABILITY STATEMENT

The original contributions presented in the study are included in the article/**Supplementary Material**, further inquiries can be directed to the corresponding author/s.

AUTHOR CONTRIBUTIONS

W-YD, BW, and G-RW designed the experiments, wrote, and revised the manuscript. W-YD and BW performed the experiments and analyzed the data. BW and G-RW contributed reagents and materials. All authors contributed to the article and approved the submitted version.

FUNDING

This study was supported by the Key Project of Inter-Government International Science and Technology Innovation Cooperation (grant no. 2019YFE0105800) and Shenzhen Science and Technology Program (grant no. KQTD20180411143628272).

SUPPLEMENTARY MATERIAL

The Supplementary Material for this article can be found online at: https://www.frontiersin.org/articles/10.3389/fnana.2021.791900/full#supplementary-material

REFERENCES

Arzuffi, R., Robledo, N., and Valdez, J. (2008). Antennal sensilla of *Toxotrypana curvicauda* (Diptera: Tephritidae). *Fla. Entomol.* 91, 669–673. doi: 10.1653/0015-4040-91.4.669

Baldock, K. C. R., Goddard, M. A., Hicks, D. M., Kunin, W. E., Mitschunas, N., Morse, H., et al. (2019). A systems approach reveals urban pollinator hotspots and conservation opportunities. *Nat. Ecol. Evol.* 3, 363–373. doi: 10.1038/s41559-018-0769-y

Bates, A. S., Schlegel, P., Roberts, R., Drummond, N., Tamimi, I., Turnbull, R., et al. (2020). Complete connectomic reconstruction of olfactory projection neurons in the fly brain. *Curr. Biol.* 30, 3183.e–3199.e. doi: 10.1016/j.cub.2020.06.042

Been, T. H., Schomaker, C. H., and Thomas, G. (1988). Olfactory sensilla on the antenna and maxillary palp of the sheep head fly, *Hydrotaea irritans* (Fallen) (Diptera: Muscidae). *Int. J. Insect Morphol. Embryol.* 17, 121–133. doi: 10.1016/0020-7322(88)90006-2

Benelli, G., Canale, A., Romano, D., Flamini, G., Tavarini, S., Martini, A., et al. (2017). Flower scent bouquet variation and bee pollinator visits in *Stevia rebaudiana* Bertoni (Asteraceae), a source of natural sweeteners. *Arthropod Plant Inte.* 11, 381–388. doi: 10.1007/s11829-016-9488-y

Bisotto-De-Oliveira, R., Redaelli, L. R., and Sant'Ana, J. (2011). Morphometry and distribution of sensilla on the antennae of *Anastrepha fraterculus* (Wiedemann) (Diptera: Tephritidae). *Neotrop. Entomol.* 40, 212–216. doi: 10.1590/s1519-566x2011000200009

Braunschmid, H., Mükisch, B., Rupp, T., Schäffler, I., Zito, P., Birtele, D., et al. (2017). Interpopulation variation in pollinators and floral scent of the lady's-slipper orchid *Cypripedium calceolus* L. *Arthropod Plant Inte.* 11, 363–379. doi: 10.1007/s11829-017-9512-x

Bruce, T. J. A., Wadhams, L. J., and Woodcock, C. M. (2005). Insect host location: a volatile situation. *Trends Plant Sci.* 10, 269–274. doi: 10.1016/j.tplants.2005.04.003

Chang, H., Liu, Y., Ai, D., Jiang, X., Dong, S., and Wang, G. (2017). A pheromone antagonist regulates optimal mating time in the moth *Helicoverpa armigera*. *Curr. Biol.* 27, 1610.e–1615.e. doi: 10.1016/j.cub.2017.04.035

Cui, W., Wang, B., Guo, M., Liu, Y., Jacquin-Joly, E., Yan, S., et al. (2018). A receptor-neuron correlate for the detection of attractive plant volatiles in *Helicoverpa assulta* (Lepidoptera: Noctuidae). *Insect Biochem. Mol.* 97, 31–39. doi: 10.1016/j.ibmb.2018.04.006

de Bruyne, M., and Baker, T. C. (2008). Odor detection in insects: volatile codes. *J. Chem. Ecol.* 34, 882–897. doi: 10.1007/s10886-008-9485-4

de Bruyne, M., Foster, K., and Carlson, J. R. (2001). Odor coding in the *Drosophila* antenna. *Neuron* 30, 537–552. doi: 10.1016/S0896-6273(01)00289-6

Dobson, H. E. M. (2006). "Relationship between floral fragrance composition and type of pollinator," in *Biology of Floral Scent*, eds N. Dudareva and E. Pichersky (Boca Raton, FL: CRC Press), 147–198.

Dötterl, S., and Vereecken, N. J. (2010). The chemical ecology and evolution of bee–flower interactions: a review and perspectives. *Can. J. Zool.* 88, 668–697. doi: 10.1139/Z10-031

Dunn, L., Lequerica, M., Reid, C. R., and Latty, T. (2020). Dual ecosystem services of syrphid flies (Diptera: Syrphidae): pollinators and biological control agents. *Pest Manag. Sci.* 76, 1973–1979. doi: 10.1002/ps.5807

Ervik, F., Tollsten, L., and Knudsen, J. T. (1999). Floral scent chemistry and pollination ecology in phytelephantoid palms (Arecaceae). *Plant Syst. Evol.* 217, 279–297. doi: 10.1007/BF00984371

Fleischer, J., Pregitzer, P., Breer, H., and Krieger, J. (2018). Access to the odor world: olfactory receptors and their role for signal transduction in insects. *Cell. Mol. Life Sci.* 75, 485–508. doi: 10.1007/s00018-017-2627-5

Gao, H., Lai, S., Zhai, Y., Lv, Z., Zheng, L., Yu, Y., et al. (2019). Comparison of the antennal sensilla and compound eye sensilla in four *Drosophila* (Diptera: Drosophilidae) species. *Fla. Entomol.* 102, 747–754. doi: 10.1653/024.102.0412

Ghaninia, M., Olsson, S. B., and Hansson, B. S. (2014). Physiological organization and topographic mapping of the antennal olfactory sensory neurons in female hawkmoths, Manduca sexta. *Chem. Senses* 39, 655–671. doi: 10.1093/chemse/bju037

Hassan, M. I., Fouda, M. A., Hammad, K. M., Basiouny, A. L., and Kamel, M. R. (2013). The ultrastructure of sensilla associated with mouthparts and antennae of *Lucilia cuprina*. *J. Egypt. Soc. Parasitol.* 43, 777–785. doi: 10.12816/0006434

Henderson, D. E. H., and Wellington, W. G. (1982). Antennal sensilla of some aphidophagous Syrphidae (Diptera): fine structure and electroantennogramme study. *Can. J. Zool.* 60, 3172–3186. doi: 10.1139/z82-403

Honda, I., Ishikawa, Y., and Matsumoto, Y. (1983). Morphological studies on the antennal sensilla of the onion fly Hylemya *Antiqua* meigen (Diptera: Anthomyiidae). *Appl. Entomol. Zool.* 18, 170–181. doi: 10.1303/aez.18.170

Hore, G., Maity, A., Naskar, A., Ansar, W., Ghosh, S., Saha, G. K., et al. (2017). Scanning electron microscopic studies on antenna of *Hemipyrellia ligurriens* (Wiedemann, 1830) (Diptera: Calliphoridae)—A blow fly species of forensic importance. *Acta Trop.* 172, 20–28. doi: 10.1016/j.actatropica.2017.04.005

Hu, F., Zhang, G., Jia, F., Dou, W., and Wang, J. (2010). Morphological characterization and distribution of antennal sensilla of six fruit flies (Diptera: Tephritidae). *Ann. Entomol. Soc. Am.* 103, 661–670. doi: 10.1603/AN09170

Hunter, F. F., and Adserballe, C. F. (1996). Cuticular structures on the antennae of *Hypoderma bovis* De Geer (Diptera: Oestridae) females. *Int. J. Insect Morphol. Embryol.* 25, 173–181. doi: 10.1016/0020-7322(95)00013-5

Isaac, C., Ravaiano, S. V., Vicari Pascini, T., and Ferreira Martins, G. (2015). The antennal sensilla of species of the Palpalis group (Diptera: Glossinidae). *J. Med. Entomol.* 52, 614–621. doi: 10.1093/jme/tjv050

Jia, H., Sun, Y., Luo, S., and Wu, K. (2019). Characterization of antennal chemosensilla and associated odorant-binding as well as chemosensory proteins in the *Eupeodes corollae* (Diptera: Syrphidae). *J. Insect Physiol.* 113, 49–58. doi: 10.1016/j.jinsphys.2018.08.002

Keesey, I. W., Knaden, M., and Hansson, B. S. (2015). Olfactory specialization in *Drosophila* suzukii supports an ecological shift in host preference from rotten to fresh fruit. *J. Chem. Ecol.* 41, 121–128. doi: 10.1007/s10886-015-0544-3

Keil, T. (1999). "Morphology and development of the peripheral olfactory organs," in *Insect Olfaction*, ed. B. S. Hanson (New York, NY: Springer Press), 5–48.

Khallaf, M. A., Cui, R., Weissflog, J., Erdogmus, M., Svatos, A., Dweck, H., et al. (2021). Large-scale characterization of sex pheromone communication systems in *Drosophila*. *Nat. Commun.* 12:4165. doi: 10.1038/s41467-021-24395-z

Larson, B. M. H., Kevan, P. G., and Inouye, D. W. (2012). Flies and flowers: taxonomic diversity of anthophiles and pollinators. *Can. Entomol.* 133, 439–465. doi: 10.4039/Ent133439-4

Leal, W. S. (2013). Odorant reception in insects: roles of receptors, binding proteins, and degrading enzymes. *Annu. Rev. Entomol.* 58, 373–391. doi: 10.1146/annurev-ento-120811-153635

Lewis, C. T. (1971). Superficial sense organs of the anennae of the fly, *Stomoxys calcitrans*. *J. Insect Physiol.* 17, 449–461. doi: 10.1016/0022-1910(71)90024-2

Li, H., Liu, W., Yang, L., Cao, H., Pelosi, P., Wang, G., et al. (2020). Aromatic volatiles and odorant receptor 25 mediate attraction of *Eupeodes corollae* to flowers. *J. Agric. Food Chem.* 68, 12212–12220. doi: 10.1021/acs.jafc.0c03854

Liu, S., Chang, H., Liu, W., Cui, W., Liu, Y., Wang, Y., et al. (2020). Essential role for SNMP1 in detection of sex pheromones in *Helicoverpa armigera*. *Insect Biochem. Mol.* 127:103485. doi: 10.1016/j.ibmb.2020.103485

Liu, X., Luo, Y., Cao, C., and Zong, S. (2012). Scanning electron microscopy of antennal sensible of *Anoplistes halodendri* halodendri and *Anoplistes halodendri* ephippium (Coleoptera: Cerambycidae). *Microsc. Res. Tech.* 75, 367–373. doi: 10.1002/jemt.21065

Liu, X. H., Li, X. Y., Li, K., and Zhang, D. (2015). Ultrastructure of antennal sensory organs of horse nasal-myiasis fly, *Rhinoestrus purpureus* (Diptera: Oestridae). *Parasitol. Res.* 114, 2527–2533. doi: 10.1007/s00436-015-4453-8

Liu, X. H., Liu, J. J., Li, X. Y., and Zhang, D. (2016). Antennal sensory organs of *Scathophaga stercoraria* (Linnaeus, 1758) (Diptera: Scathophagidae): ultramorphology and phylogenetic implications. *Zootaxa* 4067, 361–372.

Liu, Y., He, J., Zhang, R., and Chen, L. (2020). Sensilla on antenna and maxillary palp of *Neoceratitis asiatica* (Diptera: Tephritidae). *Micron* 138:102921. doi: 10.1016/j.micron.2020.102921

Mansourian, S., Enjin, A., Jirle, E. V., Ramesh, V., Rehermann, G., Becher, P. G., et al. (2018). Wild African *Drosophila* melanogaster are seasonal specialists on marula fruit. *Curr. Biol.* 28, 3960.e–3968.e. doi: 10.1016/j.cub.2018.10.033

Oh, H. W., Jeong, S. A., Kim, J., and Park, K. C. (2019). Morphological and functional heterogeneity in olfactory perception between antennae and maxillary palps in the pumpkin fruit fly, Bactrocera depressa. *Arch. Insect Biochem. Physiol.* 101:e21560. doi: 10.1002/arch.21560

Pekas, A., De Craecker, I., Boonen, S., Wäckers, F. L., and Moerkens, R. (2020). One stone; two birds: concurrent pest control and pollination services provided by aphidophagous hoverflies. *Biol. Control.* 149:104328. doi: 10.1016/j.biocontrol.2020.104328

Pezzi, M., Whitmore, D., Chicca, M., Semeraro, B., Brighi, F., and Leis, M. (2016). Ultrastructural morphology of the antenna and maxillary palp of *Sarcophaga tibialis* (Diptera: Sarcophagidae). *J. Med. Entomol.* 53, 807–814. doi: 10.1093/jme/tjw061

Prieto-Godino, L. L., Rytz, R., Bargeton, B., Abuin, L., Arguello, J. R., Peraro, M. D., et al. (2016). Olfactory receptor pseudo-pseudogenes. *Nature* 539, 93–97. doi: 10.1038/nature19824

Prieto-Godino, L. L., Rytz, R., Cruchet, S., Bargeton, B., Abuin, L., Silbering, A. F., et al. (2017). Evolution of acid-sensing olfactory circuits in *Drosophilids*. *Neuron* 93, 661.e–676.e. doi: 10.1016/j.neuron.2016.12.024

Primante, C., and Dötterl, S. (2010). A syrphid fly uses olfactory cues to find a non-yellow flower. *J. Chem. Ecol.* 36, 1207–1210. doi: 10.1007/s10886-010-9871-6

Rader, R., Cunningham, S. A., Howlett, B. G., and Inouye, D. W. (2020). Non-bee insects as visitors and pollinators of crops: biology, ecology, and management. *Annu. Rev. Entomol.* 65, 391–407. doi: 10.1146/annurev-ento-011019-025055

Renou, M., and Anton, S. (2020). Insect olfactory communication in a complex and changing world. *Curr. Opin. Insect Sci.* 42, 1–7. doi: 10.1016/j.cois.2020.04.004

Ross, K. T. A. (1992). Comparative study of the antennal sensilla of five species of root maggots: delia radicum L., D. floralis F., D. antiqua Mg., D. platura MG. (Diptera: Anthomyiidae) and Psila rosae F. (Diptera: Psilidae). *Int. J. Insect Morphol. Embryol.* 21, 175–197. doi: 10.1016/0020-7322(92)90015-f

Ruchty, M., Roces, F., and Kleineidam, C. J. (2010). Detection of minute temperature transients by thermosensitive neurons in ants. *J. Neurophysiol.* 104, 1249–1256. doi: 10.1152/jn.00390.2010

Schneider, E. S., Kleineidam, C. J., Leitinger, G., and Römer, H. (2018). Ultrastructure and electrophysiology of thermosensitive sensilla coeloconica in a tropical katydid of the genus Mecopoda (Orthoptera, Tettigoniidae). *Arthropod Struct. Dev.* 47, 482–497. doi: 10.1016/j.asd.2018.08.002

Setzu, M. D., Poddighe, S., and Angioy, A. M. (2011). Sensilla on the antennal funiculus of the blow fly, *Protophormia terraenovae* (Diptera: Calliphoridae). *Micron* 42, 471–477. doi: 10.1016/j.micron.2011.01.005

Shanbhag, S. R., Müller, B., and Steinbrecht, R. A. (1999). Atlas of olfactory organs of *Drosophila melanogaster*: 1. types, external organization, innervation and distribution of olfactory sensilla. *Int. J. Insect Morphol. Embryol.* 28, 377–397. doi: 10.1016/S0020-7322(99)00039-2

Shanbhag, S. R., Singh, K., and Singh, R. N. (1995). Fine structure and primary sensory projections of sensilla located in the sacculus of the antenna of *Drosophila melanogaster*. *Cell Tissue Res.* 282, 237–249. doi: 10.1007/BF00319115

Shields, V. D. C., and Hildebrand, J. G. (1999). Fine structure of antennal sensilla of the female sphinx moth, *Manduca sexta* (Lepidoptera: Sphingidae). II. Auriculate, coeloconic, and styliform complex sensilla. *Can. J. Zool.* 77, 302–313. doi: 10.1139/z99-003

Silva, I. M., Pereira, K. S., Spranghers, T., Zanuncio, J. C., and Serrao, J. E. (2016). Antennal sensilla and sexual dimorphism of the parasitoid *Trichospilus pupivorus* (Hymenoptera: Eulophidae). *Microsc. Microanal.* 22, 913–921. doi: 10.1017/S1431927616011314

Skevington, J. H., and Dang, P. T. (2002). Exploring the diversity of flies (Diptera). *Biodiversity* 3, 3–27. doi: 10.1080/14888386.2002.9712613

Smallegange, R. C., Kelling, F. J., and Otter, C. J. D. (2008). Types and numbers of sensilla on antennae and maxillary palps of small and large houseflies, *Musca domestica* (Diptera, Muscidae). *Microsc. Res. Tech.* 71, 880–886. doi: 10.1002/jemt.20636

Solís-Montero, L., Caceres-Garcia, S., Alavez-Rosas, D., Garcia-Crisostomo, J. F., Vega-Polanco, M., Grajales-Conesa, J., et al. (2018). Pollinator preferences for floral volatiles emitted by dimorphic anthers of a buzz-pollinated herb. *J. Chem. Ecol.* 44, 1058–1067. doi: 10.1007/s10886-018-1014-5

Soni, N., Chahda, J. S., and Carlson, J. R. (2019). Odor coding in the antenna of the tsetse fly *Glossina morsitans*. *Proc. Natl. Acad. Sci. U.S.A.* 116, 14300–14308. doi: 10.1073/pnas.1907075116

Steinbrecht, R. A. (1997). Pore structures in insect olfactory sensilla: a review of data and concepts. *Int. J. Insect Morphol. Embryol.* 26, 229–245. doi: 10.1016/S0020-7322(97)00024-X

Sukontason, K., Sukontason, K. L., Piangjai, S., Boonchu, N., Chaiwong, T., Ngern-Klun, R., et al. (2004). Antennal sensilla of some forensically important flies in families calliphoridae, sarcophagidae and muscidae. *Micron* 35, 671–679. doi: 10.1016/j.micron.2004.05.005

Tangtrakulwanich, K., Chen, H., Baxendale, F., Brewer, G., and Zhu, J. J. (2011). Characterization of olfactory sensilla of *Stomoxys calcitrans* and electrophysiological responses to odorant compounds associated with hosts and oviposition media. *Med. Vet. Entomol.* 25, 327–336. doi: 10.1111/j.1365-2915.2011.00946.x

Venkatesh, S., and Singh, R. N. (1984). Sensilla on the third antennal segment of *Drosophila melanogaster* meigen (Diptera: Drosophilidae). *Int. J. Insect Morphol. Embryol.* 13, 51–63. doi: 10.1016/0020-7322(84)90032-1

Wang, B., Liu, Y., He, K., and Wang, G. (2016). Comparison of research methods for functional characterization of insect olfactory receptors. *Sci. Rep.* 6:32806. doi: 10.1038/srep32806

Wang, J. W., Wong, A. M., Flores, J., Vosshall, L. B., and Axel, R. (2003). Two-photon calcium imaging reveals an odor-evoked map of activity in the fly brain. *Cell* 112, 271–282. doi: 10.1016/s0092-8674(03)00004-7

Wang, Q., Zhang, M., Li, K., and Zhang, D. (2012). Olfactory sensilla on antennae and maxillary palps of *Fannia hirticeps* (Stein, 1892) (Diptera: Fanniidae). *Microsc. Res. Tech.* 75, 1313–1320. doi: 10.1002/jemt.22066

Wei, J., Zhou, Q., Hall, L., Myrick, A., Hoover, K., Shields, K., et al. (2018). Olfactory sensory neurons of the Asian longhorned beetle, *Anoplophora glabripennis*, specifically responsive to its two aggregation-sex pheromone components. *J. Chem. Ecol.* 44, 637–649. doi: 10.1007/s10886-018-0978-5

Wilson, R. I. (2004). Transformation of olfactory representations in the Drosophila antennal lobe. *Science* 303, 366–370. doi: 10.1126/science.1090782

Wilson, R. I. (2013). Early olfactory processing in *Drosophila*: mechanisms and principles. *Annu. Rev. Neurosci.* 36, 217–241. doi: 10.1146/annurev-neuro-062111-150533

Wotton, K. R., Gao, B., Menz, M. H. M., Morris, R. K. A., Ball, S. G., Lim, K. S., et al. (2019). Mass seasonal migrations of hoverflies provide extensive pollination and crop protection services. *Curr. Biol.* 29, 2167.e–2173.e. doi: 10.1016/j.cub.2019.05.036

Xi, Y. Q., Yin, X. M., Zhu, C. D., Guerrieri, E., and Zhang, Y. Z. (2011). Scanning electron microscopy studies of antennal sensilla of *Ooencyrtus phongi* (Hymenoptera: Encyrtidae). *Microsc. Res. Tech.* 74, 936–945. doi: 10.1002/jemt.20979

Yao, C. A. (2005). Chemosensory coding by neurons in the coeloconic sensilla of the *Drosophila* antenna. *J. Neurosci.* 25, 8359–8367. doi: 10.1523/JNEUROSCI.2432-05.2005

Zhang, D., Li, X., Liu, X., Wang, Q., and Pape, T. (2016). The antenna of horse stomach bot flies: morphology and phylogenetic implications (Oestridae, Gasterophilinae: Gasterophilus Leach). *Sci. Rep* 6:34409. doi: 10.1038/srep34409

Zhang, D., Liu, X. H., Li, X. Y., Zhang, M., and Li, K. (2013b). Antennal sensilla of the green bottle fly, *Lucilia sericata* (Meigen) (Diptera: Calliphoridae). *Parasitol. Res.* 112, 3843–3850. doi: 10.1007/s00436-013-3573-2

Zhang, D., Liu, X. H., Wang, Q. K., and Li, K. (2014). Sensilla on the antenna of blow fly, *Triceratopyga calliphoroides* Rohdendorf (Diptera: Calliphoridae). *Parasitol. Res.* 113, 2577–2586. doi: 10.1007/s00436-014-3909-6

Zhang, D., Wang, Q., Hu, D., and Li, K. (2012b). Cuticular structures on antennae of the bot fly, *Portschinskia magnifica* (Diptera: Oestridae). *Parasitol. Res.* 111, 1651–1659. doi: 10.1007/s00436-012-3004-9

Zhang, D., Wang, Q. K., Hu, D. F., and Li, K. (2012a). Sensilla on the antennal funiculus of the horse stomach bot fly, *Gasterophilus nigricornis*. *Med. Vet. Entomol.* 26, 314–322. doi: 10.1111/j.1365-2915.2011.01007.x

Zhang, D., Wang, Q. K., Yang, Y. Z., Chen, Y. O., and Li, K. (2013a). Sensory organs of the antenna of two *Fannia* species (Diptera: Fanniidae). *Parasitol. Res.* 112, 2177–2185. doi: 10.1007/s00436-013-3377-4

Zhu, J., and Park, K. (2005). Methyl Salicylate, a soybean aphid-induced plant volatile attractive to the predator *Coccinella septempunctata*. *J. Chem. Ecol.* 31, 1733–1746. doi: 10.1007/s10886-005-5923-8

Zito, P., Rosselli, S., Bruno, M., Maggio, A., and Sajeva, M. (2019). Floral scent in *Iris planifolia* (Iridaceae) suggests food reward. *Phytochemistry* 158, 86–90. doi: 10.1016/j.phytochem.2018.11.011

Conflict of Interest: The authors declare that the research was conducted in the absence of any commercial or financial relationships that could be construed as a potential conflict of interest.

Publisher's Note: All claims expressed in this article are solely those of the authors and do not necessarily represent those of their affiliated organizations, or those of the publisher, the editors and the reviewers. Any product that may be evaluated in this article, or claim that may be made by its manufacturer, is not guaranteed or endorsed by the publisher.

Copyright © 2021 Dong, Wang and Wang. This is an open-access article distributed under the terms of the Creative Commons Attribution License (CC BY). The use, distribution or reproduction in other forums is permitted, provided the original author(s) and the copyright owner(s) are credited and that the original publication in this journal is cited, in accordance with accepted academic practice. No use, distribution or reproduction is permitted which does not comply with these terms.

frontiers in Ecology and Evolution

ORIGINAL RESEARCH
published: 08 February 2022
doi: 10.3389/fevo.2022.823119

Genome-Wide Identification of Aldehyde Oxidase Genes in Moths and Butterflies Suggests New Insights Into Their Function as Odorant-Degrading Enzymes

*Ricardo Godoy[1,2,3], Ana Mutis[2,3], Leonela Carabajal Paladino[4] and Herbert Venthur[2,3]**

[1] Programa de Doctorado en Ciencias de Recursos Naturales, Universidad de La Frontera, Temuco, Chile, [2] Centro de Investigación Biotecnológica Aplicada al Medio Ambiente (CIBAMA), Universidad de La Frontera, Temuco, Chile, [3] Laboratorio de Química Ecológica, Departamento de Ciencias Químicas y Recursos Naturales, Facultad de Ingeniería y Ciencias, Universidad de La Frontera, Temuco, Chile, [4] The Pirbright Institute, Surrey, United Kingdom

OPEN ACCESS

Edited by:
Xin-Cheng Zhao, Henan Agricultural University, China

Reviewed by:
Peng He, Guizhou University, China
Bing Wang, Institute of Plant Protection, Chinese Academy of Agricultural Sciences (CAAS), China

***Correspondence:**
Herbert Venthur
herbert.venthur@ufrontera.cl

Specialty section:
This article was submitted to Chemical Ecology, a section of the journal Frontiers in Ecology and Evolution

Received: *26 November 2021*
Accepted: *14 January 2022*
Published: *08 February 2022*

Citation:
Godoy R, Mutis A, Carabajal Paladino L and Venthur H (2022) Genome-Wide Identification of Aldehyde Oxidase Genes in Moths and Butterflies Suggests New Insights Into Their Function as Odorant-Degrading Enzymes. Front. Ecol. Evol. 10:823119. doi: 10.3389/fevo.2022.823119

Aldehyde oxidases (AOXs) are common detoxifying enzymes in several organisms. In insects, AOXs act in xenobiotic metabolism and as odorant-degrading enzymes (ODEs). These last appear as crucial enzymes in the life cycle of insects, helping to reset their olfactory system, particularly in lepidopterans, which fulfill important ecological roles (e.g., pollination or destructive life cycles). A comprehensive understanding of their olfactory system has provided opportunities to study key chemosensory proteins. However, no significant advance has been made around lepidopteran AOXs research, and even less around butterflies, a recently evolved lineage. In this study we have identified novel AOX gene families in moths and butterflies in order to understand their role as ODEs. Eighteen genomes from both moths and butterflies were used for phylogenetics, molecular evolution and sequence analyses. We identified 164 AOXs, from which 91 are new. Their phylogeny showed two main clades that are potentially related to odorant-degrading function, where both moths and butterflies have AOXs. A first ODE-related clade seems to have a non-ditrysian origin, likely related to plant volatiles. A second ODE-related clade could be more pheromone-biased. Molecular evolution analysis suggests a slight purifying selection process, though a number of sites appeared under positive selection. ODE-related AOXs have changed a phenylalanine residue by proline in the active site. Finally, this study could serve as a reference for further evolutionary and functional studies around Lepidopteran AOXs.

Keywords: Lepidoptera, insect olfaction, aldehyde oxidase, genome, phylogenetics

INTRODUCTION

The study of gene evolution in insects has provided outstanding advances in the understanding of evolutionary processes, such as expansion or contraction of gene families (Li et al., 2019). Particularly, lepidopterans represent an extraordinary target due to a clear diversification into moth and butterflies lineages (Kawahara et al., 2019). Thus, the impact of gene evolution can be seen

even within moths. For instance, regulation of desaturase genes in two sibling *Helicoverpa* species (i.e., *H. armigera* and *H. assulta*) results in reproductive isolation (Li et al., 2015). Nowadays, the enormous amount of genomic and transcriptomic datasets for insects has provided an opportunity to elucidate novel genes and their evolutionary relationships (Oppenheim et al., 2015), something that can support our understanding of ecological aspects of insects, such as behavior. For many insect species, behavior is mainly driven by olfaction. Olfaction is primarily processed by insect antennae and their small hair-like structures called sensilla, in which a set of proteins work synergistically to maintain an extremely sensitive and dynamic system (Hansson and Stensmyr, 2011; Leal, 2013; He et al., 2019). For instance, odorant-binding proteins (OBPs) and chemosensory proteins (CSPs) function as transporters that carry odorants across the sensillar lymph (Zhou, 2010; Leal, 2013). These odorants reach an heteromeric complex of receptors, such as odorant receptors (ORs), an odorant receptor co-receptor (Orco) and a sensory neuron membrane protein (SNMP), as recently reported (Zhang et al., 2020), to unleash depolarization in olfactory neuron membranes that triggers a behavioral response (Kaissling, 2013). Along with these olfactory proteins, odorant-degrading enzymes (ODEs), such as carboxylesterases (CXEs), glutathione-S-transferases (GSTs) and aldehyde oxidases (AOXs), are responsible for resetting the insect olfactory system through the degradation of odorant molecules (Chertemps and Meïbèche, 2021; Godoy et al., 2021).

Among ODEs, CXEs and GSTs have received particular attention due to their role in sex pheromone degradation in moths. For example, CXEs have been reported to degrade ester-type molecules (e.g., sex pheromones and plant volatiles) in moths *Plodia interpunctella*, *Spodoptera exigua*, *Grapholita molesta*, *Plutella xylostella,* and *Athetis lepigone* (He et al., 2014a,b,c, 2015; Zhang et al., 2017a; Liu et al., 2019; Wei et al., 2020; Wang et al., 2021a). Likewise, GSTs have been well characterized in terms of function, being the delta class likely related to odorant degrading functions (Durand et al., 2018). This is supported by the reported degrading function of *G. molesta* GST (GmolGSTd1) (Li et al., 2018) and *Cydia pomonella* GST (CpomGSTd2) (Huang et al., 2017). The AOXs, on the other hand, have received less attention so far. However, some species that use aldehydes as semiochemicals (i.e., chemicals that mediate communication between two organisms), have been studied, such as *Manduca sexta*, *Bombyx mori*, *Antheraea polyphemus*, *Amyelois transitella,* and *H. armigera*, among others (Riddiford, 1967; Kasang et al., 1978; Coffelt et al., 1979; Zhang et al., 2012). Particularly, AOXs catalyze the oxidation of aldehydes to carboxylic acids (Garattini et al., 2009; Garattini and Terao, 2012). In that sense, a few studies have functionally evaluated that process against aldehyde-based semiochemicals: an early study in *M. sexta* AOX reports that it catalyzes (*E*,*Z*)-10,12-hexadecadienal (bombykal) (Rybczynski et al., 1989), and more recently, *A. transitella* AOX2 (AtraAOX2) was reported to hydrolyze plant volatiles (e.g., propanal, hexanal, and heptanal) as well as a sex pheromone component (*Z*,*Z*)-11,13-hexadecadienal (Choo et al., 2013). Further evidence in terms of enzymatic activity of AOXs is still lacking. Nevertheless, important aspects of their function and structural features are underpinned by xanthine dehydrogenases (XDHs), an enzyme that catalyzes the oxidation of purines, pterin and aldehydes (Wang et al., 2016).

Among insects, lepidopterans have attracted special attention due to their establishment as crop pests, some with worldwide distribution. It is known that moths rely heavily on the sense of smell (Weiss, 2001), developing long distance attraction based on volatile chemicals (e.g., sex pheromones) (Chemnitz et al., 2015). In fact, hundreds of these volatiles have been identified since the first one reported for *B. mori*, the sex pheromone (*E*,*Z*)-10,12-hexadecadien-1-ol (bombykol) (Butenandt et al., 1959). On the contrary, butterflies rely heavily on visual cues and short-range chemical communication, understood as a multi-sensory integration (Costanzo and Monteiro, 2007), and hence have received less attention in terms of olfaction. Moreover, butterflies represent an interesting group for comparative studies considering their transition from moths approximately 98 Mya (million years ago) (Kawahara et al., 2019). Thus, it is believed that comparing AOXs between moths and butterflies might deepen our understanding of their odorant-degrading function.

Considering the difference in olfactory integration during the life cycle of moths and butterflies, we hypothesize that there is a specific clade of AOXs for both moths and butterflies that could be related to odorant-degrading function as well as both moth- and butterfly-specific gene expansions. Therefore, the objective of this study was to identify novel AOX genes from moths and butterflies using genomic and transcriptomic data and analyze them in terms of gene location, phylogeny, evolutionary processes, and structure.

MATERIALS AND METHODS

Data Collection

Publicly available genomic data were retrieved from NCBI Genome database[1] and InsectBase[2] for major lepidopteran families, such as Bombycidae, Sphingidae, Noctuidae, Pyralidae, Crambidae, and Plutellidae for moths, whereas Nymphalidae, Pieridae and Papilionidae were used for butterflies (**Table 1**). Each fully represented genome assembly with Reference Sequence (RefSeq) was downloaded from NCBI Assembly database at either contig, scaffold or chromosome level (**Supplementary Table 1**).

Identification of Aldehyde Oxidase Family

Bioinformatics pipeline BITACORA (Vizueta et al., 2020) was used to identify already annotated AOX genes and potentially novel related genes from both moth and butterfly genomes. A database for AOX gene family was built using reported protein sequences for lepidopterans (Rybczynski et al., 1989; Merlin et al., 2005; Pelletier et al., 2007; Choo et al., 2013; Ou et al., 2014; Zhang et al., 2014, 2017b; Yang et al., 2015; Huang et al., 2016; He et al., 2017; Xu and Liao, 2017; Wang et al., 2021b).

[1] https://www.ncbi.nlm.nih.gov/assembly

[2] http://www.insect-genome.com/

TABLE 1 | Summary of identified aldehyde oxidase genes in moths and butterflies.

Species	AOX gene annotation[a,b]				
	Total	Novel	Complete CDS	Average length (aa)	Gene annotation[c]
Moths					
B. mandarina	7	6	7	1,272	1
B. mori	9	6	9	1,266	3
M. sexta	19	16	16	1,194	3
H. armigera	8	2	8	1,335	6
S. frugiperda	20	17	19	1,259	3
O. furnacalis	8	2	8	1,298	6
P. xylostella	6	3	5	1,271	3
A. transitella	6	3	6	1,349	3
T. ni	14	3	11	1,209	11
Butterflies					
H. melpomene	2	2	2	2,523	0
P. rapae	6	2	6	1,301	4
B. anynana	11	4	10	1,282	7
D. plexippus	10	10	7	1,215	0
V. tameamea	6	5	5	1,243	1
P. aegeria	9	6	8	1,327	3
P. polytes	6	0	6	1,231	6
P. xuthus	7	4	7	1,265	4
P. machaon	7	0	6	1,281	7

[a] *Complete gene annotation available in* ***Supplementary Table 1****.*
[b] *A complete annotation table can be found in* ***Supplementary Table 1****.*
[c] *Based on Interpro, NCBI Gene database and literature searches.*
aa, aminoacids.

To identify family and structural domains for AOXs, InterPro server was used[3]. The identified profile was used to search for HMM profile in PFAM database[4] (PF01315; ID Ald_Xan_dh_C). This process increased the likelihood of identifying sequences encoding members of the AOX gene family. Further processing included the trimming of isoforms (98% cutoff) using a provided script in BITACORA pipeline. Subsequently, BLAST searches were run with the identified proteins for manual annotation. Protein domain finder CDvist[5] (Adebali et al., 2015) was used to identify conserved domains of AOXs, namely two (2Fe-2S), one flavin-containing region (FAD-binding domain) and one molybdenum cofactor/substrate-binding domain. All proteins identified in this study are provided in **Supplementary Table 1**.

Sequence Analysis and Genome Structure

The genomic organization of identified AOX genes from both moth and butterfly species that use aldehyde-based semiochemicals was analyzed based on Vogt et al. (2015) and Xu and Liao (2017) including some modifications. Moths *Bombyx mandarina*, *P. xylostella*, and *A. transitella*, and butterflies *Heliconius melpomene* and *Bicyclus anynana*, were selected for this task. Annotated gene features (in GFF3 format) were retrieved from the gene identification protocol based on the BITACORA pipeline and analyzed manually. Thus, species name as well as source, start, end, strand and attributes were used for each AOX gene. Finally, gene localization was prepared in image editor Inkscape 0.48 software.

Data Preprocessing and Transcriptome Assembly

To both take advantage of transcriptomic data and include Tortricidae and Eriocraniidae families, we retrieved antennal RNA-seq data for moth *Lobesia botrana* (data from our laboratory) and non-ditrysian moth *Eriocrania semipurpurella* (SRR5328787). FASTQ files for both moths, one containing left-pair reads and other the right-pair reads, were used for assembly. Ribosomal RNA reads were removed by mapping the libraries using Bowtie2 v.2.3.3.1 (Langmead et al., 2009) against a custom rRNA database created from insect ribosomal sequences downloaded from NCBI[6], and keeping non-mapped reads using SAMtools v.1.6 (Li et al., 2009). Low-quality reads were removed based on their q-score composition using NGSQC Toolkit v.2.3 (Patel and Jain, 2012), and high-quality reads were concatenated to build *de novo* transcriptomes using Trinity v.2.6.5 (Grabherr et al., 2011) with a *P*-value of 0.05 and fold-change value of 2.

Phylogenetic Analysis

A phylogeny for the identified AOX genes in moths and butterflies, including XDHs and AOXs from mosquitoes, beetles and bees as outgroups, was built. Full-length amino acid sequences that include conserved domains were aligned using MAFFT server[7] (Katoh et al., 2019). GUIDANCE2 server[8] was used to check consistency of the multiple sequence alignment (Sela et al., 2015). Briefly, the consistency of the alignment was measured with a score less than 0.5, in which sequences were deleted. It is worth noting that confidence scores near 1 and 0, suggest a highly and poorly consistent alignment, respectively. Finally, phylogenetic analysis was performed using maximum-likelihood method with FastTree software (Price et al., 2010). To highlight clades, specific taxa and functional evidence, the phylogenetic tree was edited using FigTree software[9] and image editor Inkscape 0.48 software.

Molecular Evolution Analysis

In order to identify putative selective pressures on AOXs, a molecular evolution analysis was performed based on the methodologies reported by Engsontia et al. (2014) and Soffan et al. (2018). Two models were used through EasyCodeML software (Gao et al., 2019) to elucidate selective pressures acting on the evolutionary process of 93 lepidopteran AOX genes, 9 XDHs and 11 AOXs from other insect orders. First, site model was applied to detect positive selection for a set of 113 sequences (Yang et al., 2000). Additionally, a branch-site model

[3] http://www.ebi.ac.uk/interpro/
[4] http://pfam.xfam.org/
[5] http://cdvist.zhulinlab.org/
[6] https://www.ncbi.nlm.nih.gov/
[7] https://mafft.cbrc.jp/alignment/server/
[8] http://guidance.tau.ac.il/ver2/
[9] http://tree.bio.ed.ac.uk/software/figtree/

was applied to test the presence of amino acids that evolved under positive selection in a specific clade represented by 8 AOX sequences (most of them functionally studied). All the amino acid sequences were aligned by ClustalW[10], and converted to DNA alignment with PAL2NAL server[11]. A maximum likelihood tree was prepared using the DNA alignment by FastTree software under default parameters. Briefly, the software estimated the ratio of normalized non-synonymous (d_N) to synonymous (d_S) (e.g., d_N/d_S or ω) substitution rate *via* the maximum likelihood method. The ω value indicates the mode of evolution, where $\omega > 1$ suggests evidence of positive selection with amino acid replacement, whereas $\omega < 1$ refers to purifying selection, and $\omega = 0$ indicates neutral selection. The specific models (M0, M3, M1a, M2a, M7, M8, and M8a) used under the "site model" method are described in detail in previous reports (Yang et al., 2000; Yang and Nielsen, 2002; Swanson et al., 2003). For the branch-site model, the 8 AOX sequences were labeled in the phylogenetic tree as foreground branch with the remaining clades as background branches. The change in ω was evaluated for a set of sites in each foreground branch through an alternative model, whereas neutral evolution was evaluated through a null model. Likelihood ratio tests (LRTs) were used to compare both models and significant results were determined using χ^2-tests. Finally, Bayes Empirical Bayes (BEB) analysis was used when LRT was significant to identify positive selected sites (PSSs) within each amino acid sequence (Yang et al., 2005).

Sequence Analysis and Protein Structure Prediction

First, a multiple sequence alignment (MSA) was built with 7 AOX sequences also used in molecular evolution analyses, belonging to *A. transitella*, *B. mori*, *P. xylostella*, *H. armigera*, *Papilio xuthus*, *Papilio machaon,* and *B. anynana*, in which PSSs were identified and indicated (**Supplementary Table 1**). Sequences from *B. mandarina* AOX5 (BmanAOX5), *Drosophila melanogaster* AOX2 (DmelAOX2) and mammal AOXs, such as *Mus musculus* AOX2 (MmAOX2) and AOX3 (MmAOX3), and *Homo sapiens* AOX1 (HsAOX1), were also included. MSA was built in Multalin server[12] and ESPript 3.0[13] (Corpet, 1988). The amino acid sequence of AtraAOX2 and BanyAOX2 were submitted to BLASTp available on the NCBI website[14] for template selection. To optimize the structural information available for AOXs, a multiple template-based homology modeling approach was considered as it was reported to increase accuracy in predicted protein models (Sokkar et al., 2011). First, multiple structure alignments were generated by SALIGN command, which is implemented in Modeler 10.1. Five hundred models of each AOX were obtained using Modeler 10.1[15]. The best models were selected according to the lowest discrete optimized protein energy (DOPE) score provided by the software. The coordinates were analyzed *via* ProCheck[16] to check stereochemical quality. Lepidopteran AOXs were visualized through PyMOL software[17]. The 3D structure of mammal AOXs were retrieved from Protein Data Bank[18] and DmelAOX2 was downloaded from AlphaFold database[19].

RESULTS

Identification and Annotation of Aldehyde Oxidase Genes

Eighteen genome assemblies were retrieved from NCBI assembly database and InsectBase server. From those, 6 were assembled at chromosome level, whereas 11 at scaffold and 1 at contig level (**Supplementary Table 1**). The use of BITACORA pipeline resulted in a raw amount of 163 putative AOX genes for moths and 100 for butterflies. After homology searches through BLAST followed by conserved domain analyses, 99 AOX genes were left for moths and 65 for butterflies. The average amino acid length of AOXs is 1272 and 1407 for moths and butterflies, respectively. On the other hand, the moth species that showed a higher number of AOX were *Spodoptera frugiperda* with 20 sequences, *M. sexta* with 19 sequences and *Trichoplusia ni* with 14. In butterflies, *B. anynana* and *Danaus plexippus* showed 11 and 10 AOX sequences, respectively. The specific number of AOX genes for each species is summarized in **Table 1**. Overall, 58 novel AOX genes were identified for moths whereas 33 AOX genes were identified for butterflies. BLAST hits for most of the novel AOX genes were either AOXs from other lepidopteran species or XDHs from the same species. In that sense, 6 new AOXs were identified for *B. mandarina* and *B. mori*, 16 for *M. sexta*, 17 for *S. frugiperda* and 10 for *D. plexippus*, as the greater numbers found. No novel AOX genes were found for butterflies *Papilio polytes* and *P. machaon*. Although most of the lepidopteran species studied here have a few annotated AOX genes, several of them are not fully annotated nor studied in terms of function. It is worth noting that the amount and length of AOX genes might be dependent on genome sequencing and annotation quality, therefore, previous estimates should be taken into account with caution.

Phylogenetic Relationships and Gene Clusters Between Moths and Butterflies

Phylogenetic analysis (**Figure 1**) suggests the presence of 5 main clades, 2 being related to either antennae specificity or odorant degradation (clades A and B in **Figure 1**). A clear diversification from insect XDHs and non-lepidopteran AOXs is observable. A clade with putative odorant-degrading function (labeled as A in **Figure 1**) appears to be a group of AOX genes evolved in ditrysian species, having the non-ditrysian moth *E. semipurpurella* EsemAOX1 at the base of the clade. Here,

[10]https://www.ebi.ac.uk/Tools/msa/clustalo/

[11]http://www.bork.embl.de/pal2nal/

[12]http://multalin.toulouse.inra.fr/multalin/

[13]https://espript.ibcp.fr/ESPript/ESPript/

[14]https://blast.ncbi.nlm.nih.gov/Blast.cgi?PAGE=Proteins

[15]http://salilab.org/modeller

[16]https://saves.mbi.ucla.edu/

[17]https://pymol.org/2/

[18]https://www.rcsb.org/

[19]https://alphafold.ebi.ac.uk/

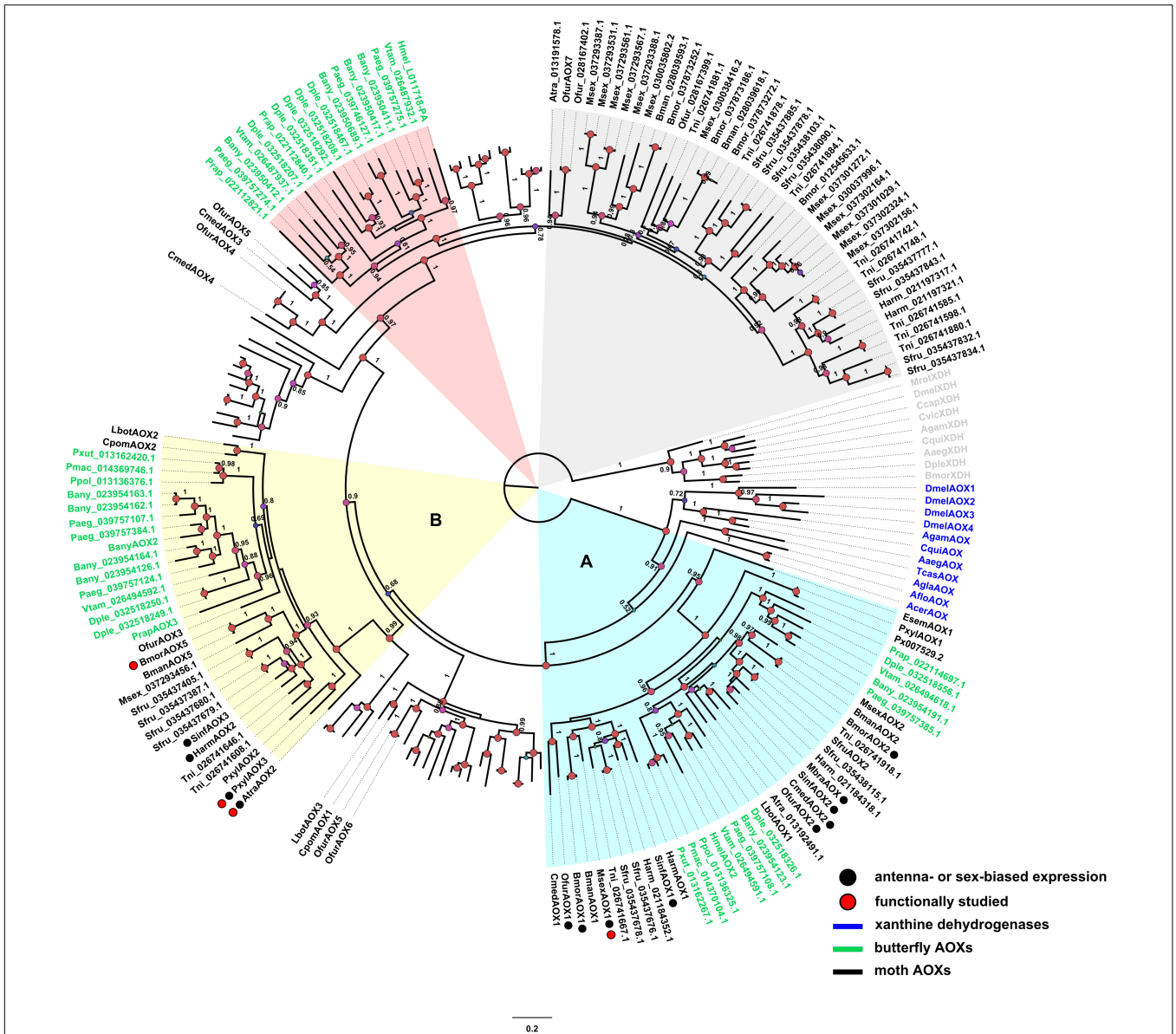

FIGURE 1 | Phylogenetic tree of AOXs identified from moth and butterfly genomes as well as some AOXs and XDHs from other insect species. Clades A (light blue) and B (yellow) are highlighted as lineage with putative ODE function and lineage with ODE function, respectively. Species in green correspond to butterflies, species in black are moths, and species in blue are AOX outgroups. The clade shaded in red color corresponds to butterfly specific AOXs with no ODE described function, and the clade shaded in gray correspond to moth specific AOXs with no ODE described function. Red circles next to the sequence name represent AOXs that have been functionally studied [MsexAOX1, (*E*,*Z*)-10,12-hexadecadienal; AtraAOX2, (*Z*,*Z*)-11,13-hexadecadienal; PxylAOX3, (*Z*)-11-hexadecenal; BmorAOX5, benzaldehyde, salicylaldehyde, vanillic aldehyde, propanal, and heptanal]. Black circles next to the sequence name indicate antennae- or sex-biased expression. Confidence scores are indicated as circles (> 70%) in nodes. All annotated genes and their amino acid sequences are in **Supplementary Table 1**.

9 moth AOX genes are reported to be enriched in antennae (**Figure 1**, species indicated with black circles next to their name), from which only *M. sexta* AOX1 (MsexAOX1) has been related to aldehyde-degrading function (Rybczynski et al., 1989). A secondary odorant degrading-related clade (labeled as B in **Figure 1**) seems to have evolved by gene duplication. This clade includes 5 moth AOX genes enriched in antennae (**Figure 1**, species indicated with black circles next to their name), and includes *A. transitella* (AtraAOX2), *P. xylostella* (PxylAOX3), and *B. mori* (BmorAOX5) which were functionally studied (Choo et al., 2013; Zhang et al., 2020; Wang et al., 2021b). Furthermore, butterfly- and moth-specific AOX lineages were identified (highlighted in red and gray, respectively, in **Figure 1**), but no reported odorant-degrading function was found for these.

Interestingly, butterflies that have aldehyde-related pheromones have AOXs present in at least one of the odorant-related clades (A or B). There are AOXs of some butterflies that are in these clades, but no aldehyde-related semiochemical

has been reported yet, such as those present in *D. plexippus*, *Pararge aegeria*, *Pieris rapae*, *P. polytes*, *P. xuthus*, *P. machaon,* and *Vanessa tameamea*. On the contrary, *H. melpomene*, that uses aldehyde-based semiochemicals, showed only 1 AOX (HmelAOX2) in clade A. Likewise, *B. anynana* (with hexadecanal as a pheromone component), has 2 AOXs in clade A, while 5 in clade B.

In terms of gene location, *B. mandarina*, *A. transitella* and *P. xylostella*, that use aldehydes as semiochemicals and have AOX genes related to ODE function, are far from other AOX genes, with the exception of PxylAOX3 (**Figure 2**). *H. melpomene* has 2 grouped AOX genes that suggest the same origin for both. Likewise, *B. anynana* has two big clusters of 4 and 7 AOX genes. Interestingly, from the bigger cluster of *B. anynana*, the 7 AOX genes were distributed in odorant-degrading clades A and B. Similarly, AOX1, AOX2 and AOX5 of *B. mandarina* that are grouped in a single cluster, are distributed in clades A and B. Besides HmelAOX2 present in clade A, gene HMEL011718-PA clustered with HmelAOX2, which appeared in the previously mentioned butterfly-specific clade (red clade in **Figure 1**).

Selective Pressures on Aldehyde Oxidase Genes

Positive selection was first evaluated for a set of 113 sequences that included XDHs and AOXs of not only butterflies and moths, but also beetles, mosquitoes, and flies (**Table 2**). The four models implemented (e.g., M3 vs. M0, M1a vs. M2a, M7 vs. M8 and M8a vs. M8) showed significant differences according to LRT analysis. Interestingly, a purifying selection was suggested as site model (M0) resulted in $\omega = 0.89$.

Additionally, a branch-site model was used to test selective pressures on specific sites (i.e., codons) among 8 closely related AOX sequences, including moths *A. transitella* AtraAOX2, *B. mori* BmorAOX5, *P. xylostella* PxylAOX3, *H. armigera* HarmAOX2 and *Sesamia inferens* SinfAOX3, and butterflies *B. anynana* BanyAOX2, *P. xuthus* PxutAOX2 and *P. machaon* PmacAOX2 (**Table 3**). As expected, most of the enzymes were found to be under positive selection at many sites. For instance, AtraAOX2 resulted in 23.5% of their amino acids as PSSs, from which 105 sites showed either $P < 0.01$ or $P < 0.001$. Similarly, 22.2% of residues in BmorAOX5, 11.9% in HarmAOX, and 11.2% in SinfAOX3 were PSSs, with more than 20 sites identified with $P < 0.001$. In terms of butterflies, BanyAOX2 resulted in PSSs distributed in 40% of the entire sequence. However, less PSSs resulted for PxutAOX2 and PmacAOX2, representing only a 2–3% of the amino acid sequence length.

Link Between Function, Primary Sequence, and Protein Structure

To complement our previous methods that included annotation, phylogeny and molecular evolution analyses, a MSA was built followed by AOX structure prediction. The MSA was based on

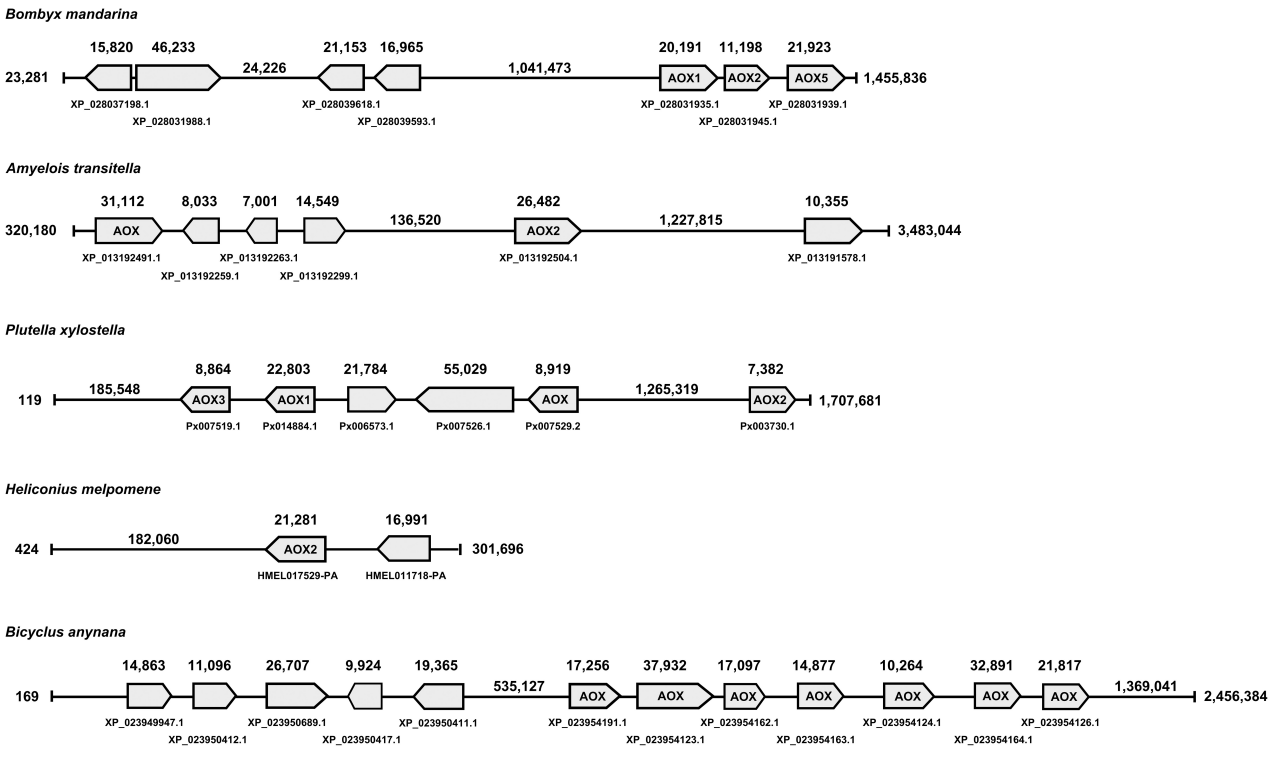

FIGURE 2 | Gene location analysis for AOXs identified from lepidopterans that use aldehydes as semiochemicals, such as moths *B. mandarina*, *A. transitella*, *P. xylostella* and butterflies *H. melpomene* and *B. anynana*.

TABLE 2 | Positive selection analysis using site model on 113 lepidopteran AOXs and XDHs sequences.

Model	np	LnL	Estimates of parameters	Models compared	LRT *p*-value
Site model					
M3	60	−10876.292891	p0: 0.46282; p1: 0.38177; p3: 0.15540; ω0: 0.24443; ω1: 1.46989; ω2: 4.81439	M3 vs. M0	0.00E + 0.00
M0	56	−11425.851842	ω: 0.89134		
M2a	59	−10882.888127	p0: 0.39310; p1: 0.41468; p2: 0.19222; ω1: 0.17566; ω2: 1.00000; ω3: 3.80060	M1a vs. M2a	0.00E + 0.00
M1a	57	−11050.821062	p0: 0.50743; p1: 0.49257; ω0: 0.15450; ω1: 1.00000		
M8	59	−10886.022772	p0: 0.78439; p: 0.53521; q: 0.46979 (p1: 0.21561); ω: 3.50001	M7 vs. M8	0.00E + 0.00
M7	57	−11067.720224	p: 0.50998; q: 0.38141		
M8a	58	−11036.136130	p0: 0.57595; p: 1.01933; q: 4.04743 (p1: 0.42405); ω: 1.00000	M8a vs. M8	0.00E + 0.00

the same 8 lepidopteran AOX sequences detailed above, as well as *B. mandarina* BmanAOX5, *D. melanogaster* DmelAOX2, and mammal AOXs *M. musculus* MmAOX2 and MmAOX3, and *H. sapiens* HsAOX1, which have been well characterized in terms of structural features and active sites.

As reference, the active site of MmAOX3 comprise Gln772, Glu1266, Lys889, Phe919 and Phe1014 (Terao et al., 2020). From those, Gln772 and Glu1266 at positions equivalent to 739 and 1209 in **Figure 3**, were found to be conserved between all AOXs (red triangles in **Figure 3**). Interestingly, Phe919 (in vertebrates) at position 884 (in Lepidoptera) in **Figure 3** was conserved among mammal AOXs, but replaced by Pro in all lepidopteran AOXs as well as DmelAOX2 (blue triangle in **Figure 3**). Lys889 (at position 855 in **Figure 3**) was also not conserved, with SinfAOX3, HarmAOX2, AtraAOX2, PmacAOX2, PxutAOX2 and PxylAOX3 having Gly, and BmorAOX5, BmanAOX5 and BanyAOX5 having Ser instead (purple triangle in **Figure 3**).

In terms of structure, we could predict the 3D arrangements for AtraAOX2 and BanyAOX2, which were used to corroborate the identified conserved residues at the active site (**Figure 4**). The active sites equivalent to MmAOX3 Gln772 and Glu1266 were identified in both Lepidoptera species as well as in DmelAOX2 and vertebrate HsAOX1. Differences in conformation were observed, which are found in large structures that have not been relaxed through molecular dynamics. Nevertheless, our results are consistent with residue locations, supporting, for instance, the role that the insect specific Pro884 plays in the active site.

DISCUSSION

In this study we identified a total of 164 AOX sequences from both moths and butterflies. In the context of an increasing amount of data from genomic studies, we have taken advantage of publicly available genome assemblies to identify and analyze AOX gene families in Lepidoptera. Particularly, AOXs are metal-containing enzymes that metabolize aldehydes into their corresponding carboxylic acids and other sub products (Krenitsky et al., 1972). Their role in insect chemosensation has been studied since 1989 when *M. sexta* AOX (MsexAOX1) was reported to catalyze (*E,Z*)-10,12-hexadecadienal (bombykal), the sex pheromone of this species (Rybczynski et al., 1989). However, reports about insect AOXs and their function toward aldehydes took more than 20 years to be published again, when *A. transitella* AOX2 (AtraAOX2) was comprehensively studied (Choo et al., 2013).

Although AOX genes have been related to metabolism of xenobiotics in mammals as well as in *Culex* mosquitoes (Hemingway et al., 2000; Coleman et al., 2002; Terao et al., 2020), recent efforts have been focused on insect AOXs that can act as ODEs in olfactory organs, such as antennae and maxillary palps. Here, we report a profile of sequences related to AOX gene family that provides new data sets for several lepidopterans (**Table 1** and **Supplementary Table 1**). For instance, our analyses revealed 5 full-length and 1 partial AOX sequences for *P. xylostella*, including the only identified AOX so far (PxylAOX3) (Wang et al., 2021b). Similarly, 9 full-length sequences were identified for *B. mori*, including BmorAOX1, BmorAOX2, and BmorAOX5, the only AOXs reported so far (Pelletier et al., 2007; Zhang et al., 2020). Likewise, we report 2 new AOXs for *H. armigera*, in which 6 AOXs had previously been reported, including HarmAOX2, suggested to be a candidate pheromone-degrading enzyme (Xu and Liao, 2017). For butterflies, no AOX-related studies have been published to our knowledge. Hence, this study would be the first to report such enzymes in this group.

In terms of number of AOXs identified in both moths and butterflies, it is interesting to notice that generalist moth species, such as *S. frugiperda*, *M. sexta* and *T. ni* resulted in the highest number of AOXs. However, we could not establish a direct relationship between number of AOXs and the condition of generalist vs. specialist species, something that has been proposed for other chemosensory proteins, such as ORs (Venthur and Zhou, 2018). Thus, we can highlight that, overall, moths resulted in a similar number of AOXs compared with butterflies, excluding *S. frugiperda*, *M. sexta,* and *T. ni*. On the one hand, the amount of identified AOXs could have been determined by the unavailability of well-assembled genomes in both moths and butterflies. On the other hand, this can also be explained because moths are largely dependent on chemosensation (at short and long range) whereas butterflies use pheromones for short range communication and visual cues (Costanzo and Monteiro, 2007). In that sense, it can be suggested that butterflies have some AOXs related to odorant degradation and to a lesser extent for the metabolism of xenobiotics. This assumption is supported by our phylogenetic analysis, where two clades related to odorant-degrading function showed the presence of both moth and butterfly AOXs.

TABLE 3 | Positive selection analysis using branch-site model on 8 lepidopteran AOX sequences.

Model	np	LnL	Estimates of parameters	LRT *p*-value[a]	PSSs[b]
Branch-site model					
#1 AtraAOX2	18	−19563.928883	p0: 0.34727; p1: 0.47396; p2a: 0.07560; p2b: 0.10317; ω0: 0.06748; ω1: 1.00000; ω2a: 0.06748; ω2b: 1.00000	0.00E + 0.00	23V, 30P, 40T, 41M, 45L, 47I, 49K, 81L, 112C, 113R, 116D, 123K, 151E, 183N, 187R, 205G, 221R, 232S, 243V, 283N, 299E, 376L, 382V, 384N, 423V, 461L, 463F, 468E, 472F, 495L, 540A, 542Q, 546S, 547E, 554G, 562A, 564E, 596G, 605A, 615V, 624P, 643R, 657V, 659V, 661V, 662L, 706M, 735S, 740H, 762I, 764E, 771A, 788T, 791I, 794C, 805Q, 807R, 810C, 826V, 833T, 840I, 842N, 862E, 874S, 875V, 879V, 884K, 889V, 893H, 900T, 903K, 920H, 925I, 935S, 941K, 942I, 964F, 989I, 1005T, 1017G, 1048L, 1053Y, 1054I, 1076R, 1079N, 1089K, 1091E, 1092M, 1099K, 1103W, 1108L, 1123K, 1126S, 1165L, 1174G, 1188I, 1189F, 1192H, 1193S, 1250V, 1254N, 1257R, 1264H, 1267A, 1289Y
#2 PxylAOX3	18	−19576.412306	p0: 0.36546; p1: 0.47336; p2a: 0.07023; p2b: 0.09096; ω0: 0.07760; ω1: 1.00000; ω2a: 0.07760; ω2b: 1.00000	0.00E + 0.00	25T, 35E, 75R, 76R, 84T, 105I, 110D, 112C, 140Q, 187R, 227S, 255I, 264A, 271D, 301Q, 308L, 312I, 313S, 317S, 319A, 336E, 339R, 343L, 354S, 380G, 391Q, 404D, 405M, 406R, 450N, 454N, 458H, 462A, 467T, 479Y, 491L, 499S, 535G, 536T, 540A, 543S, 554G, 632A, 643R, 676E, 715G, 722T, 769M, 785S, 836S, 844C, 894L, 896T, 909A, 914T, 961E, 974F, 1003M, 1020I, 1037E, 1055A, 1097T, 1107E, 1134A, 1135I, 1191K, 1219K, 1284A, 1286D
#3 BmorAOX5	18	−19563.931580	p0: 0.34710; p1: 0.47328; p2a: 0.07599; p2b: 0.10362; ω0: 0.06797; ω1: 1.00000; ω2a: 0.06797; ω2b: 1.00000	0.00E + 0.00	23V, 30P, 40T, 41M, 45L, 47I, 49K, 81L, 112C, 116D, 123K, 124E, 151E, 183N, 187R, 205G, 221R, 232S, 243V, 283N, 299E, 376L, 382V, 384N, 423V, 461L, 463F, 468E, 472F, 495L, 540A, 547E, 554G, 562A, 564E, 596G, 605A, 615V, 624P, 643R, 657V, 659V, 661V, 662L, 706M, 735S, 740H, 762I, 764E, 771A, 788T, 791I, 794C, 805Q, 807R, 810C, 826V, 833T, 840I, 842N, 862E, 874S, 875V, 879V, 884K, 889V, 893H, 900T, 903K, 920H, 925I, 935S, 941K, 942I, 964F, 989I, 1005T, 1017G, 1048L, 1053Y, 1054I, 1099K, 1103W, 1108L, 1123K, 1126S, 1165L, 1174G, 1188I, 1189F, 1192H, 1193S, 1250V, 1254N, 1257R, 1264H, 1267A, 1289Y
#4 HarmAOX2	18	−19623.819643	p0: 0.39374; p1: 0.51575; p2a: 0.03918; p2b: 0.05133; ω0: 0.08015; ω1: 1.00000; ω2a: 0.08015; ω2b: 1.00000	0.00E + 0.00	94V, 245K, 314L, 315E, 364E, 374L, 386R, 401L, 445F, 458H, 467T, 499S, 596G, 607V, 621L, 630Y, 670I, 678L, 834T, 869C, 966E, 981M, 1070V, 1104R, 1116Y, 1139Q, 1142V, 1147Y, 1190D
#5 SinfAOX3	18	−19633.400356	p0: 0.39394; p1: 0.52825; p2a: 0.03324; p2b: 0.04457; ω0: 0.07706; ω1: 1.00000; ω2a: 0.07706; ω2b: 1.00000	0.00E + 0.00	81L, 102I, 211K, 306L, 320I, 387N, 437A, 442N, 493G, 501E, 530S, 606T, 685K, 722T, 765S, 874S, 879V, 900T, 1048L, 1143L, 1198T, 1246G, 1270I, 1290E, 1295S
#6 BanyAOX2	18	−19536.056864	p0: 0.34728; p1: 0.44832; p2a: 0.08922; p2b: 0.11518; ω0: 0.06915; ω1: 1.00000; ω2a: 0.06915 ; ω2b: 1.00000	0.00E + 0.00	Supp. Info.
#7 PxutAOX2	18	−19667.749019	p0: 0.33543; p1: 0.44553; p2a: 0.09408; p2b: 0.12496; ω0: 0.06042; ω1: 1.00000; ω2a: 0.06042; ω2b: 1.00000	0.00E + 0.00	423V, 728V, 835I, 1141D
#8 PmacAOX2	18	−19668.210787	p0: 0.42216; p1: 0.54813; p2a: 0.01293; p2b: 0.01679; ω0: 0.07895; ω1: 1.00000; ω2a: 0.07895; ω2b: 1.00000	0.00E + 0.00	284Y, 486F, 725G, 730K, 934K

[a] *Significant difference according to likelihood-ratio test (LRT).*

[b] *Positive selected sites included with P > 0.99 according to Bayes Empirical Bayes (BEB) analysis. Other amino acids under positive selection with less than 0.95 of significance are included in* ***Supplementary Material****.*

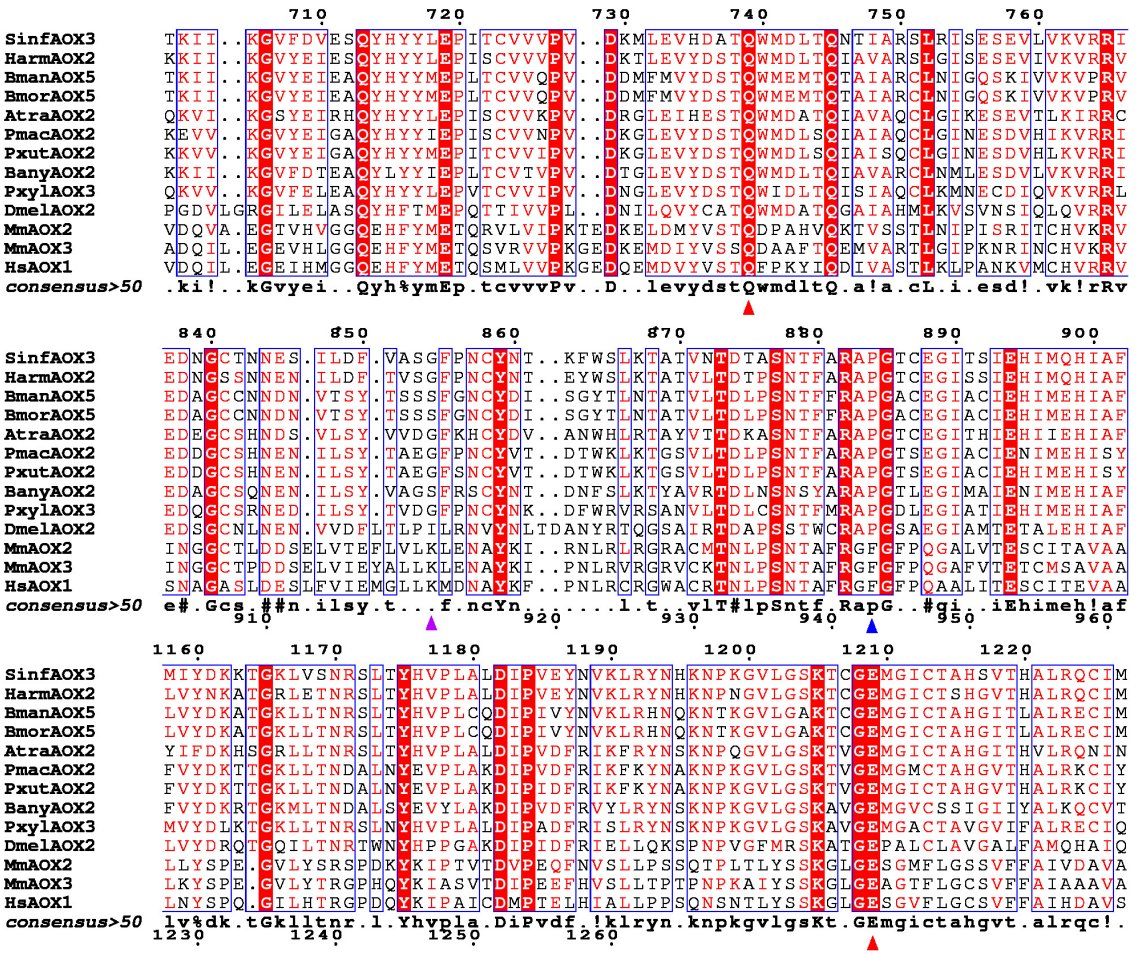

FIGURE 3 | Fragment of a multiple sequence alignment between vertebrate and invertebrate AOXs. Identical residues are highlighted in white letters with red background. Similar residues are highlighted in red and framed in blue. Triangles indicate conserved sites according to Terao et al. (2020). Red triangles show conserved residues across all analyzed species. Blue triangle shows residue conserved only in insect species. Purple triangle shows an active site with different residues within Lepidoptera species. Full alignment can be found in **Supplementary Figure 1**.

To date, two studies have reported a phylogeny for insect AOXs with focus on moths *P. xylostella* and *H. armigera* (He et al., 2017; Xu and Liao, 2017). Both analyses confirm XDHs as common ancestors followed by Dipteran AOXs, and support lepidopteran AOXs as more recently evolved enzymes. In that sense, our phylogenetic analysis is consistent with both. Furthermore, this analysis showed the two ODE-related clades already mentioned as well as a common ancestor in *E. semipurpurella* AOX1 (EsemAOX1), the only AOX identified from its antennal transcriptome. Interestingly, as an old lineage of moths (i.e., non-ditrysia), *E. semipurpurella* represents a model for evolutionary studies. Yuvaraj et al. (2017) showed that moth pheromone receptors could have evolved from plant volatile-related ORs, since two *E. semipurpurella* ORs (EsemOR3 and EsemOR5) that are phylogenetically close to plant volatile-responding ORs, respond to its sex pheromone (2*S*,6*Z*-6-nonen-2-ol), which resemble plant volatiles. The lack of more AOXs in *E. semipurpurella* could indicate that gene duplication events in other moths, and likely butterflies, happened in response to the use of more specialized aldehyde-related volatiles, such as sex pheromones. Furthermore, those that are close to EsemAOX1, in ODE-related clade (clade A in **Figure 1**), could likely be more plant volatile-biased.

It can be argued that moths with functionally studied AOXs, namely BmorAOX5, PxylAOX3 and AtraAOX2, are not strictly related to sex pheromone degradation. In fact, AtraAOX2 has not showed specificity for *A. transitella* sex pheromone [(*Z*,*Z*)-11,13-hexadecadienal], being also able to catalyze aldehyde-related plant volatiles (Choo et al., 2013). Similarly, PxylAOX3 was reported able to degrade sex pheromone (*Z*)-11-hexadecenal as well as plant-derived aldehydes, such as phenylacetaldehyde and non-anal (Wang et al., 2021b). Butterflies, *H. melpomene* with (*Z*)-9-octadecenal, octadecanal, (*Z*)-11-icosenal, icosanal and (*Z*)-13-docosenal as sex pheromone components (Darragh et al., 2017), and *B. anynana* with hexadecanal (Nieberding et al., 2008), represent the only butterflies that use aldehydes as semiochemicals in our data sets. Interestingly, one AOX (i.e., HmelAOX2) was

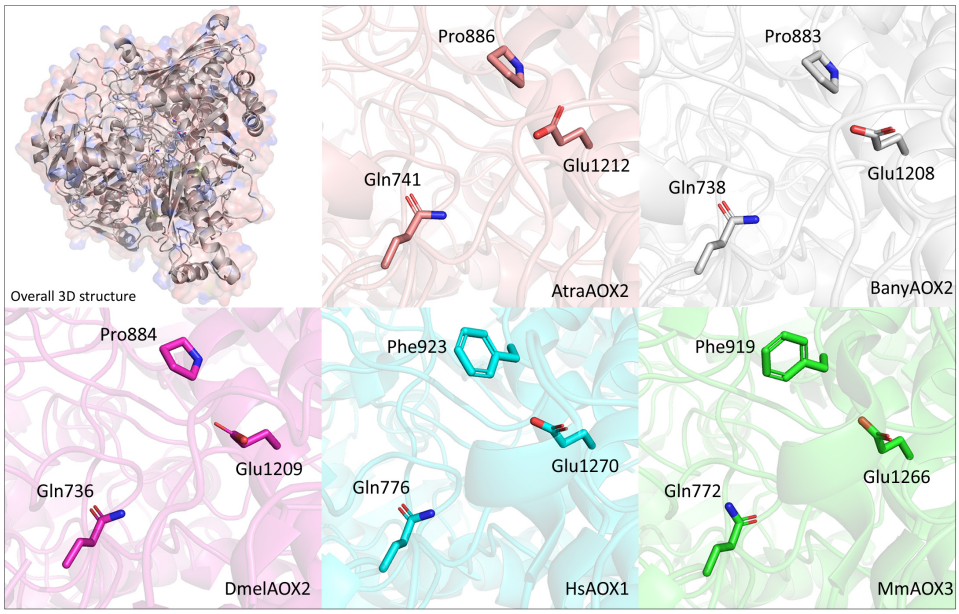

FIGURE 4 | Visualization of the location of conserved residues in 3D representations of the active site of *A. transitella* AOX2 (AtraAOX2—orange), *B. anynana* AOX2 (BanyAOX2—gray), *D. melanogaster* AOX2 (DmelAOX2—pink), *H. sapiens* AOX1 (HsAOX1—cyan) and *M. musculus* AOX3 (MmAOX3—green). Residues and their positions are indicated in each AOX. Mammal AOXs were retrieved from Protein Data Bank (https://www.rcsb.org/) and DmelAOX2 was downloaded from AlphaFold database (https://alphafold.ebi.ac.uk/).

present in an ODE-related clade according to our phylogenetic analysis, while *B. anynana* had seven. It is worth noting that *H. melpomene* as pollinator (Andersson and Dobson, 2003) and *B. anynana* as a fruit-feeding butterfly (Lewis and Wedell, 2007), are both exposed to more aldehydes emitted by plants and fruits. For *B. anynana*, it is noticeable that the seven AOXs (from a total of 12) appear to have emerged independently from the rest. Something similar to what is found in the gene location of moth species, such as *B. mandarina*, *A. transitella* and *P. xylostella*, where their AOX genes potentially related to ODE function, are far from other AOX genes, with the exception of PxylAOX3.

From the two ODE-related clades in our phylogenetic analysis, clade B resulted highly supported by both functional studies and antennal-enriched expression (**Figure 1**). The fact that AOXs from butterflies were also present in this clade, further suggests that these could use aldehyde-based volatiles as semiochemicals. Although fewer studies have exploited the semiochemistry of butterflies compared with moths, increasing evidence suggests that several species of butterflies, including *H. melpomene* and *B. anynana*, use volatiles as semiochemicals. For example, an early study reported strong antennal responses of *H. melpomene* to several tropical plant-derived volatiles, such as linalool, linalool oxide I and II, oxoisophoroneoxide and phenylacetaldehyde (Andersson and Dobson, 2003). Recently, 55 compounds exclusive of androconia (specialized units where secretory glands are found) in sympatric Pieridae butterflies that would play a role in mating orientation, were reported (Nobre et al., 2021). On the other hand, some moths and butterflies can share pheromone biosynthetic pathways. It has been reported that in *B. anynana* the synthesis of hexadecanal and (*Z*)-9-tetradecenol is mediated by conserved fatty acyl Δ11-desaturases (Liénard et al., 2014). In that sense, it is expected that other enzymes, such as AOXs, could be conserved between moths and butterflies. Therefore, it appears that AOXs in ODE-related clades could function for aldehyde-related semiochemicals whether derived from plants or conspecific species. Thus, more functional studies focused on both moths and butterflies would be necessary to support a monophyletic pheromone-degrading clade.

In general, the function of AOXs toward aldehydes might resemble the function of XDHs, which are their evolutionary ancestors (Kurosaki et al., 2013; Wang et al., 2016). High levels of similarity between vertebrate XDHs and AOXs have been reported (Terao et al., 2020). For instance, sequence identity between mammal AOXs, namely HsAOX1 and MmAOX1, reaches 83%. On the other hand, sequence identity between lepidopteran and mammal AOXs is ∼30%. More specifically, among lepidopteran AOXs, sequence identity starts decreasing at 67%. This divergence within lepidopterans is evidenced in an important amount of PSSs among those phylogenetically close AOXs that were selected for our molecular evolution analyses. Nevertheless, and as expected, residues that are conserved were not PSSs, such as those from the active site.

Our MSA analysis revealed that highly conserved residues in vertebrate AOXs, namely Glu1266, Phe919, Lys889 and Gln772, may or may not be conserved in lepidopteran and *D. melanogaster* AOXs. Thus, Glu1266 (at position 1,209 in our MSA, **Figure 3**) that is reported to be crucial for catalytic activity resulted highly conserved (Coelho et al., 2012), while Phe919 from vertebrates changes to Pro in insect AOXs (at position 884 in our MSA, **Figures 3**, **4**). It is difficult to predict the effect of

Pro instead of Phe in insect AOXs. The change from an aromatic side chain toward an aliphatic portion like the one present in Pro, might have some effects on selectivity and stability of aldehyde substrates. In our structural analyses, Pro884 was found in the active site of AtraAOX2, BanyAOX2 and DmelAOX2, keeping the region hydrophobic. In other studies, enzymes such as HCV NS5b polymerase, Pro197 along with Arg200, Cys366, Met414 and Tyr448, were reported to be crucial for ligand selectivity (Li et al., 2010). On the contrary, Pro substitutions in human carbonic anhydrase II led to an increased rigidity of the enzyme and subsequent decreased catalytic activity (Boone et al., 2015). In fact, it is well accepted that Pro restricts protein backbones with the lack of a hydrogen bond donor, disrupting α-helices (Woolfson and Williams, 1990; Van Arnam et al., 2011).

Overall, we believe this study represents the first to group a comprehensive set of AOX genes for several lepidopteran species. We have validated AOX sequences previously described and added 58 more in moths and 33 more in butterflies. We have also uncovered the potential importance of aldehydes as semiochemicals in butterflies, as reflected by the number of AOX present in this group. The information presented herein is a helpful reference for further evolutionary and functional studies in this highly biodiverse order.

DATA AVAILABILITY STATEMENT

The original contributions presented in the study are included in the article/**Supplementary Material**, further inquiries can be directed to the corresponding author.

AUTHOR CONTRIBUTIONS

RG, AM, and HV conceived the idea. RG and HV performed genome and structural analysis. LCP and AM analyzed phylogenetics and evolution data. HV and LCP wrote the manuscript. All authors contributed to the article and approved the submitted version.

FUNDING

This work was supported by Agencia Nacional de Investigación y Desarrollo (ANID) project N° 11200349 and ANID scholarship N° 21190666. LCP was supported by Wellcome Trust Investigator Award 110117/Z/15/Z.

ACKNOWLEDGMENTS

We would like to thank reviewers for the valuable comments that helped to improve this manuscript.

SUPPLEMENTARY MATERIAL

The Supplementary Material for this article can be found online at: https://www.frontiersin.org/articles/10.3389/fevo.2022.823119/full#supplementary-material

REFERENCES

Adebali, O., Ortega, D., and Zhulin, I. (2015). CDvist: a webserver for identification and visualization of conserved domains in protein sequences. *Bioinformatics* 31, 1475–1477. doi: 10.1093/bioinformatics/btu836

Andersson, S., and Dobson, H. (2003). Antennal responses to floral scents in the butterfly. *J. Chem. Ecol.* 29, 2319–2330. doi: 10.1023/A:1026278531806

Boone, C., Rasi, V., Tu, C., and McKenna, R. (2015). Structural and catalytic effects of proline substitution and surface loop deletion in the extended active site of human carbonic anhydrase II. *FEBS J.* 282, 1445–1457. doi: 10.1111/febs.13232

Butenandt, A., Beckman, R., Stamm, D., and Hecker, E. (1959). Über den sexuallockstoff des seidenspinners *Bombyx mori*. *Reindarstellung und konstitution. Z Naturforsch B.* 14, 283–284.

Chemnitz, J., Jentschke, P. C., Ayasse, M., and Steiger, S. (2015). Beyond species recognition: somatic state affects long-distance sex pheromone communication. *Proc. R. Soc. B* 282:20150832. doi: 10.1098/rspb.2015.0832

Chertemps, T., and Meïbèche, M. (2021). "19 - Odor degrading enzymes and signal termination," in *Insect Pheromone Biochemistry and Molecular Biology*, 2nd Edn, eds J. Gary, Blomquist, G. Richard, and Vogt (Cambridge, MA: Academic Press), 619–644.

Choo, Y. M., Pelletier, J., Atungulu, E., and Leal, W. S. (2013). Identification and characterization of an antennae-specific aldehyde oxidase from the navel orangeworm. *PLoS One* 8:e67794. doi: 10.1371/journal.pone.0067794

Coelho, C., Mahro, M., Trincão, J., Carvalho, A., Ramos, M., Terao, M., et al. (2012). The first mammalian aldehyde oxidase crystal structure: insights into substrate specificity. *J. Biol. Chem.* 287, 40690–40702. doi: 10.1074/jbc.M112.390419

Coffelt, J. A., Vick, K. W., Sonnet, P. E., and Doolittle, R. E. (1979). Isolation, identification, and synthesis of a female sex pheromone of the navel orangeworm, *Amyelois transitella* (Lepidoptera: Pyralidae). *J. Chem. Ecol.* 5, 955–966.

Coleman, M., Vontas, J. G., and Hemingway, J. (2002). Molecular characterization of the amplified aldehyde oxidase from insecticide resistant *Culex quinquefasciatus*. *Eur. J. Biochem.* 269, 768–779. doi: 10.1046/j.0014-2956.2001.02682.x

Corpet, F. (1988). Multiple sequence alignment with hierarchical clustering. *Nucleic Acids Res.* 16, 10881–10890. doi: 10.1093/nar/16.22.10881

Costanzo, K., and Monteiro, A. (2007). The use of chemical and visual cues in female choice in the butterfly *Bicyclus anynana*. *Proc. R. Soc. B* 274, 845–851. doi: 10.1098/rspb.2006.3729

Darragh, K., Vanjari, S., Mann, F., Gonzalez-Rojas, M. F., Morrison, C. R., Salazar, C., et al. (2017). Male sex pheromone components in Heliconius butterflies released by the androconia affect female choice. *PeerJ* 5:e3953. doi: 10.7717/peerj.3953

Durand, N., Pottier, M. A., Siaussat, D., Bozzolan, F., Maïbèche, M., and Chertemps, T. (2018). Glutathione-S-transferases in the olfactory organ of the noctuid moth Spodoptera littoralis, diversity and conservation of chemosensory clades. *Front. Physiol.* 9:1283. doi: 10.3389/fphys.2018.01283

Engsontia, P., Sangket, U., Chotigeat, W., and Satasook, C. (2014). Molecular evolution of the odorant and gustatory receptor genes in lepidopteran insects: implications for their adaptation and speciation. *J. Mol. Evol.* 79, 21–39. doi: 10.1007/s00239-014-9633-0

Gao, F., Chen, C., Arab, D. A., Du, Z., He, Y., and Ho, S. (2019). EasyCodeML: a visual tool for analysis of selection using CodeML. *Ecol. Evol.* 9, 3891–3898. doi: 10.1002/ece3.5015

Garattini, E., and Terao, M. (2012). The role of aldehyde oxidase in drug metabolism. *Expert Opin.* 8, 487–503. doi: 10.1517/17425255.2012.663352

Garattini, E., Fratelli, M., and Terao, M. (2009). The mammalian aldehyde oxidase gene family. *Hum. Genom.* 4, 119–130. doi: 10.1186/1479-7364-4-2-119

Godoy, R., Machuca, J., Venthur, H., Quiroz, A., and Mutis, A. (2021). An overview of antennal esterases in lepidoptera. *Front. Physiol.* 12:643281. doi: 10.3389/fphys.2021.643281

Grabherr, M., Haas, B. J., Yassour, M., Levin, J. Z., Thompson, D. A., Amit, I., et al. (2011). Trinity: reconstructing a full-length transcriptome without a genome from RNA-Seq data. *Nat. Biotechnol.* 29, 644–652. doi: 10.1038/nbt.1883

Hansson, B., and Stensmyr, M. (2011). Evolution of insect olfaction. *Neuron* 72, 698–711. doi: 10.1016/j.neuron.2011.11.003

He, P., Zhang, Y. N., Li, Z. Q., Yang, K., Zhu, J. Y., Liu, S. J., et al. (2014a). An antennae-enriched carboxylesterase from *Spodoptera exigua* displays degradation activity in both plant volatiles and female sex pheromones. *Insect Mol. Biol.* 23, 475–486. doi: 10.1111/imb.12095

He, P., Zhang, J., Li, Z. Q., Zhang, Y. N., Yang, K., and Dong, S. L. (2014b). Functional characterization of an antennal esterase from the noctuid moth, *Spodoptera exigua*. *Arch. Insect Biochem. Physiol.* 86, 85–99. doi: 10.1002/arch.21164

He, P., Li, Z. Q., Liu, C. C., Liu, S. J., and Dong, S. L. (2014c). Two esterases from the genus Spodoptera degrade sex pheromones and plant volatiles. *Genome* 57, 201–208. doi: 10.1139/gen-2014-0041

He, P., Zhang, Y. N., Yang, K., Li, Z. Q., and Dong, S. L. (2015). An antenna-biased carboxylesterase is specifically active to plant volatiles in *Spodoptera exigua*. *Pestic. Biochem. Physiol.* 123, 93–100.

He, P., Zhang, Y. F., Hong, D. Y., Wang, J., Wang, X. L., Zuo, L. H., et al. (2017). A reference gene set for sex pheromone biosynthesis and degradation genes from the diamondback moth, *Plutella xylostella*, based on genome and transcriptome digital gene expression analyses. *BMC Genomics* 18:219. doi: 10.1186/s12864-017-3592-y

He, P., Mang, D. Z., Wang, H., Wang, M. M., Ma, Y. F., Wang, J., et al. (2019). Molecular characterization and functional analysis of a novel candidate of cuticle carboxylesterase in *Spodoptera exigua* degrading sex pheromones and plant volatiles esters. *Pestic. Biochem. Physiol.* 163, 227–234. doi: 10.1016/j.pestbp.2019.11.022

Hemingway, J., Coleman, M., Paton, M., McCarroll, L., Vaughan, A., and DeSilva, D. (2000). Aldehyde oxidase is coamplified with the World's most common Culex mosquito insecticide resistance-associated esterases. *Insect Mol. Biol.* 9, 93–99. doi: 10.1046/j.1365-2583.2000.00160.x

Huang, X., Fan, D., Liu, L., and Feng, J. (2017). Identification and characterization of glutathione S-Transferase genes in the antennae of codling moth (Lepidoptera: Tortricidae). *Ann. Entomol. Soc. Am.* 110, 409–416. doi: 10.1093/aesa/sax041

Huang, X., Liu, L., Su, X., and Feng, J. (2016). Identification f biotransformation enzymes in the antennae of codling moth *Cydia pomonella*. *Gene* 580, 73–79. doi: 10.1016/j.gene.2016.01.008

Kaissling, K. E. (2013). Kinetics of olfactory responses might largely depend on the odorant-receptor interaction and the odorant deactivation postulated for flux detectors. *J. Comp. Physiol. A Neuroethol. Sensory Neural Behav. Physiol.* 199, 879–896. doi: 10.1007/s00359-013-0812-z

Kasang, G., Kaissling, K. E., Vostrowsky, O., and Bestmann, H. J. (1978). Bombykal, a second pheromone component of the silkworm moth *Bombyx mori* L. *Z. Angew. Chem. Int. Ed. Engl.* 17:60. doi: 10.1002/anie.197800601

Katoh, K., Rozewicki, J., and Yamada, K. D. (2019). MAFFT online service: multiple sequence alignment, interactive sequence choice and visualization. *Brief. Bioinform.* 20, 1160–1166. doi: 10.1093/bib/bbx108

Kawahara, A. Y., Plotkin, D., Espeland, M., Meusemann, K., Toussaint, E., Donath, A., et al. (2019). Phylogenomics reveals the evolutionary timing and pattern of butterflies and moths. *PNAS* 116, 22657–22663. doi: 10.1073/pnas.1907847116

Krenitsky, T. A., Neil, S. M., Elion, G. B., and Hitchings, G. H. (1972). A comparison of the specificities of xanthine oxidase and aldehyde oxidase. *Arch. Biochem. Biophys.* 150, 585–599. doi: 10.1016/0003-9861(72)90078-1

Kurosaki, M., Bolis, M., Fratelli, M., Barzago, M. M., Pattini, L., Perretta, G., et al. (2013). Structure and evolution of vertebrate aldehyde oxidases: from gene duplication to gene suppression. *Cell. Mol. Life Sci.* 70, 1807–1830. doi: 10.1007/s00018-012-1229-5

Langmead, B., Trapnell, C., Pop, M., and Salzberg, S. L. (2009). Ultrafast and memory-efficient alignment of short DNA sequences to the human genome. *Genome Biol.* 10:R25. doi: 10.1186/gb-2009-10-3-r25

Leal, W. (2013). Odorant reception in insects: roles of receptors, binding proteins, and degrading enzymes. *Annu. Rev. Entomol.* 58, 373–391. doi: 10.1146/annurev-ento-120811-153635

Lewis, Z., and Wedell, N. (2007). Effect of adult feeding on male mating behaviour in the butterfly, *Bicyclus anynana* (Lepidoptera: Nymphalidae). *J. Insect Behav.* 20, 201–213. doi: 10.1007/s10905-007-9075-2

Li, F., Zhao, X., Li, M., He, K., Huang, C., Zhou, Y., et al. (2019). Insect genomes: progress and challenges. *Insect Mol. Biol.* 28, 739–758. doi: 10.1111/imb.12599

Li, G. W., Chen, X. L., Xu, X. L., and Wu, J. X. (2018). Degradation of sex pheromone and plant volatile components by an antennal glutathione S-transferase in the oriental fruit moth, *Grapholita molesta* Busck (Lepidoptera: Tortricidae). *Arch. Insect Biochem. Physiol.* 99:e21512. doi: 10.1002/arch.21512

Li, H., Handsaker, B., Wysoker, A., Fennell, T., Ruan, J., Homar, N., et al. (2009). The sequence Alignment/Map format and SAMtools. *Bioinformatics* 25, 2078–2079. doi: 10.1093/bioinformatics/btp352

Li, T., Froeyen, M., and Herdewijn, P. (2010). Insight into ligand selectivity in HCV NS5B polymerase: molecular dynamics simulations, free energy decomposition and docking. *J. Mol. Model.* 16, 49–59. doi: 10.1007/s00894-009-0519-9

Li, Z. Q., Zhang, S. Z., Luo, J. Y., Wang, C. Y., Lv, L. M., Dong, S. L., et al. (2015). Transcriptome comparison of the sex pheromone glands from two sibling *Helicoverpa species* with opposite sex pheromone components. *Sci. Rep.* 5:9324. doi: 10.1038/srep09324

Liénard, M., Wang, H. L., Lassance, J. M., and Löfstedt, C. (2014). Sex pheromone biosynthetic pathways are conserved between moths and the butterfly *Bicyclus anynana*. *Nat. Commun.* 5:3957. doi: 10.1038/ncomms4957

Liu, H., Lei, X., Du, L., Yin, J., Shi, H., Zhang, T., et al. (2019). Antennae-specific carboxylesterase genes from Indian meal moth: Identification, tissue distribution and the response to semiochemicals. *J. Stored Prod. Res.* 84:101528. doi: 10.1016/j.jspr.2019.101528

Merlin, C., François, M. C., Bozzolan, F., Pelletier, J., Jacquin-Joly, E., and Maïbèche-Coisne, M. (2005). A new aldehyde oxidase selectivity expressed in chemosensory organs of insects. *Biochem. Biophys. Res. Commun.* 332, 4–10. doi: 10.1016/j.bbrc.2005.04.084

Nieberding, C. M., de Vos, H., Schneider, M. V., Lassance, J. M., Estramil, N., Andersson, J., et al. (2008). The male sex pheromone of the butterfly *Bicyclus anynana*: towards an evolutionary analysis. *PLoS One* 3:e2751. doi: 10.1371/journal.pone.0002751

Nobre, C. E. B., Lucas, L. A. D., Padilha, R. J. R., Navarro, D. M., Alves, L. C., and Maia, A. C. D. (2021). Specialized androconial scales conceal species-specific semiochemicals of sympatric Sulphur butterflies (Lepidoptera: Pieridae: Coliadinae). *Org. Divers Evol.* 21, 93–105. doi: 10.1007/s13127-020-00475-8

Oppenheim, S., Baker, R., Simon, S., and DeSalle, R. (2015). We can't all be supermodels: the value of comparative transcriptome to the study of non-model insects. *Insect Mol. Biol.* 24, 139–154. doi: 10.1111/imb.12154

Ou, J., Deng, H. M., Zheng, S. C., Huang, L. H., Feng, Q. L., and Liu, L. (2014). Transcriptomic analysis of developmental features of *Bombyx mori* wing disc during metamorphosis. *BMC Genomics* 15:820. doi: 10.1186/1471-2164-15-820

Patel, R., and Jain, M. (2012). NGS QC Toolkit: a toolkit for quality control of next generation sequencing data. *PLoS One* 7:e30619. doi: 10.1371/journal.pone.0030619

Pelletier, J., Bozzolan, F., Solvar, M., Françoise, M. C., Jacquin-Joly, E., and Maïbèche-Coisne, M. (2007). Identification of candidate aldehyde oxidases from the silkworm *Bombyx mori* potentially involved in antennal pheromone degradation. *Gene* 404, 31–40. doi: 10.1016/j.gene.2007.08.022

Price, M., Dehal, P., and Arkin, A. (2010). FastTree 2 – approximately maximum-likelihood trees for large alignments. *PLoS One* 5:e9490. doi: 10.1371/journal.pone.0009490

Riddiford, L. M. (1967). Trans-2-hexenal: mating stimulant for *Polyphemus moths*. *Science* 158, 139–141. doi: 10.1126/science.158.3797.139

Rybczynski, R., Reagan, J., and Lerner, M. (1989). A pheromone-degrading aldehyde oxidase in the antennae of the moth *Manduca sexta*. *J. Neurosci.* 9, 1341–1353.

Sela, I., Ashkenazy, H., Katoh, K., and Pupko, T. (2015). GUIDANCE2: accurate detection of unreliable alignment regions accounting for the uncertainty of multiple parameters. *Nucleic Acids Res.* 43, W7–W14. doi: 10.1093/nar/gkv318

Soffan, A., Subandiyah, S., Makino, H., Watanabe, T., and Horiike, T. (2018). Evolutionary analysis of the highly conserved insect odorant coreceptor (Orco) revealed a positive selection mode, implying functional flexibility. *J. Insect Sci.* 18, 1–8. doi: 10.1093/jisesa/iey120

Sokkar, P., Mohandass, S., and Ramachandran, M. (2011). Multiple templates-based homology modeling enhances structures quality of AT1 receptor: validation by molecular dynamics and antagonist docking. *J. Mol. Model.* 17, 1565–1577. doi: 10.1007/s00894-010-0860-z

Swanson, W. J., Nielsen, R., and Yang, Q. (2003). Pervasive adaptive evolution in mammalian fertilization proteins. *Mol. Biol. Evol.* 20, 18–20. doi: 10.1093/oxfordjournals.molbev.a004233

Terao, M., Garattini, E., Romão, M. J., and Leimkühler, S. (2020). Evolution, expression, and substrate specificities of aldehyde oxidase enzymes in eukaryotes. *J. Biol. Chem.* 295, 5377–5389. doi: 10.1074/jbc.REV119.007741

Van Arnam, E. B., Lester, H. A., and Dougherty, D. A. (2011). Dissecting the functions of conserved prolines within transmembrane helices of the D2 dopamine receptor. *ACS Chem. Biol.* 6, 1063–1068. doi: 10.1021/cb200153g

Venthur, H., and Zhou, J. J. (2018). Odorant receptors and odorant-binding proteins as insect pest control targets: a comparative analysis. *Front. Physiol.* 9:1163. doi: 10.3389/fphys.2018.01163

Vizueta, J., Sánchez-Gracia, A., and Rozas, J. (2020). BITACORA: a comprehensive tool for the identification and annotation of gene families in genome assemblies. *Mol. Ecol. Resour.* 20, 1445–1452. doi: 10.1111/1755-0998.13202

Vogt, R., Grosse-Wilde, E., and Zhou, J. J. (2015). The lepidoptera odorant binding protein gene family: gene gain and loss within the GOBP/PBP complex of moths and butterflies. *Insect Biochem. Mol. Biol.* 62, 142–153. doi: 10.1016/j.ibmb.2015.03.003

Wang, C. H., Zhang, C., and Hing, X. H. (2016). Xanthine dehydrogenase: an old enzyme with new knowledge and prospects. *Bioengineered* 7, 395–405. doi: 10.1080/21655979.2016.1206168

Wang, M. M., Long, G. J., Guo, H., Liu, X. Z., Wang, H., Dewer, Y., et al. (2021a). Two carboxylesterase genes in *Plutella xylostella* associated with sex pheromones and plant volatiles degradation. *Pest Manag. Sci.* 77, 2737–2746. doi: 10.1002/ps.6302

Wang, M. M., He, M., Wang, H., Ma, Y. F., Dewer, Y., Zhang, F., et al. (2021b). A candidate aldehyde oxidase in the antennae of the diamondback moth, *Plutella xylostella* (L.), is potentially involved volatiles and the detoxification of xenobiotics. *Pestic. Biochem. Phys.* 171:104726. doi: 10.1016/j.pestbp.2020.104726

Wei, H., Tan, S., Li, Z., Li, J., Moural, T. W., Zhu, F., et al. (2020). Odorant degrading carboxylesterases modulate foraging and mating behaviors of *Grapholita molesta*. *Chemosphere* 270:128647. doi: 10.1016/j.chemosphere.2020.128647

Weiss, M. R. (2001). "Vision and learning in some neglected pollinators: beetles, flies, moths and butterflies," in *Cognitive Ecology of Pollination. Animal Behavior and Floral Evolution*, eds L. Chittka and J. D. Thomson (Cambridge: Cambridge University Press).

Woolfson, D. N., and Williams, D. H. (1990). The influence of proline residues on α-helical structure. *FEBS Lett.* 277, 185–188. doi: 10.1016/0014-5793(90)80839-b

Xu, W., and Liao, Y. (2017). Identification and characterization of aldehyde oxidases (AOXs) in the cotton bollworm. *Sci. Nat.* 104:94. doi: 10.1007/s00114-017-1515-z

Yang, B., Ozaki, K., Ishikawa, Y., and Matsuo, T. (2015). Identification of candidate odorant receptors in asian corn borer ostrinia furnacalis. *PLoS One* 10:e0121261. doi: 10.1371/journal.pone.0121261

Yang, Z., and Nielsen, R. (2002). Codon-substitution models for detecting molecular adaptation at individual sites along specific lineages. *Mol. Biol. Evol.* 19, 908–917. doi: 10.1093/oxfordjournals.molbev.a004148

Yang, Z., Nielsen, R., Goldman, N., and Pedersen, A. M. (2000). Codon-substitution models for heterogeneous selection pressure at amino acid sites. *Genetics* 155, 431–449. doi: 10.1093/genetics/155.1.431

Yang, Z., Wong, W., and Nielsen, R. (2005). Bayes empirical bayes inference of amino acid sites under positive selection. *Mol. Biol. Evol.* 22, 1107–1118. doi: 10.1093/molbev/msi097

Yuvaraj, J. K., Corcoran, J. A., Andersson, M. N., Newcomb, R. D., Anderbrant, O., and Löfstedt, C. (2017). Characterization of odorant receptors from a non-ditrysian moth, *Eriocrania semipurpurella* sheds light on the origin of sex pheromone receptors in lepidoptera. *Mol. Biol. Evol.* 34, 2733–2746. doi: 10.1093/molbev/msx215

Zhang, J. P., Salcedo, C., Fang, Y. L., Zhang, R. J., and Zhang, Z. N. (2012). An overlooked component: (Z)-9-tetradecenal as a sex pheromone in *Helicoverpa armigera*. *J. Insect Physiol.* 58, 1209–1216.

Zhang, Y. N., Xia, Y. H., Zhu, J. Y., Li, S. Y., and Dong, S. L. (2014). Putative pathway of sex pheromone biosynthesis and degradation by expression patterns of genes identified from female pheromone gland and adult antenna of *Sesamia inferens* (Walker). *J. Chem. Ecol.* 40, 439–451. doi: 10.1007/s10886-014-0433-1

Zhang, Y. N., Li, Z. Q., Zhu, X. Y., Qian, J. L., Dong, Z. P., and Xu, L. (2017a). Identification and tissue distribution of carboxylesterase (CXE) genes in *Athetis lepigone* (Lepidoptera: Noctuidae) by RNA-seq. *J. Asia-Pacif. Entomol.* 20, 1150–1155.

Zhang, Y. X., Wang, W. L., Li, M. Y., Li, S. H., and Liu, S. (2017b). Identification of putative carboxylesterase and aldehyde oxidase genes from the antennae of the rice leaffolder, *Cnaphalocrocis medinalis* (Lepidoptera: Pyralidae). *J. Asia Pac. Entomol.* 20, 907–913. doi: 10.1016/j.aspen.2017.06.001

Zhang, Y., Yang, Y., Shen, G., Mao, X., Jiao, M., and Lin, Y. (2020). Identification and characterization of aldehyde oxidase 5 in the pheromone gland of the silkworm (Lepidoptera: Bombycidae). *J. Insect Sci.* 20, 1–10. doi: 10.1093/jisesa/ieaa132

Zhou, J. J. (2010). *Odorant-Binding Proteins in Insects*, 1st Edn. Burlington, VT: Elsevier Inc. doi: 10.1016/S0083-6729(10)83010-9

Conflict of Interest: The authors declare that the research was conducted in the absence of any commercial or financial relationships that could be construed as a potential conflict of interest.

Publisher's Note: All claims expressed in this article are solely those of the authors and do not necessarily represent those of their affiliated organizations, or those of the publisher, the editors and the reviewers. Any product that may be evaluated in this article, or claim that may be made by its manufacturer, is not guaranteed or endorsed by the publisher.

Copyright © 2022 Godoy, Mutis, Carabajal Paladino and Venthur. This is an open-access article distributed under the terms of the Creative Commons Attribution License (CC BY). The use, distribution or reproduction in other forums is permitted, provided the original author(s) and the copyright owner(s) are credited and that the original publication in this journal is cited, in accordance with accepted academic practice. No use, distribution or reproduction is permitted which does not comply with these terms.

frontiers in Ecology and Evolution

REVIEW
published: 15 February 2022
doi: 10.3389/fevo.2022.797287

Sex Pheromone Receptors of Lepidopteran Insects

Chan Yang[1], Jie Cheng[2], Jingyu Lin[2], Yuan Zheng[1], Xiao Yu[2] and Jinpeng Sun[1,3]**

[1] Key Laboratory of Molecular Cardiovascular Science, Ministry of Education, Department of Physiology and Pathophysiology, School of Basic Medical Sciences, Peking University, Beijing, China, [2] Key Laboratory Experimental Teratology of the Ministry of Education and Department of Physiology, School of Basic Medical Sciences, Shandong University, Jinan, China, [3] Key Laboratory Experimental Teratology of the Ministry of Education and Department of Biochemistry and Molecular Biology, School of Basic Medical Sciences, Shandong University, Jinan, China

The sex pheromone receptors (SPRs) of Lepidopteran insects play important roles in chemical communication. In the sex pheromone detection processes, sex pheromone molecule (SPM), SPR, co-receptor (Orco), pheromone binding protein (PBP), sensory neuron membrane protein (SNMP), and pheromone degradation enzyme (PDE) play individual and cooperative roles. Commonly known as butterfly and moth, the Lepidopteran insects are widely distributed throughout the world, most of which are pests. Comprehensive knowledge of the SPRs of Lepidopteran insects would help the development of sex lure technology and the sex communication pathway research. In this review, we summarized SPR/Orco information from 10 families of Lepidopteran insects from corresponding studies. According to the research progress in the literature, we speculated the evolution of SPRs/Orcos and phylogenetically analyzed the Lepidopteran SPRs and Orcos with the neighbor-joining tree and further concluded the relationship between the cluster of SPRs and their ligands; we analyzed the predicted structural features of SPRs and gave our prediction results of SPRs and Orcos with Consensus Constrained TOPology Prediction (CCTOP) and SwissModel; we summarized the functional characterization of Lepidopteran SPRs and SPR-ligand interaction and then described the progress in the sex pheromone signaling pathways and metabotropic ion channel. Further studies are needed to work out the cryo-electron microscopy (EM) structure of SPR and the SPR-ligand docking pattern in a biophysical perspective, which will directly facilitate the understanding of sex pheromone signal transduction pathways and provide guidance in the sex lure technology in field pest control.

Keywords: sex pheromone receptor, structure, signal transduction, Lepidopteran insects, evolution, function

OPEN ACCESS

Edited by:
Rui Tang,
Institute of Zoology, Guangdong Academy of Sciences, Chinese Academy of Sciences (CAS), China

Reviewed by:
Cong Huang,
Agricultural Genomics Institute at Shenzhen, Chinese Academy of Agricultural Sciences (CAAS), China
Zhongzhen Wu,
Zhongkai University of Agriculture and Engineering, China

****Correspondence:***
Xiao Yu
yuxiao@sdu.edu.cn
Jinpeng Sun
sunjinpeng@sdu.edu.cn

Specialty section:
This article was submitted to Chemical Ecology, a section of the journal Frontiers in Ecology and Evolution

Received: *18 October 2021*
Accepted: *04 January 2022*
Published: *15 February 2022*

Citation:
Yang C, Cheng J, Lin J, Zheng Y, Yu X and Sun J (2022) Sex Pheromone Receptors of Lepidopteran Insects. Front. Ecol. Evol. 10:797287. doi: 10.3389/fevo.2022.797287

INTRODUCTION

Belonging to general odorant receptors, insect sex pheromone receptors (SPRs) are expressed by olfactory sensory neurons (OSNs) and can detect volatile sex pheromones or other chemical signals to coordinate their social behaviors such as mating, reproduction, and alarming (Fleischer and Krieger, 2018). In the sex pheromone detection processes, sex pheromone molecule (SPM), SPR, co-receptor (Orco), pheromone binding protein (PBP), sensory neuron membrane protein (SNMP), and pheromone degradation enzyme (PDE) play individual and cooperative roles (Leal, 2013).

Usually, SPM was released from female insects and then sensed by specific SPR of conspecific male insects; meanwhile, the specific PBP surrounding the SPR transports the SPM to SPR and increases the magnitude of SPR response to SPM (Grosse-Wilde et al., 2006; Krieger et al., 2009); Orco was expressed in the same OSN of SPR and had been reported to increase the response strength of SPR to SPM through an ionotropic channel or a metabotropic channel (Nakagawa et al., 2005). After a series of elusive signal transduction pathways, the PDE contributes to the signal inactivation through degrading the SPM (Leal, 2013). Above all, the native mechanism of sex pheromone reception and signal transduction has not been fully elucidated until present.

Commonly known as butterfly and moth, the Lepidopteran insects are widely distributed throughout the world. In recent years, many odorant receptors had been characterized following the public annotation of *Drosophila melanogaster* odorant receptor family based on the whole-genome data (Wang and Anderson, 2010). Importantly, several SPRs have been deorphanized in *Bombyx mori* and other insect species according to the analysis of antennal transcriptome data (Nakagawa et al., 2005). As a consequence, sex attractants have been used as sex lures to wipe out pests without using chemical insecticides (Witzgall et al., 2010), and this environment-friendly pest control policy had been growing up gradually.

In this review, we summarized SPR and Orco information from 10 families (i.e., Bombycidae, Plutellidae, Sphingidae, Saturniidae, Geometridae, Nymphalidae, Noctuidae, Tortricidae, Pyralidae, and Crambidae) of Lepidopteran insects (Krieger et al., 2004, 2005; Sakurai et al., 2004; Miura et al., 2005; Nakagawa et al., 2005; Grosse-Wilde et al., 2007, 2010, 2011; Mitsuno et al., 2008; Jordan et al., 2009; Patch et al., 2009; Zhang et al., 2009, 2010, 2013, 2014, 2015; Wanner et al., 2010; Legeai et al., 2011; Wang et al., 2011; Yasukochi et al., 2011; Zhan et al., 2011; Bengtsson et al., 2012; Carraher et al., 2012; Leary et al., 2012; Liu et al., 2012, 2014; Montagne et al., 2012; Xu et al., 2012, 2015; Liu C. et al., 2013; Liu Y. et al., 2013; Sun et al., 2013; Wu et al., 2013; Zhang and Lofstedt, 2013; Jiang et al., 2014; Corcoran et al., 2015; De Fouchier et al., 2015; Feng et al., 2015; Garczynski and Leal, 2015; Lin et al., 2015; Steinwender et al., 2015; Chang et al., 2016; Ge et al., 2016; Jia et al., 2016; Walker et al., 2016; Zhang D. D. et al., 2016; Zhang Y. N. et al., 2016; Gonzalez et al., 2017; Li et al., 2017; Wicher et al., 2017; Yang S. et al., 2017; Du et al., 2018; Grapputo et al., 2018; Rojas et al., 2018; **Table 1**). Among all the Lepidopteran SPRs, several of them have been characterized to be sex pheromone sensing receptors. First of all, we reviewed the phylogenetic analyses of Lepidopteran SPRs, and the evolution of the summarized Lepidopteran SPRs was analyzed through MEGA X (Whelan and Goldman, 2001; Kumar et al., 2018). Second, we reviewed the transmembrane predictions of Lepidopteran SPRs, and the protein structure of Lepidopteran SPRs was predicted by online software Consensus Constrained TOPology Prediction (CCTOP) (Dobson et al., 2015) and SwissModel (Bertoni et al., 2017; Bienert et al., 2017; Waterhouse et al., 2018; Guex et al., 2019; Studer et al., 2020). Third, the interaction of Lepidopteran SPM and SPR was reviewed. Finally, the research status of downstream signaling responses and ligand-gated ion channels by the coupling of SPR and Orco was depicted.

Evolution of Lepidopteran Sex Pheromone Receptors

The olfactory receptor (OR) repertoire of several Lepidopteran species was usually phylogenetically analyzed, and SPRs always belong to the same clade. The neighbor-joining tree of sequences of all identified ORs of *Heliothis virescens* revealed a very high degree of diversity, i.e., a group that comprises 6 SPRs has at least 40% of their amino acids in common (Krieger et al., 2004). The neighbor-joining tree of *H. virescens* OR repertoires and BmOR1/3/4/5/6 receptors showed apparent relatedness of SPRs in *B. mori* and *H. virescens* (Krieger et al., 2005). The phylogenetic tree of *B. mori* and *H. virescens* ORs and also PxylOR1/3/4 and DindOR1/3 showed that pheromone receptors were clustered and were different from that of the Or83b family (Mitsuno et al., 2008; Patch et al., 2009). The phylogenetic analysis of *B. mori*, *Manduca sexta*, *Helicoverpa armigera*, and *H. virescens* ORs and PxylOR1/3/4/5/6/7 shows that the 6 candidate SPRs cluster together in the group of SPRs (Sun et al., 2013). SPRs formed a single subgroup in a phylogenetic tree by the ORs of *B. mori*, *H. armigera*, *H. virescens*, and *Plutella xylostella*, and the Orcos of the four species form a clade (Yang S. et al., 2017). The phylogenetic analysis of *B. mori*, *H. armigera*, and *H. virescens* ORs and PxylOR1/3/4/5/6/7/8/41/45 shows that the 8 candidate SPRs cluster together in the group of SPRs, and they are phylogenetically distinct from general odorant receptors (Liu et al., 2018). Neighbor-joining tree based on MUSCLE multiple sequence alignment of MsexOR1-5 and *B. mori* and *H. virescens* ORs shows that MsexOR1-4 belongs to the subgroup of SPRs, and a highly conserved Or83b group was indicated (Grosse-Wilde et al., 2010, 2011). The neighbor-joining tree including the ORs of *B. mori*, *H. virescens*, and MsexOR1 and ApolOR1/AperOR1 revealed that ApolOR1/AperOR1 are categorized in the subfamily of the candidate and functionally verified SPRs (Forstner et al., 2009). A phylogenetic analysis that was performed using candidate SexiOR and OR repertoires from *H. armigera*, *Helicoverpa assulta*, *Spodoptera littoralis*, and *B. mori* revealed a highly conserved Orco that was clustered with orthologs from all four of these species, and another group of relatively conserved SexiOR6/11/13/16 belongs to the same clade as SPRs (Du et al., 2018).

The phylogenetic tree that contained 21 OR sequences from *Sesamia inferens*, 43 from *M. sexta*, 21 from *H. virescens*, and 60 from *B. mori*, SinfOR2 was clustered with other Lepidopteran Orco sequences, and three SinfOR21/27/29 were clustered in the Lepidopteran SPR clade (Zhang Y. N. et al., 2016). A phylogenetic tree using a dataset containing all AlepOR sequences and all HassOR, HarmOR, HvirOR, and BmOR sequences revealed that AlepOrco was clustered with other Lepidopteran Orco sequences, and four AlepOR3/4/5/6 with full-length open reading frame (ORFs) were clustered in the Lepidopteran SPR clade (Zhang Y. N. et al., 2016). Multiple alignments of *H. armigera* SPRs and their homologs in *H. virescens* showed that the orthologous SPRs in these two insects had a high similarity. The phylogenetic analyses

TABLE 1 | The CCTOP results of SPRs and Orcos from 10 families in Lepidopteran insects.

Family	Species	Receptors	Genbank ID	CCTOP	HMMTOP	Memsat	Octopus	Philius	Phobius	Pro	Prodiv	Scampi	ScampiMsa	TMHMM
Bombycidae	*Bombyx mori* (Sakurai et al., 2004; Krieger et al., 2005; Nakagawa et al., 2005)	BmOR1	NP_001036875.1	I-6-I	I-7-O	I-8-I	I-7-O	I-8-I	I-6-I	I-8-I	I-9-O	I-6-I	I-6-I	O-7-I
		BmOR3	NP_001036925.1	I-4-I	I-5-O	I-7-O	I-6-I	I-4-I	I-4-I	I-6-I	I-7-O	I-6-I	I-6-I	I-4-I
		BmOR4	NP_001036926.1	I-6-I	O-4-O	O-7-I	O-5-I	I-7-O	I-6-I	I-6-I	I-7-O	O-6-O	I-7-O	I-6-I
		BmOR5	NP_001036927.1	I-7-O	I-7-O	I-8-I	I-7-O	I-5-O	I-6-I	I-6-I	I-7-O	I-6-I	I-7-O	I-8-I
		BmOR7	NP_001106227.1	I-7-O	O-8-O	I-8-I	I-6-I	I-4-I	I-5-O	I-6-I	I-7-O	I-6-I	I-7-O	I-5-O
		BmOR9	NP_001116805.1	I-8-I	O-6-O	I-8-I	O-4-O	I-7-O	I-7-O	I-6-I	I-6-I	I-7-O	I-7-O	I-6-I
		BmOR2*	CAD88206.1	I-7-O	O-8-O	I-7-O	I-7-O	I-7-O	I-7-O	I-6-I	I-7-O	I-7-O	I-7-O	I-7-O
	Bombyx mandarina (Zhang et al., 2009)	BmanOR1	ACT34880.1	I-6-I	O-4-O	I-8-I	I-7-O	I-8-I	I-6-I	I-8-I	I-9-O	I-6-I	I-6-I	O-7-I
		BmanOR3	ACT34882.1	I-6-I	I-5-O	I-7-O	I-6-I	I-4-I	I-4-I	I-6-I	I-7-O	I-6-I	I-6-I	O-4-O
		BmanOrco*	XP_028043387.1	I-7-O	O-8-O	I-7-O	I-7-O	I-7-O	I-7-O	I-6-I	I-7-O	I-7-O	I-7-O	I-7-O
Plutellidae	*Plutella xylostella* (Mitsuno et al., 2008; Sun et al., 2013; Yang S. et al., 2017; Liu et al., 2018)	PxylOR1	AGK43824.1	I-4-I	I-6-I	O-7-I	I-6-I	I-4-I	I-4-I	I-4-I	I-6-I	I-5-O	I-6-I	I-4-I
		PxylOR3	AGK43825.1	I-6-I	I-7-O	I-7-O	I-6-I	I-6-I	I-6-I	I-4-I	I-7-O	I-6-I	I-6-I	I-6-I
		PxylOR4	AGK43826.1	I-6-I	I-7-O	I-7-O	I-6-I	I-6-I	I-6-I	I-4-I	I-9-O	I-6-I	I-6-I	I-6-I
		PxylOR5	AGK43827.1	I-6-I	I-7-O	I-6-I	O-5-I	I-6-I	O-7-I	I-4-I	I-6-I	I-7-O	I-6-I	I-6-I
		PxylOR6	AGK43828.1	I-4-I	O-4-O	I-6-I	O-5-I	I-7-O	I-4-I	I-2-I	I-7-O	I-6-I	I-7-O	I-4-I
		PxylOR7	AGK43829.1	I-4-I	O-4-O	I-8-I	O-5-I	I-4-I	I-4-I	I-4-I	I-8-I	I-7-O	I-6-I	O-3-I
		PxylOR8	ASA39901.1	I-6-I	I-7-O	I-7-O	O-5-I	I-7-O	I-6-I	I-4-I	I-7-O	I-7-O	O-8-O	O-5-I
		PxylOR41	ASA39902.1	I-6-I	I-7-O	I-8-I	I-5-O	I-6-I	I-4-I	I-4-I	I-7-O	O-5-I	I-6-I	I-4-I
		PxylOR45	ASA39903.1	I-6-I	I-7-O	I-5-O	I-5-O	I-6-I	O-7-I	I-4-I	I-7-O	O-4-O	I-5-O	I-6-I
		PxylOr83b*	NP_001296031.1	I-7-O	O-8-O	I-7-O	I-7-O	I-7-O	I-7-O	I-6-I	I-7-O	I-7-O	I-7-O	I-7-O
Sphingidae	*Manduca sexta* (Patch et al., 2009; Grosse-Wilde et al., 2010, 2011; Wicher et al., 2017)	MsexOR1	CUQ99387.1	I-6-I	I-8-I	I-7-O	I-6-I	I-4-I	I-4-I	I-6-I	I-7-O	I-6-I	I-7-O	I-5-O
/		MsexOR4	CUQ99388.1	I-6-I	O-2-O	O-7-I	I-6-I	I-6-I	I-4-I	I-4-I	I-7-O	I-6-I	I-6-I	O-4-O
		MsexOrco*	CUQ99422.1	I-7-O	O-8-O	I-7-O	I-7-O	I-7-O	I-7-O	I-6-I	I-7-O	I-8-I	I-7-O	I-7-O
Saturniidae	*Antheraea pernyi* (Forstner et al., 2009; Li et al., 2020)	AperOR1	CBH19583.1	I-6-I	I-6-I	I-6-I	I-7-O	I-6-I	I-6-I	I-6-I	I-7-O	I-7-O	I-6-I	I-8-I
		AperOR2*	CAD88205.1	I-7-O	O-8-O	I-7-O	I-7-O	I-7-O	I-7-O	I-6-I	I-7-O	I-7-O	I-7-O	O-8-O
	Antheraea polyphemus (Forstner et al., 2009; Li et al., 2020)	ApolOR1	CBH19582.1	I-7-O	I-8-I	I-8-I	I-7-O	I-8-I	I-6-I	I-6-I	I-7-O	I-7-O	I-7-O	I-8-I
		ApolOR2*	CAD88205.1	I-7-O	O-8-O	I-7-O	I-7-O	I-7-O	I-7-O	I-6-I	I-7-O	I-7-O	I-7-O	O-8-O
Geometridae	*Operophtera brumata* (Zhang D. D. et al., 2016; Li et al., 2018)	ObruOR1	AJF20961.1	I-6-I	I-6-I	I-8-I	I-6-I	I-4-I	I-6-I	I-5-O	I-7-O	I-6-I	I-6-I	I-5-O
		ObruOrco*	AJF20962.1	I-7-O	O-8-O	I-8-I	I-7-O	I-7-O	I-7-O	I-6-I	I-7-O	I-7-O	I-7-O	I-7-O
	Ectropis grisescens (Li et al., 2017, 2018)	EgriOR31												
		EgriOrco*												
Nymphalidae	*Danaus plexippus* (Zhan et al., 2011)	DpleOR1	OWR49463.1	O-5-I	O-4-O	I-8-I	O-6-O	I-6-I	O-5-I	I-4-I	I-7-O	O-8-O	I-7-O	O-5-I
		DpleOR2*	OWR42934.1	I-7-O	I-7-O	I-8-I	I-7-O	I-7-O	I-7-O	I-6-I	I-7-O	I-7-O	I-7-O	

(Continued)

TABLE 1 | (Continued)

Family	Species	Receptors	Genbank ID	CCTOP	HMMTOP	Memsat	Octopus	Philius	Phobius	Pro	Prodiv	Scampi	ScampiMsa	TMHMM
Noctuidae	*Mythimna separata* (Mitsuno et al., 2008; Jiang et al., 2019, 2020; Tang et al., 2020)	MsepOR2	QEI49013.1	I-6-I	I-6-I	I-8-I	O-8-O	I-5-O	O-5-I	I-4-I	I-7-O	O-7-I	O-7-I	I-3-O
		MsepOR3	QEI49012.1	I-7-O	I-6-I	I-8-I	I-7-O	I-5-O	I-7-O	I-4-I	I-7-O	I-6-I	I-7-O	I-6-I
		MsepOrco*	QEI49014.1	I-7-O	I-7-O	I-7-O	I-7-O	I-7-O	I-7-O	I-6-I	I-7-O	I-7-O	I-7-O	I-7-O
	Heliothis virescens (Krieger et al., 2004; Grosse-Wilde et al., 2007; Wang et al., 2011)	HvirOR6	CAD31948.1	I-6-I	I-8-I	I-8-I	I-6-I	I-8-I	I-6-I	I-6-I	I-8-I	I-6-I	O-7-I	I-6-I
		HvirOR11	CAG38112.1	I-6-I	O-8-O	I-7-O	I-6-I	I-6-I	I-6-I	I-5-O	I-7-O	I-6-I	I-6-I	I-6-I
		HvirOR13	CAG38114.1	I-5-O	I-4-I	I-7-O	O-5-I	I-5-O	I-5-O	I-4-I	I-7-O	O-8-O	I-7-O	I-5-O
		HvirOR14	CAG38115.1	I-6-I	I-8-I	I-7-O	I-5-O	I-6-I	I-4-I	I-4-I	I-7-O	I-5-O	I-6-I	I-5-O
		HvirOR15	CAG38116.1	O-5-I	O-6-O	O-8-O	I-7-O	I-6-I	O-5-I	I-6-I	O-8-O	O-7-I	O-7-I	I-4-I
		HvirOR16	CAG38117.1	I-6-I	O-7-I	I-7-O	I-6-I	I-5-O	I-4-I	I-6-I	I-7-O	I-6-I	O-7-I	I-3-O
		HvirOR2*	CAD31851.1	I-7-O	I-7-O	I-7-O	I-7-O	I-7-O	I-7-O	I-6-I	I-7-O	O-8-O	I-7-O	I-7-O
	Spodoptera littoralis (Legeai et al., 2011; Montagne et al., 2012; De Fouchier et al., 2015)	SlitOR6	ACL81183.1	I-6-I	I-9-O	I-7-O	I-6-I	I-2-I	O-3-I	I-4-I	I-7-O	I-4-I	I-6-I	O-2-O
		SlitOR11	ACL81180.1	I-6-I	O-8-O	I-7-O	I-6-I	I-6-I	I-6-I	O-4-O	I-7-O	I-6-I	I-6-I	O-7-I
		SlitOR13	ACL81181.1	I-7-O	I-6-I	I-7-O	I-6-I	I-7-O	I-7-O	I-4-I	I-7-O	I-7-O	I-7-O	I-5-O
		SlitOR16	ACL81182.1	I-6-I	O-8-O	O-9-I	I-6-I	I-5-O	O-5-I	I-6-I	O-9-I	I-6-I	I-6-I	I-4-I
		SlitOR83b*	ACJ06648.1	I-7-O	I-7-O	I-7-O	I-7-O	I-7-O	I-7-O	I-6-I	I-7-O	I-7-O	I-7-O	I-7-O
	Spodoptera exigua (De Fouchier et al., 2015; Du et al., 2018; Zhang et al., 2018)	SexiOR6	AGH58119.1	I-4-I	O-5-L	O-6-O	I-5-O	I-5-O	I-4-I	I-2-I	I-8-I	I-6-I	I-6-I	I-5-O
		SexiOR11	AGH58120.1	I-6-I	O-8-O	I-7-O	I-6-I	I-6-I	I-6-I	O-4-O	I-7-O	I-6-I	I-6-I	O-7-I
		SexiOR13	AGH58121.1	I-7-O	I-6-I	I-7-O	I-6-I	I-7-O	I-7-O	I-4-I	I-7-O	I-6-I	I-7-O	I-5-O
		SexiOR16	AGH58122.1	I-6-I	O-9-I	O-9-I	I-6-I	I-6-I	O-5-I	O-6-I	I-7-O	I-6-I	I-6-I	I-4-I
		SexiOR2*	AAW52583.1	I-7-O	O-8-O	I-7-O	I-7-O	I-7-O	I-7-O	I-6-I	I-7-O	I-7-O	I-7-O	I-7-O
	Sesamia inferens (Zhang et al., 2013, 2014)	SinfOR21	AGY14579.2	I-6-I	O-7-I	I-8-I	O-5-I	I-6-I	I-8-I	I-6-I	I-7-O	I-6-I	O-7-I	I-3-O
		SinfOR27	AGY14585.2	I-4-I	I-8-I	I-7-O	O-6-O	I-4-I	I-4-I	I-6-I	I-7-O	I-6-I	I-7-O	I-5-O
		SinfOR29	AGY14587.2	I-4-I	I-5-O	I-7-O	I-7-O	I-4-I	O-5-I	I-4-I	I-7-O	O-7-I	O-7-I	I-4-I
		SinfOR2*	AGY14565.1	I-7-O	I-7-O	I-7-O	I-7-O	I-7-O	I-7-O	I-6-I	I-7-O	I-7-O	I-7-O	I-7-O
	Athetis lepigone (Zhang Y. N. et al., 2016, Zhang et al., 2019)	AlepOR3	AOE48008.1	I-6-I	I-6-I	I-8-I	I-7-O	I-8-I	I-4-I	I-6-I	I-7-O	I-6-I	I-6-I	I-6-I
		AlepOR4	AOE48009.1	I-6-I	I-8-I	O-6-O	O-6-O	I-6-I	I-4-I	I-6-I	I-7-O	I-6-I	I-8-I	I-4-I
		AlepOR5	AOE48010.1	I-6-I	I-6-I	I-7-O	I-6-I	I-6-I	O-5-I	I-6-I	I-7-O	O-7-I	O-8-O	I-4-I
		AlepOR6	AOE48011.1	I-6-I	I-8-I	I-8-I	I-6-I	I-6-I	I-6-I	I-4-I	I-7-O	I-6-I	I-6-I	I-8-I
		AlepOrco*	AOE48007.1	I-7-O	I-7-O	I-7-O	I-7-O	I-7-O	I-7-O	I-6-I	I-7-O	I-7-O	I-7-O	I-7-O
	Helicoverpa armigera (Zhang et al., 2010; Liu et al., 2012, Liu Y. et al., 2013; Liu et al., 2014; Jiang et al., 2014; Chang et al., 2016)	HarmOR1	ACS45304.1	I-7-O	I-5-O	I-8-I	O-5-I	I-5-O	O-6-O	I-4-I	I-7-O	I-6-I	I-7-O	O-4-O
		HarmOR2	ACS45305.1	I-6-I	O-8-O	I-7-O	I-6-I	I-6-I	I-6-I	I-5-O	I-7-O	I-6-I	I-6-I	I-6-I
		HarmOR3	ACS45306.1	I-6-I	O-7-I	I-7-O	O-5-I	I-5-O	I-4-I	I-6-I	I-7-O	I-6-I	O-7-I	O-4-O

(Continued)

TABLE 1 | (Continued)

Family	Species	Receptors	Genbank ID	CCTOP	HMMTOP	Memsat	Octopus	Philius	Phobius	Pro	Prodiv	Scampi	ScampiMsa	TMHMM
		HarmOR6	AIG51854.1	I-8-I	O-9-I	I-8-I	I-6-I	I-7-O	I-8-I	I-6-I	I-7-O	I-6-I	I-6-I	I-8-I
		HarmOR11	AIG51859.1	I-6-I	O-8-O	I-7-O	I-6-I	I-6-I	I-6-I	I-5-O	I-7-O	I-6-I	I-6-I	I-6-I
		HarmOR13	AIG51861.1	I-7-O	I-5-O	O-8-O	O-6-O	I-5-O	O-6-O	I-2-I	I-7-O	I-6-I	I-7-O	O-4-O
		HarmOR14	AJG42377.1	I-4-I	O-4-O	I-7-O	I-6-I	I-4-I	I-4-I	O-5-I	I-7-O	I-6-I	I-6-I	I-4-I
		HarmOR15	AIG51863.1	I-6-I	O-9-I	I-7-O	I-7-O	I-6-I	I-4-I	I-6-I	I-7-O	I-6-I	I-6-I	I-4-I
		HarmOR16	QLF97404.1	I-6-I	O-8-O	I-8-I	I-6-I	I-5-O	I-4-I	I-6-I	I-7-O	I-6-I	O-7-I	I-3-O
		HarmOR6-1	AGK90000.1	I-8-I	I-8-I	I-8-I	I-7-O	I-7-O	I-8-I	I-6-I	I-7-O	I-6-I	I-6-I	I-5-O
		HarmOR14a	AGK90005.1	I-4-I	I-4-I	I-7-O	I-7-O	I-4-I	I-4-I	I-6-I	I-7-O	I-5-O	O-7-I	I-4-I
		HarmOR14b	AGK90006.1	I-4-I	O-2-2	I-6-I	I-6-I	I-4-I	I-4-I	I-6-I	I-7-O	I-6-I	I-8-I	I-4-I
		HarmOr83b*	ADQ13177.1	I-7-O	I-7-O	I-7-O	I-7-O	I-7-O	I-7-O	I-6-I	I-7-O	O-8-O	I-7-O	I-7-O
	Helicoverpa assulta (Zhang et al., 2010; Jiang et al., 2014; Xu et al., 2015; Chang et al., 2016)	HassOR1	ACS45307.1	I-7-O	I-7-O	I-8-I	O-6-O	I-5-O	O-6-O	I-2-I	I-7-O	I-6-I	I-7-O	O-7-I
		HassOR2	ACS45308.1	I-6-I	O-8-O	I-7-O	I-6-I	I-6-I	I-6-I	I-5-O	I-7-O	I-6-I	I-6-I	I-6-I
		HassOR3	ACS45309.1	I-6-I	I-6-I	I-7-O	I-6-I	I-5-O	I-4-I	I-6-I	I-7-O	I-6-I	I-6-I	O-4-O
		HassOR6	AGK90014.1	I-6-I	I-8-I	I-8-I	I-6-I	I-6-I	I-6-I	I-6-I	I-7-O	O-7-I	I-6-I	I-8-I
		HassOR11	AJD81549.1	I-6-I	I-7-O	I-7-O	I-6-I	I-6-I	I-6-I	I-5-O	I-7-O	I-6-I	I-6-I	I-6-I
		HassOR13	AJD81551.1	I-7-O	I-5-O	I-8-I	O-6-O	I-5-O	I-7-O	I-2-I	I-7-O	I-6-I	I-7-O	O-7-I
		HassOR14	AHI44516.1	I-4-I	O-3-I	I-7-O	I-6-I	I-4-I	I-4-I	I-4-I	I-7-O	I-5-O	O-7-I	I-4-I
		HassOR14b	AGK90019.1	I-4-I	O-7-I	I-7-O	I-7-O	I-4-I	I-4-I	I-6-I	I-7-O	I-5-O	I-6-I	I-4-I
		HassOR15	AJD81553.1											
		HassOR16	AJD81554.1	I-6-I	I-6-I	I-7-O	I-7-O	I-4-I	I-4-I	I-6-I	I-7-O	I-6-I	I-6-I	O-4-O
		HassOr83b*	ABU45983.2	I-7-O	I-7-O	I-7-O	I-7-O	I-7-O	I-7-O	I-6-I	I-7-O	O-8-O	I-7-O	I-7-O
	Agrotis segetum (Zhang and Lofstedt, 2013)	AsegOR1	AGS41441.1	I-5-O	I-6-I	O-8-O	I-7-O	I-5-O	O-5-I	I-4-I	I-7-O	O-7-I	O-8-O	I-4-I
		AsegOR3	AGS41442.1	I-6-I	O-6-O	I-7-O	O-5-I	I-6-I	O-5-I	I-4-I	I-7-O	I-6-I	I-6-I	O-7-I
		AsegOR4	AGS41443.1	I-7-O	I-7-O	I-8-I	I-6-I	I-5-O	O-4-O	I-6-I	I-7-O	I-5-O	I-6-I	O-6-O
		AsegOR5	AGS41444.1	I-4-I	I-8-I	I-8-I	I-6-I	I-6-I	O-5-I	I-4-I	I-7-O	I-6-I	O-7-I	I-4-I
		AsegOR6	AGS41445.1	I-6-I	I-8-I	O-8-O	I-6-I	I-6-I	O-5-I	I-4-I	I-7-O	O-7-I	O-7-I	O-4-O
		AsegOR7	AGS41446.1	I-4-I	O-9-I	I-8-I	I-7-O	I-5-O	I-4-I	I-6-I	I-7-O	O-7-I	I-7-O	I-4-I
		AsegOR8	AGS41447.1	I-7-O	I-8-I	O-8-O	I-7-O	I-6-I	O-5-I	I-4-I	I-7-O	O-7-I	O-8-O	I-5-O
		AsegOR9	AGS41448.1	I-6-I	O-7-I	I-7-O	I-7-O	I-6-I	I-5-O	I-4-I	I-7-O	O-7-I	O-8-O	I-5-O
		AsegOR10	AGS41449.1	O-7-I	I-8-I	I-7-O	I-5-O	O-7-I	O-5-I	O-7-I	O-9-I	O-7-I	O-7-I	I-4-I
		AsegOrco*	AGS41440.1	I-7-O	O-8-O	I-7-O	I-7-O	I-7-O	I-7-O	I-6-I	I-7-O	I-7-O	I-7-O	I-7-O
	Spodoptera litura (Wu et al., 2013; Feng et al., 2015; Lin et al., 2015; Zhang et al., 2015)	SlituOR6	AGI96748.1	I-6-I	I-9-O	I-7-O	I-6-I	I-3-O	O-3-I	I-4-I	I-7-O	I-4-I	I-6-I	O-2-O
		SlituOR11	AGI96749.1	I-6-I	O-8-O	I-7-O	I-6-I	I-6-I	I-6-I	I-5-O	I-7-O	I-6-I	I-6-I	O-7-I
		SlituOR13	AGI96750.1	I-7-O	I-6-I	I-7-O	I-6-I	I-7-O	I-7-O	I-6-I	I-7-O	I-7-O	I-7-O	I-5-O
		SlituOR16	AGI96751.1	I-4-I	O-9-I	O-9-I	I-7-O	I-5-O	O-5-I	I-6-I	I-7-O	O-7-I	O-7-I	I-4-I
		SlituOrco*	XP_022831582.1	I-7-O	O-8-O	I-7-O	I-7-O	I-7-O	I-7-O	I-6-I	I-7-O	I-7-O	I-7-O	I-7-O

(Continued)

TABLE 1 | (Continued)

Family	Species	Receptors	Genbank ID	CCTOP	HMMTOP	Memsat	Octopus	Philius	Phobius	Pro	Prodiv	Scampi	ScampiMsa	TMHMM
Tortricidae	*Ctenopseustis obliquana* (Steinwender et al., 2015; Grapputo et al., 2018)	CoblOR1	AIT71977.1	I-5-O	I-1-O	O-7-I	I-4-I	I-5-O	I-5-O	I-2-I	I-7-O	I-5-O	I-6-I	O-4-O
		CoblOR6	AIT71981.1	I-3-O	I-1-O	O-7-I	I-4-I	I-3-O	I-2-I	I-2-I	I-7-O	I-3-O	I-6-I	I-1-O
		CoblOR7	AIT71982.1	I-4-I	I-1-O	O-7-I	I-4-I	I-5-O	I-4-I	I-5-O	I-6-I	I-5-O	I-7-O	I-4-I
		CoblOR22	AIT71991.1	I-5-O	O-5-I	O-7-I	I-5-O	I-5-O	O-6-O	I-4-I	O-7-I	I-5-O	I-5-O	I-5-O
		CoblOR45a	AIT72004.1	I-6-I	I-2-I	O-7-I	I-7-O	I-3-O	I-2-I	I-2-I	I-6-I	I-7-O	I-6-I	I-1-O
		CoblOR45b	AIT72005.1	I-4-I	I-3-O	I-8-I	O-5-I	I-5-O	I-2-I	I-2-I	I-8-I	I-7-O	I-6-I	I-4-I
		CoblOrco*	AIT72022.1	I-7-O	O-8-O	I-7-O	I-7-O	I-7-O	I-7-O	I-6-I	I-7-O	I-7-O	I-7-O	I-7-O
	Epiphyas postvittana (Jordan et al., 2009; Corcoran et al., 2015)	EposOR1	ACJ12927	I-6-I	O-2-O	O-7-I	O-5-I	I-4-I	I-2-I	I-2-I	I-6-I	I-3-O	I-6-I	I-3-O
		EposOR6	JAI18060.1	I-4-I	I-5-O	I-6-I	I-5-O	I-4-I	I-4-I	I-4-I	I-7-O	I-6-I	I-6-I	I-4-I
		EposOR7	JAI18059.1	I-6-I	O-5-I	I-8-I	I-5-O	I-4-I	I-5-O	I-4-I	I-7-O	I-7-O	I-6-I	I-6-I
		EposOR21	JAI18051.1	I-6-I	I-7-O	O-7-I	I-6-I	O-7-I	O-7-I	I-6-I	I-7-O	I-7-O	I-6-I	I-6-I
		EposOR22	JAI18050.1	I-5-O	O-8-O	I-7-O	I-5-O	I-5-O	I-5-O	I-4-I	I-7-O	I-6-I	I-6-I	I-5-O
		EposOR41	JAI18032.1	I-6-I	I-1-O	I-8-I	O-6-O	I-5-O	I-3-O	I-2-I	I-7-O	I-7-O	I-6-I	I-4-I
		EposOR43	JAI18030.1	I-6-I	I-1-O	O-6-O	O-6-O	I-6-I	I-6-I	I-3-O	I-8-I	I-6-I	I-6-I	I-6-I
		EposOR45	JAI18028.1	I-6-I	I-2-I	I-6-I	I-4-I	I-4-I	I-6-I	I-4-I	I-8-I	I-4-I	I-6-I	I-6-I
		EposOR2*	ACJ12928.2	I-7-O	I-7-O	I-7-O	I-7-O	I-7-O	I-7-O	I-6-I	I-7-O	I-7-O	I-7-O	I-7-O
	Cydia pomonella (Bengtsson et al., 2012; Walker et al., 2016; Tian et al., 2020)	CpomOR1	AFC91714.1	I-6-I	O-4-O	I-8-I	I-7-O	I-6-I	O-5-I	I-4-I	I-6-I	O-6-O	O-7-I	I-5-O
		CpomOR2a	AFC91715.2	I-6-I	O-4-O	I-7-O	I-6-I	I-5-O	I-6-I	I-6-I	I-7-O	I-6-I	I-6-I	I-5-O
		CpomOR2b	JAP38462.1	I-5-O	O-5-I	I-7-O	I-6-I	I-5-O	I-5-O	I-6-I	I-7-O	I-6-I	I-6-I	I-5-O
		CpomOR2c	JAP38461.1	I-6-I	I-5-O	I-8-I	I-6-I	I-4-I	I-4-I	O-7-I	I-7-O	I-6-I	I-6-I	I-5-O
		CpomOR3	AFC91713.2	I-6-I	I-7-O	I-7-O	O-6-O	I-6-I	I-6-I	I-6-I	I-7-O	I-6-I	I-6-I	I-6-I
		CpomOR4	AFC91716.2	O-7-I	O-4-O	O-8-O	I-7-O	O-5-I	O-5-I	O-7-I	O-8-O	I-5-O	I-6-I	O-6-O
		CpomOR5	JAP38459.1	I-6-I	I-2-I	I-8-I	I-7-O	I-6-I	O-7-I	I-6-I	I-7-O	I-6-I	I-6-I	I-7-O
		CpomOR6a	AFC91711.2	I-6-I	I-6-I	O-7-I	I-3-O	I-5-O	O-5-I	I-3-O	I-7-O	I-6-I	I-6-I	I-3-O
		CpomOR6b	JAP38458.1	I-7-O	I-7-O	I-7-O	I-4-I	I-5-O	O-6-O	I-3-O	I-7-O	I-7-O	I-7-O	I-5-O
		CpomOR7	JAP38457.1	I-6-I	I-7-O	I-8-I	O-5-I	I-7-O	I-6-I	I-4-I	I-7-O	I-7-O	I-6-I	I-7-O
		CpomOR8	JAP38456.1	I-6-I	I-6-I	I-7-O	I-7-O	I-6-I	I-6-I	I-6-I	I-7-O	I-7-O	I-6-I	I-7-O
		CpomOR9	JAP38455.1	I-6-I	I-6-I	I-8-I	I-3-O	I-6-I	I-6-I	I-2-I	I-6-I	I-7-O	I-7-O	O-4-O
		CpomOR21	JAP38451.1											
		CpomOR22	AFC91723.2	I-6-I	O-6-O	I-7-O	I-6-I	I-5-O	I-5-O	I-6-I	I-7-O	I-5-O	I-6-I	I-6-I
		CpomOrco*	AFC91712.1	I-7-O	I-7-O	I-7-O	I-7-O	I-7-O	I-5-O	I-6-I	I-7-O	I-7-O	I-7-O	I-7-O
	Cydia fagiglandana (Gonzalez et al., 2017)	CfagOR1	AST36293.1	I-6-I	I-6-I	I-8-I	I-6-I	I-6-I	I-5-O	I-6-I	I-7-O	I-5-O	I-6-I	I-6-I
		CfagOR2.1	AST36294.1											
		CfagOR2.2	AST36295.1											
		CfagOR3	AST36296.1	I-5-O	I-6-I	I-7-O	I-5-O	I-5-O	I-4-I	I-5-O	I-7-O	I-6-I	I-6-I	I-5-O
		CfagOR4	AST36297.1	O-4-O	I-6-I	O-7-I	O-6-O	I-3-O	O-4-O	I-4-I	I-7-O	I-6-I	I-8-I	O-4-O
		CfagOR5.1	AST36298.1	I-6-I	I-6-I	O-8-O	I-7-O	I-6-I	I-6-I	I-6-I	I-7-O	I-5-O	I-6-I	I-6-I
		CfagOR5.2	AST36299.1											

(Continued)

TABLE 1 | (Continued)

Family	Species	Receptors	Genbank ID	CCTOP	HMMTOP	Memsat	Octopus	Philius	Phobius	Pro	Prodiv	Scampi	ScampiMsa	TMHMM
		CfagOR6	AST36300.1	I-6-I	I-6-I	O-6-O	I-4-I	I-5-O	O-5-I	I-4-I	I-7-O	I-7-O	I-6-I	O-4-O
		CfagOR7	AST36301.1	I-6-I	I-7-O	I-7-O	O-5-I	I-6-I	I-6-I	I-4-I	I-7-O	I-6-I	I-6-I	I-6-I
		CfagOR8	AST36302.1	I-4-I	O-5-I	I-8-I	O-6-O	I-4-I	I-4-I	I-2-I	I-7-O	I-6-I	I-6-I	I-5-O
		CfagOrco*	AST36341.1	I-7-O	I-7-O	I-7-O	I-7-O	I-7-O	I-7-O	I-6-I	I-7-O	I-7-O	I-7-O	I-7-O
	Ctenopseustis herana (Steinwender et al., 2015; Grapputo et al., 2018)	CherOR1a	AIT69867.1	I-6-I	I-3-O	O-7-I	I-6-I	I-4-I	I-6-I	I-2-I	I-9-O	I-6-I	I-6-I	I-5-O
		CherOR1b	AIT69868.1	I-5-O	I-3-O	O-7-I	O-4-O	I-5-O	I-5-O	I-2-I	I-7-O	I-5-O	I-6-I	I-5-O
		CherOR6	AIT69872.1	I-3-O	I-1-O	O-7-I	I-4-I	I-3-O	I-2-I	I-2-I	I-7-O	I-3-O	I-6-I	I-1-O
		CherOR7	AIT69873.1	I-4-I	I-2-I	I-7-O	I-6-I	I-5-O	I-4-I	I-3-O	I-5-O	I-5-O	I-6-I	I-4-I
		CherOR45	AIT69894.1	I-6-I	O-3-I	O-7-I	O-6-O	I-5-O	I-4-I	I-2-I	I-8-I	I-7-O	I-6-I	I-6-I
		CherOrco*	AIT69913.1	I-7-O	O-8-O	I-7-O	I-7-O	I-7-O	I-7-O	I-6-I	I-7-O	I-7-O	I-7-O	I-7-O
	Planotortrix octo (Steinwender et al., 2016; Grapputo et al., 2018)	PoctOR1	AJF23780.1	I-5-O	I-1-O	I-8-I	O-4-O	I-5-O	I-5-O	I-5-O	I-7-O	I-5-O	I-6-I	I-5-O
		PoctOR6	AJF23784.1	I-5-O	I-1-O	I-8-I	I-4-I	I-5-O	I-3-O	I-2-I	I-8-I	I-4-I	I-6-I	I-1-O
		PoctOR7	AJF23785.1	I-4-I	I-1-O	I-6-I	I-4-I	I-5-O	I-4-I	I-4-I	I-7-O	I-5-O	I-7-O	I-4-I
		PoctOR21	AJF23792.1	I-6-I	I-5-O	I-8-I	I-5-O	I-4-I	I-6-I	I-2-I	I-7-O	I-5-O	I-6-I	I-6-I
		PoctOR22	AJF23793.1	O-6-O	O-7-I	O-7-I	I-5-O	O-6-O	O-6-O	O-5-I	O-7-I	O-7-I	O-6-O	I-5-O
		PoctOR45	AJF23806.1	I-6-I	I-2-I	I-8-I	O-5-I	I-5-O	I-4-I	I-4-I	I-6-I	I-7-O	I-6-I	I-3-O
		PoctOrco*	AJF23826.1	I-7-O	O-8-O	I-7-O	I-7-O	I-7-O	I-7-O	I-6-I	I-7-O	I-7-O	I-7-O	I-7-O
	Planotortrix excessana (Steinwender et al., 2016; Grapputo et al., 2018)	PexcOR1	AJE25866.1	I-5-O	I-3-O	I-8-I	O-4-O	I-5-O	I-5-O	I-5-O	I-7-O	I-5-O	I-6-I	I-5-O
		PexcOR7	AJE25869.1	I-5-O	I-2-I	I-8-I	I-5-O	I-5-O	I-4-I	I-4-I	I-5-O	I-6-I	I-7-O	I-5-O
		PexcOR22	AJE25877.1	I-5-O	O-5-I	I-8-I	I-5-O	I-5-O	I-5-O	I-4-I	I-6-I	I-6-I	I-6-I	I-4-I
		PexcOR45	AJE25890.1	I-7-O	O-4-O	I-7-O	I-6-I	I-5-O	I-6-I	I-4-I	I-7-O	I-7-O	I-7-O	I-6-I
		PexcOrco*	AJE25910.1											
	Hedya nubiferana (Grapputo et al., 2018)	HnubOR2.1	AST36245.1	I-6-I	I-7-O	I-7-O	I-4-I	I-6-I	I-6-I	I-4-I	I-8-I	I-7-O	I-7-O	I-6-I
		HnubOR2.2	AST36246.1	I-6-I	O-6-O	I-8-I	I-4-I	I-6-I	I-8-I	I-4-I	I-7-O	I-7-O	I-6-I	I-8-I
		HnubOR3	AST36247.1	I-5-O	I-8-I	I-8-I	I-5-O	I-5-O	I-5-O	I-3-O	I-8-I	I-7-O	I-6-I	I-8-I
		HnubOR6	AST36248.1											
		HnubOR8.1	AST36249.1	I-7-O	I-6-I	O-7-I	I-7-O	I-5-O	I-5-O	I-4-I	I-7-O	I-6-I	I-7-O	I-6-I
		HnubOR8.2	AST36250.1	I-5-O	I-5-O	O-7-I	I-5-O	I-5-O	I-4-I	I-5-O	I-6-I	I-5-O	I-7-O	I-5-O
		HnubOrco*	AST36292.1											
	Cydia nigricana (Gonzalez et al., 2017)	CnigOR1	AST36373.1	I-6-I	I-6-I	O-7-I	I-6-I	I-6-I	I-5-O	I-6-I	I-7-O	I-5-O	I-6-I	I-5-O
		CnigOR2	AST36374.1	I-6-I	I-5-O	I-8-I	I-7-O	I-4-I	O-5-I	I-6-I	I-7-O	I-5-O	I-6-I	I-5-O
		CnigOR5	AST36376.1	I-6-I	I-6-I	O-8-O	I-7-O	I-6-I	I-6-I	I-6-I	I-7-O	I-5-O	I-6-I	I-6-I
		CnigOR6	AST36377.1	O-6-O	I-6-I	O-6-O	O-6-O	I-5-O	O-3-I	I-4-I	I-7-O	I-7-O	I-7-O	O-4-O
		CnigOR7	AST36378.1	I-7-O	O-5-I	I-8-I	I-5-O	I-5-O	I-7-O	I-2-I	I-7-O	I-7-O	I-6-I	I-7-O
		CnigOR8	AST36379.1	I-7-O	I-6-I	I-7-O	O-6-O	I-5-O	I-6-I	I-4-I	I-7-O	I-6-I	I-7-O	I-5-O
		CnigOR9	AST36380.1	I-6-I	O-8-O	I-7-O	O-5-I	I-4-I	I-4-I	I-4-I	I-7-O	I-7-O	I-6-I	O-4-O
		CnigOrco*	AST36420.1	I-7-O	I-7-O	I-7-O	I-7-O	I-7-O	I-7-O	I-6-I	I-7-O	I-7-O	I-7-O	I-7-O

(Continued)

TABLE 1 | (Continued)

Family	Species	Receptors	Genbank ID	CCTOP	HMMTOP	Memsat	Octopus	Philius	Phobius	Pro	Prodiv	Scampi	ScampiMsa	TMHMM
	Lobesia botrana (Rojas et al., 2018)	LobOR1	AXF48756.1	I-6-I	O-5-I	I-8-I	O-5-I	I-6-I	O-7-I	I-6-I	I-7-O	I-9-O	O-7-I	I-6-I
		LobOR2.1	AXF48757.1											
		LobOR2.2	AXF48758.1	O-4-O	O-4-O	I-6-I	O-3-I	I-4-I	I-4-I	I-4-I	I-4-I	I-3-O	I-4-I	I-4-I
		LobOR2.3	AXF48759.1	I-5-O	I-5-O	I-5-O	I-5-O	I-6-I	I-6-I	I-4-I	I-6-I	I-5-O	I-5-O	I-5-O
		LobOR2.4	AXF48760.1	I-6-I	I-8-I	I-7-O	I-6-I	I-4-I	I-4-I	I-6-I	I-7-O	I-6-I	I-6-I	I-6-I
		LobOR3.1	AXF48761.1											
		LobOR4.2	AXF48764.1											
		LobOR6	AXF48766.1											
		LobOR38.2	AXF48785.1											
		LobOR76	AXF48812.1											
		LobOrco*	AXF48755.1	I-7-O	I-7-O	I-7-O	I-7-O	I-7-O	I-7-O	I-6-I	I-7-O	I-7-O	I-7-O	I-7-O
	Planotortrix notophaea (Carraher et al., 2012)	PnotOR1	AET06153.1											
		PnotOR2*	AET06159.1											
Pyralidae	*Amyelois transitella* (Xu et al., 2012; Garczynski and Leal, 2015)	AtraOR1	AFP54146.1	I-6-I	I-5-O	I-8-I	O-4-O	I-4-I	I-6-I	I-4-I	I-6-I	I-6-I	I-6-I	I-4-I
		AtraOR3	AFP54147.1	I-5-O	I-7-O	I-8-I	O-4-O	I-5-O	O-6-O	I-4-I	I-8-I	O-6-O	O-5-I	I-4-I
		AtraOR4	AFP66948.1	I-6-I	I-7-O	I-8-I	I-7-O	I-6-I	I-6-I	I-6-I	I-7-O	I-6-I	I-6-I	I-6-I
		AtraOR4A	AFP66949.1	I-7-O	I-7-O	I-7-O	I-6-I	I-7-O	I-6-I	I-7-O	I-7-O	I-6-I	I-7-O	I-6-I
		AtraOrco*	AFP54145.1	I-7-O	O-8-O	I-8-I	I-7-O	I-7-O	I-7-O	I-6-I	I-7-O	I-7-O	I-7-O	I-7-O
Crambidae	*Diaphania indica* (Mitsuno et al., 2008)	DindOR1	BAG71417.1	I-6-I	O-6-O	I-8-I	O-5-I	I-8-I	O-5-I	I-4-I	I-7-O	I-7-O	I-7-O	I-6-I
		DindOR3	BAG71424.1	I-6-I	I-5-O	I-7-O	I-6-I	I-6-I	I-7-I	I-6-I	I-7-O	O-8-O	I-8-I	I-5-O
		DindOR2*	BAG71418.1	I-7-O	O-8-O	I-7-O	I-7-O	I-7-O	I-7-O	I-6-I	I-7-O	I-7-O	I-7-O	I-7-O
	Ostrinia latipennis (Miura et al., 2009)	OlatOR1	BAH57981.1	I-7-O	I-7-O	I-8-I	I-7-O	I-4-I	I-7-O	I-4-I	I-7-O	I-7-O	I-6-I	I-4-I
		OlatOR3	BAI66617.1											
		OlatOR4	BAI66618.1											
		OlatOR5a	BAI66619.1											
		OlatOR5b	BAI66620.1											
		OlatOR7	BAI66621.1											
		OlatOR8	BAI66622.1											
		OlatOR2*	BAH57974.1	I-7-O	O-8-O	I-7-O	I-7-O	I-7-O	I-7-O	I-6-I	I-7-O	I-7-O	I-7-O	I-7-O
	Ostrinia nubilalis (Miura et al., 2009, 2010; Wanner et al., 2010; Yasukochi et al., 2011; Leary et al., 2012)	OnubOR1	BAH57980.1											
		OnubOR3	BAI66623.1											
		OnubOR4	BAI66624.1											
		OnubOR5	BAI66625.3											
		OnubOR6	BAI66626.1											
		OnubOR7	BAI66627.1											
		OnubOR8	BAJ61934.1	I-7-O	I-7-O	I-7-O	O-5-I	I-5-O	I-7-O	I-5-O	I-7-O	I-7-O	I-7-O	O-7-I

(Continued)

TABLE 1 | (Continued)

Family	Species	Receptors	Genbank ID	CCTOP	HMMTOP	Memsat	Octopus	Philius	Phobius	Pro	Prodiv	Scampi	ScampiMsa	TMHMM
		OnubOR2*	ADB89179.1	I-7-O	I-7-O	I-7-O	I-7-O	I-7-O	I-7-O	I-6-I	I-7-O	I-7-O	I-7-O	I-7-O
	Conogethes punctiferalis (Ge et al., 2016; Jia et al., 2016)	CpunOR1	ARO76407.1	I-6-I	I-7-O	I-7-O	I-6-I	I-6-I	I-4-I	I-4-I	O-9-I	I-6-I	I-7-O	I-4-I
		CpunOR3	ARO76409.1	I-4-I	O-4-O	I-5-O	I-4-I	I-4-I	I-2-I	I-4-I	I-5-O	I-4-I	I-4-I	O-4-O
		CpunOR4	ARO76410.1											
		CpunOR5	ARO76411.1	I-7-O	I-6-I	O-7-I	I-7-O	I-7-O	I-6-I	I-4-I	I-7-O	I-8-I	I-9-O	I-4-I
		CpunOR6	ARO76412.1											
		CpunOR7	ARO76413.1	I-6-I	O-6-O	I-6-I	O-8-O	I-5-O	I-6-I	I-6-I	I-6-I	I-8-I	O-8-O	O-7-I
		CpunOR8	ARO76414.1	I-6-I	I-5-O	I-8-I	I-6-I	I-6-I	O-5-I	I-4-I	I-7-O	I-7-O	I-7-O	I-6-I
		CpunOR9	ARO76415.1	I-6-I	O-5-I	I-8-I	I-6-I	I-5-O	O-6-O	I-4-I	I-7-O	I-5-O	I-6-I	I-6-I
		CpunOR2*	ARO76408.1	I-7-O	O-8-O	I-7-O	I-7-O	I-7-O	I-7-O	I-6-I	I-7-O	I-7-O	I-7-O	I-7-O
	Ostrinia furnacalis (Miura et al., 2009, 2010; Leary et al., 2012)	OfurOR1	BAH57982.1	I-5-O	I-6-I	I-8-I	O-6-O	I-5-O	I-5-O	I-5-O	I-7-O	I-7-O	I-7-O	I-5-O
		OfurOR3	AFK30395.1	I-7-O	O-4-O	I-7-O	O-5-I	I-7-O	I-7-O	I-6-I	I-7-O	I-7-O	I-7-O	O-6-O
		OfurOR4	AFK30397.1	I-6-I	I-6-I	O-7-I	I-7-O	I-5-O	I-8-I	I-6-I	I-7-O	I-6-I	I-6-I	I-5-O
		OfurOR5	BAI66613.1											
		OfurOR6	AFK30403.1	I-7-O	I-7-O	I-7-O	I-7-O	I-7-O	I-7-O	I-3-O	I-7-O	I-7-O	I-6-I	O-7-I
		OfurOR7	AGG91649.1	I-4-I	O-4-O	O-9-I	I-4-I	I-4-I	O-5-I	I-2-I	I-9-O	I-7-O	I-7-O	I-2-I
		OfurOR8	AGG91650.1	I-5-O	I-7-O	I-7-O	O-4-O	I-5-O	I-7-O	I-5-O	I-7-O	I-7-O	I-7-O	I-5-O
		OfurOR2*	AGG91643.1	I-7-O	O-8-O	I-7-O	I-7-O	I-7-O	I-7-O	I-6-I	I-7-O	I-7-O	I-7-O	I-7-O
	Ostrinia scapulalis (Miura et al., 2009, 2010)	OscaOR1	BAH57975.1	I-5-O	I-7-O	I-8-I	I-7-O	I-5-O	I-5-O	I-2-I	I-7-O	I-6-I	I-7-O	I-5-O
		OscaOR3	BAI66604.1	I-7-O	I-6-I	O-7-I	I-7-O	I-5-O	I-9-O	I-6-I	I-7-O	I-6-I	I-6-I	I-5-O
		OscaOR4	BAI66605.1	O-6-O	O-6-O	O-6-O	O-5-I	I-7-O	I-7-O	I-4-I	I-7-O	I-7-O	I-7-O	O-6-O
		OscaOR5	BAI66607.1	I-7-O	I-7-O	I-7-O	I-7-O	I-7-O	I-5-O	I-5-O	I-9-O	I-7-O	I-7-O	I-7-O
		OscaOR6	BAI66608.1	I-7-O	I-7-O	O-6-O	I-7-O	I-7-O	I-7-O	I-5-O	I-7-O	I-7-O	I-7-O	I-7-O
		OscaOR7	BAI66609.1	I-6-I	O-6-O	O-8-O	I-6-I	I-6-I	O-5-I	I-3-O	I-6-I	I-7-O	O-8-O	I-6-I
		OscaOR8	BAI66610.1	I-7-O	I-7-O	I-7-O	O-5-I	I-5-O	I-7-O	I-5-O	I-7-O	I-7-O	I-7-O	O-7-I
		OscaOR2*	BAH57973.1	I-7-O	O-8-O	I-7-O	I-7-O	I-7-O	I-7-O	I-6-I	I-7-O	I-7-O	I-7-O	I-7-O
	Ostrinia palustris (Miura et al., 2009, 2010)	OpalOR1	BAH57978.1	I-5-O	I-7-O	I-8-I	I-7-O	I-5-O	I-5-O	I-4-I	I-7-O	I-6-I	I-7-O	I-3-O
		OpalOR3	BAI66634.1											
		OpalOR4	BAI66635.1											
		OpalOR7	BAI66636.1											
		OpalOR8	BAI66637.3											
		OpalOR2*	BAJ23262.1											
	Ostrinia ovalipennis (Miura et al., 2009, 2010)	OovaOR1	BAH57979.1	I-7-O	I-7-O	I-8-I	I-7-O	I-4-I	I-7-O	I-4-I	I-7-O	I-7-O	I-6-I	I-4-I
		OovaOR3	BAI66629.3											
		OovaOR4	BAI66630.1											
		OovaOR5	BAI66631.1											
		OovaOR7	BAI66631.1											
		OovaOR8	BAI66633.1											

(Continued)

TABLE 1 | (Continued)

Family	Species	Receptors	Genbank ID	CCTOP	HMMTOP	Memsat	Octopus	Philius	Phobius	Pro	Prodiv	Scampi	ScampiMsa	TMHMM
		OvaOR2*	BAJ23264.1											
	Ostrinia zaguliaevi (Miura et al., 2009, 2010)	OzagOR1	BAH57976.1	I-5-O	I-6-I	I-8-I	I-8-O	I-5-O	I-5-O	I-4-I	I-7-O	I-6-I	I-7-O	O-4-O
		OzagOR3	BAI66638.1											
		OzagOR4	BAI66639.1											
		OzagOR5	BAI66640.1											
		OzagOR7	BAI66642.1											
		OzagOR8	BAI66643.1											
		OzagOR2*	BAJ23265.1											
	Ostrinia zealis (Miura et al., 2009, 2010)	OzeaOR1	BAH57977.1	I-5-O	I-6-I	O-7-I	O-6-O	I-5-O	I-5-O	I-3-O	I-7-O	I-7-O	I-7-O	O-4-O
		OzeaOR3a	BAI66644.1											
		OzeaOR3b	BAI66645.1											
		OzeaOR4	BAI66646.1											
		OzeaOR6	BAI66647.1											
		OzeaOR7	BAI66648.1											
		OzeaOR8	BAI66649.1											
		OzeaOR2*	BAJ23260.1											

"" represents the Orco of each species.*

I/O-n-I/O: "n" represents the transmembrane number of certain PR predicted by CCTOP et al; "I" means Intracellular, "O" means Extracellular; the "I/O" in front of "n" means the N terminus location, and the "I/O" behind "n" means the C terminus location.

showed that these SPRs were clustered together with other *B. mori* and *H. virescens* SPRs separated from general odorant receptors (Liu Y. et al., 2013). All identified chemosensory receptors of *H. armigera* and *H. assulta* were used to construct a phylogenetic tree with the known ORs of *H. virescens*, HvOrco, HarmOrco, and HassOrco which were grouped together in a single lineage named the Orco subfamily. OR6/11/13/14/15/16 from the three species were clustered in the SPR subfamily, which included the functionally identified SPRs in *H. virescens* (Jiang et al., 2014). Notably, 10 OR sequences were used in the phylogenetic analysis with another 41 *H. assulta* ORs identified, 68 *B. mori* ORs, and 60 *H. armigera* ORs. One group of ORs which was formed by 7 *B. mori* SPRs, 7 *H. armigera* SPRs, and 7 HassORs was identified as the SPR group (Xu et al., 2015).

In a neighbor-joining tree including OR repertoires of *Ctenopseustis obliquana*, *Ctenopseustis herana*, and *Epiphyas postvittana*, of which the clade predicted to contain the SPRs of many moth species is well supported by the bootstrap analysis (Steinwender et al., 2015). The phylogenetic analysis of the EposORs was performed against comprehensive OR datasets from *B. mori*, *H. virescens*, and *C. pomonella*, in which 8 receptors (EposOR1/6/7/21/22/41/43/45) fall into a well-supported clade that contains SPRs from other moth species, including BmOR1/3 and HvirOR6/13/14/16 (Corcoran et al., 2015). In the sequence similarity analysis of the *C. pomonella* ORs, the OR repertoires of *B. mori*, *H. virescens*, *M. sexta*, *S. littoralis*, and several ORs, Cpom1/3/4/5/6 are grouped in a conserved clade containing Lepidopteran SPRs, and Orco forms a clade (Bengtsson et al., 2012).

The *C. pomonella* ORs are presented phylogenetically within the context of other tortricid moth species (*C. obliquana*, *C. herana*, and *E. postvittana*) from which large OR repertoires have been published, along with *B. mori* ORs serving as a Lepidopteran out-group, Orco clade, and SPR clade (Walker et al., 2016). The phylogenetic analyses of odorant receptors from *Planotortrix octo*, *Planotortrix excessana*, *C. obliquana*, *C. herana*, and *E. postvittana* showed that the tree is rooted with Orco, and the SPR clade is formed (Steinwender et al., 2016). The phylogenetic relationships of odorant receptors from *L. botrana* and other insects, such as *C. pomonella*, *E. postvittana*, *B. mori*, *Ostrinia nubilalis*, *Spodoptera exigua*, *S. littoralis*, *P. xylostella*, *H. armigera*, and *H. assulta*, indicated that 10 LbotOR sequences were predicted to be closely related to the SPR clade proposed for *C. pomonella*, *B. mori*, *M. sexta*, *S. littoralis*, and *O. nubilalis* (Rojas et al., 2018). In the phylogenetic tree of odorant receptors, orthologous OR1s of the genus *Ostrinia* formed a clade, and the OR1 group was included in a single lineage of the SPR subfamily (Miura et al., 2009). In the phylogenetic tree of ORs constructed using the sequences of 162 ORs from *B. mori*, *Ostrinia furnacalis*, and *Conogethes punctiferalis*, the OR sequences were clustered into SPRs, Orco, and other divergent ORs (Ge et al., 2016). In a neighbor-joining tree of 130 OR sequences built from three different Lepidoptera species, including *C. punctiferlis*, *B. mori*, and *O. furnacalis*, the Orco was clustered with other Lepidoptera Orco sequences (Jia et al., 2016).

The SPRs of Lepidopteran insects had been phylogenetically analyzed in several studies. The phylogeny of Lepidopteran

SPRs shows four orthologous clades, in which a cluster only contains candidate SPRs of noctuid species, and paralogous SPRs from Cluster I differ dramatically in ligand selectivity and sensitivity (Zhang Y. N. et al., 2016). The neighbor-joining analysis of highly conserved Noctuidae SPRs and their ligands had been summarized (Jiang et al., 2019, 2020). In a maximum-likelihood phylogeny of Lepidopteran candidate SPRs from Yponomeutoidea, Pyraloidea, Tortricoidea, Papilionoidea, Bombycoidea, and Noctuoidea, SPRs were grouped into 5 different paralogous lineages, i.e., each containing SPRs from different Lepidopteran superfamilies (De Fouchier et al., 2015). The phylogenetic tree showed that the SPRs of different moths were clustered into four branches; while the moth Orcos were clustered into one branch that was separated from the SPRs (Zhang et al., 2014, Zhang Y. N. et al., 2016). Phylogenetic analysis constructed with 10 SPRs from *Cydia fagiglandana*, 7 SPRs from *Hedya nubiferana*, 8 SPRs from *B. mori*, 6 SPRs from *E. postvittana*, and 14 SPRs from *C. pomonella* revealed that the four genes (i.e., CpomOR1, CpomOR2a, CpomOR5, and CpomOR7) were clustered with Lepidopteran SPRs (Tian et al., 2020). In the phylogenetic tree of SPR subfamily proteins, OR1/3/4/5/6/7/8 of different *Ostrinia* species, respectively, formed a clade (Miura et al., 2010). The phylogenetic relationship of OnOR1-6 with SPRs from the superfamily of Bombycoidea, Noctuoidea, Pyraloidea, Yponomeutoidea, and Tortricoidea suggests that there is no clear relationship between the phylogeny of SPRs and their ligand (Wanner et al., 2010). In a phylogenetic tree, the OR4,5,8 genes of several *Ostrinia* moths and the OnOr6 gene formed a definite clade, which did not include any known SPRs of other Lepidoptera (Yasukochi et al., 2011). The neighbor-joining phylogenetic tree of SPRs of 8 *Ostrinia* species forms 5 orthologous lineages, i.e., each with 100% bootstrap support, belonging to the Lepidopteran SPR lineage (Leary et al., 2012).

In our summary, the phylogenetic tree of 256 SPRs and Orcos showed some similar information as former reports (**Figure 1**). The Orcos of 40 species from 10 families of Lepidoptera form a clade with a bootstrap value of 100 distinct from SPRs, indicating the high conservation of Orcos, implied the fixed function of Orcos (Zhang et al., 2019). In the Orco clade, only the 10 Orcos from Noctuidae are in a single branch; the Orcos from Tortricidae are distributed in two branches, with one branch clustered with Orcos from Crambidae and Plutellidae. As to SPRs, SPRs from Noctuidae, Tortricidae, and Crambidae are with the major number, and there is no strict affiliation between SPRs and families.

We then summarized some SPRs and their corresponding ligands (**Figure 2**), and the branch position of each SPRs are the same as in **Figure 1**. The 10 SPRs share the same ligand Z11-16:Ald; AtraOR3, MsepOR3, HvirOR13, HassOR1/13, and HarmOR1/13 are in a branch with a bootstrap support value of 99; and PxylOR1, HvirOR16, HassOR14b, and DindOR1 are in different clusters. Z11-16:Ald is the pheromone component of *H. armigera*, *H. assulta*, *H. virescens*, and *P. xylostella*. SexiOR13/SlitOR13/SlituOR13/SinfOR27 and SlitOR6/SlituOR6 are tuned to the ligand Z9,E12-14:OAC, which is the pheromone component of the 3 corresponding species. E10,Z12-16:Ald is the ligand of BmOR3 and MsexOR1 on the same branch with a bootstrap value of 99; AlepOR3 and AlepOR4 are both tuned to Z7-12:Ac, which is their corresponding pheromone component. HarmOR16, HvirOR16, and SinfOR21 are dispersed on different branches but share one ligand Z11-16:OH. PxylOR4/41/AlepOR4, OnubOR1/3/OfurOR3, and OnubOR5/OscaOR3, respectively, tune to their corresponding major ligands Z9-14:Ac, E12-14:OAc, and Z12-14:OAc. OscaOR1/OlatOR1/OovaOR1/OscaOR3 are tuned to E11-14:OH. As the SPRs from Tortricidae, CpomOR2a, and CpomOR5 are tuned to E8,E10-12:Ac, CoblOR7 and CherOR7 both tuned to Z8-14:OAc. Similar to former research (Wanner et al., 2010), there is no clear relationship between the phylogeny of SPRs and their ligands.

Structure of Lepidopteran Sex Pheromone Receptors

Several studies have predicted the transmembrane and topology of Lepidopteran SPRs and Orcos. The sequence analysis of PxylOR1/3/4 and DindOR1/3 by transmembrane domain prediction tools TMpred and TMHMM indicated that proteins coded by the genes possess the seven transmembrane domains that are the characteristics of the G protein-coupled receptors (GPCR) superfamily (Mitsuno et al., 2008). TMHMM2.0 was used for the prediction of transmembrane domains of PxylOR8/41/45, and these SPRs contain seven putative transmembrane domains (Liu et al., 2018). As with ORs from other insects, SexiOR3 hypothetically contains seven transmembrane domains with a predicted intracellular N-terminus and an extracellular C-terminus by TMHMM Server version 2.0 (Liu C. et al., 2013). SinfOR21/27/29 predicted to have the typical characteristics of an OR, including seven putative transmembrane domains, an intracellular N-terminus, and an extracellular C-terminus by TMHMM2.0 (Zhang et al., 2014). Predicted by the Phobius and MANSAT3, the SlituOR3 has seven transmembrane domains (Lin et al., 2015). According to TMBase and the SFINX package, SlituOR6/11/13/16 were predicted to possess 7 transmembrane domains (Zhang et al., 2015). The predicted transmembrane topology of CoblOR7 and CherOR7 was using SPLIT 4.0 at the transmembrane prediction server (Steinwender et al., 2015). Through TMHMM2.0, TMAP, and TMpred, EposOR1 was predicted to contain 7 transmembrane domains and an intracellular N-terminus with the exception of TMpred (Jordan et al., 2009). SlitOrco and other Noctuidae of the Orcos of Lepidoptera insects were predicted with seven transmembrane domains by TMHMM2.0 (Wu et al., 2013).

The transmembrane topology of the SPRs and Orcos of Lepidopteran insects was predicted by online software CCTOP (Dobson et al., 2015), and the structural features of these receptors according to these predictions were speculated (**Table 1**). All the SPRs showed no significant common features (such as transmembrane numbers) according to the

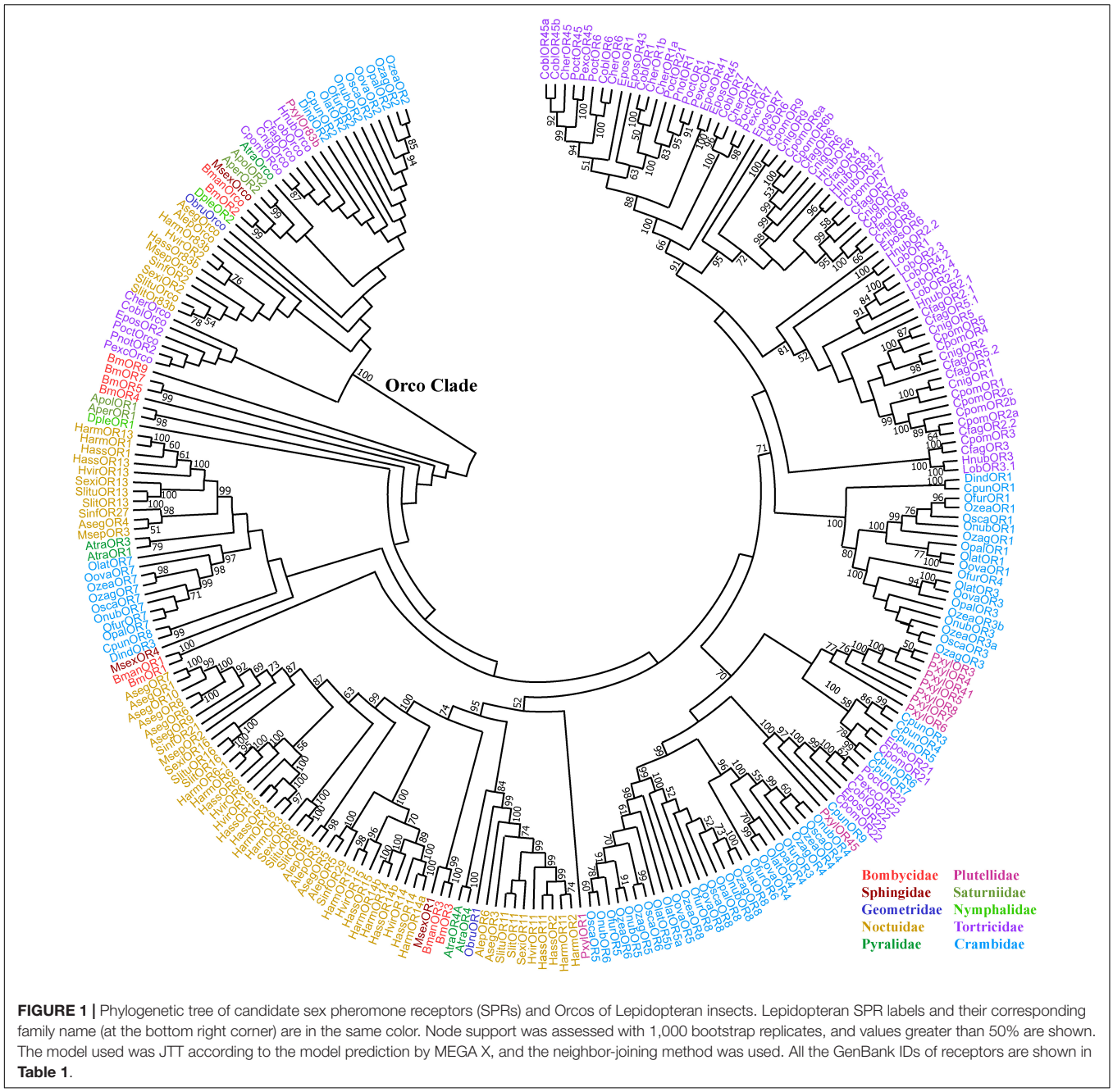

FIGURE 1 | Phylogenetic tree of candidate sex pheromone receptors (SPRs) and Orcos of Lepidopteran insects. Lepidopteran SPR labels and their corresponding family name (at the bottom right corner) are in the same color. Node support was assessed with 1,000 bootstrap replicates, and values greater than 50% are shown. The model used was JTT according to the model prediction by MEGA X, and the neighbor-joining method was used. All the GenBank IDs of receptors are shown in **Table 1**.

CCTOP prediction results, but the intracellular N-terminus and extracellular C-terminus locations of these SPRs were similar to the previous reports of Lepidopteran insects (Mitsuno et al., 2008). The single-particle cryo-electron microscopy (EM) structure of an Orco homomer from the parasitic *fig wasp* at 3.5 Å resolution had been reported, which confirmed the predicted topology of the Orco in Lepidopteran insects (Butterwick et al., 2018). Through SwissModel online predictions, the cryo-EM structures of the Orco mentioned earlier (SMTL ID: 6c70.1) were the best templates of all the SPRs according to sequence identities, and thus, all the receptors have similar structural characteristics with 7 transmembrane helixes, of which BmOR3 is shown in **Figure 3** as a sample.

Characterization and Interaction of Sex Pheromone Receptors and Specific Sex Pheromone Molecules

The functional characterization of SPRs in Lepidopteran insects can be divided into two types, namely, *in vivo* and *in vitro*. Almost all the Lepidopteran SPRs were characterized through classical *in vitro* electrophysiological recording (i.e., two-electrode voltage-clamp) of heterologous expression system on

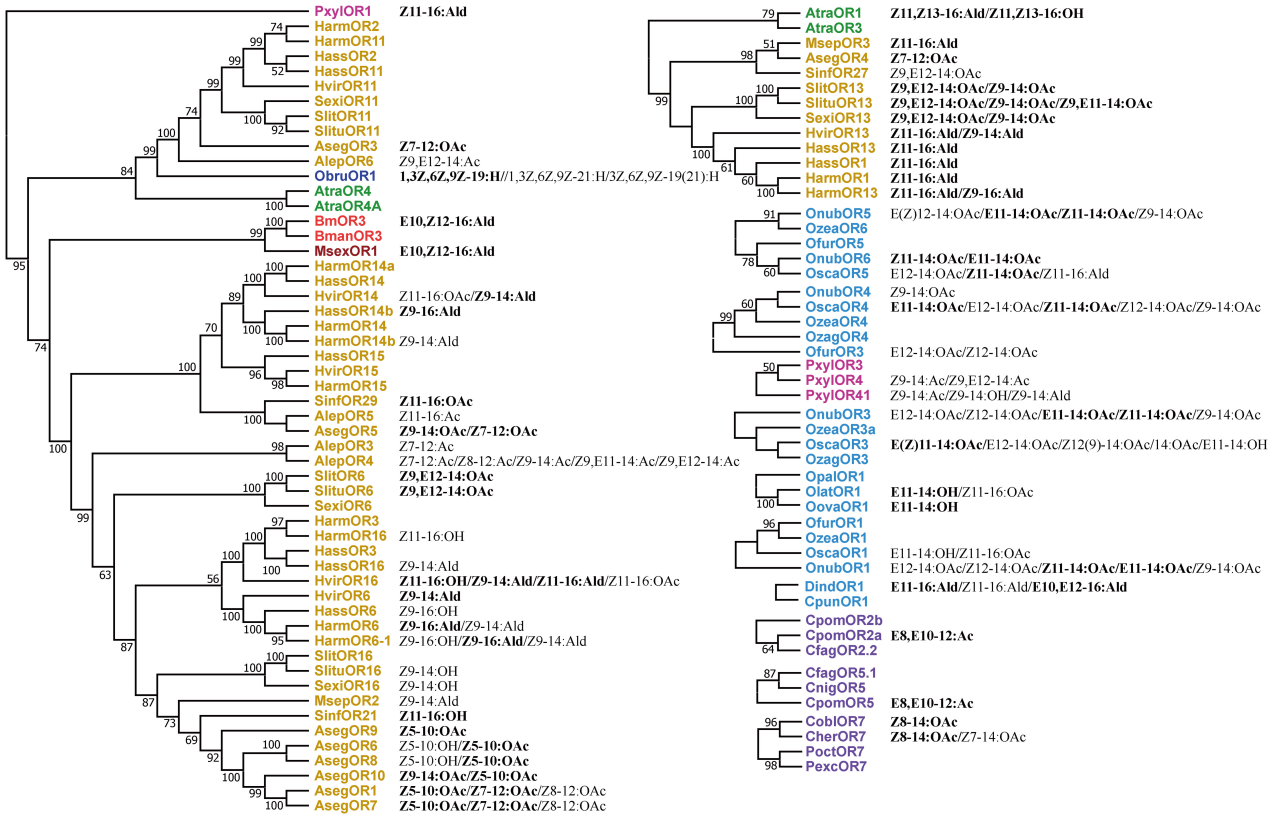

FIGURE 2 | Lepidopteran SPRs and their ligands in the form of phylogenetic branches. Lepidopteran SPR labels and their corresponding family name are in the same color as shown in **Figure 1**. The ligands of SPRs are on the right side of each SPR, among which the chemical compound in bold is the sex pheromone molecule (SPM) of the corresponding species.

SPM activation. The two-electrode voltage-clamp recording was conducted in Xenopus oocytes coinjected with complementary RNAs encoding BmOR1 and BmOR2 to test the bombykol-inducing current response (Nakagawa et al., 2005). The similar method was used in a specific pheromone detection of PxylOR1/4/8/41/45 (Sun et al., 2013; Liu et al., 2018), MsexOR1 (Wicher et al., 2017), EgirOR1 (Li et al., 2017), MsepOR2/3 (Jiang et al., 2019, 2020), HvirOR6/13/14/16 (Wang et al., 2011), SexiOR13/16 (Liu C. et al., 2013), SinfOR21/29 (Zhang et al., 2014), AlepOR3/4/6 (Zhang et al., 2019), HarmORs/HassORs (Liu Y. et al., 2013; Liu et al., 2014; Jiang et al., 2014; Xu et al., 2015), AsegOR1/4/5/6/9 (Zhang and Lofstedt, 2013), SlituOR6/13/16 (Zhang et al., 2015), CpomOR2a/5 (Tian et al., 2020), AtraOR1/3 (Xu et al., 2012), and OlatOR1/OovaOR1/OscaOR1/3/4/5 (Miura et al., 2009, 2010). HEK293/sf9 cell calcium assay verified the sex pheromone component of ApolOR1, HassOR13, CoblOR7, and CherOR7 (Forstner et al., 2009; Jordan et al., 2009; Liu et al., 2014; Steinwender et al., 2015; Xu et al., 2015). In calcium imaging, calcium indicator Fluo-AM was used to detect the ion flow response induced by a specific ligand. In sf9 cells, endogenous Orco was provided to SPRs. Recent research adopted the Bioluminescence Resonance Energy Transfer (BRET)-based calcium sensor CalfluxVTN to detect ligand (Gu et al., 2009). *In vivo*, it means that the heterologous expression system is *Drosophila* antennae. In the characterization of *S. littoralis* SPRs, SlitOR6/SlitOR13 was expressed in a majority of *Drosophila* OSN in addition to endogenous receptors, and the responses to SPM stimuli were monitored by electroantennography, or *Drosophila* OR67d was replaced with SlitOR6 and the response was monitored by single sensillum recordings (Montagne et al., 2012; De Fouchier et al., 2015).

The interaction of SPR and specific SPM can be classified into receptor-ligand interaction in the perspective of biophysics, and the affinity between receptor and ligand is usually quantified by receptor-ligand complex dissociation constant Kd. According to **Figure 2**, most SPRs are tuned not only to the SPMs of their corresponding species but also to the SPMs of sibling species/analogs and antagonists, with different response amplitudes or different SPR-ligand affinities. In some researches, amino acid mutations of SPRs are responsible for the alteration of ligands. HarmOR14b and HassOR14b share 90% identities, and F232I + T355I are the key mutations that alter HassOR14b tuning to Z9-16:Ald to HarmOR14b tuning to Z9-14:Ald (Yang K. et al., 2017), which indicates that 232 and 355 are key residues in SPR and ligand docking. In *Ostrinia* species, OR3 amino acid mutation A148T in TM3 domain alters the pheromone recognition pattern by selectively reducing

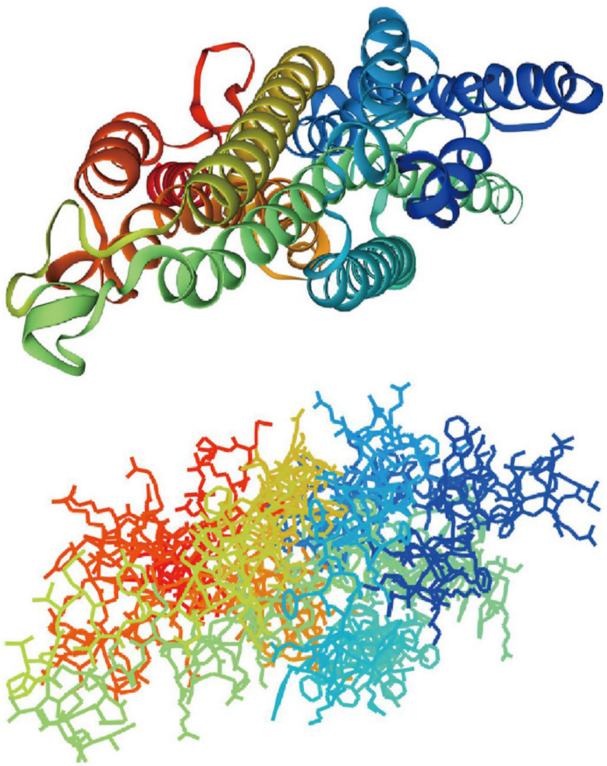

FIGURE 3 | Predicted structure of Lepidopteran SPRs BmOR3 and Orcos through SwissModel. In total, 7 transmembrane helixes were colored rainbow in the form of silk ribbon (Cartoon) and lines.

the E11-14:OAc response (EC50 of the dose-response curve) approximately 14-fold (Leary et al., 2012). Until present, no researches about SPR mutation and SPM recognition in a species have been reported. From the abovementioned studies, we can speculate that SPR and ligand docking pattern and the structure of SPR-ligand will be the future direction in SPR-ligand interaction studies.

Downstream Signaling Pathways of Sex Pheromone Receptors

Early research revealed the presence of G-protein, belonging to the Gαq family, in antennal preparations (especially the pheromone-sensitive sensilla trichodea) of *B.mori and Antheraea pernyi*, implied a participation of G-protein of the Gαq family in the signal transduction of OR cells in moths (Laue et al., 1997; Nakagawa et al., 2005). The bombykol stimulation of *Xenopus laevis* oocytes expressing BmOR-1 and BmGαq elicited robust dose-dependent inward Ca^{2+}-dependent Cl^{-} currents on two-electrode voltage-clamp recordings, demonstrating that the binding of bombykol to BmOR-1 leads to the activation of a BmGαq-mediated signaling cascade (Sakurai et al., 2004). MsexOR1 and MsexOrco coexpressed in HEK293 and CHO cells caused bombykal-dependent increases in the intracellular free Ca^{2+} concentration, and inhibitor evidence showed that phospholipase C (PLC) and protein kinase C (PKC) activities are involved in the bombykal-receptor-mediated Ca^{2+} signals of hawk moths. It could be hypothesized that MsexOrs couple to Gαq proteins, requiring the activation of PLC for pheromone transduction (Wicher et al., 2017). Immunocytochemistry research showed that anti-Gαq and anti-Gαs antisera stained the inner and outer dendritic segments of the putative OR neuron in male and female antennae, which suggested that each subunit mediates a subset of the odorant response (Miura et al., 2005). In addition, a computational model of the insect pheromone transduction cascade had been used to calculate the presence of the G-protein pathway in pheromone detection (Gu et al., 2009). Furthermore, recent research showed that in HEK293A cells expressing BmOR3 and human Gαi, the dose-dependent coupling of BmOR3 and Gαi on bombykal stimulation was detected through BRET (Lin et al., 2021). From the biophysical perspective, a conservation residue W103 in transmembrane 2 of BmOR3 is the key that determines receptor-Gi coupling (Lin et al., 2021). Pretreatment with specific Gi inhibitor PTX had no significant effects on bombykal-induced BmOR3-BmOrco complex formation or complex-regulated calcium influx, suggesting that Gi coupling and BmOrco coupling are the two independent processes in the case of BmOR3 (Lin et al., 2021).

The GPCRs usually direct the recruitment, activation, and scaffolding of the cytoplasmic signaling complexes *via* two multifunctional adaptor and transducer molecules, β-arrestins 1 and 2, and arrestins also function to activate signaling cascades independently of G-protein activation or mediate receptor desensitization (Lefkowitz and Shenoy, 2005; DeWire et al., 2007). Individual arrestins had been reported to function in both olfactory and visual pathways in Dipteran insects (Merrill et al., 2001) but not in Lepidopteran insects. Recent research reported that bombykal robustly stimulated the recruitment of human α-arrestin-1/2 and *B. mori* intrinsic arrestin to BmOR3 in HEK293A cells in a concentration-dependent manner, and the arrestin, in turn, regulated BmOR3 internalization (Lin et al., 2021). Bombykal also induced downstream kinase (i.e., ERK, SRC, AKT, and JNK) activation (phosphorylation) through arrestin (Lin et al., 2021). These results confirmed the arrestin-mediated signaling downstream of BmOR3. The knockdown of β-arrestins significantly reduced bombykal-induced calcium influx through BmOR3-BmOR2, which was accompanied by the collapse of the receptor complex, suggesting that the α-arrestins mediate Ca^{2+} response mainly by regulating the structural and functional integrity of the BmOR3-BmOR2 complex (Lin et al., 2021). The summarized researches show that insect pheromone receptors may both have G-protein and arrestin downstream pathways (**Figure 4**).

Metabotropic Ion Channel by the Coupling of Lepidopteran Sex Pheromone Receptors and Orcos

BmOR1 and BmOR3 of *B. mori* are mutually exclusively expressed in a pair of adjacent pheromone-sensitive neurons of male antennae, and both of which are coexpressed

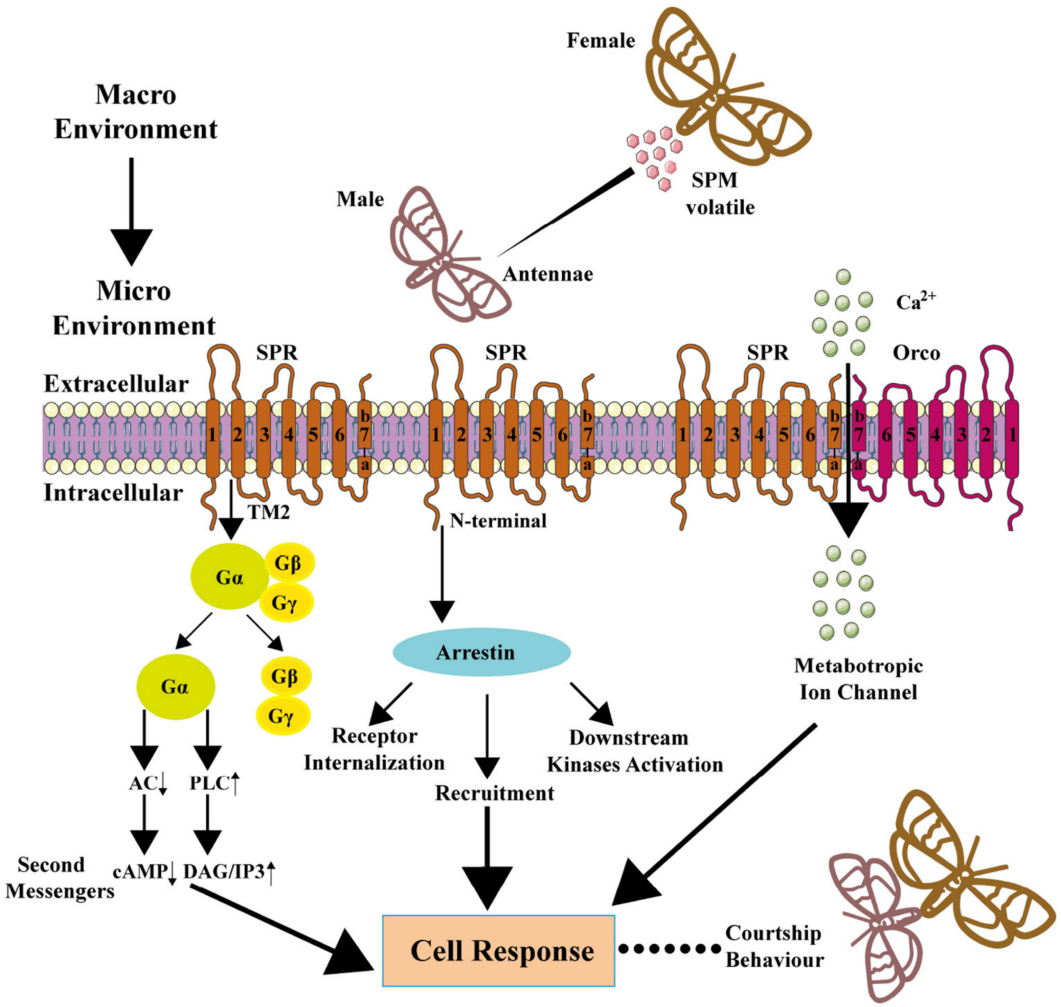

FIGURE 4 | Downstream signaling pathway of SPR and metabotropic channel of SPR-Orco. In macro environment, male insects sense the SPM released by female insects through an olfactory sensory neuron in antennae, and SPM works as an agonist to SPR, and signal transduction leads to ultimate mating behavior.

with the highly conserved insect Orco. Heterologous cells coexpressing BmOR2 can greatly enhance the sensitivity of BmOR1 to bombykol, and the current-voltage analysis showed that bombykol activated a non-selective cation channel in oocytes expressing BmOR1 and BmOR2, which is different from Ca^{2+}-activated Cl^{-} channel through BmGαq, and the non-selective cation channel activity in response to bombykol was also observed when BmOR1 was coexpressed with HvirOR2 or Or83b (Whelan and Goldman, 2001; Nakagawa et al., 2005; **Figure 4**). As reported in MsexOR1, the PLC/PKC activity is a prerequisite to bombykal-receptor-mediated Ca^{2+} signals in HEK293 and CHO cells, and it could be hypothesized that MsexOR1 and MsexOrco need to be phosphorylated before they can be gated by bombykal as an ionotropic odor receptor-ion channel complex (Wicher et al., 2017).

In a recent study, the BmOR3-BmOR2 combination elicited a response to bombykal and showed similar channel properties, and the coupling of BmOR3 and BmOR2 forms a cation channel with the detection of calcium influx (Lin et al., 2021). From the view of biophysics, there was also physical interaction between BmOR3 and its Orco BmOR2. On bombykal stimulation, the cytoplasmic parts intracellular loop 1 (ICL1), ICL2, and ICL3 moved away from the N-terminus, while the C-terminal helical kink moved close to the N-terminus of BmOR3. On the contrary, the lower part of loop7a-7b moved away from the N-terminus in BmOR2. ICL1, ICL2, and ICL3 also moved away from the N-terminus of BmOR2 (Lin et al., 2021). The replacement of transmembrane 7 in both receptors confirmed its indispensable role in BmOR3-BmOrco coupling for ionotropic functions (Lin et al., 2021). Several key motifs determine the BmOR3-BmOR2 coupling, the charged residue pair of BmOR3-E403 and BmOrco-K437 represents an important "ionic lock" in regard to mediating BmOR3-BmOrco coupling, and the hydrophobic patches F428/F433 of BmOR3 and zipper Y464/V467/L468/L471 of BmOrco are spatially close to each other, suggesting that they

might form hydrophobic interactions (Lin et al., 2021). These reports suggest that the coupling of both SPR and Orco plays a vital role in sex pheromone signal detection and transduction.

There is some evidence that the SPR-Orco channel is metabotropic but not ionotropic. In *M. sexta*, the agonist induced SPR to activate the Gq-signaling pathway (Nakagawa et al., 2005; Nolte et al., 2013, 2016; Wicher et al., 2017). In *B. mori*, the SPM elicited G-protein and arrestin pathway, and arrestin knockdown had an effect on ion influx (Lin et al., 2021). Thus, we presume that the SPR-Orco coupling forms a metabotropic channel as before (Fleischer and Krieger, 2018). Both the metabotropic channel and the downstream signaling of SPR may be teamwork in sex pheromone signal transduction (**Figure 4**).

FUTURE DIRECTIONS

By using the mature technology in transcriptome sequencing and bioinformatic analyses, more sex pheromone components and SPRs of Lepidopteran insects are needed to be identified and characterized, which will help the development of sex lure technology and its usage in pest control.

Further researches are needed to work out the cryo-EM structure of SPR and the SPR-ligand docking pattern in a biophysical perspective, which will directly facilitate the understanding of sex pheromone signal transduction pathways and provide guidance in the sex lure technology in field pest control.

AUTHOR CONTRIBUTIONS

JS and XY proposed the title of the review and provided funding required. CY wrote the original draft, performed the data processing, and prepared figures. JC, JL, and YZ contributed to review editing. All authors contributed to the article and approved the submitted version.

FUNDING

This work was primarily supported by the National Science Fund for Excellent Young Scholars Grant (81822008 to XY), the National Science Fund for Distinguished Young Scholars Grant (81825022 to JS), and the National Natural Science Foundation of China (31671197 to XY and 81773704 to JS).

REFERENCES

Bengtsson, J. M., Trona, F., Montagne, N., Anfora, G., Ignell, R., Witzgall, P., et al. (2012). Putative chemosensory receptors of the codling moth, *Cydia pomonella*, identified by antennal transcriptome analysis. *PLoS One* 7:e31620. doi: 10.1371/journal.pone.0031620

Bertoni, M., Kiefer, F., Biasini, M., Bordoli, L., and Schwede, T. (2017). Modeling protein quaternary structure of homo- and hetero-oligomers beyond binary interactions by homology. *Sci. Rep.* 7:10480. doi: 10.1038/s41598-017-09654-8

Bienert, S., Waterhouse, A., de Beer, T. A. P., Tauriello, G., Studer, G., Bordoli, L., et al. (2017). The SWISS-MODEL Repository - new features and functionality. *Nucleic Acids Res.* 45, D313–D319. doi: 10.1093/nar/gkw1132

Butterwick, J. A., Del Marmol, J., Kim, K. H., Kahlson, M. A., Rogow, J. A., Walz, T., et al. (2018). Cryo-EM structure of the insect olfactory receptor Orco. *Nature* 560, 447–452. doi: 10.1038/s41586-018-0420-8

Carraher, C., Authier, A., Steinwender, B., and Newcomb, R. D. (2012). Sequence comparisons of odorant receptors among tortricid moths reveal different rates of molecular evolution among family members. *PLoS One* 7:e38391. doi: 10.1371/journal.pone.0038391

Chang, H., Guo, M., Wang, B., Liu, Y., Dong, S., and Wang, G. (2016). Sensillar expression and responses of olfactory receptors reveal different peripheral coding in two *Helicoverpa species* using the same pheromone components. *Sci. Rep.* 6:18742. doi: 10.1038/srep18742

Corcoran, J. A., Jordan, M. D., Thrimawithana, A. H., Crowhurst, R. N., and Newcomb, R. D. (2015). The peripheral olfactory repertoire of the lightbrown apple moth, *Epiphyas postvittana*. *PLoS One* 10:e0128596. doi: 10.1371/journal.pone.0128596

De Fouchier, A., Sun, X., Monsempes, C., Mirabeau, O., Jacquin-Joly, E., and Montagné, N. (2015). Evolution of two receptors detecting the same pheromone compound in crop pest moths of the genus Spodoptera. *Front. Ecol. Evol.* 3:95. doi: 10.3389/fevo.2015.00095

DeWire, S. M., Ahn, S., Lefkowitz, R. J., and Shenoy, S. K. (2007). Beta-arrestins and cell signaling. *Annu. Rev. Physiol.* 69, 483–510.

Dobson, L., Reményi, I., and Tusnády, G. E. (2015). CCTOP: a consensus constrained TOPology prediction web server. *Nucleic Acids Res.* 43, W408–W412. doi: 10.1093/nar/gkv451

Du, L. X., Liu, Y., Zhang, J., Gao, X. W., Wang, B., and Wang, G. R. (2018). Identification and characterization of chemosensory genes in the antennal transcriptome of Spodoptera exigua. *Comp. Biochem. Physiol. Part D Genom. Proteom.* 27, 54–65. doi: 10.1016/j.cbd.2018.05.001

Feng, B., Lin, X., Zheng, K., Qian, K., Chang, Y., and Du, Y. (2015). Transcriptome and expression profiling analysis link patterns of gene expression to antennal responses in *Spodoptera litura*. *BMC Genomics* 16:269. doi: 10.1186/s12864-015-1375-x

Fleischer, J., and Krieger, J. (2018). Insect pheromone receptors - key elements in sensing intraspecific chemical signals. *Front. Cell Neurosci.* 12:425. doi: 10.3389/fncel.2018.00425

Forstner, M., Breer, H., and Krieger, J. (2009). A receptor and binding protein interplay in the detection of a distinct pheromone component in the silkmoth *Antheraea polyphemus*. *Int. J. Biol. Sci.* 5, 745–757. doi: 10.7150/ijbs.5.745

Garczynski, S. F., and Leal, W. S. (2015). Alternative splicing produces two transcripts encoding female-biased pheromone subfamily receptors in the navel orangeworm, *Amyelois transitella*. *Front. Ecol. Evol.* 3:115. doi: 10.3389/fevo.2015.00115

Ge, X., Zhang, T. T., Wang, Z. Y., He, K. L., and Bai, S. X. (2016). Identification of putative chemosensory receptor genes from yellow peach moth *Conogethes punctiferalis* (Guenée) antennae transcriptome. *Sci. Rep.* 6, 32636–32648. doi: 10.1038/srep32636

Gonzalez, F., Witzgall, P., and Walker, W. B. (2017). Antennal transcriptomes of three tortricid moths reveal putative conserved chemosensory receptors for social and habitat olfactory cues. *Sci. Rep.* 7, 41829–41840. doi: 10.1038/srep41829

Grapputo, A., Thrimawithana, A. H., Steinwender, B., and Newcomb, R. D. (2018). Differential gene expression in the evolution of sex pheromone communication in New Zealand's endemic leafroller moths of the genera Ctenopseustis and Planotortrix. *BMC Genomics* 19:94. doi: 10.1186/s12864-018-4451-1

Grosse-Wilde, E., Gohl, T., Bouche, E., Breer, H., and Krieger, J. (2007). Candidate pheromone receptors provide the basis for the response of distinct antennal neurons to pheromonal compounds. *Eur. J. Neurosci.* 25, 2364–2373. doi: 10.1111/j.1460-9568.2007.05512.x

Grosse-Wilde, E., Kuebler, L. S., Bucks, S., Vogel, H., Wicher, D., and Hansson, B. S. (2011). Antennal transcriptome of *Manduca sexta*. *PNAS* 108, 7449–7454.

Grosse-Wilde, E., Stieber, R., Forstner, M., Krieger, J., Wicher, D., and Hansson, B. S. (2010). Sex-specific odorant receptors of the tobacco hornworm manduca sexta. *Front. Cell Neurosci.* 4:22. doi: 10.3389/fncel.2010.00022

Grosse-Wilde, E., Svatos, A., and Krieger, J. (2006). A pheromone-binding protein mediates the bombykol-induced activation of a pheromone receptor in vitro. *Chem. Senses* 31, 547–555. doi: 10.1093/chemse/bjj059

Gu, Y., Lucas, P., and Rospars, J. (2009). Computational model of the insect pheromone transduction cascade. *PLoS Comput. Biol.* 5:e1000321. doi: 10.1371/journal.pcbi.1000321

Guex, N., Peitsch, M. C., and Schwede, T. (2019). Automated comparative protein structure modeling with SWISS-MODEL and Swiss-PdbViewer: a historical perspective. *Electrophoresis* 30, S162–S173. doi: 10.1002/elps.200900140

Jia, X. J., Wang, H. X., Yan, Z. G., Zhang, M. Z., Wei, C. H., Qin, X. C., et al. (2016). Antennal transcriptome and differential expression of olfactory genes in the yellow peach moth, *Conogethes punctiferalis* (Lepidoptera: Crambidae). *Sci. Rep.* 6, 29067–29082. doi: 10.1038/srep29067

Jiang, N. J., Tang, R., Guo, H., Ning, C., Li, J. C., Wu, H., et al. (2020). Olfactory coding of intra- and interspecific pheromonal messages by the male *Mythimna separata* in North China. *Insect Biochem. Mol. Biol.* 125:103439. doi: 10.1016/j.ibmb.2020.103439

Jiang, N. J., Tang, R., Wu, H., Xu, M., Ning, C., Huang, L. Q., et al. (2019). Dissecting sex pheromone communication of *Mythimna separata* (Walker) in North China from receptor molecules and antennal lobes to behavior. *Insect Biochem. Mol. Biol.* 111:103176. doi: 10.1016/j.ibmb.2019.103176

Jiang, X. J., Guo, H., Di, C., Yu, S., Zhu, L., Huang, L. Q., et al. (2014). Sequence similarity and functional comparisons of pheromone receptor orthologs in two closely related *Helicoverpa species*. *Insect Biochem. Mol. Biol.* 48, 63–74. doi: 10.1016/j.ibmb.2014.02.010

Jordan, M. D., Anderson, A., Begum, D., Carraher, C., Authier, A., Marshall, S. D., et al. (2009). Odorant receptors from the light brown apple moth (*Epiphyas postvittana*) recognize important volatile compounds produced by plants. *Chem. Senses* 34, 383–394. doi: 10.1093/chemse/bjp010

Krieger, J., Gondesen, I., Forstner, M., Gohl, T., Dewer, Y., and Breer, H. (2009). HR11 and HR13 receptor-expressing neurons are housed together in pheromone-responsive sensilla trichodea of male *Heliothis virescens*. *Chem. Senses* 34, 469–477. doi: 10.1093/chemse/bjp012

Krieger, J., Grosse-Wilde, E., Gohl, T., and Breer, H. (2005). Candidate pheromone receptors of the silkmoth *Bombyx mori*. *Eur. J. Neurosci.* 21, 2167–2176.

Krieger, J., Grosse-Wilde, E., Gohl, T., Dewer, Y. M. E., Raming, K., and Breer, H. (2004). Genes encoding candidate pheromone receptors in a moth (*Heliothis virescens*). *PNAS* 101, 11845–11850. doi: 10.1073/pnas.0403052101

Kumar, S., Stecher, G., Li, M., Knyaz, C., and Tamura, K. (2018). MEGA X: molecular evolutionary genetics analysis across computing platforms. *Mol. Biol. Evol.* 35, 1547–1549. doi: 10.1093/molbev/msy096

Laue, M., Maida, R., and Redkozubov, A. (1997). G-protein activation, identification and immunolocalization in pheromone-sensitive sensilla trichodea of moths. *Cell Tissue Res.* 288, 149–158. doi: 10.1007/s004410050802

Leal, W. S. (2013). Odorant reception in insects: roles of receptors, binding proteins, and degrading enzymes. *Annu. Rev. Entomol.* 58, 373–391. doi: 10.1146/annurev-ento-120811-153635

Leary, G. P., Allen, J. E., Bunger, P. L., Luginbill, J. B., Linn, C. E., Macallister, I. E., et al. (2012). Single mutation to a sex pheromone receptor provides adaptive specificity between closely related moth species. *PNAS* 109, 14081–14086. doi: 10.1073/pnas.1204661109

Lefkowitz, R. J., and Shenoy, S. K. (2005). Transduction of receptor signals by β-Arrestins. *Science* 308, 512–517. doi: 10.1126/science.1109237

Legeai, F., Malpel, S., Montagné, N., Monsempes, C., Cousserans, F., Merlin, C., et al. (2011). An expressed Sequence Tag collection from the male antennae of the Noctuid moth *Spodoptera littoralis*: a resource for olfactory and pheromone detection research. *BMC Genomics* 12:86. doi: 10.1186/1471-2164-12-86

Li, J., Wang, X., and Zhang, L. (2020). Sex pheromones and olfactory proteins in Antheraea moths: *A. pernyi* and *A. polyphemus* (Lepidoptera: Saturniidae). *Arch. Insect Biochem. Physiol.* 105, 1–10. doi: 10.1002/arch.21729

Li, Z. Q., Cai, X. M., Luo, Z. X., Bian, L., Xin, Z. J., Chu, B., et al. (2018). Comparison of olfactory genes in two ectropis species: emphasis on candidates involved in the detection of Type-II Sex pheromones. *Front. Physiol.* 9:1602. doi: 10.3389/fphys.2018.01602

Li, Z. Q., Luo, Z. X., Cai, X. M., Bian, L., Xin, Z. J., Liu, Y., et al. (2017). Chemosensory gene families in ectropis grisescens and candidates for detection of Type-II sex pheromones. *Front. Physiol.* 8:953. doi: 10.3389/fphys.2017.00953

Lin, J. Y., Yang, Z., Yang, C., Du, J. X., Yang, F., Cheng, J., et al. (2021). An ionic lock and a hydrophobic zipper mediate the coupling between an insect pheromone receptor BmOR3 and downstream effectors. *J. Biol. Chem.* 297:101160. doi: 10.1016/j.jbc.2021.101160

Lin, X., Zhang, Q., Wu, Z., and Du, Y. (2015). Identification and differential expression of a candidate sex pheromone receptor in natural populations of *Spodoptera litura*. *PLoS One* 10:e0131407. doi: 10.1371/journal.pone.0131407

Liu, C., Liu, Y., Walker, W. B., Dong, S., and Wang, G. (2013). Identification and functional characterization of sex pheromone receptors in beet armyworm *Spodoptera exigua* (Hubner). *Insect Biochem. Mol. Biol.* 43, 747–754. doi: 10.1016/j.ibmb.2013.05.009

Liu, N. Y., Xu, W., Papanicolaou, A., Dong, S. L., and Anderson, A. (2014). Identification and characterization of three chemosensory receptor families in the cotton bollworm *Helicoverpa armigera*. *BMC Genomics* 15:597. doi: 10.1186/1471-2164-15-597

Liu, Y., Gu, S., Zhang, Y., Guo, Y., and Wang, G. (2012). Candidate olfaction genes identified within the *Helicoverpa armigera* antennal transcriptome. *PLoS One* 7:e48260. doi: 10.1371/journal.pone.0048260

Liu, Y., Liu, C., Lin, K., and Wang, G. (2013). Functional specificity of sex pheromone receptors in the cotton bollworm *Helicoverpa armigera*. *PLoS One* 8:e62094. doi: 10.1371/journal.pone.0062094

Liu, Y., Liu, Y., Jiang, X., and Wang, G. (2018). Cloning and functional characterization of three new pheromone receptors from the diamondback moth, *Plutella xylostella*. *J. Insect Physiol.* 107, 14–22. doi: 10.1016/j.jinsphys.2018.02.005

Merrill, C. E., Riesgo-Escovar, J., Pitts, R. J., Kafatos, F. C., Carlson, J. R., and Zwiebel, L. J. (2001). Visual arrestins in olfactory pathways of *Drosophila* and the malaria vector mosquito *Anopheles gambiae*. *PNAS* 99, 1633–1638. doi: 10.1073/pnas.022505499

Mitsuno, H., Sakurai, T., Murai, M., Yasuda, T., Kugimiya, S., Ozawa, R., et al. (2008). Identification of receptors of main sex-pheromone components of three *Lepidopteran species*. *Eur. J. Neurosci.* 28, 893–902. doi: 10.1111/j.1460-9568.2008.06429.x

Miura, N., Atsumi, S., Tabunoki, H., and Sato, R. (2005). expression and localization of three G protein alpha subunits, Go, Gq, and Gs, in adult antennae of the silkmoth (*Bombyx mori*). *J. Comp. Neurol.* 485, 143–152. doi: 10.1002/cne.20488

Miura, N., Nakagawa, T., Tatsuki, S., Touhara, K., and Ishikawa, Y. (2009). A male-specific odorant receptor conserved through the evolution of sex pheromones in *Ostrinia* moth *species*. *Int. J. Biol. Sci.* 5, 319–330. doi: 10.7150/ijbs.5.319

Miura, N., Nakagawa, T., Touhara, K., and Ishikawa, Y. (2010). Broadly and narrowly tuned odorant receptors are involved in female sex pheromone reception in *Ostrinia moths*. *Insect Biochem. Mol. Biol.* 40, 64–73. doi: 10.1016/j.ibmb.2009.12.011

Montagne, N., Chertemps, T., Brigaud, I., Francois, A., Francois, M. C., Fouchier, A., et al. (2012). Functional characterization of a sex pheromone receptor in the pest moth *Spodoptera littoralis* by heterologous expression in *Drosophila*. *Eur. J. Neurosci.* 36, 2588–2596. doi: 10.1111/j.1460-9568.2012.08183.x

Nakagawa, T., Sakurai, T., Nishioka, T., and Touhara, K. (2005). Insect sex-pheromone signals mediated by specific combinations of olfactory receptors. *Science* 307, 1638–1641. doi: 10.1126/science.1106267

Nolte, A., Funk, N. W., Mukunda, L., Gawalek, P., Werckenthin, A., Hansson, B. S., et al. (2013). In situ tip-recordings found no evidence for an Orco-based ionotropic mechanism of pheromone-transduction in *Manduca sexta*. *PLoS One* 8:e62648. doi: 10.1371/journal.pone.0062648

Nolte, A., Gawalek, P., Koerte, S., Wei, H., Schumann, R., Werckenthin, A., et al. (2016). No evidence for ionotropic pheromone transduction in the hawkmoth *Manduca sexta*. *PLoS One* 11:e0166060. doi: 10.1371/journal.pone.0166060

Patch, H. M., Velarde, R. A., Walden, K. K., and Robertson, H. M. (2009). A candidate pheromone receptor and two odorant receptors of the hawkmoth *Manduca sexta*. *Chem. Senses* 34, 305–316. doi: 10.1093/chemse/bjp002

Rojas, V., Jimenez, H., Palma-Millanao, R., Gonzalez-Gonzalez, A., Machuca, J., Godoy, R., et al. (2018). Analysis of the grapevine moth *Lobesia botrana* antennal transcriptome and expression of odorant-binding and chemosensory proteins. *Comp. Biochem. Physiol. Part D* 27, 1–12. doi: 10.1016/j.cbd.2018.04.003

Sakurai, T., Nakagawa, T., Mitsuno, H., Mori, H., Endo, Y., Tanoue, S., et al. (2004). Identification and functional characterization of a sex pheromone receptor

in the silkmoth *Bombyx mori*. *PNAS* 101, 16653–16658. doi: 10.1073/pnas.0407596101

Steinwender, B., Crowhurst, R. N., Thrimawithana, A. H., and Newcomb, R. D. (2015). Pheromone receptor evolution in the cryptic leafroller species, *Ctenopseustis obliquana* and *C. herana*. *J. Mol. Evol.* 80, 42–56. doi: 10.1007/s00239-014-9650-z

Steinwender, B., Thrimawithana, A. H., Crowhurst, R., and Newcomb, R. D. (2016). Odorant receptors of the New Zealand Endemic leafroller moth species *Planotortrix octo* and *P. excessana*. *PLoS One* 11:e0152147. doi: 10.1371/journal.pone.0152147

Studer, G., Rempfer, C., Waterhouse, A. M., Gumienny, G., Haas, J., and Schwede, T. (2020). QMEANDisCo - distance constraints applied on model quality estimation. *Bioinformatics* 36, 1765–1771.

Sun, M., Liu, Y., Walker, W. B., Liu, C., Lin, K., Gu, S., et al. (2013). Identification and characterization of pheromone receptors and interplay between receptors and pheromone binding proteins in the diamondback moth, *Plutella xyllostella*. *PLoS One* 8:e62098. doi: 10.1371/journal.pone.0062098

Tang, R., Jiang, N. J., Ning, C., Li, G. C., Huang, L. Q., and Wang, C. Z. (2020). The olfactory reception of acetic acid and ionotropic receptors in the *Oriental armyworm*, *Mythimna separata* Walker. *Insect Biochem. Mol. Biol.* 118:103312. doi: 10.1016/j.ibmb.2019.103312

Tian, K., Liu, W., Feng, L. K., Huang, T. Y., Wang, G. R., and Lin, K. J. (2020). Functional characterization of pheromone receptor candidates in codling moth *Cydia pomonella* (Lepidoptera: Tortricidae). *Insect Sci.* 28, 445–456. doi: 10.1111/1744-7917.12775

Walker, W. B., Gonzalez, F., Garczynski, S. F., and Witzgall, P. (2016). The chemosensory receptors of codling moth Cydia pomonella-expression in larvae and adults. *Sci. Rep.* 6, 23518–23534. doi: 10.1038/srep23518

Wang, G., Vasquez, G. M., Schal, C., Zwiebel, L. J., and Gould, F. (2011). Functional characterization of pheromone receptors in the tobacco budworm *Heliothis virescens*. *Insect Mol. Biol.* 20, 125–133. doi: 10.1111/j.1365-2583.2010.01045.x

Wang, L., and Anderson, D. J. (2010). Identification of an aggression-promoting pheromone and its receptor neurons in *Drosophila*. *Nature* 463, 227–231. doi: 10.1038/nature08678

Wanner, K. W., Nichols, A. S., Allen, J. E., Bunger, P. L., Garczynski, S. F., Linn, C. E., et al. (2010). Sex pheromone receptor specificity in the European corn borer moth, *Ostrinia nubilalis*. *PLoS One* 5:e8685. doi: 10.1371/journal.pone.0008685

Waterhouse, A., Bertoni, M., Bienert, S., Studer, G., Tauriello, G., Gumienny, R., et al. (2018). SWISS-MODEL: homology modelling of protein structures and complexes. *Nucleic Acids Res.* 46, W296–W303. doi: 10.1093/nar/gky427

Whelan, S., and Goldman, N. (2001). A general empirical model of protein evolution derived from multiple protein families using a maximum-likelihood approach. *Mol. Biol. Evol.* 18, 691–699. doi: 10.1093/oxfordjournals.molbev.a003851

Wicher, D., Morinaga, S., Halty-deLeon, L., Funk, N., Hansson, B., Touhara, K., et al. (2017). Identification and characterization of the bombykal receptor in the hawkmoth *Manduca sexta*. *J. Exp. Biol.* 220, 1781–1786. doi: 10.1242/jeb.154260

Witzgall, P., Kirsch, P., and Cork, A. (2010). Sex pheromones and their impact on pest management. *J. Chem. Ecol.* 36, 80–100. doi: 10.1007/s10886-009-9737-y

Wu, Z. N., Chen, X., Du, Y. J., Zhou, J. J., and ZhuGe, Q. C. (2013). Molecular identification and characterization of the *Orco orthologue* of *Spodoptera litura*. *Insect Sci.* 20, 175–182. doi: 10.1111/j.1744-7917.2011.01483.x

Xu, P., Garczynski, S. F., Atungulu, E., Syed, Z., Choo, Y. M., Vidal, D. M., et al. (2012). Moth sex pheromone receptors and deceitful parapheromones. *PLoS One* 7:e41653. doi: 10.1371/journal.pone.0041653

Xu, W., Papanicolaou, A., Liu, N. Y., Dong, S. L., and Anderson, A. (2015). Chemosensory receptor genes in the Oriental tobacco budworm *Helicoverpa assulta*. *Insect Mol. Biol.* 24, 253–263. doi: 10.1111/imb.12153

Yang, K., Ning, C., and Wang, C. Z. (2017). Two single-point mutations shift the ligand selectivity of a pheromone receptor between two closely related moth species. *eLife* 6:e29100.

Yang, S., Cao, D., Wang, G., and Liu, Y. (2017). Identification of genes involved in chemoreception in *Plutella xyllostella* by antennal transcriptome analysis. *Sci. Rep.* 7:11941. doi: 10.1038/s41598-017-11646-7

Yasukochi, Y., Miura, N., Nakano, R., Sahara, K., and Ishikawa, Y. (2011). Sex-linked pheromone receptor genes of the European corn borer, *Ostrinia nubilalis*, are in tandem arrays. *PLoS One* 6:e18843. doi: 10.1371/journal.pone.0018843

Zhan, S., Merlin, C., Boore, J. L., and Reppert, S. M. (2011). The monarch butterfly genome yields insights into long-distance migration. *Cell* 147, 1171–1185. doi: 10.1016/j.cell.2011.09.052

Zhang, D. D., and Lofstedt, C. (2013). Functional evolution of a multigene family: orthologous and paralogous pheromone receptor genes in the turnip moth, *Agrotis segetum*. *PLoS One* 8:e77345. doi: 10.1371/journal.pone.0077345

Zhang, D. D., Wang, H. L., Schultze, A., Fross, H., Francke, W., Krieger, J., et al. (2016). Receptor for detection of a Type II sex pheromone in the winter moth *Operophtera brumata*. *Sci. Rep.* 6:18576. doi: 10.1038/srep18576

Zhang, D. D., Zhu, K. Y., and Wang, C. Z. (2010). Sequencing and characterization of six cDNAs putatively encoding three pairs of pheromone receptors in two sibling species, *Helicoverpa armigera* and *Helicoverpa assulta*. *J. Insect Physiol.* 56, 586–593. doi: 10.1016/j.jinsphys.2009.12.002

Zhang, J., Yan, S., Liu, Y., Jacquin-Joly, E., Dong, S., and Wang, G. (2015). Identification and functional characterization of sex pheromone receptors in the common cutworm (*Spodoptera litura*). *Chem. Senses* 40, 7–16. doi: 10.1093/chemse/bju052

Zhang, S. X., Xu, S. Q., Kong, L. F., Sima, Y. H., and Cui, W. Z. (2009). Cloning of pbp1, or1 and or3 from wild silkworm *Bombyx mandarina* and evolutional analysis with the orthologous genes of domesticated silkworm *Bombyx mori*. *Acta Entomol. Sinica* 52, 917–922.

Zhang, Y. N., Du, L. X., Xu, J. W., Wang, B., Zhang, X. Q., Yan, Q., et al. (2019). Functional characterization of four sex pheromone receptors in the newly discovered maize pest *Athetis lepigone*. *J. Insect Physiol.* 113, 59–66. doi: 10.1016/j.jinsphys.2018.08.009

Zhang, Y. N., Jin, J. Y., Jin, R., Xia, Y. H., Zhou, J. J., Deng, J. Y., et al. (2013). Differential expression patterns in chemosensory and non-chemosensory tissues of putative chemosensory genes identified by transcriptome analysis of insect pest the purple stem borer Sesamia inferens (Walker). *PLoS One* 8:e69715. doi: 10.1371/journal.pone.0069715

Zhang, Y.N., Ma, J. F., Sun, L., Dong, Z. P., Li, Z. Q., Zhu, X. Y., et al. (2016). Molecular identification and sex distribution of two chemosensory receptor families in *Athetis lepigone* by antennal transcriptome analysis. *J. Asia-Pac Entomol.* 19, 571–580. doi: 10.1016/j.aspen.2016.05.009

Zhang, Y. N., Qian, J. L., Xu, J. W., Zhu, X. Y., Li, M. Y., Xu, X. X., et al. (2018). Identification of chemosensory genes based on the transcriptomic analysis of six different chemosensory organs in *Spodoptera exigua*. *Front. Physiol.* 9:432. doi: 10.3389/fphys.2018.00432

Zhang, Y. N., Zhang, J., Yan, S. W., Chang, H. T., Liu, Y., Wang, G. R., et al. (2014). Functional characterization of sex pheromone receptors in the purple stem borer. Sesamia inferens (Walker). *Insect Mol. Biol.* 23, 611–620.

Conflict of Interest: The authors declare that the research was conducted in the absence of any commercial or financial relationships that could be construed as a potential conflict of interest.

Publisher's Note: All claims expressed in this article are solely those of the authors and do not necessarily represent those of their affiliated organizations, or those of the publisher, the editors and the reviewers. Any product that may be evaluated in this article, or claim that may be made by its manufacturer, is not guaranteed or endorsed by the publisher.

Copyright © 2022 Yang, Cheng, Lin, Zheng, Yu and Sun. This is an open-access article distributed under the terms of the Creative Commons Attribution License (CC BY). The use, distribution or reproduction in other forums is permitted, provided the original author(s) and the copyright owner(s) are credited and that the original publication in this journal is cited, in accordance with accepted academic practice. No use, distribution or reproduction is permitted which does not comply with these terms.

frontiers | Frontiers in Ecology and Evolution

CORRECTION
published: 14 April 2022
doi: 10.3389/fevo.2022.900818

Corrigendum: Sex Pheromone Receptors of Lepidopteran Insects

Chan Yang[1], Jie Cheng[2], Jingyu Lin[2], Yuan Zheng[1], Xiao Yu[2] and Jinpeng Sun[1,3]**

[1] Key Laboratory of Molecular Cardiovascular Science, Ministry of Education, Department of Physiology and Pathophysiology, School of Basic Medical Sciences, Peking University, Beijing, China, [2] Key Laboratory Experimental Teratology of the Ministry of Education and Department of Physiology, School of Basic Medical Sciences, Shandong University, Jinan, China, [3] Key Laboratory Experimental Teratology of the Ministry of Education and Department of Biochemistry and Molecular Biology, School of Basic Medical Sciences, Shandong University, Jinan, China

Keywords: sex pheromone receptor, structure, signal transduction, Lepidopteran insects, evolution, function

A Corrigendum on

Sex Pheromone Receptors of Lepidopteran Insects
by Yang, C., Cheng, J., Lin, J., Zheng, Y., Yu, X., and Sun, J. (2022). Front. Ecol. Evol. 10:797287. doi: 10.3389/fevo.2022.797287

In the original article, the sentence "The identified SPRs and their specific sex pheromone ligands were summarized (Table 1)." should have been removed.

A correction has been made to **Introduction**, paragraph 3:

"In this review, we summarized SPR and Orco information from 10 families (i.e., Bombycidae, Plutellidae, Sphingidae, Saturniidae, Geometridae, Nymphalidae, Noctuidae, Tortricidae, Pyralidae, and Crambidae) of Lepidopteran insects (Krieger et al., 2004, 2005; Sakurai et al., 2004; Miura et al., 2005; Nakagawa et al., 2005; Grosse-Wilde et al., 2007, 2010, 2011; Mitsuno et al., 2008; Jordan et al., 2009; Patch et al., 2009; Zhang et al., 2009, 2010, 2013, 2014, 2015; Wanner et al., 2010; Legeai et al., 2011; Wang et al., 2011; Yasukochi et al., 2011; Zhan et al., 2011; Bengtsson et al., 2012; Carraher et al., 2012; Leary et al., 2012; Liu et al., 2012, 2014; Montagne et al., 2012; Xu et al., 2012, 2015; Liu C. et al., 2013; Liu Y. et al., 2013; Sun et al., 2013; Wu et al., 2013; Zhang and Lofstedt, 2013; Jiang et al., 2014; Corcoran et al., 2015; De Fouchier et al., 2015; Feng et al., 2015; Garczynski and Leal, 2015; Lin et al., 2015; Steinwender et al., 2015; Chang et al., 2016; Ge et al., 2016; Jia et al., 2016; Walker et al., 2016; Zhang D.D. et al., 2016; Zhang Y.N. et al., 2016; Gonzalez et al., 2017; Li et al., 2017; Wicher et al., 2017; Yang et al., 2017; Du et al., 2018; Grapputo et al., 2018; Rojas et al., 2018; Table 1). Among all the Lepidopteran SPRs, several of them have been characterized to be sex pheromone sensing receptors. First of all, we reviewed the phylogenetic analyses of Lepidopteran SPRs, and the evolution of the summarized Lepidopteran SPRs was analyzed through MEGA X (Whelan and Goldman, 2001; Kumar et al., 2018). Second, we reviewed the transmembrane predictions of Lepidopteran SPRs, and the protein structure of Lepidopteran SPRs was predicted by online software Consensus Constrained TOPology Prediction (CCTOP) (Dobson et al., 2015) and SwissModel (Bertoni et al., 2017; Bienert et al., 2017; Waterhouse et al., 2018; Guex et al., 2019; Studer et al., 2020). Third, the interaction of Lepidopteran SPM and SPR was reviewed. Finally, the research status of downstream signaling responses and ligand-gated ion channels by the coupling of SPR and Orco was depicted."

In the original article, **Figures 3** and **4** did not match their captions because the figures were erroneously interchanged. The corrected **Figures 3** and **4** with their captions appear below.

In the original article, the citation "[18]" should have been replaced with "Wicher et al., 2017". The citation has now been inserted in "*Downstream Signaling Pathways of Sex Pheromone Receptors*", paragraph 1 and should read:

OPEN ACCESS

Edited and reviewed by:
Rui Tang,
Guangdong Academy of Science (CAS), China

***Correspondence:**
Xiao Yu
yuxiao@sdu.edu.cn
Jinpeng Sun
sunjinpeng@sdu.edu.cn

Specialty section:
This article was submitted to Chemical Ecology, a section of the journal Frontiers in Ecology and Evolution

Received: *21 March 2022*
Accepted: *23 March 2022*
Published: *14 April 2022*

Citation:
Yang C, Cheng J, Lin J, Zheng Y, Yu X and Sun J (2022) Corrigendum: Sex Pheromone Receptors of Lepidopteran Insects. Front. Ecol. Evol. 10:900818. doi: 10.3389/fevo.2022.900818

"Early research revealed the presence of G-protein, belonging to the Gαq family, in antennal preparations (especially the pheromone-sensitive sensilla trichodea) of *B. mori* and *Antheraea pernyi*, implied a participation of G-protein of the Gαq family in the signal transduction of OR cells in moths (Laue et al., 1997; Nakagawa et al., 2005). The bombykol stimulation of *Xenopus laevis* oocytes expressing BmOR-1 and BmGαq elicited robust dose-dependent inward Ca^{2+}-dependent Cl^- currents on two-electrode voltage-clamp recordings, demonstrating that the binding of bombykol to BmOR-1 leads to the activation of a BmGαq-mediated signaling cascade (Sakurai et al., 2004). MsexOR1 and MsexOrco coexpressed in HEK293 and CHO cells caused bombykal-dependent increases in the intracellular free Ca^{2+} concentration, and inhibitor evidence showed that phospholipase C (PLC) and protein kinase C (PKC) activities are involved in the bombykal-receptor-mediated Ca^{2+} signals of hawk moths. It could be hypothesized that MsexOrs couple to Gαq proteins, requiring the activation of PLC for pheromone transduction (Wicher et al., 2017). Immunocytochemistry research showed that anti-Gαq and anti-Gαs antisera stained the inner and outer dendritic segments of the putative OR neuron in male and female antennae, which suggested that each subunit mediates a subset of the odorant response (Miura et al., 2005). In addition, a computational model of the insect pheromone transduction cascade had been used to calculate the presence of the G-protein pathway in pheromone detection (Gu et al., 2009). Furthermore, recent research showed that in HEK293A cells expressing BmOR3 and human Gαi, the dose-dependent coupling of BmOR3 and Gαi on bombykal stimulation was detected through BRET (Lin et al., 2021). From the biophysical perspective, a conservation residue W103 in transmembrane 2 of BmOR3 is the key that determines receptor-Gi coupling (Lin et al., 2021). Pretreatment with specific Gi inhibitor PTX had no significant effects on bombykal-induced BmOR3-BmOrco complex formation or complex-regulated calcium influx, suggesting that Gi coupling and BmOrco coupling are the two independent processes in the case of BmOR3 (Lin et al., 2021)."

Due to a production error, bombykol was erroneously described as the agonist of MsexOR1 and BmOR3; the correct agonist is bombykal.

A correction has been made to *"Downstream Signaling Pathways of Sex Pheromone Receptors"*, paragraphs 1 and 2:

"Early research revealed the presence of G-protein, belonging to the Gαq family, in antennal preparations (especially the pheromone-sensitive sensilla trichodea) of *B. mori* and *Antheraea pernyi*, implied a participation of G-protein of the Gαq family in the signal transduction of OR cells in moths (Laue et al., 1997; Nakagawa et al., 2005). The bombykol stimulation of *Xenopus laevis* oocytes expressing BmOR-1 and BmGαq elicited robust dose-dependent inward Ca^{2+}-dependent Cl^- currents on two-electrode voltage-clamp recordings, demonstrating that the binding of bombykol to BmOR-1 leads to the activation of a BmGαq-mediated signaling cascade (Sakurai et al., 2004). MsexOR1 and MsexOrco coexpressed in HEK293 and CHO cells caused bombykal-dependent increases in the intracellular free Ca^{2+} concentration, and inhibitor evidence showed that phospholipase C (PLC) and protein kinase C (PKC) activities are involved in the bombykal-receptor-mediated Ca^{2+} signals of hawk moths. It could be hypothesized that MsexORs couple to Gαq proteins, requiring the activation of PLC for pheromone transduction (Wicher et al., 2017). Immunocytochemistry research showed that anti-Gαq and anti-Gαs antisera stained the inner and outer dendritic segments of the putative OR neuron in male and female antennae, which suggested that each subunit mediates a subset of the odorant response (Miura et al., 2005). In addition, a computational model of the insect pheromone transduction cascade had been used to calculate the presence of the G-protein pathway in pheromone detection (Gu et al., 2009). Furthermore, recent research showed that in HEK293A cells expressing BmOR3 and human Gαi, the dose-dependent coupling of BmOR3 and Gαi on bombykal stimulation was detected through BRET (Lin et al., 2021). From the biophysical perspective, a conservation residue W103 in transmembrane 2 of BmOR3 is the key that determines receptor-Gi coupling (Lin et al., 2021). Pretreatment with specific Gi inhibitor PTX had no significant effects on bombykal-induced BmOR3-BmOrco complex formation or complex-regulated calcium influx, suggesting that Gi coupling and BmOrco coupling are the two independent processes in the case of BmOR3 (Lin et al., 2021).

The GPCRs usually direct the recruitment, activation, and scaffolding of the cytoplasmic signaling complexes *via* two multifunctional adaptor and transducer molecules, β-arrestins 1 and 2, and arrestins also function to activate signaling cascades independently of G-protein activation or mediate receptor desensitization (Lefkowitz and Shenoy, 2005; DeWire et al., 2007). Individual arrestins had been reported to function in both olfactory and visual pathways in Dipteran insects (Merrill et al., 2001) but not in Lepidopteran insects. Recent research reported that bombykal robustly stimulated the recruitment of human β-arrestin-1/2 and *B. mori* intrinsic arrestin to BmOR3 in HEK293A cells in a concentration-dependent manner, and the arrestin, in turn, regulated BmOR3 internalization (Lin et al., 2021). Bombykal also induced downstream kinase (i.e., ERK, SRC, AKT, and JNK) activation (phosphorylation) through arrestin (Lin et al., 2021). These results confirmed the arrestin-mediated signaling downstream of BmOR3. The knockdown of β-arrestins significantly reduced bombykal-induced calcium influx through BmOR3-BmOR2, which was accompanied by the collapse of the receptor complex, suggesting that the β-arrestins mediate Ca2+ response mainly by regulating the structural and functional integrity of the BmOR3-BmOR2 complex (Lin et al., 2021). The summarized researches show that insect pheromone receptors may both have G-protein and arrestin downstream pathways (**Figure 4**)."

The same correction has also been made to *"Metabotropic Ion Channel by the Coupling of Lepidopteran Sex Pheromone Receptors and Orcos"*, paragraphs 1 and 2:

"BmOR1 and BmOR3 of *B. mori* are mutually exclusively expressed in a pair of adjacent pheromone-sensitive neurons of male antennae, and both of which are coexpressed with the highly conserved insect Orco. Heterologous cells coexpressing BmOR2 can greatly enhance the sensitivity of BmOR1 to bombykol, and

the current-voltage analysis showed that bombykol activated a non-selective cation channel in oocytes expressing BmOR1 and BmOR2, which is different from Ca^{2+}-activated Cl^- channel through BmGαq, and the non-selective cation channel activity in response to bombykol was also observed when BmOR1 was coexpressed with HvirOR2 or Or83b (Whelan and Goldman, 2001; Nakagawa et al., 2005; **Figure 4**). As reported in MsexOR1, the PLC/PKC activity is a prerequisite to bombykal-receptor-mediated Ca2+ signals in HEK293 and CHO cells, and it could be hypothesized that MsexOR1 and MsexOrco need to be phosphorylated before they can be gated by bombykal as an ionotropic odor receptor-ion channel complex (Wicher et al., 2017).

In a recent study, the BmOR3-BmOR2 combination elicited a response to bombykal and showed similar channel properties, and the coupling of BmOR3 and BmOR2 forms a cation channel with the detection of calcium influx (Lin et al., 2021). From the view of biophysics, there was also physical interaction between BmOR3 and its Orco BmOR2. On bombykal stimulation, the cytoplasmic parts intracellular loop 1 (ICL1), ICL2, and ICL3 moved away from the N-terminus, while the C-terminal helical kink moved close to the N-terminus of BmOR3. On the contrary, the lower part of loop7a-7b moved away from the N-terminus in BmOR2. ICL1, ICL2, and ICL3 also moved away from the N-terminus of BmOR2 (Lin et al., 2021). The replacement of transmembrane 7 in both receptors confirmed its indispensable role in BmOR3-BmOrco coupling for ionotropic functions (Lin et al., 2021). Several key motifs determine the BmOR3-BmOR2 coupling, the charged residue pair of BmOR3-E403 and BmOrco-K437 represents an important "ionic lock" in regard to mediating BmOR3-BmOrco coupling, and the hydrophobic patches F428/F433 of BmOR3 and zipper Y464/V467/L468/L471 of BmOrco are spatially close to each other, suggesting that they might form hydrophobic interactions (Lin et al., 2021). These reports suggest that the coupling of both SPR and Orco plays a vital role in sex pheromone signal detection and transduction."

The authors and publisher apologize for these errors and state that this does not change the scientific conclusions of the article in any way. The original article has been updated.

REFERENCES

Bengtsson, J. M., Trona, F., Montagne, N., Anfora, G., Ignell, R., Witzgall, P., et al. (2012). Putative chemosensory receptors of the codling moth, *Cydia pomonella*, identified by antennal transcriptome analysis. *PLoS One* 7:e31620. doi: 10.1371/journal.pone.0031620

Bertoni, M., Kiefer, F., Biasini, M., Bordoli, L., and Schwede, T. (2017). Modeling protein quaternary structure of homo- and hetero-oligomers beyond binary interactions by homology. *Sci. Rep.* 7:10480. doi: 10.1038/s41598-017-09654-8

Bienert, S., Waterhouse, A., de Beer, T. A. P., Tauriello, G., Studer, G., Bordoli, L., et al. (2017). The SWISS-MODEL Repository - new features and functionality. *Nucleic Acids Res.* 45, D313–D319. doi: 10.1093/nar/gkw1132

Carraher, C., Authier, A., Steinwender, B., and Newcomb, R. D. (2012). Sequence comparisons of odorant receptors among tortricid moths reveal different rates of molecular evolution among family members. *PLoS One* 7:e38391. doi: 10.1371/journal.pone.0038391

Chang, H., Guo, M., Wang, B., Liu, Y., Dong, S., and Wang, G. (2016). Sensillar expression and responses of olfactory receptors reveal different peripheral coding in two *Helicoverpa species* using the same pheromone components. *Sci. Rep.* 6:18742. doi: 10.1038/srep18742

Corcoran, J. A., Jordan, M. D., Thrimawithana, A. H., Crowhurst, R. N., and Newcomb, R. D. (2015). The peripheral olfactory repertoire of the lightbrown apple moth, *Epiphyas postvittana*. *PLoS One* 10:e0128596. doi: 10.1371/journal.pone.0128596

De Fouchier, A., Sun, X., Monsempes, C., Mirabeau, O., Jacquin-Joly, E., and Montagné, N. (2015). Evolution of two receptors detecting the same pheromone compound in crop pest moths of the genus Spodoptera. *Front. Ecol. Evol.* 3:95. doi: 10.3389/fevo.2015.00095

DeWire, S. M., Ahn, S., Lefkowitz, R. J., and Shenoy, S. K. (2007). Beta-arrestins and cell signaling. *Annu. Rev. Physiol.* 69, 483–510.

Dobson, L., Reményi, I., and Tusnády, G. E. (2015). CCTOP: a consensus constrained TOPology prediction web server. *Nucleic Acids Res.* 43, W408–W412. doi: 10.1093/nar/gkv451

Du, L. X., Liu, Y., Zhang, J., Gao, X. W., Wang, B., and Wang, G. R. (2018). Identification and characterization of chemosensory genes in the antennal transcriptome of Spodoptera exigua. *Comp. Biochem. Physiol. Part D Genom. Proteom.* 27, 54–65. doi: 10.1016/j.cbd.2018.05.001

Feng, B., Lin, X., Zheng, K., Qian, K., Chang, Y., and Du, Y. (2015). Transcriptome and expression profiling analysis link patterns of gene expression to antennal responses in *Spodoptera litura*. *BMC Genomics* 16:269. doi: 10.1186/s12864-015-1375-x

Garczynski, S. F., and Leal, W. S. (2015). Alternative splicing produces two transcripts encoding female-biased pheromone subfamily receptors in the navel orangeworm, *Amyelois transitella*. *Front. Ecol. Evol.* 3:115. doi: 10.3389/fevo.2015.00115

Ge, X., Zhang, T. T., Wang, Z. Y., He, K. L., and Bai, S. X. (2016). Identification of putative chemosensory receptor genes from yellow peach moth *Conogethes punctiferalis* (Guenée) antennae transcriptome. *Sci. Rep.* 6, 32636–32648. doi: 10.1038/srep32636

Gonzalez, F., Witzgall, P., and Walker, W. B. (2017). Antennal transcriptomes of three tortricid moths reveal putative conserved chemosensory receptors for social and habitat olfactory cues. *Sci. Rep.* 7, 41829–41840. doi: 10.1038/srep41829

Grapputo, A., Thrimawithana, A. H., Steinwender, B., and Newcomb, R. D. (2018). Differential gene expression in the evolution of sex pheromone communication in New Zealand's endemic leafroller moths of the genera Ctenopseustis and Planotortrix. *BMC Genomics* 19:94. doi: 10.1186/s12864-018-4451-1

Grosse-Wilde, E., Gohl, T., Bouche, E., Breer, H., and Krieger, J. (2007). Candidate pheromone receptors provide the basis for the response of distinct antennal neurons to pheromonal compounds. *Eur. J. Neurosci.* 25, 2364–2373. doi: 10.1111/j.1460-9568.2007.05512.x

Grosse-Wilde, E., Kuebler, L. S., Bucks, S., Vogel, H., Wicher, D., and Hansson, B. S. (2011). Antennal transcriptome of *Manduca sexta*. *PNAS* 108, 7449–7454.

Grosse-Wilde, E., Stieber, R., Forstner, M., Krieger, J., Wicher, D., and Hansson, B. S. (2010). Sex-specific odorant receptors of the tobacco hornworm manduca sexta. *Front. Cell Neurosci.* 4:22. doi: 10.3389/fncel.2010.00022

Gu, Y., Lucas, P., and Rospars, J. (2009). Computational model of the insect pheromone transduction cascade. *PLoS Comput. Biol.* 5:e1000321. doi: 10.1371/journal.pcbi.1000321

Guex, N., Peitsch, M. C., and Schwede, T. (2019). Automated comparative protein structure modeling with SWISS-MODEL and Swiss-PdbViewer: a historical perspective. *Electrophoresis* 30, S162–S173. doi: 10.1002/elps.200900140

Jia, X. J., Wang, H. X., Yan, Z. G., Zhang, M. Z., Wei, C. H., Qin, X. C., et al. (2016). Antennal transcriptome and differential expression of olfactory genes in the yellow peach moth, *Conogethes punctiferalis* (Lepidoptera: Crambidae). *Sci. Rep.* 6, 29067–29082. doi: 10.1038/srep29067

Jiang, X. J., Guo, H., Di, C., Yu, S., Zhu, L., Huang, L. Q., et al. (2014). Sequence similarity and functional comparisons of pheromone receptor orthologs in two closely related *Helicoverpa species*. *Insect Biochem. Mol. Biol.* 48, 63–74. doi: 10.1016/j.ibmb.2014.02.010

Jordan, M. D., Anderson, A., Begum, D., Carraher, C., Authier, A., Marshall, S. D., et al. (2009). Odorant receptors from the light brown apple moth

(*Epiphyas postvittana*) recognize important volatile compounds produced by plants. *Chem. Senses* 34, 383–394. doi: 10.1093/chemse/bjp010

Krieger, J., Grosse-Wilde, E., Gohl, T., and Breer, H. (2005). Candidate pheromone receptors of the silkmoth *Bombyx mori*. *Eur. J. Neurosci.* 21, 2167–2176.

Krieger, J., Grosse-Wilde, E., Gohl, T., Dewer, Y. M. E., Raming, K., and Breer, H. (2004). Genes encoding candidate pheromone receptors in a moth (*Heliothis virescens*). *PNAS* 101, 11845–11850. doi: 10.1073/pnas.0403052101

Kumar, S., Stecher, G., Li, M., Knyaz, C., and Tamura, K. (2018). MEGA X: molecular evolutionary genetics analysis across computing platforms. *Mol. Biol. Evol.* 35, 1547–1549. doi: 10.1093/molbev/msy096

Laue, M., Maida, R., and Redkozubov, A. (1997). G-protein activation, identification and immunolocalization in pheromone-sensitive sensilla trichodea of moths. *Cell Tissue Res.* 288, 149–158. doi: 10.1007/s004410050802

Leary, G. P., Allen, J. E., Bunger, P. L., Luginbill, J. B., Linn, C. E., Macallister, I. E., et al. (2012). Single mutation to a sex pheromone receptor provides adaptive specificity between closely related moth species. *PNAS* 109, 14081–14086. doi: 10.1073/pnas.1204661109

Lefkowitz, R. J., and Shenoy, S. K. (2005). Transduction of receptor signals by β-Arrestins. *Science* 308, 512–517. doi: 10.1126/science.1109237

Legeai, F., Malpel, S., Montagné, N., Monsempes, C., Cousserans, F., Merlin, C., et al. (2011). An expressed Sequence Tag collection from the male antennae of the Noctuid moth *Spodoptera littoralis*: a resource for olfactory and pheromone detection research. *BMC Genomics* 12:86. doi: 10.1186/1471-2164-12-86

Li, Z. Q., Luo, Z. X., Cai, X. M., Bian, L., Xin, Z. J., Liu, Y., et al. (2017). Chemosensory gene families in ectropis grisescens and candidates for detection of Type-II sex pheromones. *Front. Physiol.* 8:953. doi: 10.3389/fphys.2017.00953

Lin, J. Y., Yang, Z., Yang, C., Du, J. X., Yang, F., Cheng, J., et al. (2021). An ionic lock and a hydrophobic zipper mediate the coupling between an insect pheromone receptor BmOR3 and downstream effectors. *J. Biol. Chem.* 297:101160. doi: 10.1016/j.jbc.2021.101160

Lin, X., Zhang, Q., Wu, Z., and Du, Y. (2015). Identification and differential expression of a candidate sex pheromone receptor in natural populations of *Spodoptera litura*. *PLoS One* 10:e0131407. doi: 10.1371/journal.pone.0131407

Liu, C., Liu, Y., Walker, W. B., Dong, S., and Wang, G. (2013). Identification and functional characterization of sex pheromone receptors in beet armyworm *Spodoptera exigua* (Hubner). *Insect Biochem. Mol. Biol.* 43, 747–754. doi: 10.1016/j.ibmb.2013.05.009

Liu, N. Y., Xu, W., Papanicolaou, A., Dong, S. L., and Anderson, A. (2014). Identification and characterization of three chemosensory receptor families in the cotton bollworm *Helicoverpa armigera*. *BMC Genomics* 15:597. doi: 10.1186/1471-2164-15-597

Liu, Y., Gu, S., Zhang, Y., Guo, Y., and Wang, G. (2012). Candidate olfaction genes identified within the *Helicoverpa armigera* antennal transcriptome. *PLoS One* 7:e48260. doi: 10.1371/journal.pone.0048260

Liu, Y., Liu, C., Lin, K., and Wang, G. (2013). Functional specificity of sex pheromone receptors in the cotton bollworm *Helicoverpa armigera*. *PLoS One* 8:e62094. doi: 10.1371/journal.pone.0062094

Merrill, C. E., Riesgo-Escovar, J., Pitts, R. J., Kafatos, F. C., Carlson, J. R., and Zwiebel, L. J. (2001). Visual arrestins in olfactory pathways of *Drosophila* and the malaria vector mosquito *Anopheles gambiae*. *PNAS* 99, 1633–1638. doi: 10.1073/pnas.022505499

Mitsuno, H., Sakurai, T., Murai, M., Yasuda, T., Kugimiya, S., Ozawa, R., et al. (2008). Identification of receptors of main sex-pheromone components of three *Lepidopteran species*. *Eur. J. Neurosci.* 28, 893–902. doi: 10.1111/j.1460-9568.2008.06429.x

Miura, N., Atsumi, S., Tabunoki, H., and Sato, R. (2005). Expression and localization of three G protein alpha subunits, Go, Gq, and Gs, in adult antennae of the silkmoth (*Bombyx mori*). *J. Comp. Neurol.* 485, 143–152. doi: 10.1002/cne.20488

Montagne, N., Chertemps, T., Brigaud, I., Francois, A., Francois, M. C., Fouchier, A., et al. (2012). Functional characterization of a sex pheromone receptor in the pest moth *Spodoptera littoralis* by heterologous expression in *Drosophila*. *Eur. J. Neurosci.* 36, 2588–2596. doi: 10.1111/j.1460-9568.2012.08183.x

Nakagawa, T., Sakurai, T., Nishioka, T., and Touhara, K. (2005). Insect sex-pheromone signals mediated by specific combinations of olfactory receptors. *Science* 307, 1638–1641. doi: 10.1126/science.1106267

Patch, H. M., Velarde, R. A., Walden, K. K., and Robertson, H. M. (2009). A candidate pheromone receptor and two odorant receptors of the hawkmoth *Manduca sexta*. *Chem. Senses* 34, 305–316. doi: 10.1093/chemse/bjp002

Rojas, V., Jimenez, H., Palma-Millanao, R., Gonzalez-Gonzalez, A., Machuca, J., Godoy, R., et al. (2018). Analysis of the grapevine moth *Lobesia botrana* antennal transcriptome and expression of odorant-binding and chemosensory proteins. *Comp. Biochem. Physiol. Part D* 27, 1–12. doi: 10.1016/j.cbd.2018.04.003

Sakurai, T., Nakagawa, T., Mitsuno, H., Mori, H., Endo, Y., Tanoue, S., et al. (2004). Identification and functional characterization of a sex pheromone receptor in the silkmoth *Bombyx mori*. *PNAS* 101, 16653–16658. doi: 10.1073/pnas.0407596101

Steinwender, B., Crowhurst, R. N., Thrimawithana, A. H., and Newcomb, R. D. (2015). Pheromone receptor evolution in the cryptic leafroller species, *Ctenopseustis obliquana* and *C. herana*. *J. Mol. Evol.* 80, 42–56. doi: 10.1007/s00239-014-9650-z

Studer, G., Rempfer, C., Waterhouse, A. M., Gumienny, G., Haas, J., and Schwede, T. (2020). QMEANDisCo - distance constraints applied on model quality estimation. *Bioinformatics* 36, 1765–1771.

Sun, M., Liu, Y., Walker, W. B., Liu, C., Lin, K., Gu, S., et al. (2013). Identification and characterization of pheromone receptors and interplay between receptors and pheromone binding proteins in the diamondback moth, *Plutella xyllostella*. *PLoS One* 8:e62098. doi: 10.1371/journal.pone.0062098

Walker, W. B., Gonzalez, F., Garczynski, S. F., and Witzgall, P. (2016). The chemosensory receptors of codling moth Cydia pomonella-expression in larvae and adults. *Sci. Rep.* 6, 23518–23534. doi: 10.1038/srep23518

Wang, G., Vasquez, G. M., Schal, C., Zwiebel, L. J., and Gould, F. (2011). Functional characterization of pheromone receptors in the tobacco budworm *Heliothis virescens*. *Insect Mol. Biol.* 20, 125–133. doi: 10.1111/j.1365-2583.2010.01045.x

Wanner, K. W., Nichols, A. S., Allen, J. E., Bunger, P. L., Garczynski, S. F., Linn, C. E., et al. (2010). Sex pheromone receptor specificity in the European corn borer moth, *Ostrinia nubilalis*. *PLoS One* 5:e8685. doi: 10.1371/journal.pone.0008685

Waterhouse, A., Bertoni, M., Bienert, S., Studer, G., Tauriello, G., Gumienny, R., et al. (2018). SWISS-MODEL: homology modelling of protein structures and complexes. *Nucleic Acids Res.* 46, W296–W303. doi: 10.1093/nar/gky427

Whelan, S., and Goldman, N. (2001). A general empirical model of protein evolution derived from multiple protein families using a maximum-likelihood approach. *Mol. Biol. Evol.* 18, 691–699. doi: 10.1093/oxfordjournals.molbev.a003851

Wicher, D., Morinaga, S., Halty-deLeon, L., Funk, N., Hansson, B., Touhara, K., et al. (2017). Identification and characterization of the bombykal receptor in the hawkmoth *Manduca sexta*. *J. Exp. Biol.* 220, 1781–1786. doi: 10.1242/jeb.154260

Wu, Z. N., Chen, X., Du, Y. J., Zhou, J. J., and ZhuGe, Q. C. (2013). Molecular identification and characterization of the *Orco orthologue* of *Spodoptera litura*. *Insect Sci.* 20, 175–182. doi: 10.1111/j.1744-7917.2011.01483.x

Xu, P., Garczynski, S. F., Atungulu, E., Syed, Z., Choo, Y. M., Vidal, D. M., et al. (2012). Moth sex pheromone receptors and deceitful parapheromones. *PLoS One* 7:e41653. doi: 10.1371/journal.pone.0041653

Xu, W., Papanicolaou, A., Liu, N. Y., Dong, S. L., and Anderson, A. (2015). Chemosensory receptor genes in the Oriental tobacco budworm *Helicoverpa assulta*. *Insect Mol. Biol.* 24, 253–263. doi: 10.1111/imb.12153

Yang, S., Cao, D., Wang, G., and Liu, Y. (2017). Identification of genes involved in chemoreception in *Plutella xyllostella* by antennal transcriptome analysis. *Sci. Rep.* 7:11941. doi: 10.1038/s41598-017-11646-7

Yasukochi, Y., Miura, N., Nakano, R., Sahara, K., and Ishikawa, Y. (2011). Sex-linked pheromone receptor genes of the European corn borer, *Ostrinia nubilalis*, are in tandem arrays. *PLoS One* 6:e18843. doi: 10.1371/journal.pone.0018843

Zhan, S., Merlin, C., Boore, J. L., and Reppert, S. M. (2011). The monarch butterfly genome yields insights into long-distance migration. *Cell* 147, 1171–1185. doi: 10.1016/j.cell.2011.09.052

Zhang, D.D., Wang, H. L., Schultze, A., Fross, H., Francke, W., Krieger, J., et al. (2016). Receptor for detection of a Type II sex pheromone in the winter moth *Operophtera brumata*. *Sci. Rep.* 6:18576. doi: 10.1038/srep18576

Zhang, D. D., and Lofstedt, C. (2013). Functional evolution of a multigene family: orthologous and paralogous pheromone receptor genes in the turnip moth, *Agrotis segetum*. *PLoS One* 8:e77345. doi: 10.1371/journal.pone.0077345

Zhang, D. D., Zhu, K. Y., and Wang, C. Z. (2010). Sequencing and characterization of six cDNAs putatively encoding three pairs of pheromone receptors in two sibling species, *Helicoverpa armigera* and *Helicoverpa assulta*. *J. Insect Physiol.* 56, 586–593. doi: 10.1016/j.jinsphys.2009.12.002

Zhang, J., Yan, S., Liu, Y., Jacquin-Joly, E., Dong, S., and Wang, G. (2015). Identification and functional characterization of sex pheromone receptors in the common cutworm (*Spodoptera litura*). *Chem. Senses* 40, 7–16. doi: 10.1093/chemse/bju052

Zhang, S. X., Xu, S. Q., Kong, L. F., Sima, Y. H., and Cui, W. Z. (2009). Cloning of pbp1, or1 and or3 from wild silkworm *Bombyx mandarina* and evolutional analysis with the orthologous genes of domesticated silkworm *Bombyx mori*. *Acta Entomol. Sinica* 52, 917–922.

Zhang, Y.N., Ma, J. F., Sun, L., Dong, Z. P., Li, Z. Q., Zhu, X. Y., et al. (2016). Molecular identification and sex distribution of two chemosensory receptor families in *Athetis lepigone* by antennal transcriptome analysis. *J. Asia-Pac Entomol.* 19, 571–580. doi: 10.1016/j.aspen.2016.05.009

Zhang, Y. N., Jin, J. Y., Jin, R., Xia, Y. H., Zhou, J. J., Deng, J. Y., et al. (2013). Differential expression patterns in chemosensory and non-chemosensory tissues of putative chemosensory genes identified by transcriptome analysis of insect pest the purple stem borer Sesamia inferens (Walker). *PLoS One* 8:e69715. doi: 10.1371/journal.pone.0069715

Zhang, Y. N., Zhang, J., Yan, S. W., Chang, H. T., Liu, Y., Wang, G. R., et al. (2014). Functional characterization of sex pheromone receptors in the purple stem borer. Sesamia inferens (Walker). *Insect Mol. Biol.* 23, 611–620.

Publisher's Note: All claims expressed in this article are solely those of the authors and do not necessarily represent those of their affiliated organizations, or those of the publisher, the editors and the reviewers. Any product that may be evaluated in this article, or claim that may be made by its manufacturer, is not guaranteed or endorsed by the publisher.

Copyright © 2022 Yang, Cheng, Lin, Zheng, Yu and Sun. This is an open-access article distributed under the terms of the Creative Commons Attribution License (CC BY). The use, distribution or reproduction in other forums is permitted, provided the original author(s) and the copyright owner(s) are credited and that the original publication in this journal is cited, in accordance with accepted academic practice. No use, distribution or reproduction is permitted which does not comply with these terms.

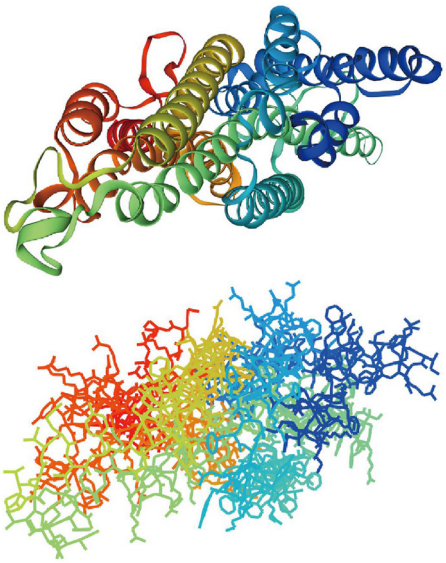

FIGURE 3 | Predicted structure of Lepidopteran SPRs BmOR3 and Orcos through SwissModel. In total, 7 transmembrane helixes were colored rainbow in the form of silk ribbon (Cartoon) and lines.

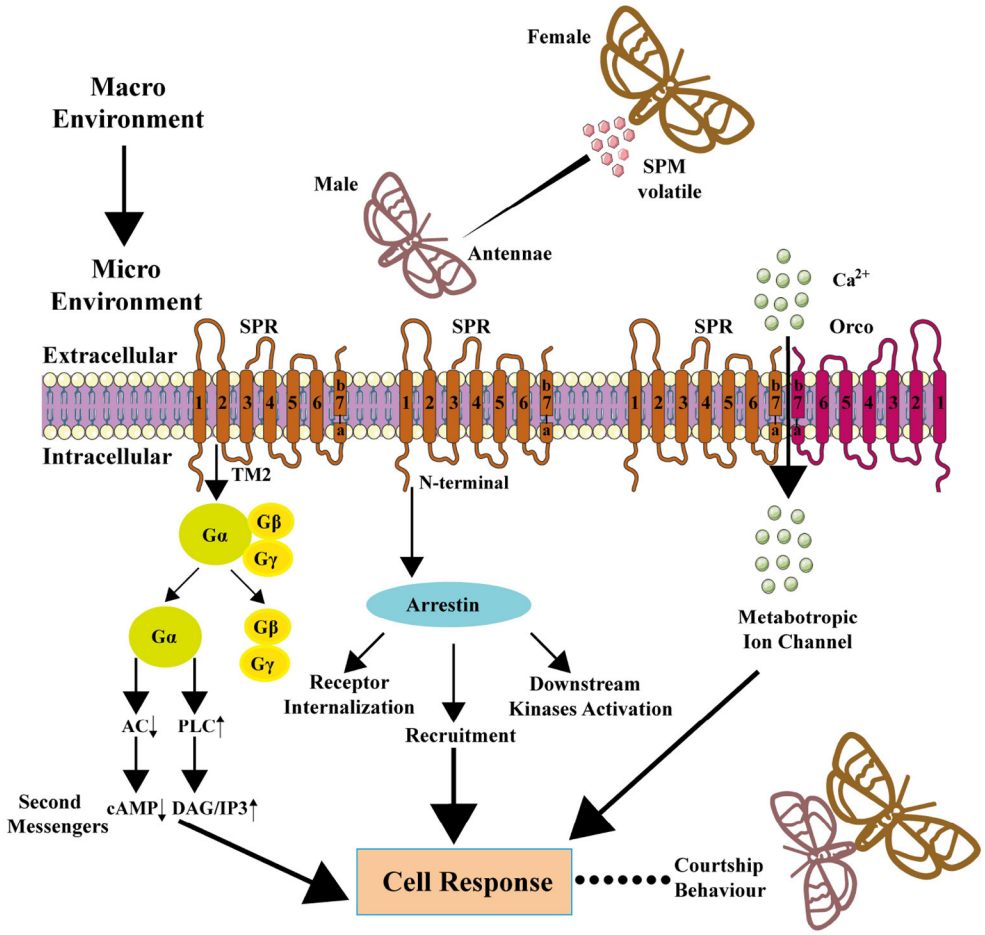

FIGURE 4 | Downstream signaling pathway of SPR and metabotropic channel of SPR-Orco. In macro environment, male insects sense the SPM released by female insects through an olfactory sensory neuron in antennae, and SPM works as an agonist to SPR, and signal transduction leads to ultimate mating behavior.

frontiers in Physiology

ORIGINAL RESEARCH
published: 28 February 2022
doi: 10.3389/fphys.2022.839559

Identification of Odorant-Binding and Chemosensory Protein Genes in *Mythimna separata* Adult Brains Using Transcriptome Analyses

*Wen-Bo Chen[1†], Li-Xiao Du[2†], Xiao-Yan Gao[1], Long-Long Sun[1], Lin-Lin Chen[1], Gui-Ying Xie[1], Shi-Heng An[1] and Xin-Cheng Zhao[1]**

[1] Henan International Joint Laboratory of Green Pest Control, College of Plant Protection, Henan Agricultural University, Zhengzhou, China, [2] State Key Laboratory for Biology of Plant Diseases and Insect Pests, Institute of Plant Protection, Chinese Academy of Agricultural Sciences, Beijing, China

Large numbers of chemosensory genes have been identified in the peripheral sensory organs of the pest *Mythimna separata* (Walker) to increase our understanding of chemoreception-related molecular mechanisms and to identify molecular targets for pest control. Chemosensory-related genes are expressed in various tissues, including non-sensory organs, and they play diverse roles. To better understand the functions of chemosensory-related genes in non-sensory organs, transcriptomic analyses of *M. separata* brains were performed. In total, 29 odorant-binding proteins (OBPs) and 16 chemosensory proteins (CSPs) putative genes were identified in the transcriptomic data set. The further examination of sex- and tissue-specific expression using RT-PCR suggested that eight *OBPs* (*OBP5*, *-7*, *-11*, *-13*, *-16*, *-18*, *-21*, and *-24*) and eight *CSPs* (*CSP2–4*, *-8*, *CSP10–12*, and *-15*) genes were expressed in the brain. Furthermore, bands representing most *OBPs* and *CSPs* could be detected in antennae, except for a few that underwent sex-biased expression in abdomens, legs, or wings. An RT-qPCR analysis of the expression profiles of six *OBPs* (*OBP3–5*, *-9*, *-10*, and *-16*) and two *CSPs* (*CSP3* and *CSP4*) in different tissues and sexes indicated that *OBP16* was highly expressed in male brain, and *CSP3* and *CSP4* were female-biased and highly expressed in brain. The expression levels of *OBP5* and *OBP10* in brain were not significantly different between the sexes. The findings expand our current understanding of the expression patterns of *OBP*s and *CSP*s in *M. separata* sensory and non-sensory tissues. These results provide valuable reference data for exploring novel functions of OBPs and CSPs in *M. separata* and may help in developing effective biological control strategies for managing this pest by exploring novel molecular targets.

Keywords: *Mythimna separata*, brain transcriptome, chemosensory genes, chemosensory protein, non-sensory organ, odorant binding protein

OPEN ACCESS

Edited by:
Ya-Nan Zhang,
Huaibei Normal University, China

Reviewed by:
Dingze Mang,
Tokyo University of Agriculture and Technology, Japan
Peng-Fei Lu,
Beijing Forestry University, China

***Correspondence:**
Xin-Cheng Zhao
xincheng@henau.edu.cn

† These authors have contributed equally to this work

Specialty section:
This article was submitted to Invertebrate Physiology, a section of the journal Frontiers in Physiology

Received: *20 December 2021*
Accepted: *24 January 2022*
Published: *28 February 2022*

Citation:
Chen W-B, Du L-X, Gao X-Y, Sun L-L, Chen L-L, Xie G-Y, An S-H and Zhao X-C (2022) Identification of Odorant-Binding and Chemosensory Protein Genes in Mythimna separata Adult Brains Using Transcriptome Analyses. Front. Physiol. 13:839559. doi: 10.3389/fphys.2022.839559

INTRODUCTION

The oriental armyworm *Mythimna separata* (Walker) is a migratory and polyphagous pest species in China and other parts of Asia and Oceania (Jiang et al., 2011, 2014; Liu et al., 2016). The larvae of *M. separata* feed on more than 300 kinds of crops, including wheat, rice, corn, and cotton, resulting in serious yield losses. As with many other moth species, the *M. separata* adults rely heavily on

olfaction to find host plants for food and mates for reproduction. To find the optimal chemical attractants for the control of the pest, the olfactory mechanisms of *M. separata* have been explored in many studies at the behavior, electrophysiology, and molecular levels (Mitsuno et al., 2008; Jiang et al., 2019, 2020; Wang et al., 2021). Thanks to advances in transcriptome sequencing techniques, a large number of chemosensory genes of *M. separata*, including genes for olfactory receptors (ORs), ionotropic receptors (IRs), sensory neuron membrane proteins, odorant-binding proteins (OBPs), and chemosensory proteins (CSPs), have been identified (Bian et al., 2017; Chang X. Q. et al., 2017; He et al., 2017; Liu et al., 2017; Du et al., 2018). The functions of some chemosensory-related proteins in *M. separata*, such as ORs, IRs, and CSPs, have also been well examined, and they are involved in sex pheromone, host volatiles and acid sensing (Mitsuno et al., 2008; Younas et al., 2018a,b, 2021; Zhang et al., 2019; Jiang et al., 2020; Tang et al., 2020; Wang et al., 2021). In addition to these proteins having known functional specificities, there is a large number of proteins of unknown specificity still awaiting experimental testing.

In general, chemosensory genes are expressed in the chemosensory organs of insects (Liu et al., 2012, 2015; Gu et al., 2013; Xiao et al., 2017; Li et al., 2020). However, chemosensory-related proteins are also present in various tissues and play diverse roles (Pelosi et al., 2017). Some insect chemosensory receptors have been identified in non-sensory organs, and their new physiological functions have been further clarified. For example, several gustatory receptors are expressed in the brains of *Drosophila* and *Bombyx mori*, and they are involved in the sensing of internal sugar and fructose nutrient cues, proprioception, hygroreception, and other sensory modalities (Thorne and Amrein, 2010; Miyamoto et al., 2012, Miyamoto and Amrein, 2014; Mang et al., 2016a,b). A subset of ORs are expressed in the testes of the malaria-causing mosquito, and their functions may be associated with sperm activation (Pitts et al., 2014). The OBPs and CSPs are small water-soluble proteins containing a hydrophobic pocket for ligand binding, and they mainly mediate the first step of olfactory signal transmission, which has been widely proven (Pelosi et al., 2017). In addition, the OBPs and CSPs have been detected in various tissues other than olfactory organs. For example, *CSPs* have been identified in the pheromone glands of *Mamestra brassicae* and *B. mori* (Jacquin-Joly et al., 2001; Dani et al., 2011). The *OBP10* of *Helicoverpa armigera* was found on the egg surface (Sun et al., 2012), and *OBPs* and *CSPs* have been detected in the seminal fluids of *Drosophila melanogaster*, *Aedes aegypti* and *Apis mellifera* (Li et al., 2008; Takemori and Yamamoto, 2009; Baer et al., 2012). They have also been identified in venom glands of the parasitic wasps *Leptopilina heterotoma* and *Pteromalus puparum* (Heavner et al., 2013; Wang et al., 2015), in the eye of *H. armigera* (Zhu et al., 2016), and in the ovaries and eggshells of *A. aegypti* (Costa-da-Silva et al., 2013; Marinotti et al., 2014). These proteins may be involved in carrying semiochemicals that have various roles, such as in reproduction, regeneration, development, nutrition, anti-inflammatory action, and vision (Pelosi et al., 2017).

The chemosensory genes of *M. separata* identified from the transcriptomes of a head, antenna, palp, and proboscis also revealed that they have multiple points of origination (Bian et al., 2017; Chang X. Q. et al., 2017; He et al., 2017; Liu et al., 2017; Du et al., 2018). The antennal transcriptomes of *M. separata* revealed 37 OBPs and 14 CSPs in one study, and 32 OBPs and 16 CSPs in another (Chang X. Q. et al., 2017; He et al., 2017). Two studies of *M. separata* head transcriptomes revealed 50 OBPs and 22 CSPs, and 38 OBPs and 18 CSPs, respectively (Bian et al., 2017; Liu et al., 2017). More chemosensory genes in head compared with antennal transcriptomes may indicate that some of the genes are expressed in the brain. Previously, some chemosensory proteins, such as OBPs, CSPs, ORs, and gustatory receptors, were identified in insect brain tissues, and it was hypothesized that these proteins performed important unknown physiological functions as well as the specific known physiological functions (Miyamoto et al., 2012, Miyamoto and Amrein, 2014; Mang et al., 2016a,b; Walker et al., 2019; Wang et al., 2020).

In the present study, RNA-Seq was applied to mine *OBPs* and *CSPs* genes from the brain transcriptome of *M. separata*, and then semi-quantitative RT-PCR and RT-qPCR were used to confirm the expression patterns of *OBPs* and *CSPs* in different sexes and tissues. The findings serve as a foundation for exploring novel functions of chemosensory genes in insect brains and provide new pest control targets.

MATERIALS AND METHODS

Insects Rearing and Tissue Collection

Larvae of *M. separata* were collected in Xinxiang, Henan Province, China. The colony was reared on an artificial diet in the laboratory and maintained under the conditions of 27 ± 1°C, 75 ± 5% relative humidity, and a 14-h/10-h light/dark cycle. Pupae of different sexes were separated in glass Petri dishes before eclosion. Adult moths were provided with sucrose solution 10% (v/v). Brains, antennae, wings, legs and abdomens of unmated moths were collected 2–4 days after eclosion, immediately frozen in liquid nitrogen, and stored at −70°C for RNA extraction.

cDNA Library Construction and Transcriptome Sequencing

Total RNA extracted from brains of approximately 600 adult males and females independently were used to construct separately three female and three male cDNA libraries. The libraries were sequenced using the PE100 strategy on the Illumina HiSeq^{TM} 2000 platform (Illumina, San Diego, CA, United States) at Novogene Bioinformatics Technology Co. Ltd. (Beijing, China). Briefly, mRNA was purified from total RNA using magnetic beads with Oligo (dT), and then, it was fragmented into short fragments after adding fragmentation buffer. First-strand cDNA was synthesized using random hexamer primer and M-MuLV reverse transcriptase (RNase H). Subsequently, the second-strand cDNA was synthesized using DNA polymerase I and RNase H. The double-stranded cDNA was purified using the AMPure XP system (Beckman Coulter, Beverly, MA, United States). NEBNext Adaptors having a hairpin loop structure were ligated to prepare for hybridization after the adenylation of the DNA fragments' 3′ ends. Library fragments

were purified using the AMPure XP system for selecting preferentially cDNA fragments of 150–200 bp. Then, the selected fragments were used as templates for PCR amplification. PCR products were also purified using the AMPure XP system, and library quality was assessed on an Agilent 2100 Bioanalyzer and with a Q-PCR system.

Brain Transcriptome Assembly and Functional Annotation

A *de novo* transcriptome was assembled using the paired-reads mode with default parameters using the short-read program Trinity (Grabherr et al., 2011). Trinity outputs were clustered using TGICL (Pertea et al., 2003). The consensus cluster sequences and singletons made up the final unigene dataset. The generation of unigenes was performed using BLASTx and BLASTn programs against the public databases, with an E-value threshold of 10^{-5}. GO terms were extracted from the best hits obtained from BLASTx against the NR database using the Blast2GO program (Conesa et al., 2005). A GO functional classification of all the unigenes was performed using WEGO software.[1] KOG and KEGG annotations were performed using Blastall software against the KOG[2] and KEGG[3] databases, respectively.

Identification of Putative *OBPs* and *CSPs* Genes

Candidate unigenes encoding putative *OBPs* and *CSPs* were selected on the basis of the NR annotation results in the remote server. All the candidate chemosensory genes were further manually checked using the BLASTx program. The open reading frame (ORF) of each candidate unigene was predicted using the ORF finder tool.[4] The putative signal peptides of OBP and CSP protein sequences were predicted using SignalP 4.1.[5] In addition, all the candidate genes were compared with previously reported sequences using the BLASTn program (with an E-value threshold of 10^{-5}) to identify novel *OBPs* and *CSPs* genes (Du et al., 2018). These genes were named in accordance with gene naming rules by adding a suffix with a number to indicate the descending order of their coding region lengths.

Phylogenetic Analyses of Odorant-Binding Protein and Chemosensory Protein Family Proteins

Multiple alignments of amino acid sequences were performed using the online prediction website MAFFT.[6] The phylogenetic trees were constructed using the maximum-likelihood method with a bootstrap analysis of 1,000 replicates and the JTT with Freqs. (+F) Substitution Model using MEGA5.2 (Tamura et al., 2011). The phylogenetic trees were visualized using FigTree v1.4.3.[7] OBPs data sets contained 29 candidate OBPs from *M. separata*, and 150 from other Lepidopteran moths, including *B. mori* (Gong et al., 2009), *H. armigera* (Liu et al., 2012), *Helicoverpa assulta* (Chang H. et al., 2017), *Spodoptera exigua* (Liu et al., 2015), *Heliothis virescens* (Vogel et al., 2010), and *Spodoptera litura* (Gu et al., 2015). CSPs data sets contained 16 putative CSPs from *M. separata*, and 72 from other Lepidopteran moths, including *B. mori* (Gong et al., 2009), *H. assulta* (Chang H. et al., 2017), *H. armigera* (Zhang J. et al., 2015), *H. virescens* (Picimbon et al., 2001), *Agrotis ipsion* (Gu et al., 2014), *S. litura* (Zhang Y. N. et al., 2015), and *S. exigua* (Liu et al., 2015). The amino acid sequences used in the phylogenetic analyses are listed in **Supplementary Materials 1, 2**.

Tissue- and Sex-Specific Expression Analyses of *OBPs* and *CSPs*

To confirm the expression profiles of the identified *OBPs* and *CSPs* genes, semi-quantitative PCR (RT-PCR) was performed. Total RNA was isolated from brains, antennae, wings, legs, and abdomens of 50–60 adults and extracted using TRIzol reagent (Invitrogen, Carlsbad, CA, United States) following the manufacturer's instructions. Single-stranded cDNA templates were synthesized from 1 μg of total RNA from various tissue samples using the FastKing gDNA Dispelling RT SuperMix (TianGen, Beijing, China). Specific primers of predicted *OBPs* and *CSPs* genes were designed using Premier 5.0 (**Supplementary Material 3** and **Supplementary Table 1**). PCR reactions were carried out using equal amounts of cDNA (200 ng) template. The β-*actin* (GenBank Acc. GQ856238.1) of *M. separata* was selected as the reference gene to test the integrity of the cDNA templates and also the expression quantification of the target genes. The PCR was performed in a Mastercycler® (Eppendorf, Hamburg, Germany) under the following conditions: 94°C for 5 min, 25–33 cycles (depending on the expression level of each gene) of 94°C for 30 s, 56°C for 30 s, and 72°C for 30 s, followed by a final extension at 72°C for 10 min. PCR products were analyzed on 1.0% agarose gels and visualized after staining with ethidium bromide.

The RT-qPCR analysis was conducted using an ABI QuantStudio3 (Applied Biosystems, Carlsbad, CA, United States). The specific RT-qPCR primers were designed using Beacon Designer 8.13 (PREMIER Biosoft International, CA, United States) (**Supplementary Material 3** and **Supplementary Table 2**). Two reference genes, β-*actin* (GenBank Acc. GQ856238.1) and glyceraldehyde-3-phosphate dehydrogenase (*gapdh*) (GenBank Acc. HM055756.1) were used to normalize target gene expression. The amplification efficiencies of the target and reference gene primers were evaluated using a four-fold serial dilution of cDNA templates from adult antennae. Reactions for each sample (20 μl) consisted of 10 μl of SuperReal PreMix Plus (TianGen, Beijing, China), 0.5 μl of each primer (10 μM), 0.4 μl of Rox reference dye, 1 μl of sample cDNA, and 7.6 μl of sterilized ultrapure water. Amplification conditions were an initial denaturation at 95°C for 3 min, followed by 40 cycles of 95°C for 15 s, and a single

[1] http://wego.genomics.org.cn/cgi-bin/wego/index.pl
[2] http://www.ncbi.nlm.nih.gov/COG/
[3] http://www.genome.jp/kegg/
[4] http://www.ncbi.nlm.nih.gov/gorf/gorf.html
[5] http://www.cbs.dtu.dk/services/SignalP/
[6] https://www.ebi.ac.uk/Tools/msa/mafft/
[7] http://tree.bio.ed.ac.uk/software/figtree/

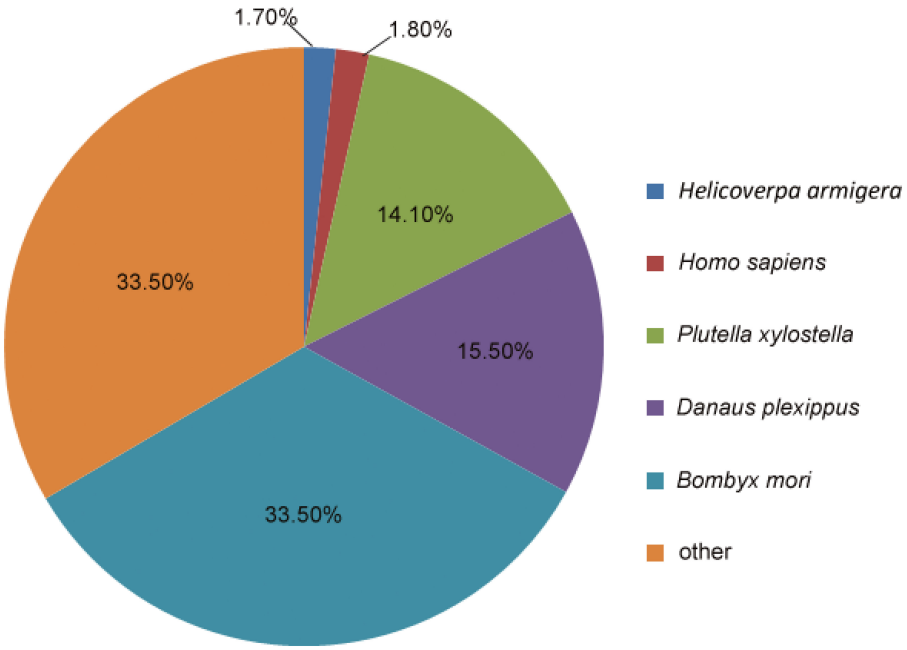

FIGURE 1 | Proportional homology distribution among other insect species based on the best BLAST hits against the NR database for the assembled unigenes from the *Mythimna separata* brain transcriptomes.

step for annealing and extension was performed at 60°C for 30 s. The PCR products were heated to 95°C for 15 s, cooled to 60°C for 1 min, heated to 95°C for 30 s, and cooled to 60°C for 15 s to determine the dissociation curves. The RT-qPCR reaction of each sample was performed in three technical replicates and three biological replicates. Then, we used the relative quantitation method ($2^{-\Delta\Delta CT}$) (Livak and Schmittgen, 2001) to evaluate quantitative variation. Transcript amounts were standardized to 1 using the sample from adult male brain. Data were analyzed using Data Processing System software version 9.5 (Tang and Zhang, 2013). A one-way analysis of variance with Tukey's multiple comparison test was performed to analyze differences in gene expression levels among multiple samples, and $p < 0.05$ was considered to be significant.

RESULTS

An Overview of Brain Transcriptomes

Six adult brain cDNA libraries, three for females and three for males of *M. separata*, were constructed and sequenced using the Illumina HiSeq^{TM} 2000 platform. As a result, 61,283,994, 59,876,048, and 68,196,054 raw reads were produced from the three separate female brain samples; and 46,814,292, 60,931,890, and 43,177,818 raw reads were produced from the three separate male brain samples. After trimming the adaptor sequences, contaminating sequences, and low quality sequences, 56,689,466, 54,841,746, and 62,601,386 clean reads of the three separate female brain samples, and 43,297,968, 56,087,138, and 40,004,380 clean reads of the three separate male brain samples, remained for the following assembly (**Supplementary Material 3** and **Supplementary Table 3**). Subsequently, all the clean reads were assembled together and generated 132,516 unigenes with lengths ranging from 201 to 28,894 bp, with a mean length of 579 bp.

Homology Searches and Functional Annotation of *Mythimna separata* Brain Unigenes

Homology searches querying the 132,516 unigenes against other insect species were performed using the BLASTx and BLASTn programs, with the E-value cut-off of $1.0E^{-5}$. In total, 27,594 unigenes (20.82%) had BLASTx hits in the NR database, and 12,499 unigenes (9.43%) had BLASTn hits in the NT database. Among the annotated unigenes, 4445 (3.35%) were annotated in all of the databases [NR, NT, KO (KEGG ontology), SwissProt, protein family (PFAM), GO, and KOG], whereas 35,484 (26.77%) were annotated in at least one database (**Supplementary Material 3** and **Supplementary Table 4**). The analysis showed that most *M. separata* protein sequences were orthologs of proteins in *B. mori* (33.5%), *Danaus plexippus* (15.5%), and *Plutella xylostella* (14.1%) (**Figure 1**).

According to the GO category analysis, only 21,188 (15.99%) assembled unigenes corresponded to different functional groups. Because one unigene can align to multiple GO categories, 54,623 (41.22%) unigenes were assigned to biological process, 33,526 (25.30%) to cellular component, and 23,545 (17.77%) to molecular function. In the molecular function category, the terms of binding and catalytic activity were the most represented. In the cellular component terms, cell and cell part were the most abundant. In the biological process category, cellular

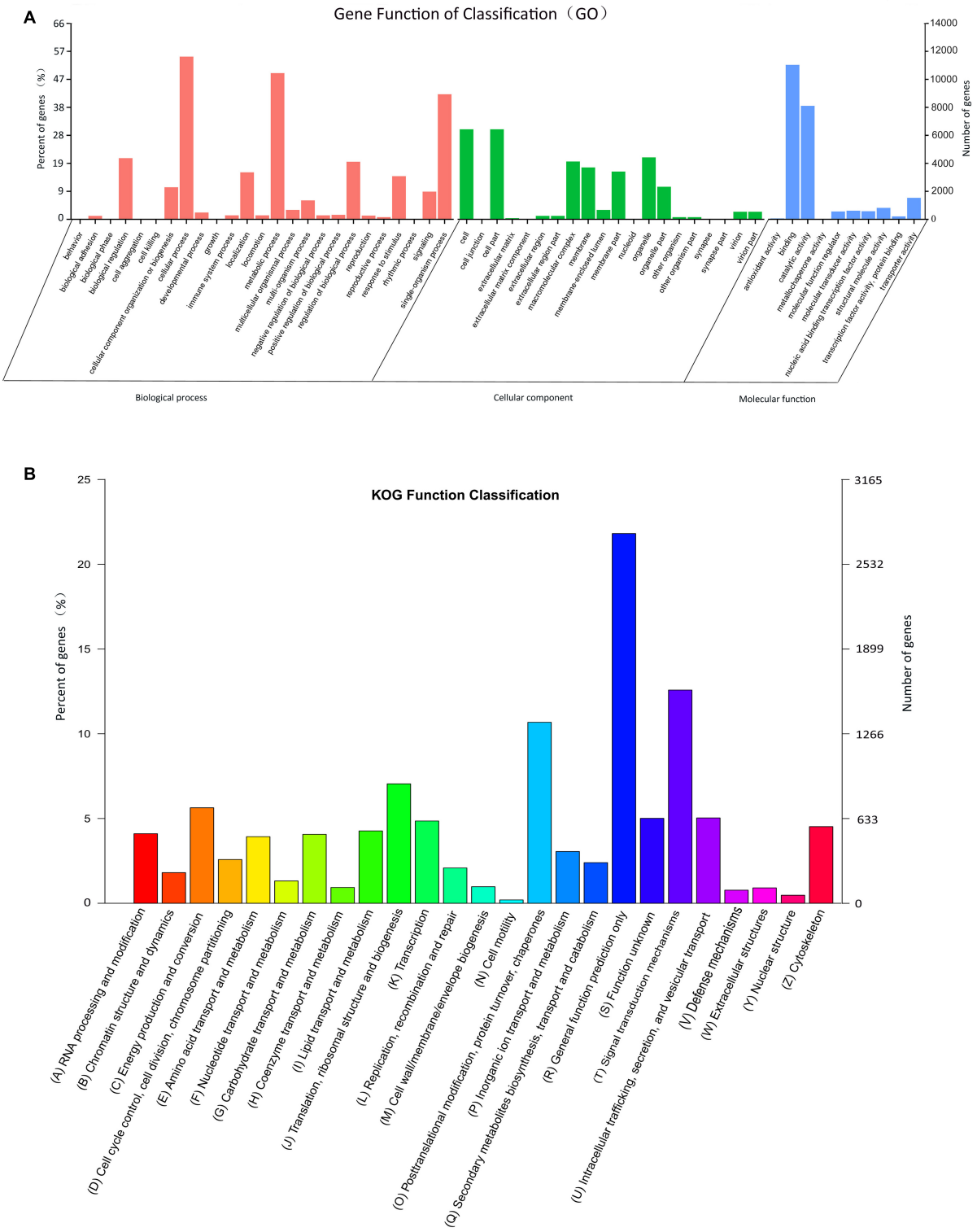

FIGURE 2 | Histograms of gene ontology (GO) classifications **(A)** and clusters of orthologous groups of proteins (KOG) **(B)**. **(A)** The GO classifications are summarized into three main categories: biological processes, cellular component, and molecular function. The right *y*-axis indicates the number of genes in a category, and the left *y*-axis indicates the percentage of genes in a specific term in that main category. **(B)** The *x*-axis indicates 26 categories. The left *y*-axis indicates the percentage of a specific gene classification in that main category, and the right *y*-axis indicates the number of genes in a category.

TABLE 1 | Odorant-binding proteins identified in *Mythimna separata* brain transcriptomes.

Gene name	Accession number	Unigene ID	Gene length (bp)	ORF (aa)	Complete ORF	SP (aa)	Blastx best hit (name/species)	Reference ID	E-value	Identity (%)
GOBP1	MH175135	c123103_g1	532	145	N	N	general odorant binding protein 1 [*Agrotis segetum*]	ABI24159.1	4.00E-87	96
GOBP2	MH175137	c110784_g1	489	162	Y	1–21	general odorant-binding protein 2 [*Helicoverpa armigera*]	XP_021192653.1	1.00E-29	89
PBP1	MH168089	c10667_g1	417	139	N	N	pheromone binding protein 1 precursor [*Mamestra brassicae*]	AAC05702.2	1.00E-86	87
PBP2	MH168090	c32738_g1	939	168	N	1–25	pheromone binding protein [*Mythimna separata*]	BAG71416.1	1.00E-116	98
OBP1	MH175126	c6219_g1	1111	334	Y	1–20	odorant binding protein 9 [*Spodoptera litura*]	ALD65883.1	4.00E-102	85
OBP2	MH175116	c69119_g1	1181	252	Y	1–19	odorant binding protein 23 [*Spodoptera exigua*]	AKT26500.1	1.00E-155	82
OBP3	MH175122	c63834_g1	915	237	Y	1–19	odorant binding protein 25 [*Spodoptera exigua*]	AKT26502.1	2.00E-96	62
OBP4	MH175112	c99468_g1	773	197	Y	1–17	odorant-binding protein 19 [*Helicoverpa assulta*]	AGC92793.1	1.00E-76	60
OBP5	MH175118	c66723_g2	943	183	Y	1–17	odorant binding protein 1 [*Agrotis ipsilon*]	AGR39564.1	1.00E-86	70
OBP6	MH175138	c136846_g1	663	168	Y	1–20	odorant binding protein [*Spodoptera exigua*]	ADY17882.1	2.00E-76	71
OBP7	MH175117	c68084_g1	605	156	N	N	odorant binding protein 1 [*Agrotis ipsilon*]	AGR39564.1	1.00E-73	75
OBP8	MH175127	c59109_g1	573	153	Y	1–17	antennal binding protein 7 [*Antheraea yamamai*]	ADO95155.1	3.00E-09	33
OBP9	MH168091	c63533_g1	578	146	Y	1–21	pheromone binding protein 4 [*Mamestra brassicae*]	AAL66739.1	1.00E-82	84
OBP10	MH175123	c62882_g1	562	146	Y	1–16	odorant binding protein 6 [*Agrotis ipsilon*]	AGR39569.1	2.00E-76	86
OBP11	MH175124	c62557_g1	799	145	Y	1–21	OBP13 [*Sesamia inferens*]	AGS36753.1	2.00E-22	41
OBP12	MH175131	c44266_g1	492	141	Y	1–18	odorant binding protein 8 [*Spodoptera exigua*]	AGH70104.1	1.00E-80	88
OBP13	MH175130	c49279_g1	660	139	Y	1–21	SexiOBP13 [*Spodoptera exigua*]	AGP03459.1	8.00E-24	39
OBP14	MH183292	c29765_g1	417	138	Y	1–17	odorant binding protein 5 [*Agrotis ipsilon*]	AGR39568.1	4.00E-31	75
OBP15	MH175125	c62413_g1	1164	137	Y	1–20	general odorant-binding protein 56a-like [*Helicoverpa armigera*]	XP_021196568.1	1.00E-55	80
OBP16	MH175119	c64285_g1	839	133	Y	1–16	odorant binding protein 9 [*Spodoptera exigua*]	AGH70105.1	2.00E-77	89
OBP17	MH175120	c64152_g2	1016	132	N	N	odorant-binding protein 2 precursor [*Bombyx mori*]	NP_001140186.1	4.00E-68	74
OBP18	MH175133	c34278_g1	366	110	N	1–19	odorant binding protein 2 [*Agrotis ipsilon*]	AGR39565.1	2.00E-16	36
OBP19	MH175129	c5297_g1	430	107	N	N	antennal binding protein [*Heliothis virescens*]	CAC33574.1	2.00E-49	74
OBP20	MH175134	c141343_g1	265	88	N	1–20	OBP5 [*Helicoverpa armigera*]	AEB54581.1	1.00E-23	74
OBP21	MH175139	c100957_g1	261	86	N	1–19	OBP9 [*Helicoverpa armigera*]	AEB54592.1	4.00E-23	48
OBP22	MH175113	c97924_g1	227	71	N	1–18	general odorant-binding protein 28a [*Helicoverpa armigera*]	XP_021194660.1	2.00E-29	67
OBP23	MH175136	c109617_g1	322	69	N	N	odorant binding protein 22 [*Spodoptera exigua*]	AKT26499.1	1.00E-37	91
OBP24	MH175128	c57242_g1	228	50	N	1–16	odorant binding protein 9 [*Spodoptera exigua*]	AGH70105.1	7.00E-22	86
OBP25	MH175114	c93169_g1	213	44	N	N	odorant-binding protein 9 [*Helicoverpa assulta*]	AGC92789.1	5.00E-06	55

ORF, open reading frame; SP, signal peptides; aa, amino acid.

FIGURE 3 | Multiple alignment of amino acid sequences of OBPs from *M. separata*. In the sequence alignments, only the proteins with full-length ORFs were selected. Conserved cysteine residues are highlighted, and signal peptides are boxed in red.

process, metabolic process, and single-organism process were most abundant (**Figure 2A**).

In the obtained KOG functional annotation, 12,672 unigenes were categorized into 26 functional groups (**Figure 2B**). "General function prediction only" was the largest group (2764, 21.81%), followed by the "Signal transduction mechanism (1594, 12.58%) and Posttranslational modification, protein turnover, chaperones" (1353, 10.68%) groups, and "Cell motility" (25, 0.20%) was the smallest group.

Identification of Putative *OBPs* and *CSPs* Genes

In the *M. separata* brain transcriptomes, 29 *OBP*s were annotated on the basis of the TBLASTN results. Among them, 16 OBPs contained intact ORFs, with lengths ranging from 133 to 334 amino acids (**Table 1**). Based on the numbers and locations of the conserved cysteines, the OBPs were classified into three categories, Classic, Pluc-C, and Minus-C OBPs families. Seven full-length OBPs (GOBP2, OBP6, OBP9, OBP11–13, and OBP15) had the typical six conserved cysteines and spacing, forming the Classic OBPs family. Three full-length OBPs (OBP4, -5, and -10) belonged to the Pluc-C OBPs family, having additional two, three, and six cysteines located downstream of the conserved C6. The remaining six full-length OBPs (OBP1–3, -8, -14, and -16) belonged to the Minus-C OBPs family. OBP1 lacked conserved cysteine C1; OBP2 had none of the typical six conserved cysteines; OBP3 only had conserved cysteines C1 and C6; and OBP8, -14, and -16 lacked the conserved cysteines C2 and C5 (**Figure 3**). Compared with our earlier identified OBPs in *M. separata* (Du et al., 2018), many of them shared high sequence identity levels, ranging from 80 to 100%. However, OBP2, -3, -17, and -23 shared a no more than 36% sequence identity (**Supplementary Material 3** and **Supplementary Table 5**).

Sixteen transcripts encoding candidate CSPs were identified. Among them, 14 CSPs contained intact ORFs, with lengths ranging from 106 to 290 amino acids (**Table 2**). These identified full-length CSPs proteins included a signal peptide and four highly conserved cysteine profiles (C1-X6-C2-X18-C3-X2-C4, where X represents any amino acid) (**Figure 4**). The CSP15 and CSP16 amino acid sequences were incomplete due to the lack of a 3′ or 5′ terminus. Compared with previously identified CSPs (Du et al., 2018), most of them shared high sequence identity levels, ranging from 74 to 100%. However, there were two CSPs, CSP9 and CSP12, that shared less than a 41% sequence identity (**Supplementary Material 3** and **Supplementary Table 5**).

Phylogenetic Analysis of Odorant-Binding Proteins and Chemosensory Proteins

All the putative OBPs clustered with at least one lepidopteran ortholog in the phylogenetic tree (**Figure 5**). The identified GOBP and PBP protein sequences in brain clustered into the GOBP and PBP clades in the phylogenetic tree, respectively. OBP5 and OBP7 shared a 68.28% sequences identity and clustered together. OBP11 and OBP18 only shared a 29.66% similarity, but they also clustered together. With OBP13, they formed a clade containing *Slit*OBP25. All the candidate CSPs proteins clustered with at least one lepidopteran ortholog in the phylogenetic tree (**Figure 6**). CSP3 and CSP15 shared a 67.97% sequences identity, and formed a clade with *Aips*CSP7. CSP7 and CSP16 shared a 45.60% sequences identity and clustered together.

Expression Profiles of Putative *OBPs* and *CSPs* Genes

The RT-PCR expression profiles indicated that the majority of *OBPs* genes were expressed in the antennae. *OBP5*, *-7*, *-11*, *-13*, *-16*, *-18*, *-21*, and *-24* were detected in the brain. Among them, *OBP5*, *-7*, *-11*, and *-13* showed male brain-biased expression, whereas *OBP21* showed female brain-biased expression. *OBP16*, *-18*, and *-24* were expressed in both female and male brains. *OBP5*, *-7*, and *-11* were also detected in the antennae and abdomens. *OBP13* could be detected in the abdomens. *OBP16* and *OBP24* were detected in the antennae, abdomens, and legs. *OBP18* could be detected in all the tissues, and *OBP21* was detected in the legs and wings (**Figure 7**). The RT-PCR expression profiles indicated that most *CSPs* genes were expressed in all the examined tissues

TABLE 2 | Chemosensory proteins identified in brain transcriptomes of *Mythimna separata*.

Gene name	Accession number	Unigene ID	Gene Length (bp)	ORF (aa)	complete ORF	SP (aa)	Blastx best hit (name/species)	reference ID	E-value	Identity (%)
CSP1	MH175144	c71325_g1	1178	290	Y	1–16	chemosensory protein 14 [*Spodoptera exigua*]	AKT26490.1	5.00E-139	79
CSP2	MH175147	c67550_g1	860	128	Y	1–18	chemosensory protein 3 [*Agrotis ipsilon*]	AGR39573.1	6.00E-64	83
CSP3	MH175149	c65965_g1	735	128	Y	1–16	chemosensory protein [*Mamestra brassicae*]	AAF71289.1	1.00E-58	80
CSP4	MH175145	c69441_g1	1605	127	Y	1–18	chemosensory protein 6 [*Agrotis ipsilon*]	AGR39576.1	1.00E-69	99
CSP5	MH175150	c65547_g1	990	127	Y	1–18	putative chemosensory protein [*Sesamia inferens*]	AGY49267.1	9.00E-61	80
CSP6	MH175155	c58863_g1	384	127	Y	1–18	chemosensory protein 8 [*Athetis dissimilis*]	AND82450.1	2.00E-55	81
CSP7	MH175158	c42045_g1	547	125	Y	1–16	putative chemosensory protein [*Sesamia inferens*]	AGY49266.1	8.00E-41	60
CSP8	MH175151	c65068_g1	1009	124	Y	1–16	chemosensory protein 2 [*Athetis dissimilis*]	AND82444.1	2.00E-74	86
CSP9	MH175152	c64033_g1	949	123	Y	1–19	chemosensory protein 3 [*Athetis dissimilis*]	AND82445.1	6.00E-65	94
CSP10	MH175154	c60888_g1	860	122	Y	1–16	chemosensory protein 10 [*Athetis dissimilis*]	AND82452.1	9.00E-79	97
CSP11	MH175153	c63211_g1	587	120	Y	1–16	putative chemosensory protein CSP12 [*Spodoptera litura*]	ALJ30223.1	3.00E-62	88
CSP12	MH175142	c92712_g1	392	114	Y	1–19	chemosensory protein [*Artemia franciscana*]	ABY62738.1	4.00E-76	96
CSP13	MH175146	c69155_g1	1665	107	Y	1–18	chemosensory protein 5 [*Agrotis ipsilon*]	AGR39575.1	2.00E-54	97
CSP14	MH175143	c75033_g3	1250	106	Y	1–16	chemosensory protein 5 [*Athetis dissimilis*]	AND82447.1	5.00E-61	91
CSP15	MH175157	c47311_g1	363	103	N	1–16	chemosensory protein [*Mamestra brassicae*]	AAF71289.1	8.00E-46	83
CSP16	MH175156	c52173_g1	359	77	N	N	putative chemosensory protein [*Sesamia inferens*]	AGY49266.1	8.00E-43	62

ORF, open reading frame; SP, signal peptides; aa, amino acid.

(**Figure 7**). Three *CSP* genes, *CSP2–4*, were expressed in female brain. *CSP8* was detected in male brain, and *CSP10–12*, and *CSP15* were detected in both female and male brains (original gel images of RT-PCR can be found in **Supplementary Material 4**).

To confirm the RT-PCR results, RT-qPCR was performed to measure quantitatively the expression levels of six *OBPs* (*OBP3–5*, *-9*, *-10*, and *-16*) and 2 *CSPs* (*CSP3* and *CSP4*) genes in the various tissues (**Figure 8**). The RT-qPCR results were mostly consistent with the RT-PCR results. They confirmed that *OBP5*, *OBP16*, *CSP3,* and *CSP4* were expressed in brain, and further revealed that *OBP10*, which was not detected by RT-PCR, was also expressed in brain. The expression levels of *OBP5* and *OBP10* in brain were not significantly different between the sexes ($p > 0.05$), whereas that of *OBP16* was three times higher in male brain than in female brain ($p < 0.05$). The expression levels of *CSP3* and *CSP4* were 40 and 24 times higher in female brain than in the male, respectively ($p < 0.05$).

DISCUSSION

In the present study, we first sequenced and analyzed the transcriptomes of adult male and female *M. seperata* brains. Among the 132,516 unigenes identified, only 15.98% were annotated to one or more GO term, and only 20.82% had homologous matches to entries in the NCBI NR protein database. This was similar to other lepidopteran species (Liu et al., 2012; Zhang Y. N. et al., 2015), indicating that a large number of *M. seperata* genes are either non-coding or homologs of genes that have not been annotated to GO terms. Importantly, we identified 29 *OBPs* and 16 *CSPs* putative genes in the data set, providing valuable reference data for exploring novel functions of chemosensory genes in *M. separata*.

The number of *OBPs* obtained in this study was less than the number identified from the antennal (37 and 32) and head (50 and 38) transcriptomes of *M. separata* (Bian et al., 2017; Chang X. Q. et al., 2017; He et al., 2017; Liu et al., 2017). Here, we identified two novel OBPs (OBP2 and OBP3) and two OBPs (OBP17 and OBP23) that share a no more than 36% sequence identity compared with our earlier identified 38 OBPs from the antennae, labial palps, and proboscises transcriptomes of *M. separata* (Du et al., 2018). The other OBPs shared high sequences identity levels, ranging from 80% to 100% (**Supplementary Material 3** and **Supplementary Table 5**). The small number of *OBPs* identified in brain may be because *OBPs* genes are mainly expressed in antennae, mouth organs, and other chemosensory structures. We identified 16 *CSPs* in the adult brain transcriptome, which is comparable with the numbers identified from earlier reported antennal transcriptomes, 14 and 16 *CSPs* reported by Chang X. Q. et al. (2017) and He et al. (2017), respectively, and head transcriptomes of *M. separate*, 18 *CSPs* reported by Liu et al. (2017), but fewer than the numbers identified in other head transcriptomes (22 *CSPs*) by Bian et al. (2017) and our earlier analyzed antennae, labial palps, and proboscises transcriptomes (38 *CSPs*) (Du et al., 2018). However, we also found that two CSPs (CSP9 and CSP12) shared less than a 41% sequence identity compared with our earlier

FIGURE 4 | Multiple alignment of amino acid sequences of CSPs from *M. separata*. In the sequence alignments, the C-terminus of CSP15 and N-terminus of CSP16 are truncated. Four conserved residues are highlighted, and signal peptides are boxed in red.

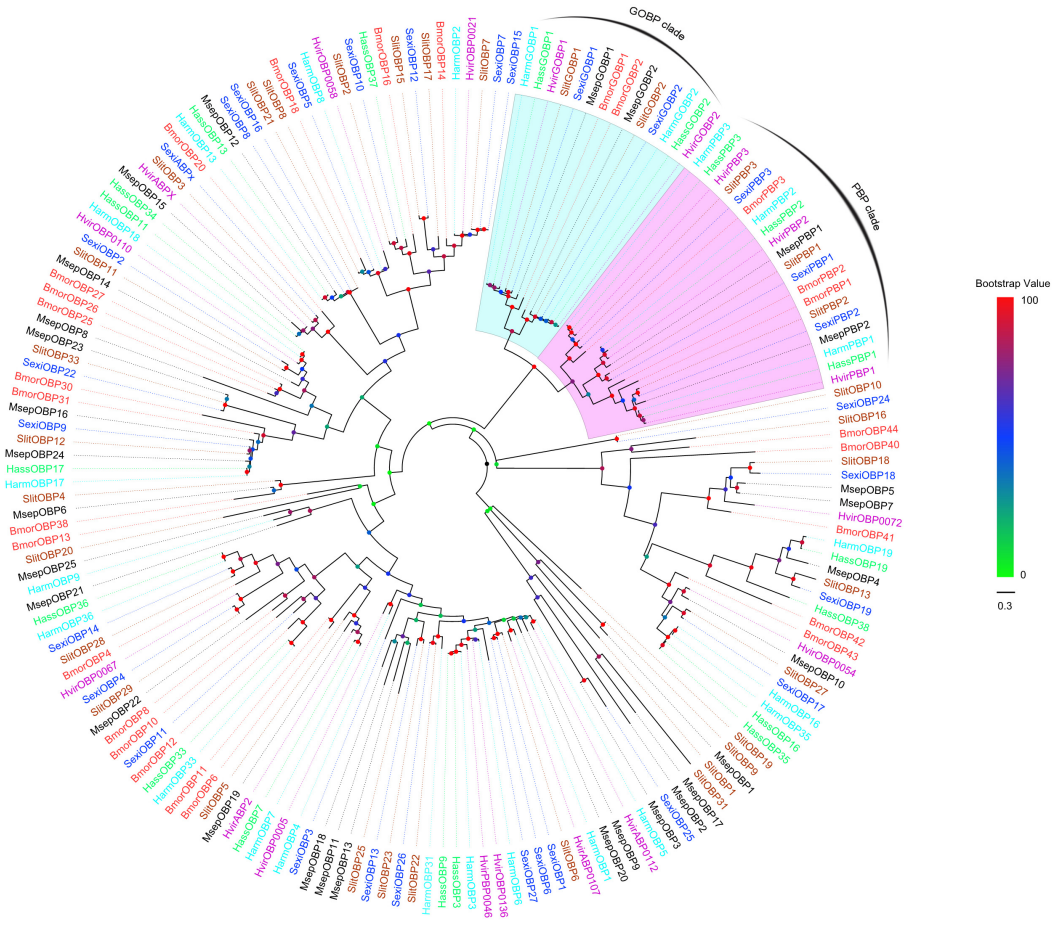

FIGURE 5 | Phylogenetic tree of putative OBPs from lepidopteran species. This tree was constructed using MEGA5.2 based on alignment results of MAFFT. Msep: *Mythimna separata* (black); Harm: *Helicoverpa armigera* (cyan); Hass: *Helicoverpa assulta* (green); Bmor: *Bombyx mori* (red); Hvir: *Heliothis virescens* (dark violet); Sexi: *Spodoptera exigua* (blue) Slit: *Spodoptera litura* (sandy brown). The clades in violet and light cyan represent general odorant-binding proteins and pheromone-binding proteins, respectively.

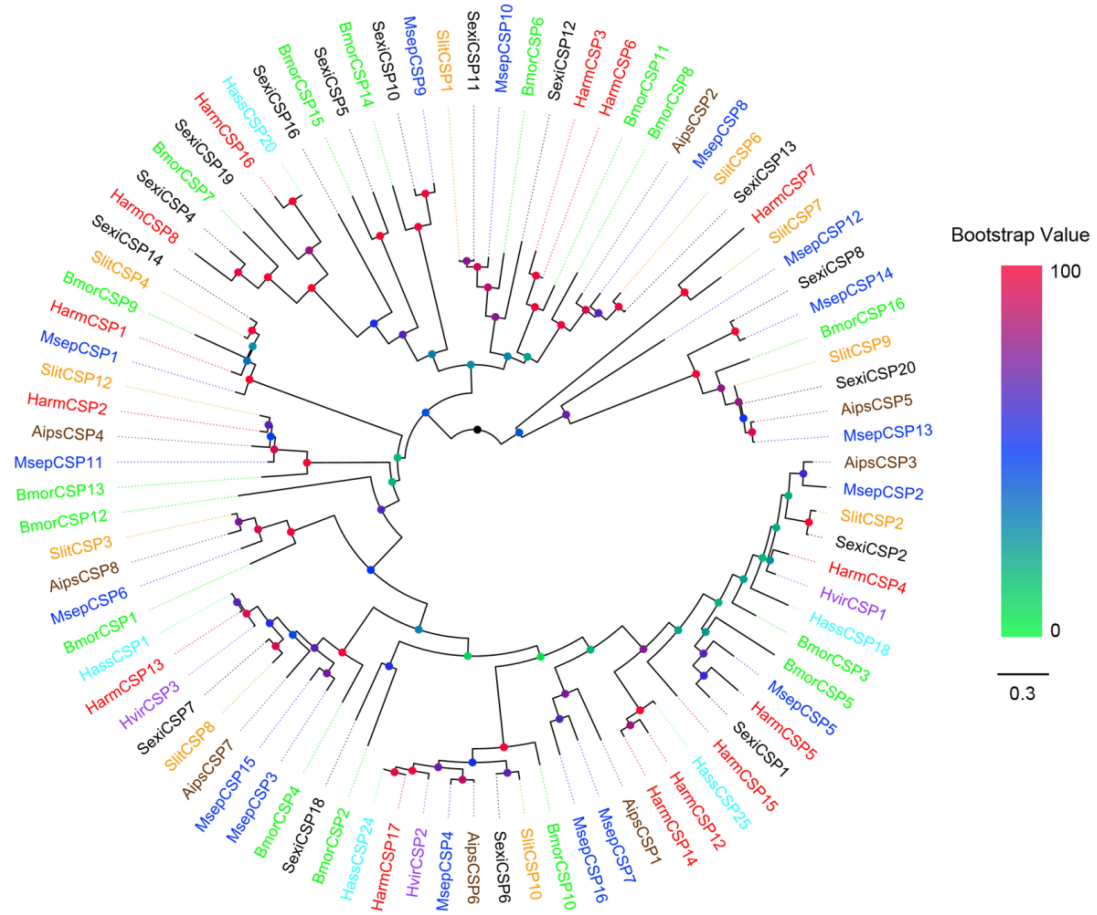

FIGURE 6 | Phylogenetic tree of putative CSPs from lepidopteran species. This tree was constructed using MEGA5.2 based on alignment results of MAFFT. Msep: *Mythimna separata* (blue); Aips: *Agrotis ipsilon* (brown); Harm: *Helicoverpa armigera* (red); Hvir: *Heliothis virescens* (dark orchid); Hass: *Helicoverpa assulta* (cyan); Bmor: *Bombyx mori* (green); Slit: *Spodoptera litura* (orange); Sexi: *Spodoptera exigua* (black).

identified CSPs. Most other CSPs shared high sequence identity levels, ranging from 74 to 100% (**Supplementary Material 3** and **Supplementary Table 5**). The novel and relatively low sequence homology levels of OBPs and CSPs identified in the present study may indicate that they are specifically expressed and function in the brain, and their ligand-binding functions need to be investigated in the future.

The further examination of sex- and tissue-specific expression using RT-PCR confirmed that eight *OBP*s (*OBP5*, *-7*, *-11*, *-13*, *-16*, *-18*, *-21*, and *-24*) and eight *CSP*s (*CSP2–4*, *-8*, *CSP10–12*, and *-15*) were expressed in brain. The RT-qPCR results indicated that *OBP5*, *OBP10*, *OBP16*, *CSP3,* and *CSP4* have relatively abundant and sex-biased expression levels in adult brain. These findings in *M. separata* brain are consistent with previous research on other insect species. For example, at least two *OBP*s and three *CSP*s were identified in the brain of *Spodoptera littoralis*. The genes with relatively abundant expression levels in the brain were *SlitOBP4*, *SlitPBP2*, *SlitCSP1*, *SlitCSP2*, and *SlitCSP8* (Walker et al., 2019). Four OBPs were identified in the brain transcriptome of *Vespa velutina* (Wang et al., 2020). In the brain of *Adelphocoris lineolatus*, *AlinOBP14* was identified (Tian et al., 2021). In *A. mellifera*, there are six *CSPs* and most have been detected in the brain (Liu et al., 2020). Indeed, several studies have reported their putative physiological functions as carriers for endogenous compounds in brain. *In situ* hybridization with mRNA of *AlinOBP14* showed that the gene was expressed in the antennal lobe of the brain and fluorescence-based competitive-binding assays showed that juvenile hormone and the precursors of the hormone bound to the AlinOBP14 protein (Sun et al., 2019; Tian et al., 2021). Therefore, AlinOBP14 in the antennal lobes of *A. lineolatus* might function as a carrier of endogenous compounds, including juvenile hormone and hormone precursors. Juvenile hormone affects the responsiveness of olfactory interneurons in the antennal lobe and is likely involved in the plasticity of the insect brain (Anton and Gadenne, 1999). The possible roles of CSPs in the nervous system has also been demonstrated using gene knockout assays. A CSP *AmelGB10389* knockout in honey bee resulted in abnormal brain development, which suggests the CSPs may play roles in neuronal plasticity (Maleszka et al., 2007; Liu et al., 2020). The CSPs may function as carriers of lipids and juvenile hormone to modulate olfactory responses,

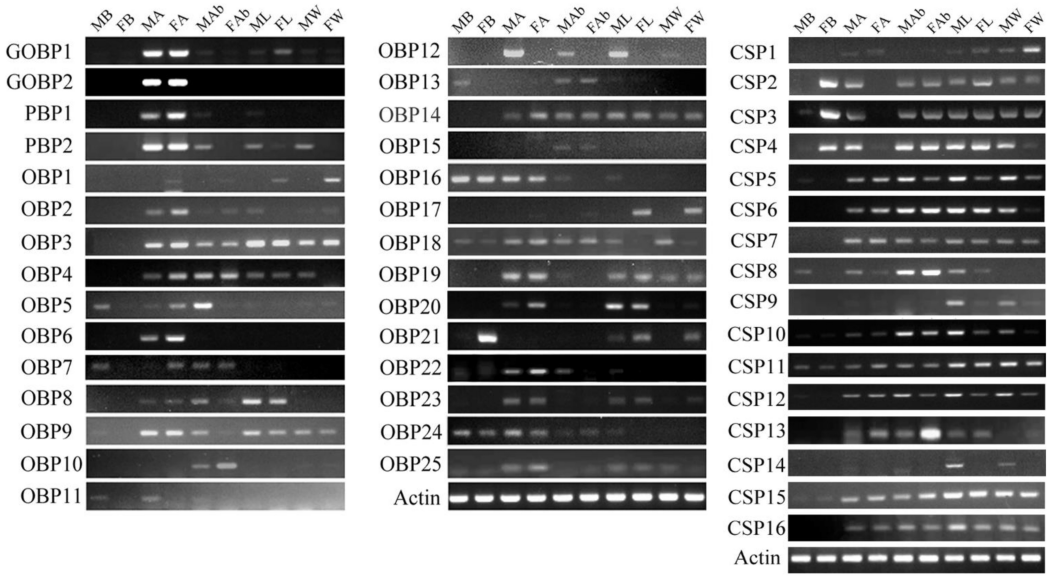

FIGURE 7 | *Mythimna separata OBPs* and *CSPs* transcript levels in different tissues of male and female adults as evaluated by RT-PCR. MB: male brains; FB: female brains; MA: male antennae; FA: female antennae; MAb: male abdomens; FAb: female abdomens; ML: male legs; FL: female legs; MW: male wings; FW: female wings.

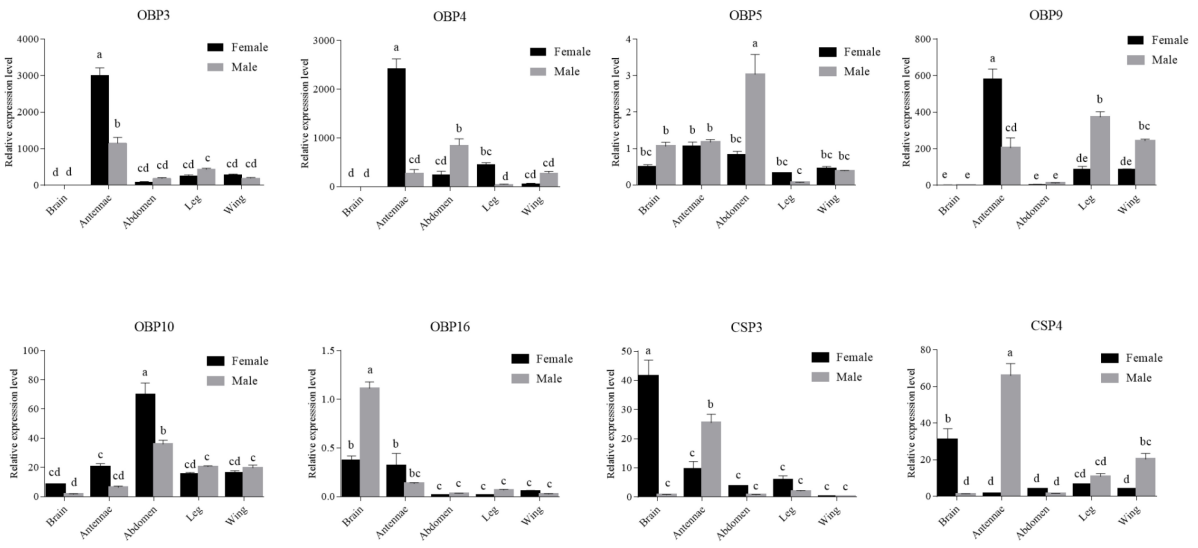

FIGURE 8 | Six *OBPs* and two *CSPs* transcript levels in different tissues of both sexes as evaluated by RT-qPCR. The internal controls β-*actin* and *gapdh* were used to normalize transcript levels in each sample. The standard error is represented by the error bar, and the different letters above each bar denote significant differences ($p < 0.05$).

olfactory learning, and memorization in the antennal lobe and mushroom body neuropiles (Liu et al., 2020). The expression of CSPs in the neural systems of insects may function, by controlling diacylglycerol and protein phosphorylation, in neuroplasticity, neurogenesis, synaptogenesis, the formation of new synapses, and the generation of new neuron connections (Liu et al., 2020).

*OBP*s and *CSP*s are typically expressed in chemosensory structures, such as antennae and mouth organs, and their proteins function as carriers of odorants in insect chemoreception (Pelosi et al., 2017). However, OBPs and CSPs proteins in other insect species are endowed with multiple functions in the non-sensory organs of the insect body, such as pheromone delivery, solubilization of nutrients, development, and insecticide resistance (Pelosi et al., 2017). The varying expression patterns of *OBPs* and *CSPs* genes across tissues of *M. separata* may also suggest that their proteins play broader physiological roles in addition to carrying odorants. In particular, in the present study, the expression of several *OBP*s and *CSP*s

in *M. separata* brain may expand our current understanding of the expression patterns of chemosensory genes in insect non-sensory tissues, and the results establish a foundation for further studies on the novel functions of chemosensory genes in non-sensory tissues of *M. separata*.

DATA AVAILABILITY STATEMENT

The datasets presented in this study can be found in online repositories. The names of the repository/repositories and accession number(s) can be found below: https://www.ncbi.nlm.nih.gov/sra/PRJNA793072.

AUTHOR CONTRIBUTIONS

W-BC and X-CZ conceived and designed the experiments, wrote the manuscript. W-BC, L-XD, and X-CZ performed the experiments. X-YG, L-LS, L-LC, G-YX, and S-HA analyzed the data. All authors have read and approved the manuscript for publication.

FUNDING

This study was funded by grants from the National Natural Science Foundation of China (Nos. 32130089 and 32001912), Department of Science and Technology of Henan Province Key Research and Development and Promotion Special Projects (No. 202102110226), and the Support Program for Young Talents in Henan Province (No. 2020HYTP043).

SUPPLEMENTARY MATERIAL

The Supplementary Material for this article can be found online at: https://www.frontiersin.org/articles/10.3389/fphys.2022.839559/full#supplementary-material

REFERENCES

Anton, S., and Gadenne, C. (1999). Effect of juvenile hormone on the central nervous processing of sex pheromone in an insect. *Proc. Natl. Acad. Sci. U.S.A.* 96, 5764–5767. doi: 10.1073/pnas.96.10.5764

Baer, B., Zareie, R., Paynter, E., Poland, V., Millar, A. H. (2012). Seminal fluid proteins differ in abundance between genetic lineages of honeybees. *J. Proteomics* 75, 5646–5653. doi: 10.1016/j.jprot.2012.08.002

Bian, H. X., Ma, H. F., Zheng, X. X., Peng, M. H., Li, Y. P., Su, J. F., et al. (2017). Characterization of the adult head transcriptome and identification of migration and olfaction genes in the oriental armyworm mythimna separata. *Sci. Rep.* 7:2324. doi: 10.1038/s41598-017-02513-6

Chang, H., Dong, A., Zhang, J., Dong, S., Liu, Y., and Wang, G. (2017). Candidate odorant binding proteins and chemosensory proteins in the larval chemosensory tissues of two closely related noctuidae moths, *Helicoverpa armigera* and H. assulta. *PLoS One* 12:e0179243. doi: 10.1371/journal.pone.0179243

Chang, X. Q., Nie, X. P., Zhang, Z., Zeng, F. F., Lv, L., Zhang, S., et al. (2017). De novo, analysis of the oriental armyworm, *Mythimna separata*, antennal transcriptome and expression patterns of odorant-binding proteins. *Comput. Biochem. Phys.* 22, 120–130. doi: 10.1016/j.cbd.2017.03.001

Conesa, A., Götz, S., García-Gómez, J. M., Terol, J., Talón, M., and Robles, M. (2005). Blast2GO: a universal tool for annotation, visualization and analysis in functional genomics research. *Bioinformatics* 21, 3674–3676. doi: 10.1093/bioinformatics/bti610

Costa-da-Silva, A. L., Kojin, B. B., Marinotti, O., James, A. A., and Capurro, M. L. (2013). Expression and accumulation of the two-domain odorant-binding protein AaegOBP45 in the ovaries of blood-fed *Aedes aegypti*. *Parasite Vector* 6:364. doi: 10.1186/1756-3305-6-364

Dani, F. R., Michelucci, E., Francese, S., Mastrobuoni, G., Cappellozza, S., La Marca, G., et al. (2011). Odorant-binding proteins and chemosensory proteins in pheromone detection and release in the silkmoth bombyx mori. *Chem. Senses* 36, 335–344. doi: 10.1093/chemse/bjq137

Du, L., Zhao, X., Liang, X., Gao, X., Liu, Y., and Wang, G. (2018). Identification of candidate chemosensory genes in *Mythimna separata* by transcriptomic analysis. *BMC Genom.* 19:518. doi: 10.1186/s12864-018-4898-0

Gong, D. P., Zhang, H. J., Zhao, P., Xia, Q. Y., and Xiang, Z. H. (2009). The odorant binding protein gene family from the genome of silkworm, bombyx mori. *BMC Genom.* 10:332. doi: 10.1186/1471-2164-10-332

Grabherr, M. G., Haas, B. J., Yassour, M., Levin, J. Z., Thompson, D. A., Amit, I., et al. (2011). Full length transcriptome assembly from RNA-Seq data without a reference genome. *Nat. Biotechnol.* 29:644. doi: 10.1038/nbt.1883

Gu, S. H., Sun, L., Yang, R. N., Wu, K. M., Guo, Y. Y., Li, X. C., et al. (2014). Molecular characterization and differential expression of olfactory genes in the antennae of the black cutworm moth *Agrotis ipsilon*. *PLoS. One* 9:e103420. doi: 10.1371/journal.pone.0103420

Gu, S. H., Wu, K. M., Gu, Y. Y., Pickett, J. A., Field, L. M., Zhou, J. J., et al. (2013). Identification of genes expressed in the sex pheromone gland of the black cutworm *Agrotis ipsilon* with putative roles in sex pheromone biosynthesis and transport. *BMC Genom.* 14:636. doi: 10.1186/1471-2164-14-636

Gu, S. H., Zhou, J. J., Gao, S., Wang, D. H., Li, X. C., Guo, Y. Y., et al. (2015). Identification and comparative expression analysis of odorant binding protein genes in the tobacco cutworm *Spodoptera litura*. *Sci. Rep.* 5:13800. doi: 10.1038/srep13800

He, Y. Q., Feng, B., Guo, Q. S., and Du, Y. (2017). Age influences the olfactory profiles of the migratory oriental armyworm *Mythimna separata* at the molecular level. *BMC Genom.* 18:32. doi: 10.1186/s12864-016-3427-2

Heavner, M. E., Gueguen, G., Rajwani, R., Pagan, P. E., Small, C., and Govind, S. (2013). Partial venom gland transcriptome of a drosophila parasitoid wasp, *Leptopilina heterotoma*, reveals novel and shared bioactive profiles with stinging hymenoptera. *Gene* 526, 195–204. doi: 10.1016/j.gene.2013.04.080

Jacquin-Joly, E., Vogt, R. G., FranÇois, M. C., and Nagnan-Le Meillour, P. (2001). Functional and expression pattern analysis of chemosensory proteins expressed in antennae and pheromonal gland of mamestra brassicae. *Chem. Senses* 26, 833–844. doi: 10.1093/chemse/26.7.833

Jiang, N. J., Tang, R., Guo, H., Ning, C., Li, J. C., Wu, H., et al. (2020). Olfactory coding of intra- and interspecific pheromonal messages by the male mythimna separata in north China. *Insect Biochem. Mol. Biol.* 125:103439. doi: 10.1016/j.ibmb.2020.103439

Jiang, N. J., Tang, R., Wu, H., Xu, M., Ning, C., Huang, L. Q., et al. (2019). Dissecting sex pheromone communication of mythimna separata (walker) in north China from receptor molecules and antennal lobes to behavior. *Insect Biochem. Mol. Biol.* 111:103176. doi: 10.1016/j.ibmb.2019.103176

Jiang, X., Luo, L., Zhang, L., Sappington, T. W., and Hu, Y. (2011). Regulation of migration in mythimna separata (walker) in China: a review integrating environmental, physiological, hormonal, genetic, and molecular factors. *Environ. Entomol.* 40, 516–533. doi: 10.1603/EN10199

Jiang, X., Zhang, L., Cheng, Y., and Luo, L. (2014). Current status and trends in research on the oriental armyworm, *Mythimna separata* (walker) in China. *Chin. J. Appl. Entomol.* 51, 881–889.

Li, S., Picimbon, J. F., Ji, S. D., Kan, Y. C., Qiao, C. L., Zhou, J. J., et al. (2008). Multiple functions of an odorant-binding protein in the mosquito *Aedes aegypti*. *Biochem. Bioph. Res.* 372, 464–468. doi: 10.1016/j.bbrc.2008.05.064

Li, Z., Zhang, Y., An, X., Wang, Q., Khashaveh, A., Gu, S., et al. (2020). Identication of leg chemosensory genes and sensilla in the *Apolygus lucorum*. *Front. Physiol.* 11:276.

Liu, G., Xuan, N., Rajashekar, B., Arnaud, P., Offmann, B., and Picimbon, J.-F. (2020). Comprehensive history of CSP genes: evolution, phylogenetic distribution and functions. *Genes* 11:413. doi: 10.3390/genes11040413

Liu, N. Y., Zhang, T., Ye, Z. F., Li, F., and Dong, S. L. (2015). Identification and characterization of candidate chemosensory gene families from spodoptera exigua developmental transcriptomes. *Int. J. Biol. Sci.* 11, 1036–1048. doi: 10.7150/ijbs.12020

Liu, Y., Gu, S., Zhang, Y., Guo, Y., and Wang, G. (2012). Candidate olfaction genes identified within the *Helicoverpa armigera* antennal transcriptome. *PLoS One* 7:e48260. doi: 10.1371/journal.pone.0048260

Liu, Y., Qi, M., Chi, Y., and Wuriyanghan, H. (2016). De novo assembly of the transcriptome for oriental armyworm *Mythimna separata* (lepidoptera: noctuidae) and analysis on insecticide resistance-related genes. *J. Insect Sci.* 16:92. doi: 10.1093/jisesa/iew079

Liu, Z., Wang, X., Lei, C., and Zhu, F. (2017). Sensory genes identification with head transcriptome of the migratory armyworm, *Mythimna separata*. *Sci. Rep.* 7:46033. doi: 10.1038/srep46033

Livak, K. J., and Schmittgen, T. D. (2001). Analysis of relative gene expression data using real-time quantitative PCR and the 2-ΔΔCT method. *Methods* 25, 402–408. doi: 10.1006/meth.2001.1262

Maleszka, J., Forêt, S., Saint, R., and Maleszka, R. (2007). RNAi-induced phenotypes suggest a novel role for a chemosensory protein CSP5 in the development of embryonic integument in the honeybee *Apis mellifera*. *Dev. Genes Evol.* 217, 189–196. doi: 10.1007/s00427-006-0127-y

Mang, D., Shu, M., Endo, H., Yoshizawa, Y., Nagata, S., Kikuta, S., et al. (2016a). Expression of a sugar clade gustatory receptor, BmGr6, in the oral sensory organs, midgut, and central nervous system of larvae of the silkworm bombyx mori. *Insect Biochem. Mol. Biol.* 70, 85–98. doi: 10.1016/j.ibmb.2015.12.008

Mang, D., Shu, M., Tanaka, S., Nagata, S., Takada, T., Endo, H., et al. (2016b). Expression of the fructose receptor BmGr9 and its involvement in the promotion of feeding, suggested by its co-expression with neuropeptide F1 in Bombyx mori. *Insect Biochem. Mol. Biol.* 75, 58–69. doi: 10.1016/j.ibmb.2016.06.001

Marinotti, O., Ngo, T., Kojin, B. B., Chou, S. P., Nguyen, B., Juhn, J., et al. (2014). Integrated proteomic and transcriptomic analysis of the *Aedes aegypti* eggshell. *BMC Dev. Biol.* 14:15. doi: 10.1186/1471-213X-14-15

Mitsuno, H., Sakurai, T., Murai, M., Yasuda, T., Kugimiya, S., Ozawa, R., et al. (2008). Identification of receptors of main sex-pheromone components of three *Lepidopteran species*. *Eur. J. Neurosci.* 28, 893–902. doi: 10.1111/j.1460-9568.2008.06429.x

Miyamoto, T., and Amrein, H. (2014). Diverse roles for the drosophila fructose sensor Gr43a. *Fly* 8, 19–25. doi: 10.4161/fly.27241

Miyamoto, T., Slone, J., Song, X., and Amrein, H. (2012). A fructose receptor functions as a nutrient sensor in the drosophila brain. *Cell* 151, 1113–1125. doi: 10.1016/j.cell.2012.10.024

Pelosi, P., Iovinella, I., Zhu, J., Wang, G., and Dani, F. R. (2017). Beyond chemoreception: diverse tasks of soluble olfactory proteins in insects. *Biol. Rev.* 93, 184–200. doi: 10.1111/brv.12339

Pertea, G., Huang, X., Liang, F., Antonescu, V., Sultana, R., Karamycheva, S., et al. (2003). TIGR gene indices clustering tools (TGICL): a software system for fast clustering of large EST datasets. *Bioinformatics* 19, 651–652. doi: 10.1093/bioinformatics/btg034

Picimbon, J. F., Dietrich, K., Krieger, J., and Breer, H. (2001). Identity and expression pattern of chemosensory proteins in *Heliothis virescens* (lepidoptera, noctuidae). *Insect Biochem. Mol. Biol.* 31, 1173–1181. doi: 10.1016/s0965-1748(01)00063-7

Pitts, R. J., Liu, C., Zhou, X., Malpartida, J. C., and Zwiebel, L. J. (2014). Odorant receptor mediated sperm activation in disease vector mosquitoes. *Proc. Natl. Acad. Sci. U.S.A.* 111, 2566–2571. doi: 10.1073/pnas.1322923111

Sun, L., Li, Y., Zhang, Z., Guo, H., Xiao, Q., Wang, Q., et al. (2019). Expression patterns and ligand binding characterization of plus-C odorant-binding protein 14 from *Adelphocoris lineolatus* (goeze). *Comput. Biochem. Physiol.* 227, 75–82. doi: 10.1016/j.cbpb.2018.10.001

Sun, Y. L., Huang, L. Q., Pelosi, P., and Wang, C. Z. (2012). Expression in antennae and reproductive organs suggests a dual role of an odorant-binding protein in two sibling *Helicoverpa species*. *PLoS One* 7:e30040. doi: 10.1371/journal.pone.0030040

Takemori, N., and Yamamoto, M. T. (2009). Proteome mapping of the drosophila melanogaster male reproductive system. *Proteomics* 9, 2484–2493. doi: 10.1002/pmic.200800795

Tamura, K., Peterson, D., Peterson, N., Stecher, G., Nei, M., and Kumar, S. (2011). MEGA5: molecular evolutionary genetics analysis using maximum likelihood, evolutionary distance, and maximum parsimony methods. *Mol. Biol. Evol.* 28, 2731–2739. doi: 10.1093/molbev/msr121

Tang, Q. Y., and Zhang, C. X. (2013). Data processing system (DPS) software with experimental design, statistical analysis and data mining developed for use in entomological research. *Insect Sci.* 20, 254–260. doi: 10.1111/j.1744-7917.2012.01519.x

Tang, R., Jiang, N. J., Ning, C., Li, G. C., Huang, L. Q., and Wang, C. Z. (2020). The olfactory reception of acetic acid and ionotropic receptors in the *Oriental armyworm*, *Mythimna separata* walker. *Insect Biochem. Mol. Biol.* 118:103312. doi: 10.1016/j.ibmb.2019.103312

Thorne, N., and Amrein, H. (2010). Atypical expression of drosophila gustatory receptor genes in sensory and central neurons. *J. Comput. Neurol.* 506, 548–568. doi: 10.1002/cne.21547

Tian, W., Zhang, T., Gu, S., Guo, Y., Gao, X., and Zhang, Y. (2021). OBP14 (odorant-binding-protein) sensing in *Adelphocoris lineolatus* based on peptide nucleic acid and grapheme oxide. *Insects* 12:422. doi: 10.3390/insects12050422

Vogel, H., Heidel, A. J., Heckel, D. G., and Groot, A. T. (2010). Transcriptome analysis of the sex pheromone gland of the noctuid moth *Heliothis virescens*. *BMC Genom.* 11:29. doi: 10.1186/1471-2164-11-29

Walker, W. B., Roy, A., Anderson, P., Schlyter, F., and Larsson, M. C. (2019). Transcriptome analysis of gene families involved in chemosensory function in *Spodoptera littoralis* (lepidoptera: noctuidae). *BMC Genom.* 20:428. doi: 10.1186/s12864-019-5815-x

Wang, C., Wang, B., and Wang, G. (2021). Functional characterization of sex pheromone neurons and receptors in the armyworm, *Mythimna separata* (walker). *Front. Neuroanat.* 15:673420. doi: 10.3389/fnana.2021.673420

Wang, L., Zhu, J. Y., Qian, C., Fang, Q., and Ye, G. Y. (2015). Venom of the parasitoid wasp pteromalus puparum contains an odorant binding protein. *Arch. Insect Biochem.* 88, 101–110. doi: 10.1002/arch.21206

Wang, M., Li, H., Zheng, H., Zhao, L., Xue, X., and Wu, L. (2020). De novo transcriptomic resources in the brain of vespa velutina for invasion control. *Insects* 11:101. doi: 10.3390/insects11020101

Xiao, Y., Sun, L., Ma, X. Y., Dong, K., Liu, H. W., Wang, Q., et al. (2017). Identification and characterization of the distinct expression profiles of candidate chemosensory membrane proteins in the antennal transcriptome of *Adelphocoris lineolatus* (goeze). *Insect Mol. Biol.* 26, 74–91. doi: 10.1111/imb.12272

Younas, A., Waris, M. I., Chang, X. Q., Shaaban, M., Abdelnabby, H., Tahir ul Qamar, M., et al. (2018a). A chemosensory protein MsepCSP5 involved in chemoreception of oriental armyworm *Mythimna separata*. *Int. J. Biol. Sci.* 14, 1935–1949. doi: 10.7150/ijbs.27315

Younas, A., Waris, M. I., Tahir ul Qamar, M., Shaaban, M., Prager, S. M., and Wang, M. Q. (2018b). Functional analysis of the chemosensory protein MsepCSP8 from the oriental armyworm *Mythimna separata*. *Front. Physiol.* 9:872. doi: 10.3389/fphys.2018.00872

Younas, A., Waris, M. I., Shaaban, M., Tahir ul Qamar, M., and Wang, M. Q. (2021). Appraisal of Msep CSP14 for chemosensory functions in *Mythimna separata*. *Insect Sci.* 1–15. doi: 10.1111/1744-7917.12909

Zhang, J., Wang, B., Dong, S., Cao, D., Dong, J., Walker, W. B., et al. (2015). Antennal transcriptome analysis and comparison of chemosensory gene families in two closely related noctuidae moths, *Helicoverpa armigera* and H. assulta. *PLoS One* 10:e0117054. doi: 10.1371/journal.pone.0117054

Zhang, K., Feng, Y., Du, L., Gao, S., Yan, H., Li, K., et al. (2019). Functional analysis of MsepOR13 in the oriental armyworm *Mythimna*

separata (walker). *Front. Physiol.* 10:367. doi: 10.3389/fphys.2019.00367

Zhang, Y. N., Zhu, X. Y., Fang, L. P., He, P., Wang, Z. Q., Chen, G., et al. (2015). Identification and expression profiles of sex pheromone biosynthesis and transport related genes in *Spodoptera litura*. *PLoS One* 10:e0140019. doi: 10.1371/journal.pone.0140019

Zhu, J., Iovinella, I., Dani, F. R., Liu, Y. L., Huang, L. Q., Liu, Y., et al. (2016). Conserved chemosensory proteins in the proboscis and eyes of Lepidoptera. *Int. J. Biol. Sci.* 11, 1394–1404. doi: 10.7150/ijbs.16517

Conflict of Interest: The authors declare that the research was conducted in the absence of any commercial or financial relationships that could be construed as a potential conflict of interest.

Publisher's Note: All claims expressed in this article are solely those of the authors and do not necessarily represent those of their affiliated organizations, or those of the publisher, the editors and the reviewers. Any product that may be evaluated in this article, or claim that may be made by its manufacturer, is not guaranteed or endorsed by the publisher.

Copyright © 2022 Chen, Du, Gao, Sun, Chen, Xie, An and Zhao. This is an open-access article distributed under the terms of the Creative Commons Attribution License (CC BY). The use, distribution or reproduction in other forums is permitted, provided the original author(s) and the copyright owner(s) are credited and that the original publication in this journal is cited, in accordance with accepted academic practice. No use, distribution or reproduction is permitted which does not comply with these terms.

frontiers in Physiology

ORIGINAL RESEARCH
published: 28 February 2022
doi: 10.3389/fphys.2022.847895

Characterization of Antennal Chemosensilla and Associated Chemosensory Genes in the Orange Spiny Whitefly, *Aleurocanthus spiniferus* (Quaintanca)

Yu-Qing Gao[1†], Zhen-Zhen Chen[1†], Meng-Yuan Liu[1], Chang-Yuan Song[1], Zhi-Fei Jia[1], Fang-Hua Liu[1], Cheng Qu[2], Youssef Dewer[3], Hai-Peng Zhao[1], Yong-Yu Xu[1] and Zhi-Wei Kang[1]**

[1] College of Plant Protection, Shandong Agricultural University, Tai'an, China, [2] Beijing Key Laboratory of Environment Friendly Management on Fruit Diseases and Pests in North China, Institute of Plant and Environment Protection, Beijing Academy of Agriculture and Forestry Sciences, Beijing, China, [3] Phytotoxicity Research Department, Central Agricultural Pesticide Laboratory, Agricultural Research Center, Giza, Egypt

OPEN ACCESS

Edited by:
Xin-Cheng Zhao,
Henan Agricultural University, China

Reviewed by:
Herbert Venthur,
University of La Frontera, Chile
Zhao-Qun Li,
Tea Research Institute (CAAS), China

***Correspondence:**
Yong-Yu Xu
xuyy@sdau.edu.cn
Zhi-Wei Kang
zwkang2010@126.com

[†] These authors have contributed equally to this work

Specialty section:
This article was submitted to Invertebrate Physiology, a section of the journal Frontiers in Physiology

Received: 03 January 2022
Accepted: 20 January 2022
Published: 28 February 2022

Citation:
Gao Y-Q, Chen Z-Z, Liu M-Y, Song C-Y, Jia Z-F, Liu F-H, Qu C, Dewer Y, Zhao H-P, Xu Y-Y and Kang Z-W (2022) Characterization of Antennal Chemosensilla and Associated Chemosensory Genes in the Orange Spiny Whitefly, Aleurocanthus spiniferus (Quaintanca). Front. Physiol. 13:847895. doi: 10.3389/fphys.2022.847895

The insect chemosensory system plays an important role in many aspects of insects' behaviors necessary for their survival. Despite the complexity of this system, an increasing number of studies have begun to understand its structure and function in different insect species. Nonetheless, the chemosensory system in the orange spiny whitefly *Aleurocanthus spiniferus*, as one of the most destructive insect pests of citrus in tropical Asia, has not been investigated yet. In this study, the sensillum types, morphologies and distributions of the male and female antennae of *A. spiniferus* were characterized using scanning electron microscopy. In both sexes, six different sensilla types were observed: trichodea sensilla, chaetica sensilla, microtrichia sensilla, coeloconic sensilla, basiconic sensilla, and finger-like sensilla. Moreover, we identified a total of 48 chemosensory genes, including 5 odorant-binding proteins (OBPs), 12 chemosensory proteins (CSPs), 3 sensory neuron membrane proteins (SNMPs), 6 odorant receptors (ORs), 8 gustatory receptors (GRs), and 14 ionotropic receptors (IRs) using transcriptome data analysis. Tissue-specific transcriptome analysis of these genes showed predominantly expression in the head (including antennae), whereas CSPs were broadly expressed in both head (including the antennae) and body tissue of adult *A. spiniferus*. In addition, the expression profiling of selected chemosensory genes at different developmental stages was examined by quantitative real time-PCR which was mapped to the transcriptome. We found that the majority of these genes were highly expressed in adults, while *AspiORco*, *AspiGR1*, *AspiGR2*, and *AspiIR4* genes were only detected in the pupal stage. Together, this study provides a basis for future chemosensory and genomic studies in *A. spiniferus* and closely related species. Furthermore, this study not only provides insights for further research on the molecular mechanisms of *A. spiniferus*-plant interactions but also provides extensive potential targets for pest control.

Keywords: *Aleurocanthus spiniferus*, transcriptome, antennal sensilla, chemosensory genes, expression patterns

INTRODUCTION

In insects, the chemosensory system is extremely critical for detecting and discriminating specific chemical signals in the environment necessary for their survival and reproduction (Hallem et al., 2006; Knolhoff and Heckel, 2014; Kang et al., 2020). The insect peripheral chemosensory system comprises odorant receptors (ORs), gustatory receptors (GRs), ionotropic receptors (IRs), odorant binding proteins (OBPs), chemosensory proteins (CSPs), and sensory neuron membrane proteins (SNMPs) (Fleischer et al., 2018; Sun et al., 2020; Liu et al., 2021). These protein families have been identified from a large number of insect species, however, they still remain unidentified from several insect species.

Odorant binding proteins are small soluble olfactory proteins which are thought to be responsible for transporting hydrophobic odor molecules through the sensillum lymph to odorant receptors, which are housed on the dendritic membrane of olfactory sensory neurons (Wang et al., 2020; Tian et al., 2021). Previous studies have shown that OBPs are expressed selectively in different types of sensilla on the antenna, which are considered the minimum functional units for chemoreception. In general, OBPs show higher binding affinities with ligands *in vitro*. For instance, *ApisOBP3* and *SaveOBP7* showed a high binding affinity with aphid alarm pheromone, (E)-beta-farnesene, whereas, *ApisOBP1*, *ApisOBP3*, *ApisOBP8*, *ApisOBP7*, and *SaveOBP7* showed a high binding affinity with plant volatiles (Qiao et al., 2009; Zhong et al., 2012).

Chemosensory proteins represent another class of small soluble proteins abundant in the lymph of chemosensilla (Pelosi et al., 2006). They are also broadly expressed in various organs, such as palps, proboscis, legs, wings, eyes, and pheromone glands (Hua et al., 2012, 2013; Gu et al., 2013; Liu et al., 2014; Zhu et al., 2016; Li et al., 2020). CSPs are different from OBPs in amino acid sequence and structure, but appear to be similar in functions, although better evidence is needed to clarify their role in olfaction (Calvello et al., 2005; Tian et al., 2021). The first CSP protein was discovered in the regenerating legs of the American cockroach, *Periplaneta americana* (Nomura et al., 1992). OS-D, a related CSP, was later cloned from *Drosophila melanogaster* antennae and is thought to be involved in pheromone binding (Mckenna et al., 1994). More insect CSP genes have recently been identified and characterized as a result of the completion of diverse insect genome sequences (Pelosi et al., 2017). Various numbers of CSP genes have been identified in different insect species. For instance, 4 CSPs were reported in *D. melanogaster*, six in *Apis mellifera* (Forêt et al., 2007), and 20 in *Bombyx mori* (Gong et al., 2007), 70 in *Locusta migratoria* (Picimbon et al., 2000), 43 in *Aedes aegypti* (Mei et al., 2018), three in *Heliothis virescens* (Picimbon et al., 2001) and 27 in *Helicoverpa armigera* (Agnihotri et al., 2021).

Odorant receptors were the first insect chemosensory receptor family which were identified using a bioinformatics screen of the *D. melanogaster* genome (Gao and Chess, 1999). The typical ORs are seven-transmembrane receptors with a reversed membrane topology. In general, ORs have a wide variety of odor affinities, and a single odorant molecule may bind to a number of olfactory receptors with variable affinities, which are dependent on physio-chemical features of molecules such as their molecular weights (Buck, 2004). Once the odorant interacts with the odorant receptor, it undergoes structural modifications and binds and activates the olfactory-type G protein on the inside of the olfactory receptor neuron. Activated olfactory receptors trigger nerve impulses that transmit information about the odor to the brain (Fleischer et al., 2018).

In insect gustatory organs, gustatory receptors GRs are a large gene family, which are implicated in host-seeking (Hallem et al., 2006; Agnihotri et al., 2016). Most of these GR proteins have the typical structure of seven transmembrane domains, were initially identified in the *D. melanogaster* genome based on a bioinformatic approach (Clyne et al., 2000). Further studies discovered that *D. melanogaster* has 68 gustatory receptor proteins, which are encoded by 60 gustatory receptor genes by alternative splicing (Dunipace et al., 2001; Scott et al., 2001; Robertson et al., 2003). The amino acid sequences of most gustatory receptor proteins are quite diverse, with just 8–12% sequence similarity. Some of this variance might help to increase the diversity of GRs' responses to ligands (Robertson et al., 2003). GRs were classified as sugar receptors, CO_2 receptors, GR43a-like receptors, bitter receptors, sex pheromone receptors, and unknown receptors based on the ligands to which they respond (Jones et al., 2007; Sato et al., 2011). With the development of insect genome sequencing, insect GR genes have been discovered in an increasing number of species: *Anopheles gambiae* has 52 Gr genes that encode 76 GR proteins (Hill et al., 2002), and *A. aegypti* has 79 GR genes that encode 114 GR proteins (Kent et al., 2008). *Bombyx mori* and *Tribolium castaneum* have 65 and 220 GR genes, respectively (Richards et al., 2008; Wanner and Robertson, 2008). Among all insect species investigated, *H. armigera* had the second-highest number of GR genes (197) (Xu et al., 2016).

Compared to other chemosensory gene families, SNMPs are a small family where only one or two members have been reported (SNMP1 and SNMP2). SNMP1 is found to be co-expressed with pheromone receptors in pheromone responsive neurons and seems to be an indicator of pheromone-responsive neurons (Jiang et al., 2016; Fleischer et al., 2018; Zhang et al., 2018). In contrast, SNMP2 is expressed in cells surrounding the neuron clusters supporting cells (Jiang et al., 2016). Recently, a novel SNMP gene, SNMP3 was found specifically expressed in the larval midgut of (*B. mori*), which assumed to be involved in the immune response to virus and bacterial infections (Zhang et al., 2018).

The orange spiny whitefly *Aleurocanthus spiniferus* is a serious insect pest of citrus, grapes and tea plants (Tang et al., 2015; Nugnes et al., 2020; Radonjić and Hrnčić, 2021). It also causes significant damage to more than 90 plant species from 38 families widely distributed throughout the world (Tang et al., 2015; Radonjić and Hrnčić, 2021). Due to the serious damage caused by this pest, it has been reported as quarantine pest in many countries (EPPO A2 list[1]). To date, there are limited studies on *A. spiniferus* that are mainly focused on population dynamics, insecticide selections, biological control and color plates (Mokrane et al., 2020; Nugnes et al., 2020; Tian et al., 2020). In this study, we investigated the structure,

[1]https://www.eppo.int/ACTIVITIES/plant_quarantine/A2_list

distribution, and abundance of the antennal sensilla in the adult male and female *A. spiniferus* by scanning electron microscopy. Transcriptome sequencing of *A. spiniferus* was performed to identify the candidate chemosensory genes. Moreover, tissue expression patterns of the putative chemosensory genes were assessed by quantitative real-time PCR (qPCR). These findings provide a basis for future chemosensory and genomic studies in *A. spiniferus* and closely related species.

MATERIALS AND METHODS

Insect Materials

In this study, *A. spiniferus* were collected form tea cultivar 'Huangjinya' (*Camellia sinensis*) that were maintained in the greenhouse in Jinan, Shandong, China. Due to the low sex ratio of male, we are unable to get high quality and quantity of RNAs from male head tissues. Thus, we conducted the transcriptome analysis with the mixture of male and female head and bodies tissues. Heads with antennae (200 heads per replicate) and bodies only with thoraxes, legs, wings and abdomens (50 bodies per replicate) were dissected, collected in liquid nitrogen and then subjected to RNA extractions using RNAiso (Takara Bio, Tokyo, Japan) according to the manufacturer's instructions. The RNA integrity was verified by 1% agarose gel electrophoresis and the quantity was assessed with a Nanodrop ND-2000 spectrophotometer (Nanodrop Technologies, Wilmington, DE, United States).

Scanning Electron Microscopy

Approximately 50 female and male adults were used for the identification of antennal sensilla using scanning electron microscopy (SEM). Experiments were conducted followed the method previously descried by Zhang et al. (2015). Whole bodies of *A. spiniferus* were putted into 1.5 ml clean Eppendorf tubes and washed twice using 0.1 M phosphate-buffered saline (PBS, pH 7.2) each for 5 min. After the preliminary cleaning, all of these samples were transferred into ultrasonic bath for deep cleaning (250 W, 30 s). Cleaned samples were fixed in 2.5% glutaraldehyde at 4°C overnight. After the fixation, all samples were washed five times in PBS (0.1 M, pH 7.2) for 20 min each, and then incubated in osmium tetroxide for 15 h. Dehydration of all samples was conducted in ethanol series (45%, 55%, 75%, 85%, 95% for 30 min each, and 100% for 14 h). Then, all samples were transferred into new Eppendorf tubes with 0.5 ml 100% ethanol for 7 h. Dehydrated samples were rinsed in isoamyl acetate for 1 h each. Finally, all samples were dried, mounted on aluminum stubs and gold coated. Antennal sensilla were observed and recorded using ZEISS Ultra-55 Scanning Electron Microscope (Carl Zeiss Meditec, Oberkochen, Baden-Württemberg, Germany). Student's *t*-test was used for the comparison of the difference between male and female ($P < 0.05$).

Transcriptome Sequences

Three biological replicates of high quality and quantity RNAs from heads and bodies of *A. spiniferus* were subjected to cDNA library construction and sequencing on the Illumina, Inc. (San Diego, CA, United States) by Novogene Bioinformatics Technology Co., Ltd. (Beijing, China). Clean data (clean reads) were obtained by removing adapter-containing reads, higher N rate reads (N rates > 10%), and low-quality reads (50% bases with *Q*-score $\leq$ 5) from the raw data (raw reads) using in-house Perl scripts. Clean read assembly was carried out with the short-read assembly program Trinity with min_kmer_cov set to 2 by default and all other parameters set default. The annotation of unigenes was performed by NCBI BLASTx search against the Nr protein database, with an *E*-value threshold of 1×10^{-5}. The blast results were then imported into the Blast2GO pipeline for GO annotation. The longest open reading frame ORF for each unigene was determined by the NCBI ORF Finder tool[2]. Differential expression analysis was performed using the DESeq2 R package (1.20.0). DESeq2 provides statistical routines for determining differential expression in digital gene expression data using a model based on the negative binomial distribution. The resulting *P*-values were adjusted using the Benjamini and Hochberg's approach for controlling the false discovery rate. Genes with an adjusted *P*-value < 0.05 found by DESeq2 were assigned as differentially expressed. Expression levels were expressed in terms of FPKM values (fragments per kilobase per million reads), which was calculated by RSEM (RNA-Seq by Expectation-Maximization) with default parameters (Kang et al., 2017b). The sequences reported in this paper have been deposited in the GenBank SRA database (BioProject ID: PRJNA792195).

Verification of Candidate Chemosensory Genes in *Aleurocanthus spiniferus*

Genes annotated as chemosensory genes in *A. spiniferus* were further verified by BLASTp (*E*-value < 1×10^{-5} and Identity > 30%) in NCBI non-redundant protein sequences database with algorithm of PSI-BLAST. Furthermore, we also used the amino acid sequences of OBPs and CSPs of *B. tabaci* against our transcriptome database to avoid the omission of transcriptome annotation (Zeng et al., 2019). The signal peptide and conserved domains of OBPs and CSPs of *A. spiniferus* were predicted by SignalP 5.0 Server[3] and SMART (simple modular architecture research tool[4]). Transmembrane domains in ORs, GRs and IRs were predicted by TMHMM - 2.0[5].

Sequence Alignment and Phylogenetic Analysis

Sequence alignment and phylogenetic analysis were conducted as described by Zeng et al. (2019). Amino acid sequences of candidate OBPs, CSPs, SNMPs, ORs, GRs, and IRs were aligned by ClustalW used gap opening penalty 10 and gap extension penalty 0.2. The alignments were further manually edited. Phylogenetic trees were subsequently constructed by the maximum likelihood method using MEGA X based on the model WAG and gamma distributed with bootstrap 1000 (Kumar et al., 2018). The trees were further edited using the ITOL tool (Letunic and Bork, 2019). All amino acid sequences used in this work are presented in **Supplementary Table S1**.

[2]http://www.ncbi.nlm.nih.gov/gorf/gorf.html

[3]http://www.cbs.dtu.dk/services/SignalP/

[4]http://smart.emblheidelberg.de/

[5]https://services.healthtech.dtu.dk/service.php?TMHMM-2.0

TABLE 1 | Antennal length and chemosensillar distribution on the antennae of *A. spiniferus*.

	Segment		Length (μm)	The number of antennal sensillar					
				Microtrichia sensilla	Grooved surface trichodea sensilla	Chaetae sensilla	Coeloconic sensilla	Basiconic sensilla	Finger-like sensilla
Female	Total		296 ± 11*a*	More	1	7	4	1	1
	Scape		16.54 ± 1.27*a*	More	1	1	0	0	0
	Pedicel		49.26 ± 4.07*a*	More	0	6	0	0	0
		F1	101.61 ± 3.24*a*						
		F2	21.60 ± 2.52*a*						
	Flagellum	F3	21.70 ± 2.15*a*	More	0	0	4	4	1
		F4	28.58 ± 3.17*a*						
		F5	57.88 ± 3.95*a*						
Male	Total		247 ± 7*b*	More	1	7	4	4	1
	Scape		15.14 ± 0.70*b*	More	1	0	0	0	0
	Pedicel		44.01 ± 3.36*b*	More	0	5	0	0	0
		F1	78.12 ± 2.20*b*						
		F2	15.83 ± 2.02*b*						
	Flagellum	F3	24.77 ± 2.13*b*	More	0	2	4	4	1
		F4	24.77 ± 2.13*b*						
		F5	45.22 ± 2.58*b*						

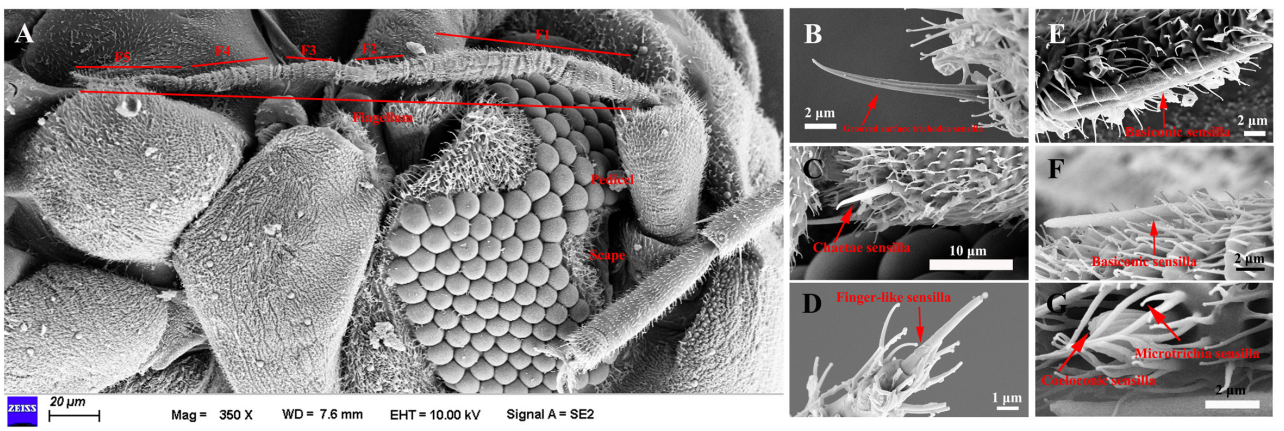

FIGURE 1 | The types of sensilla present on *A. spiniferus* antennae. **(A)** Female antenna. **(B)** Grooved surface richodea sensilla **(C)** Chaetae sensilla. **(D)** Figure-like sensilla. **(E)** Basiconic sensilla. **(F)** Basiconic sensilla. **(G)** Coeloconic and microtrichia sensilla.

TABLE 2 | Assembly summary of the *A. spiniferus* transcriptome.

Group name	Head			Body		
	1	2	3	1	2	3
Raw reads	29,663,967	28,041,038	31,218,486	29,511,378	27,409,600	30,642,126
Clean reads	29,080,717	27,293,657	30,829,257	28,968,202	26,996,849	30,291,895
GC percent	38.7%	38.8%	37.57%	40.24%	40.16%	39.3%
Total number of unigenes	75,298					
N50 length	2,355					
Max length	38,279					
Min length	301					
Mean length	782					

TABLE 3 | Candidate chemosensory genes in *A. spiniferus*.

Gene name	Unigene IDs	ORF (aa)	Signal peptide	Homology search with known proteins		
				Best blastp hit	E-value	Identity (%)
AspiOBP1	Cluster-17909.36062	143	1–23	AQS80474.1| odorant binding protein 1 [*Bemisia tabaci*]	1e-58	59.29
AspiOBP2	Cluster-17909.4418	248	1–22	XP_018902547.1| PREDICTED: uncharacterized protein LOC109034040 [*Bemisia tabaci*]	1e-89	64.29
AspiOBP3	Cluster-17909.4100	265	1–26	AQS80478.1| odorant binding protein 5 [*Bemisia tabaci*]	3e-114	83.51
AspiOBP5	Cluster-17909.46264	223	1–28	AMQ76484.1| odorant-binding protein 31 [*Apolygus lucorum*]	7e-15	33.70
AspiOBP7	Cluster-17909.17740	141	NF	XP_018909253.1| PREDICTED: uncharacterized protein LOC109038604 [*Bemisia tabaci*]	2e-68	84.56
AspiCSP2	Cluster-17909.27950	133	1–19	XP_018914249.1| PREDICTED: ejaculatory bulb-specific protein 3-like [*Bemisia tabaci*]	1e-72	83.46
AspiCSP3	Cluster-17909.9823	132	1–20	AIT38537.1| chemosensory protein 3 [*Bemisia tabaci*]	2e-50	61.54
AspiCSP4	Cluster-17909.11369	109	1–20	XP_018912154.1| PREDICTED: ejaculatory bulb-specific protein 3-like [*Bemisia tabaci*]	5e-45	68.81
AspiCSP5	Cluster-17909.27981	173	1–17	AQS80473.1| chemosensory protein 13 [*Bemisia tabaci*]	4e-59	56.82
AspiCSP7	Cluster-17909.18369	125	1–20	ANJ43349.1| chemosensory protein 4 [*Bemisia tabaci*]	2e-54	64.34
AspiCSP8	Cluster-17909.18168	140	1–27	XP_018914236.1| PREDICTED: ejaculatory bulb-specific protein 3-like [*Bemisia tabaci*]	5e-44	58.12
AspiCSP9	Cluster-17909.19859	124	1–20	XP_018898412.1| PREDICTED: ejaculatory bulb-specific protein 3-like [*Bemisia tabaci*]	7e-62	78.23
AspiCSP10	Cluster-17909.8133	136	1–22	XP_018914236.1| PREDICTED: ejaculatory bulb-specific protein 3-like [*Bemisia tabaci*]	3e-57	66.91
AspiCSP12	Cluster-17909.30984	132	NF	XP_018916537.1| PREDICTED: ejaculatory bulb-specific protein 3-like [*Bemisia tabaci*]	4e-46	57.03
AspiCSP14	Cluster-11558.0	142	1–22	XP_018912701.1| PREDICTED: ejaculatory bulb-specific protein 3-like [*Bemisia tabaci*]	9e-74	89.44
AspiCSP15	Cluster-17909.27059	109	NF	XP_018916603.1| PREDICTED: ejaculatory bulb-specific protein 3-like [*Bemisia tabaci*]	2e-69	92.59
AspiCSP16	Cluster-17909.35439	149	1–21	XP_018913601.1| PREDICTED: ejaculatory bulb-specific protein 3-like [*Bemisia tabaci*]	8e-66	76.12
AspiSNMP1	Cluster-17909.47564	494		XP_018916083.1| PREDICTED: sensory neuron membrane protein 1-like [*Bemisia tabaci*]	0.0	66.87
AspiSNMP2.1	Cluster-17909.2178	564		XP_018909770.1| PREDICTED: sensory neuron membrane protein 2-like [*Bemisia tabaci*]	0.0	59.96
AspiSNMP2.2	Cluster-17909.23140	457		XP_018914385.1| PREDICTED: sensory neuron membrane protein 2-like [*Bemisia tabaci*]	0.0	79.21
AspiORco	Cluster-17909.2187	472		XP_018916513.1| PREDICTED: odorant receptor coreceptor [*Bemisia tabaci*]	0.0	76.82
AspiOR2	Cluster-17909.26288	423		XP_018901087.1| PREDICTED: uncharacterized protein LOC109033105 [*Bemisia tabaci*]	1e-35	31.05
AspiOR3	Cluster-15455.0	418		XP_018901080.1| PREDICTED: uncharacterized protein LOC109033100 [*Bemisia tabaci*]	3e-24	41.50
AspiOR4	Cluster-17909.52227	179		XP_018901080.1| PREDICTED: uncharacterized protein LOC109033100 [*Bemisia tabaci*]	6e-15	32.65
AspiOR5	Cluster-17909.1519	272		XP_018901080.1| PREDICTED: uncharacterized protein LOC109033100 [*Bemisia tabaci*]	6e-18	36.62
AspiOR6	Cluster-17909.15899	138		XP_018901202.1| PREDICTED: uncharacterized protein LOC109033177 [*Bemisia tabaci*]	2e-19	39.69
AspiGR1	Cluster-17909.53621	239		XP_018917335.1| PREDICTED: uncharacterized protein LOC109044210 [*Bemisia tabaci*]	1e-49	65.32
AspiGR2	Cluster-17909.51990	136		XP_016657079.2| gustatory receptor for sugar taste 64a-like [*Acyrthosiphon pisum*]	4e-14	42.11

(Continued)

TABLE 3 | (Continued)

Gene name	Unigene IDs	ORF (aa)	Signal peptide	Homology search with known proteins		
				Best blastp hit	E-value	Identity (%)
AspiGR3	Cluster-18904.0	176		XP_018903763.1| PREDICTED: gustatory receptor for sugar taste 64f-like [*Bemisia tabaci*]	2e-116	96.00
AspiGR4	Cluster-18974.0	184		XP_018910036.1| PREDICTED: uncharacterized protein LOC109039135 [*Bemisia tabaci*]	3e-110	97.09
AspiGR5	Cluster-17909.6070	108		XP_018910041.1| PREDICTED: gustatory receptor for sugar taste 43a-like [*Bemisia tabaci*]	3e-23	65.75
AspiGR6	Cluster-17909.19648	97		XP_025419807.1| gustatory receptor for sugar taste 61a-like [*Sipha flava*]	2e-17	49.44
AspiGR7	Cluster-14878.0	87		XP_018910041.1| PREDICTED: gustatory receptor for sugar taste 43a-like [*Bemisia tabaci*]	3e-40	89.74
AspiGR8	Cluster-17909.12848	73		XP_027845934.1| gustatory receptor for sugar taste 61a-like isoform X2 [*Aphis gossypii*]	1e-08	50.00
AspiIR1	Cluster-14132.0	416		XP_018902736.1| PREDICTED: uncharacterized protein LOC109034187 [*Bemisia tabaci*]	4e-131	55.85
AspiIR2	Cluster-8053.0	267		XP_018916090.1| PREDICTED: glutamate receptor ionotropic, delta-1 [*Bemisia tabaci*]	1e-162	88.35
AspiIR3	Cluster-17909.2243	605		XP_018911141.1| PREDICTED: ionotropic receptor 25a [*Bemisia tabaci*]	0.0	86.28
AspiIR4	Cluster-17909.4915	603		XP_018908639.1| PREDICTED: ionotropic receptor 21a [*Bemisia tabaci*]	0.0	72.12
AspiIR5	Cluster-17909.17580	286		XP_018909625.1| PREDICTED: glutamate receptor ionotropic, kainate 4-like [*Bemisia tabaci*]	1e-157	79.23%
AspiIR6	Cluster-17909.52928	909		XP_018900134.1| PREDICTED: glutamate receptor ionotropic, kainate 3-like [*Bemisia tabaci*]	0.0	89.99
AspiIR7	Cluster-3371.0	548		XP_018918104.1| PREDICTED: glutamate receptor ionotropic, delta-2 [*Bemisia tabaci*]	0.0	81.93
AspiIR8	Cluster-17909.14487	580		XP_018911078.1| PREDICTED: glutamate receptor ionotropic, kainate 2-like isoform X1 [*Bemisia tabaci*]	0.0	98.02
AspiIR9	Cluster-17909.54060	549		XP_018904379.1| PREDICTED: uncharacterized protein LOC109035262 [*Bemisia tabaci*]	0.0	74.50
AspiIR10	Cluster-17909.50436	912		XP_018907677.1| PREDICTED: glutamate receptor ionotropic, kainate 2-like isoform X2 [*Bemisia tabaci*]	0.0	91.28
AspiIR11	Cluster-17909.4133	919		XP_018914442.1| PREDICTED: glutamate receptor ionotropic, kainate 2 [*Bemisia tabaci*]	0.0	97.26
AspiIR12	Cluster-17909.605	893		XP_018906951.1| PREDICTED: glutamate receptor 1-like [*Bemisia tabaci*]	0.0	94.97
AspiIR13	Cluster-11154.0	1051		XP_018917922.1| PREDICTED: uncharacterized protein LOC109044571 isoform X1 [*Bemisia tabaci*]	0.0	85.46
AspiNmdar1	Cluster-17909.33013	981		XP_018899297.1| PREDICTED: glutamate [NMDA] receptor subunit 1 isoform X1 [*Bemisia tabaci*]	0.0	96.74

Expression Pattern Analysis of Chemosensory Genes by Quantitative Real-Time Polymerase Chain Reaction

RNAs of *A. spiniferus* from different tissues (heads and bodies) and developmental stages (second nymphs, third nymphs, puparia/fourth nymphs, female adults and male adults) were extracted by RNAiso (Takara Bio., Tokyo, Japan). The cDNA was synthesized from total RNA using FastQuant RT Kit (With gDNase) (Tiangen, Beijing, China) according to the standard manufacturer's protocol. Gene-specific primers were designed by Primer Premier 6 (PREMIER Biosoft International, Palo Alto, CA, United States), which are listed in **Supplementary Table S2**. qPCR reaction was conducted in a total volume of 20 μL containing: 10 μL of 50× SYBR Premix Ex Taq, 0.8 μL of primer (10 mM), 0.8 μL of sample cDNA, and 7.6 μL sterilized ultra-pure grade H_2O. The cycling conditions were as follows: 95°C for 30 s, followed by 40 cycles of 95°C for 5 s and 55°C for 30 s. Three technical and three biological replicates were used for each sample. Relative quantification was performed using the Comparative $2^{-\Delta\Delta CT}$ method (Livak and Schmittgen, 2001). Transcription levels of these chemosensory genes were normalized by reference gene RPS28 (Kang et al., 2017a; Kong et al., 2021). Heatmaps of chemosensory genes were constructed by pheatmap in R 4.0.4 as Liu et al. (2020) reported. Differences of selected chemosensory genes between male and female were subjected to Student's *t*-test ($P < 0.05$), while one-way analysis of variance (ANOVA) followed by separation of

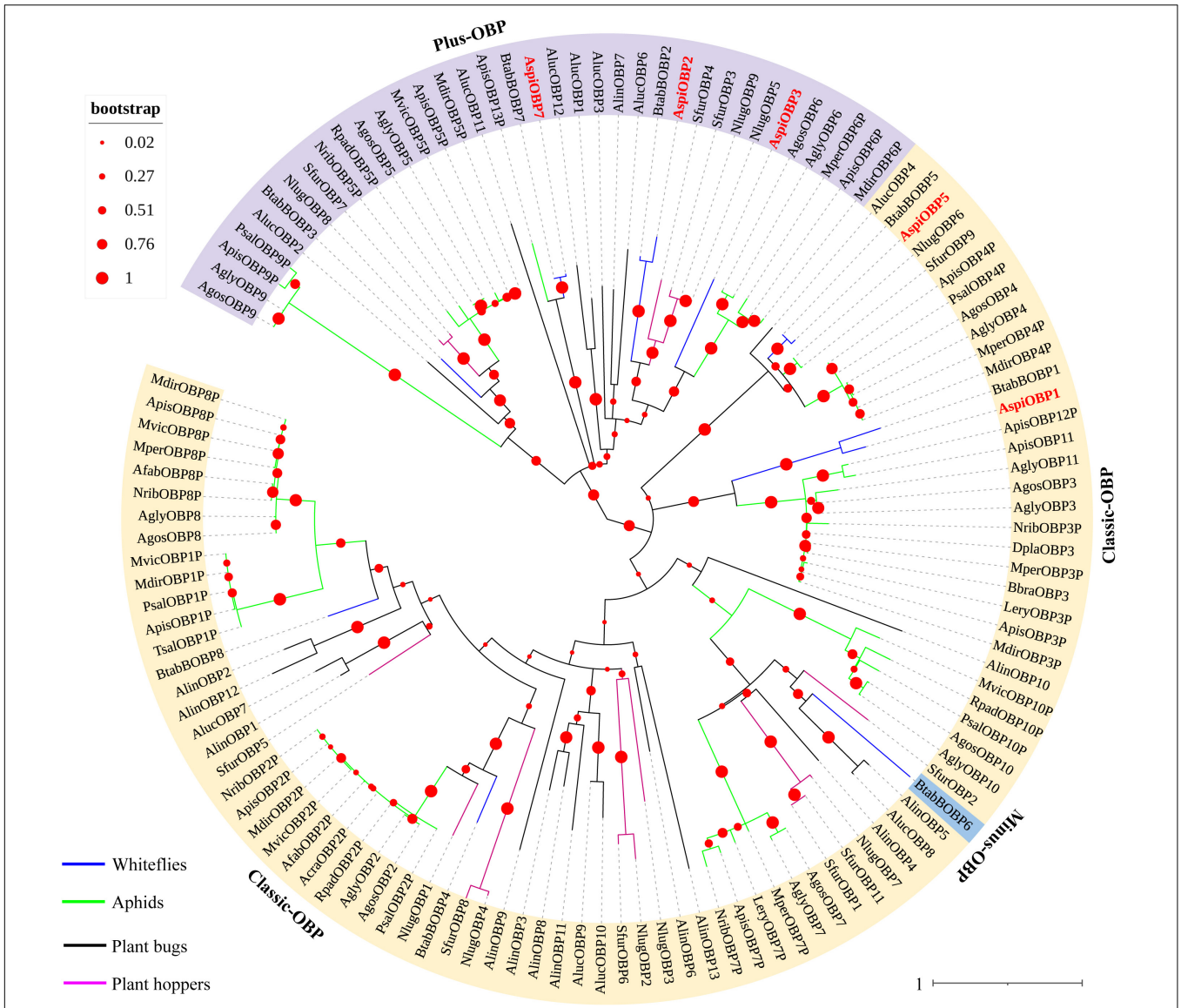

FIGURE 2 | Phylogenetic analysis of putative odorant-binding proteins (OBPs) of *A. spiniferus*. The phylogenetic tree was built using OBP sequences from whitefly species (Btab, *Bemisia tabaci*; Aspi, *A. spiniferus*), aphid species (Apis, *Acyrthosiphon pisum*; Mper, *Myzus persicae*; Agos, *Aphis gossypii*; Psal, *Pterocomma salicis*; Agly, *Aphis glycines*; Mdir, *Metopolophium dirhodum*; Mvic, *Megoura viciae*; Bbra, *Brevicoryne brassicae*; Lery, *Lipaphis erysimi*; Afab, *Aphis fabae*; Acra, *Aphis craccivora*; Tsal, *Tuberolachnus salignus*; Dpla, *Drepanosiphum platanoidis*; Nrib, *Nasonovia ribisnigri*; Rpad, *Rhopalosiphum padi*), plant hoppers (Sfur, *Sogatella furcifera*; Nlug, *Nilaparvata lugens*), and plant bugs (Aluc, *Apolygus lucorum*; Alin, *Adelphocoris lineolatus*).

means with the Fisher's protected least significant difference (LSD) test ($P < 0.05$) was used for the difference among the different developmental stages.

RESULTS

Morphology of Antennal Sensilla of *Aleurocanthus spiniferus*

The length of female antennae was significantly longer than that of male (**Table 1**). Six different sensilla types were observed: trichodea sensilla, chaetica sensilla, microtrichia sensilla, coeloconic sensilla, basiconic sensilla, and finger-like sensilla. There was no difference of the distribution and structure of other sensilla between the two sexes (**Figure 1A**). Grooved surface trichodea sensilla were only found on the scape (**Figure 1B** and **Table 1**). Chaetae sensilla presented on the scape and pedicel female *A. spiniferus*, while it was found on the pedicel and flagellum (**Figure 1C** and **Table 1**). Finger-like sensilla was only found on the tips of the fifth flagellum of *A. spiniferus* (**Figure 1D** and **Table 1**). Basiconic sensilla looks like a sword and was found on the flagellar subsegment 5 (**Figures 1E,F** and **Table 1**). Coeloconic sensilla were surrounded by microtrichia sensilla, and microtrichia sensilla were the most abundant and

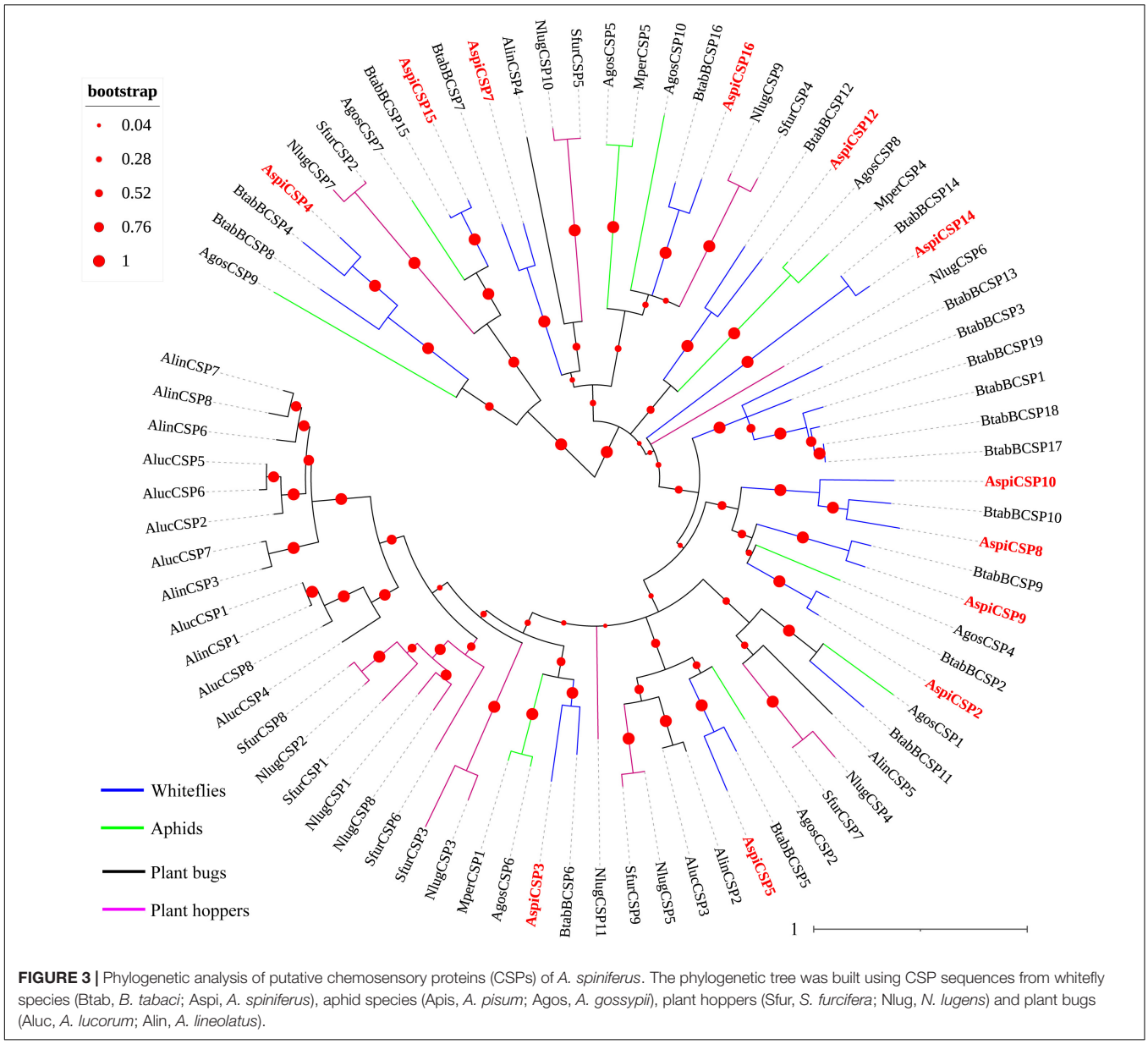

FIGURE 3 | Phylogenetic analysis of putative chemosensory proteins (CSPs) of *A. spiniferus*. The phylogenetic tree was built using CSP sequences from whitefly species (Btab, *B. tabaci*; Aspi, *A. spiniferus*), aphid species (Apis, *A. pisum*; Agos, *A. gossypii*), plant hoppers (Sfur, *S. furcifera*; Nlug, *N. lugens*) and plant bugs (Aluc, *A. lucorum*; Alin, *A. lineolatus*).

widely distributed sensilla on the entire antennae of *A. spiniferus* (**Figure 1G** and **Table 1**).

Transcriptome Analysis Data of *Aleurocanthus spiniferus*

The transcriptome data was presented in **Table 2**. The total number of unigenes was 75298. Max, Min, and mean length were 38279, 301, and 782 bp, respectively (**Table 2**). GC percent of sequences from bodies showed a little bit higher than that from heads (**Table 2**). Homology analyses results showed that the most similar sequences of 75.1% sequences were from *B. tabaci* (**Supplementary Figure S1**). Functional annotation was performed using NR, NT, KO, Swissprot, PFAM, GO, and KOG databases (**Supplementary Table S3**). Based on the GO categorization, differential expressed genes were enriched in protein metabolic process, hydrolase activity, cellular protein metabolic process, intracellular non-membrane-bounded organelle, non-membrane-bounded organelle and translation (**Supplementary Figure S2**).

Putative Chemosensory Genes in *Aleurocanthus spiniferus*

In this study, a total of five transcripts encoding candidate OBPs were identified in the transcriptome of *A. spiniferus* (**Table 3**). The number of putative OBPs was a little bit lower than that identified in the genome of *B. tabaci* (eight OBPs). All of the putative OBPs had full-length ORFs, and only *AspiOBP7* without signal peptide (**Table 3**). A phylogenetic tree was constructed using the identified OBPs from whiteflies (*A. spiniferus* and *B. tabaci*), aphids (*Acyrthosiphon pisum*,

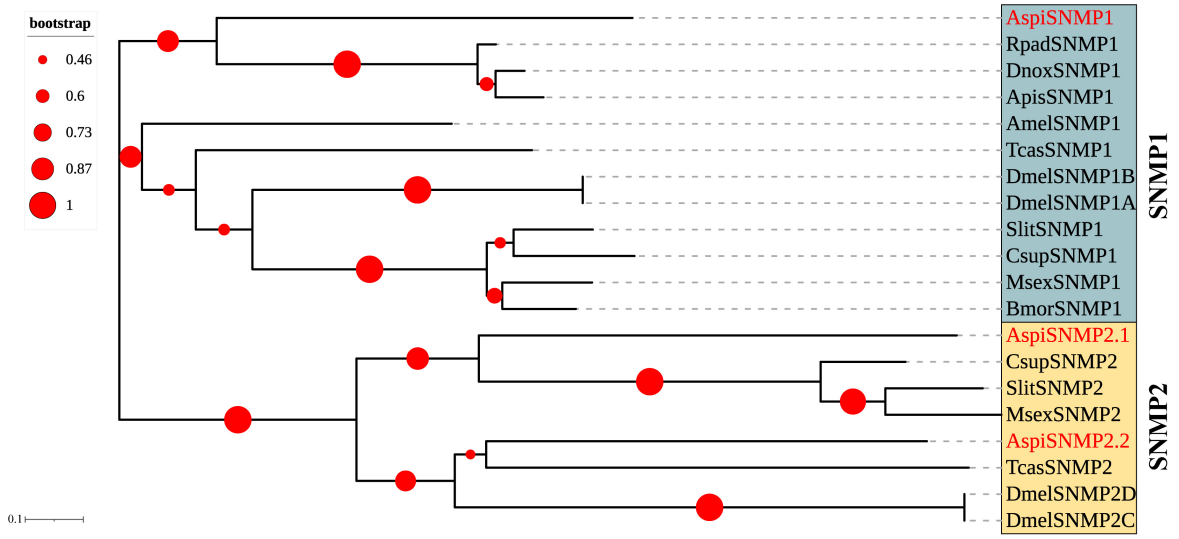

FIGURE 4 | Phylogenetic analysis of putative sensory neuron membrane proteins of *A. spiniferus*.

Aphis glycines, *Brevicoryne brassicae*, *Metopolophium dirhodum*, *Rhopalosiphum padi*, *Lipaphis erysimi*, *Aphis fabae*, *Aphis craccivora*, *Tuberolachnus salignus*, *Myzus persicae*, *Aphis gossypii, Drepanosiphum platanoidis*, and *Nasonovia ribisnigri*), plant bugs (*Apolygus lucorum* and *Adelphocoris lineolatus*) and plant hoppers (*Nilaparvata lugens* and *Sogatella furcifera*) (**Figure 2** and **Supplementary Figure S3**). In the phylogenetic tree, *AspiOBP1*, *AspiOBP2*, *AspiOBP5*, and *AspiOBP7* were clustered with OBPs from *B. tabaci*, while *AspiOBP3* was clustered with OBPs from aphids (**Figure 2**).

We identified 12 candidate CSPs in *A. spiniferus* (**Table 3**) and the number of putative CSPs identified was also lower than that in *B. tabaci* (19 CSPs). Of the 12 putative CSPs, all of them had full-length ORFs, and only *AspiCSP12* and *AspiCSP15* without signal peptide. To analyze the relationship between the CSPs in the different species, a phylogenetic tree was constructed and is presented in **Figure 3**, which includes the identified CSPs from whiteflies (*A. spiniferus* and *B. tabaci*), aphids (*A. gossypii* and *M. persicae*), plant bugs (*A. lucorum* and *A. lineolatus*) and plant hoppers (*N. lugens* and *S. furcifera*). In the phylogenetic tree, all of the identified CSPs were clustered with CSPs in *B. tabaci* (**Figure 3**).

Interestingly, there were three SNMPs identified in *A. spiniferus* that were significantly different from other Hemipteran insects (**Table 3**). The best hits by homology search in NCBI of these SNMPs were SNMPs from *B. tabaci* (**Table 3**). The phylogenetic tree showed that there were two distinct cluster SNMP1 (*AspiSNMP1*) and SNMP2 (*AspiSNMP2.1* and *AspiSNMP2.2*; **Figure 4**).

We identified transcripts encoding six putative ORs (**Table 3**). Among these candidate ORs, *AspiORco*, *AspiOR2*, and *AspiOR3* likely represented full-length genes, encoding proteins made up of more than 400 amino acids (**Table 3**). In the phylogenetic tree, *AspiORco*, *AgosOrco1*, *RapdOrco1*, and *ApisOR1* were clustered in a specific subgroup called odorant co-receptor (Orco) with four transmembrane domains (**Figure 5** and **Supplementary Table S4**). Rest of these identified ORs was clustered in a specific subgroup (**Figure 5**).

For GRs, in this study, we identified eight candidate GRs from the transcriptome of *A. spiniferus* (**Table 3**). A phylogenetic tree was constructed with sequences from whitefly (*A. spiniferus*), aphids (*A. pisum* and *R. padi*) and fly (*D. melanogaster*). *AspiGR14* was clustered with *DmelGR63a* and *DmelGR21a* as a CO_2 receptor, while *AspiGR3* were found in a clade with sugar receptors, which included GRs identified from *D. melanogaster*, *A. pisum*, and *R. padi* (**Figure 6**).

Fourteen putative IRs were identified from the transcriptome of *A. spiniferus* (**Table 3**). Among them, only *AspiIR2*, *AspiIR5*, and *AspiIR8* were found to be a part of the full-length gene. The E-values for *AspiIR3*, *AspiIR4*, *AspiIR6*, *AspiIR7*, *AspiIR8*, *AspiIR9*, *AspiIR10*, *AspiIR11*, *AspiIR12*, *AspiIR13*, and *AspiNmdar1* were zero as compared to the amino acid sequences of these genes in *B. tabaci* (**Table 3**). In the phylogenetic tree, almost all of these IRs were clustered in a known group, such as IR8a/IR25a (*AspiIR3*), IR21a (*AspiIR4*), IR40a (*AspiIR5*), IR75 (*AspiIR9*), IR76b (*AspiIR7*), IR93a (*AspiIR1* and *AspiIR2*), and NMDA iGluRs (*AspiNmdar1*) (**Figure 7**).

Expression Profiles of Chemosensory Genes

Expression results of these selected chemosensory genes in different developmental stages showed that *AspiOBP1* and *AspiIR9* were more strongly expressed in nymphs than that in puparia and adults whereas expression of *AspiOBP3* and *AspiCSP12* in puparia and adults were significantly higher than that in nymphs (**Figure 8**). Surprisingly, *AspiORco*, *AspiOR2*, *AspiGR1*, *AspiGR3*, and *AspiIR4* showed highest expression profiles in puparia among the developmental stages (**Figure 8**). On the contrary, *AspiCSP10*, *AspiIR2*, and *AspiIR3* had the lowest

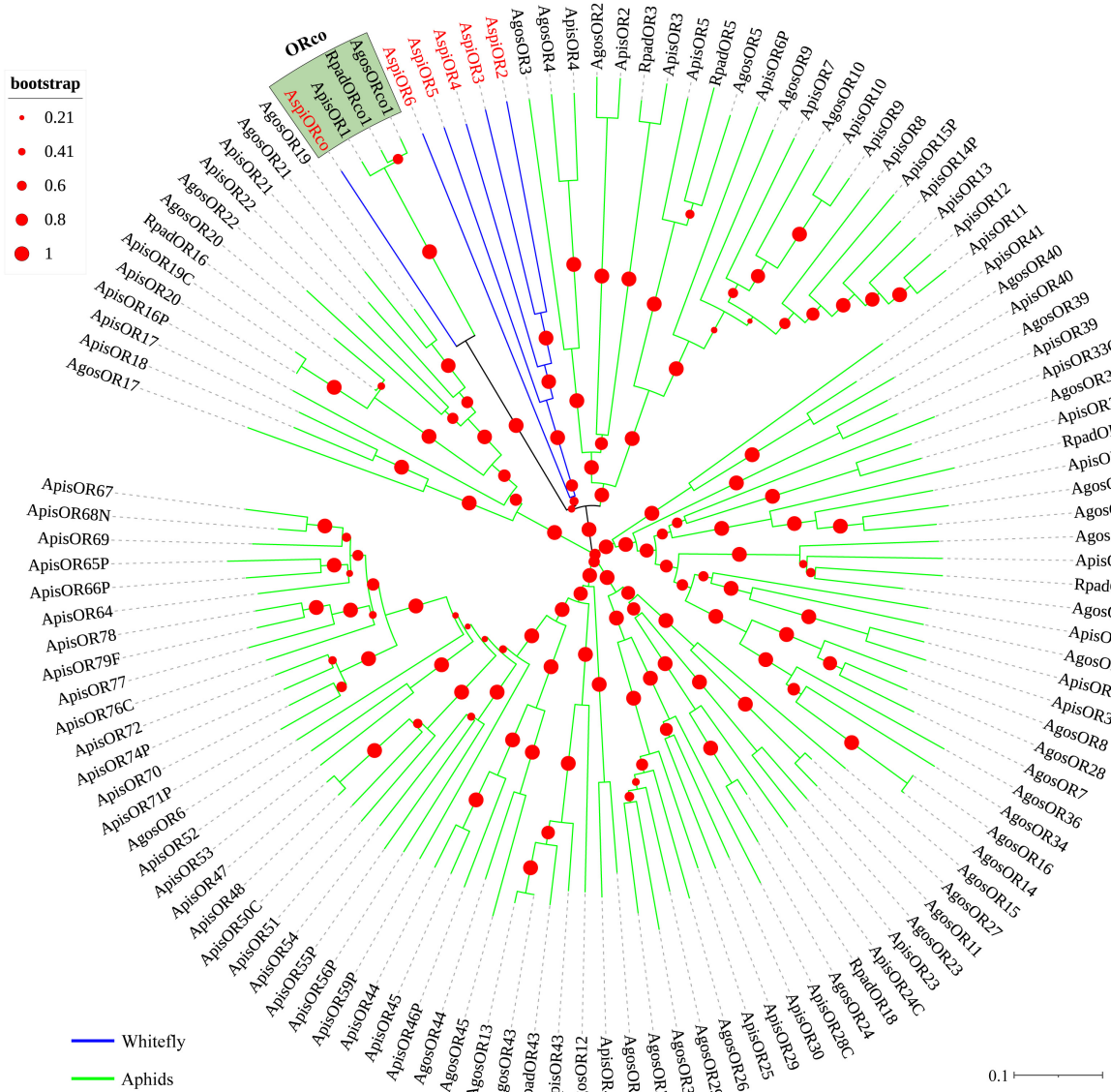

FIGURE 5 | Phylogenetic analysis of putative odorant receptors (ORs) of *A. spiniferus*. The phylogenetic tree was built using OR sequences from whitefly specie (Aspi, *A. spiniferus*) and aphid species (Apis, *A. pisum*; Rpad, *R. padi*; Agos, *A. gossypii*).

expression in puparia. The expression of *AspiOBP2* and *AspiIR5* were significantly higher than that in nymphs and puparia (**Figure 8**). *AspiGR6*, *AspiGR8*, *AspiIR8*, and *AspiIR13* presented a higher expression in nymphs and puparia than that in adults (**Figure 8**). The expression of *AspiIR11* in second instar was significantly higher than other developmental stages (**Figure 8**).

Based on the transcriptome results, we found that all of OBPs and SNMPs, and major of ORs and IRs were more considerably expressed in head than in bodies (**Figure 9A**). Meanwhile, only five of 12 CSPs were predominately expressed in heads, and four of 12 CSPs highly expressed in bodies (**Figure 9A**). In addition, there were only two of eight GRs showed significant tissue-specific expression patterns (**Figure 9A**). qPCR validation of selected chemosensory genes showed that expressions of *AspiOBP1*, *AspiOBP2*, *AspiOBP3*, *AspiCSP10*, *AspiORco*, *AspiOR2*, *AspiGR1*, *AspiGR6*, *AspiGR8*, *AspiNmdar1*, *AspiIR2*, *AspiIR3*, *AspiIR4*, *AspiIR7*, *AspiIR8*, *AspiIR9*, *AspiIR11*, and *AspiIR13* in heads were significantly higher than that in bodies, while *AspiCSP12*, *AspiGR3*, *AspiGR4*, and *AspiIR5* were predominantly expressed in bodies (**Figure 9B**). There was no difference of the expression of *ApisOR3* and *AspiOR5* between heads and bodies (**Figure 9B**).

DISCUSSION

Insects have a complex chemosensory system that accurately perceives external chemicals and plays a pivotal role in many

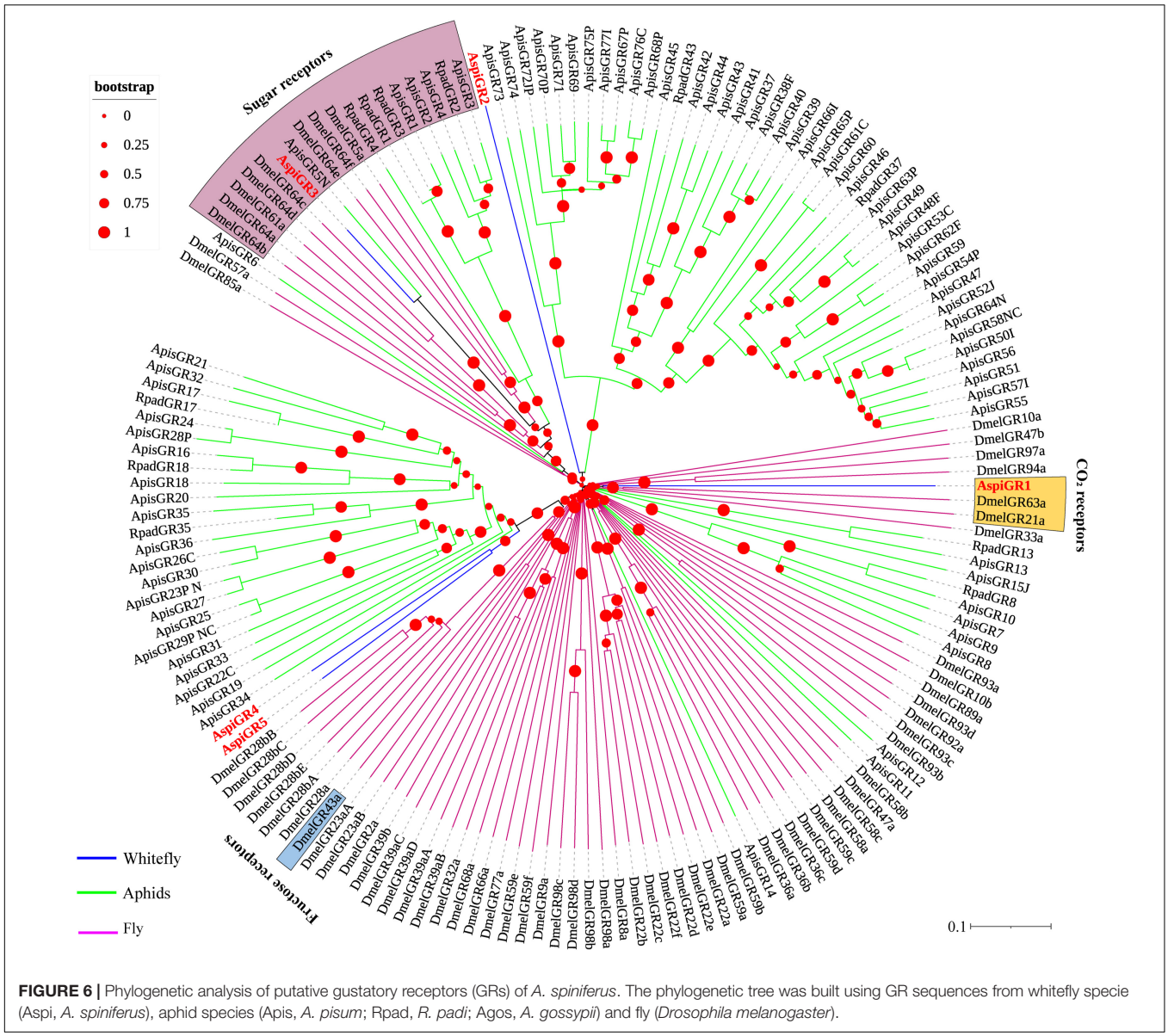

FIGURE 6 | Phylogenetic analysis of putative gustatory receptors (GRs) of *A. spiniferus*. The phylogenetic tree was built using GR sequences from whitefly specie (Aspi, *A. spiniferus*), aphid species (Apis, *A. pisum*; Rpad, *R. padi*; Agos, *A. gossypii*) and fly (*Drosophila melanogaster*).

insect life activities. Several studies have been conducted to understand the structure and function of the chemosensory system in different insect species, however, the chemosensory system in the orange spiny whitefly, *A. spiniferus* has not been investigated yet. The present study is the first report identifying the various types and distribution of the sensilla on the adult male and female antenna of *A. spiniferus.* Consistent with the results of two cryptic *B. tabaci* specie, length of male antenna was significantly longer than that of females, which was caused by the obviously smaller bodies of male *A. spiniferus* (Zhang et al., 2015). Furthermore, there was no differences in the composition and number of antennal sensilla between males and females. Contrary with that, in two cryptic *B. tabaci* specie, males had more chaetae sensilla (7) than females (5) (Zhang et al., 2015). Interestingly, in *A. spiniferus*, distribution of chaetae sensilla between males and females was different. In females, chaetae sensilla was observed in scape (1) and pedicel (6), while in males chaetae sensilla was found in pedicel (5) and flagellum (2). Differences of the distribution of chaetae sensilla might be involved in the different behaviors between males and females of *A. spiniferus*.

In this study, we systematically identified and chemosensory genes in *A. spiniferus* via transcriptomic analyses. A total of 48 candidate chemosensory genes including 5 OBPs, 12 CSPs, 3 SNMPs, 6 ORs, 8 GRs, and 14 IRs were predicted. The number of identified chemosensory receptors was close to *B. tabaci* that contains 9 OBPs, 18 CSPs, 7 ORs, and 17 GRs, but significantly lower than that in other hemipterans (*A. pisum*: 79 ORs, 77 GRs, 15 OBPs, and 1 SNMP; *A. gossypii*: 45 ORs, 14 IRs, 9 OBPs, 9 CSPs, and 1 SNMPs) (Chen et al., 2016; Wang et al., 2017; Xie et al., 2017; Zeng et al., 2019). However, the total number of OBPs and CSPs in whiteflies showed no contractions or expansion when compared with other hemipteran insects (Zeng et al., 2019).

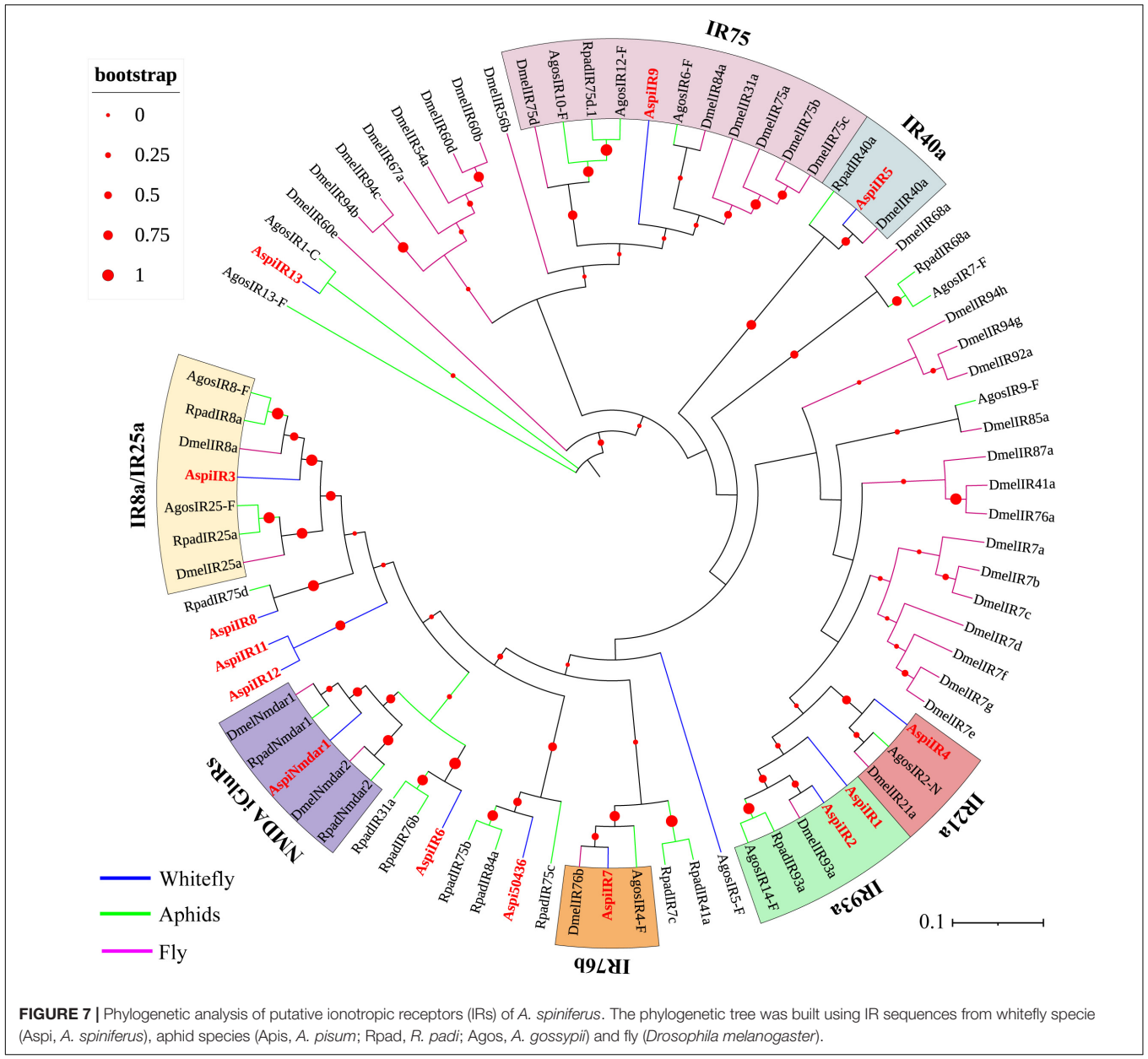

FIGURE 7 | Phylogenetic analysis of putative ionotropic receptors (IRs) of *A. spiniferus*. The phylogenetic tree was built using IR sequences from whitefly specie (Aspi, *A. spiniferus*), aphid species (Apis, *A. pisum*; Rpad, *R. padi*; Agos, *A. gossypii*) and fly (*Drosophila melanogaster*).

The reduction of numbers of ORs and GRs in whiteflies might result from their polyphagia and strong detoxification systems (Chen et al., 2016; Xie et al., 2017). Thereby, less ORs and GRs are enough for them to find their suitable host plants. In addition, as the number of IRs was similar with other insects, we speculated that IRs may work as ORs and GRs. Thus, the functional investigations about ORs, GRs and IRs are needed to figure out the reason of this phenomenon.

In this study, we found that all of these five OBPs were predominately expressed in the head. Expression of *AspiOBP1*, *AspiOBP2*, and *AspiOBP3* across developmental stages showed that *AspiOBP1* was more highly expressed in nymphs than that in pupae and adults whereas the expression of *AspiOBP3* in pupae and adults was significantly higher than that in nymphs. *AspiOBP2* was abundantly expressed in adults. Similarly, in *Sitophilus zeamais*, *SzeaOBP1* showed highest expression at larval stage, while the expression of *SzeaOBP28* at pupae and adult stage was significantly higher than that at larval stage (Zhang Y. et al., 2019). Furthermore, *SzeaOBP1* showed broader binding affinity for plant volatile compounds than *SzeaOBP28* (Zhang Y. et al., 2019). Silencing *SzeaOBP1* reduced the preference of *S. zeamais* to its preferred volatiles (Zhang Y. et al., 2019). In *B. tabaci*, *BtabOBP1*, *BtabOBP2*, *BtabOBP3*, *BtabOBP4*, *BtabOBP7*, and *BtabOBP8* were highly expressed in heads whereas *BtabOBP5* predominately expressed in legs and wings. *BtabOBP1*, *BtabOBP3*, and *BtabOBP4* have been demonstrated to bind oviposition repellent volatile, β-ionone and various volatiles to its specific chemosensory receptor

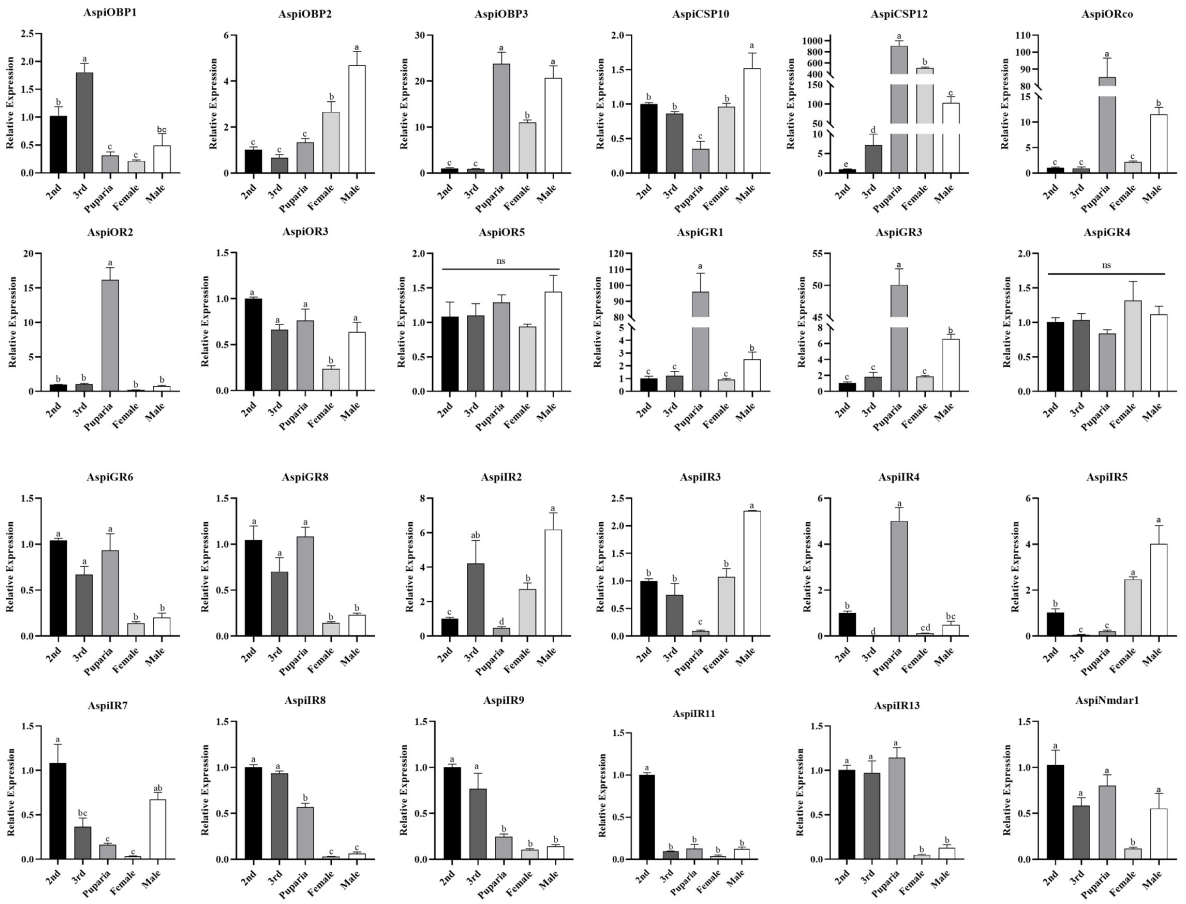

FIGURE 8 | Quantitative real-time polymerase chain reaction (qPCR)-based expression profiling of selected chemosensory genes in different developmental stages of *A. spiniferus*.

(Li et al., 2019; Wang et al., 2020). Knockdown of *BtabOBP3* in *B. tabaci* by RNAi resulted in a reverse olfactory behavior to β-ionone (Wang et al., 2020). Furthermore, silencing *BtabOBP3* also reduced the preference of *B. tabaci* on ToCV-infected tomato plants and the ToCV transmission rate of *B. tabaci* (Shi et al., 2019). Besides the function of odorants perception, OBPs also have been found to been involved in other insect physiological process. For example, the adult *A. lineolatus* head predominately expressed *AlinOBP14* showed a pronounced binding affinity for insect juvenile hormone III (Sun et al., 2019). In *N. lugens*, knockdown of the gene for *NlugOBP3* not only reduced the response rate to seeding volatiles but also resulted in strikingly high nymph mortality (He et al., 2011).

Unlike the expression of OBPs is focused in the antennae or other olfactory sensilla in most insects, CSPs were found to be broadly expressed in various tissues including antennae, wings, legs and abdomen (Hua et al., 2013; Yang et al., 2014). For example, *AlucCSP2* and *AlucCSP3* of *A. lucorum* were specifically expressed in female wings, and showed high binding affinities with cotton secondary metabolites including gossypol, tannings, quercetin and rutin hydrate (Hua et al., 2013). In *N. lugens*, none of CSPs was predominately expressed in antennae (Yang et al., 2014). Leg highly expressed *CSP3* and *CSP8* of *N. lugens* strongly bound to plant volatiles (Waris et al., 2018). Injected with *dsNlugCSP8* significantly reduced the attractive responses of *N. lugens* to nerolidol and hexanal (Waris et al., 2018). Furthermore, CSPs are also known to be involved in insecticide resistance. Overexpressing *AgosCSP5* on *Drosophila* files showed higher resistance and survival in response to imidacloprid and cypermethrin than control flies (Li et al., 2021). In *B. tabaci* and *Ophraella communa*, *BtabCSP11* and *OcomCSP12* were strongly expressed in the female abdomen and ovary respectively, and both of them are involved in the reproduction (Ma et al., 2019; Zeng et al., 2020). Consistent with these results, in this work, we found *AspiCSP12* was specifically expressed in female bodies. Additionally, *AspiCSP12* also showed higher expression levels at puparia and adult stages than that in nymphs. However, AspiCSP10 showed lowest transcript abundance in puparia, and there was no difference of this gene between nymphs and adults. All of these results indicate that *AspiCSP12* might have other physiological functions rather than just being involved in odorant perception.

Recently, more research has been focused on the function of three chemosensory receptor types: ORs, GRs, and IRs

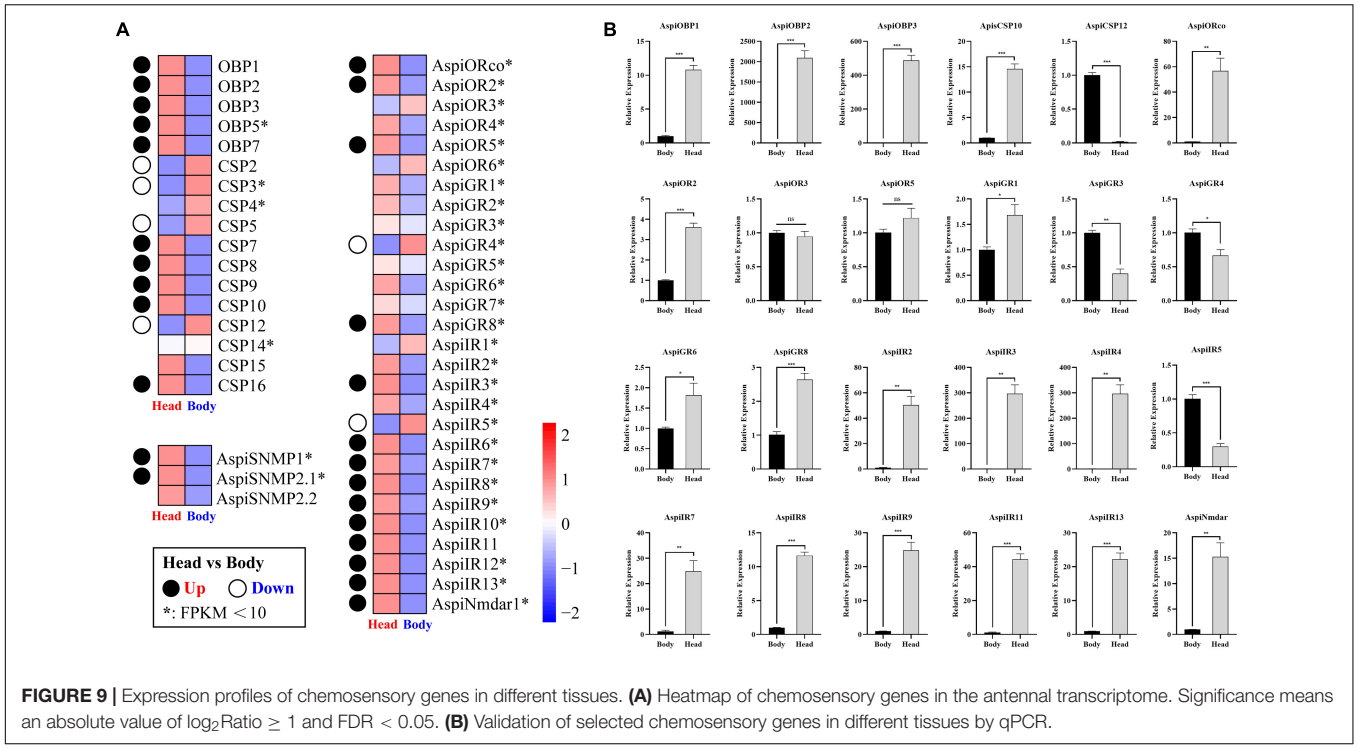

FIGURE 9 | Expression profiles of chemosensory genes in different tissues. **(A)** Heatmap of chemosensory genes in the antennal transcriptome. Significance means an absolute value of $\log_2$Ratio ≥ 1 and FDR < 0.05. **(B)** Validation of selected chemosensory genes in different tissues by qPCR.

(Zhang R.B. et al., 2017; Yang et al., 2020, 2021). In this study, we identified six ORs in the *A. spiniferus* transcriptome. Among of these ORs, *AspiORco*, *AspiOR2*, and *AspiOR5* were predominately expressed in head whereas other ORs showed broadly expressed in heads and bodies. Furthermore, the expression of *ORco* was significantly higher in male and puparia than that in other stages. Similar results were observed in aphids, and knockdown of *SaveORco* in *S. avenae* disrupted its response to plant volatiles and the aphid alarm pheromone, (E)-β-farnesene (Fan et al., 2015; Kang et al., 2018). Besides the *ORco*, in *A. pisum*, *ApisOR5* is known as an essential receptor for its alarm pheromone E-β-farnesene, and *ApisOR4* is involved in the recognition of plant volatiles (Zhang R.B. et al., 2017; Zhang R.B. et al., 2019). Silencing *CquiOR114/117* in female *Culex quinquefasciatus* significantly impaired the blood feeding behavior (Wu et al., 2020). All of these results indicated that ORs especially for *AspiORco*, *AspiOR2*, and *AspiOR5* in *A. spiniferus* might be involved in the plant volatiles perception.

As phloem-feeding insects, whiteflies can be affected and even killed by the phytochemicals in plant phloem sap, such as amino acids, sugars and other metabolites (Cui et al., 2017; Hasanuzzaman et al., 2018; Xia et al., 2021). To cope with this, whiteflies assess the suitability of a potential host plant and select the best plant as well as the best feeding region on the plant (Döring, 2014; Cui et al., 2017; Hu and Tsai, 2020). For example, the content of phenolic glycosides and amino acids in cottonwood leaves varies with their developmental stage and its host aphid *Chaitophorous populicola* was able to detect the difference and to track the preferred leaf stages to optimize its feeding (Gould et al., 2007). In *M. persicae*, the high glutamine concentration stimulated the feeding behavior (Cao et al., 2017). Overexpressing *PrapGR28* from *Pieris rapae* in *Drosophila* files resulted in a strong preference to the food with sinigrin whereas the wild-type (WT) files showed avoidance (Yang et al., 2021). In *B. mori*, *BmorGR66* mutant showed no significant feeding preference for both mulberry leaves and Mongolian oak leaves, while WT *B. mori* did not eat Mongolian oak leaves (Zhang Z.J. et al., 2019). Apart from the GRs, some IRs are also expressed in gustatory organs and are involved in gustation perception (Zhang et al., 2021). For example, IRs expressed in *D. melanogaster* leg sensilla also showed a response to food components such as sugar, salts, polyamines and bitter compounds (Ling et al., 2014; Hussain et al., 2016). In *H. armigera*, knockout of *IR8a* reduced the EAG responses and trend behavior to acetic acid (Zhang et al., 2021). Additionally, IR8a was found to be essential to detect human odors and water detection in *Aedes aegypti* (Raji et al., 2019a,b). Meanwhile, *IR40a*, *IR93a* and *IR25a* mediate the humidity preference in *D. melanogaster* (Enjin et al., 2016). Furthermore, IR25a and IR93a are also involved in the detection of temperature. Interestingly, *Nmdars* have been implicated in associative learning and memory in *D. melanogaster* and are essential factors for male offspring production in *Diploptera punctata* (Xia et al., 2005; Huang et al., 2015). Based on the *A. spiniferus* transcriptome, putative receptors for sugar in GRs, *IR8a*, *IR40a*, *IR93a*, and *Nmdars* were predicted according to the phylogenetic analyses. Almost all of GRs except *AspiGR4* were widely expressed in heads and bodies whilst major of IRs exhibited higher expression in heads than that in bodies. Expressions of selected GRs and IRs showed that the highest expression of *AspiGR1*, *AspiGR3*, and *AspiIR4* were at puparia.

AspiIR5, which was clustered as *IR40a*, had higher expression in adults than that in nymphs and puparia. All of these results indicated that GRs and IRs in *A. spiniferus* might be involved in various biological processes and have critical roles in the survival.

Taken together, in this study, we systemically identified six types of sensilla on antennae of including grooved surface trichodea sensilla, chaetae sensilla, microtrichia sensilla, coeloconic sensilla, basiconic sensilla and finger-like sensilla via SEM and a total of 48 chemosensory genes in *A. spiniferus* including 5 OBPs, 12 CSPs, 3 SNMPs, 6 ORs, 8 GRs, and 14 IRs. Based on the transcriptome data, we developed a tissue-specific expression profile for each of the identified chemosensory genes in *A. spiniferus*, which might reveal an initial prediction of these genes' function. Furthermore, we also analyzed the expression of 24 selected chemosensory genes across the developmental stages. In summary, this study not only provides strong background information and initial understanding on the chemosensory systems in host reception of this polyphagous insect but also provides extensive potential targets for pest control. In future, the further investigation about which gene is the key factor of plant perception and the suitable pest management target is needed to be done.

DATA AVAILABILITY STATEMENT

The datasets presented in the study are deposited in the Genbank SRA database, accession number PRJNA792195. Our data has now been released in NCBI (https://www.ncbi.nlm.nih.gov/bioproject/PRJNA792195).

AUTHOR CONTRIBUTIONS

Z-WK designed the research, analyzed transcriptome data, constructed phylogenetic trees, and wrote the manuscript. Z-WK, Y-QG, and M-YL collected sample. Y-QG, Z-ZC, and C-YS performed SEM experiment. Y-QG, Z-ZC, and F-HL conducted qPCR and analyzed qPCR results. YD, H-PZ, Y-YX, and CQ edited the manuscript. Y-YX and Z-WK revised the manuscript. All authors contributed to the article and approved the submitted version.

FUNDING

This research was funded by the Modern Tea Industry Technology System of Shandong Province (SDAIT-19-04).

ACKNOWLEDGMENTS

We sincerely thank all staff and students in the Laboratory of Insect Ecology and Physiology (Shandong Agricultural University). We also appreciate the constructive comments from the reviewers which greatly improved the quality of our paper.

SUPPLEMENTARY MATERIAL

The Supplementary Material for this article can be found online at: https://www.frontiersin.org/articles/10.3389/fphys.2022.847895/full#supplementary-material

Supplementary Figure S1 | Homology analyses results. The BLASTx annotations of *A. spiniferus* antenna transcripts. **(A)** E-value distribution. **(B)** Similarity distribution. **(C)** Species distribution.

Supplementary Figure S2 | Functional annotation of *A. spiniferus* transcripts based on gene ontology (GO) categorization.

Supplementary Figure S3 | Alignment of OBPs **(A)** and CSPs **(B)** of *A. spiniferus*.

Supplementary Table S1 | Amino acid sequences of chemosensory genes from *A. spiniferus* and other insects that used for phylogenetic analyses.

Supplementary Table S2 | Primers used in this work.

Supplementary Table S3 | Summary of *A. spiniferus* transcriptome annotation.

Supplementary Table S4 | Transmembrane domains in ORs, GRs and IRs.

REFERENCES

Agnihotri, A., Liu, N. Y., and Xu, W. (2021). Chemosensory proteins (CSPs) in the cotton bollworm *Helicoverpa armigera*. *Insects* 13:29. doi: 10.3390/insects13010029

Agnihotri, A. R., Roy, A. A., and Joshi, R. S. (2016). Gustatory receptors in Lepidoptera: chemosensation and beyond. *Insect Mol. Biol.* 25, 519–529. doi: 10.1111/imb.12246

Buck, L. B. (2004). Olfactory receptors and odor coding in mammals. *Nutr. Rev.* 62, S184–S188. doi: 10.1301/nr.2004.nov.S184-S188

Calvello, M., Brandazza, A., Navarrini, A., Dani, F. R., Turillazzi, S., Felicioli, A., et al. (2005). Expression of odorant-binding proteins and chemosensory proteins in some Hymenoptera. *Insect Biochem. Mol. Biol.* 35, 297–307. doi: 10.1016/j.ibmb.2005.01.002

Cao, H. H., Zhanga, Z. F., Wang, X. F., and Liu, T. X. (2017). Nutrition outweighs defense: *myzus persicae* (green peach aphid) prefers and performs better on young leaves of cabbage. *BioRxiv [Preprint]* doi: 10.1101/085159

Chen, W., Hasegawa, D. K., Kaur, N., Kliot, A., Pinheiro, P. V., Luan, J. B., et al. (2016). The draft genome of whitefly *Bemisia tabaci* MEAM1, a global crop pest, provides novel insights into virus transmission, host adaptation, and insecticide resistance. *BMC Biol.* 14:110. doi: 10.1186/s12915-016-0321-y

Clyne, P. J., Warr, C. G., and Carlson, J. R. (2000). Candidate taste receptors in *Drosophila*. *Science* 287, 1830–1834. doi: 10.1126/science.287.5459.1830

Cui, H. Y., Guo, L. T., Wang, S. L., Xie, W., Jiao, X., Wu, Q. J., et al. (2017). The ability to manipulate plant glucosinolates and nutrients explains the better performance of *Bemisia tabaci* Middle East-Asia Minor 1 than Mediterranean on cabbage plants. *Ecol. Evol.* 7, 6141–6150. doi: 10.1002/ece3.2921

Döring, T. F. (2014). How aphids find their host plants, and how they don't. *Ann. Appl. Biol.* 165, 3–26. doi: 10.1111/aab.12142

Dunipace, L., Meister, S., McNealy, C., and Amrein, H. (2001). Spatially restricted expression of candidate taste receptors in the *Drosophila* gustatory system. *Curr. Biol.* 11, 822–835. doi: 10.1016/S0960-9822(01)00258-5

Enjin, A., Zaharieva, E. E., Frank, D. D., Mansourian, S., Suh, G. S., Gallio, M., et al. (2016). Humidity sensing in *Drosophila*. *Curr. Biol.* 26, 1352–1358. doi: 10.1016/j.cub.2016.03.049

Fan, J., Zhang, Y., Francis, F., Cheng, D. F., Sun, J. R., and Chen, J. L. (2015). Orco mediates olfactory behaviors and winged morph differentiation induced by alarm pheromone in the grain aphid, Sitobion avenae. *Insect Biochem. Mol. Biol.* 64, 16–24. doi: 10.1016/j.ibmb.2015.07.006

Fleischer, J., Pregitzer, P., Breer, H., and Krieger, J. (2018). Access to the odor world: olfactory receptors and their role for signal transduction in insects. *Cell Mol. Life Sci.* 75, 485–508. doi: 10.1007/s00018-017-2627-5

Forêt, S., Wanner, K. W., and Maleszka, R. (2007). Chemosensory proteins in the honey bee: insights from the annotated genome, comparative analyses and expressional profiling. *Insect Biochem. Mol. Biol.* 37, 19–28. doi: 10.1016/j.ibmb.2006.09.009

Gao, Q., and Chess, A. (1999). Identification of candidate Drosophila olfactory receptors from genomic DNA sequence. *Genomics* 60, 31–39. doi: 10.1006/geno.1999.5894

Gong, D. P., Zhang, H. J., Zhao, P., Lin, Y., Xia, Q. Y., and Xiang, Z. H. (2007). Identification and expression pattern of the chemosensory protein gene family in the silkworm, *Bombyx mori*. *Insect Biochem. Mol. Biol.* 37, 266–277. doi: 10.1016/j.ibmb.2006.11.012

Gould, G., Rifleman, P., Perez, A., and Coleman, J. S. (2007). Variation in Eastern cottonwood (*Populus deltoides* Bartr.) phloem sap content caused by leaf development may affect feeding site selection behavior of the aphid, *Chaitophorous populicola* Thomas (Homoptera: aphididae). *Environ. Entomol.* 36, 1212–1225.

Gu, S. H., Wu, K. M., Guo, Y. Y., Pickett, J. A., Field, L. M., Zhou, J. J., et al. (2013). Identification of genes expressed in the sex pheromone gland of the black cutworm *Agrotis ipsilon* with putative roles in sex pheromone biosynthesis and transport. *BMC Genomics* 14:636. doi: 10.1186/1471-2164-14-636

Hallem, E. A., Dahanukar, A., and Carlson, J. R. (2006). Insect odor and taste receptors. *Annu. Rev. Entomol.* 51, 113–135. doi: 10.1146/annurev.ento.51.051705.113646

Hasanuzzaman, A. T. M., Islam, M. N., Liu, F. H., Cao, H. H., and Liu, T. X. (2018). Leaf chemical compositions of different eggplant varieties affect performance of *Bemisia tabaci* (Hemiptera: aleyrodidae) nymphs and adults. *J. Econ. Entomol.* 111, 445–453. doi: 10.1093/jee/tox333

He, P., Zhang, J., Liu, N. Y., Zhang, Y. N., Yang, K., and Dong, S. L. (2011). Distinct expression profiles and different functions of odorant binding proteins in *Nilaparvata lugens* Stal. *PLoS One* 6:e28921. doi: 10.1371/journal.pone.0028921

Hill, C. A., Fox, A. N., Pitts, R. J., Kent, L. B., Tan, P. L., Chrystal, M. A., et al. (2002). G protein coupled receptors in *Anopheles gambiae*. *Science* 298, 176–178. doi: 10.1126/science.1076196

Hu, F. Y., and Tsai, C. W. (2020). Nutritional relationship between *Bemisia tabaci* and its primary endosymbiont, *Portiera aleyrodidarum*, during host plant acclimation. *Insects* 11:498. doi: 10.3390/insects11080498

Hua, J. F., Zhang, S., Cui, J. J., Wang, D. J., Wang, C. Y., Luo, J. Y., et al. (2012). Identification and binding characterization of three odorant binding proteins and one chemosensory protein from *Apolygus lucorum* (Meyer-Dur). *J. Chem. Ecol.* 38, 1163–1170. doi: 10.1007/s10886-012-0178-7

Hua, J. F., Zhang, S., Cui, J. J., Wang, D. J., Wang, C. Y., Luo, J. Y., et al. (2013). Functional characterizations of one odorant binding protein and three chemosensory proteins from *Apolygus lucorum* (Meyer-Dur) (Hemiptera: miridae) legs. *J. Insect Physiol.* 59, 690–696. doi: 10.1016/j.jinsphys.2013.04.013

Huang, J., Hult, E. F., Marchal, E., and Tobe, S. S. (2015). Identification and characterization of the NMDA receptor and its role in regulating reproduction in the cockroach *Diploptera punctata*. *J. Exp. Biol.* 218, 983–990. doi: 10.1242/jeb.115154

Hussain, A., Zhang, M., Ucpunar, H. K., Svensson, T., Quillery, E., Gompel, N., et al. (2016). Ionotropic chemosensory receptors mediate the taste and smell of polyamines. *PLoS Biol.* 14:e1002454. doi: 10.1371/journal.pbio.1002454

Jiang, X., Pregitzer, P., Grosse-Wilde, E., Breer, H., and Krieger, J. (2016). Identification and characterization of two "Sensory Neuron Membrane Proteins" (SNMPs) of the desert locust, *Schistocerca gregaria* (Orthoptera: acrididae). *J. Insect Sci.* 16:33. doi: 10.1093/jisesa/iew015

Jones, W. D., Cayirlioglu, P., Kadow, I. G., and Vosshall, L. B. (2007). Two chemosensory receptors together mediate carbon dioxide detection in *Drosophila*. *Nature* 445, 86–90. doi: 10.1038/nature05466

Kang, Z. W., Liu, F. H., Pang, R. P., Yu, W. B., Tan, X. L., Zheng, Z. Q., et al. (2018). The identification and expression analysis of candidate chemosensory genes in the bird cherry-oat aphid *Rhopalosiphum padi* (L.). *Bull. Entomol. Res.* 108, 645–657. doi: 10.1017/S0007485317001171

Kang, Z. W., Tian, H. G., Liu, F. H., Liu, X., Jing, X. F., and Liu, T. X. (2017b). Identification and expression analysis of chemosensory receptor genes in an aphid endoparasitoid *Aphidius gifuensis*. *Sci. Rep.* 7:3939. doi: 10.1038/s41598-017-03988-z

Kang, Z. W., Liu, F. H., Tian, H. G., Zhang, M. Z., Guo, S. S., and Liu, T. X. (2017a). Evaluation of the reference genes for expression analysis using quantitative real-time polymerase chain reaction in the green peach aphid, *Myzus persicae*. *Insect Sci.* 24, 222–234. doi: 10.1111/1744-7917.12310

Kang, Z. W., Liu, F. H., Xu, Y. Y., Cheng, J. H., Lin, X. L., Jing, X. F., et al. (2020). Identification of candidate odorant-degrading enzyme genes in the antennal transcriptome of *Aphidius gifuensis*. *Entomol. Res* 51, 36–54. doi: 10.1111/1748-5967.12489

Kent, L. B., Walden, K. K. O., and Robertson, H. M. (2008). The gr family of candidate gustatory and olfactory receptors in the yellow-fever mosquito *Aedes aegypti*. *Chem. Senses* 33, 79–93. doi: 10.1093/chemse/bjm067

Knolhoff, L. M., and Heckel, D. G. (2014). Behavioral assays for studies of host plant choice and adaptation in herbivorous insects. *Annu. Rev. Entomol.* 59, 263–278. doi: 10.1146/annurev-ento-011613-161945

Kong, X., Li, Z. X., Gao, Y. Q., Liu, F. H., Chen, Z. Z., Tian, H. G., et al. (2021). Genome-wide identification of neuropeptides and their receptors in an aphid endoparasitoid wasp, *Aphidius gifuensi*. *Insects* 12:745. doi: 10.3390/insects12080745

Kumar, S., Stecher, G., Li, M., Knyaz, C., and Tamura, K. (2018). MEGA X: molecular evolutionary genetics analysis across computing platforms. *Mol. Biol. Evol.* 35, 1547–1549. doi: 10.1093/molbev/msy096

Letunic, I., and Bork, P. (2019). Interactive Tree Of Life (iTOL) v4: recent updates and new developments. *Nucleic Acids Res.* 47, W256–W259. doi: 10.1093/nar/gkz239

Li, F., Venthur, H., Wang, S., Homem, R. A., and Zhou, J. J. (2021). Evidence for the involvement of the chemosensory protein *Agoscsp5* in resistance to insecticides in the cotton aphid, *Aphis gossypii*. *Insects* 12:335. doi: 10.3390/insects12040335

Li, F. Q., Li, D., Dewer, Y., Qu, C., Yang, Z., Tian, J., et al. (2019). Discrimination of oviposition deterrent volatile β-ionone by odorant-binding proteins 1 and 4 in the whitefly *Bemisia tabaci*. *Biomolecules* 9:563. doi: 10.3390/biom9100563

Li, Z. B., Zhang, Y. Y., An, X. K., Wang, Q., Khashaveh, A., Gu, S. H., et al. (2020). Identification of leg chemosensory genes and sensilla in the *Apolygus lucorum*. *Front. Physiol.* 11:276. doi: 10.3389/fphys.2020.00276

Ling, F., Dahanukar, A., Weiss, L. A., Kwon, J. Y., and Carlson, J. R. (2014). The molecular and cellular basis of taste coding in the legs of *Drosophila*. *J. Neurosci.* 34, 7148–7164. doi: 10.1523/JNEUROSCI.0649-14.2014

Liu, F. H., Wickham, J. D., Cao, Q. J., Lu, M., and Sun, J. H. (2020). An invasive beetle–fungus complex is maintained by fungal nutritional-compensation mediated by bacterial volatiles. *ISME J.* 14, 1–14. doi: 10.1038/s41396-020-00740-w

Liu, J. B., Liu, H., Yi, J. Q., Mao, Y. K., Li, J., Sun, D. L., et al. (2021). Transcriptome characterization and expression analysis of chemosensory genes in *Chilo sacchariphagus* (Lepidoptera Crambidae), a key pest of sugarcane. *Front. Physiol.* 12:636353. doi: 10.3389/fphys.2021.636353

Liu, Y. L., Guo, H., Huang, L. Q., Pelosi, P., and Wang, C. Z. (2014). Unique function of a chemosensory protein in the proboscis of two *Helicoverpa* species. *J. Exp. Biol.* 217, 1821–1826. doi: 10.1242/jeb.102020

Livak, K. J., and Schmittgen, T. D. (2001). Analysis of relative gene expression data using real-time quantitative PCR and the $2^{-\Delta\Delta CT}$ method. *Methods* 25, 402–408. doi: 10.1006/meth.2001.1262

Ma, C., Cui, S., Tian, Z., Zhang, Y., Chen, G., Gao, X., et al. (2019). *OcomCSP12*, a chemosensory protein expressed specifically by ovary, mediates reproduction in *Ophraella communa* (Coleoptera: chrysomelidae). *Front. Physiol.* 10:1290. doi: 10.3389/fphys.2019.01290

Mckenna, M. P., Hekmatscafe, D. S., Gaines, P., and Carlson, J. R. (1994). Putative *Drosophila* pheromone-binding proteins expressed in a subregion of the olfactory system. *J. Biol. Chem.* 269, 16340–16347. doi: 10.1016/S0021-9258(17)34013-9

Mei, T., Fu, W. B., Li, B., He, Z. B., and Chen, B. (2018). Comparative genomics of chemosensory protein genes (CSPs) in twenty-two mosquito species (Diptera: culicidae): identification, characterization, and evolution. *PLoS One* 13:e0190412. doi: 10.1371/journal.pone.0190412

Mokrane, S., Cavallo, G., Tortorici, F., Romero, E., Fereres, A., Djelouah, K., et al. (2020). Behavioral effects induced by organic insecticides can be exploited for a sustainable control of the orange spiny whitefly *Aleurocanthus spiniferus*. *Sci. Rep.* 10:15746. doi: 10.1038/s41598-020-72972-x

Nomura, A., Kawasaki, K., Kubo, T., and Natori, S. (1992). Purification and localization of p10, a novel protein that increases in nymphal regenerating Legs of *Periplaneta americana* (American Cockroach). *Int. J. Dev. Biol.* 36, 391–398.

Nugnes, F., Laudonia, S., Jesu, G., Jansen, M. G. M., Bernardo, U., and Porcelli, F. (2020). *Aleurocanthus spiniferus* (Hemiptera: aleyrodidae) in some european countries: diffusion, hosts, molecular characterization, and natural enemies. *Insects* 11:42. doi: 10.3390/insects11010042

Pelosi, P., Iovinella, I., Zhu, J., Wang, G. R., and Dani, F. R. (2017). Beyond chemoreception: diverse tasks of soluble olfactory proteins in insects. *Biol. Rev.* 93, 184–200. doi: 10.1111/brv.12339

Pelosi, P., Zhou, J. J., Ban, L. P., and Calvello, M. (2006). Soluble proteins in insect chemical communication. *Cell Mol. Life Sci.* 63, 1658–1676. doi: 10.1007/s00018-005-5607-0

Picimbon, J. F., Dietrich, K., Breer, H., and Krieger, J. (2000). Chemosensory proteins of Locusta migratoria (Orthoptera: acrididae). *Insect Biochem. Mol. Biol.* 30, 233–241. doi: 10.1016/S0965-1748(99)00121-6

Picimbon, J. F., Dietrich, K., Krieger, J., and Breer, H. (2001). Identity and expression pattern of chemosensory proteins in *Heliothis virescens* (Lepidoptera, Noctuidae). *Insect Biochem. Mol. Biol.* 31, 1173–1181. doi: 10.1016/S0965-1748(01)00063-7

Qiao, H., Tuccori, E., He, X., Gazzano, A., Field, L., Zhou, J. J., et al. (2009). Discrimination of alarm pheromone (E)-β-farnesene by aphid odorant-binding proteins. *Insect Biochem. Mol. Biol.* 39, 414–419. doi: 10.1016/j.ibmb.2009.03.004

Radonjić, S., and Hrnčić, S. (2021). Spreading of *Aleurocanthus spiniferus* (Quaintance) (Hemiptera: aleyrodidae) in coastal area of Montenegro. *Acta Hortic.* 1308, 311–318. doi: 10.17660/ActaHortic.2021.1308.44

Raji, J. I., Gonzalez, S., and DeGennaro, M. (2019a). *Aedes aegypti* Ir8a mutant female mosquitoes show increased attraction to standing water. *Commun. Integr. Biol.* 12, 181–186. doi: 10.1080/19420889.2019.1681063

Raji, J. I., Melo, N., Castillo, J. S., Gonzalez, S., Saldana, V., Stensmyr, M. C., et al. (2019b). *Aedes aegypti* mosquitoes detect acidic volatiles found in human odor using the IR8a pathway. *Curr. Biol.* 29, 1253.e1257–1262.e1257. doi: 10.1016/j.cub.2019.02.045

Richards, S., Gibbs, R. A., Weinstock, G. M., Brown, S. J., Denell, R., Beeman, R. W., et al. (2008). The genome of the model beetle and pest *Tribolium castaneum*. *Nature* 452, 949–955. doi: 10.5167/uzh-2931

Robertson, H. M., Warr, C. G., and Carlson, J. R. (2003). Molecular evolution of the insect chemoreceptor gene superfamily in *Drosophila melanogaster*. *Proc. Natl. Acad. Sci. U.S.A.* 100, 14537–14542. doi: 10.1073/pnas.2335847100

Sato, K., Tanaka, K., and Touhara, K. (2011). Sugar-regulated cation channel formed by an insect gustatory receptor. *Proc. Natl. Acad. Sci. U.S.A.* 108, 11680–11685. doi: 10.1073/pnas.1019622108

Scott, K., Brady, R., Cravchik, A., Morozov, P., Rzhetsky, A., Zuker, C., et al. (2001). chemosensory gene family encoding candidate gustatory and olfactory receptors in *Drosophila*. *Cell* 104, 661–673. doi: 10.1016/S0092-8674(01)00263-X

Shi, X. B., Wang, X. Z., Zhang, D. Y., Zhang, Z. H., Zhang, Z., Cheng, J., et al. (2019). Silencing of odorant-binding protein gene OBP3 using RNA interference reduced virus transmission of tomato chlorosis virus. *Int. J. Mol. Sci.* 20:4969. doi: 10.3390/ijms20204969

Sun, D. D., Huang, Y., Qin, Z. J., Zhan, H. X., Zhang, J. P., Liu, Y., et al. (2020). Identification of candidate olfactory genes in the antennal transcriptome of the stink bug *Halyomorpha halys*. *Front. Physiol.* 11:876. doi: 10.3389/fphys.2020.00876

Sun, L., Li, Y., Zhang, Z., Guo, H., Xiao, Q., Wang, Q., et al. (2019). Expression patterns and ligand binding characterization of Plus-C odorant-binding protein 14 from *Adelphocoris lineolatus* (Goeze). *Comp. Biochem. Physiol. B* 227, 75–82. doi: 10.1016/j.cbpb.2018.10.001

Tang, X. T., Tao, H. H., and Du, Y. Z. (2015). Microsatellite-based analysis of the genetic structure and diversity of *Aleurocanthus spiniferus* (Hemiptera: aleyrodidae) from tea plants in China. *Gene* 560, 107–113. doi: 10.1016/j.gene.2015.01.050

Tian, J. H., Zhan, H. X., Dewer, Y., Zhang, B. Y., Qu, C., Luo, C., et al. (2021). Whitefly network analysis reveals gene modules involved in host plant selection, development and evolution. *Front. Physiol.* 12:656649. doi: 10.3389/fphys.2021.656649

Tian, Y. Y., Chen, Z. J., Huang, X. Q., Zhang, L. X., and Zhang, Z. Q. (2020). Evaluation of botanicals for management of piercing-sucking pests and the effect on beneficial arthropod populations in tea trees *Camellia sinensis* (L.) O. Kuntze (Theaceae). *J. Insect Sci.* 20:27. doi: 10.1093/jisesa/ieaa101

Wang, R., Hu, Y., Wei, P., Qu, C., and Luo, C. (2020). Molecular and functional characterization of one odorant-binding protein gene OBP3 in *Bemisia tabaci* (Hemiptera: aleyrodidae). *J. Econ. Entomol.* 113, 299–305. doi: 10.1093/jee/toz248

Wang, R., Li, F. Q., Zhang, W., Zhang, X. M., Qu, C., Tetreau, G., et al. (2017). Identification and expression profile analysis of odorant binding protein and chemosensory protein genes in *Bemisia tabaci* MED by head transcriptome. *PLoS One* 12:e0171739. doi: 10.1371/journal.pone.0171739

Wanner, K. W., and Robertson, H. M. (2008). The gustatory receptor family in the silkworm moth *Bombyx mori* is characterized by a large expansion of a single lineage of putative bitter receptors. *Insect Mol. Biol.* 17, 621–629. doi: 10.1111/j.1365-2583.2008.00836.x

Waris, M. I., Younas, A., Ui Qamar, M. T., Hao, L., Ameen, A., Ali, S., et al. (2018). Silencing of chemosensory protein gene NlugCSP8 by RNAi induces declining behavioral responses of *Nilaparvata lugens*. *Front. Physiol.* 9:379. doi: 10.3389/fphys.2018.00379

Wu, Q., Li, C. X., Liu, Q. M., Guo, X. X., Shi, Q. M., Zhang, H. D., et al. (2020). RNA interference of odorant receptor CquiOR114/117 affects blood-feeding behavior in *Culex quinquefasciatus*. *Acta Trop.* 204:105343. doi: 10.1016/j.actatropica.2020.105343

Xia, J. X., Guo, Z. J., Yang, Z. Z., Han, H. L., Wang, S. L., Xu, H. F., et al. (2021). Whitefly hijacks a plant detoxification gene that neutralizes plant toxins. *Cell* 184, 1693.e1617–1705.e1617. doi: 10.1016/j.cell.2021.02.014

Xia, S., Miyashita, T., Fu, T. F., Lin, W. Y., Wu, C. L., Pyzocha, L., et al. (2005). NMDA receptors mediate olfactory learning and memory in *Drosophila*. *Curr. Biol.* 15, 603–615. doi: 10.1016/j.cub.2005.02.059

Xie, W., Chen, C. H., Yang, Z. Z., Guo, L. T., Yang, X., Wang, D., et al. (2017). Genome sequencing of the sweetpotato whitefly *Bemisia tabaci* MED/Q. *Gigascience* 6, 1–7. doi: 10.1093/gigascience/gix018

Xu, W., Papanicolaou, A., Zhang, H. J., and Anderson, A. (2016). Expansion of a bitter taste receptor family in a polyphagous insect herbivore. *Sci. Rep.* 6:23666. doi: 10.1038/srep23666

Yang, J., Guo, H., Jiang, N. J., Tang, R., Li, G. C., Huang, L. Q., et al. (2021). Identification of a gustatory receptor tuned to sinigrin in the cabbage butterfly *Pieris rapae*. *PLoS Genet.* 17:e1009527. doi: 10.1371/journal.pgen.1009527

Yang, K., Gong, X. L., Li, G. C., Huang, L. Q., Ning, C., and Wang, C. Z. (2020). A gustatory receptor tuned to the steroid plant hormone brassinolide in *Plutella xylostella* (Lepidoptera: plutellidae). *eLife* 9:e64114. doi: 10.7554/eLife.64114

Yang, K., He, P., and Dong, S. L. (2014). Different expression profiles suggest functional differentiation among chemosensory proteins in *Nilaparvata lugens* (Hemiptera: delphacidae). *J. Insect Sci.* 14:270. doi: 10.1093/jisesa/ieu132

Zeng, Y., Merchant, A., Wu, Q. J., Wang, S. L., Kong, L., Zhou, X. G., et al. (2020). A chemosensory protein BtabCSP11 mediates reproduction in *Bemisia tabaci*. *Front. Physiol.* 11:709. doi: 10.3389/fphys.2020.00709

Zeng, Y., Yang, Y. T., Wu, Q. J., Wang, S. L., Xie, W., and Zhang, Y. J. (2019). Genome-wide analysis of odorant-binding proteins and chemosensory proteins in the sweet potato whitefly, *Bemisia tabaci*. *Insect Sci.* 26, 620–634. doi: 10.1111/1744-7917.12576

Zhang, H. J., Xu, W., Chen, Q. M., Sun, L. N., Anderson, A., Xia, Q. Y., et al. (2018). Functional characterization of sensory neuron membrane proteins (SNMPs). *bioRxiv [Preprint]* doi: 10.1101/262154

Zhang, R. B., Liu, Y., Yan, S. C., and Wang, G. R. (2019). Identification and functional characterization of an odorant receptor in pea aphid, *Acyrthosiphon pisum*. *Insect Sci.* 26, 58–67. doi: 10.1111/1744-7917.12510

Zhang, Y., Shen, C., Xia, D. S., Wang, J., and Tang, Q. F. (2019). Characterization of the expression and functions of two odorant-binding proteins of *Sitophilus zeamais* Motschulsky (Coleoptera: curculionoidea). *Insects* 10:409. doi: 10.3390/insects10110409

Zhang, Z. J., Zhang, S. S., Niu, B. L., Ji, D. F., Liu, X. J., Li, M. W., et al. (2019). A determining factor for insect feeding preference in the silkworm, *Bombyx mori*. *PLoS Biol.* 17:e3000162. doi: 10.1371/journal.pbio.3000162

Zhang, R. B., Wang, B., Grossi, G., Falabella, P., Liu, Y., Yan, S. C., et al. (2017). Molecular basis of alarm pheromone detection in aphids. *Curr. Biol.* 27, 55–61. doi: 10.1016/j.cub.2016.10.013

Zhang, X. M., Wang, S., Li, S., Luo, C., Li, Y. X., and Zhang, F. (2015). Comparison of the antennal sensilla ultrastructure of two cryptic species in *Bemisia tabaci*. *PLoS One* 10:e0121820. doi: 10.1371/journal.pone.0121820

Zhang, X. X., Yang, B., Sun, D. D., Guo, M. B., Zhang, J., and Wang, G. R. (2021). Ionotropic receptor 8a is involved in the attraction of *Helicoverpa armigera* to acetic acid. *Insect Sci. [Online ahead of print]* doi: 10.1111/1744-7917.12962

Zhong, T., Yin, J., Deng, S., Li, K., and Cao, Y. (2012). Fluorescence competition assay for the assessment of green leaf volatiles and trans-beta-farnesene bound to three odorant-binding proteins in the wheat aphid *Sitobion avenae* (Fabricius). *J. Insect Physiol.* 58, 771–781. doi: 10.1016/j.jinsphys.2012.01.011

Zhu, J., Iovinella, I., Dani, F. R., Liu, Y. L., Huang, L. Q., Liu, Y., et al. (2016). Conserved chemosensory proteins in the proboscis and eyes of *Lepidoptera*. *Int. J. Biol. Sci.* 12, 1394–1404. doi: 10.7150/ijbs.16517

Conflict of Interest: The authors declare that the research was conducted in the absence of any commercial or financial relationships that could be construed as a potential conflict of interest.

Publisher's Note: All claims expressed in this article are solely those of the authors and do not necessarily represent those of their affiliated organizations, or those of the publisher, the editors and the reviewers. Any product that may be evaluated in this article, or claim that may be made by its manufacturer, is not guaranteed or endorsed by the publisher.

Copyright © 2022 Gao, Chen, Liu, Song, Jia, Liu, Qu, Dewer, Zhao, Xu and Kang. This is an open-access article distributed under the terms of the Creative Commons Attribution License (CC BY). The use, distribution or reproduction in other forums is permitted, provided the original author(s) and the copyright owner(s) are credited and that the original publication in this journal is cited, in accordance with accepted academic practice. No use, distribution or reproduction is permitted which does not comply with these terms.

frontiers in Neuroanatomy

ORIGINAL RESEARCH
published: 10 March 2022
doi: 10.3389/fnana.2022.844171

Serotonergic Neurons in the Brain and Gnathal Ganglion of Larval *Spodoptera frugiperda*

Jia-Jia Zhang†, Long-Long Sun†, Ya-Nan Wang, Gui-Ying Xie, Shi-Heng An, Wen-Bo Chen, Qing-Bo Tang* and Xin-Cheng Zhao*

Henan International Joint Laboratory of Green Pest Control, College of Plant Protection, Henan Agricultural University, Zhengzhou, China

The fall armyworm *Spodoptera frugiperda* (*S. frugiperda*) (Lepidoptera: Noctuidae) is a worldwide, disruptive, agricultural pest species. The larvae of *S. frugiperda* feed on seedling, leave, and kernel of crops with chewing mouthparts, resulting in reduced crop yields. Serotonin is an important biogenic amine acting as a neural circuit modulator known to mediate lots of behaviors including feeding in insects. In order to explore the serotonergic neural network in the nervous system of larval *S. frugiperda*, we performed immunohistochemical experiments to examine the neuropil structure of the brain and the gnathal ganglion with antisynapsin and to examine their serotonergic neurons with antiserotonin serum. Our data show that the brain of larval *S. frugiperda* contains three neuromeres: the tritocerebrum, the deutocerebrum, and the protocerebrum. The gnathal ganglion also contains three neuromeres: the mandibular neuromere, the maxillary neuromere, and the labial neuromere. There are about 40 serotonergic neurons in the brain and about 24 serotonergic neurons in the gnathal ganglion. Most of these neurons are wide-field neurons giving off processes in several neuropils of the brain and the gnathal ganglion. Serotonergic neuron processes are mainly present in the protocerebrum. A pair of serotonergic neurons associated with the deutocerebrum has arborizations in the contralateral antennal lobe and bilateral superior lateral protocerebra. In the gnathal ganglion, the serotonergic neuron processes are also widespread throughout the neuropil and some process projections extend to the tritocerebrum. These findings on the serotonergic neuron network in larval *S. frugiperda* allow us to explore the important roles of serotonin in feeding and find a potential approach to modulate the feeding behavior of the gluttonous pest and reduce its damage.

Keywords: brain, gnathal ganglion, immunoreactivity, neuropils, serotonin, *Spodoptera frugiperda*, taste

OPEN ACCESS

Edited by:
Jean-Pierre Hornung, University of Lausanne, Switzerland

Reviewed by:
Shigehiro Namiki, The University of Tokyo, Japan
David Krantz, University of California, Los Angeles, United States
Elizabeth Knapp, University of California, Los Angeles, United States, contributed to the review of DK

****Correspondence:***
Wen-Bo Chen
wenbochen@henau.edu.cn
Qing-Bo Tang
qingbotang@126.com

† These authors have contributed equally to this work

Received: *27 December 2021*
Accepted: *31 January 2022*
Published: *10 March 2022*

Citation:
Zhang J-J, Sun L-L, Wang Y-N, Xie G-Y, An S-H, Chen W-B, Tang Q-B and Zhao X-C (2022) Serotonergic Neurons in the Brain and Gnathal Ganglion of Larval Spodoptera frugiperda. Front. Neuroanat. 16:844171. doi: 10.3389/fnana.2022.844171

INTRODUCTION

The fall armyworm (FAW) *Spodoptera frugiperda* (*S. frugiperda*) (Lepidoptera: Noctuidae) is a disruptive agricultural pest species and shows a high potential to cause crop yield loss due to its polyphagy, gluttony, high mobility, and high reproductivity. FAW can feed on more than 80 crops, including maize, wheat, sorghum, millet, sugarcane, vegetable crops, and cotton (Montezano et al., 2018). Larvae of FAW can feed on seedlings, leaves, developing tassel, and kernel with chewing

mouthparts, which could reduce the photosynthetic area, grain quality, and ultimately reduce the yield. FAW is native to the Americas, but has now spread globally. In China, FAW was first found in southeast of Yunnan Province in 2019 and rapidly spreads through eastern China (Wu et al., 2019, 2021). Once this pest species is established in a country or area, it may not be possible to eradicate it because of its high adaptation. It is necessary to develop the strategies for the sustainable control of *S. frugiperda* by exploring any potential target at the levels of molecule, physiology, and behavior.

Serotonin [5-hydroxytryptamine (5-HT)] is a biogenic amine, acting as neurotransimitter, neuromodulator, or neurohormone in a wide range of organisms, including insects (Nässel, 1988; Vleugels et al., 2015). The immunohistochemical experiments with serotonin antiserum showed that serotonergic neurons of insect species are limited in number, but the project processes were widely distributed in both the peripheral and the central nervous system (Klemm et al., 1984; Lange et al., 1988; Nässel, 1988; Homberg and Hildebrand, 1989a,b; Breidbach, 1990; Boleli and Paulino-Simões, 1999; Leitinger et al., 1999; Settembrini and Villar, 2004; Dacks et al., 2006; Liu et al., 2011; Huser et al., 2012; van der Woude and Smid, 2017; Tang et al., 2019; Tierney, 2020). The widespread serotonergic neurons are involved in multiple effects in a variety of behaviors and physiological activities, including vision, olfaction, audition, feeding, flight, aggregation, aggression, sleep, learning and memory, circadian rhythms, immunity, stress, metabolism, growth, and reproduction (Kloppenburg and Mercer, 2008; Anstey et al., 2009; Qi et al., 2014, 2016; Tang et al., 2019; Tierney, 2020).

Particularly, the modulation of serotonin on feeding-related processes has been intensively studied in several insect species, including locust, aphid (Kaufmann et al., 2004), bugs (Orchard, 2006), bees (French et al., 2014), mosquitoes (Novak and Rowley, 1994), and flies (Haselton et al., 2009; Albin et al., 2015; Schoofs et al., 2018; Lyu et al., 2021). The serotonergic modulation is involved in feeding states, e.g., hunger and satiety and in a sequence of discrete events of feeding, such as, food detection, salivary secretion, food intake, and ingestion of food (Tierney, 2020). Elevated serotonin inhibited the proboscis extension, decreased feeding time, and reduced sucrose consumption in cockroach, honeybees, ants, mosquitoes, blow fly, and fresh fly (Cohen, 2001; Dacks et al., 2003; Haselton et al., 2009; Falibene et al., 2012; French et al., 2014; Kinney et al., 2014). Injected serotonin showed synergistic suppression of pymetrozine, an insecticide for aphid and locust (Kaufmann et al., 2004). These reports supported the association between serotonin and satiety. In some experiments, however, serotonin was also found to be associated with hunger. Activation of a subset of serotonergic neurons in the brain of *Drosophila* could increase food intake (Albin et al., 2015). Depletion of serotonin in bug *Rhodnius prolixus* and mosquito *Aedes triseriatus* suppressed blood intake (Cook and Orchard, 1990; Novak and Rowley, 1994).

Recently, measurements of high-performance liquid chromatography showed that serotonin is present in the brain and the digestive tract of larval *S. frugiperda* (Oyarzabal-Armendariz et al., 2021). After fed with azadirachtin, the amount of serotonin increased in the larval *S. frugiperda* brain, but decreased in the intestine. The increased serotonin could alter activities in memory, learning, sleep, and locomotor, while the decreased serotonin reduce the peristalsis movements (Oyarzabal-Armendariz et al., 2021). Therefore, the antifeedant and repellent effects of azadirachtin on *S. frugiperda* might be mediated by serotonin signal (Lin et al., 2021; Oyarzabal-Armendariz et al., 2021). Here, we performed immunohistochemistry with antiserotonin serum to examine the distribution of serotonergic neurons in the central nervous system of larval *S. frugiperda*. We provide the first comprehensive description of the serotonergic neuronal network in *S. frugiperda* larvae, which is essential for understanding the neural mechanism of feeding-related modulation.

MATERIALS AND METHODS

Insects

Larval *S. frugiperda* was reared on an artificial diet (wheat bran 40 g, yeast powder 34 g, casein 25 g, sorbic acid 2 g, corn meal 100 g, vitamin composite powders 4 g, methylparaben 4 g, agar 18 g, and distilled water 900 ml) in the laboratory under 16/8 light/dark, at 27 ± 1°C and 75% relative humidity. Larvae at the second day of 5th instar were used for the immunohistochemistry experiments. Adults were fed on a 10% sucrose solution.

Immunohistochemistry for Synapsin and Serotonin

In order to examine the distribution of serotonin-immunoreactive neurons in the brain and the gnathal ganglion, immunohistochemistry with the antisynapsin for labeling the neuropil structure and antiserotonin for labeling the serotonergic neurons was performed. The detailed procedures were described in previous studies (Zhao et al., 2016; Tang et al., 2019). The preparations were dissected. The brain and the gnathal ganglion were isolated from the insect body in Ringer's solution (150 mM NaCl, 3 mM $CaCl_2$, 3 mM KCl, 25 mM sucrose, and 10 mM N-tris(hydroxymethyl)methyl-2-aminoethanesulfonic acid, pH 6.9) and fixed in 4% paraformaldehyde (PFA) solution (4% PFA in 0.1 M phosphate buffer) for 2–4 h at room temperature. Followed the rinse with phosphate-buffered saline (PBS) (684 mM NaCl, 13 mM KCl, 50.7 mM Na_2HPO_4, and 5 mM KH_2PO_4, pH 7.4) for 6 times, each time 10 min, the brain and the gnathal ganglion were preincubated in 10% normal goat serum (NGS) (Sigma Aldrich, St Louis, Mosby, United States) in PBS containing 0.5% Triton X-100 (PBST) for 3 h at room temperature to minimize the non-specific staining. Next, the brain and the gnathal ganglion were incubated in the primary antibodies, anti-SYNORF1 (1:100, Developmental Studies Hybridoma Bank, University of Iowa, Iowa City, Iowa, United States) and antiserotonin serum (1:4,000, Immunostar Incorporation, Hudson, Wisconsin, United States), in PBST containing 5% NGS for 5 days at 4°C. After that, the samples were rinsed with PBS for 6 × 20 min and then incubated in the secondary antibodies, Alexa Fluor 488 conjugated goat antimouse (1:400, Invitrogen, Eugene, Oregon, United States) and Alexa Fluor

633 conjugated goat antirabbit (1:400, Invitrogen, Eugene, Oregon, United States) in PBST containing 5% NGS for 3 days at 4°C. Finally, the samples were rinsed 6 × 20 min with PBS, dehydrated in a series ethanol (50, 70, 90, and 96% and 2 × 100%, 10 min each time), cleared in methyl salicylate, and mounted in Permount.

Image Data Acquisition and Analysis

All the images were obtained by laser scanning confocal microscope (Nikon A1, Japan) with 10X/2.2 air objective. Fluorescent dyes of Alexa Fluor 488 and Alexa Fluor 633 were excited by a 488-nm Argon laser and a 633-nm HeNe laser, respectively. The resolution of image is 1,024 × 1,024 and the interval is 2–3 μm. The value of high voltage (HV) is set at 35–50 and the laser intensity and other parameters are adjusted during scanning.

Confocal image data format was converted into tag image file format by Image J software [version 1.53f51, National Institutes of Health (NIH), United States]. Software of Amira version 5.3 (Visage Imaging, Fürth, Germany) was then used to analyze the image stacks. Neuropil structures and nerves were reconstructed by using the tool of LabelField of Amira and serotonin-immunoreactive neurons were reconstructed by using the module of SkeletonTree. Volumes of neuropils and cell bodies were measured by using the tool of TissueStatistics. Adobe Photoshop was used to adjust color, brightness, and contrast of confocal image when necessary and the image panels were edited by Adobe Illustrator 2021 (Adobe System, San Jose, California, United States). ANOVA and the bar chart of the average diameter and volume of cell bodies were performed by using GraphPad Prism version 9.0 (GraphPad Software Incorporation, San Diego, California, United States). The nomenclature of neuroanatomical structures, serotonin-immunoreactive neurons, and abbreviations suggested by Ito et al. (2014) and Tang et al. (2019) were used for larval *S. frugiperda*.

RESULTS

In total, we performed immunohistochemical staining with anti-SYNORF1 and antiserotonin serum on 30 preparations, of which 14 preparations were stained successfully, 10 preparations were stained weakly, and six preparations were unstained. Four brains and five gnathal ganglia were used for examining the neuroanatomical structures and the distribution of serotonergic neurons.

Anatomy of Larval *Spodoptera frugiperda* Brain

The immunoreactivity of anti-SYNORF1 revealed the synapsin-enriched neuropil and that of antiserotonin revealed cell bodies and cell fibers of serotonergic neurons in the brain (**Figures 1A1–A5**, merged; B1-B5, anti-SYNORF1; C1-C5, antiserotonin). The brain of larval *S. frugiperda* contained three main neuromeres: the protocerebrum (PR), the deutocerebrum (DE), and the tritocerebrum (TR). Based upon the intensity of immunoreactivity, several prominent neuropils in the PR could be identified (**Figures 1B1–B5**). Three-dimensional reconstructions of the neuropils were also created and then their volumes and relative volumes to those of the whole brain were measured (**Figure 2**). The alpha lobe (α) was located anteriorly and pointed vertically to the dorsal surface and the beta lobe (β) was located medially and pointed horizontally to the middle line of the PR (**Figures 1B1,B2**, **2A**). The pedunculus (PED) lay in the middle of each hemisphere, forming the lobe (LOB) of mushroom body together with the α and β lobes (**Figures 1B3,B4**, **2A**). Volume of LOB is 25.44×10^4 μm^3, about 4.55% of the whole-brain neuropil (**Figures 2B,C**). The calyx (CA) was located posteriorly in the PR (**Figures 1B3,B4**, **2A**). Volume of CA is 34.54×10^4 μm^3, about 6.17% of the whole-brain neuropil (**Figures 2B,C**). The central body (CB), an unpaired neuropil, was located horizontally in the center of the PR, crossed the midline, and linked both the hemispheres (**Figures 1B3**, **2A**). Volume of CB is 2.34×10^4 μm^3, about 0.41% of the whole-brain neuropil (**Figures 2B,C**). The lateral accessory lobe (LAL) was also visible, located laterally to the mushroom body lobes (**Figures 1B3**, **2A**). Volume of LAL is 13.84×10^4 μm^3, about 2.47% of the whole-brain neuropil (**Figures 2B,C**). The protocerebral bridge (PB) was located posteriorly, on either side of middle line of the PR (**Figures 1B4**, **2A**). Volume of PB is 1.53×10^4 μm^3, about 0.27% of the whole-brain neuropil (**Figures 2B,C**). The optical lobe (OL) was located on most lateral side of the PR (**Figures 1B5**, **2A**). Volume of OL is 18.60×10^4 μm^3, about 3.33% of the whole-brain neuropil (**Figures 2B,C**). In addition to these prominent neuropils mentioned above, the PR also contained a large neuropil, referred as midbrain (MBr), which has homogeneous intensity of immunoreactivity without obvious boundaries. Volume of MBr is 397.28×10^4 μm^3, about 70.57% of the whole-brain neuropil (**Figures 2B,C**). The antennal lobe (AL), a spherical structure of the DE, was located most anteriorly of the brain (**Figures 1B1**, **2A**). The volume of AL is 14.38×10^4 μm^3, about 2.57% of the whole-brain neuropil (**Figures 2B,C**). The TR was located most ventral of the brain, at the root of circumesophageal connective, which linked the brain and the gnathal ganglion (**Figures 1B1–B3**, **2A**). Volume of the TR is 54.74×10^4 μm^3, about 9.72% of the whole-brain neuropil (**Figures 2B,C**).

Serotonergic Neurons in the Brain of Larval *Spodoptera frugiperda*

The serotonergic neurons revealed by the immunoreactivity to antiserotonin serum had their cell bodies in the cell body layer and neural fibers projected in wide regions of the neuropils and crossed the midline forming six commissures linking both the hemispheres (**Figures 1C1–C5**). All the identified cell bodies were counted and their diameters and volumes were measured (**Figures 2D–F**). There are about 40 serotonergic neurons in the brain (**Table 1**). The cell body cluster of PR-M was located in the medial region of the posterior PR and contained 18 cell bodies, nine in each hemisphere. Diameters of these cell bodies are in the range of 12.19–16.66 μm and volumes are in the range of 407–1,531 μm^3. Serotonergic neurons of PR-M were bilateral and extended widespread projection to the neuropils of the both hemisphere protocerebra via the commissures

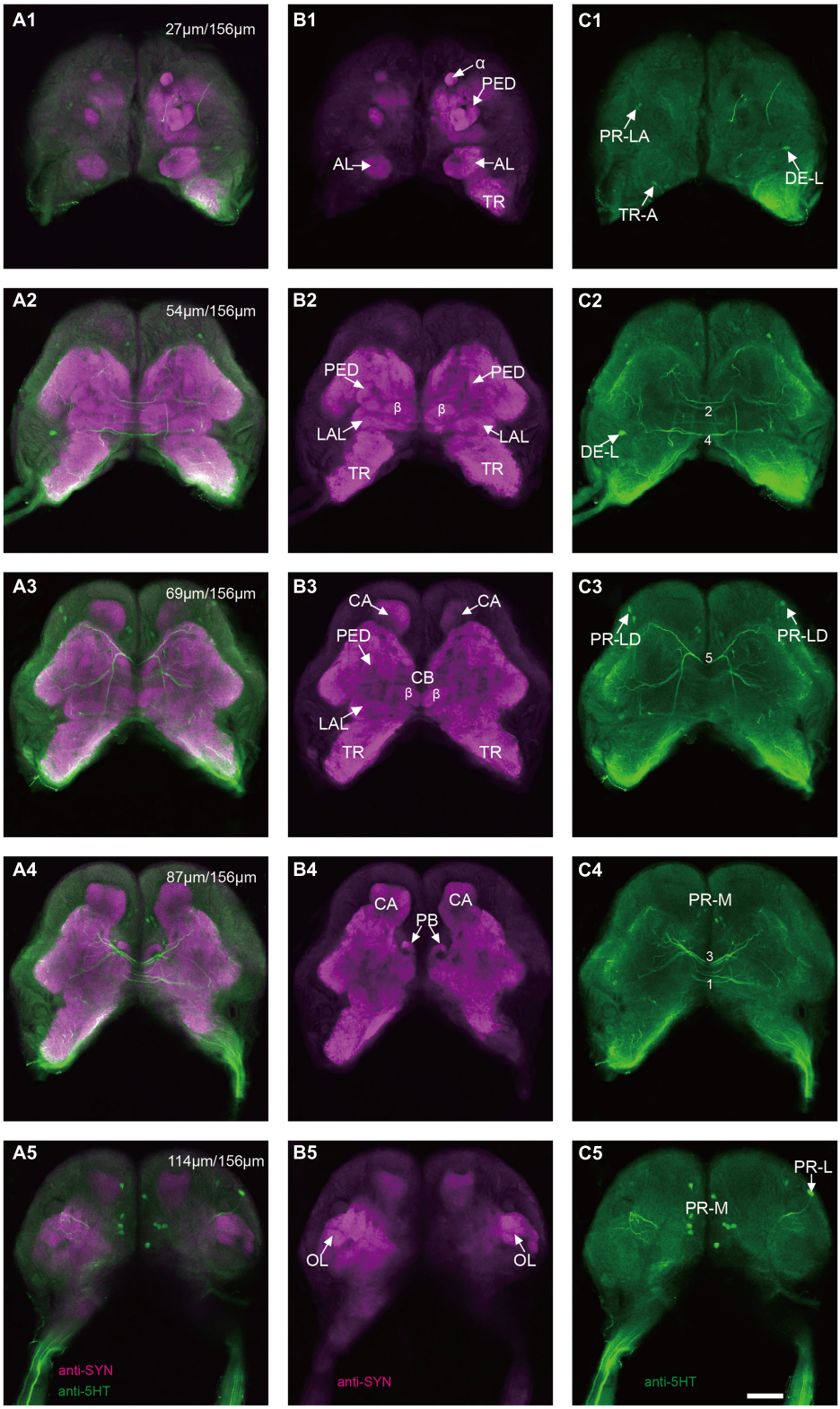

FIGURE 1 | Confocal images of the brain of *Spodoptera frugiperda* larvae. **(A1–A5)** Merged confocal image showing the neuropil (magenta) and the serotonin-immunoreactive neurons (green). **(B1–B5)** Confocal image showing the neuropils of the brain. **(C1–C5)** Confocal image showing the serotonin-immunoreactive neurons in the brain. α, alpha lobe; AL, antennal lobe; CA, calyx; CB, central body; LAL, lateral accessory lobe; OL, optic lobe; PB,: protocerebral bridge; PED, pedunculus; TR, tritocerebrum. Scale bars, 100 μm.

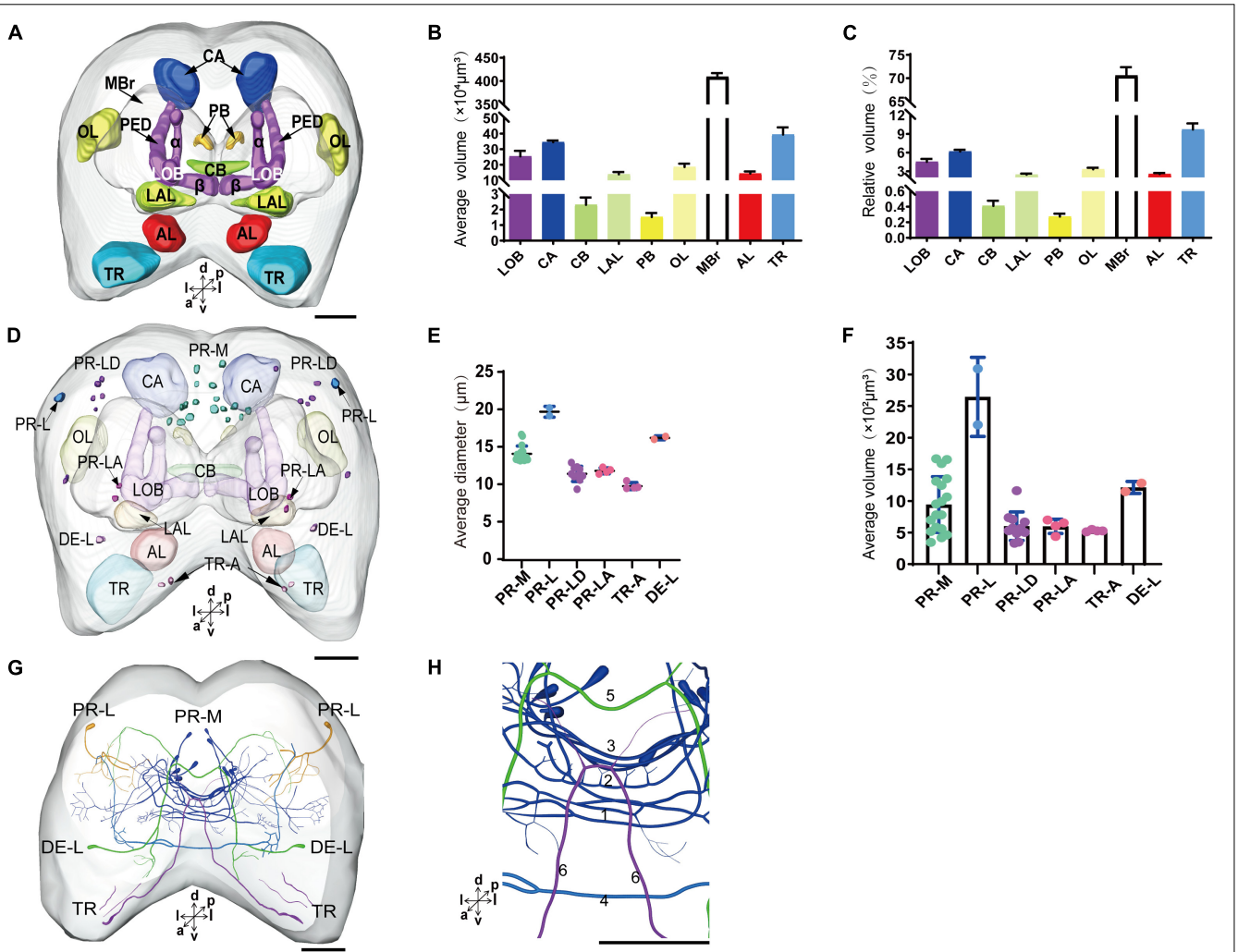

FIGURE 2 | The average and relative volume of the neuropils, the average diameter and volume of cell bodies, and the distribution of the serotonergic neuronal processes and cell bodies in the brain. **(A)** Three-dimensional reconstructions of the neuropils in the brain in frontal view. **(B,C)** The average and relative volume of the neuropils. **(D)** Reconstructions of cell bodies in the brain. **(E,F)** The average diameter and volume of cell bodies in the brain. **(G)** Reconstructed skeleton trees of the thick neuronal processes showing their projection patterns in anterior view. **(H)** Reconstructed skeleton trees of commissures 1–6 in anterior view. PR-M, PR-L, PR-LD, PR-LA, DE-L, and TR-A are cell clusters. α, alpha lobe; AL, antennal lobe; β, belta lobe; CA, calyx; CB, central body; LAL, lateral accessory lobe; LOB, mushroom body lobes; OL, optic lobe; PB, protocerebral bridge; TR, tritocerebrum. Directions: a, anterior; d, dorsal; l, lateral; m, medial; p, posterior; v, ventral. Scale bar, 100 μm.

1–3 (**Figures 2G,H**, **3**). Innervation regions of their terminals include posterior optic tubercle (POTU), anterior ventrolateral protocerebrum (AVLP), superior intermediate protocerebrum (SIP), superior medial protocerebrum (SMP), inferior medial protocerebrum (IMP), and CB (**Figure 3**). However, the neuropils of PB, CA, PED, α and β lobes, and lateral horn lack serotonergic neuron processes.

The cell body of PR-L was located in the lateral region of the lateral PR, only one in each hemisphere (**Figure 2D**). Diameters of these cell bodies are in the range of 17.31–20.01 μm and volumes are in the range of 2,199–3,089 μm^3 (**Figures 2E,F**). Its axon projected to ipsilateral regions of optic lobe, posterior lateral protocerebrum (PLP), and superior lateral protocerebrum (SLP) (**Figures 4A–C** and **Table 1**). There were 10 labeled cell bodies in the cluster of PR-LD, located dorsally to the lateral PR (**Figure 2D**). Diameters of these cell bodies are in the range of 9.15–13.81 μm and volumes are in the range of 431–1,162 μm^3 (**Figures 2E,F**). There were 4 labeled cell bodies in the cluster of PR-LA, located anteriorly to the lateral PR (**Figure 2D** and **Table 1**). Diameters of these cell bodies are in the range of 9.46–10.46 μm and volumes are in the range of 512–550 μm^3 (**Figures 2E,F**). No visible processes were observed from PR-LD and PR-LA. Two LALs were also innervated by serotonin neurons and linked by commissure 4 (**Figures 2G,H**, **4D–F**); however, the cell bodies for these serotonergic neurons were unable to be traced.

The cluster of DE-L contained only one cell body located laterally to the AL on each hemisphere (**Figure 2D** and **Table 1**).

TABLE 1 | Number, location, and innervation areas of serotonin-immunoreactive neurons in the brain and the gnathal ganglion of *Spodoptera frugiperda* larvae.

Brain/GNG	Cell body cluster	Number of neurons (n)	Location of cell body	Innervation areas
Brain	PR-M	16–18(4)	Medial region of the posterior protocerebrum	Posterior optic tubercle, anterior ventrolateral protocerebrum, superior intermediate protocerebrum, superior medial protocerebrum, inferior medial protocerebrum, and central body
	PR-L	2(4)	Lateral region of the lateral protocerebrum	Ipsilateral regions of optic lobe, posterior lateral protocerebrum, and superior lateral protocerebrum
	PR-LD	10–12(4)	Dorsally to the lateral protocerebrum	Not resolved
	PR-LA	4(4)	Anteriorly to the lateral protocerebrum	Not resolved
	TR-A	4(4)	Anteromedial tritocerebrum	Contralateral superior medial protocerebrum
GNG	GNG-AD	7(5)	Medial region of anteriodorsal gnathal ganglion	Anterior mandibular neuromere and tritocerebrum
	GNG-AV	2(5)	Anterior region of ventral gnathal ganglion	Not resolved
	GNG-M	3(5)	Median area of ventral gnathal ganglion	Not resolved
	GNG-L1	4(5)	Lateral cell body layer to the mandibular neuromere	Mandibular neuromere and tritocerebrum
	GNG-L2	4–5(5)	Lateral cell body layer to the maxillary neuromere	Maxillary neuromere and tritocerebrum
	GNG-L3	4(5)	Lateral cell body layer to the labial neuromere	Labial neuromere and tritocerebrum

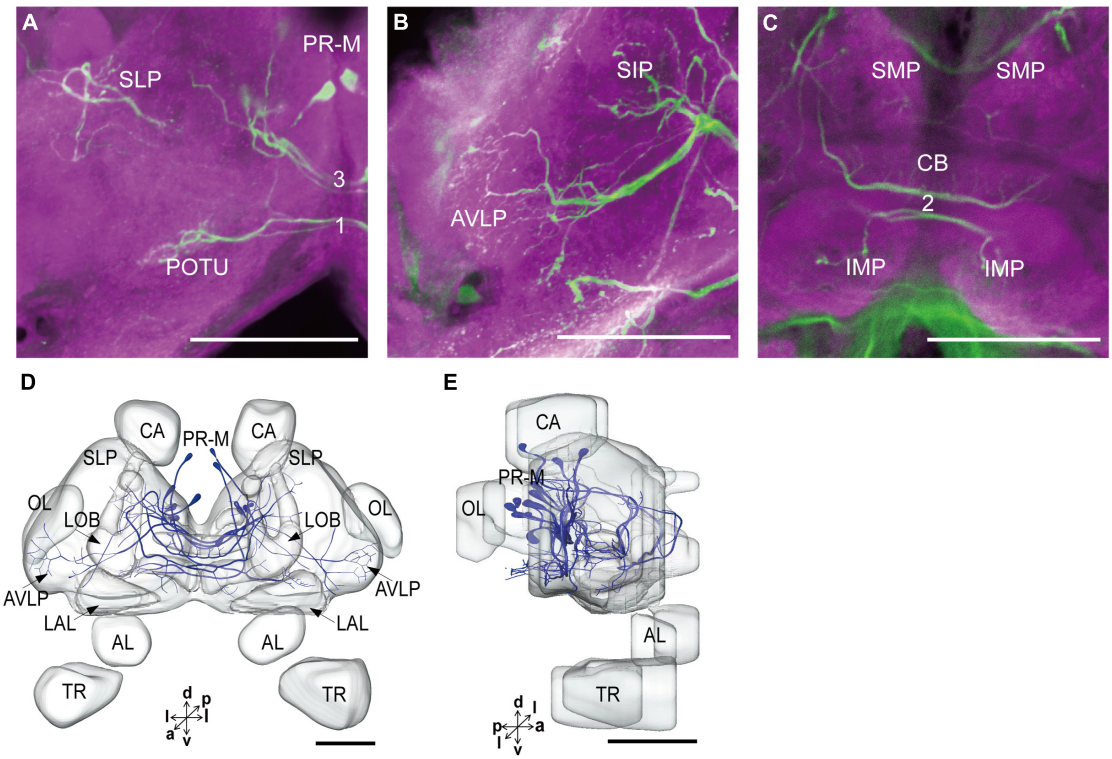

FIGURE 3 | The projection area of PR-M neurons. **(A–C)** The confocal stack images of PR-M neurons. **(D)** The anterior view of three-dimensional reconstructions of PR-M neurons. **(E)** The lateral view of three-dimensional reconstructions of PR-M neurons. AVLP, anterior ventrolateral protocerebrum; CB, central body; IMP, inferior medial protocerebrum; SLP, superior lateral protocerebrum; SMP, superior medial protocerebrum; POTU, posterior optic tubercle.PR-M is cell cluster. Directions: a, anterior; d, dorsal; l, lateral; p, posterior; v, ventral. Scale bar, 100 μm.

Diameters of these cell bodies are in the range of 15.37–16.91 μm and volumes are in the range of 1,213–1,728 μm^3 (**Figures 2E,F**). The neurites of DE-L ran dorsoposteriorly into the ipsilateral PR via medial antennal lobe tract, crossed the midline via commissure 5, and then projected via contralateral medial antennal tract to the contralateral AL. In addition, this neuron also gave rise to arborizations in both the hemispheres of SLP (**Figures 2G,H**, **5A–D** and **Table 1**).

There were four cell bodies in TR-A of both the hemispheres (**Figure 2D**). Diameters of these cell bodies are in the range of 10.92–12.57 μm and volumes are in the range of 440–715 μm^3 (**Figures 2E,F**). No visible processes, however, were

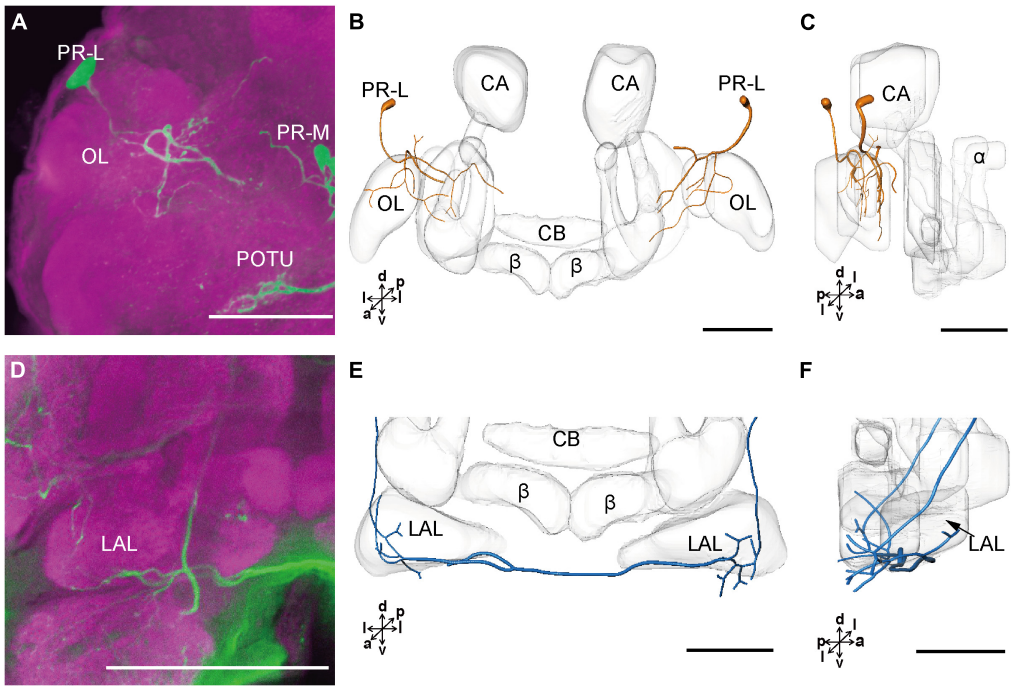

FIGURE 4 | The projection area of PR-L and LAL neurons. **(A)** The confocal stack images of PR-L neurons. **(B,C)** The anterior and lateral view of the three-dimensional reconstructions of the PR-L neurons. **(D)** The confocal stack images of LAL neuron. **(E,F)** The three-dimensional reconstructions of the LAL neurons in the anterior and lateral views. α, alpha lobe; β, belta lobe; CA, calyx; CB, central body; LAL, lateral accessory lobe; OL, optic lobe; POTU, posterior optic tubercle; PR-M and PR-L are cell clusters. Directions: a, anterior; d, dorsal; l, lateral; p, posterior; v, ventral. Scale bars, 100 μm.

observed from TR-A. The TR, indeed, contained the processes of serotonergic neurons, which were from the neurons in the gnathal ganglion via the circumesophageal connective (**Figure 5E**). In addition, a single serotonergic neuron passing the TR, projected upward along the medial side, and then crossed the midline giving off arborizations in the contralateral superior medial PR (**Figures 2G,H**, **5E,F** and **Table 1**).

Anatomy and Serotonergic Neurons of the Gnathal Ganglion of Larval *Spodoptera frugiperda*

The gnathal ganglion was composed of three neuromeres: the mandibular neuromere (MdNe), the maxillary neuromere (MxNe), and the labial neuromere (LbNe) (**Figures 6A–E**). The average volume of three neuromeres were about 87.92–105.17 × 104 μm^3 (**Figure 6F**). There were about 24 cell bodies of serotonergic neurons distributed in several clusters of GNG-AD, GNG-AV, GNG-M, and GNG-L (**Figures 6A–D,G**).

GNG-AD contained seven cell bodies, situated in the medial region of anterodorsal gnathal ganglion. Diameters of these cell bodies are in the range of 8.87–26.27 μm and volumes are in the range of 965–7,847 μm^3 (**Figures 6H,I**). These neurons sent their arborization into the TR. GNG-AV contained two cell bodies, located in the anterior region of ventral gnathal ganglion. Diameters of these cell bodies are in the range of 9.34–10.79 μm and volumes are in the range of 758–1,038 μm^3 (**Figures 6H,I**). GNG-M contained three cell bodies, located in the median area of ventral gnathal ganglion. Diameters of these cell bodies are in the range of 3.53–4.17 μm and volumes are in the range of 305–381 μm^3 (**Figures 6H,I**). No visible processes were observed from neurons of GNG-AV and GNG-AD.

Three clusters, GNG-L1, GNG-L2, and GNG-L3, were located in the lateral cell body layer to the MdNe, the MxNe, and the LbNe, respectively. Each cluster contained four cell bodies with two on each hemisphere. Diameters of these cell bodies are in the range of 8.56–14.41 μm and volumes are in the range of 607–1,799 μm^3 (**Figures 6H,I**). These neurons sent their thick axons to the contralateral hemisphere via the commissure, gave off many fine arborizations, and then projected upward to the TR through the circumesophageal connective (**Figures 6J,K** and **Table 1**).

DISCUSSION

Neuropil structures and serotonergic neurons of the brain and the gnathal ganglion of larval *S. frugiperda* were identified based upon the immuoreactivities with antisynapsin and antiserotonin serum. The gnathal ganglion of larval *S. frugiperda* is a neuropil fused with the MdNe, the MxNe, and the LbNe and the brain fused with the PR, the DE, and the TR. Within the PR, the neuropils of OL, LOB, CA, CB, PB, and LAL are prominent and easily identified. The other neuropils of the PR including the lateral PR and the superior PR account for 70.57% of the brain, showing no obvious boundaries. The prominent

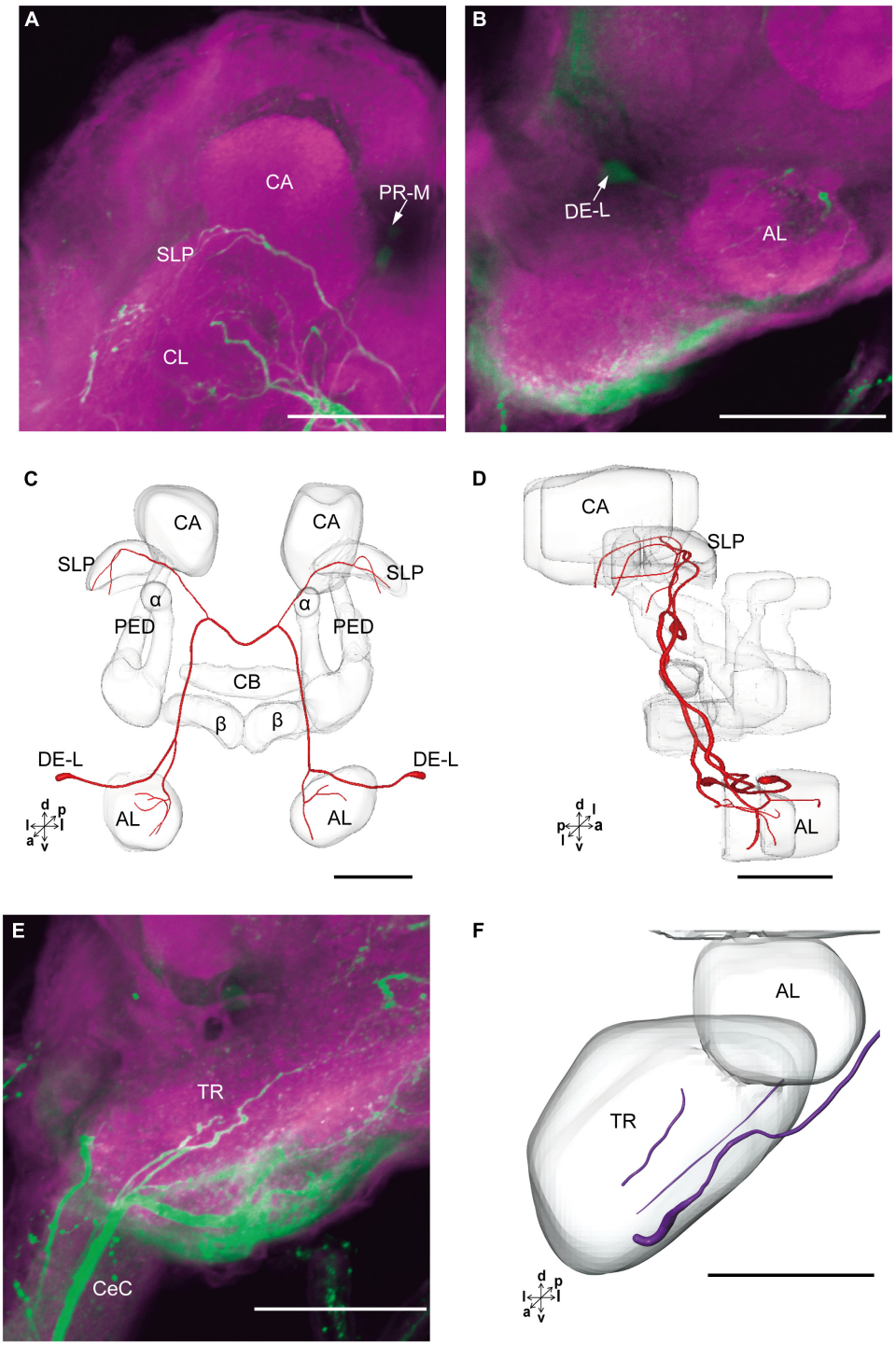

FIGURE 5 | The projection area of DE-L and TR neurons. **(A,B)** The confocal stack images of DE-L neurons. **(C,D)** The anterior and lateral views of the three-dimensional reconstructions of the DE-L neurons. **(E)** The confocal stack images of TR neuron. **(F)** The three-dimensional reconstructions of the TR neurons in anterior view. α, alpha lobe; AL, antennal lobe; β, belta lobe; CA, calyx; CB, central body; CeC, circumoesphageal connective; PED, pedunculus; SLP, superior lateral protocerebrum; PR-M and DE-L are cell clusters. Directions: a, anterior; d, dorsal; l, lateral; p, posterior; v, ventral. Scale bars, 100 μm.

neuropil of the DE is AL. Structure and spatial arrangement of the brain neuropils are similar to that of studied lepidoptera species, for instance, the monarch butterfly *Danaus plexippus*, the sphinx moth *Manduca sexta* (*M. sexta*), the cotton bollworm *Helicoverpa armigera* (*H. armigera*), and the tea geometrid *Ectropis obliqua* (*E. obliqua*) (Nordlander and Edwards, 1968;

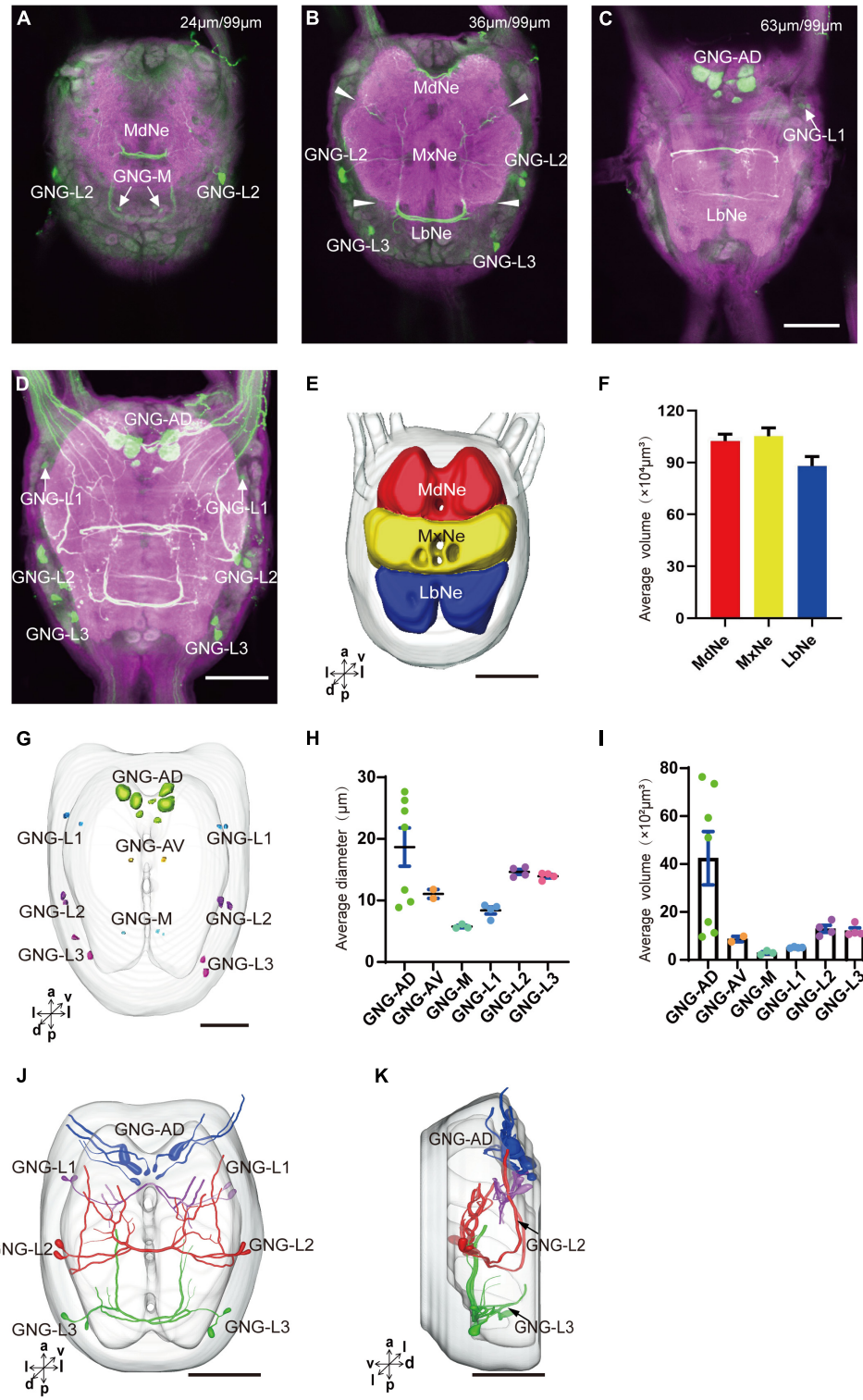

FIGURE 6 | Neuromeres, cell bodies, and processes of the serotonergic neuron in the gnathal ganglion. **(A–C)** Confocal images showing the distribution of the serotonergic neuron processes and cell bodies in the gnathal ganglion. **(D)** The confocal stack images of gnathal ganglion. **(E)** Three-dimensional reconstructions of main neuromeres in gnathal ganglion. **(F)** The average volume of main neuromeres. **(G)** The location of cell bodies in gnathal ganglion. **(H,I)** The average diameter and volume of cell bodies in gnathal ganglion. **(J,K)** Three-dimensional reconstructions of the serotonergic neurons in the cluster of gnathal ganglion in anterior and lateral view. GNG-AD, GNG-AV, GNG-M, GNG-L1, GNG-L2, and GNG-L3 are cell clusters. MdNe, mandibular neuromere, MxNe, maxillary neuromere, LbNe, labial neuromere. Directions: a, anterior; d, dorsal; l, lateral; m, medial; p, posterior; v, ventral. Scale bars, 100 μm.

Huetteroth et al., 2010; Tang et al., 2014; Xie et al., 2016). The volumes and the relative volume of the prominent neuropils are also similar to those of *H. armigera* and *E. obliqua* (Tang et al., 2014; Xie et al., 2016).

Number and Size of Serotonergic Neurons in the Brain and the Gnathal Ganglion

There are about 40 serotonergic neurons in the brain and about 24 serotonergic neurons in the gnathal ganglion of *S. frugiperda* larvae. The similar numbers were also reported in other larvae species, moths *M. sexta* (Granger et al., 1989; Griss, 1989), *H. armigera* (Tang et al., 2019), flies *Drosophila melanogaster* (*D. melanogaster*) (Vallés and White, 1988; Huser et al., 2012), *Calliphora erythrocephala* and *Sarcophaga bullata* (Nässel and Cantera, 1985), and the beetle *Tenebrio molitor* (Breidbach, 1990). In adults of *M. sexta* and *D. melanogaster*, the number of serotonergic neurons in the gnathal ganglion is also about 20 (Vallés and White, 1988; Homberg and Hildebrand, 1989a; Sitaraman et al., 2008). Similarly, in the central brain of adults of these species, e.g., brain neuropils excluding the optic lobe, the number of serotonergic neurons is about 40 in *M. sexta*, *D. melanogaster*, the honeybee *Apis mellifera* (*A. mellifera*), the wasp *Trichogramma evanescens* (*T. evanescens*), and the blood-feeding bug *Triatoma infestans* (Schürmann and Klemm, 1984; Lange et al., 1988; Vallés and White, 1988; Homberg and Hildebrand, 1989a; Sitaraman et al., 2008; van der Woude and Smid, 2017). No cell bodies of serotonergic neurons were found in the optic lobe of *S. frugiperda*. The similar results were also observed in *H. armigera* (Tang et al., 2019). However, in adults, there are about 600 serotonergic neurons located in the optic lobe of *M. sexta*, 80 in armyworm *Mythimna separata*, 100 in butterfly *Mimathyma schrenckii* (*M. schrenckii*), 40 in *D. melanogaster*, 40–60 in *A. mellifera*, and 120 in mantis *Tenodera sinensis* (Schürmann and Klemm, 1984; Vallés and White, 1988; Homberg and Hildebrand, 1989b; Leitinger et al., 1999; Niu et al., 2004; Sitaraman et al., 2008; Guo et al., 2018). The differentiation of serotonergic neurons in the optic lobe is dependent on the development of optic lobe neuropils during the metamorphosis (Nässel et al., 1987).

Cell body sizes of serotonergic neurons of *S. frugiperda* larvae were also measured. Cell bodies in diameters are about 9–20 μm in the brain and 3.5–26 μm in the gnathal ganglion. In *T. evanescens*, the diameters of cell body sizes of serotonergic neurons are about 2 μm, while in *A. mellifera*, the diameters of cell body sizes of serotonergic neurons are 8–30 μm (Schürmann and Klemm, 1984; van der Woude and Smid, 2017). Therefore, the size of serotonergic neurons in different species may be related to insect body sizes (van der Woude and Smid, 2017). Within a species, however, why the size of serotonergic neurons differ from different clusters is not clear. The size of cell body may be related to the size of arborization. For example, the cell bodies of PR-M, PR-L, and DE-L in *S. frugiperda* larvae are larger and their arborizations are spread wider. The size of cell body may also be related to the function of neurosecretion. Four serotonergic neurons of GNG-AD located in the medial gnathal ganglion are very large. Similar results were also found in locust *Schistocerca gregaria*, cockroach *Periplaneta americana*, larval *H. armigera*, and larval and adult *M. sexta* (Bishop and O'Shea, 1983; Tyrer et al., 1984; Griss, 1989; Homberg and Hildebrand, 1989a; Tang et al., 2019). Intracellular recordings from such neurons of *M. sexta* larvae revealed overshooting soma spikes of large amplitude and long duration, which suggest that these neurons are neurosecretory cells (Griss, 1989).

Innervation Patterns of Serotonergic Neurons in the Brain

In the PR, the cell bodies of serotonergic neurons of larval *S. frugiperda* are distributed mainly in four clusters: PR-M, PR-L, PR-LD, and PR-LA. The processes of PR-LD and PR-LA are invisible; probably, they are not developed yet in the present stage. In contrast, PR-M has processes projecting to wide region in the PR, including the CB, bilateral areas of superior intermediate protocerebra, superior and inferior medial protocerebra, anterior ventrolateral protocerebra, and POTU. The arborizations in these areas are quite dense. The neurons in the cluster of PR-L have processes projecting mainly to the ipsilateral posterior and superior lateral protocerebra. A few processes of these neurons project to the inner part of the ipsilateral optic lobe. Genetic manipulations demonstrated that a subset of serotonergic neurons in the anterior, medial, and lateral PR evoked hunger (Albin et al., 2015) and several serotonergic neurons in the inferior PR and the lateral PR inhibited the attraction of ethanol in adult *D. melanogaster* (Xu et al., 2016). Many processes were also found in both the LALs of larval *S. frugiperda*; however, their cell bodies were unable to be traced. The serotonergic processes in the LAL of *H. armigera* originated from the cells in the cluster of PR-A, which located in anterior region of the PR (Tang et al., 2019). The patterns of serotonergic neuron arborizations of PR-M and PR-L are similar between *S. frugiperda* and *H. armigera*. The neuropils of the PR of larval *S. frugiperda*, including PB, CA, PED, α and β lobes, and lateral horn, lack serotonergic neuron processes. Similar findings have been reported in larvae of *H. armigera*, *M. sexta*, and *D. melanogaster* (Granger et al., 1989; Huser et al., 2012; Tang et al., 2019). In contrast, the mushroom bodies of adult *M. sexta* and *D. melanogaster* contain fine serotonergic neuron processes (Homberg and Hildebrand, 1989a; Sitaraman et al., 2008). These results suggest that some serotonergic neurons in the mushroom body are remodeled during the metamorphosis from the larva to the adult. The mushroom bodies of insects are related to learning and memory activities and serotonin have been demonstrated to be involved in olfaction and place learning and memory in *D. melanogaster* (Sitaraman et al., 2008, 2012). The lack of serotonergic neuron in the larval mushroom body, however, does not suggest that serotonin plays no role in learning and memory at larval stage. Recently, a serotonin receptor, 5-HT7, was found expressing in the mushroom body of *Drosophila* larvae, which was shown to mediate the associative olfactory appetitive learning and memory (Huser et al., 2017; Ganguly et al., 2020). Whether serotonin

mediates the associative learning and memory for *S. frugiperda* in the same manner could be investigated by using molecular methods in future study.

A pair of deutocerebral serotonergic neurons DE-L of larval *S. frugiperda* has arborizations in the contralateral AL and bilateral superior lateral protocerebra, which was similar to the reports in the larvae of *M. sexta* and *H. armigera* (Kent et al., 1987; Tang et al., 2019). In adult of *M. sexta*, the branching pattern persists and expands in the AL with the development of glomeruli (Kent et al., 1987). The similar arborization patterns between larvae and adult may indicated DE-L neurons that play the same function in both the different life stages. Electrophysiological recordings demonstrated that the deutocerebral serotonergic neuron showing responses to odorants and mechanical stimuli in adult moths *Bombyx mori* (*B. mori*) and *Helicoverpa assulta* (Hill et al., 2002; Zhao and Berg, 2009). In *D. melanogaster*, these two deutocerebral serotonergic neurons could counteract the inhibition of the ethanol attraction from the serotonergic neurons of the PR (Xu et al., 2016). In *B. mori*, dye-filled DE-L neuron also gave off some arborizations in the lateral accessory lobe, but such innervation pattern was not found in larval *S. frugiperda* or other studied lepidopteran species (Dacks et al., 2006; Zhao and Berg, 2009; Tang et al., 2019).

The cells in the cluster of TR-A in the TR of larval *S. frugiperda* were also similar to that of *H. armigera* and other species (Nässel, 1988; Granger et al., 1989; Wegerhoff, 1999; Tang et al., 2019). The cell bodies were weakly stained with antiserotonin serum and their neuronal processes were not detected. Throughout the TR, however, serotonergic neuron processes are abundant and they may originate from the frontal ganglion and the gnathal ganglion. Two neurons, which linked the TR, form a commissure in the frontal of the medial PR and give off some arborizations in the SMP. The TR is the stomatogastric center. The findings of the serotonergic neuron network between the TR, the PR, and the gnathal ganglion could facilitate us to explore the roles of serotonin in feeding, for instance, food detection, food intake, and nutrient choice, and help in finding a potential approach to modulate the feeding behavior of the gluttonous pest and reduce its damage.

Serotonergic Neurons in the Gnathal Ganglion

The immunoreactivity to antiserotonin serum in the cell cluster of GNG-AV and GNG-M of larval *S. frugiperda* was weak and their processes were unable to be traced. The cluster of GNG-AD gave off processes in the most anterior of the gnathal ganglion and projected to the TR. All the three neuromeres of the gnathal ganglion of larval *S. frugiperda* contain widespread processes of serotonergic neurons originated from the cells in the cluster GNG-L. The thick processes from the cell clusters on both the sides form a horseshoe pattern, cross the midline via a commissure, and project anteriorly to the contralateral TR. Such neurons and their branching patterns show high conservation across insect taxa, which were also found in larvae of *H. armigera*, *M. sexta*, *Tenebrio molitor* (*T. molitor*) and the flies *D. melanogaster*, *Conistra erythrocephala* (*C. erythrocephala*), and *Sarcophaga bullata* (*S. bullata*) (Nässel and Cantera, 1985; Griss, 1989; Breidbach, 1990; Huser et al., 2012; Tang et al., 2019).

In adults of insect species, serotonergic neurons and their processes in the gnathal ganglion were also found in the similar patterns (Bishop and O'Shea, 1983; Tyrer et al., 1984; Rehder et al., 1987; Vallés and White, 1988; Griss, 1989; Homberg and Hildebrand, 1989a; Breidbach, 1990). Previous studies demonstrated that the serotonergic neurons in the lateral side of the gnathal ganglion facilitated the food ingestion of *D. melanogaster* larvae (Schoofs et al., 2018). In addition to the internal regulation, the serotonergic neurons of the gnathal ganglion were also involved in mediating taste detection (Yao and Scott, 2021). One class of serotonergic neurons in the gnathal ganglion responds to gustatory detection of sugars and the other class to gustatory detection of bitter compounds (Yao and Scott, 2021). As in other species, larval *S. frugiperda* possesses taste sensilla on the maxilla, responding to the stimuli sugar and bitter substances to regulate the feeding preference (Hou et al., 2020). How the serotonergic neurons in the gnathal ganglion of larval *S. frugiperda* regulate the feeding preference would be an interesting issue in the future study.

DATA AVAILABILITY STATEMENT

The raw data supporting the conclusions of this article will be made available by the authors, without undue reservation.

AUTHOR CONTRIBUTIONS

Q-BT, W-BC, and X-CZ: study concept and design. J-JZ, L-LS, Y-NW, G-YX, and W-BC: acquisition of data. J-JZ, L-LS, G-YX, W-BC, and X-CZ: analysis and interpretation of data. W-BC and X-CZ: drafting of the manuscript. Q-BT, W-BC, X-CZ, and S-HA: final manuscript. Q-BT and W-BC: obtain funding. All authors contributed to the article and approved the submitted version.

FUNDING

This study was funded by the Key Science and Technology Research Project of Henan Province of China (Grant Nos. 201300111500 and 202102110072) and the National Natural Science Foundation of China (Grant No. 32001912).

ACKNOWLEDGMENTS

We are grateful to Juan Qu for insect rearing, Ms. Meng-Li Yang and Shu-Lan Wang for help with the laser scanning confocal microscopy, and Prof. Bente G. Berg (Norwegian University of Science and Technology) for help with the Amira software.

REFERENCES

Albin, S. D., Kaun, K. R., Knapp, J. M., Chung, P., Heberlein, U., and Simpson, J. H. (2015). A subset of serotonergic neurons evokes hunger in adult Drosophila. *Curr. Biol.* 25, 2435–2440. doi: 10.1016/j.cub.2015.08.005

Anstey, M. L., Rogers, S. M., Ott, S. R., Burrows, M., and Simpson, S. J. (2009). Serotonin mediates behavioral gregarization underlying swarm formation in desert locusts. *Science* 323, 627–630. doi: 10.1126/science.1165939

Bishop, C. A., and O'Shea, M. (1983). Serotonin immunoreactive neurons in the central nervous system of an insect (*Periplaneta americana*). *J. Neurobiol.* 14, 251–269. doi: 10.1002/neu.480140402

Boleli, I. C., and Paulino-Simões, Z. L. (1999). Mapping of serotonin-immunoreactive neurons of Anastrepha obliqua Macquart larvae. *Revta Bras Zoo* 16, 1099–1107. doi: 10.1590/s0101-81751999000400019

Breidbach, O. (1990). Serotonin-immunoreactive brain interneurons persist during metamorphosis of an insect: a development study of the brain of *Tenebrio molitor* L (Coleoptera). *Cell Tissue Res.* 259, 345–360. doi: 10.1007/bf00318458

Cohen, R. W. (2001). Diet balancing in the cockroach Rhyparobia madera: does serotonin regulate this behavior? *J. Insect Behav.* 14, 99–111.

Cook, H., and Orchard, I. (1990). Effects of 5,7-DHT upon feeding and serotonin content of various tissues in *Rhodnius prolixus*. *J. Insect Physiol.* 36, 361–367. doi: 10.1016/0022-1910(90)90018-b

Dacks, A. M., Christensen, T. A., and Hildebrand, J. G. (2006). Phylogeny of a serotonin-immunoreactive neuron in the primary olfactory center of the insect brain. *J. Comp. Neurol.* 498, 727–746. doi: 10.1002/cne.21076

Dacks, A. M., Nickel, T., and Mitchell, B. K. (2003). An examination of serotonin and feeding in the flesh fly Neobellieria bullata (Sarcophagidae: Diptera). *J. Insect Behav.* 16, 1–21.

Falibene, A., Roessler, W., and Josens, R. (2012). Serotonin depresses feeding behaviour in ants. *J. Insect Physiol.* 58, 7–17. doi: 10.1016/j.jinsphys.2011.08.015

French, A. S., Simcock, K. L., Rolke, D., Gartside, S. E., Blenau, W., and Wright, G. A. (2014). The role of serotonin in feeding and gut contractions in the honeybee. *J. Insect Physiol.* 61, 8–15. doi: 10.1016/j.jinsphys.2013.12.005

Ganguly, A., Cheng, Q., Bajaj, J., and Lee, D. (2020). Serotonin receptor 5-HT7 in Drosophila mushroom body neurons mediates larval appetitive olfactory learning. *Sci. Rep.* 10:21267. doi: 10.1038/s41598-020-77910-5

Granger, N. A., Homberg, U., Henderson, P., Towel, A., and Lauder, J. M. (1989). Serotonin-immunoreactive neurons in the brain of *Manduca sexta* during larval development and larval-pupal metamorphosis. *Int. J. Dev. Neurosci.* 7, 55–72. doi: 10.1016/0736-5748(89)90044-0

Griss, C. (1989). Serotonin-immunoreactive neurons in the suboesophageal ganglion of caterpillar of the hawk moth *Manduca sexta*. *Cell Tissue Res.* 258, 101–109.

Guo, P., Ma, B. W., Zhao, X. C., Wang, G. P., and Xie, G. Y. (2018). Distribution of 5-hydroxytryptamine in the optic lobes of the oriental armyworm, *Mythomna separata* (Lepidoptera: Noctuidae). *Acta. Entomol. Sin.* 61, 668–675.

Haselton, A. T., Downer, K. E., Zylstra, J., and Stoffolano, J. J. G. (2009). Serotonin inhibits protein feeding in the blow fly *Phormia regina* (Meigen). *J. Insect Behav.* 22, 452–463. doi: 10.1007/s10905-009-9184-1

Hill, E. S., Iwano, M., Gatellier, L., and Kanzaki, R. (2002). Morphology and physiology of the serotonin-immunoreactive putative antennal lobe feedback neuron in the male silkmoth *Bombyx mori*. *Chem. Senses* 27, 475–483. doi: 10.1093/chemse/27.5.475

Homberg, U., and Hildebrand, J. G. (1989a). Serotonin-immunoreactive neurons in the median protocerebrum and suboesophageal ganglion of the sphinx moth *Manduca sexta*. *Cell Tissue Res.* 258, 1–24. doi: 10.1007/BF00223139

Homberg, U., and Hildebrand, J. G. (1989b). Serotonin-immunoreactivity in the optic lobes of the sphinx moth *Manduca sexta* and colocalization with FMRFamide and SCPB immunoreactivity. *J. Comp. Neurol.* 288, 243–253. doi: 10.1002/cne.902880204

Hou, W. H., Sun, L. L., Ma, Y., Sun, H. W., Zhang, J. J., Bai, R. E., et al. (2020). Gustatory perception and feeding preference of Spodoptera frugiperda (Lepidoptera: Noctuidae) larvae to four stimuli. *Acta Entomol. Sin.* 63, 545–557.

Huetteroth, W., el Jundi, B., el Jundi, S., and Schachtner, J. (2010). 3D-reconstructions and virtual 4D-visualization to study metamorphic brain development in the sphinx moth *Manduca sexta*. *Front. Syst. Neurosci.* 4:7. doi: 10.3389/fnsys.2010.00007

Huser, A., Eschment, M., Güllü, N., Collins, K. A. N., Böpple, K., Pankevych, L., et al. (2017). Anatomy and behavioral function of serotonin receptors in Drosophila melanogaster larvae. *PLoS One* 12:e0181865. doi: 10.1371/journal.pone.0181865

Huser, A., Rohwedder, A., Apostolopoulou, A. A., Widmann, A., Pfitzenmaier, J. E., and Maiolo, E. M. (2012). The serotonergic central nervous system of the Drosophila larva: anatomy and behavioral function. *PLoS One* 7:e47518. doi: 10.1371/journal.pone.0047518

Ito, K., Shinomiya, K., Ito, M., Armstrong, J. D., Boyan, G., and Hartenstein, V. (2014). A systematic nomenclature for the insect brain. *Neuron* 81, 755–765. doi: 10.1016/j.neuron.2013.12.017

Kaufmann, L., Schürmann, F., Yiallouros, M., Harrewijin, P., and Kayser, H. (2004). The serotonergic system is involved in feeding inhibition by pymetrozine. Comparative studies on a locust (*Locusta migratoria*) and an aphid (*Myzus persicae*). *Comp. Biochem. Physiol. Part A* 138, 469–483. doi: 10.1016/j.cca.2004.08.007

Kent, K. S., Hoskins, S. G., and Hildebrand, J. G. (1987). A novel serotonin-immunoreactive neuron in the antennal lobe of the sphinx moth *Manduca sexta* persists throughout postembryonic life. *J. Neurobiol.* 18, 451–465. doi: 10.1002/neu.480180506

Kinney, M. P., Panting, N. D., and Clark, T. M. (2014). Modulation of appetite and feeding behavior of the larval mosquito *Aedes aegypti* by the serotonin-selective reuptake inhibitor paroxetine: shifts between distinct feeding modes and the influence of feeding status. *J. Exp. Biol.* 217, 935–943. doi: 10.1242/jeb.094904

Klemm, N., Steinbusch, H. W., and Sundler, F. (1984). Distribution of serotonin-containing neurons and their pathways in the supraoesophageal ganglion of the cockroach *Periplaneta americana* (L.) as revealed by immunocytochemistry. *J. Comp. Neurol.* 225, 387–395. doi: 10.1002/cne.902250306

Kloppenburg, P., and Mercer, A. R. (2008). Serotonin modulation of moth central olfactory neurons. *Annu. Rev. Entomol.* 53, 179–190. doi: 10.1146/annurev.ento.53.103106.093408

Lange, A. B., Orchard, I., and Lloyd, R. J. (1988). Immunohistochemical and electrochemical detection of serotonin in the nervous system of the blood-feeding bug, *Rhodnius prolixus*. *Arch. Insect Biochem. Physiol.* 8, 187–201. doi: 10.1002/arch.940080305

Leitinger, G., Pabst, M. A., and Kral, K. (1999). Serotonin-immunoreactive neurones in the visual system of the praying mantis: an immunohistochemical, confocal laser scanning and electron microscopic study. *Brain Res.* 823, 11–23. doi: 10.1016/s0006-8993(98)01339-0

Lin, S., Li, S., Liu, Z., Zhang, L., Wu, H., Cheng, D., et al. (2021). Using azadirachtin to transform Spodoptera frugiperda from pest to natural enemy. *Toxins* 13:541. doi: 10.3390/toxins13080541

Liu, S. S., Li, A. Y., Witt, C. M., Perez, and de Leon, A. A. (2011). Immunohistological localization of serotonin in the the CNS and feeding system of the stable fly *Stomoxys calcitrans* L. (Diptera: Muscidae). *Arch. Insect Biochem. Physiol.* 77, 199–219. doi: 10.1002/arch.20434

Lyu, Y., Promislow, D. E. L., and Pletcher, S. D. (2021). Serotoin signaling modulates aging-associated metabolic network integrity in response to nutrient choice in *Drosophila melanogaster*. *Commun. Biol.* 4:740. doi: 10.1038/s42003-021-02260-5

Montezano, D. G., Specht, A., Sosa-Gómez, D. R., Roque-Specht, V. F., and Sousa-Silva, J. C. (2018). Host plants of *Spodoptera frugiperda* (Lepidoptera: Noctuidae) in the Americas. *Afr. Entomol.* 26, 286–300.

Nässel, D. R. (1988). Serotonin and serotonin-immunoreactive neurons in the nervous system of insects. *Prog. Neurobiol.* 30, 1–85. doi: 10.1016/0301-0082(88)90002-0

Nässel, D. R., and Cantera, R. (1985). Mapping of serotonin-immunoreactive neurons in the larval nervous system of the flies Calliphora erythrocephala and Sarcophaga bullata. a comparison with ventral ganglion in adult animals. *Cell Tissue Res.* 239, 423–434.

Nässel, D. R., Ohlsson, L., and Sivasubramanian, P. (1987). Postembryonic differentiation of serotonin-immunoreactive neurons in fleshfly optic lobes developing in situ or cultured in vivo without eye discs. *J. Comp. Neurol.* 255, 327–340. doi: 10.1002/cne.902550302

Niu, H., Li, Y. N., and Bao, X. X. (2004). Distribution of GABA and 5-HT-ergic immunoreactive neurons in the visual system of butterfly *Mimathyma screnckii*. *Acta. Zool. Sin.* 50, 770–774.

Nordlander, R. H., and Edwards, J. S. (1968). Morphology of the larval and adult brains of the monarch butterfly, *Danaus plexippus plexippus*, L. *J. Morphol.* 126, 67–94. doi: 10.1002/jmor.1051260105

Novak, M. G., and Rowley, W. A. (1994). Serotonin depletion affects blood-feeding but not host-seeking ability in *Aedes triseriatus* (Diptera: Culicidae). *J. Med. Entomol.* 31, 600–606. doi: 10.1093/jmedent/31.4.600

Orchard, I. (2006). Serotonin: a coordinator of feeding-related physiological events in the blood-gorging bug, *Rhodnius prolixus*. *Comp. Biochem. Physiol. Part A.* 144, 316–324. doi: 10.1016/j.cbpa.2005.11.010

Oyarzabal-Armendariz, E., Alquicira-Mireles, J., Zúñiga-Ruíz, B., Arreola-Ramírez, J. L., Guevara-Fefer, P., and Lara-Figueroa, C. O. (2021). Effect of *Azadirachta indica* A. Juss (Meliaceae) on the serotonin rhythm of *Spodoptera frugiperda* (Lepidoptera: Noctuidae). *Chronobiol. Int.* 38, 201–211. doi: 10.1080/07420528.2020.1858849

Qi, Y. X., Huang, J., Li, M. Q., Wu, Y. S., Xia, R. Y., and Ye, G. Y. (2016). Serotonin modulates insect hemocyte phagocytosis via two different serotonin receptors. *eLife* 5:e12241. doi: 10.7554/eLife.12241

Qi, Y. X., Wu, S. F., Huang, J., and Ye, G. Y. (2014). Advances in 5-hydroxytryptamine and its receptors in insects. *Acta Entomol. Sin.* 57, 844–859.

Rehder, V., Bicker, G., and Hammer, M. (1987). Serotonin-immunoreactive neurons in the antennal lobe and suboesophageal ganglion of the honeybee. *Cell Tissue Res.* 247, 59–66. doi: 10.1016/s0040-8166(96)80070-x

Schoofs, A., Hückesfeld, S., and Pankratz, M. J. (2018). Serotonergic network in the subesophageal zone modulates the motor pattern for food intake in Drosophila. *J. Insect Physiol.* 106, 36–46. doi: 10.1016/j.jinsphys.2017.07.007

Schürmann, F. W., and Klemm, N. (1984). Serotonin-immunoreactive neurons in the brain of the honeybee. *J. Comp. Neurol.* 225, 570–580. doi: 10.1002/cne.902250407

Settembrini, B. P., and Villar, M. J. (2004). Distribution of serotonin in the central nervous system of the blood-feeding heteropteran, *Triatoma infestans* (Heteroptera: Reduviidae). *J. Morphol.* 260, 21–32. doi: 10.1002/jmor.10211

Sitaraman, D., LaFerriere, H., Birman, S., and Zars, T. (2012). Serotonin is critical for rewarded olfactory short-term memory in Drosophila. *J. Neurogenet.* 26, 238–244. doi: 10.3109/01677063.2012.666298

Sitaraman, D., Zars, M., LaFerriere, H., Chen, Y. C., Sable-Smith, A., Kitamoto, T., et al. (2008). Serotonin is necessary for place memory in Drosophila. *Proc. Nat. Acad. Sci. USA.* 105, 5579–5584. doi: 10.1073/pnas.0710168105

Tang, Q. B., Song, W. W., Chang, Y. J., Xie, G. Y., Chen, W. B., and Zhao, X. C. (2019). Distribution of serotonin-immunoreactive neurons in the brain and gnathal ganglion of caterpillar *Helicoverpa armigera*. *Front. Neuroanatomy* 13:56. doi: 10.3389/fnana.2019.00056

Tang, Q. B., Zhan, H., Berg, B. G., Yan, F. M., and Zhao, X. C. (2014). Three dimensional reconstructions of the brain and the suboesophageal ganglion of Helicoverpa armigera (Lepidoptera: Noctuidae) Larvae. *Acta Entomol. Sin.* 57, 538–546.

Tierney, A. J. (2020). Feeding, hunger, satiety and serotonin in invertebrates. *Proc. R Soc. B.* 287:20201386. doi: 10.1098/rspb.2020.1386

Tyrer, N. M., Turner, J. D., and Altman, J. S. (1984). Identifiable neurons in the locust central nervous system that react with antibodies to serotonin. *J. Comp. Neurol.* 227, 313–330. doi: 10.1002/cne.902270303

Vallés, A. M., and White, K. (1988). Serotonin-containing neurons in Drosophila melanogaster: development and distribution. *J. Comp. Neurol.* 268, 414–428. doi: 10.1002/cne.902680310

van der Woude, E., and Smid, H. M. (2017). Maximized complexity in miniaturized brains: morphology and distribution of octopaminergic, dopaminergic and serotonergic neurons in the parasitic wasp, *Trichogramma evanescens*. *Cell Tissue Res.* 369, 477–496. doi: 10.1007/s00441-017-2642-8

Vleugels, R., Velinden, H., and Vanden Broeck, J. (2015). Serotonin, serotonin receptors and their actions in insects. *Neurotransimitter* 2:e314.

Wegerhoff, R. (1999). GABA and Serotonin immunoreactivity during postembryonic brain development in the beetle *Tenebrio molitor*. *Microsci. Res. Tech.* 45, 154–164. doi: 10.1002/(SICI)1097-0029(19990501)45:3<154::AID-JEMT3>3.0.CO;2-5

Wu, Q. L., He, L. M., Shen, X. J., Jiang, Y. Y., Liu, J., Hu, G., et al. (2019). Estimation of the potential infestation area of newly-invaded fall armyworm Spodoptera Frugiperda in the Yangtze river valley of China. *Insects* 10:298. doi: 10.3390/insects10090298

Wu, Q. L., Jiang, Y. Y., Liu, J., Hu, G., and Wu, K. M. (2021). Trajectory modeling revealed a southwest-northeast migration corridor for fall armyworm *Spodoptera frugiperda* (Lepidoptera: Noctuidae) emerging from the North China plain. *Insect Sci.* 28, 649–661. doi: 10.1111/1744-7917.12852

Xie, G. Y., Chen, J. H., Tang, Q. B., Yin, J., and Zhao, X. C. (2016). Anatomical structure of the brain of larval Ectropis obliqua (Lepidoptera: Geometridae). *Acta Entomol. Sin.* 59, 831–838.

Xu, L., He, J., Kaiser, A., Gräber, N., Schläger, L., Ritze, Y., et al. (2016). A single pair of serotonergic neurons conteracts serotonergic inhibition of ethanol attraction in Drosophila. *PLoS One* 11:e0167518. doi: 10.1371/journal.pone.0167518

Yao, Z., and Scott, K. (2021). Serotonergic neurons translate taste detection into internal nutrient regulation. *BioRxiv [Preprint]* doi: 10.1101/2021.05.13.444014

Zhao, X. C., and Berg, B. G. (2009). Morphological and physiological characteristics of the serotonin-immunoreactive neuron in the antennal lobe of the male oriental tobacco budworm, Helicoverpa assulta. *Chem. Senses* 34, 363–372. doi: 10.1093/chemse/bjp013

Zhao, X. C., Chen, Q. Y., Guo, P., Xie, G. Y., Tang, Q. B., Guo, X. R., et al. (2016). Glomerular identification in the antennal lobe of the male moth *Helicoverpa armigera*. *J. Comp. Neurol.* 524, 2993–3013. doi: 10.1002/cne.24003

Conflict of Interest: The authors declare that the research was conducted in the absence of any commercial or financial relationships that could be construed as a potential conflict of interest.

Publisher's Note: All claims expressed in this article are solely those of the authors and do not necessarily represent those of their affiliated organizations, or those of the publisher, the editors and the reviewers. Any product that may be evaluated in this article, or claim that may be made by its manufacturer, is not guaranteed or endorsed by the publisher.

Copyright © 2022 Zhang, Sun, Wang, Xie, An, Chen, Tang and Zhao. This is an open-access article distributed under the terms of the Creative Commons Attribution License (CC BY). The use, distribution or reproduction in other forums is permitted, provided the original author(s) and the copyright owner(s) are credited and that the original publication in this journal is cited, in accordance with accepted academic practice. No use, distribution or reproduction is permitted which does not comply with these terms.

frontiers | Frontiers in Physiology

ORIGINAL RESEARCH
published: 27 April 2022
doi: 10.3389/fphys.2022.900752

Functional Characterization of Odorant Binding Protein PyasOBP2 From the Jujube Bud Weevil, *Pachyrhinus yasumatsui* (Coleoptera: Curculionidae)

Bo Hong[1], *Qing Chang*[1], *Yingyan Zhai*[1], *Bowen Ren*[2] *and Feng Zhang*[1]*

[1]Bio-Agriculture Institute of Shaanxi, Xi'an, China, [2]Shaanxi Academy of Forestry, Xi'an, China

Odorant binding proteins (OBPs) play an important role in insect olfaction. The jujube bud weevil *Pachyrhinus yasumatsui* (Coleoptera: Curculionidae) is a major pest of *Zizyphus jujuba* in northern China. In the present study, based on the antennal transcriptome, an OBP gene of *P. yasumatsui* (*PyasOBP2*) was cloned by reverse transcription PCR (RT-PCR). Expression profile analyses by quantitative real-time PCR (qRT-PCR) revealed that *PyasOBP2* was highly expressed in the antennae of both male and female *P. yasumatsui* adults, while its expression was negligible in other tissues. PyasOBP2 was prokaryotically expressed, and purified by Ni-NTA resin. The fluorescence competitive binding assays with 38 plant volatiles from *Z. jujuba* showed that PyasOBP2 could bind with a broad range of plant volatiles, and had strongest binding capacities to host-plant volatiles like ethyl butyrate (K_i = 3.02 μM), 2-methyl-1-phenylpropene (K_i = 4.61 μM) and dipentene (K_i = 5.99 μM). The three dimensional structure of PyasOBP2 was predicted by homology modeling, and the crystal structure of AgamOBP1 (PDB ID: 2erb) was used as a template. The molecular docking results indicated that the amino acid residue Phe114 of PyasOBP2 could form hydrogen bonds or hydrophobic interactions with some specific ligands, so this residue might play a key role in perception of host plant volatiles. Our results provide a basis for further investigation of potential functions of PyasOBP2, and development of efficient monitoring and integrated pest management strategies of *P. yasumatsui*.

Keywords: *Pachyrhinus yasumatsui*, odorant binding protein, prokaryotic expression, host volatile, fluorescence competitive binding assay, molecular docking

OPEN ACCESS

Edited by:
Rui Tang,
Guangdong Academy of Science (CAS), China

Reviewed by:
Hao Guo,
Chinese Academy of Sciences (CAS), China
Zhongzhen Wu,
Zhongkai University of Agriculture and Engineering, China

***Correspondence:**
Feng Zhang
zhangfeng73@xab.ac.cn

Specialty section:
This article was submitted to Invertebrate Physiology, a section of the journal Frontiers in Physiology

Received: *21 March 2022*
Accepted: *06 April 2022*
Published: *27 April 2022*

Citation:
Hong B, Chang Q, Zhai Y, Ren B and Zhang F (2022) Functional Characterization of Odorant Binding Protein PyasOBP2 From the Jujube Bud Weevil, Pachyrhinus yasumatsui (Coleoptera: Curculionidae). Front. Physiol. 13:900752. doi: 10.3389/fphys.2022.900752

INTRODUCTION

In long-term interactions with external environments, insects have evolved a highly specific and sensitive olfactory system, which enables them to sense various chemical signals and undertake a series of behaviors such as mating, host location, foraging, oviposition, and predator avoidance (Justice et al., 2010; Elgar et al., 2018). The olfactory system consists of various proteins expressed during the chemoreceptive process, such as odorant binding proteins (OBPs), chemosensory proteins (CSPs), olfactory receptors (ORs), gustatory receptors (GRs), ionotropic receptor (IRs), sensory neuron membrane proteins (SNMPs), and odorant degrading enzymes (ODEs) (Vosshall et al., 1999; De Bruyne and Baker, 2008; Sanchez-Gracia et al., 2009). OBPs and CSPs are both soluble

proteins that are concentrated in the chemosensilla lymph of insects. The two kinds of proteins are able to selectively bind, and transport hydrophobic odorant molecules across the lymph to ORs located on the dendritic membrane of sensory neurons, activating the chemical signal transduction process (Laughlin et al., 2008; Leal, 2013; Pelosi et al., 2014).

In general, insect OBPs are small (about 100–200 amino acids) hydrosoluble proteins. According to distinct conserved cysteine patterns, insect OBPs can be divided into four subfamilies: "classic OBPs" with six conserved cysteine residues, "minus-C OBPs" with four conserved cysteine residues, "plus-C OBPs" with eight conserved cysteine residues, and "atypical OBPs" with six conserved cysteine residues as in "classic OBPs", but with additional cysteines in the C-terminal region (Hekmat-Scafe et al., 2002; Venthur et al., 2014; Brito et al., 2016).

Since the first insect OBP was identified from *Antheraea polyphemus* (Vogt and Riddiford, 1981), a large number of OBPs have been identified by using sequenced genomes and transcriptomes from several insect orders, including Diptera, Hymenoptera, Lepidoptera, Hemiptera, Coleoptera, and Orthoptera (Jacquin-Joly et al., 2000; Northey et al., 2016; Wu et al., 2016; Pelosi et al., 2018; Venthur and Zhou, 2018). In recent years, an increasing number of studies involving the identification and function of OBP genes in insect species have demonstrated that most insect OBPs are highly expressed in antennae, indicating that OBPs play a key role in chemoreception (Wang et al., 2019; Zhang et al., 2020). Moreover, OBPs are found to selectively bind to various volatiles emitted from host plants (Deng et al., 2012; Ju et al., 2012; Cui et al., 2018). Therefore, host volatiles play a crucial role in insect orientation and host selection, and studies on the binding characteristics of insect OBPs with volatiles will bring a better understanding of olfactory recognition mechanism at molecular levels.

The jujube bud weevil, *Pachyrhinus yasumatsui* (Kôno and Morimoto, 1960) (Coleoptera: Curculionidae), has recently become a major pest of jujube plants (*Ziziphus jujuba* Mill) in northern China, causing serious ecological damage and large economic losses (Huang and Li, 1993; Ren and Qi, 2009; Tang et al., 2013). Although being still the main tools to control *P. yasumatsui*, chemical insecticides pose serious threat to environmental and human health, and lead to pest resistance (Yang et al., 2019; Yan et al., 2020). The jujube bud weevil is an oligophagous herbivore, feeding mainly on jujube plants, so the host selection behaviors of this insect may rely on olfaction (Hong et al., 2017; Wang et al., 2017). In previous studies, *P. yasumatsui* adults were found to be significantly attracted by several volatiles emitted from jujube shoots (e.g., ocimene, α-farnesene, nonanal and methyl palmitate), based on electroantennography (EAG) and Y-tube olfactometer experiments (Yan et al., 2017; Yan et al., 2020). However, little is known about olfaction in this pest at the molecular level.

In our previous studies, 24 putative OBPs were identified from the antennal transcriptome of *Pachyrhinus yasumatsui* (unpublished), and the level of unigenes coding for OBPs was calculated using fragments per kilobase of transcript per million mapped read (FPKM) values. The FPKM values indicated that the candidate OBP gene *PyasOBP2* had the highest level in the male antennae (FPKM = 40599.96), suggesting that *PyasOBP2* was an antenna-enriched OBP gene and may be involved in the odor identification for *P. yasumatsui*. In this work, we cloned *PyasOBP2* by using RT-PCR, determined its expression profile in different tissues, and purified the recombinant protein to test its affinity with jujube volatiles by fluorescence competitive binding assays. Based on the results of ligand-binding assays, we performed three dimensional (3D) structural modeling and molecular docking to investigate the binding sites of PyasOBP2, and identify the key amino acid residues involved. Our results provide a foundation for clarifying molecular mechanisms of insect olfaction, and will serve as a reference for developing management strategies for this pest.

MATERIALS AND METHODS

Experimental Insect Samples

The pupae of *P. yasumatsui* were collected from Jiaxian County, Shaanxi, China (37°59′53″N, 110°21′07″E) in April 2020, and placed in incubators at 25 ± 1°C, 16 h light: 8 h dark cycle and 60 ± 5% RH. The emerged male and female adults were collected and

TABLE 1 | Primer pairs used for cloning, prokaryotic expression and gene expression analyses.

Primer name	Primer sequence (5′-3′)	Product size (bp)
For gene cloning		
OBP2-F	ATATTTTGATTGACAATCTAGTCAGAC	588
OBP2-R	ACTTAGATTTGGGATGCGTATT	
For qRT-PCR		
OBP2-qF	GTGGAATCACGGAGGACGA	161
OBP2-qR	ATCTTTGAATGGATACGGTTGTG	
EF1α-qF	TCCCAAGCTGATTGTGCTG	112
EF1α-qR	CAAGGGTGAAGGCGAGAAG	
Actin-qF	TGTTGCGGCTCTTGTCGT	169
Actin-qR	GCTTTGGGCTTCATCTCCTA	
For prokaryotic expression		
OBP2-eF	CGGGATCCAAGCTTACATTGCCACCAGAAT	351
OBP2-eR	CCGGAATTCCGGTTAGACGAAGAACCAATTCTCAGG	

Restriction sites are underlined.

TABLE 2 | Binding affinities of PyasOBP2 to jujube volatile ligands in fluorescence binding assays.

Ligands	Formula	CAS	Source/Purity	IC_{50}(μM)	K_i(μM)
Alcohols					
1-Penten-3-ol	$C_5H_{10}O$	616-25-1	Aladdin, >97.0%	>20	-
cis-3-Hexen-1-ol	$C_6H_{12}O$	928-96-1	Aladdin, 98.0%	8.06	6.85
trans-2-Hexen-1-ol	$C_6H_{12}O$	928-95-0	Aladdin, 97.0%	8.93	6.60
Benzyl alcohol	C_7H_8O	100-51-6	Aladdin, ≥99.5%	16.18	11.96
Eucalyptol	$C_{10}H_{18}O$	470-82-6	Aladdin, >99.5%	15.07	12.81
Linalool	$C_{10}H_{18}O$	78-70-6	Aladdin, 98.0%	11.62	9.88
Nerolidol	$C_{15}H_{26}O$	7212-44-4	Aladdin, 97.0%	7.54	6.41
Terpenoids					
Ocimene	$C_{10}H_{16}$	13877-91-3	Sigma, ≥90.0%	10.49	8.92
α-Pinene	$C_{10}H_{16}$	7785-26-4	Aladdin, ≥99.0%	10.80	9.18
Camphene	$C_{10}H_{16}$	79-92-5	Aladdin, 95.0%	8.33	7.08
α-Phellandrene	$C_{10}H_{16}$	99-83-2	Sigma, >95.0%	10.73	9.12
Myrcene	$C_{10}H_{16}$	123-35-3	Aladdin, ≥90.0%	11.80	8.92
Dipentene	$C_{10}H_{16}$	7705-14-8	Aladdin, 95.0%	7.05	5.99
3-Carene	$C_{10}H_{16}$	13466-78-9	Aladdin, >90.0%	>20	-
β-Caryophyllene	$C_{15}H_{24}$	87-44-5	Sigma, ≥98.0%	>20	-
Squalene	$C_{30}H_{50}$	111-02-4	Aladdin, 98.0%	>20	-
Esters					
Ethyl butyrate	$C_6H_{12}O_2$	105-54-4	Aladdin, ≥99.5%	3.55	3.02
Butyl acetate	$C_6H_{12}O_2$	123-86-4	Aladdin, ≥99.7%	>20	-
Ethyl 2-methylbutyrate	$C_7H_{14}O_2$	7452-79-1	Aladdin, 98.0%	>20	-
Ethyl valerate	$C_7H_{14}O_2$	539-82-2	Aladdin, ≥99.7%	>20	-
Ethyl isovalerate	$C_7H_{14}O_2$	108-64-5	Aladdin, ≥99.7%	>20	-
cis-3-Hexenyl acetate	$C_8H_{14}O_2$	3681-71-8	Aladdin, 98.0%	>20	-
cis-3-Hexenyl 3-methylbutanoate	$C_{11}H_{20}O_2$	35154-45-1	Aladdin, 97.0%	>20	-
2-Methylbutyric Acid *cis*-3-Hexen-1-yl Ester	$C_{11}H_{20}O_2$	53398-85-9	Aladdin, 98.0%	11.92	10.13
Dibutyl phthalate	$C_{16}H_{22}O_2$	84-74-2	Aladdin, >99.5%	10.46	7.73
Methyl palmitate	$C_{17}H_{34}O_2$	112-39-0	Aladdin, ≥99.0%	>20	-
Methyl oleate	$C_{19}H_{36}O_2$	112-62-9	Aladdin, ≥99.0%	>20	-
Aldehydes					
Isobutyraldehyde	C_4H_8O	78-84-2	Aladdin, >99.5%	12.99	11.04
trans-2-Hexen-1-al	$C_6H_{10}O$	6728-26-3	Aladdin, 98.0%	15.75	13.39
Caproaldehyde	$C_6H_{12}O$	66-25-1	Aladdin, ≥99.0%	10.86	8.03
Heptaldehyde	$C_7H_{14}O$	111-71-7	Aladdin, ≥98.0%	15.37	11.36
Octanal	$C_8H_{16}O$	124-13-0	Aladdin, 99.0%	7.81	6.64
Nonanal	$C_9H_{18}O$	124-19-6	Aladdin, 96.0%	15.56	13.22
Others					
Dodecane	$C_{12}H_{26}$	112-40-3	Aladdin, ≥99.5%	>20	-
2-Methyl-1-phenylpropene	$C_{10}H_{12}$	768-49-0	Aladdin, >98.0%	5.42	4.61
Benzonitrile	C_7H_5N	100-47-0	Aladdin, ≥99.5%	>20	-
Geranyl nitrile	$C_{10}H_{15}N$	5146-66-7	Aladdin, 97.0%	>20	-
Eugenol	$C_{10}H_{12}O_2$	97-53-0	Aladdin, >99.5%	>20	-

separately reared on fresh buds of *Zizyphus jujuba*. Antennae, heads (without antennae), thoraxes, abdomens, legs and wings of *P. yasumatsui* were collected from 5-d-old adults, immediately transferred to Eppendorf tubes immersed in liquid nitrogen, and stored at −80°C until RNA extraction.

RNA Extraction, cDNA Synthesis, and Gene Cloning

Total RNA was extracted with the Trizol reagent (TaKaRa Co., Dalian, China). The integrity of RNA was assessed by 1.0% agarose gel electrophoresis, and the concentration was quantified with a SimpliNano spectrophotometer (GE Healthcare, Piscataway, NJ, United States). cDNA was synthesized from total RNA (1 μg for each sample) using the PrimeScript™ 1st Strand cDNA Synthesis Kit (TaKaRa) by following the manufacturer's instructions, and cDNA samples were stored at −20°C.

The *OBP2* gene sequence was obtained from the antennal transcriptome of *P. yasumatsui* (GenBank No. SRR7871392, unpublished), and specific PCR primers were designed to amplify the coding region (**Table 1**). RT-PCR reactions were carried out by using the following conditions: 3 min at 95°C; 35 cycles of 30 s at 95°C, 30 s at 56°C, 30 s at 72°C; and 72°C for 10 min. The purified RT-PCR product was ligated into the pMD®19-T vector, and transformed into DH5α competent cells (TaKaRa) for sequencing.

Sequence and Phylogenetic Analyses

The open reading frame (ORF) of *PyasOBP2* was predicted by using the ORFfinder (https://www.ncbi.nlm.nih.gov/orffinder/). The signal peptide of the amino acid sequence of PyasOBP2 was

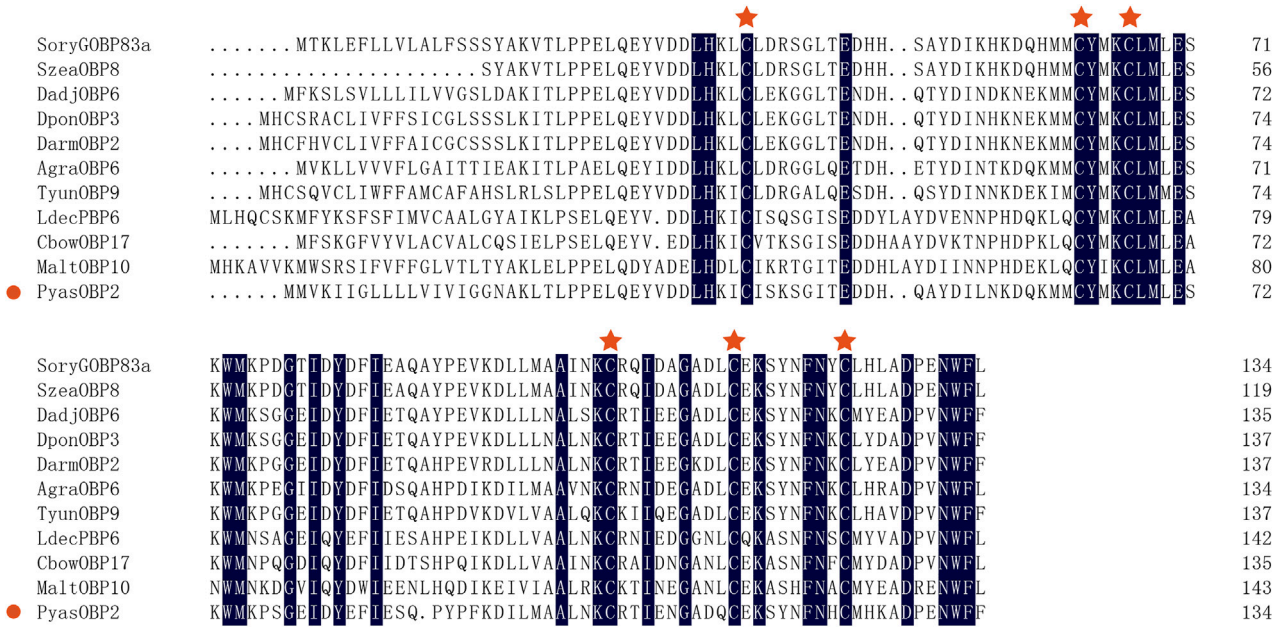

FIGURE 1 | Multiple alignments of PyasOBP2 and other OBPs from coleopterans. The conserved cysteine residues were marked with a red star. Species names and GenBank accession numbers of the ten OBPs are: *Sitophilus oryzae* (SoryGOBP83a, XP_030747957); *Sitophilus zeamais* (SzeaOBP8, QCT83262); *Dendroctonus adjunctus* (DadjOBP6, QKV34987); *Dendroctonus ponderosae* (DponOBP3, AKK25131); *Dendroctonus armandi* (DarmOBP2, AIY61045); *Anthonomus grandis* (AgraOBP6, AVI04887); *Tomicus yunnanensis* (TyunOBP9, AMP19491); *Leptinotarsa decemlineata* (LdecPBP6, XP_023024287); *Colaphellus bowringi* (CbowOBP17, ALR72505); *Monochamus alternatus* (MaltOBP10, AIX97025).

predicted using the SignalP program server (https://services.healthtech.dtu.dk/service.php?SignalP-5.0). The molecular weight and theoretical isoelectric point of PyasOBP2 was calculated with the Expasy program online (http://web.expasy.org/protparam/). Sequence alignment of PyasOBP2 with OBPs from other insects was carried out with DNAMAN 9.0 (Lynnon Biosoft, San Ramon, CA, United States). Based on amino acid sequences of PyasOBP2 and other coleopteran OBPs, phylogenetic analyses were performed in MEGA X (Kumar et al., 2018) using the neighbor-joining approach with a bootstrap replication of 1000. Finally, the phylogenetic tree was created and edited with FigTree 1.4.4 (http://tree.bio.ed.ac.uk/software/figtree/).

Tissue Expression of *PyasOBP2*

Tissue expression levels of *PyasOBP2* in *P. yasumatsui* were measured by qRT-PCR. The *EF1-α* gene (GenBank No. OK105108) and *β-actin* gene (GenBank No. OK322363) from *P. yasumatsui* were used as reference genes. Primer sequences were designed with Primer-BLAST (https://www.ncbi.nlm.nih.gov/tools/primer-blast/), and listed in **Table 1**. qRT-PCR reactions were performed with TB Green® Premix Ex Taq™ II (TaKaRa) and a StepOnePlus Real-Time PCR System (Applied Biosystems, Carlsbad, CA, United States) using the following conditions: 30 s at 95°C, followed by 40 cycles of 5 s at 95°C, 30 s at 60°C, 30 s at 72°C. Three biological replicates and three technical replicates were conducted for each gene. The expression level (L) of all the genes was calculated with **Eq. 1**. L = the expression level of all the genes, Ct = the threshold cycle value, E = amplification efficiency. The normalized expression level of *PyasOBP2* (N_{OBP2}) in different adult tissues was calculated with **Eq. 2** (Livak and Schmittgen, 2001; Vandesompele et al., 2002). Significant differences in different tissues were analyzed by one-way ANOVA, followed by the Tukey's HSD tests ($p < 0.05$ was considered statistically significant). The Student's t-test was used to compare the expressions of *PyasOBP2* between male and female adults. All the data were analyzed using the SPSS 22.0 software.

$$L = (1+E)^{-Ct} \quad (1)$$

$$N_{OBP2} = \frac{(1+E_{OBP2})^{-Ct_{OBP2}}}{\sqrt{(1+E_{EF-1\alpha})^{-Ct_{EF-1\alpha}} \times \left(1+E_{\beta-actin}\right)^{-Ct_{\beta-actin}}}} \quad (2)$$

Cloning and Construction of Recombinant Plasmids

Primers with restriction enzyme sites *BamH*I and *EcoR*I were designed with Primer Premier 5.0 (**Table 1**), and the coding region of PyasOBP2 without the signal peptide was amplified with PCR. The PCR products were ligated into the pMD®19-T vector, transformed into DH5α competent cells (TaKaRa Co., Dalian, China) and then sequenced. The correct pMD®19-T plasmids were digested by restriction enzymes (*BamH*I and *EcoR*I) (TaKaRa) for 1–2 h at 37°C, cloned into the digested pET32a vector, and then transformed into DH5α cells. The correct recombinant plasmids were transformed into BL21

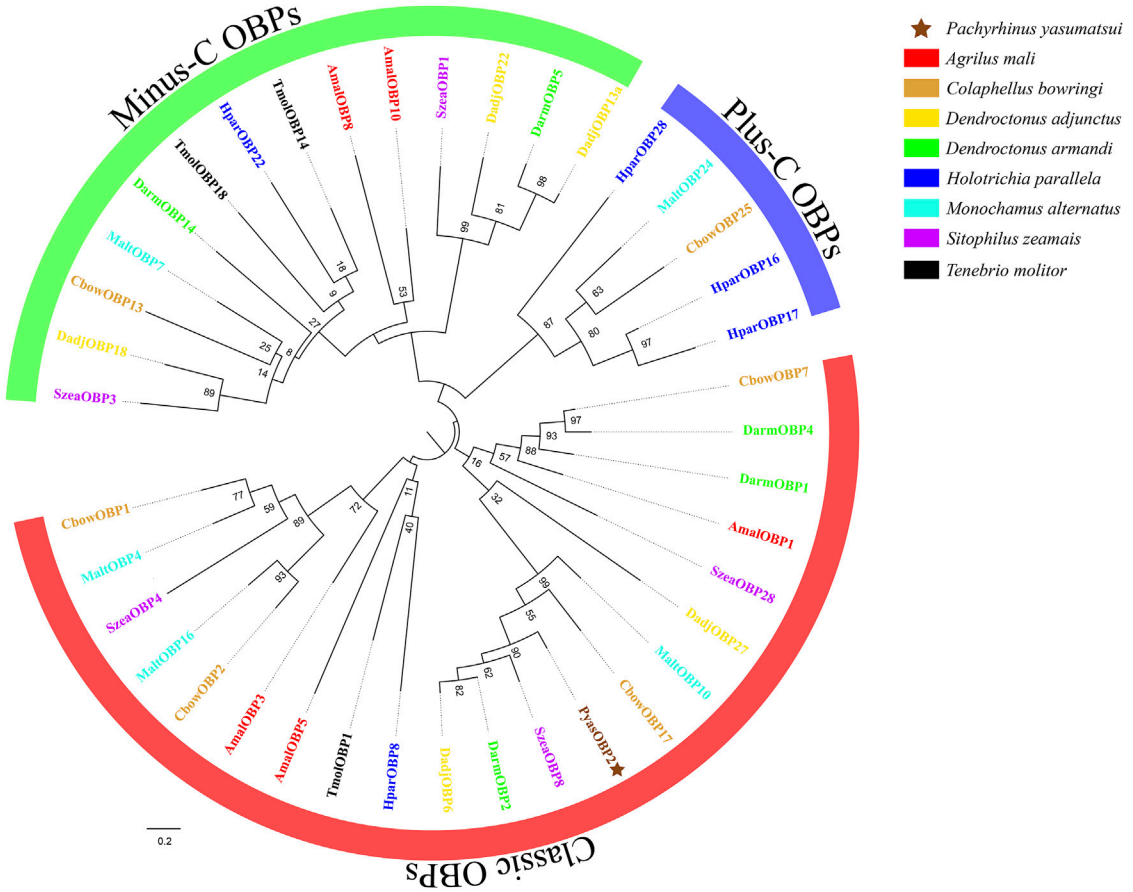

FIGURE 2 | Phylogenetic tree of PyasOBP2 and OBPs from other coleopterans. Gene names and GenBank accession numbers of 40 OBPs are as follows: *Pachyrhinus yasumatsui* (PyasOBP2, MG585343); *Agrilus mali* (AmalOBP1, AVU05010; AmalOBP3, AVU05012; AmalOBP5, AVU05014; AmalOBP8, AVU05017; AmalOBP10, AVU05019); *C. bowringi* (CbowOBP1, ALR72489; CbowOBP2, ALR72490; CbowOBP7, ALR72495; CbowOBP13, ALR72501; CbowOBP17, ALR72505; CbowOBP25, ALR72513); *D. adjunctus* (DadjOBP6, QKV34987; DadjOBP13a, QKV34993; DadjOBP18, QKV34997; DadjOBP22, QKV34999; DadjOBP27, QKV35002); *D. armandi* (DarmOBP1, AIY61044; DarmOBP2, AIY61045; DarmOBP4, ALM64966; DarmOBP5, ALM64967; DarmOBP14, ALM64972); *Holotrichia parallela* (HparOBP8, AKI84366; HparOBP16, AKI84374; HparOBP17, AKI84375; HparOBP22, AKI84380; HparOBP28, ALP75941); *M. alternatus* (MaltOBP4, AHA39269; MaltOBP7, AIX97022; MaltOBP10, AIX97025; MaltOBP16, AIX97031; MaltOBP24, AIX97039); *S. zeamais* (SzeaOBP1, QCT83255; SzeaOBP3, QCT83257; SzeaOBP4, QCT83258; SzeaOBP8, QCT83262; SzeaOBP28, QCT83282); *Tenebrio molitor* (TmolOBP1, AJM71475; TmolOBP14, AJM71488; TmolOBP18, AJM71492)

(DE3) competent cells (TaKaRa). Single colonies were cultured in liquid LB (supplemented with 100 mg/ml ampicillin) overnight at 37°C.

Prokaryotic Expression and Purification of PyasOBP2

The culture was diluted 1:100 with liquid LB, and incubated at 37°C until the OD_{600} reached a value of 0.6–0.8. Protein expression was induced by adding isopropyl-β-D-1-thiogalactopyranoside (IPTG) at a final concentration of 0.5 mM into the culture, and allowed to last for 10 h at 18°C. The bacterial cells (500 ml) were collected by centrifugation (8000 g for 10 min, 4°C), and the cell pellet was suspended with the lysis buffer (50 mg/ml Lysozyme and 20 mM Tris-HCl buffer at pH 7.4). The suspension was sonicated on ice, and centrifuged (12000 g for 30 min, 4°C) for a second time. Recombinant PyasOBP2 was examined by Sodium Dodecyl Sulfate—Polyacrylamide Gel electrophoresis (SDS-PAGE). Protein present in the supernatant was purified with a Ni-NTA His·Bind Resin column (7 Sea Biotech, Shanghai, China). The purified protein was assessed by SDS-PAGE, identified with the anti-His tag monoclonal antibody (Cwbio biotech, Beijing, China) by the Western Blot analysis, and desalted in a dialysis buffer (20 mM Tris-HCl at pH 7.4). To avoid confounding effects on subsequent experiments, His-tag was removed from the protein using a recombinant enterokinase (rEK) (Yeasen Biotech, Shanghai, China), and the concentration of the protein was assayed by the BCA protein quantification kit (Cwbio biotech, Beijing, China).

Fluorescence Binding Assays

Fluorescence competitive binding assays were carried out on an F-2700 fluorescence spectrophotometer (Hitachi, Tokyo, Japan)

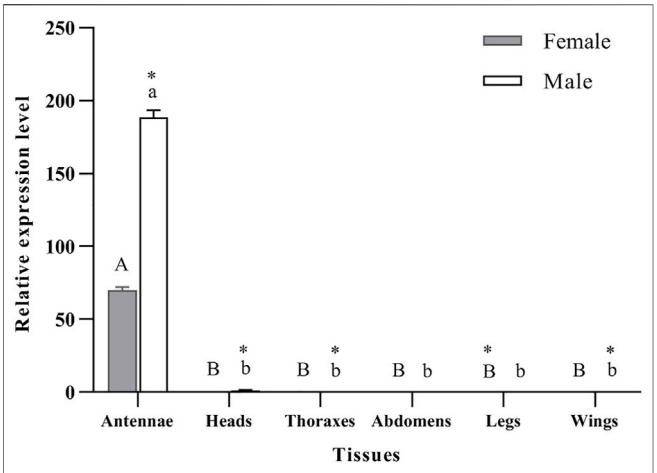

FIGURE 3 | Expression profiles of the *PyasOBP2* gene in different tissues of *Pachyrhinus yasumatsui*. The fold changes are relative to the expression levels in the legs of adult females. Different capital and lowercase letters above bars indicate significant differences among tissues of females and males, respectively. Asterisks indicate significant differences in expression levels between female and male in the same tissues.

to determine the binding affinity of PyasOBP2. 1-N-phenylnaphthylamine (1-NPN) was used as a fluorescent probe (Pelosi et al., 2006) with excitation at 337 nm, and the emission spectra were measured from 370 to 550 nm. Based on gas chromatography-mass spectrometry (GC-MS) and previous studies (Yan et al., 2017; Yan et al., 2020), 38 volatiles derived from *Z. jujuba* were selected as putative ligands for fluorescence competitive binding assays (**Table 2**). 1-NPN and all ligands used in binding assays were diluted in methanol to 1 mM stock solutions. To measure the binding affinity of PyasOBP2 with 1-NPN, PyasOBP2 solution (with a final concentration of 2 μM) was titrated with 1-NPN to final concentrations ranging from 2 to 20 μM. In ligand-binding assays, each ligand with a concentration ranging from 0 to 20 μM was added into a mixture of PyasOBP2 (2 μM) and 1-NPN (2 μM), and maximal fluorescence intensities were plotted against ligand concentrations based on three replicates.

The dissociation constant $K_{1\text{-NPN}}$ (for PyasOBP2 binding with 1-NPN) was calculated with Scatchard plotting of binding data in the GraphPad Prism 8.0 Software (Sideris et al., 1992). The dissociation constant (K_i) of each ligand was calculated with **Eq. 3**, as described by Cui et al. (2018). The ligand binding affinity to PyasOBP2 was considered as very strong ($K_i \leq 5$ μM), strong (5 μM$<K_i \leq$10 μM), moderate (10 μM$<K_i \leq$20 μM) and weak ($K_i >$20 μM) in this study.

$$K_i = IC_{50} / (1 + [1 - NPN] / K_{1-NPN}) \quad (3)$$

Three Dimensional Structural Modeling and Molecular Docking

Structural templates for PyasOBP2 were searched by using PSI-BLAST against the Protein Data Bank (PDB) database. Based on high sequence similarity with PyasOBP2, the crystal structure of AgamOBP1 from *Anopheles gambiae* (PDB ID: 2erb) was selected as a template for homology modeling using Modeller 10.1 (Webb and Sali, 2016). To obtain the reliable 3D structure of PyasOBP2, the quality of models was assessed by Verify3D and PROCHECK (https://saves.mbi.ucla.edu/).

The 3D models of selected ligands were generated and optimized using ChemBioDraw12.0 (Cousins, 2011). The molecular docking of PyasOBP2 with ligands was performed

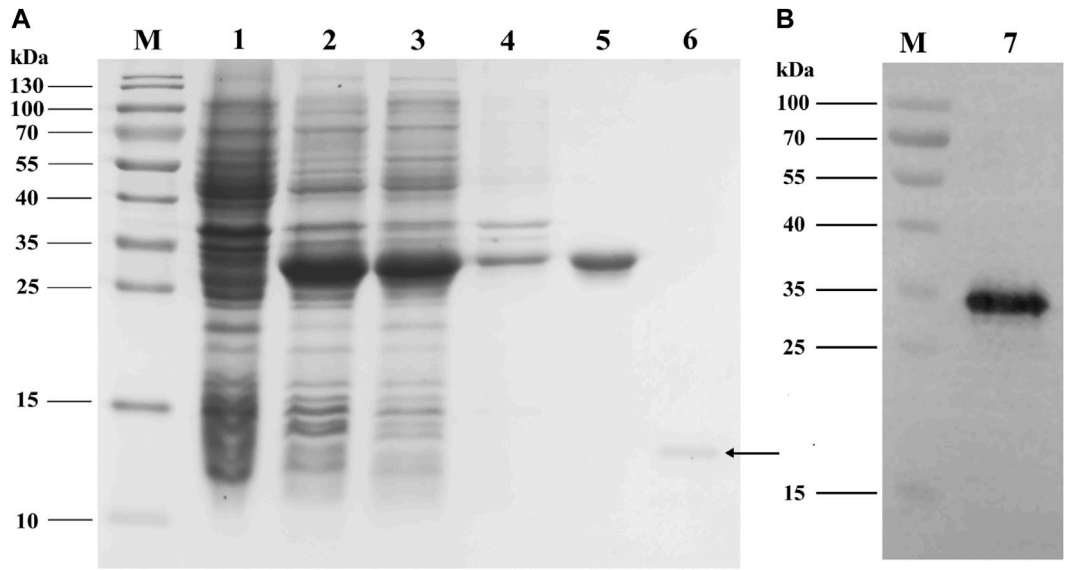

FIGURE 4 | (A) SDS-PAGE and **(B)** western blot analyses of expressed recombinant PyasOBP2. M: Protein marker; 1: Non-induced pET32a/PyasOBP2; 2: Induced pET32a/PyasOBP2; 3: Supernatant of pET32a/PyasOBP2; 4: Inclusion body of pET32a/PyasOBP2; 5: Purified PyasOBP2; 6: Re-purified PyasOBP2 after the removal of His-tag; 7: Western blot of purified PyasOBP2.

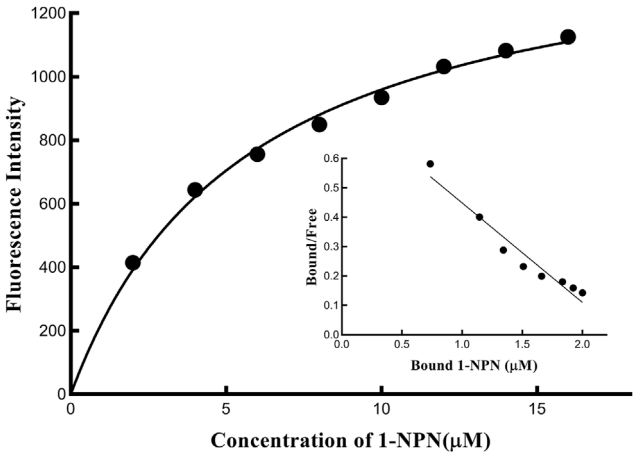

FIGURE 5 | The binding curve and Scatchard plot of PyasOBP2 with 1-NPN.

using Autodock 4.2.6 (https://autodock.scripps.edu/). LigPlot + v. 2.2.4 (https://www.ebi.ac.uk/thornton-srv/software/LigPlus/) and PyMOL v.2.5.2 (https://pymol.org/) were used to visualize 2D and 3D structures of the proteins, respectively.

RESULTS

Characterization of *PyasOBP2* cDNA

The full-length cDNA of *PyasOBP2* (GenBank No. OK322360) was obtained by RT-PCR using specific primers. The cDNA sequence of *PyasOBP2* contained a 408-bp ORF encoding 135 amino acid residues. At the N-terminus, PyasOBP2 possessed a predicted 19-residue signal peptide (**Supplementary Figure S1**). The predicted molecular weight and theoretical isoelectric point (pI) of the mature protein PyasOBP2 were 13.71 kDa and 4.98, respectively.

Sequence alignments of PyasOBP2 with ten homologous OBPs from other coleopteran insects revealed that PyasOBP2 had typical characteristics of classic OBPs with six conserved cysteine residues (C_1-X_{24}-C_2-X_3-C_3-X_{36}-C_4-X_9-C_5-X_8-C_6, X represent any amino acid except cysteine; **Supplementary Figures S1** and **Figure 1**) (Zhou, 2010). Moreover, PyasOBP2 shared the highest sequence identity (76.27%) with SoryGOBP83a and SzeaOBP8, followed by DponOBP3 (75.21% identity), DadjOBP6 (74.79% identity) and *Dendroctonus armandi* DarmOBP2 (73.50% identity). The phylogenetic tree showed that 40 coleopteran insect OBPs could be divided into three subfamilies: minus-C OBPs, classic OBPs and plus-C OBPs (**Figure 2**). Among the OBPs, the closest homolog of PyasOBP2 was SzeaOBP8, consistent with the results of multiple sequence alignments.

Expression Profiles of *PyasOBP2*

qRT-PCR was used to determine the expression levels of *PyasOBP2* in different adult tissues of both sexes of *P. yasumatsui*. For both female and male adults, *PyasOBP2* was significantly and highly expressed in antennae, but it was almost not expressed in all other tissues (**Figure 3**; ♀: $F_{5,\ 12} = 3158.41$, $p < 0.001$; ♂: $F_{5,\ 12} = 4049.09$, $p < 0.001$). Sex-biased expression of *PyasOBP2* was found in antennae, heads, thoraxes, legs, and wings. Expression levels of *PyasOBP2* in antennae ($t = 67.49$, $p < 0.001$), heads ($t = 13.92$, $p < 0.01$), thoraxes ($t = 9.26$, $p < 0.05$) and wings ($t = 6.55$, $p < 0.05$) were significantly higher in males than those in females. Whereas expression levels of *PyasOBP2* in legs were significantly higher in females than in males ($t = 112.53$, $p < 0.001$).

Expression and Purification of PyasOBP2

The analyses of SDS-PAGE (**Figure 4A**) and western blot (**Figure 4B**) showed that recombinant PyasOBP2 was successfully expressed and purified with the *E. coli* system. The recombinant PyasOBP2 with His-tag was mainly present in the supernatant after IPTG induction, and exhibited distinct bands at the size of approximately 30 kDa. PyasOBP2 after the removal of His-tag had a high purity but low concentration (0.79 mg/ml), and showed a distinct band at the size of approximately 13.5 kDa (as shown by the arrow in **Figure 4A**).

Fluorescent Competitive Binding Assays of PyasOBP2

The binding affinity of 1-NPN with the purified PyasOBP2 was measured, and the binding curve as well as corresponding Scatchard plot were drawn (**Figure 5**). Results revealed that the dissociation constant of PyasOBP2 with 1-NPN was 5.662 μM, suggesting 1-NPN is a good reporter ligand for PyasOBP2. Among 38 tested host volatiles, PyasOBP2 was found to bind to 22 volatiles (K_i<20 μM), indicating that PyasOBP2 had a broad ligand-binding affinity (**Table 2**; **Figure 6**). Among the seven tested alcohols, cis-3-hexen-1-ol, trans-2-hexen-1-ol, linalool, and nerolidol showed strong binding affinity (K_i<10 μM) for PyasOBP2 (**Figure 6A**). Among the nine tested terpenoids, six terpenoids (i.e., ocimene, α-pinene, camphene, α-phellandrene, myrcene, and dipentene) with the same molecular formula of $C_{10}H_{16}$, presented strong binding affinity for PyasOBP2 (K_i values = 5.99–9.18 μM) (**Figure 6B**). Among the eleven tested esters, only three esters, including ethyl butyrate, 2-methylbutyric acid cis-3-hexen-1-yl ester and dibutyl phthalate, displayed good binding affinity for PyasOBP2 (K_i values = 3.02–10.13 μM) (**Figure 6C**). All the six tested aldehydes showed good binding affinity for PyasOBP2 with K_i values ranging from 6.64 to 13.39 μM (**Figure 6D**). Among the five other ligands, 2-methyl-1-phenylpropene exhibited very strong binding affinity for PyasOBP2 (K_i = 4.61 μM), whereas dodecane, eugenol and two nitriles (benzonitrile and geranyl nitrile) could not bind to PyasOBP2 (**Figure 6E**).

Protein Structure Prediction and Molecular Docking

BLAST results showed that PyasOBP2 shared the highest sequence similarity (34%) and query coverage (96%) with

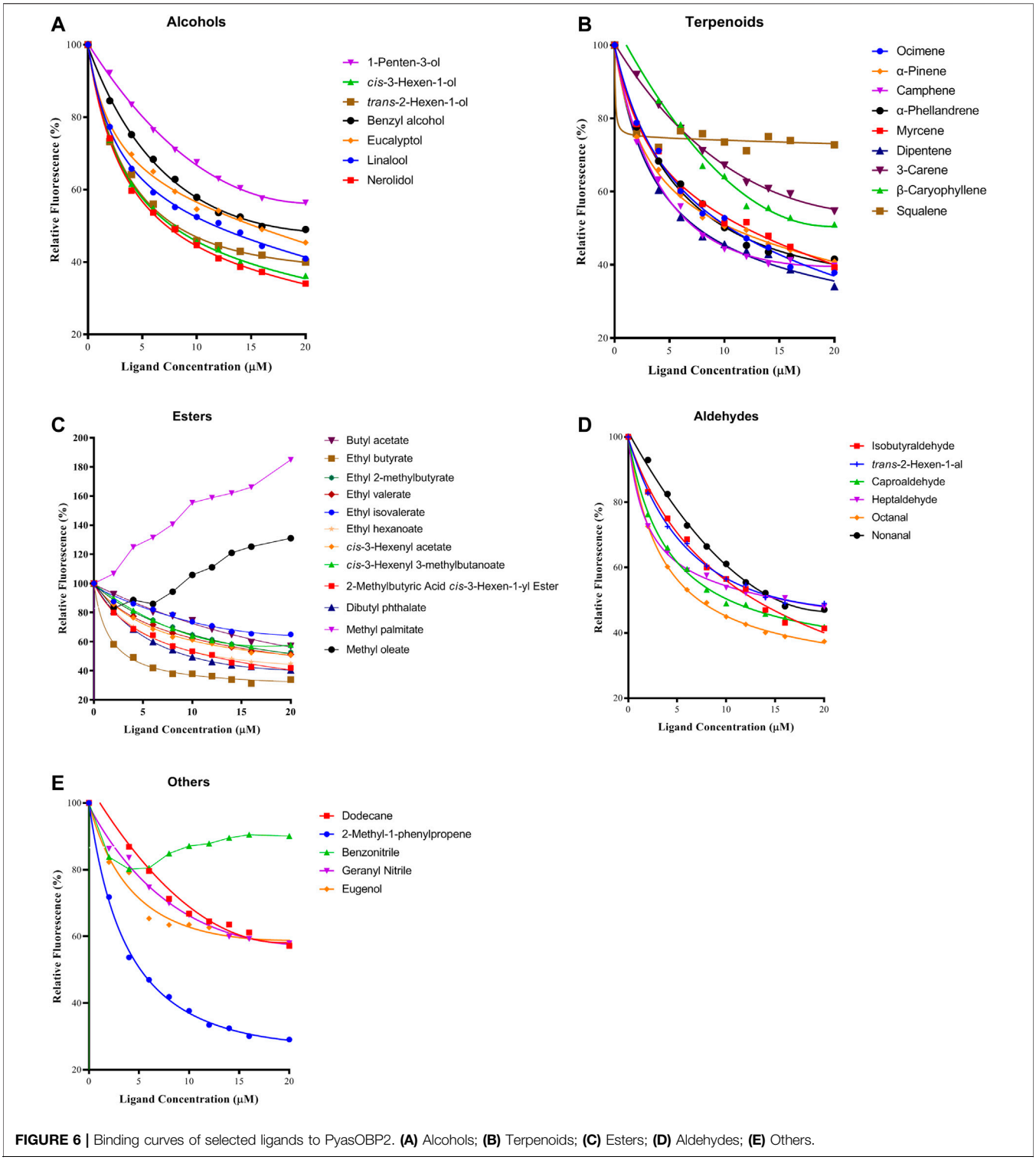

FIGURE 6 | Binding curves of selected ligands to PyasOBP2. **(A)** Alcohols; **(B)** Terpenoids; **(C)** Esters; **(D)** Aldehydes; **(E)** Others.

AgamOBP1. Therefore, *Anopheles gambiae* AgamOBP1 (2erb) was selected as the homology modeling template to generate 3D structure of PyasOBP2 (**Figure 7**). The obtained structural model of PyasOBP2 was evaluated by Verify3D and PROCHECK. In Verify3D analyses, 85.34% of residues had averaged 3D/1D score ≥ 0.2 (**Supplementary Figure S2**). The Ramachandran plot exhibited that 93.3% of amino acid residues were in most favored regions and only 1.0% of residues was in disallowed

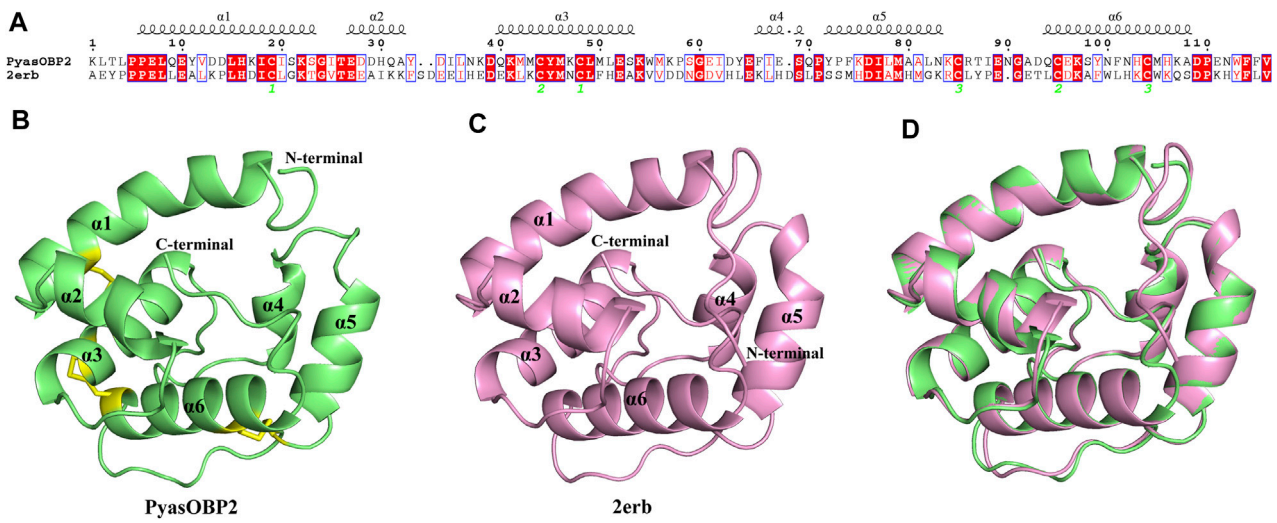

FIGURE 7 | Structural modeling of PyasOBP2. **(A)** Sequence alignment between PyasOBP2 and AgamOBP1 (2erb). **(B)** 3D structure of PyasOBP2. The N-terminal, C-terminal and six α-helices are labeled, and three disulfide bridges are colored in yellow. **(C)** 3D structure of 2erb used as the template. **(D)** Superimposed structure of PyasOBP2 and the template 2erb.

TABLE 3 | Docking results for PyasOBP2 with three ligands.

Ligandsact	Binding energy (Kcal/mol)	Residues involved in hydrogen bond	Residues involved in hydrophobic interactions	Residues involved in van der waals interactions
Ethyl butyrate	–3.71	Phe114	Met105	Asn112, Trp113
2-Methyl-1-phenylpropene	–5.85	-	Ile77, Leu78, Ala81, Met105, Phe114	Gln70, Asn112, Trp113
Dipentene	–5.92	-	Phe74, Ile77, Leu78, Ala81, Met105, Phe114	Gln70, Asn112, Trp113

regions (**Supplementary Figure S3**), suggesting that the predicted model of PyasOBP2 is reasonable and reliable (Bowie et al., 1991; Lüthy et al., 1992). The predicted 3D structure of PysOBP2 consisted of six α-helices, including α1 (Pro6-Ser23), α2 (Glu27-Ala32), α3 (Gln40-Ser53), α4 (Phe66-Ser69), α5 (Tyr72-Asn83), and α6 (Gln94-Ala108) (**Figure 7A**). Among these, five α-helices (α1, α3, α4, α5 and α6), together with three pairs of disulfide bridges (Cys19 in α1 and Cys48 in α3, Cys44 in α3 and Cys95 in α6, Cys85 in α5 and Cys104 in α6), formed the hydrophobic binding pocket (**Figure 7B**).

To further explore the characteristics of PyasOBP2 binding sites, three ligands (i.e., ethyl butyrate, 2-methyl-1-phenylpropene, and dipentene), which exhibited very high binding affinities (K_i values from 3.02 to 5.99 μM) for PyasOBP2 in binding assays were selected for molecular docking. The docking results showed that the ligands bound in the PyasOBP2 pocket with negative energy values (**Table 3**). The 2D and 3D binding interactions, as well as the optimal orientation and conformation of three ligands in the hydrophobic cavity, were shown in **Figure 8**. We found that hydrogen bonds (Phe114), hydrophobic interactions (Met105) and van der Waals interactions (Asn112, Trp113) were the main interactions involved in binding of PyasOBP2 with ethyl butyrate (**Table 3**). For binding with 2-methyl-1-phenylpropene and dipentene, similar interactions were found involving main residues of Ile77, Leu78, Ala81, Met105, Phe114, Gln70, Asn112, and Trp113. Among these residues, Ile77, Leu78, Ala81, Met105, and Phe114 were mainly involved in hydrophobic interactions, whereas Gln70, Asn112, and Trp113 contributed the most to van der Waals interactions (**Figure 8**; **Table 3**).

DISCUSSION

In the present study, we cloned and characterized the OBP gene *PyasOBP2*, based on the antennal transcriptome of *P. yasumatsui*. PyasOBP2 has an N-terminal signal peptide containing 19 amino acids, and possesses six conserved cysteine residues that follow the typical pattern of classic OBPs: C_1-X_{24}-C_2-X_3-C_3-X_{36}-C_4-X_9-C_5-X_8-C_6. Phylogenetic analyses showed that the closest homolog of PyasOBP2 was SzeaOBP8 from *S. zeamais* (76.27% sequence identity). Expression profile analyses showed that *PyasOBP2* was most highly expressed in the antennae of both males and females, but it was almost not expressed in all other tissues, implying that PyasOBP2 may play potential roles in perception of host plant

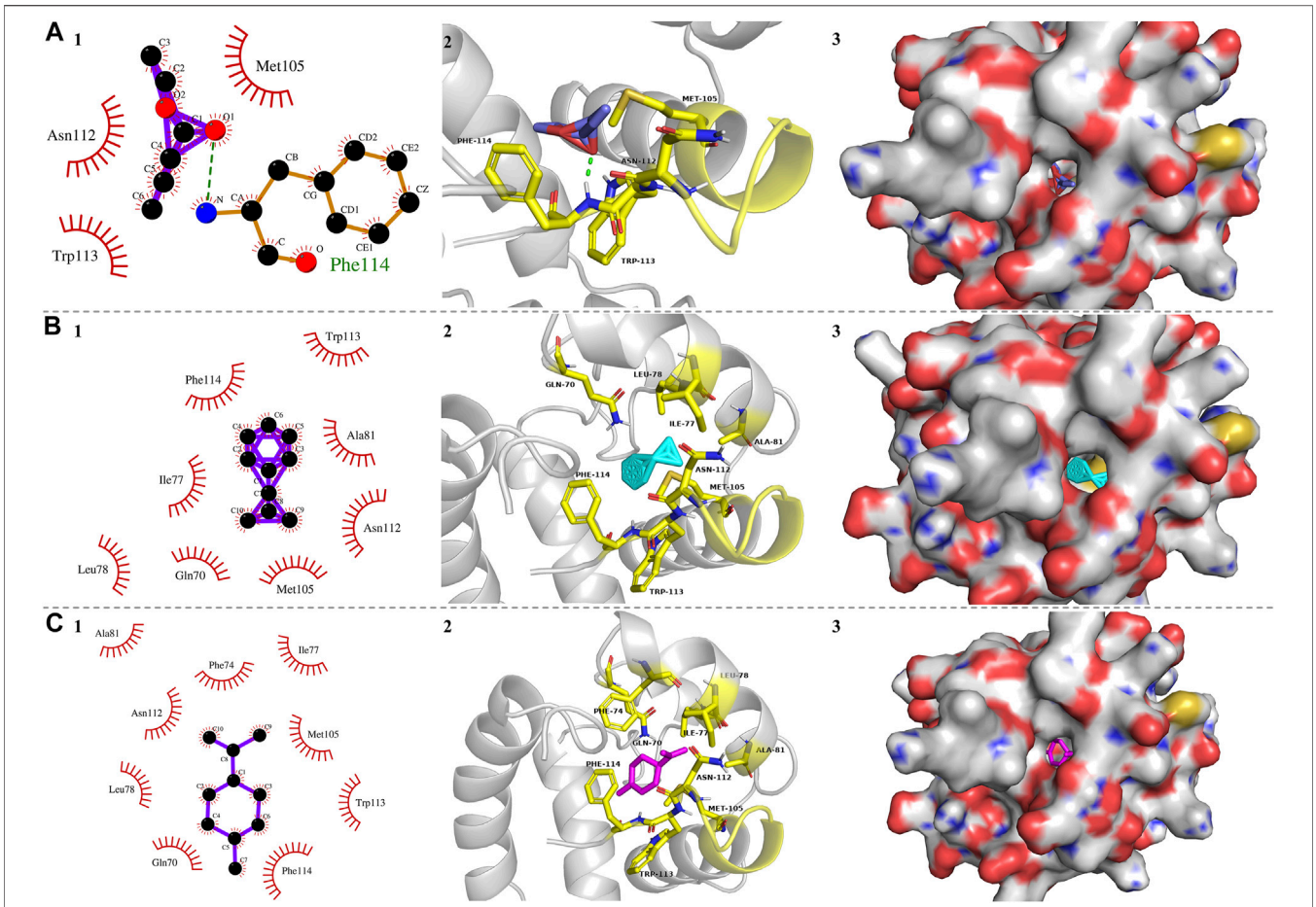

FIGURE 8 | Molecular docking of PyasOBP2 with **(A)** Ethyl butyrate, **(B)** 2-Methyl-1-phenylpropene, and **(C)** Dipentene. **(1)** Key residues of PyasOBP2 involved in main interactions (2D). The hydrogen bond was marked with green dot line. **(2)** Key residues of PyasOBP2 involved in main interactions (3D). **(3)** The optimal orientation and conformation of different ligands in the hydrophobic cavity formed by hydrophobic residues of PyasOBP2.

odors (Sun et al., 2014; Li et al., 2017; He et al., 2019). Expression levels of *PyasOBP2* in antennae were significantly higher in males than those in females. This male-biased expression suggested that PyasOBP2 may detect pheromones released by females and play the same roles as pheromone binding proteins (PBPs) (Gong et al., 2014; Khuhro et al., 2017; Cui et al., 2018). However, sex pheromones are still unknown in *P. yasumatsui*. Thus, we leave this issue as a potential direction for future work.

OBPs were thought to be capable of binding to host plant volatiles (Vogt et al., 2015; Brito et al., 2016). In this study, we characterized the binding activities of PyasOBP2 to 38 selected volatiles from *Z. jujuba*. The fluorescence competitive binding assays showed that PyasOBP2 could bind with a wide range of volatile ligands (K_i<20 μM), such as alcohols, terpenoids, esters and aldehydes, implying it had a broad ligand-binding affinity. Previous studies have proved that three plant volatiles, ocimene, nonanal and methyl palmitate, could elicite strong EAG responses in adult *P. yasumatsui* antennae (Yan et al., 2017; Yan et al., 2020). However, our results indicated that PyasOBP2 exhibited strong and moderate binding affinity with ocimene (K_i<10 μM) and nonanal (K_i<20 μM), respectively, whereas it was incapable of binding with methyl palmitate (K_i>20 μM), suggesting that an OBP could only bind with some specific odors during the process of insect chemoreception (Zhang et al., 2020), and further studies on other OBPs from *P. yasumatsui* are needed to confirm this. Additionally, PyasOBP2 showed different binding affinities to some isomers, such as dipentene (K_i<5 μM) and 3-carene (K_i>20 μM), as well as ethyl butyrate (K_i<5 μM) and butyl acetate (K_i>20 μM), and it could not bind to some volatile ligands with more than 16 carbon atoms (such as methyl palmitate, methyl oleate and squalene), indicating that the size and structure of ligands, as well as their conformational changes, could affect the binding affinity for OBPs (Sandler et al., 2000; Christina et al., 2017).

In general, the 3D structure of OBPs contains a hydrophobic binding pocket formed by several α-helices, and some residues located in the pocket can be the potential binding sites in interactions between OBPs and ligands (Sandler et al., 2000). For instance, Tyr111 of HoblOBP1 is involved in the binding of hexyl benzoate (Zhuang et al., 2014); in LstiGOBP1, Thr15, Trp43, and Val14 play a key role in the binding wtih 1-heptanol (Yin et al., 2015), and Thr9, Val111, and Val114 are

involved in the binding of dodecanol with GmolGOBP2 (Li et al., 2016). As the ligands with best binding affinity to PyasOBP2, ethyl butyrate, 2-methyl-1-phenylpropene, and dipentene were selected for docking with PyasOBP2. The molecular docking results showed that several hydrophobic residues (Leu8, Val12, Met46, Leu49, Met50, Trp55, Ile67, Gln70, Phe74, Ile77, Leu78, Ala81, Phe101, Asn102, and Met105) of PyasOBP2 could form a hydrophobic pocket important for ligand binding, and the residue Phe114 might contribute to the formation of hydrogen bonds in binding with some esters.

Except for hydrogen bonds, hydrophobic interactions and van der Waals interactions between insect OBPs and ligands are also crucial for ligand binding (Fu et al., 2018; Li et al., 2021). For binding with 2-methyl-1-phenylpropene and dipentene, Phe114 contributed the most to hydrophobic interactions. Met105 was mainly involved in hydrophobic interactions, whereas Asn112 and Trp113 might have affected the formation of van der Waals interactions in binding of PyasOBP2 with three ligands. Besides, the loop in the C-terminal of PyasOBP2 could act as a lid to cover the binding pocket, and some residues of this loop, such as Asn112, Trp113, and Phe114, could play a key role in the binding with some ligands. Similar results were reported in AgamOBP1 from *Anopheles gambiae* (Wogulis et al., 2006), HarmOBP7 from *Helicoverpa armigera* (Sun et al., 2013) and HoblOBP1 from *Holotrichia oblita* (Zhuang et al., 2014). Such a structure could function to prevent ligands from getting out of the pocket and strengthen the binding ability of PyasOBP2.

Overall, the OBP gene *PyasOBP2* from *P. yasumatsui* was reported for the first time, and this OBP demonstrated an antenna-specific expression pattern, as well as broad ligand-binding capability, providing evidence for the possible olfactory roles of OBPs in perceiving host plant odors of *P. yasumatsui*. Our molecular docking results indicated that the amino acid residue Phe114 of PyasOBP2 may be a key binding site, especially for some volatile ligands like ethyl butyrate, 2-methyl-1-phenylpropene and dipentene. In future studies, site-directed mutagenesis and RNAi experiments are needed to further clarify the importance of specific residues in PyasOBP2.

DATA AVAILABILITY STATEMENT

The original contributions presented in the study are included in the article/**Supplementary Material**, further inquiries can be directed to the corresponding author.

AUTHOR CONTRIBUTIONS

BH and FZ conceived and designed the experimental plan. BH, QC, YZ, and BR performed the experiments. BH, QC, and FZ analyzed and processed data. BH, QC, and FZ wrote and edited the manuscript.

FUNDING

This work was supported by the CAS "Light of West China" Program (Grant No. XAB2019AW15), the Doctoral Start-up Fund of Shaanxi Academy of Sciences (Grant No. 2020K-31), and Science and Technology Innovation Program of Shaanxi Academy of Forestry (Grant No. SXLK2020-0216).

ACKNOWLEDGMENTS

The authors would like to thank Guangwei Li (Shaanxi Province Key Laboratory of Jujube, Yan'an University, China) for his assistance in fluorescence competitive binding assays and Prof. Deguang Liu (Key Laboratory of Applied Entomology, Northwest A&F University, China) for his helpful suggestions on our initial manuscript.

SUPPLEMENTARY MATERIAL

The Supplementary Material for this article can be found online at: https://www.frontiersin.org/articles/10.3389/fphys.2022.900752/full#supplementary-material

REFERENCES

Bowie, J. U., Lüthy, R., and Eisenberg, D. (1991). A Method to Identify Protein Sequences that Fold into a Known Three-Dimensional Structure. *Science* 253 (5016), 164–170. doi:10.1126/science.1853201

Brito, N. F., Moreira, M. F., and Melo, A. C. A. (2016). A Look inside Odorant-Binding Proteins in Insect Chemoreception. *J. Insect Physiol.* 95, 51–65. doi:10.1016/j.jinsphys.2016.09.008

Cousins, K. R. (2011). Computer Review of Chemdraw Ultra 12.0. *J. Am. Chem. Soc.* 133, 8388. doi:10.1021/ja204075s

Cui, X., Liu, D., Sun, K., He, Y., and Shi, X. (2018). Expression Profiles and Functional Characterization of Two Odorant-Binding Proteins from the Apple Buprestid Beetle *Agrilus mali* (Coleoptera: Buprestidae). *J. Econ. Entomol.* 111, 1420–1432. doi:10.1093/jee/toy066

De Bruyne, M., and Baker, T. C. (2008). Odor Detection in Insects: Volatile Codes. *J. Chem. Ecol.* 34, 882–897. doi:10.1007/s10886-008-9485-4

Deng, S., Yin, J., Zhong, T., Cao, Y., and Li, K. (2012). Function and Immunocytochemical Localization of Two Novel Odorant-Binding Proteins in Olfactory Sensilla of the Scarab Beetle Holotrichia Oblita Faldermann (Coleoptera: Scarabaeidae). *Chem. Senses* 37, 141–150. doi:10.1093/chemse/bjr084

Drakou, C. E., Tsitsanou, K. E., Potamitis, C., Fessas, D., Zervou, M., and Zographos, S. E. (2017). The crystal Structure of the AgamOBP1Icaridin Complex Reveals Alternative Binding Modes and Stereo-Selective Repellent Recognition. *Cell. Mol. Life Sci.* 74, 319–338. doi:10.1007/s00018-016-2335-6

Elgar, M. A., Zhang, D., Wang, Q., Wittwer, B., Thi Pham, H., Johnson, T. L., et al. (2018). Insect Antennal Morphology: the Evolution of Diverse Solutions to Odorant Perception. *Yale J. Biol. Med.* 91, 457–469. Available at: https://pubmed.ncbi.nlm.nih.gov/30588211/

Fu, X.-B., Zhang, Y.-L., Qiu, Y.-L., Song, X.-M., Wu, F., Feng, Y.-L., et al. (2018). Physicochemical Basis and Comparison of Two Type II Sex Pheromone Components Binding with Pheromone-Binding Protein 2 from tea Geometrid, *Ectropis Obliqua*. *J. Agric. Food Chem.* 66, 13084–13095. doi:10.1021/acs.jafc.8b04510

Gong, Z.-J., Miao, J., Duan, Y., Jiang, Y.-L., Li, T., and Wu, Y.-Q. (2014). Identification and Expression Profile Analysis of Putative Odorant-Binding

Proteins in *Sitodiplosis Mosellana* (Gehin) (Diptera: Cecidomyiidae). *Biochem. Biophysical Res. Commun.* 444, 164–170. doi:10.1016/j.bbrc.2014.01.036

He, P., Chen, G. L., Li, S., Wang, J., Ma, Y. F., Pan, Y. F., et al. (2019). Evolution and Functional Analysis of Odorant-binding Proteins in Three rice Planthoppers: Nilaparvata Lugens , Sogatella Furcifera , and Laodelphax Striatellus. *Pest Manag. Sci.* 75, 1606–1620. doi:10.1002/ps.5277

Hekmat-Scafe, D. S., Scafe, C. R., McKinney, A. J., and Tanouye, M. A. (2002). Genome-wide Analysis of the Odorant-Binding Protein Gene Family in *Drosophila melanogaster*. *Genome Res.* 12, 1357–1369. doi:10.1101/gr.239402

Hong, B., Zhang, F., Li, Y. M., Zhang, S. L., and Chen, Z. J. (2017). Spatial distribution of *Scythropus yasumatsui* Kono et Morimoto adults in jujube orchard of Northern Shaanxi. *Plant Prot.* 43 (6), 113–117. doi:10.3969/j.issn.0529-1542.2017.06.018

Huang, W. Z., and Li, D. Z. (1993). Studies on Spatial Distribution Pattern of *Scythropus Yasumatsui* Larvae. *Chin. B. Entomol.* 6, 348–350. Available at: https://kns.cnki.net/kcms/detail/detail.aspx?dbcode=CJFD&dbname=CJFD9093&filename=KCZS199306013&uniplatform=NZKPT&v=8xA0Ljt-7XfzvypQEMsH6gyBzrhAV9O21YXnzFHz5JgTjqY3C9Ui6jU24jV0nBEd

Jacquin-Joly, E., Bohbot, J., Francois, M.-C., Cain, A.-H., and Nagnan-Le Meillour, P. (2000). Characterization of the General Odorant-Binding Protein 2 in the Molecular Coding of Odorants in *Mamestra Brassicae*. *FEBS J.* 267 (22), 6708–6714. doi:10.1046/j.1432-1327.2000.01772.x

Ju, Q., Qu, M.-j., Wang, Y., Jiang, X.-j., Li, X., Dong, S.-l., et al. (2012). Molecular and Biochemical Characterization of Two Odorant-Binding Proteins from Dark Black Chafer, *Holotrichia Parallela*. *Genome* 55, 537–546. doi:10.1139/g2012-042

Justice, R. W., Biessmann, H., Walter, M. F., Dimitratos, S. D., and Woods, D. F. (2003). Genomics Spawns Novel Approaches to Mosquito Control. *BioEssays* 25 (10), 1011–1020. doi:10.1002/bies.10331

Khuhro, S. A., Liao, H., Dong, X.-T., Yu, Q., Yan, Q., and Dong, S.-L. (2017). Two General Odorant Binding Proteins Display High Bindings to Both Host Plant Volatiles and Sex Pheromones in a Pyralid Moth *Chilo Suppressalis* (Lepidoptera: Pyralidae). *J. Asia-Pacific Entomol.* 20, 521–528. doi:10.1016/j.aspen.2017.02.015

Kôno, H., and Morimoto, K. (1960). Curculionidae from Shansi, North China (Coleoptera). *Mushi* 34 (2), 71–87. Available at: https://ukrbin.com/literature.php?id=1068&action=reltaxa

Kumar, S., Stecher, G., Li, M., Knyaz, C., and Tamura, K. (2018). MEGA X: Molecular Evolutionary Genetics Analysis across Computing Platforms. *Mol. Biol. Evol.* 35, 1547–1549. doi:10.1093/molbev/msy096

Laughlin, J. D., Ha, T. S., Jones, D. N. M., and Smith, D. P. (2008). Activation of Pheromone-Sensitive Neurons Is Mediated by Conformational Activation of Pheromone-Binding Protein. *Cell* 133, 1255–1265. doi:10.1016/j.cell.2008.04.046

Leal, W. S. (2013). Odorant Reception in Insects: Roles of Receptors, Binding Proteins, and Degrading Enzymes. *Annu. Rev. Entomol.* 58, 373–391. doi:10.1146/annurev-ento-120811-153635

Li, G., Chen, X., Li, B., Zhang, G., Li, Y., and Wu, J. (2016). Binding Properties of General Odorant Binding Proteins from the oriental Fruit Moth, *Grapholita Molesta* (Busck) (Lepidoptera: Tortricidae). *PLoS ONE* 11, e0155096. doi:10.1371/journal.pone.0155096

Li, L., Zhou, Y.-T., Tan, Y., Zhou, X.-R., and Pang, B.-P. (2017). Identification of Odorant-Binding Protein Genes inGaleruca daurica(Coleoptera: Chrysomelidae) and Analysis of Their Expression Profiles. *Bull. Entomol. Res.* 107, 550–561. doi:10.1017/S0007485317000402

Li, D., Li, C., and Liu, D. (2021). Analyses of Structural Dynamics Revealed Flexible Binding Mechanism for the Agrilus mali Odorant Binding Protein 8 towards Plant Volatiles. *Pest Manag. Sci.* 77 (4), 1642–1653. doi:10.1002/ps.6184

Livak, K. J., and Schmittgen, T. D. (2001). Analysis of Relative Gene Expression Data Using Real-Time Quantitative PCR and the $2^{-\Delta\Delta CT}$ Method. *Methods* 25, 402–408. doi:10.1006/meth.2001.1262

Lüthy, R., Bowie, J. U., and Eisenberg, D. (1992). Assessment of Protein Models with Three-Dimensional Profiles. *Nature* 356 (6364), 83–85. doi:10.1016/S0076-6879(97)77022-8

Northey, T., Venthur, H., De Biasio, F., Chauviac, F.-X., Cole, A., Ribeiro, K. A. L., et al. (2016). Crystal Structures and Binding Dynamics of Odorant-Binding Protein 3 from Two Aphid Species *Megoura Viciae* and *Nasonovia Ribisnigri*. *Sci. Rep.* 6, 24739. doi:10.1038/srep24739

Pelosi, P., Zhou, J.-J., Ban, L. P., and Calvello, M. (2006). Soluble Proteins in Insect Chemical Communication. *Cell. Mol. Life Sci.* 63, 1658–1676. doi:10.1007/s00018-005-5607-0

Pelosi, P., Iovinella, I., Felicioli, A., and Dani, F. R. (2014). Soluble Proteins of Chemical Communication: an Overview across Arthropods. *Front. Physiol.* 5, 320. doi:10.3389/fphys.2014.00320

Pelosi, P., Iovinella, I., Zhu, J., Wang, G., and Dani, F. R. (2018). Beyond Chemoreception: Diverse Tasks of Soluble Olfactory Proteins in Insects. *Biol. Rev.* 93, 184–200. doi:10.1111/brv.12339

Ren, D. Z., and Qi, X. Y. (2009). Preliminary Study on the Control of *Scythropus Yasumatsui* in Northern Shaanxi. *J. Hebei Agric. Sci.* 13 (6), 40–41. doi:10.3969/j.issn.1088-1631.2009.06.019

Sánchez-Gracia, A., Vieira, F. G., and Rozas, J. (2009). Molecular Evolution of the Major Chemosensory Gene Families in Insects. *Heredity* 103, 208–216. doi:10.1038/hdy.2009.55

Sandler, B. H., Nikonova, L., Leal, W. S., and Clardy, J. (2000). Sexual Attraction in the Silkworm Moth: Structure of the Pheromone-Binding-Protein-Bombykol Complex. *Chem. Biol.* 7, 143–151. doi:10.1016/S1074-5521(00)00078-8

Sideris, E. E., Valsami, G. N., Koupparis, M. A., and Macheras, P. E. (1992). Determination of Association Constants in Cyclodextrin/drug Complexation Using the Scatchard Plot: Application to Beta-Cyclodextrinanilinonaphthalenesulfonates. *Pharm. Res.* 09, 1568–1574. doi:10.1023/a:1015808307322

Sun, Y.-L., Huang, L.-Q., Pelosi, P., and Wang, C.-Z. (2013). A Lysine at the C-Terminus of an Odorant-Binding Protein Is Involved in Binding Aldehyde Pheromone Components in Two Helicoverpa Species. *PLoS ONE* 8, e55132. doi:10.1371/journal.pone.0055132

Sun, L., Xiao, H.-J., Gu, S.-H., Zhou, J.-J., Guo, Y.-Y., Liu, Z.-W., et al. (2014). The Antenna-specific Odorant-Binding Protein AlinOBP13 of the Alfalfa Plant bugAdelphocoris Lineolatusis Expressed Specifically in Basiconic Sensilla and Has High Binding Affinity to Terpenoids. *Insect Mol. Biol.* 23, 417–434. doi:10.1111/imb.12089

Tang, X. L., Zhao, H. Z., and Zhang, X. W. (2013). Techniques for the Control of *Scythropus Yasumatsui* in the Northern Shaanxi. *Shaanxi For. Sci. Technol.* 4, 131–132. doi:10.3969/j.issn.1001-2117.2013.04.044

Vandesompele, J., De Preter, K., Pattyn, F., Poppe, B., Van Roy, N., De Paepe, A., et al. (2002). Accurate Normalization of Real-Time Quantitative RT-PCR Data by Genometric Averaging of Multiple Internal Control Genes. *Genome Biol.* 3, research0034. RESEARCH0034. doi:10.1186/gb-2002-3-7-research0034

Venthur, H., Mutis, A., Zhou, J.-J., and Quiroz, A. (2014). Ligand Binding and Homology Modelling of Insect Odorant-Binding Proteins. *Physiol. Entomol.* 39, 183–198. doi:10.1111/phen.12066

Venthur, H., and Zhou, J.-J. (2018). Odorant Receptors and Odorant-Binding Proteins as Insect Pest Control Targets: a Comparative Analysis. *Front. Physiol.* 9, 1163. doi:10.3389/fphys.2018.01163

Vogt, R. G., Große-Wilde, E., and Zhou, J.-J. (2015). The Lepidoptera Odorant Binding Protein Gene Family: Gene Gain and Loss within the GOBP/PBP Complex of Moths and Butterflies. *Insect Biochem. Mol. Biol.* 62, 142–153. doi:10.1016/j.ibmb.2015.03.003

Vogt, R. G., and Riddiford, L. M. (1981). Pheromone Binding and Inactivation by Moth Antennae. *Nature* 293, 161–163. doi:10.1038/293161a0

Vosshall, L. B., Amrein, H., Morozov, P. S., Rzhetsky, A., and Axel, R. (1999). A Spatial Map of Olfactory Receptor Expression in the Drosophila Antenna. *Cell* 96, 725–736. doi:10.1016/S0092-8674(00)80582-6

Wang, J. L., Hong, B., Chen, Z. J., Lian, Z. M., Zhang, S. L., Li, Y. M., et al. (2017). The Olfactory Response of *Scythropus Yasumatsui* to Volatiles of Different Jujube Cultivars. *J. Environ. Entomol.* 39 (6), 1273–1280. doi:10.3969/j.issn.1674-0858.2017.06.12

Wang, H., Chen, H., Wang, Z., Liu, J., Zhang, X., Li, C., et al. (2019). Molecular Identification, Expression, and Functional Analysis of a General Odorant-Binding Protein 1 of Asian Citrus Psyllid. *Environ. Entomol.* 48 (1), 245–252. doi:10.1093/ee/nvy179

Webb, B., and Sali, A. (2016). Comparative Protein Structure Modeling Using Modeller. *Curr. Protoc. Protein Sci.* 86, 2–37. doi:10.1002/cpps.20

Wogulis, M., Morgan, T., Ishida, Y., Leal, W. S., and Wilson, D. K. (2006). The crystal Structure of an Odorant Binding Protein from *Anopheles gambiae*:

Evidence for a Common Ligand Release Mechanism. *Biochem. Biophysical Res. Commun.* 339, 157–164. doi:10.1016/j.bbrc.2005.10.191

Wu, Z., Lin, J., Zhang, H., and Zeng, X. (2016). BdorOBP83a-2 Mediates Responses of the oriental Fruit Fly to Semiochemicals. *Front. Physiol.* 7, 452. doi:10.3389/fphys.2016.00452

Yan, X. F., Liu, Y. H., Li, G., Qiang, D. H., and Xu, Y. P. (2017). EAG and Olfactory Behavioral Responses of *Scythropus Yasumatsui* to Volatiles from the Zizyphus Jujube. *Chin. J. Appl. Entomol.* 54 (4), 621–628. doi:10.7679/j.issn.2095-1353.2017.076

Yan, X. F., Liu, Y. H., Wang, Y. W., Li, G., Jing, R., and Yang, Y. J. (2020). EAG and Behavioral Responses of *Scythropus Yasumatsui* (Coleoptera: Curculionidae) to Volatiles from the Common Jujube (*Zizyphus Jujuba*). *Acta Entomol. Sin.* 63 (8), 981–991. doi:10.16380/j.kcxb.2020.08.008

Yang, B., Zhang, N., Yan, X. F., Liu, Y. H., Lv, P. B., and Shen, J. (2019). Control efficiency of several pesticides on *Scythropus yasumatsui* Kono et Morimoto. *J. Shanxi Agric. Sci.* 47 (4), 668–672. doi:10.3969/j.issn.1002-2481.2019.04.41

Yin, J., Zhuang, X., Wang, Q., Cao, Y., Zhang, S., Xiao, C., et al. (2015). Three Amino Acid Residues of an Odorant-Binding Protein Are Involved in Binding Odours inLoxostege sticticalisL. *Insect Mol. Biol.* 24 (5), 528–538. doi:10.1111/imb.12179

Zhang, F., Merchant, A., Zhao, Z., Zhang, Y., Zhang, J., Zhang, Q., et al. (2020). Characterization of MaltOBP1, a Minus-C Odorant-Binding Protein, from the Japanese Pine Sawyer Beetle, *Monochamus Alternatus* Hope (Coleoptera: Cerambycidae). *Front. Physiol.* 11, 212. doi:10.3389/fphys.2020.00212

Zhou, J.-J. (2010). Odorant-binding Proteins in Insects. *Vitam. Horm.* 83, 241–272. doi:10.1016/S0083-6729(10)83010-9

Zhuang, X., Wang, Q., Wang, B., Zhong, T., Cao, Y., Li, K., et al. (2014). Prediction of the Key Binding Site of Odorant-Binding Protein ofHolotrichia Oblita Faldermann (Coleoptera: Scarabaeida). *Insect Mol. Biol.* 23 (3), 381–390. doi:10.1111/imb.12088

Conflict of Interest: The authors declare that the research was conducted in the absence of any commercial or financial relationships that could be construed as a potential conflict of interest.

Publisher's Note: All claims expressed in this article are solely those of the authors and do not necessarily represent those of their affiliated organizations, or those of the publisher, the editors and the reviewers. Any product that may be evaluated in this article, or claim that may be made by its manufacturer, is not guaranteed or endorsed by the publisher.

Copyright © 2022 Hong, Chang, Zhai, Ren and Zhang. This is an open-access article distributed under the terms of the Creative Commons Attribution License (CC BY). The use, distribution or reproduction in other forums is permitted, provided the original author(s) and the copyright owner(s) are credited and that the original publication in this journal is cited, in accordance with accepted academic practice. No use, distribution or reproduction is permitted which does not comply with these terms.

frontiers | Frontiers in Physiology

ORIGINAL RESEARCH
published: 04 May 2022
doi: 10.3389/fphys.2022.877133

Spatial Expression Analysis of Odorant Binding Proteins in Both Sexes of the Aphid Parasitoid *Aphidius gifuensis* and Their Ligand Binding Properties

Xin Jiang[1,2†], *Yaoguo Qin*[1,3†], *Jun Jiang*[1], *Yun Xu*[4], *Frédéric Francis*[2], *Jia Fan*[1*] and *Julian Chen*[1*]

[1]State Key Laboratory for Biology of Plant Diseases and Insect Pests, Institute of Plant Protection, Chinese Academy of Agricultural Sciences, Beijing, China, [2]Functional and Evolutionary Entomology, Gembloux Agro-Bio Tech, University of Liège, Gembloux, Belgium, [3]Department of Entomology and MOA Key Laboratory for Monitoring and Environment-Friendly Control of Crop Pests, College of Plant Protection, China Agricultural University, Beijing, China, [4]Agricultural Environment and Resources Institute of YAAS, Kunming, China

OPEN ACCESS

Edited by:
Rui Tang,
Guangdong Academy of Science (CAS), China

Reviewed by:
Hao Guo,
Chinese Academy of Sciences (CAS), China
Peng He,
Guizhou University, China

***Correspondence:**
Jia Fan
jfan@ippcaas.cn
Julian Chen
chenjulian@caas.cn

[†]These authors have contributed equally to this work

Specialty section:
This article was submitted to Invertebrate Physiology, a section of the journal Frontiers in Physiology

Received: 16 February 2022
Accepted: 18 March 2022
Published: 04 May 2022

Citation:
Jiang X, Qin Y, Jiang J, Xu Y, Francis F, Fan J and Chen J (2022) Spatial Expression Analysis of Odorant Binding Proteins in Both Sexes of the Aphid Parasitoid Aphidius gifuensis and Their Ligand Binding Properties. Front. Physiol. 13:877133. doi: 10.3389/fphys.2022.877133

In China, *Aphidius gifuensis* is one of the most common endoparasitoids of the green peach aphid *Myzus persicae* and grain aphid *Sitobion miscanthi* in the field. Insect odorant-binding proteins (OBPs) play vital roles in odor perception during feeding, host searching, mating and oviposition. In addition, some OBPs are involved in other physiological processes such as gustation and reproduction. In the present study, a comparative antennal transcriptomic analysis was applied between male and female *A. gifuensis*. The spatial expression patterns among antennae, heads, thoraxes, abdomens and legs of OBPs in both sexes were further profiled. Fifteen *AgifOBP*s were predicted, and 14 of them were identified by gene cloning, including 12 classic OBPs and 2 min-C OBPs. As expected, all OBPs were mainly expressed at high levels in antennae, heads or legs which are sensory organs and tissues. Finally, ligand binding properties of 2 OBPs (AgifOBP7 and AgifOBP9) were further evaluated. Female leg specifically expressed AgifOBP9 displays a broad and high binding property to aphid alarm pheromones, plant green volatiles and aphid sex pheromones (Ki < 10 μM). However, female leg specifically expressed AgifOBP7 displays poor affinity for all tested ligands except CAU-II-11 ((E)-3,7-dimethylocta-2,6-dien-1-yl-2-hydroxy-3-methoxybenzoate), a reported (E)-β-farnesene (EBF) analog with an exceptionally high binding affinity (Ki = 1.07 ± 0.08 μM). In summary, we reported the spatial expression pattern of the OBP repertoire in *A. gifuensis*, and further studied the binding properties of OBP7 and OBP9, which are mainly expressed in female legs, laying the foundation for the dissection of the contribution of OBPs to chemosensation in *A. gifuensis*.

Keywords: *Aphidifus gifuensis*, transcriptome, odorant binding protein, spatial expression pattern, fluorescence binding assay

INTRODUCTION

Aphidius gifuensis is one of the most common endoparasitoids of green peach aphid *Myzus persicae* and grain aphid *Sitobion miscanthi* in China. *S. miscanthi* is also habitually called *Sitobion avenae* in China (Zhang, 1999; Jiang et al., 2019), and is the undisputed dominant Chinese dominant pest of wheat. Aphids has long been the most damaging pest of crops and vegetables, causing yield and quality losses by stealing nutrients, transferring plant viruses, and excreting honeydew to block plant photosynthesis (Wu, 2002). In Yunnan and many other areas of China, *M. persicae* on tobacco has been successfully controlled by artificially released *A. gifuensis* as a powerful biocontrol tool (Ohta and Honda, 2010; Yang et al., 2009).

The behavioral response of insects to olfactory cues is essentially driven by feeding, reproduction and habitat selection (Pelosi et al., 2014). Molecular odorants enter the sensilla through pores and spread inside the hemolymph on the antennae due to odorant-binding proteins (OBPs) and/or chemosensory proteins (CSPs) (Pelosi et al., 2006; Leal, 2013). These odorants are then transported to olfactory receptors (ORs), ionotropic receptors (IRs), or sensory neuron membrane proteins (SNMPs), from which the chemical signals will be transmitted into electrophysiological signals for the brain (Leal, 2013; Pelosi et al., 2018). Insect OBPs were initially discovered in antennae of the moth *Antheraea polyphemus* (Vogt and Riddiford, 1981). Their wide distributions in antennal sensilla indicated the first link of OBPs in the signal chain of odorant perception (Xu et al., 2009). OBPs are tiny, globular, water-soluble proteins with a molecular weight of 10–30 kDa (Pelosi et al., 2005). The presence of six highly conserved cysteine residues, which are paired in three interlocking disulfide bridges to maintain the protein's tertiary structure, is a common feature of classical OBPs (Pelosi et al., 2014). OBPs act as shuttles for hydrophobic odor molecules, transporting them through the sensillum lymph to odorant receptors (Zhou et al., 2010). After initiating receptors, OBPs may also concentrate odorants in the sensillum lymph and swiftly destroy odorant molecules (Vogt and Riddiford, 1981; Leal, 2013). The prediction of the whole OBP family in species became quite simple due to the availability of more insect genomes and transcriptomes using next-generation sequencing techniques. However, the number of OBPs in Hymenoptera varies; for example, *Apis mellifera* has 21 OBPs, *Microplitis mediator* has 18 OBPs, *Pieris rapae* has 14 OBPs, *Spodoptera exigua* has 34 OBPs, *Cotesia vestalis* has 20 OBPs, and 90 OBPs were predicted in *Nasonia vitripennis* (Forêt and Maleszka, 2006; Vieira et al., 2012; Liu et al., 2015; Peng et al., 2017; Li et al., 2020; Liu et al., 2020; Zhou et al., 2021). Insect OBPs not only are expressed in the chemosensory system, but also occur in nonsensory tissues and organs, such as the cornicles (Wang et al., 2021a), thoraxes (Xue et al., 2016; Gao et al., 2018; Wang et al., 2019), reproductive organs (Li et al., 2008; Sun et al., 2012b), mandibular glands (Iovinella et al., 2011), salivary glands (Zhang et al., 2017), and wings (Calvello et al., 2003; Pelosi et al., 2005; Wang et al., 2021b). Some insect OBPs have physiological functions other than binding odorants. For example, the sperm carrier function of OBPs has been reported in the male reproductive apparatus of mosquitoes (Li et al., 2008). Moreover, one OBP expressed by male moths is found on the surface of fertilized eggs, which functions to avoid cannibalistic behaviors among larvae (Sun et al., 2012b). Therefore, spatial expression patterns would be helpful to classify and analyze the possible functions of OBPs.

Herbivore-induced volatiles (HIPVs), green leaf volatiles (GLVs), and pheromones such as the aphid alarm pheromone E-beta-farnesene (EBF) are used by natural enemies to find their prey during predation and parasitism (Dong et al., 2008; CMD De Moraes et al., 1998; Buitenhuis et al., 2004). *A. gifuensis* evolved a comprehensive chemosensory system to effectively detect the semiochemical cues of its host and plants (Yang et al., 2009). For example, *A. gifuensis* can distinguish healthy, mechanically damaged, and aphid-infested plants (Dong et al., 2008). Additionally, both female and male *A. gifuensis* were reported to present a positive electroantennogram (EAG) response to EBF and many tobacco volatiles, including trans-2-hexenal, methyl salicylate, benzaldehyde, cis-3-hexen-1-ol, and 1-hexanal (Song et al., 2021a). The volatile sex pheromone has also been shown to be released by female *Aphidius*, causing intense sexual orientation in males (Fan et al., 2018). OBPs, CSPs and chemosensory receptors in *A. gifuensis* have been widely predicted based on transcriptome data (Kang et al., 2017; Fan et al., 2018). However, there is still a paucity of information on the expression profiles of odorant binding proteins in various sensory organs of *A. gifuensis*. Sequence identification is critical for further functional studies, not to mention the mechanisms of host foraging and mating behavior which are completely unknown.

In the present study, we performed gene prediction, identification, expression profiling of *AgifOBPs* and further performed a ligand competitive binding test on their recombinant proteins expressed in a prokaryotic expression system to discover two leg-specifically expressed OBPs (AgifOBP7 and AgifOBP9) in *A. gifuensis* as follows: 1) used *A. gifuensis* antennal transcriptome to predict *AgifOBPs*; 2) we identified *AgifOBPs* and profiled their spatial expression patterns among tissues and organs of both sexes; and 3) we revealed a partial mechanism of olfactory perception based on the ligand competitive binding test.

MATERIALS AND METHODS

Insect Rearing and Tissue Collection

The laboratory population of *Aphidius gifuensis* was the same as that previously described by Fan et al., 2018. The mummies were collected and placed separately in Petri dishes (3.5 cm in diameter). Newly emerged (within 0–12 h) *Aphidius* were transferred to larger Petri dishes (9 cm in diameter and 2 cm in height) for another 24 h, and the two groups were divided by sex. Cotton balls dipped in a 25% aqueous solution of sucrose were constantly supplied as the diet for adult wasps. Approximately 500 pairs of antennae from each sex were collected for RNA sequencing. In total, for each replication of qRT-PCR, 100 antennae, 50 heads, 50 thorax, 50 abdomens, and

300 legs were collected. Three replicates were conducted for sampling. The dissected tissues were immediately frozen in liquid nitrogen and stored at −80°C.

Total RNA Extraction and Synthesis of the First Chain of cDNA

Total RNA was extracted using TRIzol reagent and combined with micro total RNA extraction kit (Tianmo, Beijing, China) following the manufacturer's instructions. The frozen tissues were homogenized with a liquid nitrogen cooled mortar and ground with a pestle into very fine dust. Homogenized tissues were treated with 1 ml of TRIzol reagent (Invitrogen, Carlsbad, CA, United States). RNA degradation and contamination were monitored on 2% agarose gels. RNA purity was checked using a Nanodrop ND-1000 spectrophotometer (NanoDrop products, Wilmington, DE, United States). The RNA concentration was measured using a spectrophotometer RNA Nano 6000 Assay Kit of the Agilent Bioanalyzer 2,100 system (Agilent Technologies, CA, United States). Individual total RNA was isolated and cDNA was synthesized using the TRUEscript RT kit (LanY Science & Technology, Beijing, China) following the manufacturer's protocol.

Transcriptome Sequencing, Assembly and Functional Annotation

A total of 3 μg of RNA sample with standard quality ratios (1.8 < OD260/280 < 2.1) was purified using poly-T oligo-attached magnetic beads. Divalent cations under elevated temperature in NEBNext First Strand Synthesis Reaction Buffer (5×) were used for fragmentation. Single-stranded (ss) cDNA was synthesized using a random hexamer primer, M-MuLV Reverse Transcriptase and DNA Polymerase I and RNase H (NEB, United States). The 3′ ends of the DNA fragments were adenylated and the NEBNext Adaptor was ligated to the fragments for hybridization. The library fragments were purified with the AMPure XP system (Beckman Coulter, Beverly, MA, United States) to size select cDNA fragments ~150–200 bp in length. Then, 3 μl of USER Enzyme (NEB, United States) was used with size-selected, adaptor-ligated cDNA at 37°C for 15 min followed by 5 min at 95°C prior to PCR. PCR was performed with Phusion High-Fidelity DNA polymerase, Universal PCR primers and Index (X) Primer. The products were purified (AMPure XP system), and library quality was assessed using the Agilent Bioanalyzer 2,100 system (Agilent Technologies, CA, United States). Clustering of the index-coded samples was performed on a cBot Cluster Generation System using TruSeq PE Cluster Kit v3-cBot-HS (Illumina, China) according to the manufacturer's instructions. The library preparations were sequenced on an Illumina HiSeq 2,500 platform and paired-end reads (the sequencing strategy was PE125) were generated after cluster generation. After sequencing, the raw reads were processed to remove low quality and adaptor sequences by ng_qc, and then assembled into unigenes using Trinity r20140413p1 min_kmer_cov:2 and other default parameters (Grabherr et al., 2011). Then the unigenes were annotated using seven databases, including the nonredundant protein sequence (Nr, e-value = $1e^{-5}$), nonredundant nucleotide (Nt, e-value = $1e^{-5}$), Pfam (e-value = 0.01), Clusters of Orthologous Groups (KOG/COG, e-value = $1e^{-3}$), Swiss-Prot (e-value = $1e^{-5}$), Kyoto Encyclopedia of Genes and Genomes (KEGG, e-value = $1e^{-10}$) and Gene Ontology (GO, e-value = $1e^{-6}$) databases.

OBP Gene Prediction and Identification

The available sequences of *OBPs* from Hymenoptera species were used as "query" sequences to identify candidate unigenes that code OBPs in the *A. gifuensis* antennal transcriptome with the TBLASTn program with an e-value threshold of 10^{-5}. The sequences that fit the criteria were considered candidate OBPs. The open reading frames were searched by ORF finder (http://www.ncbi.nlm.nih.gov.orffinder/). The putative N-terminal signal peptides were predicted using the SignalP V4.1 program (http://www.cbs.dtu.dk/services/SignalP-4.1/) following the default parameters. Alignments of amino acid sequences were performed with Clustal Omega (https://www.ebi.ac.uk/Tools/msa/clustalo/) and edited using DNAMAN (Lynnon Biosoft San Ramon, CA, United States) software. According to the DEG results, the mean FPKM values for each gene in the antennae of males and females were then log-transformed ["$\log_2$ (FPKM +1)"]. A heat map was generated using TBtools (Chen et al., 2020). A phylogenetic tree was constructed by MEGA11 using the maximum likelihood method with a LG + mode to analyze the relationship of OBPs among species and reveal clues of their function (Tamura et al., 2021). Values indicated at the nodes are bootstrap values based on 1,000 replicates presented with 95% cutoff. The orthologous protein sequences from the genomes and transcriptomes of the following Hymenoptera species were used in the analysis: *Apis mellifera* (Forêt and Maleszka, 2006); *M. mediator* (Zhang et al., 2009; Peng et al., 2017); *M. pulchricornis* (Sheng, et al., 2017) and *Aulacocentrum confusum* (Li et al., 2021). The amino acids of the sequences used are listed in **Supplementary Material S1**. A circular phylogenetic tree was then generated and taxonomically color-coded using the online tool iTOL (https://itol.embl.de/itol.cgi). To identify the sequences of all candidate *AgifOBPs*, gene-specific primers (**Supplementary Table S3**) were designed with Primer 5.0 (http://frodo.wi.mit.edu/primer5/). Polymerase chain reactions were conducted on an Eppendorf Mastercycler® gradient PCR machine using 2×TransStart FastPfu PCR SuperMix (Trans, Beijing, China) and antennal cDNA as a template. An initial denaturation step at 95°C for 5 min followed by 35 cycles of 95°C for 35 s, 58°C as a melting temperature for 35 s, and 72°C for 45 s, and a final extension at 72°C for 10 min. The PCR products were electrophoresed on 2% agarose gels and stained with ethidium bromide to ensure that the correct products were amplified. All targeted PCR products were purified using the AxyPrep PCR clean up Kit (CORING, Jiangshu, China), and then cloned into the pEASY Blunt clone vector (Trans, Beijing, China). After transformation of *Escherichia coli* DH5α competent cells with the ligation products, positive colonies were selected by PCR using the plasmid primers M13 F and M13 R and

sequenced at San bo Biotech (Beijing, China). Individual clones confirmed to contain the desired sequence were incubated in LB/ampicillin medium.

Spatial Expression Pattern of AgifOBPs

To explore the expression characteristics of the *AgifOBPs*, RT-qPCR with an ABI 7500 real-time PCR system (Applied Biosystems Fosters City CA, United States) was conducted with cDNAs prepared from each tissue of male and female *Aphidius*. Briefly, 0.6 μl of both forward primer (10 μmol/L) and reverse primer (10 μmol/L) (**Supplementary Table S4**) were used in a 20-μl reaction containing 10 μl of 2x SuperReal PreMix Plus, 2 μl of cDNA (from 250 ng of total RNA), 0.4 μl of 50x ROX reference dye, and 6.4 μl of ribonuclease-free ddH_2O following the instructions provided with the SuperReal PreMix Plus (SYBR Green) kit (FP205) (Tiangen, Beijing, China). The PCR program was as follows: initial 15-min step at 95°C, 40 cycles of denaturation at 95°C for 15 s, annealing at 60°C for 32 s and elongation at 72°C for 1 min and finally a 10-min step at 72°C. For melting curve analysis, a dissociation step cycle was added automatically. The amplification efficiency was calculated using the equation: E = [10(-1/slope)-1] ×100%, in which the slope was derived by plotting the cycle threshold (Ct) value against five 2-fold serial dilutions. Only primers with 95–105% amplification efficiencies were used for subsequent data analysis. Relative quantification was performed according to the $2^{-\Delta\Delta Ct}$ method (Livak and Schmittgen, 2001). β-Actin and (nicotinamide adenine dinucleotide) NADH were used as reference genes to normalize the data. All qRT-PCR analyses were performed in three technical and biological replications.

Prokaryotic Expression and Purification of AgifOBP7 and AgifOBP9

The prokaryotic expression and purification procedures were consistent with previous studies (Prestwich, 1993; Wang et al., 2021a). Gene-specific primers were designed to clone the full-length cDNAs encoding mature AgifOBP proteins. The PCR products were first cloned into the pEASY-T1 clone vector (TransGen Biotech, Beijing, China), and then excised and subcloned into the bacterial expression vector pET28a (+) (Novagen, Madison, WI) between the Nde I and EcoR I restriction sites, and reconstructed plasmids were verified by sequencing. The recombinant AgifOBP7 and AgifOBP9 in the present study contain no histidine-tagged peptide at the N-terminus.

Protein expression was induced by adding isopropyl-1-thio-b-D-galactopyranoside (IPTG) to a final concentration of 1 mM when the culture reached an OD_{600} value of 0.6. Cells were incubated for an additional 12 h at 28°C and then harvested by centrifugation and sonicated at a low temperature (ice-water mixture). After centrifugation, the bands obtained were checked by 15% SDS–PAGE for their correspondence to the predicted molecular masses of the proteins. They were solubilized according to protocols for the effective rebuilding of the recombinant OBPs in their active forms (Prestwich, 1993). The soluble proteins were then purified by anion-exchange chromatography with RESOURCE Q15 HP column (GE HEALTH CARE, United States) and gel filtration [Superdex 75 10/300 GL column (GE HEALTH CARE, United States)], The crude extracts were passed over a pre-equilibrated RESOURCE Q15 HP column (20 mM Tris-HCl, pH 8.5), and then washed and eluted with Buffer B (20 mM Tris-HCL, 1 M NaCl, pH 8.5). And finally with two rounds of gel filtration through a Superdex 75 10/300 GL column., those eluted proteins were collected and analyzed by 15% SDS-PAGE, and then, several successive dialyzes were performed: 1) at 4°C for 3 h, against 2 L of storage buffer (20 mM Tris-HCl, pH 8.5), 2) at 4°C for 3 h, against 2 L storage buffer (20 mM Tris-HCl, pH 8.5), and 3) at 4°C against 2 L of storage buffer (20 mM Tris-HCl, pH 8.5) overnight. Finally, the desalted protein samples were ultracentrifuged for 30 min using 3-kDa ultrafiltration at 4°C, and 5,000 rpm. Protein samples were analyzed by SDS-PAGE after every purification step, the concentration of purified protein was determined by a Protein Assay kit (Qubit™ Protein Assay kit, Q33211, Invitrogen), and the purified AgifOBPs were analyzed by mass spectrometry (LC–MS). The purity and concentration of the soluble proteins were evaluated using SDS–PAGE. Finally, stock solutions of AgifOBP7 and AgifOBP9 were collected and kept at −20°C in Tris–HCl (50 mM, pH 7.4).

Fluorescence Competitive Binding Assays

To investigate the ligand-binding property of two AgifOBPs, five groups of competitive ligands were used: 1) aphid alarm pheromone components, including EBF, (-)-α-pinene, (-)-β-pinene and (+)-limonene which are released by other aphids following natural enemy predation or physical damage (Francis et al., 2005; Song et al., 2021b), 2) main components of the aphid sex pheromone: (4aSR,7SR,7aRS)-Nepetalactone; 3) green leaf volatiles of wheat: (Z)-3-hexen-1-ol; 4) aphid-induced plant volatiles (methyl salicylate, and 6-methyl-5-hepten-2-one); and 5) an EBF derivative artificial chemical, namely CAU-II-11, ((E)-3,7-dimethylocta-2,6-dien-1-yl-2-hydroxy-3-methoxybenzoate), which showed a high affinity for aphid EBF- binding proteins (OBP3/7/9, Qin et al., 2020), and was used to investigate the binding properties of purified AgifOBP7 and AgifOBP9. The classes, CAS numbers and purity of the chemicals used in this study are listed in **Table 1**.

Fluorescence intensity was recorded in a right angle configuration on a Lengguang 970CRT spectrofluorimeter (Shanghai Jingmi, China) at room temperature using a 1 cm light path fluorimeter quartz cuvette. A slit width of 10 nm was selected for both excitation and emission. The measured fluorescence intensities were corrected for both blank signals due to protein emission and scattered excitation light. The spectral data were processed using the software 970CRT 2.0l. Fluorescence binding experiments were conducted in 50 μM Tris-HCl buffer, pH 7.4, at room temperature. The binding affinity for N-phenyl-1-naphthylamine (1-NPN) was determined by adding aliquots of a 1 mM stock solution of 1-NPN dissolved in

TABLE 1 | Binding affinities of AgifOBP7 and AgifOBP9 for candidate ligands, evaluated in displacement binding assays using the fluorescent probe, 1-NPN.

No	Code	CAS	Purity	OBP7		OBP9	
				IC50	Ki(μM)	IC50	Ki(μM)
1	(E)-β-Farnesene	18,794–84–8	≥85%	>30	20.30 ± 1.99	17.83 ± 1.69	4.60 ± 0.43
2	(-)-α-Pinene	80–56–8	≥95%	>30	>30	24.10 ± 3.42	6.22 ± 0.88
3	(-)-β-Pinene	19,902–08–0	≥99%	>30	>30	11.86 ± 1.27	3.06 ± 0.33
4	(+)-Limonene	138–86–3	≥95%	>30	>30	12.85 ± 0.25	3.32 ± 0.06
5	(4aSR 7SR 7aRS)-Nepetalactone	21,651–62–7	≥80%	>30	16.12 ± 3.49	9.03 ± 0.31	2.33 ± 0.08
6	6-Methyl-5-hepten-2-one	110–93–0	≥99%	>30	>30	22.32 ± 3.38	5.76 ± 0.87
7	cis-3-Hexenol	928–96–1	≥97%	>30	>30	17.01 ± 0.33	4.39 ± 0.09
8	Methyl salicylate	119–36–8	≥99%	>30	>30	13.31 ± 2.99	3.43 ± 0.77
9	CAU-II-11	-	≥98%	18.56 ± 1.73	8.50 ± 0.73	4.15 ± 0.33	1.07 ± 0.08

spectrophotometric grade methanol into a 2 μM protein sample. The fluorescence of 1-NPN was excited at 337 nm, and emission was recorded between 350 and 500 nm. Spectra were recorded with a high-speed scan. All ligands used in competitive experiments were dissolved in spectrophotometric grade methanol. In competition assays, aliquots of the competing ligands were added into a 2 μM protein solution in the presence of a given concentration of 1-NPN. To estimate the binding affinities of each AgifOBP for a variety of different ligands, we monitored the decrease in 1-NPN fluorescence due to the ability of different odorants to displace 1-NPN and determined the Ki value for each compound. To determine the dissociation constants, the intensity values corresponding to the maximum fluorescence emissions were plotted against the cumulative 1-NPN concentration. The amount of bound ligand was calculated from the fluorescence intensity values by assuming that the protein was 100% active, with a stoichiometry of 1:1 protein: ligand at saturation. The curves were linearized using Scatchard plots. The value of $K_{1\text{-NPN}}$ was estimated on a direct plot by nonlinear regression with an equation corresponding to a single binding site using Prism 7 (GraphPad Software, Inc., United States), and the IC_{50} was defined as the concentration of a competitor that caused a 50% reduction in fluorescence intensity. The dissociation constants of the inhibitors (Ki) were calculated according to the formula Ki = [IC50]/(1+[1-NPN]/$K_{1\text{-NPN}}$), in which [1-NPN] represents the free 1-NPN concentration and $K_{1\text{-NPN}}$ represents the dissociation constant for AgifOBPs/1-NPN (Ban et al., 2003; Zhong et al., 2012; Sun et al., 2016; Fan et al., 2017; Qin et al., 2020; Wang et al., 2021b). All fluorescence competitive binding assays were performed in three independent replicates, and Ki dates are present as means ± SD.

Statistical Analyses

For qRT-PCR analyses, the differences between means of biological replicates were tested using two-way ANOVA followed by multiple comparisons tests regardless of rows and columns using GraphPad Prism version 7.0.0 for Windows (GraphPad, Software, San Diego, California United States, www.graphpad.com). Differences between means for experiments with more than two treatments were distinguished using Tukey's honestly significant difference (HSD) test at the $p < 0.05$ significance level.

RESULTS

Overview of Transcriptomes

A total of 2.22 and 2.30 million raw reads were obtained from *A. gifuensis* antennae libraries from females and males, respectively. The data presented in the study that was deposited in the Sequence Read Archive (SRA) repository, the accession number are SRR18251541 and SRR18251542. After removal of low-quality, adaptor, and contaminating sequences, 3.31 and 3.03 million clean reads were retained (**Supplementary Table S1**) and assembled into 81,235 distinct transcripts (mean length = 661 bp) and 65,854 unigenes (mean length = 568 bp). The length distribution presented in (**Supplementary Figure S1**). In total, 18,408 (27.95% of all 65,854 unigenes), 5,625 (8.54%), 7,551 (40.92%), 12,484 (18.95%), 15,070 (22.88%), 15,951 (24.22%) and 9,462 (14.36%) transcripts from *A. gifuensis* antennae were annotated using the Nr, Nt, KO, Swiss-Prot, Pfam, GO and KOG databases, respectively (**Supplementary Table S2**). The most abundant GO terms were biological process terms, with *AgifOBP3* corresponding to the cellular process and *AgifOBP15* grouped with the membrane. The cluster for cellular process was the second largest group. Most transcripts that corresponded to molecular function were related to binding and catalytic activity (**Supplementary Figure S2**). In the KOG classification, unigenes clustered into 26 categories (**Supplementary Figure S3**). Among these categories, general function prediction was the dominant category, followed by signal transduction and posttranslational modification, protein turnover and chaperon. All the unigenes annotated in the KO database were assigned to the 5 biological pathways described in the KEGG database: cellular processes, environmental information processing, genetic information processing, metabolism, and organismal systems (**Supplementary Figure S4**). The most common pathway was metabolism followed by genetic information processing, organismal systems and cellular processes. Signal transduction was involved in 940 genes in the environmental information processing group.

OBP Prediction and Phylogenetic Analysis

Fifteen putative OBPs with complete open reading frames were predicted from the antennal transcriptome data. We mainly named them following Fan's work (Fan et al., 2018). *AgifOBP10* with a partial ORF reported by Fan is missing

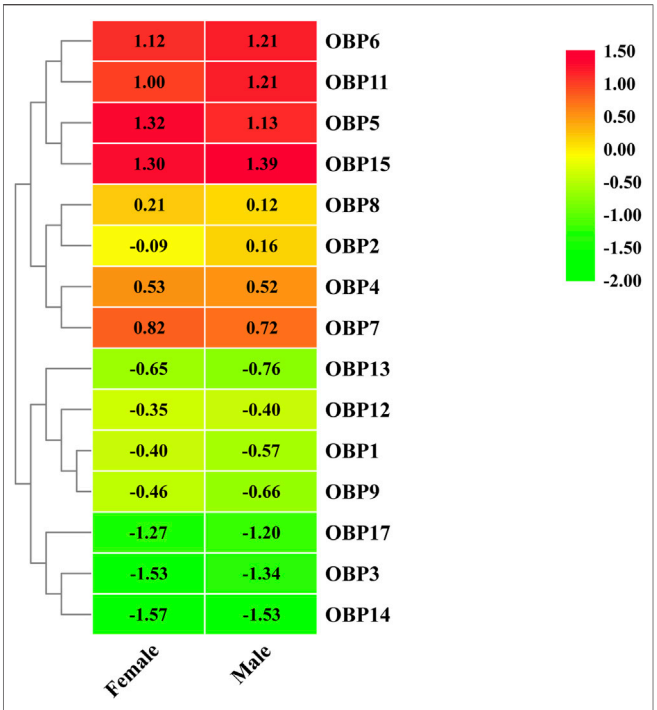

FIGURE 1 | Heatmap of differentially expressed OBP genes between females and males based on FPKM values of antennae transcriptomes.

here. All OBP transcripts were confirmed by molecular cloning, followed by sequencing, except for *AgifOBP14*. All 15 OBPs have the characteristic of insect OBP sequence motif (Yuan et al., 2015), and 12 *Agif*OBPs (*AgifOBP1-3,5–9,11,13,14,15*) of them have the classic OBP Cys motif (C_1-$X_{22\text{-}32}$-C_2-X_3-C_3-$X_{36\text{-}46}$-C_4-$X_{8\text{-}14}$-C_5-X_8-C_6) (Xu et al., 2009), while 3 *AgifOB*Ps (*AgifOBP4/12/17*) belong to the minus-C OBP Cys motif with four or five conserved cysteines (**Supplementary Figure S5**). The heatmap in **Figure 1** illustrates that OBP5, OBP6, OBP11, and OBP15 were highly expressed genes in both sex antennae but OBP3/14/17 showed relatively low expression levels. The phylogenetic tree of Hymenoptera OBPs was built using MEGA11 (maximum likelihood method with an LG model) OBP sequences from 5 different species (*A. gifuensis*, *A. mellifera*, *M. mediator*, *M. pulchricornis* and *A. confusum*). *A. gifuensis* OBPs are clustered together to form three homologous subgroups (lineages). Among them, OBP1, OBP5, OBP7, OBP9 andOBP17 were in one subgroup, OBP2, OBP3, OBP6, OBP8 and OBP11-OBP15 were in the other subgroup, and OBP4 fell into the third subgroup. The results showed that AgifOBP*s* almost spread across in clades without species specificity (**Figure 2**). Among these AgifOBPs, AgifOBP4 was found in the MpulOBP4 clade. AgifOBP6 exhibited a rather high similarity to other orthologs such as AmelOBP6, MmedOBP6 and MpulOBP6. AgifOBP8 also showed a high similarity to MmedOBP8 and MpulOBP8 (**Figure 2**).

Spatial Expression Pattern of *AgifOBPs*

Compared to other tissues or organs, 8 of the 14 OBPs, namely, *AgifOBP3, AgifOBP5, AgifOBP6, AgifOBP7, AgifOBP8, AgifOBP11, AgifOBP12* and *AgifOBP15,* maintained higher expression in antennae (**Figures 3**, **4**; $p < 0.05$). *AgifOBP17* was highly expressed in the head. *AgifOBP1/2/7/9* were expressed in legs with significantly higher expression levels (**Figures 3**, **4**, $p < 0.05$). The other two *OBPs*, *AgifOBP4* and *AgifOBP13* were widely expressed among tissues and organs.

Specifically, *AgifOBP3/5/6/11/12/15* were specifically expressed in antennae. Among them, the expression levels of AgifOBP3/11 were even higher in male antennae. However, *AgifOBP12/15* were even higher in female antennae, and *AgifOBP6* showed no difference in antennae of both sexes. Moreover, *AgifOBP1/2/4/5/7/9/15* showed relatively higher expression levels in legs (**Figures 3**, **4**). Among them, *AgifOBP2* was specifically expressed in female legs. And *AgifOBP7/9/15* were expressed at comparatively higher levels in female legs. In contrast, *AgifOBP1/4/5* were expressed at higher levels in male legs. Notably *AgifOBP7* was female specific and was expressed directly in female antennae and legs. In males, *AigfOBP8* was specifically expressed in antennae. In females, it was relatively highly expressed in both the antennae and abdomen. We also found that the highest level of *AgifOBP17* was in the heads of both sexes. Although both *AgifOBP4* and *AgifOBP13* were widely expressed, *AgifOBP4* showed an even higher expression level in thoraxes of both females and males. *AgifOBP13* expression was significantly higher in the male abdomen. In addition, *AgifOBP1* and *AgifOBP9* were specifically or highly expressed in the legs of both male and female *A. gifuensis*. *AgifOBP2* was significantly expressed in the legs of females (**Figure 4**, $p < 0.05$).

In summary, *AgifOBP3/5/6/11/12/15* were antennal specifically expressed OBPs. *AgifOBP2/9* were specifically expressed OBPs in legs. *AgifOBP17* is an OBP specifically in the head (**Figure 3**, $p < 0.05$). In addition, *AgifOBP5/7* were female specific OBPs. *AgifOBP8* expression was significantly higher in the antennae of males and in both the antennae and abdomen of females (**Figure 4**, $p < 0.05$).

Expression and Purification of AgifOBP7 and AgifOBP9

AgifOBP7 and AgifOBP9 were successfully expressed in the inclusion bodies using a bacterial system. After a dissolving and refolding treatment, the refolded AgifOBP7 and AgifOBP9 were purified with yields of 0.25 mg/ml as soluble proteins (**Figures 5A,B**). More than 15 mg of purified AgifOBP7 and AgifOBP9 was obtained using RESOURCE Q15 affinity columns, with the His-tag removed. The theoretical molecular weight values for AgifOBP7 and AgifOBP9 were very close to the measured values (AgifOBP7, 13.401 kDa; AgifOBP9, 12.498 kDa). The purified protein samples were further identified by LC–MS/MS (data not shown).

Fluorescence Competitive Binding Assays

To investigate the role of two OBPs in the odor perception of aphids, we chose alarm pheromones (EBF, (-)-α-pinene, (-)-β-pinene, (+)-limonene, EBF derivative (CAU-II-11), aphid sexual pheromones (4aSR 7SR 7aRS)-nepetalactone as well as volatiles of

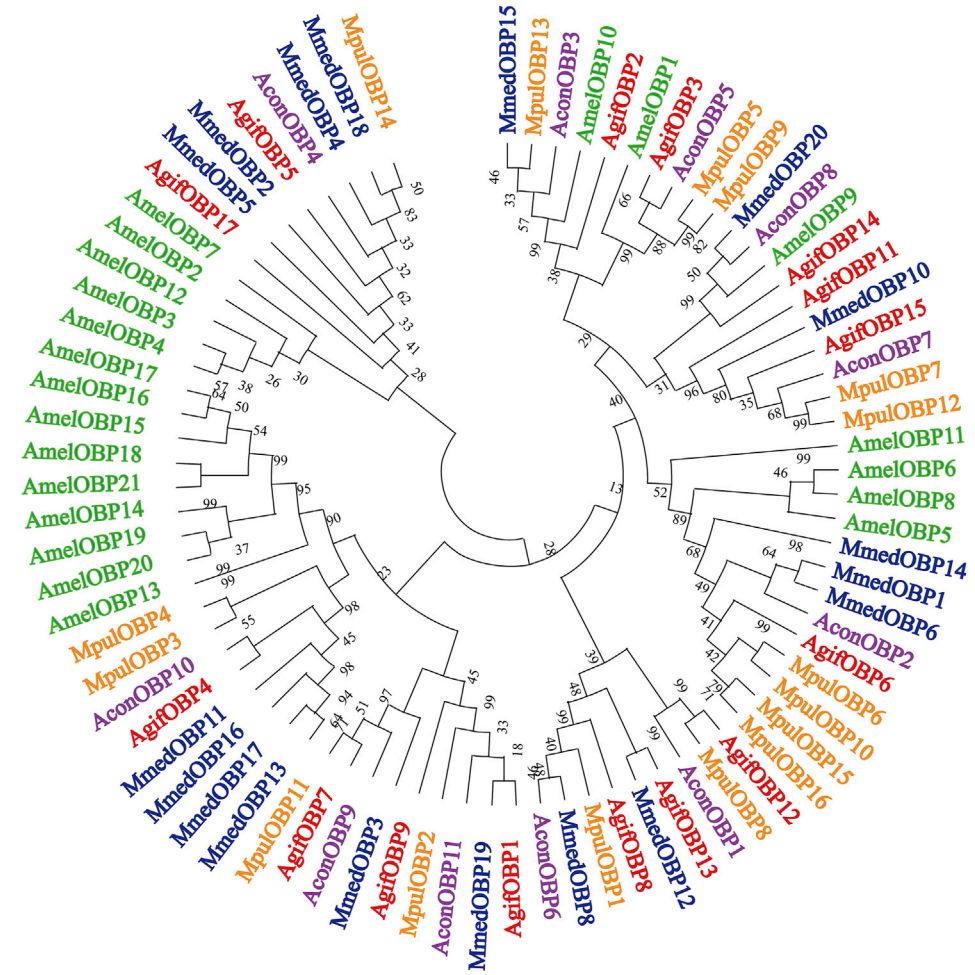

FIGURE 2 | Phylogenetic relationships of target parasitoid putative OBPs and 66 putative other hymenopteran OBPs; detailed relationships of the putative *AgifOBPs* (in red), *MmedOBPs* (in blue), *AmelOBPs* (in green), *MpulOBPs* (in orange), and *AconOBPs* (in purple). The trees were constructed with MEGA 11 using an LG + model and bootstrap support was calculated with 1,000 rapid bootstrap replicates with a 95% cutoff. The species names are abbreviated with four letters, and their full names with all accession numbers of the OBP amino acid sequences are provided in **Supplementary Material S1**.

wheat green leaf (cis-3-hexen-1-ol) and aphid induced plant main volatiles (methyl salicylate, 6-methyl-5-hepten-2-one) as the candidate ligands for fluorescence competitive binding assays (**Table 1**). We first tested the binding affinities of both OBPs to the fluorescent probe N-phenyl-1-naphthylamine (1-NPN) as previously reported (Qiao et al., 2009; Fan et al., 2017). The dissociation constants of AgifOBP7/1-NPN and the AgifOBP9/1-NPN complex were 1.69 ± 0.27 μM and 0.69 ± 0.24 μM respectively (**Figures 5C,D**).

In a subsequent experiment, we used a fluorescence competitive binding assay to determine the binding affinities of AgifOBP7 and AgifOBP9 to different odorants. Based on the binding curves, we calculated the median inhibitory concentration (IC50) and dissociation constant (Ki) values (**Table 1**). Among the tested odorants, EBF, (-)-α-pinene, (-)-β-pinene, (+)-limonene, (4aSR 7SR 7aRS)-nepetalactone; cis-3-hexen-1-ol, methyl salicylate and 6-methyl-5-hepten-2-one displayed relatively high binding affinities (Ki < 10 μM) to AgifOBP9 (**Figure 5F**). Interestingly, among all the tested odorants, CAU-II-11 bound most strongly (Ki = 1.07 ± 0.08 μM) to AgifOBP9 (**Table 1**), which is the derivative of EBF (Ki = 4.60 ± 0.43 μM). However, this was not the case with AgifOBP7, which only displayed weak binding with EBF (Ki = 20.30 ± 1.99) and (4aSR 7SR 7aRS)-nepetalactone (Ki = 16.12 ± 3.49), not much with (-)-α-pinene, (-)-β-pinene, (+)-limonene, cis-3-hexen-1-ol, methyl salicylate and 6-methyl-5-hepten-2-one. CAU-II-11, like AgifOBP9, showed the strongest binding affinity (Ki = 1.07 ± 0.08 μM) to AgifOBP7 among the examined odorants (**Figure 5E**; **Table 1**).

DISCUSSION

Odorant-binding proteins are classically defined as olfactory soluble proteins (Vogt, R. G., & Riddiford, L. M, 1981; Pelosi, 2006) and play an essential role in habitat searching and finding

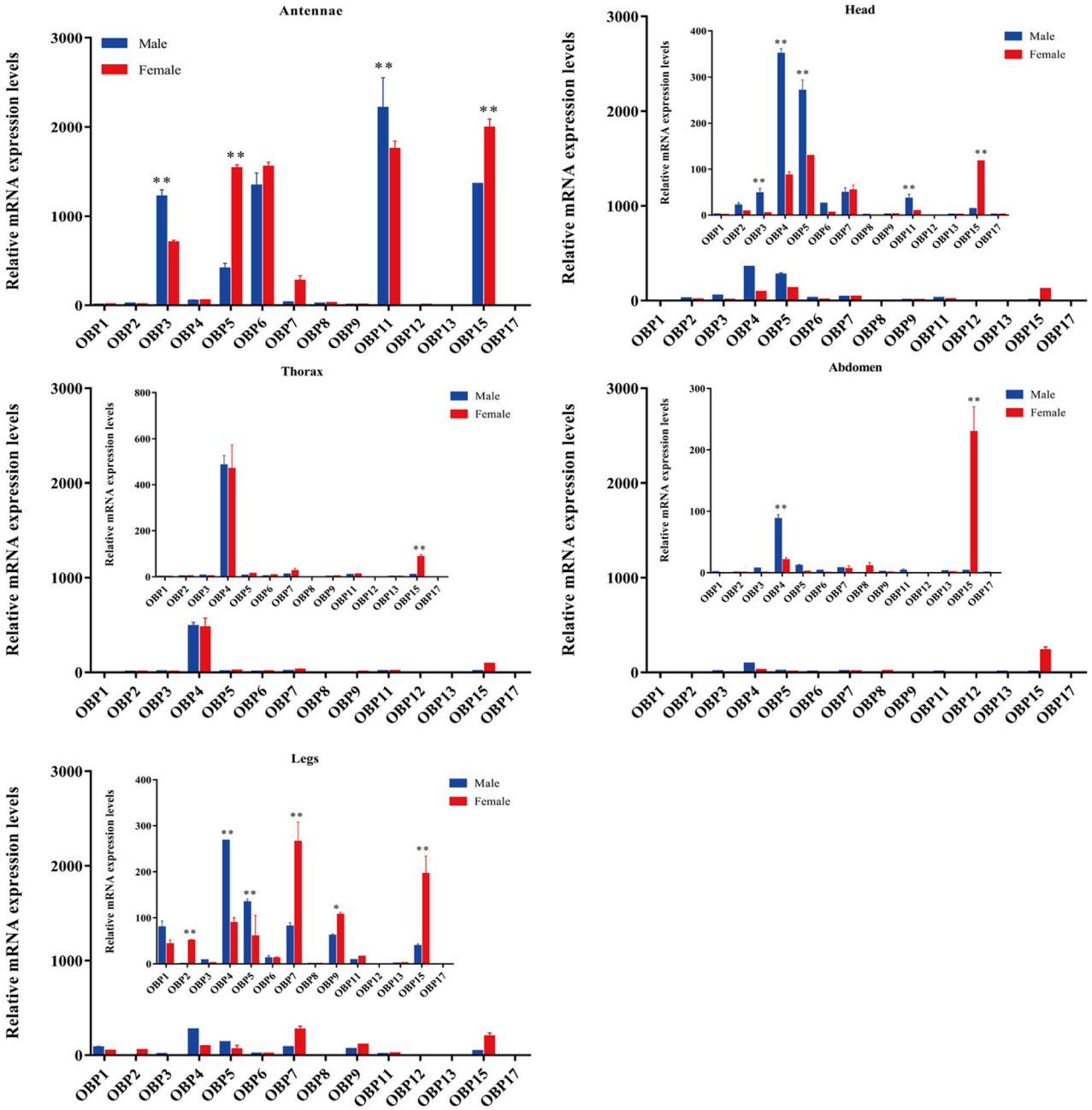

FIGURE 3 | The relative expression patterns of different *AgifOBP* genes in different tissues of males and females as measured by quantitative real-time polymerase chain reaction. The fold changes are relative to the transcript levels of OBP13 in the male thorax. The NADH and ACTIN genes were used as references to normalize the expression of each tested gene. The data are presented as the mean ± SD. The asterisk * and ** above the bars indicate significant differences at $p < 0.05$; and $p < 0.01$, respectively, according to two-way ANOVA.

suitable mates. With the increase in insect genome projects and transcriptome sequencing projects, large numbers of OBPs have recently been identified in different insect species. In the present study, we constructed a cDNA library from the antennae of the endoparasitoid *A. gifuensis* for transcriptome sequencing and categorized the potential function of the odorant binding protein genes by bioinformatics approaches.

OBP Prediction, Cloning and Phylogenetic Analysis

Fourteen OBPs in the *A. gifuensis* antennae transcriptome were identified in the present study. This number is similar to those in *A. mellifera* (Forêt and Maleszka, 2006), *M. mediator* (Zhang et al., 2009; Peng et al., 2017), *Meteorus pulchricornis* (Sheng et al., 2017), *Cotesia vestalis* (Zhou et al., 2021) and *Aulacocentrum*

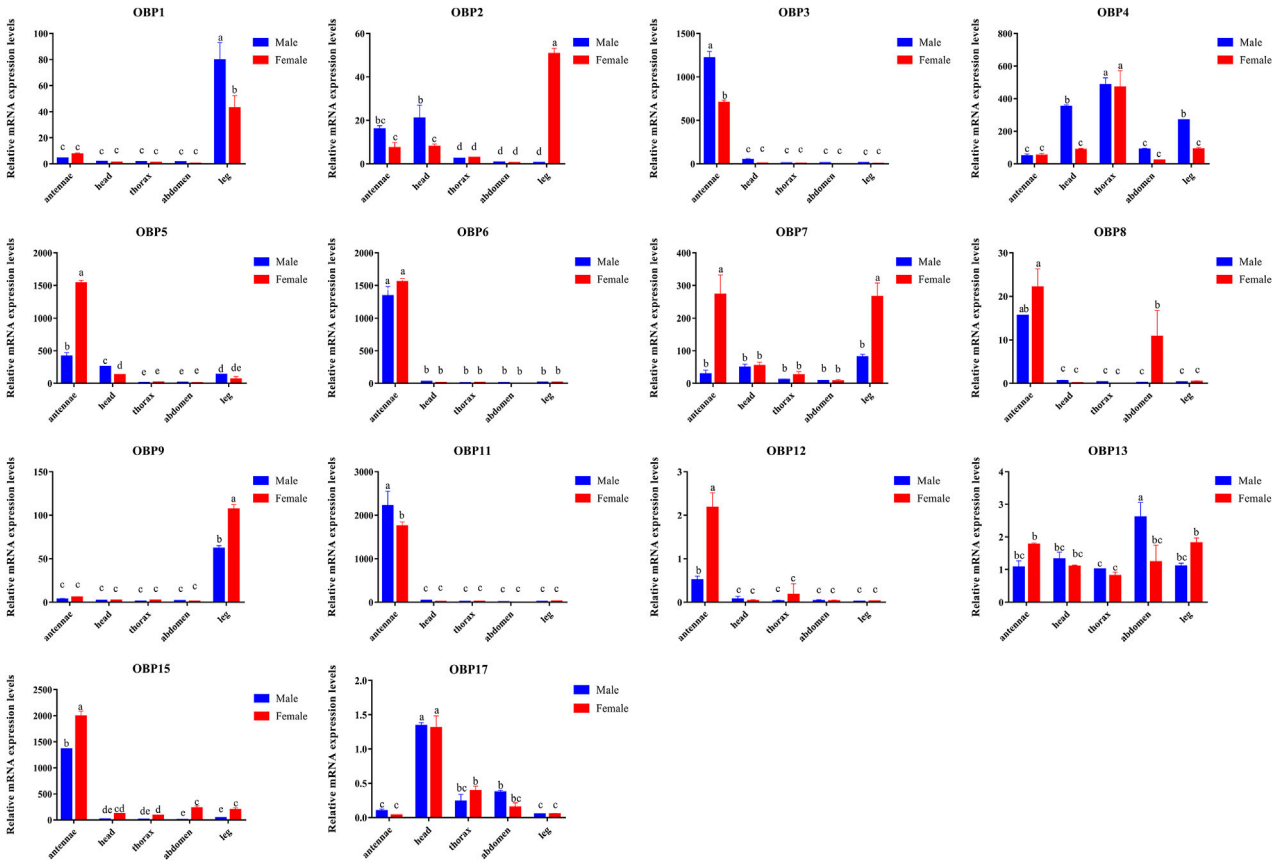

FIGURE 4 | Relative expression of *AgifOBP* genes in the different tissues of male and female *A. gifuensis* as measured by quantitative real-time polymerase chain reaction. Relative fold changes were normalized to the transcript levels in the male thorax. The NADH and ACTIN genes were used as references to normalize the expression of each tested gene. The standard error is represented by the error bar ($n = 3$) and the different lowercase letters (a, b, c, d, e) indicate significant differences in transcript abundances (two-way ANOVA followed by Tukey's HSD multiple comparison test, $p < 0.05$).

confusum (Li et al., 2021), therefore indicating that there are similar OBP numbers in Hymenoptera insects.

The phylogenetic tree of these *AgifOBPs*, together with OBPs from 4 hymenopteran species, showed that the *AgifOBPs* segregate into the orthologous clades of the other species, rather than into *A. gifuensis* paralogous clades. *AgifOBP4* was found in the *MpulOBP4* clade, whereas *AconOBP4*, *MmedOBP4*, and *AmelOBP4* were clustered in the other one clade. *AgifOBP6* and *AgifOBP8* were present in the three wasps of *A. gifuensis*, *M. mediator* and *M. pulchricornis,* but their orthologs were rarely found in *Apis mellifera* (**Figure 2**). This also suggests that these *AgifOBPs* might play different roles in odor recognition or have roles other than olfaction. The comparatively conserved OBPs in hymenoptera wasps, particularly in parasitoid wasps implied that their function could be limited to the common olfactory physiology of these insects. Some study results on natural enemies of aphids support this hypothesis. For example, aphid OBP7 orthologs have been widely reported to have their affinities with the alarm pheromone EBF (Sun et al., 2012a; Zhong et al., 2012; Fan et al., 2017; Qin et al., 2020). *CpalOBP10* in lacewing *Chrysopa pallens*, an aphid predator, belongs to the same lineage as aphid OBP7 such as in *S. avenae* and in *A. pisum,* and its affinity for EBF was also consistent with that of aphid OBP7 orthologs (Li et al., 2017; Li et al., 2019).

Spatial Expression Pattern

The spatial expression profile of *AgifOBPs* was verified using qPCR. Our data revealed that five *OBPs*, namely *AgifOBP3*, *AgifOBP5*, *AgifOBP6*, *AgifOBP11*, and AgifOBP15, were expressed at a high level in the antennae (**Figures 3**, **4**), while four *OBPs*, *AgifOBP2*, *AgifOBP4*, *AgifOBP7* and *AgifOBP8*, were expressed at a medium level, and seven *OBPs*, *AgifOBP1*, *AgifOBP9*, *AgifOBP12/13*, and *AgifOBP17*, were expressed at a low level in the antennae (**Figures 3**, **4**). The antennal specific *OBPs* (**Figure 4**) suggest their function of recognizing and binding odorants from the environment. Six *OBPs*, *AgifOBP2, AgifOBP4, AgifOBP5, AgifOBP7, AgifOBP13* and *AgifOBP17,* showed expression patterns among sensory and nonsensory organs, indicating their possible multiple functions in olfactory perception as well as other physiological processes such as development and reproduction. Both *AgifOBP1* and *AgifOBP9* showed higher expression levels in the legs than the other four tissues (antennae, heads, thorax and abdomen), which could be related to the adaptation of *A. gifuensis* during migration as we

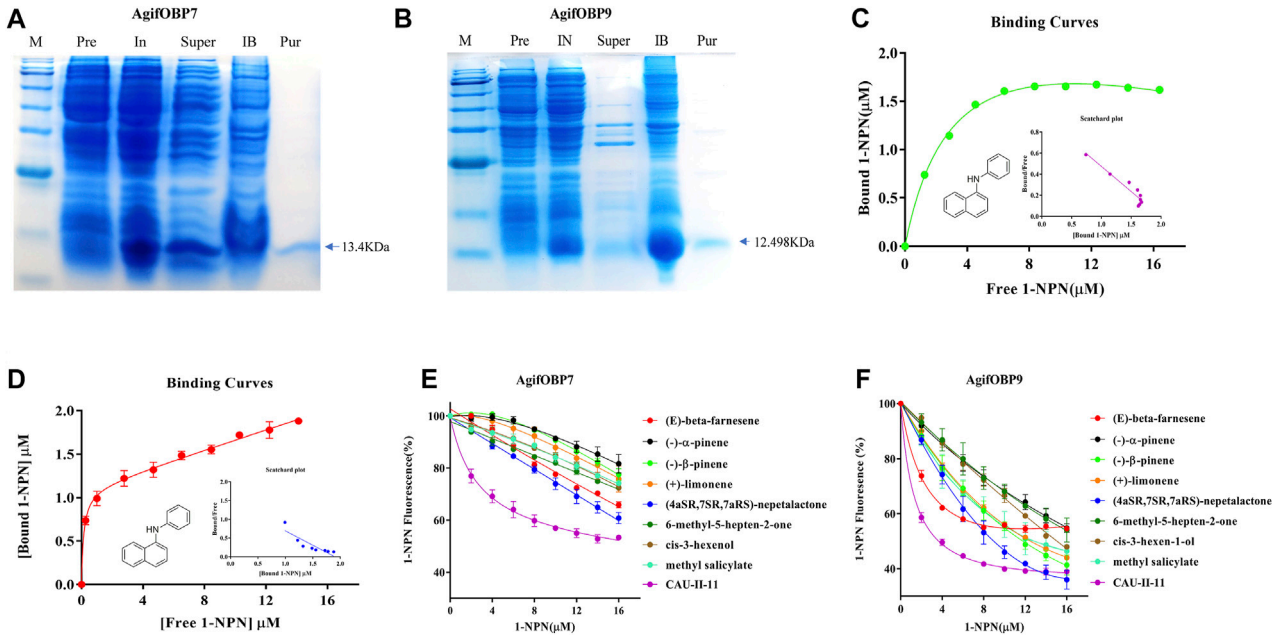

FIGURE 5 | Expression and binding properties of AgifOBP7 and AgifOBP9 with candidate ligands. **(A)** Expression and purification of AgifOBP7, **(B)** Expression and purification of AgifOBP9. Line M: molecular weight PR 1910 (11–180 KDa) Marker, 11, 17, 25, 35, 48, 63, 75, 100, 135, 180 KDa; IN: Induced pET-28a (+)/AgifOBP7/9; Super: pET-28a (+)/AgifOBP7/9 Supernatant; IB: pET-28a (+)/AgifOBP7/9 Inclusion body; Pur: Purified pET-28a (+)/AgifOBP7/9 without His-tag. **(C,D)** Binding curves of AgifOBP7 and AgifOBP9 with N-phenyl-1-naphthylamine (1-NPN) in 50 mM Tris-HCl buffer (pH 7.4). **(E,F)** Competitive binding curves of AgifOBP7 and AgifOBP9 to components of aphid alarm pheromones ((E)-beta-farnesene, (-)-α-pinene, (-)-β-pinene, (+)-limonene, (E)-beta-farnesene derivative (CAU-II-11); aphid sexual pheromone (4aSR 7SR 7aRS)-nepetalactone, the volatiles of wheat green leaf (cis-3-hexen-1-ol) and aphid induced plant main volatiles (methyl salicylate, 6-methyl-5-hepten-2-one). A mixture of the recombinant protein and N-phenyl-1-naphthylamine (1-NPN) in 50 mM Tris-HCl buffer (pH 7.4) at the concentration of 2 μM was titrated with 1 mM solutions of each competing ligand to a final concentration range of 2–16 μM. Fluorescence values are presented as percent of the values in the absence of competitor. Date are the means ± SD of three independent experiments.

have discussed in our previous study (Xue et al., 2016), and might be involved in the procedure of taste or volatile perception or be related to olfactory sensilla on the legs (Yasukawa et al., 2010; Harada et al., 2012). A similar condition was also found for *AgifOBP5*, which is expressed in small amounts in the head and leg, in addition to being expressed abundantly in antennae.

Apart from antennae, alternatively, these OBPs expressed in other tissues may be responsible for corresponding functions. For example, *NlugOBP3* is highly expressed in the abdomen of *Nilaparvata lugens* and may be involved in juvenile hormone transport and play an important role in metamorphosis (He et al., 2011). Insect OBPs have been reported to act as carrier proteins in the male reproductive apparatus of mosquitoes (Li et al., 2008). After mating, the OBPs expressed by male moths are found on the surface of fertilized eggs, which helps the larvae to avoid cannibalistic behaviors (Sun et al., 2012b). For parasitic wasps, *AconOBP8* was reported to be expressed predominantly in the abdomen (Li et al., 2021). Similar expression patterns of OBPs in the nonolfactory tissues were observed in *Sclerodermus sp.* (Zhou et al., 2015) and *M. pulchricornis* (Sheng et al., 2017). In our present study, qPCR analysis revealed that *AgifOBP8* was also expressed in the female abdomen, and it can be speculated that *OBP8* may potentially function as a pheromone-binding protein for identifying a particular signal such as the sex pheromone component in mating or oviposition behaviors, although the active component of sex pheromone in this species is still unclear.

The results obtained by qPCR are consistent with antennal transcriptome based differential expression analysis (heatmap, **Figure 1**). Nonetheless, any discrepancy between qPCR and differential expression analysis results illustrate the poor performance of showing local details by omics big data analysis.

Ligand-Binding Properties

Table 1 indicates that the proteins AgifOBP7 and AgifOBP9 have broad binding activities across the aphid alarm pheromone components, aphid sex pheromone, green leaf volatiles, aphid-induced plant volatiles and EBF derivatives. AgifOBP9 showed higher binding activities than AgifOBP7 with all the five types of compounds. Similar results have been found in its prey aphid *A. pisum*, in which ApisOBP9 also exhibited higher affinities with all the compounds than ApisOBP7 (Qin et al., 2020), although there is no evolutionary homology between the two species. For AgifOBP7 and AgifOBP9, EBF derivatives had higher binding properties than the lead EBF and other compounds. These results are consistent with studies on the characterized OBPs of ApisOBP1, ApisOBP3, and ApisOBP6-OBP10 in *A. pisum* (Sun et al., 2012a; Qin et al., 2020). Both proteins show preferential binding to several related compounds. AgifOBP7 bound the above five types of compounds from strong to

weak: EBF derivative, aphid sex pheromone main component, aphid alarm pheromone component EBF, and other alarm pheromone components, green leaf volatile and induced plant volatiles. AgifOBP9, bound the above five types of compounds from strong to weak: EBF derivative, aphid sex pheromone main component, aphid alarm pheromone component (-)-β-pinene and (+)-limonene, induced plant volatile methyl salicylate, green leaf volatile (Z)-3-hexen-1-ol, alarm pheromone component EBF, induced plant volatile 6-methyl-5-hepten-2-one and alarm pheromone component (-)-α-pinene. Our results suggest that there are substantial differences in their interactions such that AgifOBP7binds strongly to aphid pheromone components and derivatives and binds weakly to the others, which is similar to OBP7 in *S. avenea* (Zhong et al., 2012); and AgifOBP9 broadly binds to all kinds of compounds, which is likely OBP9 in *M. persicae* (Wang et al., 2021a).

As the natural enemy of aphids, *A. gifuensis* locates aphids using the cues of aphid pheromones and plant volatiles (Powell et al., 1998; Kang et al., 2017). Our results indicate that AgifOBP7 is specific to aphid pheromone components and EBF derivatives, and that AgifOBP9 has a broad spectrum of binding to compounds. Other OBPs in aphid natural enemies also bound to aphid pheromone components and plant volatiles. For example, OBP3, OBP4, OBP6, OBP7, OBP9, and OBP10 in *Chrysopa pallens* bind plant volatiles and aphid alarm pheromone EBF, and, OBP10 specifically binds EBF (Li, et al., 2017; Li et al., 2019). The new OBPs from the aphid natural enemy *Eupeodes corollae*, OBP12, OBP15 and OBP16 also bound with EBF and plant volatiles, among which OBP12 and OBP15 strongly bound EBF (Wang et al., 2022).

Many natural enemies such as *Aphidius ervi*, *Aphidius uzbekistanicus*, and *Adalia bipunctata* are attracted to EBF (Buitenhuis et al., 2004). To confirm the functions suggested by the phylogenetic tree and tissue expression profiles, AgifOBP7 and AgifOBP9 were selected to perform a potential functional study. Overall, the odorants exhibited relatively high binding affinities (Ki < 10 μM) to *AgifOBP9* (**Figure 5F**; **Table 1**). Interestingly, among all the tested odorants, CAU-II-11 had the strongest binding affinity (Ki = 1.07 ± 0.08 μM) to AgifOBP9 (**Table 1**), which is the derivative of EBF (Ki = 4.60 ± 0.43 μM). This finding is in line with prior research on ApisOBP3/7/9 using CAU-II-11 (Qin et al., 2020). This result further supports that both aphid-induced volatiles as well as EBF are used by *A. gifuensis* in aphid location and that AgifOBP9 may be involved in this process.

In summary, we first predicted 15 *OBPs* based on the antennal transcriptome of both male and female *A. gifuensis*. Fourteen of these OBPs were verified by gene cloning. Furthermore, their detailed spatial expression pattern showed that most *OBPs* are mainly expressed in the sensory organs, but some are widely expressed in various tissues or organs such as the thorax and abdomen. Finally, at least one female particularly expressing OBP (AgifOBP9) showed affinity to EBF in a fluorescence competition experiment, which further indicated the likely molecular basement of sensing the aphid alarm pheromone at the molecular level in *A. gifuensis*. In addition, what cannot be ignored is the presence of *OBPs* expressed in other nonsensory organs such as the abdomen, which supports the existence of carrier transport functions other than for foreign chemicals and therefore broader ligand ranges of wasp *OBPs*. Our findings may shed insight into parasitic wasps' olfactory sensitivity to host hints, as olfactory organs recognize pheromones and odorant substances that influence both host hunting and oviposition activities and will help us better understand parasitic wasp host forging and mating behaviors, which will aid in the strengthening and better utilization of *A. gifuensis* as a powerful and natural biocontrol strategy. As a result, we anticipate that additional research into the aforementioned topics will improve the efficacy of parasitoid-based biological control approaches against aphid pests.

DATA AVAILABILITY STATEMENT

The data presented in the study was deposited in the Sequence Read Archive (SRA) repository, the accession number are SRR18251541 and SRR18251542.

AUTHOR CONTRIBUTIONS

XJ and JF collected the insect organs or tissues, analyzed the transcriptome data, performed the molecular experiments such as RNA extraction, gene cloning and qPCR, and wrote the draft. JF and YQ assembled the RNA seq data. XJ and YX established the insect laboratory population. FF discussed the data. JF conceived and designed the study, and performed the personalized bioinformatic analysis. JC organized and directed the project. All authors contributed to the manuscript revision.

FUNDING

The National Natural Science Foundation of China (31801739), National Key Research and Development Program of China (2021YFE0115600, 2017YFD0201700), and China's Donation to the CABI Development Fund.

SUPPLEMENTARY MATERIAL

The Supplementary Material for this article can be found online at: https://www.frontiersin.org/articles/10.3389/fphys.2022.877133/full#supplementary-material

REFERENCES

Ban, L., Scaloni, A., D'Ambrosio, C., Zhang, L., Yan, Y., and Pelosi, P. (2003). Biochemical Characterization and Bacterial Expression of an Odorant-Binding Protein from *Locusta migratoria*. *Cell Mol. Life Sci. (Cmls)* 60 (2), 390–400. doi:10.1007/s000180300032

Buitenhuis, R., Mcneil, J. N., Boivin, G., and Brodeur, J. (2004). The Role of honeydew in Host Searching of Aphid Hyperparasitoids. *J. Chem. Ecol.* 30 (2), 273–285. doi:10.1023/b:joec.0000017977.39957.97

Calvello, M., Guerra, N., Brandazza, A., D'Ambrosio, C., Scaloni, A., Dani, F. R., et al. (2003). Soluble Proteins of Chemical Communication in the Social Wasp *Polistes dominulus*. *Cell Mol. Life Sci. (Cmls)* 60, 1933–1943. doi:10.1007/s00018-003-3186-5

Chen, C., Chen, H., Zhang, Y., Thomas, H. R., Frank, M. H., He, Y., et al. (2020). TBtools: An Integrative Toolkit Developed for Interactive Analyses of Big Biological Data. *Mol. Plant* 13 (8), 1194–1202. doi:10.1016/j.molp.2020.06.009

De Moraes, C. M., Lewis, W. J., Paré, P. W., Alborn, H. T., and Tumlinson, J. H. (1998). Herbivore-infested Plants Selectively Attract Parasitoids. *Nature* 393 (6685), 570–573. doi:10.1038/31219

Dong, W. X., Zhang, F., Fang, Y. L., and Zhang, Z. N. (2008). Electroantennogram Responses of Aphid Parasitoid *Aphidius Gifuensis* to Aphid Pheromones and Host-Plant Volatiles. *Chin. J. Ecol.* 27 (4), 591–595. doi:10.3724/SP.J.1141.2008.00438

Fan, J., Xue, W., Duan, H., Jiang, X., Zhang, Y., Yu, W., et al. (2017). Identification of an Intraspecific Alarm Pheromone and Two Conserved Odorant-Binding Proteins Associated with (E)-β-farnesene Perception in Aphid Rhopalosiphum Padi. *J. Insect Physiol.* 101, 151–160. doi:10.1016/j.jinsphys.2017.07.014

Fan, J., Zhang, Q., Xu, Q., Xue, W., Han, Z., Sun, J., et al. (2018). Differential Expression Analysis of Olfactory Genes Based on a Combination of Sequencing Platforms and Behavioral Investigations in *Aphidius Gifuensis*. *Front. Physiol.* 9, 1679. doi:10.3389/fphys.2018.01679

Forêt, S., and Maleszka, R. (2006). Function and Evolution of a Gene Family Encoding Odorant Binding-like Proteins in a Social Insect, the Honey Bee (*Apis mellifera*). *Genome Res.* 16 (11), 1404–1413. doi:10.1101/gr.5075706

Francis, F., Vandermoten, S., Verheggen, F., Lognay, G., and Haubruge, E. (2005). Is the (E)-β-farnesene Only Volatile Terpenoid in Aphids? *J. Appl. Entomol.* 129 (1), 6–11. doi:10.1111/j.1439-0418.2005.00925.x

Gao, X.-K., Zhang, S., Luo, J.-Y., Wang, C.-Y., Lü, L.-M., Zhang, L.-J., et al. (2018). Molecular Characterization and Ligand-Binding Properties of Six Odorant-Binding Proteins (OBPs) from Aphis Gossypii. *J. Asia-Pacific Entomol.* 21, 914–925. doi:10.1016/j.aspen.2018.07.004

Grabherr, M. G., Haas, B. J., Yassour, M., Levin, J. Z., Thompson, D. A., Amit, I., et al. (2011). Full-length Transcriptome Assembly from Rna-Seq Data without a Reference Genome. *Nat. Biotechnol.* 29 (7), 644–652. doi:10.1038/nbt.1883

Harada, E., Nakagawa, J., Asano, T., Taoka, M., Sorimachi, H., Ito, Y., et al. (2012). Functional evolution of duplicated odorant-binding protein genes, Obp57d and Obp57e, in Drosophila. *PLoS One* 7 (1), e29710. doi:10.1371/journal.pone.0029710

He, P., Zhang, J., Liu, N.-Y., Zhang, Y.-N., Yang, K., and Dong, S.-L. (2011). Distinct Expression Profiles and Different Functions of Odorant Binding Proteins in *Nilaparvata lugens* Stål. *PLoS One* 6 (12), e28921. doi:10.1371/journal.pone.0028921

Iovinella, I., Dani, F. R., Niccolini, A., Sagona, S., Michelucci, E., Gazzano, A., et al. (2011). Differential Expression of Odorant-Binding Proteins in the Mandibular Glands of the Honey Bee According to Caste and Age. *J. Proteome Res.* 10, 3439–3449. doi:10.1021/pr2000754

Jiang, X., Zhang, Q., Qin, Y., Yin, H., Zhang, S., Li, Q., et al. (2019). A Chromosome-Level Draft Genome of the Grain Aphid Sitobion Miscanthi. *Sitobion miscanthiGigascience* 8 (8), giz101. doi:10.1093/gigascience/giz101

Kang, Z.-W., Tian, H.-G., Liu, F.-H., Liu, X., Jing, X.-F., and Liu, T.-X. (2017). Identification and Expression Analysis of Chemosensory Receptor Genes in an Aphid Endoparasitoid *Aphidius Gifuensis*. *Sci. Rep.* 7 (1), 3939. doi:10.1038/s41598-017-03988-z

Leal, W. S. (2013). Odorant Reception in Insects: Roles of Receptors, Binding Proteins, and Degrading Enzymes. *Annu. Rev. Entomol.* 58, 373–391. doi:10.1146/annurev-ento-120811-153635

Li, M.-Y., Jiang, X.-Y., Qi, Y.-Z., Huang, Y.-J., Li, S.-G., and Liu, S. (2020). Identification and Expression Profiles of 14 Odorant-Binding Protein Genes from *Pieris Rapae* (Lepidoptera: Pieridae). *J. Insect Sci.* 20 (5), 2. doi:10.1093/jisesa/ieaa087

Li, S., Picimbon, J.-F., Ji, S., Kan, Y., Chuanling, Q., Zhou, J.-J., et al. (2008). Multiple Functions of an Odorant-Binding Protein in the Mosquito *Aedes aegypti*. *Biochem. Biophysical Res. Commun.* 372 (3), 464–468. doi:10.1016/j.bbrc.2008.05.064

Li, T.-T., Liu, W.-C., Zhu, J., Yang, Y.-H., Ma, C., Lu, C., et al. (2019). Crystal Structure and Ligand Identification of Odorant Binding Protein 4 in the Natural Predator *Chrysopa Pallens*. *Int. J. Biol. Macromolecules* 141, 1004–1012. doi:10.1016/j.ijbiomac.2019.09.043

Li, Y.-j., Chen, H.-c., Hong, T.-l., Yan, M.-w., Wang, J., Shao, Z.-m., et al. (2021). Identification of Chemosensory Genes by Antennal Transcriptome Analysis and Expression Profiles of Odorant-Binding Proteins in Parasitoid Wasp *Aulacocentrum Confusum*. *Comp. Biochem. Physiol. D: Genomics Proteomics* 40, 100881. doi:10.1016/j.cbd.2021.100881

Li, Z.-Q., Zhang, S., Cai, X.-M., Luo, J.-Y., Dong, S.-L., Cui, J.-J., et al. (2017). Three Odorant Binding Proteins May Regulate the Behavioural Response of Chrysopa Pallens to Plant Volatiles and the Aphid Alarm Pheromone (E)-β-farnesene. *Insect Mol. Biol.* 26 (3), 255–265. doi:10.1111/imb.12295

Liu, N.-Y., Zhang, T., Ye, Z.-F., Li, F., and Dong, S.-L. (2015). Identification and Characterization of Candidate Chemosensory Gene Families from *Spodoptera Exigua* Developmental Transcriptomes. *Int. J. Biol. Sci.* 11 (9), 1036–1048. doi:10.7150/ijbs.12020

Liu, Y., Du, L., Zhu, Y., Yang, S., Zhou, Q., Wang, G., et al. (2020). Identification and Sex-Biased Profiles of Candidate Olfactory Genes in the Antennal Transcriptome of the Parasitoid Wasp *Cotesia Vestalis*. *Comp. Biochem. Physiol. Part D: Genomics Proteomics* 34, 100657. doi:10.1016/j.cbd.2020.100657

Livak, K. J., and Schmittgen, T. D. (2001). Analysis of Relative Gene Expression Data Using Real-Time Quantitative PCR and the 2−ΔΔCT Method. *Methods* 25 (4), 402–408. doi:10.1006/meth.2001.1262.Prestwich

Ohta, I., and Honda, K.-i. (2010). Use of *Sitobion Akebiae* (Hemiptera: Aphididae) as an Alternative Host Aphid for a Banker-Plant System Using an Indigenous Parasitoid, *Aphidius Gifuensis* (Hymenoptera: Braconidae). *Appl. Entomol. Zool.* 45 (2), 233–238. doi:10.1303/aez.2010.233

Pelosi, P., Calvello, M., and Ban, L. (2005). Diversity of Odorant-Binding Proteins and Chemosensory Proteins in Insects. *Chem. Senses* 30 (Suppl. 1), i291–i292. doi:10.1093/chemse/bjh229

Pelosi, P., Iovinella, I., Felicioli, A., and Dani, F. R. (2014). Soluble Proteins of Chemical Communication: an Overview across Arthropods. *Front. Physiol.* 5, 320. doi:10.3389/fphys.2014.00320

Pelosi, P., Iovinella, I., Zhu, J., Wang, G., and Dani, F. R. (2018). Beyond Chemoreception: Diverse Tasks of Soluble Olfactory Proteins in Insects. *Biol. Rev.* 93 (1), 184–200. doi:10.1111/brv.12339

Pelosi, P., Zhou, J.-J., Ban, L. P., and Calvello, M. (2006). Soluble Proteins in Insect Chemical Communication. *Cell. Mol. Life Sci.* 63 (14), 1658–1676. doi:10.1007/s00018-005-5607-0

Peng, Y., Wang, S.-N., Li, K.-M., Liu, J.-T., Zheng, Y., Shan, S., et al. (2017). Identification of Odorant Binding Proteins and Chemosensory Proteins in *Microplitis Mediator* as Well as Functional Characterization of Chemosensory Protein 3. *PLoS One* 12 (7), e0180775. doi:10.1371/journal.pone.0180775

Powell, W., Pennacchio, F., Poppy, G. M., and Tremblay, E. (1998). Strategies Involved in the Location of Hosts by the ParasitoidAphidius erviHaliday (Hymenoptera: Braconidae: Aphidiinae). *Biol. Control.* 11, 104–112. doi:10.1006/bcon.1997.0584

Prestwich, G. D. (1993). Bacterial Expression and Photoaffinity Labeling of a Pheromone Binding Protein. *Protein Sci.* 2, 420–428. doi:10.1002/pro.5560020314

Qiao, H., Tuccori, E., He, X., Gazzano, A., Field, L., Zhou, J.-J., et al. (2009). Discrimination of Alarm Pheromone (E)-β-farnesene by Aphid Odorant-Binding Proteins. *Insect Biochem. Mol. Biol.* 39 (5-6), 414–419. doi:10.1016/j.ibmb.2009.03.004

Qin, Y. G., Yang, Z. K., Song, D. L., Wang, Q., Gu, S. H., Li, W. H., et al. (2020). Bioactivities of Synthetic Salicylate-substituted Carboxyl (E)-β-Farnesene Derivatives as Ecofriendly Agrochemicals and Their Binding Mechanism

with Potential Targets in Aphid Olfactory System. *Pest Manag. Sci.* 76 (7), 2465–2472. doi:10.1002/ps.5787

Sheng, S., Liao, C.-W., Zheng, Y., Zhou, Y., Xu, Y., Song, W.-M., et al. (2017). Candidate Chemosensory Genes Identified in the Endoparasitoid *Meteorus Pulchricornis* (Hymenoptera: Braconidae) by Antennal Transcriptome Analysis. *Comp. Biochem. Physiol. Part D: Genomics Proteomics* 22, 20–31. doi:10.1016/j.cbd.2017.01.002

Song, X., Qin, Y.-G., Yin, Y., and Li, Z.-X. (2021a). Identification and Behavioral Assays of Alarm Pheromone in the Vetch Aphid *Megoura Viciae*. *J. Chem. Ecol.* 47 (8-9), 740–746. doi:10.1007/s10886-021-01297-4

Song, Y., Liu, C., Cai, P., Chen, W., Guo, Y., Lin, J., et al. (2021b). Host-Seeking Behavior of *Aphidius Gifuensis* (Hymenoptera: Braconidae) Modulated by Chemical Cues within a Tritrophic Context. *J. Insect Sci.* 21 (3), 9. doi:10.1093/jisesa/ieab036

Sun, L., Wei, Y., Zhang, D.-D., Ma, X.-Y., Xiao, Y., Zhang, Y.-N., et al. (2016). The Mouthparts Enriched Odorant Binding Protein 11 of the Alfalfa Plant Bug *Adelphocoris Lineolatus* Displays a Preferential Binding Behavior to Host Plant Secondary Metabolites. *Front. Physiol.* 7, 201. doi:10.3389/fphys.2016.00201

Sun, Y.-L., Huang, L.-Q., Pelosi, P., and Wang, C.-Z. (2012b). Expression in Antennae and Reproductive Organs Suggests a Dual Role of an Odorant-Binding Protein in Two Sibling Helicoverpa Species. *Plos One* 7 (1), e30040. doi:10.1371/journal.pone.0030040

Sun, Y. F., De Biasio, F., Qiao, H. L., Iovinella, I., Yang, S. X., Ling, Y., et al. (2012a). Two Odorant-Binding Proteins Mediate the Behavioural Response of Aphids to the Alarm Pheromone (E)-ß-farnesene and Structural Analogues. *PLoS One* 7 (3), e32759. doi:10.1371/journal.pone.0032759

Tamura, K., Stecher, G., and Kumar, S. (2021). MEGA11: Molecular Evolutionary Genetics Analysis Version 11. *Mol. Biol. Evol.* 38 (7), 3022–3027. doi:10.1093/molbev/msab120

Vieira, F. G., Forêt, S., He, X., Rozas, J., Field, L. M., and Zhou, J.-J. (2012). Unique Features of Odorant-Binding Proteins of the Parasitoid Wasp *Nasonia vitripennis* Revealed by Genome Annotation and Comparative Analyses. *PLoS One* 7 (8), e43034. doi:10.1371/journal.pone.0043034

Vogt, R. G., and Riddiford, L. M. (1981). Pheromone Binding and Inactivation by Moth Antennae. *Nature* 293 (5828), 161–163. doi:10.1038/293161a0

Wang, B., Dong, W., Li, H., D'Onofrio, C., Bai, P., Chen, R., et al. (2022). Molecular Basis of (E)-β-farnesene-mediated Aphid Location in the Predator Eupeodes Corollae. *Curr. Biol.* 32 (21), 951–962. doi:10.1016/j.cub.2021.12.054

Wang, L., Bi, Y. D., Liu, M., Li, W., Liu, M., Di, S. F., et al. (2019). Identification and Expression Profiles Analysis of Odorant-binding Proteins in Soybean Aphid, Aphis Glycines (Hemiptera: Aphididae). *Insect Sci.* 27, 1019–1030. doi:10.1111/1744-7917.1270910.1111/1744-7917.12709

Wang, L., Yin, H., Zhu, Z., Yang, S., and Fan, J. (2021a). A Detailed Spatial Expression Analysis of Wing Phenotypes Reveals Novel Patterns of Odorant Binding Proteins in the Soybean Aphid, *Aphis Glycines*. *Front. Physiol.* 12, 702973. doi:10.3389/fphys.2021.702973

Wang, Q., Liu, J.-T., Zhang, Y.-J., Chen, J.-L., Li, X.-C., Liang, P., et al. (2021b). Coordinative Mediation of the Response to Alarm Pheromones by Three Odorant Binding Proteins in the green Peach Aphid *Myzus persicae*. *Insect Biochem. Mol. Biol.* 130, 103528. doi:10.1016/j.ibmb.2021.103528

Wu, J. X. (2002). *Agricultural Entomology*. Beijing: China Agriculture Press.

Xu, X., Xu, W., Ishida, Y., Li, Y., Leal, W. S., and Ames, J. B. (2009). 1H, 15N, and 13C Chemical Shift Assignments of the Mosquito Odorant Binding Protein-1 (CquiOBP1) Bound to the Mosquito Oviposition Pheromone. *Biomol. NMR Assign* 3 (2), 195–197. doi:10.1007/s12104-009-9173-5

Xue, W., Fan, J., Zhang, Y., Xu, Q., Han, Z., Sun, J., et al. (2016). Identification and Expression Analysis of Candidate Odorant-Binding Protein and Chemosensory Protein Genes by Antennal Transcriptome of *Sitobion Avenae*. *PLoS One* 11 (8), e0161839. doi:10.1371/journal.pone.0161839

Yang, S., Xu, R., Yang, S.-Y., and Kuang, R.-P. (2009). Olfactory Responses of Aphidius *gifuensis* to Odors of Host Plants and Aphid-Plant Complexes. *Insect Sci.* 16 (6), 503–510. doi:10.1111/j.1744-7917.2009.01282.x

Yang, S., Wei, J., Yang, S., and Kuang, R. (2011). Current Status and Future Trends of Augmentative Release of Aphidius Gifuensis for Control of Myzus Persicae in China Yunnan Province. *Journal of the Entomological Research Society* 13 (3), 87–99.

Yasukawa, J., Tomioka, S., Aigaki, T., and Matsuo, T. (2010). Evolution of expression patterns of two odorant-binding protein genes, obp57d and obp57e, in drosophila. *Gene* 467 (1-2), 25–34. doi:10.1016/j.gene.2010.07.006

Yuan, H.-B., Ding, Y.-X., Gu, S.-H., Sun, L., Zhu, X.-Q., Liu, H.-W., et al. (2015). Molecular Characterization and Expression Profiling of Odorant-Binding Proteins in *Apolygus Lucorum*. *PLoS ONE* 10 (10), e0140562. doi:10.1371/journal.pone.0140562

Zhang, G. (1999). *Aphids in Agriculture and Forestry of Northwest China*. 1st ed. Beijing: China Environmental Science.

Zhang, S., Zhang, Y.-J., Su, H.-H., Gao, X.-W., and Guo, Y.-Y. (2009). Identification and Expression Pattern of Putative Odorant-Binding Proteins and Chemosensory Proteins in Antennae of the *Microplitis Mediator* (Hymenoptera: Braconidae). *Chem. Senses* 34 (6), 503–512. doi:10.1093/chemse/bjp027

Zhang, Y., Fan, J., Sun, J., Francis, F., and Chen, J. (2017). Transcriptome Analysis of the Salivary Glands of the Grain Aphid, Sitobion Avenae. *Sci. Rep.* 7 (1), 15911. doi:10.1038/s41598-017-16092-z

Zhong, T., Yin, J., Deng, S., Li, K., and Cao, Y. (2012). Fluorescence Competition Assay for the Assessment of green Leaf Volatiles and Trans-β-farnesene Bound to Three Odorant-Binding Proteins in the Wheat Aphid Sitobion Avenae (Fabricius). *J. Insect Physiol.* 58 (6), 771–781. doi:10.1016/j.jinsphys.2012.01.011

Zhou, C.-X., Min, S.-F., Yan-Long, T., and Wang, M.-Q. (2015). Analysis of Antennal Transcriptome and Odorant Binding Protein Expression Profiles of the Recently Identified Parasitoid Wasp, Sclerodermus Sp. *Comp. Biochem. Physiol. Part D: Genomics Proteomics* 16, 10–19. doi:10.1016/j.cbd.2015.06.003

Zhou, J.-J., Vieira, F. G., He, X.-L., Smadja, C., Liu, R., Rozas, J., et al. (2010). Genome Annotation and Comparative Analyses of the Odorant-Binding Proteins and Chemosensory Proteins in the Pea Aphid *Acyrthosiphon pisum*. *Insect Mol. Biol.* 19 (Suppl. 2), 113–122. doi:10.1111/j.1365-2583.2009.00919.x

Zhou, Y. N., Xie, S., Chen, J. N., Wang, Z. H., Yang, P., Zhou, S. C., et al. (2021). Expression and Functional Characterization of Odorant-Binding Protein Genes in the Endoparasitic Wasp Cotesia Vestalis. *Insect Sci.* 28 (5), 1354–1368. doi:10.1111/1744-7917.12861

Conflict of Interest: The authors declare that the research was conducted in the absence of any commercial or financial relationships that could be construed as a potential conflict of interest.

Publisher's Note: All claims expressed in this article are solely those of the authors and do not necessarily represent those of their affiliated organizations or those of the publisher, the editors, and the reviewers. Any product that may be evaluated in this article, or claim that may be made by its manufacturer, is not guaranteed or endorsed by the publisher.

Copyright © 2022 Jiang, Qin, Jiang, Xu, Francis, Fan and Chen. This is an open-access article distributed under the terms of the Creative Commons Attribution License (CC BY). The use, distribution or reproduction in other forums is permitted, provided the original author(s) and the copyright owner(s) are credited and that the original publication in this journal is cited, in accordance with accepted academic practice. No use, distribution or reproduction is permitted which does not comply with these terms.

Advantages of publishing in Frontiers

OPEN ACCESS
Articles are free to read for greatest visibility and readership

FAST PUBLICATION
Around 90 days from submission to decision

HIGH QUALITY PEER-REVIEW
Rigorous, collaborative, and constructive peer-review

TRANSPARENT PEER-REVIEW
Editors and reviewers acknowledged by name on published articles

Frontiers
Avenue du Tribunal-Fédéral 34
1005 Lausanne | Switzerland

Visit us: www.frontiersin.org
Contact us: frontiersin.org/about/contact

REPRODUCIBILITY OF RESEARCH
Support open data and methods to enhance research reproducibility

DIGITAL PUBLISHING
Articles designed for optimal readership across devices

FOLLOW US
@frontiersin

IMPACT METRICS
Advanced article metrics track visibility across digital media

EXTENSIVE PROMOTION
Marketing and promotion of impactful research

LOOP RESEARCH NETWORK
Our network increases your article's readership